Proceedings of the I·R·E

A Journal of Communications and Electronic Engineering

(Including the WAVES AND ELECTRONS Section)

September, 1949

Volume 37 Number 9

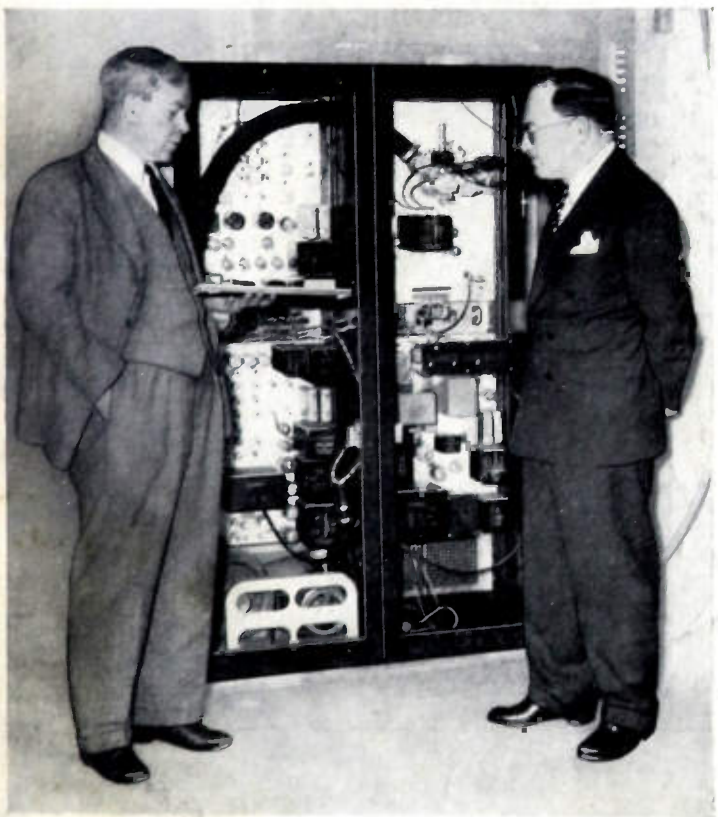

Hazeltine Electronic Corp.

AIR-NAVIGATION BEACON

Magnetostriction delay lines are used with pairs of pulses separated up to 90 microseconds in ground station equipment enabling airplanes to determine their distance from known points.

PROCEEDINGS OF THE I.R.E.

Waves and Electrons Section

TABLE OF CONTENTS FOLLOWS PAGE 32A

The Institute of Radio Engineers


AMPEREX
is FIRST again
with the most extensive line of
production-standardized, self-quenching
RADIATION
COUNTER TUBES
AMPEREX has the most complete line of standardized types of radiation counter tubes that are actual production line models. If you are working on anything which requires radiation counter tubes, chances are that Amperex can fit you neatly with a tube from our regular line. Save time...save money...write today for detailed Amperex literature.
re-tube with Amperex...
AMPEREX ELECTRONIC CORP.
25 WASHINGTON STREET, BROOKLYN 1, N. Y.
In Canada and Newfoundland: Rogers Majestic Limited
11-19 Brentcliffe Road, Leaside, Toronto, Ontario, Canada

Chicago Welcomes Electronic Engineers

Edgewater Beach Hotel, Chicago home of the National Electronics Conference. NEC Board of Directors, left to right, W. C. White of G.E. Research Laboratories; Karl Kramer (Sec.) of Jensen Manufacturing Co.; Prof. G. H. Fett, (NEC Pres.) University of Illinois; A. W. Graf. (Chairman of Board) Chicago; Prof. L. T. DeVore, (Program Chairman) University of Illinois.

NATIONAL ELECTRONICS CONFERENCE

The 1949 annual NATIONAL ELECTRONICS CONFERENCE will be held Monday through Wednesday, September 26-27-28, at the Edgewater Beach Hotel in Chicago, Ill.

Jointly sponsored by the Chicago Section of the Institute of Radio Engineers and the local section of AIEE, together with Illinois Institute of Technology, Northwestern University and the University of Illinois, its program of technical papers is directed toward electronics, particularly the first day, but with some attention to communication subjects, vacuum tubes and circuits on Tuesday and Wednesday.

50 leading firms will exhibit electronic equipment in the East and West Lounges. Admission to exhibits is by invitation. Registration for technical sessions is $3.00. Advance registration may be sent to "National Electronics Conference, Karl Kramer, Secy., 852 East 83rd St., Chicago 19, Ill." A special, advance price of $14.25 will cover registration, the three daily luncheons, and Volume 5 of the "Proceedings of the National Electronics Conference" (separately sold for $4.00). Make check payable to "National Electronics Conference, Inc," and mail before September 12th.

The Institute of Radio Engineers will have a service and information booth in the exhibits.

Calendar of COMING EVENTS

1949 IRE West Coast Convention, San Francisco, Calif., August 30-September 2

National Instrument Conference and Exhibit

A five day conference on instrumentation will be conducted by The Instrument Society of America at St. Louis, Mo. All sessions and exhibits will be in the beautiful Municipal Auditorium. IRE is a co-sponsor and Region V members may attend without registration cost.

September 12-16 1949

1949 National Electronics Conference, Chicago, Ill., September 26-28

National Radio Exhibition, Olympia, London, England, September 28 to October 28

AIEE Midwest General Meeting, Cincinnati, Ohio, October 17-21

Radio Fall Meeting, Syracuse, N.Y., October 31, November 1-2

1949 Nucleonics Symposium, New York City, October 31, November 1-2

IRE-URSI Fall Meeting, Washington, D.C., October 31, November 1-2

Audio Fair, Hotel New Yorker, New York City, October 27-28-29, 1949, sponsored by the Audio Engineering Society.

Second Annual Nucleonics Symposium October 31 to November 2, 1949 at Hotel Commodore, New York. IRE/AIEE

Southwestern IRE Conference, Baker Hotel, Dallas, Texas, December 9-10, 1949.

1950 IRE National Convention, New York, N.Y., March 6-9

IRE Regional Meetings Accelerate Electronic Progress!

PROCEEDINGS OF THE I.R.E. September, 1949, Vol. 37, No. 9. Published monthly in two sections by The Institute of Radio Engineers, Inc., at 1 East 79 Street, New York 21, N.Y. Price $2.25 per copy. Subscriptions: United States and Canada, $18.00 a year; foreign countries $19.00 a year. Entered as second class matter, October 26, 1927, at the post office at Menasha, Wisconsin, under the act of March 3, 1879. Acceptance for mailing at a special rate of postage is provided for in the act of February 28, 1925, embodied in Paragraph 4, Section 412, P. L. and R., authorized October 26, 1927.

Table of contents will be found following page 32A

Save Chassis Space!

and Improve Performance!

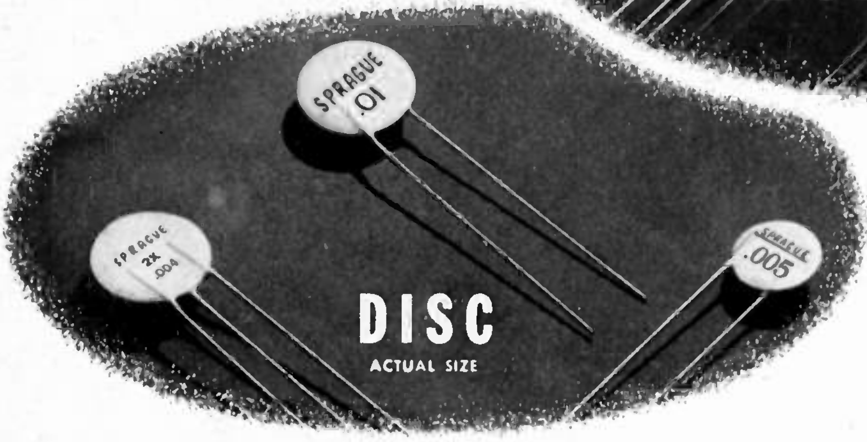

Reduce Assembly Operations!

SPRAGUE High-K Ceramic Capacitors

—— HERLEC ——

● Sprague-Herlec high-K ceramic capacitors for bypass and coupling applications offer the designer of television and F-M receivers savings in both chassis space and in component and wiring costs.

● Disc Types 29C and 36C capacitors are extremely small round wafer-shaped units. Mounted across miniature tube sockets with extremely short leads, they result in improved v-h-f bypassing. Both single and dual capacitors are available on one disc.

● Bulplate Type 34C multiple capacitors are rectangular wafers with as many as five capacitor sections. One rugged, ceramic Bulplate may combine into a single, compact integral assembly all the capacitors and related wiring in one or more stages of electronic circuits. In combination with miniature resistors, Bulplates make more stable and reliable network assemblies than do completely printed R-C circuits. Closer electrical tolerances are more economically obtained and circuits may operate at a higher power level.

● All Sprague-Herlec ceramic capacitors are protected by a tough, moisture-resistant insulating coating.

● A constant and reliable supply of capacitors is assured by operation of two manufacturing plants in two widely separated locations.

● *Write for Engineering Bulletin 601A today!*

SPRAGUE ELECTRIC CO. NORTH ADAMS MASSACHUSETTS

PIONEERS IN ELECTRIC AND ELECTRONIC DEVELOPMENT

THE HERLEC CORPORATION • MILWAUKEE 3, WISCONSIN
(Wholly owned Sprague Subsidiary)

-hp- Precision Voltmeters...
FAST ACCURATE READINGS
2 cps to 700 mc

-hp- MODEL 400C

ANOTHER -*hp*- SERVICE

Person-to-Person Help With Your Measuring Problems

Almost anywhere in America, -*hp*- field representatives can give you personal help with your measuring problems. They have complete data on -*hp*- instruments, their performance, servicing and adaptability. Call the nearest -*hp*- field representative whenever, wherever you need help with a measuring problem.

BOSTON, MASSACHUSETTS
Burlingame Associates
270 Commonwealth Ave.
KEnmore 6-8100

CHICAGO 6, ILLINOIS
Alfred Crossley & Associates
549 W. Randolph St.
State 7444

CLEVELAND 12, OHIO
M. P. Odell
1748 Northfield Avenue
Potomac 6960

DALLAS 5, TEXAS
Earl W. Lipscomb
4433 Stanford Street
Logan 6-5097

DENVER 10, COLORADO
Ronald G. Bowen
1896 So. Humboldt Street
Spruce 9368

FORT MYERS, FLORIDA
Arthur Lynch and Associates
P. O. Box 466
Fort Myers 1269M

HIGH POINT, NORTH CAROLINA
Bivins & Caldwell
Room 807, Security Bank Building
Phone 3672

LOS ANGELES 46, CALIFORNIA
Norman B. Neely Enterprises
7422 Melrose Avenue
Whitney 1147

NEW YORK 7, NEW YORK
Burlingame Associates
11 Park Place
Digby 9-1240

SAN FRANCISCO 3, CALIFORNIA
Norman B. Neely Enterprises
954 Howard Street
Douglas 2-2609

TORONTO 1, CANADA
Atlas Radio Corporation, Ltd.
560 King Street West
Waverley 4761

WASHINGTON 9, D. C.
Burlingame Associates
2017 S. Street N. W.
Decatur 8000

From 2 cycles to 700 megacycles, there's an accurate, easy-to-operate -*hp*- voltmeter to fit every voltage measurement requirement. You can choose from 5 precision voltmeters (including a battery-operated instrument) the ones which precisely fill your measuring need. Each has the familiar -*hp*- characteristics of high sensitivity, wide range, versatility, compact size, and time-saving ease of operation. These -*hp*- precision voltmeters are used by radio stations, manufacturers, research laboratories and scientific men throughout the world.

INSTRUMENT	FREQ. RANGE	VOLTAGE RANGE	ACCURACY	INPUT IMPEDANCE	PRICE
-hp- 400A	10 cps to 1 mc	.005 to 300 v 9 ranges	Within 3%	1 meg., 16 $\mu\mu$fd shunt	$185.00
-hp- 400B	2 cps to 100 kc	.005 to 300 v 9 ranges	Within 3%	10 meg., 20 $\mu\mu$fd shunt	195.00
-hp- 400C	20 cps to 2 mc	.0001 v to 300 v 12 ranges	Within 3%	10 meg., 15 $\mu\mu$fd shunt	200.00
-hp- 404A (Battery Op'd.)	2 cps to 50 kc	.0005 v to 300 v 11 ranges	Within 5%	10 meg., 20 $\mu\mu$fd shunt	185.00
-hp- 410A	20 cps to 700 mc	0.1 v to 300 v 7 ranges	Within 3%	10 meg., 1.3 $\mu\mu$fd shunt	245.00

For complete data on any -hp- instrument, write direct to factory or contact the nearest -hp- technical representative.

HEWLETT-PACKARD CO.
1876-D PAGE MILL ROAD · PALO ALTO, CALIFORNIA
Export Agents: Frazar & Hansen, Ltd.
301 Clay Street, San Francisco 11, California, U.S.A.

hp laboratory instruments
FOR SPEED AND ACCURACY

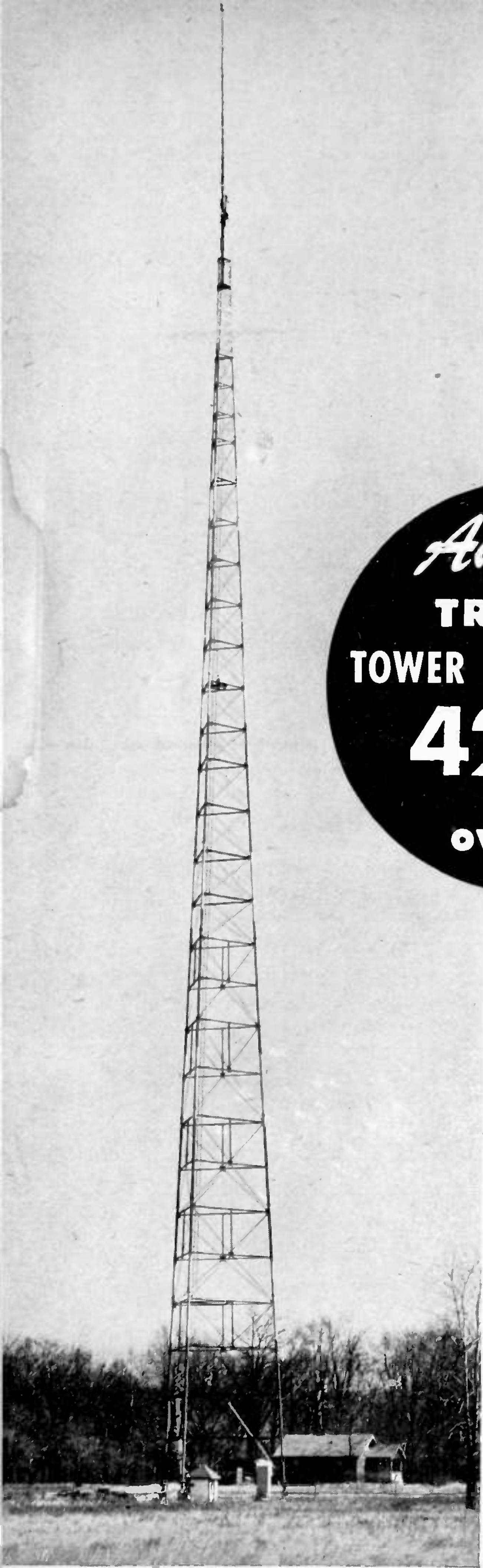

Reaching far out for Royal Oak...
WEXL-FM at Royal Oak, Michigan

● Metropolitan Detroit dialers are enjoying royal reception of WEXL-FM programs beamed from atop a new Truscon Radio Tower. Standing sturdy and strong as an oak, this Truscon Type H-30 Self-Supporting Tower, supporting an 8-bay General Electric FM antenna, rises to an overall height of 425 feet.

The Royal Oak Broadcasting Company is another in the long list of station operators who have turned to Truscon for the solution to their tower problems. In this case, blustery Great Lakes winters and blistering midwestern sun presented wide extremes of wind and weather. Still,

Another
TRUSCON
TOWER OF STRENGTH
425 FT.
HIGH
OVERALL

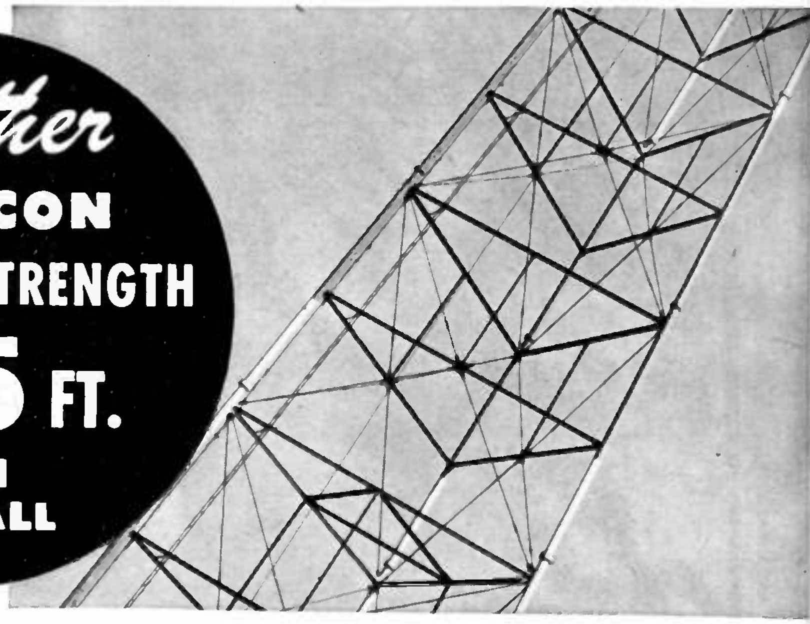

Truscon engineering and construction skills combined to deliver the tower which *exactly meets the demands of those purely local conditions.*

Truscon engineers are prepared to answer the tower problems of your particular project. They'll design and build your tower tall or small . . . guyed or self-supporting . . . uniform or tapered cross-section . . . for AM, FM or TV operation. Call in your nearby Truscon representative, or write our home office in Youngstown, Ohio, for consultation without obligation.

TRUSCON STEEL COMPANY
YOUNGSTOWN 1, OHIO
Subsidiary of Republic Steel Corporation

TRUSCON
SELF-SUPPORTING
AND UNIFORM
CROSS SECTION GUYED
TOWERS

A transient signal...

IMAGINED AT 4 KV... *but*... IMAGED AT 14 KV!

Du Mont Oscillography <u>shows</u> the difference...

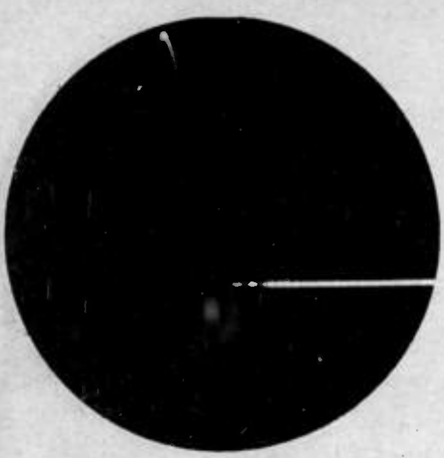

At low operating voltages the cathode-ray tube will respond to a high-speed transient signal, but—only at high voltages is the light output sufficient to SEE and *RECORD it.*

Du Mont high-voltage Oscillography shows you the difference with these actual (unretouched) oscillograms, and here's how it's done:

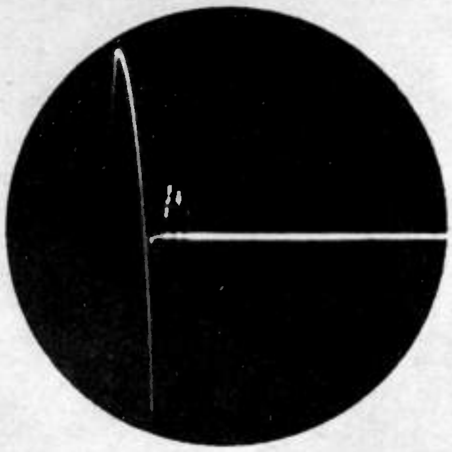

...with DU MONT HIGH-VOLTAGE CATHODE-RAY TUBES

Type 5RP-A is an intensifier-type, high-voltage cathode-ray tube featuring multiple accelerating electrodes for use with accelerating potentials up to 25,000 volts, without serious loss in deflection sensitivity. Writing rates in excess of 280 inches per microsecond have been recorded with this tube.

Type 5XP- has operating characteristics identical with those of the Type 5RP-A except for increased deflection sensitivity in one direction, provided by specially designed deflection plates. Especially suited for use with wide-band amplifiers. Types 5RP-A and 5XP- alike are capable of sufficient light output to allow projected oscillograms. Type 5XP- is interchangeable with Type 5RP-A except for slightly greater overall length.

...with these HIGH-VOLTAGE CATHODE-RAY INSTRUMENTS

Type 280-A is a high-voltage oscillograph for precision measurement of time. Originally designed to measure the composite television signal, it has found applications in many other fields. Time intervals of .025 microsecond can be measured, using time base variable from 1 to 15,000 microseconds. Calibrated delay circuit accurately delays sweep from 4 to 1,000 microseconds. Video-amplifier circuits provide uniform response up to 10 megacycles. Internal power supply provides accelerating potential up to 14,000 volts to a Type 5XP- tube.

Type 281-A is a basic cathode-ray indicator utilizing Type 5RP-A tube. Provision made for either capacitive or direct-coupling to all deflection plates. Displays single transient writing speeds up to 210 inches per microsecond. Internal power supply provides overall accelerating potential of 8,000 volts; external power supply can be used for higher voltages. The Type 286-A Power Supply is especially designed for use with the Type 281-A indicator, supplying overall accelerating potenial of 29,000 volts.

Type 250-AH is a high-voltage version of the versatile Type 250-A. High-voltage Type 5RP-A tube replaces Type 5CP-A. Provision is made for external high-voltage power supply. Type 250-AH is capable of recording writing speeds ten times those recorded by the Type 250-A. Using Type 263-B Power Supply, accelerating potentials as high as 13,000 volts may be applied. Sufficient light output to project oscillograms up to 30 feet with Type 2542 Projection Lens.

Type 248-A oscillograph is a favorite for high-frequency research. Self-contained, it offers a medium-voltage oscillograph for investigating pulses containing high-frequency components. Vertical amplifiers uniform in response within 30% from 20 cycles to 5 megacycles per second.

With addition of Type 263-B Power Supply, the Type 248-A becomes a high-voltage oscillograph for observation and photography of transients of short duration and extremely low repetition rates. Accelerating potentials up to 14,000 volts may be applied to a Type 5RP-A tube.

...with these HIGH-VOLTAGE POWER SUPPLIES

Type 286-A is a regulated rectified R-F type high-voltage power supply with adjustable output from 18,000 to 25,000 volts. Designed for use with Type 281-A indicator or wherever additional high voltage is required. Meter indicates output voltage.

Type 263-B is also a rectified R-F high-voltage power supply delivering from 6,000 to 12,000 volts. Designed for use with oscillographs employing 5RP-A or 5XP- tubes. Light in weight. Meter indicates output voltage.

For further details and prices, just address . . .

DUMONT *for Oscillography*

ALLEN B. DU MONT LABORATORIES, INC., *INSTRUMENT DIVISION*, 1000 MAIN AVENUE, CLIFTON, NEW JERSEY

Electronic Manufacturers

Specify HI-Q COMPONENTS–

for Dependable Performance

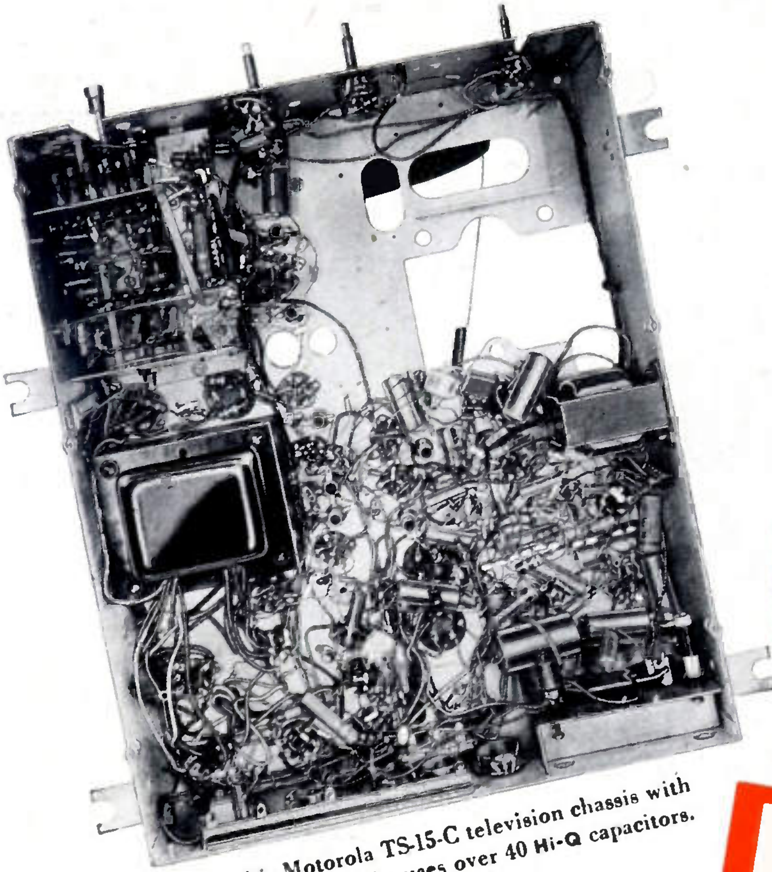

This Motorola TS-15-C television chassis with 12" picture tube uses over 40 **Hi-Q** capacitors.

● Motorola and practically all the rest of the industry's big names are among the more than 200 users of **Hi-Q** Components. They know from experience that they can depend upon **Hi-Q** for fine quality and strict adherance to ratings and tolerances . . . that **Hi-Q** contributes to the performance and long life of any electronic circuit.

Our engineers are always available to work with you in the development and production of capacitors, trimmers, resistors and choke coils to meet your specific needs. Write, wire or phone whenever you have a question concerning them.

Hi-Q general purpose ceramic capacitors have proven superior to mica and paper condensers of corresponding values. They are available in ratings of 5 mmf to 33,000 mmf. **Hi-Q** disc capacitors are high dielectric by-pass, blocking or coupling capacitors designed for use where their physical shape is more adaptable than tubular units.

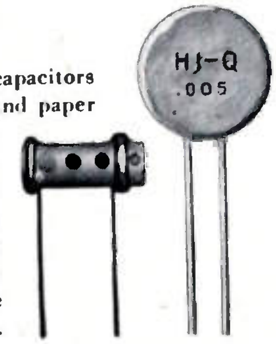

HI-Q COMPONENTS BETTER 4 WAYS

PRECISION Tested step by step from raw material to finished product. Accuracy guaranteed to your specified tolerance.

UNIFORMITY Constancy of quality is maintained over entire production through continuous manufacturing controls.

DEPENDABILITY Interpret this factor in terms of your customers' satisfaction . . . Year after year of trouble-free performance. Our Hi-Q makes your product better.

MINIATURIZATION The smallest BIG VALUE components in the business make possible space saving factors which reduce your production costs . . . increase your profits.

JOBBERS—ADDRESS: ROOM 1332
101 Park Ave., New York, N. Y.

HI-Q *Electrical Reactance Corp.*
FRANKLINVILLE, N. Y.

Plants: Franklinville, N. Y.— Jessup, Pa.— Myrtle Beach, S. C.
Sales Offices: New York, Philadelphia, Detroit, Chicago, Los Angeles

ELECTRONICS

Designers

Now..higher voltage

from

GENERAL ELECTRIC

SELENIUM STACKS

using new 18-volt (D-C) cells

New process for depositing selenium gives rectifier stacks greater uniformity, higher efficiency and longer useful life.

Here's real news for rectifier users. G.E.'s new 18-volt selenium cells, made by a special evaporation process which deposits selenium on the aluminum base with greater uniformity than otherwise possible, give you these advantages:

GREATER OUTPUT—With 50% more output than the standard 12-volt cells, the new design can be used for any application except those few which demand 24-hour, year-around service.

HIGHER EFFICIENCY—Not only is the initial efficiency higher, but more uniform coating keeps it high during the life of the stack.

SAVING IN SPACE—About one-quarter less space is required for the same output.

LOWER COST—Depending on the voltage across the stack, the 18-volt cells can save 25% in cost compared to standard 12-volt cells.

Selenium stacks are available in several standard sizes. Output in d-c voltage ranges from 18 to 126; applied a-c voltage, from 26 to 161 Bulletin GEA-5258 will give you detailed information. Send for it today:

STYLED FOR READABILITY
BUILT FOR RELIABILITY

This brand-new line of 2½-inch thin panel instruments has streamlined features which will give your panels a "new look." Arc lines have been eliminated,

GENERAL ELECTRIC

Digest

TIMELY HIGHLIGHTS ON G-E COMPONENTS

leaving only the upright scale divisions. New tapered pointer helps eye focus only on the reading. All but essential markings are masked by attractive case.

Internal mechanism is designed for extra reliability. High coercive Alnico magnet assures proper alignment, even under severe operating conditions. Large air gap reduces danger of stickiness caused by foreign particles. A variety of types and ratings in round or square cases are available for use in radio, television or testing equipment. Get complete details from Bulletin GEC-368.

DESIGNED FOR YOUR REQUIREMENTS

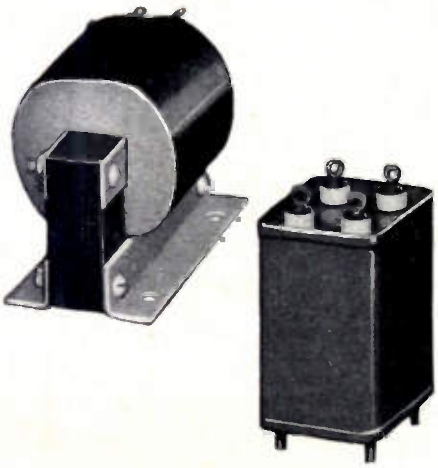

General Electric pulse transformers for radar and associated applications are designed to perform dependably in extremes of operating conditions. Many ratings in current production are of a special nature—designed to keep pace with rapidly changing requirements of the industry. However, for certain applications, they can be built to the specifications of electronic equipment manufacturers. Types available include interstage transformers, blocking oscillator transformers, charging chokes, current transformers, and pulse thyratron grid transformers. For a listing of available designs and ratings, send for bulletin GEC-481.

THEY'RE SMALL BUT THEY CAN TAKE IT

Cast-glass bushings with sealed-in nickel-steel hardware can be readily welded, soldered, or brazed directly to the apparatus, thus eliminating gaskets and providing a better seal. Small, compact structure often makes possible reduction of over-all size and weight of equipment. Practically unaffected by weathering, micro-organisms, and thermal shock, they're particularly well suited for use in electronic equipment and in installations where operating conditions are severe. Available in ratings up to 8.6 kv and for currents to 1200 amperes. Check Bul. GEA-5093.

RELY ON THESE FOR STABILITY

Fixed paper-dielectric capacitors are manufactured in accordance with joint Army-Navy specification JAN-C-25. They're constructed with thin Kraft paper, oil or Pyranol* impregnated, for stable characteristics and high dielectric strength. Plates are aluminum foil; special bushing construction provides for short internal leads, prevents possible grounds and short circuits. Cases have permanent hermetic seal.

Case style CP 63 (shown above) is rated 0.1–0.1 muf and 1000 volts. Other ratings range from .01 muf to 15 muf and from 100 to 12,500 volts. Write for detailed description and operating data in bulletin GEA-4357A.
*Reg. U.S. Pat. Off.

DOES A BIG JOB IN CLOSE QUARTERS

G.E.'s midget soldering iron can do a big job with only one-fourth the wattage usually used. This handy 6-volt, 25-watt iron is only 8 inches long with 1/8" or 1/4" tips and weighs but 1 3/4 ounces. Designed for close-quarter, pin-point precision soldering, the "midget" offers you all these advantages: low cost soldering; "finger-tip" operation; quick, continuous heat; easy renewal; long life; low maintenance. A real aid in designing radios, instruments, meters, electric appliances, and many other products requiring precision soldering. Available from stock. Check bulletin GEA-4519.

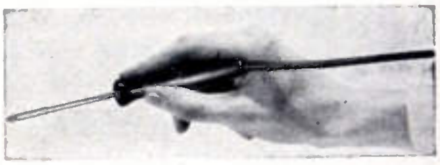

General Electric Company, Section G667-2
Apparatus Department, Schenectady, N. Y.
Please send me the following bulletins:

- ☐ GEA-4357A D-C Capacitors
- ☐ GEA-4519 Midget Soldering Iron
- ☐ GEA-5093 Glass Bushings
- ☐ GEA-5258 Selenium Stacks
- ☐ GEC-368 Panel Instruments
- ☐ GEC-481 Pulse Transformers

NAME ....

COMPANY ....

ADDRESS ....

CITY .... STATE ....

MARION ... helps Polytechnic Research and Development ...

... monitor microwave oscillator operation

The PRD Type 801 Universal Klystron Power Supply is a new and versatile instrument. It was produced by Polytechnic Research and Development Company of Brooklyn for operating the many high voltage klystron tubes which are used as sources of microwave energy in the fields of Radar, Radio Relay and Microwave Spectroscopy.

When PRD developed the Type 801 it needed two extremely accurate, matched indicating instruments for measuring Beam Current and Beam Voltage. Because PRD had previous experience with Marion and because Marion is so well known for foolproof, troublefree instruments of this kind . . . at reasonable cost, it was natural that PRD should turn to Marion. Marion's Standard Type 53SN was selected. This is a 3½" instrument, noted for accuracy and readability.

When you want standard or special purpose instruments for electrical indicating or measuring, we invite you to turn to us. Our long experience in helping others leads us to believe that we can help you too.

the name MARION means the most in meters

ASK US FOR FURTHER INFORMATION

M·E·I

MARION ELECTRICAL INSTRUMENT COMPANY

MANCHESTER, NEW HAMPSHIRE

Export Division, 458 Broadway, New York 13, U. S. A., Cables MORHANEX

IN CANADA: THE ASTRAL ELECTRIC COMPANY, SCARBORO BLUFFS, ONTARIO

On Land, Sea, and Air

Mallory Vibrators Are Relied Upon For Complete Dependability

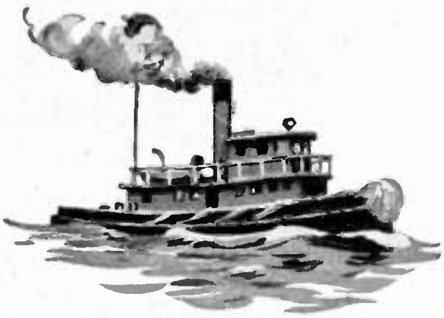

Whatever your vibrator application, the odds are that a standard Mallory Vibrator already is performing a similar job. The illustrations on this page are only a few of many examples where Mallory Vibrators are giving dependable service.

Mallory engineering skill, long experience, and complete adherence to quality ideals mean that Mallory Vibrators will give you longer life and less trouble.

More Mallory Vibrators are used in original equipment than all other makes combined. Why take a chance on anything less than this standard of excellence?

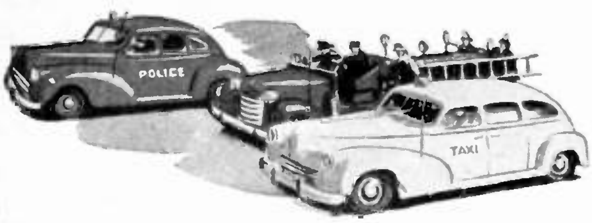

Send complete technical details of your problem. Mallory will supply the answer.

Vibrators and Vibrapack* Power Supplies

P. R. MALLORY & CO. Inc.

MALLORY

P. R. MALLORY & CO., Inc., INDIANAPOLIS 6, INDIANA

SERVING INDUSTRY WITH

Capacitors
Contacts
Controls
Rectifiers
Switches
Vibrators
Power Supplies
Resistance Welding Materials

*Reg. U. S. Pat. Off.

KILOVOLTS for KLYSTRONS

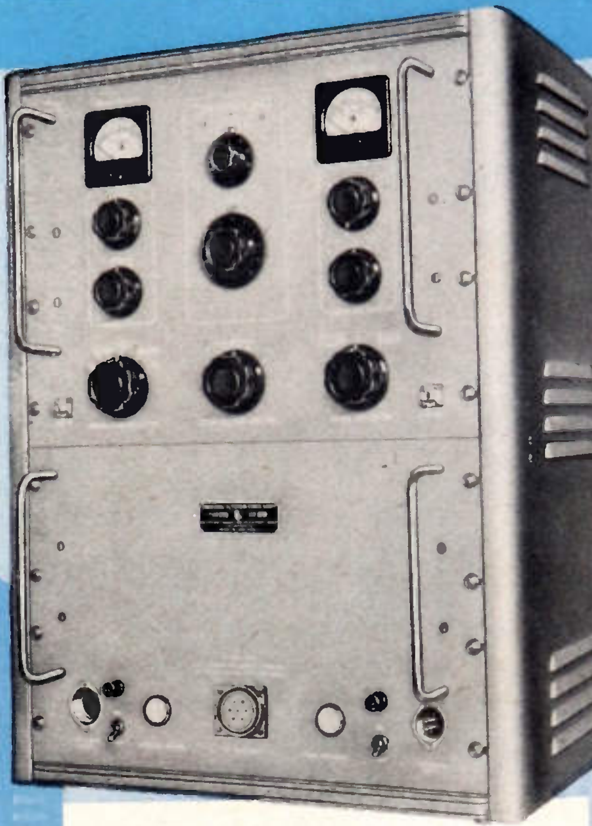

NEW PRD

POWER SUPPLY for microwave oscillators

PRICE
$1250.00
F.O.B. BROOKLYN, N.Y.

DIRECT READING CONTROLS
— coarse and fine — allow repeller voltage to be accurately adjusted from −20 to −750 volts.

CONTINUOUSLY VARIABLE
carefully regulated beam voltage supply provides cathode-to-grounded-anode potential in two ranges with choice of operation from 800 to 1500 volts at 65 ma or to 3600 volts at 25 ma.

GRID VOLTAGE
may be varied continuously from —300 volts to a positive value limited by the klystron grid current.

PANEL METERS
Indicate beam voltage and current directly.

The Type 801 Universal Klystron Power Supply has been developed by PRD to meet the increasing need of research and production engineers for a unit to operate the many high voltage klystrons now in use throughout the microwave spectrum.

Provision is made for c-w, square-wave, sawtooth, and external modulation of conventional internal cavity klystrons, external cavity oscillators, and the new millimeter tubes now coming into use in microwave spectroscopy.

Excellent voltage stabilization guarantees a maximum of oscillator frequency stability. Carefully controlled modulation wave-shapes insure accuracy of standing wave measurements and spectrum analysis when made with oscillators powered by this supply.

Polytechnic RESEARCH
& DEVELOPMENT COMPANY, Inc.
202 TILLARY ST., BROOKLYN 2, NEW YORK

JUST OFF THE PRESS!
The new 95-page catalog describing the complete PRD line of microwave test equipment is now available— write for your copy today to Dept. X.

News—New Products

These manufacturers have invited PROCEEDINGS readers to write for literature and further technical information. Please mention your I.R.E. affiliation.

New Plug-In Audio Amplifiers

The design of new AM, FM and Television audio amplifiers has been announced by the **Transmitter Div., General Electric Co.**, Electronics Park, Syracuse, N. Y.

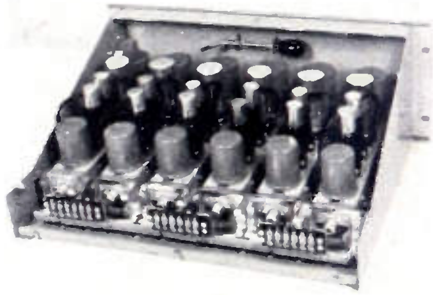

The amplifiers plug into Cannon receptacles mounted at the rear of the trays. The trays fit into a shelf which can be mounted in any standard 19 inch cabinet or relay rack.

Included are the Type BA-1-C Pre-Amplifier with its' Type FA-22-A Tray, the Type BA-12-A Program/Monitor Amplifier with its' Type FA-22-B Tray, and the Type FA-23-A Shelf which will accommodate up to six of the pre-amplifiers, and up to four of the program-monitor amplifiers.

The Type BA-1-C Pre-Amplifier may be used as a microphone or transcription pre-amplifier, booster amplifier, medium-level line amplifier, or as an isolation amplifier.

The Type BA-12-A Program/Monitor Amplifier may be used as a program or line amplifier, a monitoring amplifier, or an isolation amplifier.

New Diffusion Pump

A new oil-diffusion type vacuum pump, the HV-1, is in mass production by **Eitel-McCullough, Inc.**, 189 San Mateo Ave., San Bruno, Calif.

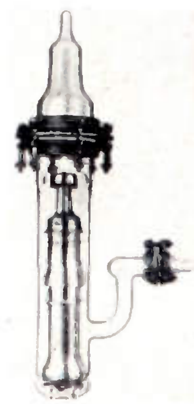

The HV-1 was originally designed by Eimac engineers for their own use in vacuum-tube manufacturing. It will deliver up to 67 liters per second, and has an attainable vacuum of 4×10^{-7} mm Hg.

The manufacturer states that expansion in the fields of nuclear science, research, and material processing in vacuum applications should find many applications for this pump.

(Continued on page 26A)


NEXT BEST THING
TO A
"SKY-HOOK!"
"Sky-hooks" being expensive and somewhat impractical, why not start from the ground up with a Blaw-Knox tower to obtain support for your high-riding FM and TV antennas?
Blaw-Knox, having built towers since spark-gap days, makes available to electronic engineers a degree of practical experience unequalled in this field. So, when you want the next best thing to a sky-hook, call Blaw-Knox.
[Shown here is a Blaw-Knox special 417 ft. Type H-40 Heavy Duty tower for Station WHIO, Dayton, Ohio. This tower was designed to support an RCA combination 4-section pylon, plus a 6-section TV antenna and station call letters.]
BLAW-KNOX DIVISION
OF BLAW-KNOX COMPANY
2037 Farmers Bank Building • Pittsburgh 22, Pa.
Distributed by
Graybar
OFFICES IN 100 PRINCIPAL CITIES
BLAW-KNOX
ANTENNA
TOWERS

These manufacturers have invited PROCEEDINGS readers to write for literature and further technical information. Please mention your I.R.E. affiliation.

(Continued from page 22A)

Precision Asbestos Tubing

Originally designed by **Precision Paper Tube Co.**, 2045 W. Charleston St., Chicago 47, Ill., as a heat resistant base for coils and bobbins, this new asbestos tubing has other potentialities in the industry.

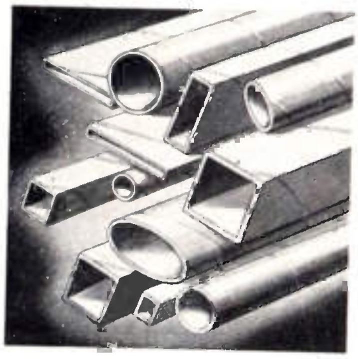

Because it is unaffected by high temperatures, this tubing could be used as insulation and as a dielectric, in such units as heaters, thermal heating devices, for insulating rods, etc.

The tube is made by spirally winding prepared asbestos tape to predetermined sizes around a mandrel, and then diformed into shape. This tubing can be supplied in any length, with wall thicknesses from 0.10 inch.

New Power Supply

The Model B, a recently designed dc power supply that employs new type heavy duty selenium rectifiers, and has a wide range variable voltage control, and damped volt and ammeter, is now available from **Electro Products Labs., Inc.**, 549 W. Randolph St., Chicago 6, Ill.

This source will deliver from 3 to 9 volts with a rating of 6 volts at 20 amperes continuous, and 35 amperes instantaneous, from 50 to 60cps 115 volt supply.

The Model B was primarily designed for testing or operating automobile radio receivers, but it will also test faulty vibrators, push button solenoids, 6-volt battery type receivers, and will provide over and under voltage operating conditions for all auto radio receivers.

(Continued on page 30A)

You haven't seen this before!

AEROVOX TYPE '87

AEROCON

SELF-MOLDED PLASTIC TUBULAR

● Brand *new!* Looks like a paper tubular yet *is entirely different*. This plastic tubular is *molded in its own paper tube*. That means a tubular approaching the performance of the molded-plastic capacitor yet available at a price closer to the conventional paper tubular.

For example: In a typical TV receiver using some 30 molded-plastic capacitors, the Type '87 Aerocon scores a saving of 50 cents! And without sacrificing top performance!

It's all due to another exclusive Aerovox development—Aerolene—the combination impregnating-sealing material already featured in Aerovox Duranite tubulars in general use.

So here's real *performance insurance* for those TV, auto-radio, oscillograph and other severe-service requirements. And at irresistible price, too.

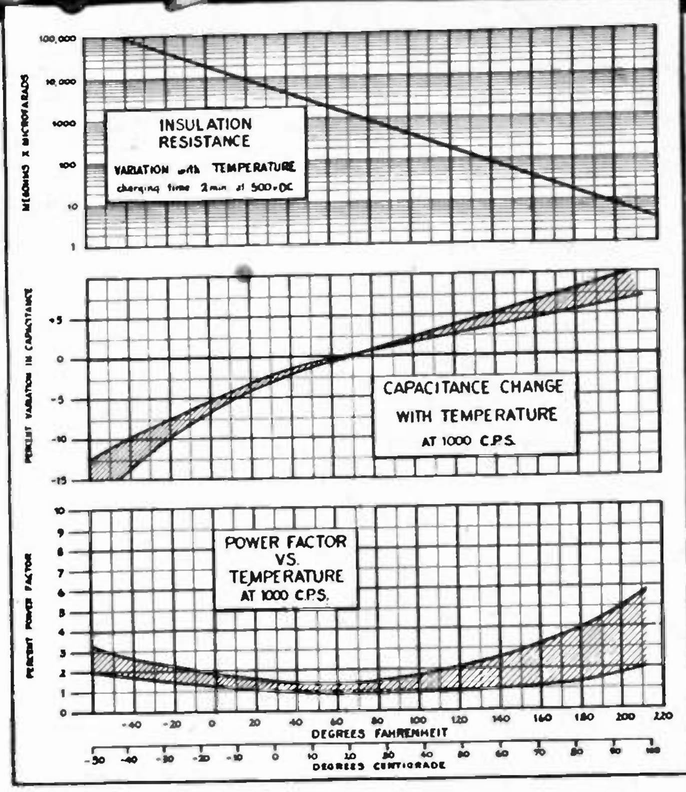

Samples, ratings, quotations available on request

AEROCON CHECK LIST

- ✔ Paper-tube tubular but with ends sealed with rock-hard Aerolene.
- ✔ Aerolene impregnant eliminates stocking and using of both wax and oil capacitors. One impregnant does work of both.
- ✔ Absence of impregnating oils and waxes eliminates dripping or cracking of wax coating which interaction might cause.
- ✔ Equal to or even smaller than molded units.
- ✔ Heat- and humidity-resistant qualities of the order of the best plastic tubulars.
- ✔ Can be used without drips at 212°F.
- ✔ Dielectric strength maintained at elevated temperatures. Rated voltages based on 212°F. operation.
- ✔ No softening of dip wax to become gummy, tacky, dirty or dark.
- ✔ Unimpaired by sub-zero operation. Capacitance increases slightly with temperature rise.
- ✔ Extremely high initial insulation resistance. Units recover insulation resistance upon heating.

AEROVOX capacitors

FOR RADIO-ELECTRONIC AND INDUSTRIAL APPLICATIONS

AEROVOX CORPORATION, NEW BEDFORD, MASS., U.S.A.

SALES OFFICES IN ALL PRINCIPAL CITIES • Export: 13 E. 40th ST., NEW YORK 16, N. Y.

Cable: 'ARLAB' • In Canada: AEROVOX CANADA LTD., HAMILTON, ONT.

News—New Products

These manufacturers have invited PROCEEDINGS readers to write for literature and further technical information. Please mention your I.R.E. affiliation.

(Continued from page 26A)

New Pre-Set Type Industrial Counter

A new series of presettable high-speed electronic counters for industrial applications, with counting rates of 10,000 per minute, and operating from photoelectric or magnetic pickup sources, may be purchased from the manufacturer **Airlectron, Inc.**, P.O. Box 151, Caldwell, N. J.

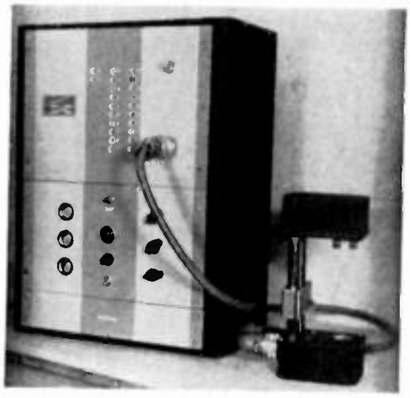

Various models are designed for pre-set ranges of from 1 to 999 gross with decade selection and direct reading count indication (shown in illustration); fixed preselection of any four quantities; and for decade selection of any number up to 10,000.

The output circuits of these counters may be connected so as to start and stop machine operation, switch loading chutes, or perform functions associated with counting.

Special timers are furnished if desired for use in rate determination or the precise measurement of rotational speeds.

Dimensions: 14" wide, 10" high, and 8" deep.

Turnover Type Pickup

A new turnover type phonograph pickup with double needle cartridge, which plays 33⅓, 45, and 78 rpm records at the same pressure, has been manufactured by **Astatic Corp.**, Conneaut, Ohio.

The pickup is the Model CLD, which employs Model LQD cartridge. All three recordings are played at 8 grams pressure. The needles may be removed by light prying with a knife point or small screw driver; this may be performed without removing the cartridge.

When using a 78 rpm Audio-Tone test record, output voltages are 1.2 volts at 1,000 cps, and with a 33⅓ rpm Columbia 281 record, 0.9 volt at 1,000 cps.

(Continued on page 58A)

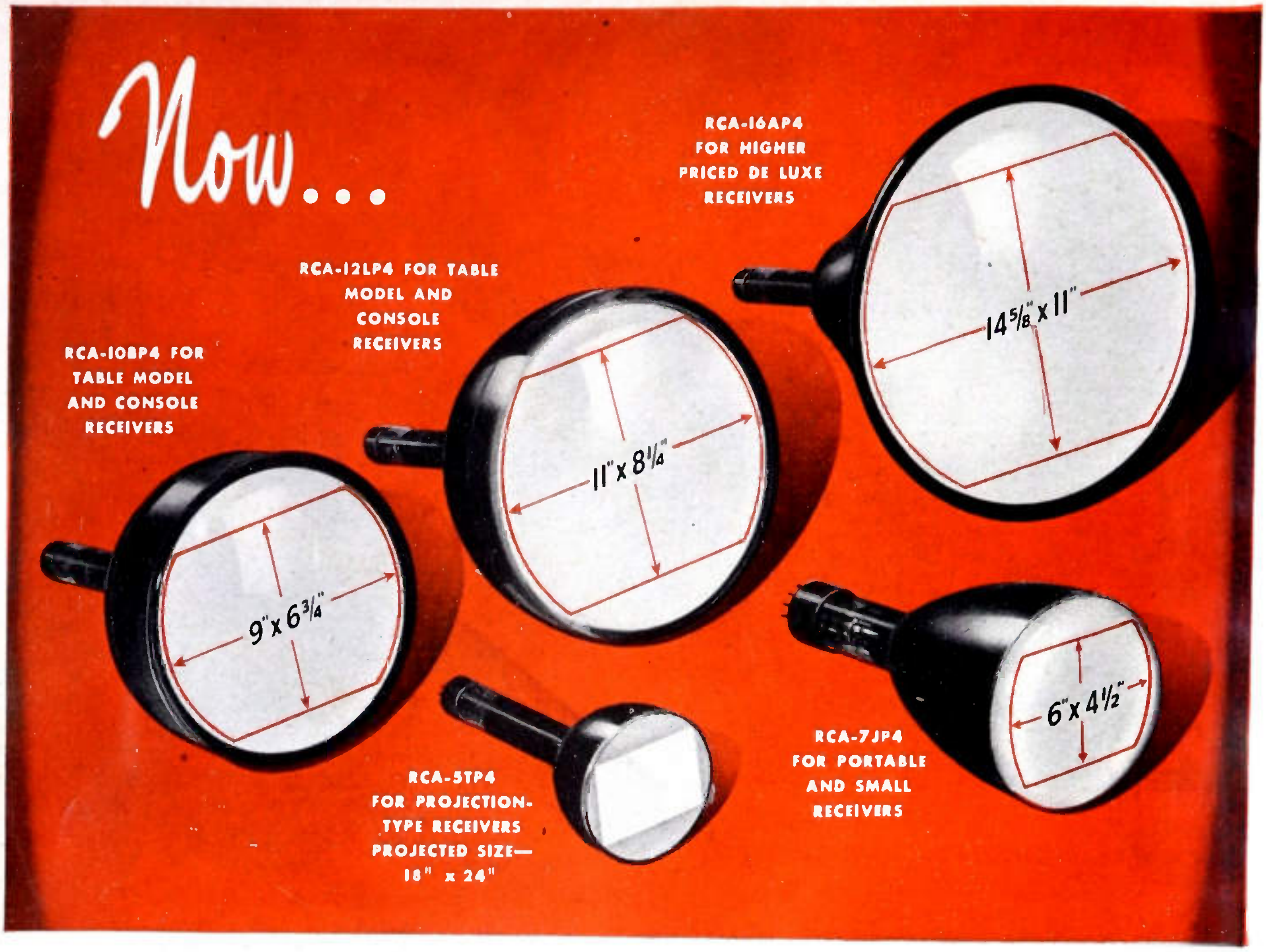

THE FOUNTAINHEAD OF MODERN TUBE DEVELOPMENT IS RCA

. . . the five most popular kinescopes —from one dependable source

RCA now has a popular type of kinescope to accommodate television receiver designs in practically every class and price range.

Concentrated production on these five accepted types results in longer production runs, which in turn, make possible lower cost, more uniform, and better quality tubes for our customers.

All five types are currently being mass-produced at the famed RCA tube plant in Lancaster, Pennsylvania. In addition, a large new plant is under construction at Marion, Indiana, where the production will be centered on the RCA-16-inch metal-cone kinescope.

RCA Application Engineers are ready to cooperate with you in applying these kinescopes and their associated components to your specific designs. For further information write RCA, Commercial Engineering, Section 47IR, Harrison, N.J.

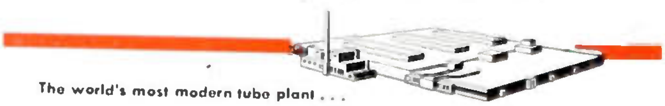

The world's most modern tube plant . . .

RCA, LANCASTER, PA.

RADIO CORPORATION of AMERICA

ELECTRON TUBES **HARRISON, N.J.**

PROCEEDINGS OF THE I.R.E.

(Including the WAVES AND ELECTRONS Section)

Published Monthly by

The Institute of Radio Engineers, Inc.

VOLUME 37 — *September, 1949* — NUMBER 9

Changes of address (with advance notice of fifteen days) and communications regarding subscriptions and payments should be mailed to the Secretary of the Institute, at 450 Ahnaip St., Menasha, Wisconsin, or 1 East 79 Street, New York 21, N. Y.

PROCEEDINGS OF THE I.R.E.

INSTITUTE NEWS AND RADIO NOTES SECTION

WAVES AND ELECTRONS SECTION

Responsibility for the contents of papers published in the PROCEEDINGS OF THE I.R.E. rests upon the authors. Statements made in papers are not binding on the Institute or its members.

† Deceased

Julius A. Stratton

DIRECTOR, 1948–1950

Julius Adams Stratton was born on May 18, 1901, in Seattle, Washington. In 1919 he entered the University of Washington, but transferred the following year to the Massachusetts Institute of Technology. After receiving the bachelor of science degree in electrical engineering from MIT in 1923, he spent the next year studying at the Universities of Grenoble and Toulouse in France.

Dr. Stratton returned to MIT in 1924 to act as research assistant in the Communications Laboratory for two years. During this period he received the master's degree in electrical engineering, in 1925. Returning to Europe in 1926, he was granted the doctor of science degree from the Technische Hochschule, in Zurich, Switzerland, in 1927. The following year he continued his studies in physics at the University of Munich.

In 1928 Dr. Stratton returned to the United States and was appointed assistant professor of engineering at MIT. He was transferred to the physics department four years later. When the Radiation Laboratory was established at MIT in 1940, he became a staff member, with the rank of full professor.

From 1942 to 1947, Dr. Stratton acted as expert consultant in the office of the Secretary of War. Meanwhile, in 1945, MIT established the Research Laboratory of Electronics, and appointed Dr. Stratton its head. He was also Chairman of the Committee on Electronics, Research, and Development from 1946 to 1947; and, for his services rendered during the war, was awarded the Medal for Merit by the Secretary of War.

A Director of the Armed Forces Communications Association, Dr. Stratton is a Fellow of the American Physical Society and the American Academy of Arts and Sciences. He became a Member of the Institute in 1942, a Senior Member in 1943, and a Fellow in 1945.

Institute Publication Policy

The Institute of Radio Engineers has consistently and successfully placed before its membership technical material of professional quality covering, broadly, the communications and electronics field. Despite the steadily shrinking purchasing power of money, and the consequent abnormal rise in the cost of paper, printing, and all other elements entering into the publication of the PROCEEDINGS OF THE I.R.E., the Institute has met the needs of the membership for major professional publications in its field. Frequently technical and industrial advantages arise from the PROCEEDINGS papers, not only promptly, but also many years after their initial publication. In fact, the value of the PROCEEDINGS OF THE I.R.E. to its readers grows steadily from the date of publication.

With the unparalleled expansion of the communications and electronics field, there has been a correspondingly rapid rise in the number of papers submitted for publication in the PROCEEDINGS. In order to publish acceptable papers with a justifiable amount of space in the PROCEEDINGS, it is necessary that a co-ordinated publication policy shall be developed and applied. There was therefore established the Editorial Administrative Committee, which considers all papers that have been found broadly acceptable for publication by the editorial readers from the Papers Review Committee and the Board of Editors. In order to avoid previous undue delays in publication, it is inevitable that some papers cannot be included in the PROCEEDINGS, and many others must be substantially condensed, in justice to the authors and readers as a group. The Editorial Administrative Committee acts along these lines on a judicial and impartial basis. Its deliberations follow careful consideration of each paper by at least four editorial readers, and sometimes more. It is encouraging to find that agreement among the editorial readers and among the members of the Editorial Administrative Committee is high.

The Institute continues to need papers which set forth novel discoveries or developments in clear fashion, and which, it is hoped, will contribute to the upbuilding of communications and electronic techniques and equipment. It has been widely felt among the membership that clear descriptions in words or through diagrams are to be preferred to a mathematical discussion if the sense of the paper can thus be adequately presented. Most readers hope to go through a paper and understand its significance without the necessity for absorbing a large number of complex equations. Of course all realize that many major contributions require that mathematics be utilized in order that future workers in that particular field can pursue the subject further. Particularly is this the case for the final formula giving the desired results. Many members have suggested, however, that wherever possible such mathematical expositions should be in the form of an appendix rather than scattered through the body of the paper. The Editorial Administrative Committee also considers it an obligation of the author to document his paper by substituting references to earlier material for repetition of such material.

The prospective authors of papers are urged to submit these for consideration for PROCEEDINGS publication. Preferred papers will deal with original material of basic nature, of considerable importance to a fair number of the PROCEEDINGS readers, of actual or potentially useful nature, and of the minimum length consistent with clarity of presentation of the truly novel fundamentals of the subject matter. The more nearly a submitted paper meets these requirements, the more welcome it will be for consideration for publication in the PROCEEDINGS.

The Institute accordingly asks the submission of such papers, so that the quality of the PROCEEDINGS may be maintained, excessive use of textual space may be avoided, and delays in publication may be substantially reduced. The understanding and co-operation of prospective authors are accordingly most earnestly solicited.

—*The Editor*

Double-Stream Amplifiers*

J. R. PIERCE†, FELLOW, IRE

Summary—**This paper presents expressions useful in evaluating the gain of a double-stream amplifier having thin concentric electron streams of different velocity and input and output gaps across which both streams pass.**

1. Introduction

A NEW HIGH-FREQUENCY AMPLIFIER has been described recently.[1–4] In this device there are two closely coupled streams of electrons with slightly different velocities. These two electron streams support a space-charge wave which travels with a velocity lying between the two electron velocities, and which increases in amplitude with distance as it travels. Use can be made of this increasing wave in obtaining amplification. The increasing wave can be set up by means of a helix or resonator which forms the input circuit. After the wave has increased as much as is desired, an amplified output can be obtained by means of a helix or resonator which acts as an output circuit.

The double-stream amplifier has many attractive features. For instance, the two electron streams need be close to one another, but need not be close to a long metallic circuit. Also, a high gain can be attained in a relatively short distance. In order to evaluate the new device, however, it is necessary to know how close the electron streams must be to one another, and what over-all gain may be expected in a given physical structure. It is the purpose of this paper to carry the theory far enough so that the over-all performance of a particular structure can be calculated and so that the importance of various parameters such as separation of the electron streams can be evaluated.

In the structure to be analyzed, which is shown in Fig. 1, the two streams are velocity modulated in passing across the gap between the grids of input resonator R_1, which is fed by input line L_1. This velocity modulation sets up an increasing space-charge wave. The wave grows in the space between input resonator R_1 and output resonator R_2. The convection current associated with the wave excites resonator R_2 and so transfers power to the output line L_2. The electron streams are collected on an anode A.

* Decimal classification: R132×R339.2. Original manuscript received by the Institute, February 9, 1949; revised manuscript received, June 10, 1949.

† Bell Telephone Laboratories, Inc., New York, N. Y.

[1] J. R. Pierce and W. B. Hebenstreit, "A new type of high-frequency amplifier," *Bell Sys. Tech. Jour.*, vol. 28, pp. 33–51; January, 1949.

[2] A. V. Hollenberg, "Experimental observation of amplification by interaction between two electron streams," *Bell Sys. Tech. Jour.*, vol. 28, pp. 52–58; January, 1949.

[3] A. V. Haeff, "The electron wave tube," Proc. I.R.E., vol. 37, pp. 4–10; January, 1949.

[4] L. E. Neergard, "Analysis of a simple model of two-beam growing-wave tube," *RCA Rev.*, vol. 9, pp. 585–601; December, 1948.

2. Motion of the Electrons

One problem in the analysis of double-stream amplifiers is to express the ac charge in the electron stream in terms of the fields acting on the electrons. In order to save space, expressions derived elsewhere will be used.

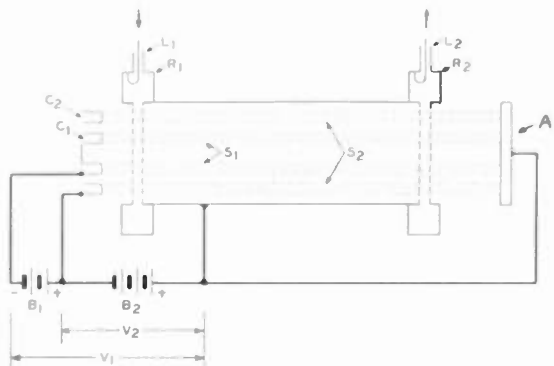

Fig. 1—A double-stream amplifier using concentric tubular electron streams and resonators as input and output circuits.

These are linearized (small signal) expressions derived assuming 1. nonrelativistic equations of motion, 2. a static electric field derivable from a potential, and 3. the same potential for all electrons at a given cross section of the beam. This would be essentially true for a thin tubular beam, 4. no electron motion perpendicular to the direction of electron flow. MKS units are used. All quantities are assumed to vary with time and distance as $\exp j(\omega t-\beta z)$.

The following additional nomenclature will be used:

ϵ_0 = dielectric constant of vacuum $\epsilon_0=8.85\times10^{-12}$ farad/meter

η = charge-to-mass ratio of the electron $\eta=1.76\times10^{11}$ coulomb/kilogram

I_{01}, I_{02} = dc currents

u_1, u_2 = dc velocities

ρ_{01}, ρ_{02} = dc linear charge densities $\rho_{01}=-I_1/u_1$, $\rho_{02}=-I_2/u_2$

ρ_1, ρ_2 = ac linear charge densities

v_1, v_2 = ac velocities

V_{01}, V_{02} = dc voltages with respect to the cathodes $u_1=\sqrt{\eta V_{01}}$, $u_2=\sqrt{2\eta V_{02}}$

$\beta_1=\omega/u_1$, $\beta_2=\omega/u_2$.

By use of the equations of motion and continuity ρ_1 and ρ_2, the linear charge densities in the two streams, have been shown to be[1]

$$\rho_1=\frac{I_{01}\beta^2}{2u_1V_{01}\left[\beta\left(1+\frac{b}{2}\right)-\beta\right]^2} \tag{1}$$

$$\rho_2 = \frac{I_{02}\beta^2}{2u_1V_{01}\left[\beta\left(1 - \frac{b}{2}\right) - \beta\right]^2} \cdot \tag{2}$$

Here b is the fractional velocity separation

$$b = \frac{2(u_1 - u_2)}{u_1 + u_2} \tag{3}$$

and u_0 is a sort of mean velocity specified by a mean potential V_0

$$u_0 = \sqrt{2\eta V_0} = \frac{2u_1u_2}{u_1 + u_2} \tag{4}$$

and β_0 is a phase constant related to u_0

$$\beta = \frac{\omega}{u_0} \cdot \tag{5}$$

We shall treat only a special case, that in which

$$\frac{I_{01}}{u_1V_{01}} = \frac{I_{02}}{u_2V_{02}} = \frac{I_0}{u_0V_0} \cdot \tag{6}$$

Here I_0 is a sort of mean current which, together with u_0, specifies the ratios I_{01}/u_1V_{01} and I_{02}/u_2V_{02}, which appear in (1) and (2).

In terms of these new quantities, the expression for the total ac charge density ρ is, from (1) and (2)

$$\rho = \rho_1 + \rho_2 = \frac{I_0\beta^2}{2u_0V_0}\left[\frac{1}{\left[\beta_0\left(1 - \frac{b}{2}\right) - \beta\right]^2} + \frac{1}{\left[\beta_0\left(1 + \frac{b}{2}\right) - \beta\right]^2}\right]V. \tag{7}$$

Equation (7) is a *ballistical* equation telling what charge density ρ is produced when the flow is bunched by a voltage V. To solve our problem, that is, to solve for the phase constant β, we must associate (7) with a *circuit* equation which tells us what voltage V the charge density produces.

3. Circuit Equation

Here it will simply be assumed that the ac voltage is proportional to the ac charge, as in a capacitance. The factor of proportionality p may be called a coefficient of induction

$$V = p\rho. \tag{8}$$

For a tubular beam, p will be a function of beam radius and of β. As we are interested in values of β lying in a small range about β_0, we will make a further approximation, and assume p to have the value it would have for $\beta = \beta_0$. This makes p a real constant.

The evaluation of p is merely a problem in electrostatics; this is a simple problem in certain cases. For instance, for a thin tubular beam in free space, one finds

$$p = F(\beta_0 a)/\epsilon_0 \tag{9}$$

$$F(\beta_0 a) = \frac{I_0(\beta_0 a)K_0(\beta_0 a)}{2\pi} \cdot \tag{10}$$

Here I_0 and K_0 are modified Bessel functions. In Fig. 2, $F(\beta_0 a)$ is plotted versus $\beta_0 a$.

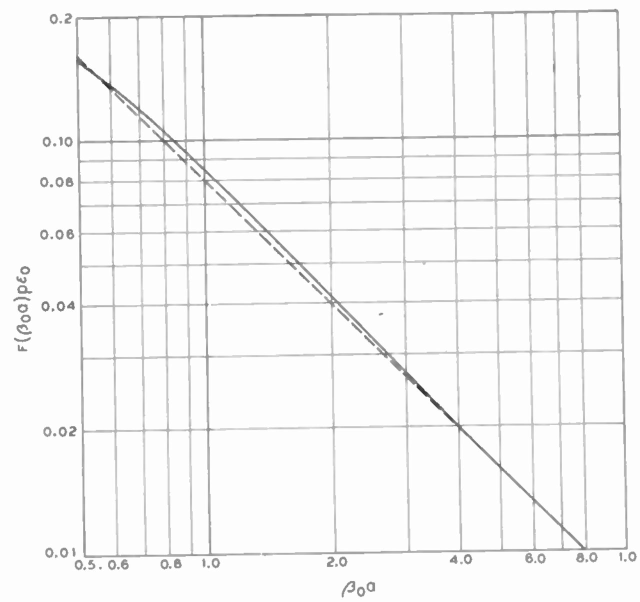

Fig. 2—Function $F(\beta_0 a)$ versus radius of beam in radians, $\beta_0 a$. The ordinate is also equal to $p\epsilon_0$, where p is the coefficient of induction for a thin tubular beam. The straight dashed line is $1/4\pi\beta_0 a$, which $F(\beta_0 a)$ approaches for large values of $\beta_0 a$.

In actually using a tubular beam, a tubular outer conductor must be used. The presence of such an outer conductor will reduce p somewhat. We can get an idea of the seriousness of this reduction by considering the case of a plane electron beam a distance d from a parallel plane conductor. In this case, we find the ratio R of the field produced by a given charge to the field which

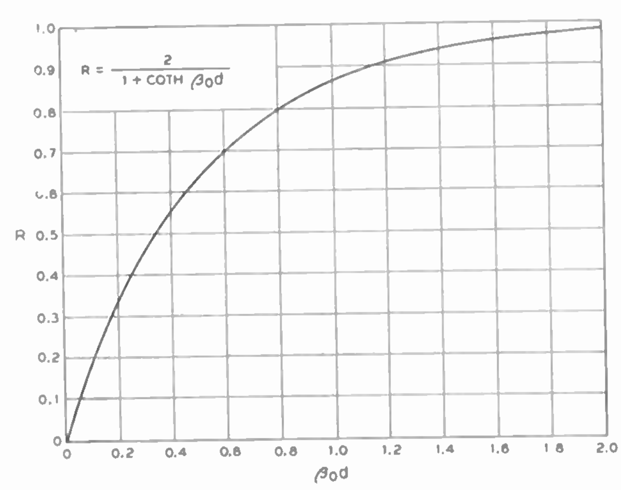

Fig. 3—Factor R, by which the coefficient of induction for a plane electron stream is reduced by the presence of a conducting plane a distance d away, plotted versus $\beta_0 d$, the separation of the stream and the plane in radians. This factor R may also be used in connection with sufficiently large tubular beams with a tubular shield.

would be produced if the conducting plane were removed to be

$$R = \frac{2}{1 + \coth \beta_0 d}. \tag{11}$$

In Fig. 3, R is plotted versus $\beta_0 d$. We see that for $\beta_0 d$ larger than 1.5, the conducting plane has little effect. Presumably, an outer tubular conductor more than 1.5 radians away from a tubular beam would have little effect. For reasonably large values of $\beta_0 a$ (perhaps $\beta_0 a = 1.5$ or larger), R can be used as a correction factor in connection with (10) in obtaining p for a tubular beam with a tubular outer conductor.

4. Combined Equation and Solution

Let us combine (7) with (8). We obtain

$$\frac{1}{[(1 - b/2) - \beta/\beta_0]^2} + \frac{1}{[(1 + b/2) - \beta/\beta_0]^2} = \frac{1}{U^2} \tag{12}$$

$$U^2 = \frac{(\beta/\beta_0)^2 I_0 p}{2u_0 V_0} = \frac{(\beta/\beta_0)^2 (p\epsilon_0) I_0}{2^{3/2}\eta^{1/2}\epsilon_0 V_0^{3/2}}. \tag{13}$$

In assuming p to be a constant over the range considered, we assumed β to be nearly equal to β_0. Hence, in (13) we will replace $(\beta/\beta_0)^2$ by unity, giving the approximate relation

$$U^2 = \frac{(p\epsilon_0) I_0}{2^{3/2}\eta^{1/2}\epsilon_0 V_0^{3/2}} = 9.52 \times 10^4 p\epsilon_0 I_0 / V_0^{3/2}. \tag{14}$$

In solving (12) it is convenient to let

$$\beta = \beta_0(1 + \delta) \tag{15}$$

$$U_M^2 = b^2/8. \tag{16}$$

We then obtain

$$\delta = \pm j\frac{b}{2}\left[\pm (U/2U_M)\sqrt{(U^2/U_M^2) + 8} - (U^2/2U_M^2) - 1\right]^{1/2}. \tag{17}$$

We see that δ/b is a function of U/U_M only.

In terms of δ, the amplitude varies with distance as

$$\exp(-j\beta_0 - j\beta_0\delta).$$

We see that the increasing wave, if there is one, is given by the plus signs. The rate of increase in db per wavelength per unit b, which will be called A, is

$$A = 20(\log_{10} e)(2\pi)\left(\frac{-j\delta}{b}\right) = 27.3\left[(U/2U_M)\sqrt{(U^2/U_M^2) + 8} - (U^2/2U_M^2) - 1\right]^{1/2}. \tag{18}$$

In Fig. 4, A is plotted versus $(U/U_M)^2$.

From (14) and (16) the abscissa is

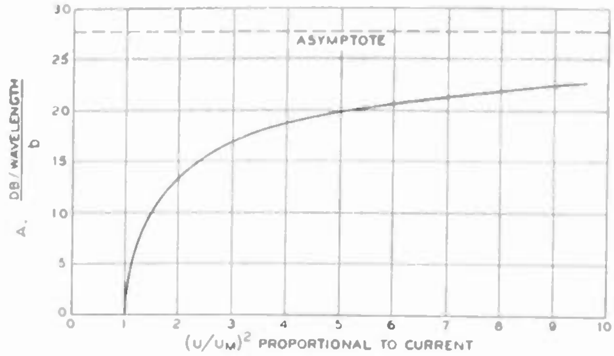

Fig. 4—Factor A, giving db per wavelength per unit b, versus $(U/U_M)^2$, which is also the ratio of beam current to the critical current which will just give an increasing wave.

$$(U/U_M)^2 = 7.61 \times 10^5 p\epsilon_0 I_0 / b^2 V_0^{3/2}. \tag{19}$$

For a given geometry, that is, for a given value of $p\epsilon_0$, and for given values of b and V_0, $(U/U_M)^2$ varies directly as the current. Hence, increasing the abscissa is equivalent to increasing the current. For currents below some critical current I_M given by

$$(U/U_M)^2 = 1$$

$$I_M = 1.313 \times 10^{-6} b^2 V_0^{3/2} / p\epsilon_0 \tag{20}$$

there is no increasing wave. As the current is raised above this value, the gain gradually rises and approaches asymptotically 27.3b db/wavelength.

5. Boundary Conditions

So far the rate of increase of the increasing wave has been evaluated in terms of I_0, V_0, $p\epsilon_0$, and b. In this section, we will consider the initial amplitude of the increasing wave which is set up by velocity modulating the electron streams, and the convection current associated with the increasing wave. In considering these matters, expressions for velocity and convection current will be written in terms of quantities already defined. For instance,[1]

$$v_1 = \frac{\eta(\beta/\beta_0)(1 - b/2)}{u_0(b/2 + \delta)}. \tag{21}$$

We have already replaced β/β_0 by unity in some of our expressions. We may as well do so here. For the increasing wave we can have $|\delta| \ll 1$ only when $b/2$ is not very small; for the unattenuated waves $|\delta| \ll 1$ only when $b/2 \ll 1$. Hence, we will assume $b/2 \ll 1$. We can write (21) approximately, with some rearrangement, as

$$(b/2)v_1 = \frac{\eta}{u_0(1 + 2\delta/b)} V \tag{22}$$

and similarly

$$(b/2)v_2 = \frac{-\eta}{u_0(1 - 2\delta/b)} V. \tag{23}$$

Let q_1 and q_2 be the convection currents of the two streams. We have the general relation

$$\frac{\partial q_1}{\partial z} = -\frac{\partial \rho_1}{\partial t}$$

$$q_1 = \frac{\omega}{\beta}\rho_1. \tag{24}$$

We have,[1] using the same approximations as before,

$$(b/2)^2 q_1 = \frac{-I_0}{2V_0(1+2\delta/b)^2} V \tag{25}$$

$$(b/2)^2 q_2 = \frac{-I_0}{2V_0(1-2\delta/b)^2} V. \tag{26}$$

If the first stream is velocity-modulated by a voltage V_i, the initial velocity will be

$$v_1 = \frac{u_1}{2}\frac{V_i}{V}. \tag{27}$$

In accordance with the approximation we have made $(b/2 \ll 1)$ we will replace u_1 by u_{01}. Then we obtain as the initial velocities

$$v_1 = v_2 = \frac{u_0}{2}\frac{V_i}{V} = \frac{\eta V_i}{u_0}. \tag{28}$$

The initial convection currents will be zero.

Let us denote the V's for the four waves and the four values of δ for the four waves (which we obtain from (18)) by the subscripts I, II, III, and IV. We will use the subscript I for the increasing wave (given by the + signs in (18)). We see from (22), (23), and (28) that

$$\sum_{N=1}^{IV} \frac{V_N}{(1+2\delta_N/b)} = bV_i/2 \tag{29}$$

$$\sum_{N=1}^{IV} \frac{V_N}{(1-2\delta_N/b)} = -bV_i/2 \tag{30}$$

and from (25), (26), and the fact that the initial convection currents are zero

$$\sum_{N=I}^{IV} \frac{V_N}{(1+2\delta_N/b)^2} = 0 \tag{31}$$

$$\sum_{N=I}^{IV} \frac{V_N}{(1-2\delta_N/b)^2} = 0. \tag{32}$$

We can solve these equations, obtaining $2V_I/bV_i$, where V_I is the voltage associated with the increasing wave, as a function of $(U/U_M)^2$.

We are more interested in $|q|$, the magnitude of the total convection current, (q_1+q_2), associated with the increasing wave. From (25) and (26) we obtain

$$\frac{|q|}{V_i} = \frac{I_0}{bV_0}G \tag{33}$$

$$G = \left|\frac{1}{(1+2\delta_I/b)^2} + \frac{1}{(1-2\delta_I/b)^2}\right|\left(\frac{2V_I}{bV_i}\right). \tag{34}$$

We note that both δ_I/b and $2V_I/bV_i$ are functions of $(U/U_M)^2$ only. The function G is plotted versus $(U/U_M)^2$ in Fig. 5.

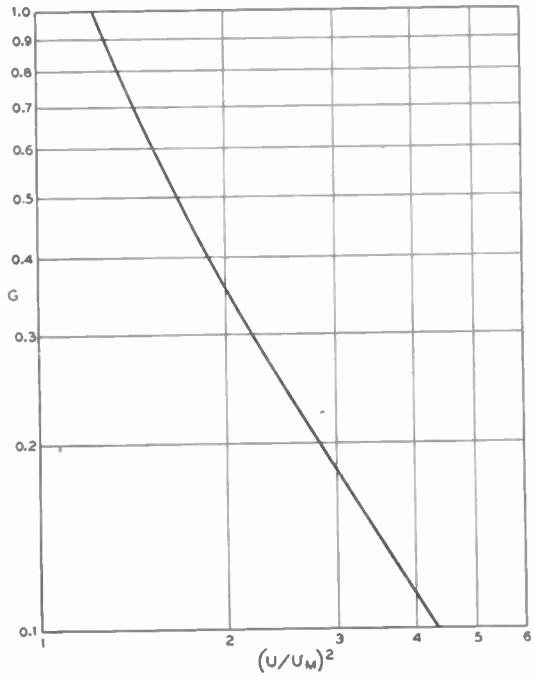

Fig. 5—A conductance factor G versus $(U/U_M)^2$. The ratio of initial convection current in the increasing wave to the voltage velocity-modulating both streams is $(I_0/bV_0)G$.

The quantity $|q|/V_i$ is a conductance. If the tube is long enough so that at the output the increasing wave is large compared with the three other waves, the transconductance of the tube g_m is, neglecting the effect transit time across the gaps (gap factor),

$$g_m = \frac{I_0}{bV_0} G 10^{bAN/20}. \tag{35}$$

Here N is the number of beam wavelengths between the gaps. G and A are functions of $(U/U_M)^2$. The number of beam wavelengths is the number of free-space wavelengths times c/u_0, where c is the velocity of light, and

$$c/u_0 = 505/\sqrt{V_0}. \tag{36}$$

6. Separation of the Electron Streams

So far we have assumed that the same field acts on both electron streams. We will now consider a case in which all the electrons in stream 1 are acted on by an ac potential V_1 and all electrons in stream 2 are acted on by a potential V_2. Such would be the case, for instance; for thin concentric electron streams.

In this case we have three coefficients of induction, p_1, p_2, and p_m, which appear in the following relation between charge densities and potentials

$$V_1 = p_1\rho_1 + p_m\rho_2 \tag{37}$$

$$V_2 = p_2\rho_2 + p_m\rho_1. \tag{38}$$

The p's will be taken as real constants.

We will now have in place of (1) and (2)

$$\rho_1 = \frac{\eta I_{01}}{u_1^3} \frac{\beta^2}{(\beta_1 - \beta)^2} V_1 = a_1 V_1 \tag{39}$$

$$\rho_2 = \frac{\eta I_{02}}{u_2^3} \frac{\beta^2}{(\beta_2 - \beta)^2} V_2 = a_2 V_2. \tag{40}$$

As written, (39) and (40) define the parameters a_1 and a_2, which relate charge densities to the voltages producing them. We can now write (37) and (38)

$$V_1 = p_1 a_1 V_1 + p_m a_2 V_2 \tag{41}$$

$$V_2 = p_2 a_2 V_2 + p_m a_1 V_1. \tag{42}$$

By eliminating the V's we obtain

$$(1 - p_1 a_1)(1 - p_2 a_2) = p_m^2 a_1 a_2. \tag{43}$$

We will consider the special case in which

$$\frac{\eta p_1 I_{01}}{u_1^3} = \frac{\eta p_2 I_{02}}{u_2^3} = \frac{p_0 I_0}{2u_0 V_0} = K^2. \tag{44}$$

The quantities u_0 and V_0 will have the same meaning as before. The product $p_0 I_0$ can be regarded as a single parameter.

By introducing b and δ as before, we obtain

$$\frac{1}{(\delta - b/2)^2} + \frac{1}{(\delta + b/2)^2} = \frac{1}{K^2(1+\delta)^2}\left[1 + \frac{K^4(1+\delta)^4\left(1 - \dfrac{p_m^2}{p_1 p_2}\right)}{(\delta - b/2)^2(\delta + b/2)^2}\right]. \tag{45}$$

As before, we will neglect δ with respect to unity. We will now let

$$\frac{1}{U^2} = \frac{1}{K^2}\left[1 + \frac{K^4\left(1 - \dfrac{p_m^2}{p_1 p_2}\right)}{(\delta^2 - (b/2)^2)^2}\right]. \tag{46}$$

In terms of U, (45) can be rewritten

$$\frac{1}{(\delta - b/2)^2} + \frac{1}{(\delta + b/2)^2} = \frac{1}{U^2}. \tag{47}$$

This is the same as (12), and the solutions are given by (17).

If we substitute the value of δ for the increasing wave (using the + signs in (17)) into (46), we obtain

$$\frac{1}{K^4} - \frac{1}{K^2 U^2} + \frac{(1 - p_m^2/p_1 p_2)}{U^4(1 - \sqrt{1 + 8(U_M/U)^2})^2} = 0. \tag{48}$$

Let

$$\alpha = (U/U_M)^2 \tag{49}$$

and

$$1 - p_m^2/p_1 p_2 = S. \tag{50}$$

We obtain on solving (48)

$$\frac{U_M^2}{K^2} = \frac{1}{2\alpha}\left(1 + \sqrt{1 - \frac{4S}{(1 - \sqrt{1 + 8/\alpha})^2}}\right). \tag{51}$$

In (50), S is a measure of the separation of the electron streams. For coincident electron streams, $p_m = p_1 = p_2$ and $S = 0$. For infinitely remote (uncoupled) streams, $p_m = 0$ and $S = 1$. If the streams are coincident, so that $S = 0$,

$$\frac{U_M^2}{U^2} = \frac{U_M^2}{K^2}. \tag{52}$$

That is, U and K are equal and the solution is equivalent to that for coincident streams.

Suppose we use, for comparison, a case in which $S = 0$ (coincident streams). The ratio of the actual current to current which would just give gain if S were zero is K^2/U_M^2. The ratio of *effective* current to critical current is α. We can use (51) to plot α (which must be entered as the abscissa in Fig. 4 to obtain A) versus K^2/U_M^2, the ratio of actual current to a critical current calculated setting $S = 0$. Such a plot is shown in Fig. 6.

It is helpful in considering Fig. 6 to express the abscissa, K^2/U_M^2, by means of (49) and (44) as

$$\frac{K^2}{U_M^2} = \frac{2p_0 J_0}{(b/2)^2 u_0 V_0}. \tag{53}$$

Thus, the abscissa is proportional to current.

The gain per wavelength is proportional to δ_I, the value for δ for the increasing wave, and δ_I can be obtained by means of (18)

$$\delta_I = j\frac{b\sqrt{\alpha}}{2\sqrt{2}}(\sqrt{1 + 8/\alpha} - 2/\alpha - 1)^{1/2}. \tag{54}$$

Actually, in obtaining the gain per wavelength per unit b, α may be used as the abscissa in Fig. 4.

Let us consider the curves of Fig. 6. We see that for $S = 0$ the plot is a 45° line; in this case $U = K$. For finite values of the parameter S, the effective current at first rises as current is increased, and then falls. There is thus a maximum value of effective current.

If we examine (51) we see that α has its maximum value at

$$1 - \frac{4S^2}{(1 - \sqrt{1 + 8/\alpha})^2} = 0. \tag{55}$$

A larger value of α would, from (51), imply a complex current. The maximum value of α, obtained from (55) is

$$\alpha_{\max} = \frac{8}{[(1 + 2S)^2 - 1]}. \tag{56}$$

We see from (51) and (55) that this value occurs at a current ratio

$$K^2/U_M^2 = 2\alpha. \tag{57}$$

The currents for this maximum can be obtained using (53) and (44). As S approaches unity, α_{max} approaches unity (no gain) and K^2/U_M^2 approaches 2.

We are now in a position to obtain the gain versus current for separated electron streams, and we can obtain the maximum gain in terms of S from (56) and (54). It remains to evaluate this parameter in some physical case.

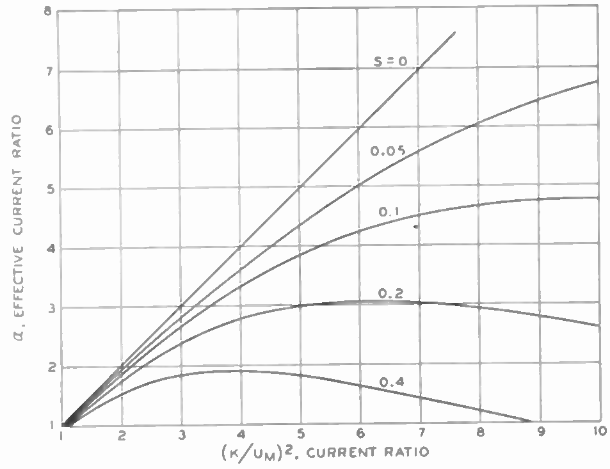

Fig. 6—A curve for separated streams, giving $\alpha=(U/U_M)^2$, the effective current ratio, versus $(K/U_M)^2$, a current ratio for various values of beam separation parameter S.

Sometimes two thin hollow cylindrical beams are used. The writer has treated this case and found that for such beams

$$S = 1 - \frac{I_0(\beta_0 a)K_0(\beta_0 b)}{K_0(\beta_0 a)I_0(\beta_0 b)} \tag{58}$$

Here a and b are the radii of the inner and outer beams. A much simpler expression is adequate when $\beta_0 a$ and $\beta_0 b$ are sufficiently large so that the beams may be regarded as essentially plane. For a plane sheet of impressed charge of phase constant β_0, the potential falls off normal to the sheet as exp $(-\beta_0 d)$ where d is distance from the sheet. Hence, we see at once that

$$p_m/p_1 = p_m/p_2 = e^{-\beta_0 d}$$
$$S = 1 - e^{-2\beta_0 d} \tag{59}$$

where $\beta_0 d$ is the separation between the current sheets in radians. The parameter S is plotted versus $\beta_0 d$ in Fig. 7. The maximum gain per wavelength per unit b is plotted versus $\beta_0 d$ in Fig. 8.

To give an idea of the separations involved, it may be pointed out that for 1,000 volts and 4,000 Mc, 1 radian corresponds to 0.030 inches.

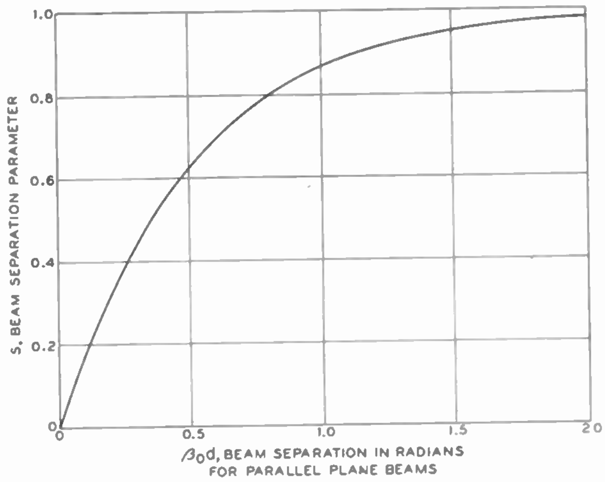

Fig. 7—Beam separation parameter S versus beam separation in radians $\beta_0 d$ for parallel plane beams separated by a distance d. This curve is also applicable to large concentric tubular beams separated radially by a distance d.

In computing gain for separated tubular streams, it is necessary to know not only S, but p_1 and p_2 as well. These coefficients of induction can be computed by applying the formulas of section 3 to each stream separately.

The boundary conditions for separated streams have not been worked out.

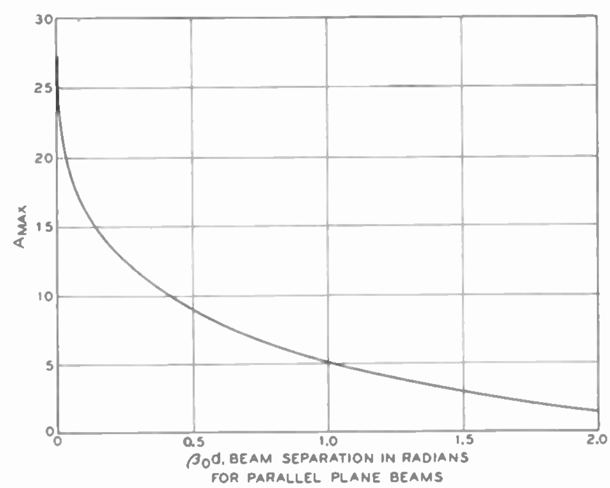

Fig. 8—A_{max}, the maximum gain per wavelength per unit b, plotted versus $\beta_0 d$, the beam separation in radians, for parallel plane beams or for large concentric tubular beams.

Part II—Investigations of High-Frequency Echoes*

H. A. HESS†

Summary—**Oscillographic high-speed records of high-frequency telegraph signals (10 to 20 Mc) which show periodic variations in the field strength are investigated in this paper. A movement of the ionospheric reflector is considered as the cause of Doppler shifts, which are measured within the amplitudes of interfering radio waves between two consecutive minima. The long-distance propagation which usually occurs over multiple paths in the transmission, indicates shifts of 0.1 to 0.5 cps; 2.4 cps were measured at the interference of direct and indirect signal of VIS, Sydney, Australia, on 16,450 kc. Routes passing the auroral zones are characterized by the occurrence of "cleft signals" with shifts between 5 and 30 cps.**

I. Introduction

The author's[1] previous paper contains investigations of time-interval measurements between long-distance signals and their echoes. It was intended to find an explanation for the highly constant values of a complete high-frequency circuit around the globe, which vary between 0.13760 and 0.13805 second. The complete circulating signal travels on paths between 41,280 and 41,420 km; about 1,300 km greater than the earth's circuit. Interferences of waves coming from multiple paths in the transmission, and the uniform variations of the phases are considered as the cause for divergences within the measured time intervals. The shape of the signals is influenced within fractions of 1 second, and this fact seems to be an occasion for errors in the measurements.[2] An analysis[3,4] of the signals in their individual wave components gives a new possibility to explore the kind of the ionospheric propagation.

Schmidt's theory[5,6] of a sliding-wave propagation along an ionospheric limit layer has been discussed by Dieminger, Hamberger, and Rawer,[7] as well as by Lassen.[8] These scientists explain the high-frequency propagation over long distances, and the occurrence of signals which travel repeatedly around the globe, by multiple reflections between the *F* layer and the earth's surface.

According to Griffiths,[9] Doppler shifts of about 0.5 cps were perceived at the normal frequency of WWV, 15,000 kc, National Bureau of Standards, Washington, D. C. during observations at Tatsfield, England, in December, 1945. The author found, by his recent studies, many measurable shifts on the interference of high-frequency signals, which were recorded on film rolls at Frederikshavn, 57°26′N, 10°29′E, and at Randers, 56°31′N, 10°02′E, during the period 1942 to 1945. The apparatus used were described in the previous paper. The accuracy for time-interval measurements, surveyed by a 500 cps normal frequency, was in the order of $5 \cdot 10^{-5}$ seconds, if the velocity of the films was greater than two meters per second.

II. Investigation of Radio-Wave Interferences

An interference of two waves with the same frequency either effects an intensification, or a diminution of the resulting amplitude, according to the existing phase conditions. Morse signals are interrupted coherent waves. Their beginning and closing makes possible the analysis of multiple paths in the transmission, by measuring the time intervals between the successively arriving waves.

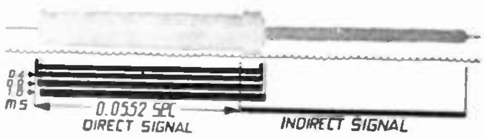

Fig. 1—Direct signal (multiple paths) and indirect signal of LSA, Monte Grande, Argentina, 17,600 kc.

Fig. 1 shows an oscillographic record of the unmodulated signal of LSA3, Monte Grande, Argentina, 17,600 kc, on October 10, 1944, 11^h54 Central European time (CET), at Randers, as an exquisite case of an involved multipath phenomenon. The direct signal arrived probably on four paths within time intervals of 0.4, 0.9, and 1.6 milliseconds between the component which arrives first, or detours of about 120, 270, and 480 km. The end of the direct signal is overlapped by the beginning indirect signal, which travels along the reverse great-circle path, and reaches the receiver after the time difference of $t_i = 0.0552$ second, measured between the first component of the direct signal. Employing the equation:[10] $d = u/2(1 - t_i/t_u)$, where $u = 40{,}024$ km (earth's circuit), and $t_u = 0.13778$ second (time interval

* Decimal classification: R112.4. Original manuscript received by the Institute, July 13, 1948; revised manuscript received, March 18, 1949.

† Schad-Str. 24, 14a-ULM (Donau), Germany.

[1] H. A. Hess, "Investigations of high-frequency echoes," Proc. I.R.E., vol. 36, pp. 981–992; August, 1948.

[2] H. A. Hess, "Messungen an Funksignalen," *Das Elektron*, vol. 2, pp. 312–321; December, 1948.

[3] H. A. Hess, "Das Kurzwellenecho," *Funk und Ton*, no. 2, pp. 57–65; no. 5, pp. 244–253; and no. 7, pp. 334–344; 1948.

[4] H. A. Hess, "Über den periodischen Schwund bei der Kurzwellenübertragung," *Funk und Ton*; to be published.

[5] O. v. Schmidt, "Neue Erklärung des Kurzwellenumlaufes um die Erde," *Z. Tech. Phys.*, vol. 17, p. 443; 1936.

[6] H. A. Hess, "Untersuchungen an Kurzwellen-Echosignalen," *Z. Naturf.*, vol. 1, p. 499; September, 1947.

[7] L. Hamberger and K. Rawer, "Zur Fernausbreitung der Kurzwellen," *Z. Naturf.*, vol. 2a, p. 521; September, 1947.

[8] H. Lassen, "Die Ausbreitung der Kurzwellen-Echosignale," *Funk und Ton*, p. 420; August, 1948.

[9] H. V. Griffiths, "Doppler effect in propagation," *Wireless Eng.*, vol. 24, pp. 162–167; June, 1947.

[10] See p. 982 of footnote reference 1.

of the complete high-frequency circuit), a distance of 11,995 km is obtained. The true distance between Monte Grande and Randers is 12,010 km.

Fig. 2—Direct signal of WKO, Rocky Point, N. Y., 15,970 kc. (Two paths with different phase conditions).

Fig. 2 is a record of the unmodulated direct signal of WKO Rocky Point, N. Y., 15,970 kc on November 8, 1944, 14^{h}08 CET at Randers with two transmission paths. The first wave is characterized by a rather low field strength, while the second retarded component arrived after 0.35 millisecond, and represents a detour of 105 km between both paths. Since 15,970 kc is considered as a rather high transmission frequency with regard to the conditions of 1944 during the minimum of the sun-spot cycle, the propagation occurred under flat angles of incidence toward the horizon; 3° at two hops, and 9° at three hops between earth's surface and F layer coincide well with the measured detour of 105 km. The recorded case indicates opposite phases of the interfering waves, since the end of the second component is characterized by an increase of the amplitude. Variations of the phase conditions are generally observed within a few seconds, and minima alternating with maxima make possible the study of Doppler shifts on the film rolls which had a length of 10 meters.

These investigations demonstrate that measurements between the components, which arrive first, of the direct signals and the indirect circulating signals should only permit exact distance determinations. The weak first components frequently did not appear on all recorded signals of North American stations, probably because of the various and fortuitous sensitivity of the receiver. Their absence principally must be considered as the cause of the errors in the measurements which were found to diverge within a range of about 60 km.

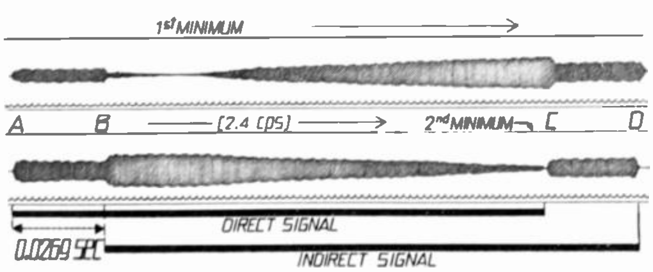

Fig. 3—Doppler-shift studies at the interference of direct and indirect signal of VIS, Sydney, Australia, 16,450 kc.

Fig. 3 shows a record of two consecutive slightly modulate signals of VIS, Sydney, Australia, 16,450 kc on November 8, 1944, 10^{h}05 CET at Randers. Both signals consisting of two interfering waves represent the direct signals A–C and the indirect signal B–D with a measurable time difference of $t_i = 0.0269$ second. The distance between Sydney and Randers is 16,110 km. The not overlapped parts of the direct and the indirect signals have approximately equal field strengths, while previously and subsequently the amplitudes are different. Thus, a sharp minimum occurs during the interference period B–C on both recorded signals. The time interval of 0.42 second between these two consecutive minima means a Doppler shift of 2.4 cps in the frequency between direct and indirect signals.

Since a moved reflector is considered to effect the sinusoidal variations in the amplitudes of the interfering sky waves, the Doppler shifts are given by the equation:

$$f_d = \frac{v}{c} \cdot f,$$

where $f = 16{,}450$ kc is the rf used, v generally expresses a velocity (in this case: the path difference within 1 second), and $c = 299{,}776$ km is the velocity of the electromagnetic waves. The measured frequency shift $f_d = 2.4$ cps is equivalent with a path difference of 43 meters per second. For a long distance propagation, however, the angles of incidence are oblique toward the vertically moved F layer, and the Doppler shift is given by the equation

$$f_d = \frac{2 \cdot v}{c} \cdot f \cdot \sin(\alpha + \gamma), \quad \text{where}$$

α is the angle of incidence toward the horizon, γ the half angular width of a single hop between the earth's surface and a F layer reflection, and v the vertical velocity of the F layer.

The geographical distance between Sydney and Randers is about 16,000 km on the direct path, and about 24,000 km on the reverse path. Direct signal and indirect signals travels on ionospheric paths of 16,548 and 24,822 km, if the assumption of six and nine ionospheric reflections is made. The sum 41,370 km, or a time of 0.1379 second for the completely circulating signal is well in accordance with the average value $t_u = 0.13778$ second.

For the case that the F layer should ascend along the direct path, and descend along the reverse path, 15 effective reflections may be regarded. The equation:

$$v = 1/15 \cdot c \cdot \frac{f_d}{2 \cdot f \sin(\alpha + \gamma)}$$

may approximately give an average value for the velocity of an individual point of the reflecting F layer. $\angle\alpha = 4°20'$, and $\angle\gamma = 12°$ were calculated for a direct propagation in six hops, like as for a reverse propagation in nine hops with regard to a F layer height of 250 km. A velocity of 5 meters per second is obtained for the F layer. This average value may be corrected by the experience that the velocity of the F layer can not be homogeneous at every point along the direct and reverse path.

The ionospheric conditions actually are more involved than a simple calculation would sufficiently explain them. The direct and reverse great-circle path is

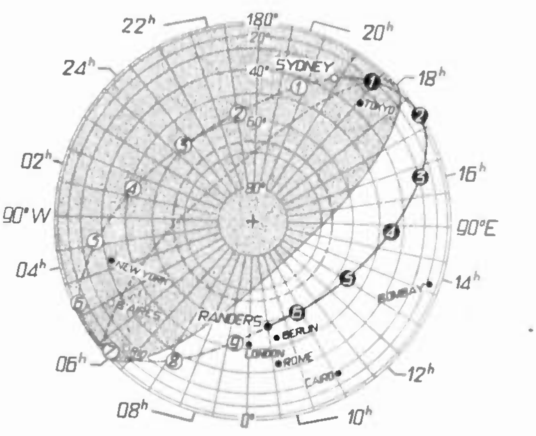

Fig. 4—Direct and reverse great-circle path between Sydney and Randers, and illumination of the globe on November 8, 10^h00, Central European time.

illustrated in Fig. 4, together with the illumination of the globe on November 8, 10^h00 CET. The points of probable ionospheric reflections which are marked with numbers along the direct and reverse path are distributed on different times of the day and seasons. According to the general experiences with the vertical incidence sounding, an ascending layer seems possible at the points 1, 2, 3, 4, and 5 along the direct path, while the movement at point 6 is probably a descending one. Along the indirect path, a slight ascending occurred at points 1, 2, 3, 4, and 5 (summer-night conditions) while certainly an effective descending occurred at points 6, 7, 8, and 9 because of sunrise.

In the case that the great-circle line between transmitter and receiver passes the auroral zone, strongly marked fluctuations within the signal amplitudes were observed. Fig. 5 represents the routes on the earth's globe which are characterized by the occurrence of "cleft signals." Filled-out points are positions on the northern hemisphere, and circles on the southern hemisphere. Both magnetic poles and the auroral zone on the northern hemisphere are marked. The auroral center has been found by many observers[11] on polar lights to be in northwestern Greenland (78°N, 68°W), in the middle between the magnetic and geographical pole. Similar conditions are supposed on the southern hemisphere. Cleft signals are observed in Europe from stations in Hawaii, Alaska, and the western North America. They also occur on routes between eastern North America and East Asia, as well as between South Africa and New Zealand on the southern hemisphere.

Fig. 6 shows that three selected film records with cleft signals of KQF, Kailua, Hawaii, on 13,495 kc, made at Randers, Denmark. The signal amplitudes are characterized by a sinusoidal course between minima and

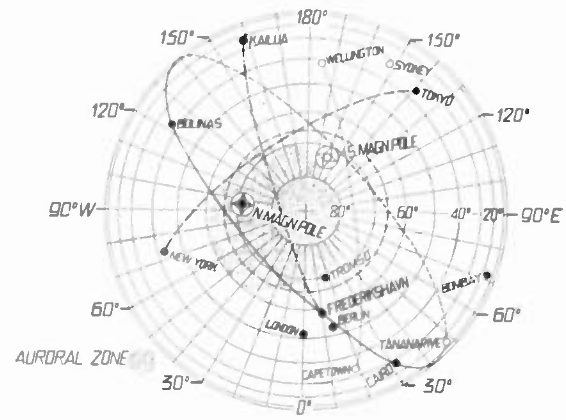

Fig. 5—Routes across the auroral zone.

maxima. (a) is the record of August 31, 1944, 08^h07 CET. A sharp minimum and maximum of two interfering waves occurred within 80 milliseconds, indicating a Doppler shift of 6 cps. The signal itself is slightly modulated with 360 cps. (b) represents two deep minima in a record of August 24, 1944, 08^h35 CET within 43 milliseconds, and indicates a Doppler shift of 23 cps.

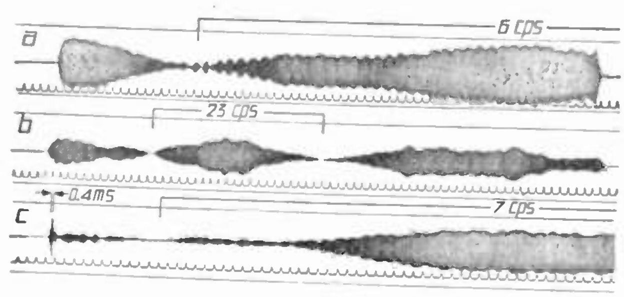

Fig. 6—Cleft signals of KQF, Kailua, Hawaii, 13,495 kc.

Since the minima do not occur within the same time intervals, the signal might be shaped by more than two interfering waves. The distorted 360-cps signal modulation is also a reason to suppose an interference of multiple waves. (c) The record of August 15, 1944, 08^h40 CET shows a pulse structure at the commencement of the signal, which lasts 0.4 millisecond, followed by a deep minimum. The maximum occurring after 75 milliseconds indicates a Doppler shift of 7 cps. The strong short pulse is actually the wave which arrives first, overlapped after 0.4 millisecond by the retarded component which has an opposite phase. With regard to

[11] L. Harang, "Das Polarlicht," *Akadem. Verlagsges.* (Leipzig), pp. 4–13; 1940.

the frequencies used of 15 Mc, the measured Doppler shifts between 5 and 30 cps indicate velocities of 100 to 500 meters per second.

Indirect signals did not occur at KQF, Hawaii. This kind of echoes, however, was found on records of stations in California and Madagascar. The recording place, Frederikshavn, and these two positions are on the same great-circle line, which passes the proximity of the northern and the southern magnetic pole, as shown in Fig. 5. Figs. 7(a) and (b) are records of the direct and the indirect signals of KPH, Bolinas, Calif., 12,735 kc on January 20, 1942, 15h20 CET, and FZT, Tananarive, Madagascar, 17,890 kc on April 27, 1942, 09h30 CET. The cleft direct signal from California passed the northern auroral zone, and the cleft indirect signal from Madagascar passed the southern and the northern auroral zone. Doppler shifts of 15 and 12 cps were measured. It is striking that the indirect signal from California is normal, though it has passed the auroral zone on the southern hemisphere. This probably is an evidence that no interference of multiple waves occurred, as a case of a single-path propagation.

(a)

(b)

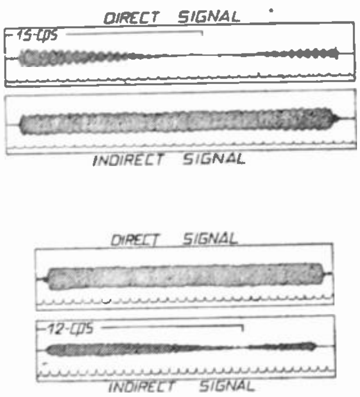

Fig. 7—(a) Cleft direct signal and normal indirect signal from California; and (b) normal direct signal and cleft indirect signal from Madagascar.

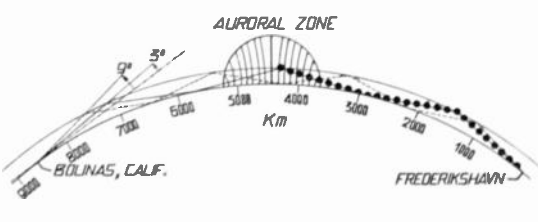

Fig. 8—Three- and four-hops propagation between Bolinas and Frederikshavn across the auroral zone.

A profile shown in Fig. 8 enables an investigation of the ionospheric transmission between Bolinas and Frederikshavn. The true distance is 8,571 km. With regard to the conditions in 1944, 12,735 kc was a rather high frequency, reflected from the F layer under angles beteen 0° and 10° toward the horizon. The propagation is considered to occur along two paths, in three and four hops with angles of 3° and 9°. The detour between both paths is 100 km. One ionospheric reflector of the first path is situated within the auroral zone, while two reflectors of the second path are more distant from the turbulence zone. Both waves evidently are affected by shifts, and decline from the transmitter frequency.

III. Conclusions

On the basis of these investigations, the long distance propagation is explained by repeatedly reflected waves between ionosphere and earth's surface. An absorbing, refracting, and reflecting influence of the E layer is possible on the long-distance propagation. It can be neglected for a transmission near the critical F frequency, insomuch as no abnormal E ionization occurs. The sun's radiation effects the daily course of the F layer ionization, connected with the variations of the virtual height. An F layer velocity between 0 and 10 meters per second, concluded from Doppler shifts found in the long-distance propagation, coincides well with the experiences of the vertical incidence sounding. Signals unmodulated or slightly modulated only permit exact Doppler-shift measurements, while strongly modulated signals and pulses are unsuited. Cleft signals, characterized by shifts between 5 and 30 cps, indicate a multiple-path propagation and a strong turbulence of the ionosphere within the auroral zone, since a velocity of 100 to 500 meters per second cannot be explained with the regular uniformly ascending or descending movement of the F layer in lower geographical latitudes. A radiation of electrically charged particles, probably from the sun, which is deflected by the earth's magnetic field to the zones of the magnetic poles, is regarded to cause this turbulence. Waves reflected from the ionosphere are split in ordinary and extraordinary components by the earth's magnetic field; circularly polarized at the poles, and linearly at the equator. Probably the frequency shifts of both components reflected within the auroral zone are also different, and it seems, that they are much stronger absorbed after repeated ionospheric reflections. The formation of ionized layers[12] within the auroral zone is much involved, and depends on many unknown factors, as shown by the occurrence of the sporadic F layer.[13]

Since the occurrence of Doppler shifts indicates a vertically moved ionospheric reflector, no definite limit exists between the F layer and the vacuum. Therefore, there are no arguments which should confirm the "sliding-wave" conclusions, to explain the highly constant time intervals of repeatedly circulating signals.

[12] L. Harang, "Experimental studies on the reflection of radio waves from ionized regions," *Geofys. Publik.* (Oslo), vol. 13, no. 4; 1942.

[13] O. Burkard, "A sporadic F layer," *Terr. Mag. Atmo. Elec.*, vol. 53, no. 1; 1948.

Microwave Filter Theory and Design*

J. HESSEL†, SENIOR MEMBER, IRE, G. GOUBAU†, AND L. R. BATTERSBY†

Summary—**The first part of this paper gives the theory of waveguide filters with arbitrary identical links, and their matching to a line. The treatment differs from that previously presented in the literature, in that the electromagnetic state of the impedors and transducers is described by relations between the incident and reflected waves. This simplifies the analysis of all waveguide systems, because each transformation by a line section results only in a phase shift of these waves. Each filter stage is characterized by two angles which can be determined by simple measurements. The formulas which describe the insertion properties of the filters are given in terms of these angles.**

The second part gives the application of the theory to direct and quarter-wave coupled band-pass iris filters. The design data are given, including correction factors for irises of finite thickness. Measured insertion loss curves of direct couples filters constructed, show good agreement with the theoretical.

Table of Symbols

a = wide dimension of a rectangular waveguide
$a_{11}a_{12}$ = coefficients of a transducer matrix
b, b_d = relative 3-db bandwidth without and with dissipation loss; also narrow dimension of a rectangular waveguide
d_0 = diameter of a circular iris
d_{11} = diameter of a slit iris
D = distance between two irises
f = frequency
f_0 = center frequency
f_c = cutoff frequency of the waveguide
F_0 = factor for calculation of circular irises
F_{11} = factor for calculation of slit irises
g = transmission constant
$j = \sqrt{-1}$
L = insertion loss
m = integer
n = number of stages

$$p = \frac{\cos \psi}{\cos \phi}$$

$$q = \frac{\sin \psi}{\sin \phi}$$

Q = quality of an unloaded cavity
$\vec{u}$, $\overleftarrow{u}$ = amplitudes of guide waves
w_z = characteristic reflection factor of a transducer
z = normalized impedance
Z_0 = characteristic impedance of a waveguide
α, β, γ = factors characterizing the frequency response
δ = iris thickness
ϵ = factor characterizing the dissipation loss
θ = transmission phaseshift
λ = free-space wavelength
λ_g = wavelength in a guide
λ_c = cutoff wavelength
ν = half relative 3-db bandwidth
σ = factor characterizing the dissipation loss
τ = ratio between 3-db bandwidth of n stage filter to 3-db bandwidth of one single stage
ϕ = aperture of an iris, characteristic of a transducer
ψ = characteristic of a transducer
$\bar{\psi}$ = phase length of a guide section.

PART I. MICROWAVE FILTER THEORY

1. Introduction

THE COMPONENTS of microwave equipments are connected by waveguides or concentric lines, and their electromagnetic states are determined by incoming and outgoing waves. There are linear relations between these waves which, in the case of transducers, can be written in the form:

$$\begin{pmatrix} \vec{u}_1 \\ \overleftarrow{u}_1 \end{pmatrix} = \begin{pmatrix} a_{11} & a_{12} \\ a_{21} & a_{22} \end{pmatrix} \times \begin{pmatrix} \vec{u}_2 \\ \overleftarrow{u}_2 \end{pmatrix}; \tag{1}$$

$\vec{u}_1$ and $\overleftarrow{u}_1$ are the complex amplitudes of the incoming and outgoing waves on one side, and $\overleftarrow{u}_2$ and $\vec{u}_2$ the amplitudes of the corresponding waves on the other side of the transducer (Fig. 1).

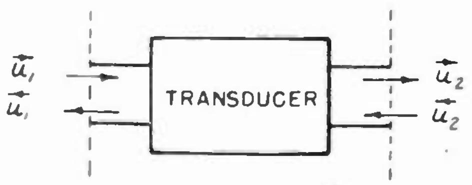

Fig. 1—Block diagram of a transducer. The arrows indicate the direction of the incoming and outgoing waves.

The characterization of microwave transducers by "Wave Matrices" (a) as defined in (1) is very useful for the analysis of microwave systems. The matrix elements a_{ik} are closely related to the reflection and transmission coefficients, and can be determined more directly than the coefficients of an impedance or admittance matrix. Heretofore, wave matrices have not found much application in the analysis of transmission line circuits, such as filters. To our knowledge, all publications relating to filter design are based on lumped element theory[1] which requires, as an intermediate

* Decimal classification: R143.2×R310. Original manuscript received by the Institute, July 22, 1948; revised manuscript received, March 31, 1949.

† Coles Signal Laboratory, Signal Corps Engineering Laboratories, Red Bank, N. J.

[1] G. L. Ragan, "Microwave Transmission Circuits," MIT Radiation Lab. Series, vol. 9, McGraw-Hill Book Co., New York, N. Y., 1948; chaps. 9 and 10.

step, the determination of equivalent circuits. This intermediate step is eliminated by the use of wave matrices. Some information about wave matrices may be obtained from the Radiation Laboratory Series.[2] A more elaborate treatment of the wave matrix theory will be contained in a monograph now being published.[3]

In the following the wave matrices are used for the analysis of transmission line filters with identical stages, including their matching transformers.

2. Characteristics of Symmetrical Transducers

There are several possible characterizations for a transducer. It is obvious that a characterization is desirable which is based on measurable quantities, such as reflection and transmission coefficients, and which is at the same time convenient for the analysis. Thus we write the wave matrix for an arbitrary symmetrical transducer in the form:

$$(a) \equiv \frac{j}{\sin\phi}\begin{pmatrix} -e^{j\psi} & -\cos\phi \\ \cos\phi & e^{-j\psi} \end{pmatrix}$$

$$-\frac{\pi}{2} < Re\,[\phi] < +\frac{\pi}{2}. \qquad (2)$$

The angles ϕ and ψ are the quantities which may be introduced as characteristics of the transducer. They are real if the dissipation losses are negligible; otherwise they contain an imaginary part. In terms of ϕ and ψ, the reflection and transmission coefficients become:

$$\left(\frac{\overleftarrow{u_1}}{\overrightarrow{u_1}}\right)_{\text{for } \overleftarrow{u}_2=0} = -\cos\phi\, e^{-j\psi},$$

$$\left(\frac{\overleftarrow{u_2}}{\overrightarrow{u_1}}\right)_{\text{for } \overleftarrow{u}_2=0} = j\sin\phi\, e^{-j\psi}. \qquad (3)$$

For negligible losses we see ϕ is a measure of the absolute value of the reflection coefficient $\cos\phi$ and of the transmission coefficient $|\sin\phi|$. ψ is a measure of their arguments.

If a transducer consists of a plane thin iris only, ψ is equal to ϕ. Therefore, ϕ can be used as the only characteristic of an iris, and it will be called in the following the "aperture" of the iris. ϕ is connected with the normalized impedance z by the relation:

$$z = \frac{j}{2}\tan\phi. \qquad (4)$$

It can be shown that every symmetrical transducer is equivalent to an iris with an aperture ϕ (defined by (3)) and line sections on both sides, the length of which is $\frac{1}{2}(\psi-\phi)$. This is also true if dissipation is considered, then the iris and the line sections must be dissipative, i.e., ϕ and ψ complex.

If a transducer is inserted in a system, and the reflection factor measured on the output side of the transducer is $w_2 = \overleftarrow{u_2}/\overrightarrow{u_2}$, the transformed reflection factor $w_1 = \overleftarrow{u_1}/\overrightarrow{u_1}$, which appears on the input side is, with regard to eq. (1) and (2):

$$w_1 = -\frac{\cos\phi + w_2 e^{-j\psi}}{e^{j\psi} + w_2\cos\phi}. \qquad (5)$$

There is a certain value of $w_2 = w_z$ which remains unchanged by the transducer; this means $w_1 = w_2 = w_z$. w_z, which may be called the "characteristic reflection factor" of the transducer, is found from (5) to be:

$$w_z = -p \pm \sqrt{p^2 - 1} \quad \text{where} \quad p = \frac{\cos\psi}{\cos\phi}. \qquad (6)$$

The transmission constant g of the transducer defined by: $e^g = (\overrightarrow{u_1}/\overrightarrow{u_2})_{\text{for } w_1=w_2=w_z}$ becomes:

$$e^g = q \mp j\sqrt{1 - q^2} \quad \text{where} \quad q = \frac{\sin\psi}{\sin\phi}. \qquad (7)$$

Regarding the signs of the roots in (6) and (7), the following statements can be made: The upper sign of (6) corresponds to the upper sign in (7) if we state that $\sqrt{\sin^2\phi} = +\sin\phi$, $\sqrt{\cos^2\phi} = +\cos\phi$. Furthermore, the law of conservation of energy stipulates that $|w_z|$ can never be greater than 1, and the real part of g never positive.

If dissipation is negligible (ϕ and ψ real) we see from (7) that g is purely imaginary for $|q| < 1$ or ψ is between the limits:

$$m\pi - |\phi| < \psi < m\pi + |\phi| \quad m = 0, 1, 2, 3, \cdots. \qquad (8)$$

At the same time w_z is real (see (6)). If the transducer is loaded by a system the reflection factor of which is $w_2 = w_z$, the passing wave undergoes only a shift in phase; its amplitude remains unchanged. In the range:

$$(m+1)\pi - |\phi| > \psi > m\pi + |\phi|, \qquad (9)$$

g contains a real part and w_z becomes complex with the absolute value 1. In this case the passing wave is attenuated, if the transducer is loaded with $w_2 = w_z$. Equations (8) and (9) determine the passing and rejection ranges of the transducer.

The characteristic reflection factor of a transducer has a meaning similar to characteristic impedance in the usual four-terminal theory.

3. Filter with Identical Links

Consider a filter of n identical symmetrical transducers (Fig. 2). The equations for such a ladder may be

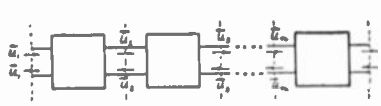

Fig. 2—Block diagram of a filter with identical stages.

[2] See pp. 551-554 of footnote reference 1.

[3] G. Goubau, R. Hornerjager, R. Muller, and Ch. Schmelzer, "Elektromagnetische Wellenleiter und Hohlraume," Wissenschaft., Verlagsges., Stuttgart, Germany.

written in the form:

$$\begin{pmatrix} \overrightarrow{u_1} \\ \overleftarrow{u_1} \end{pmatrix} = \begin{pmatrix} a_{11} & a_{12} \\ a_{21} & a_{22} \end{pmatrix} \times \begin{pmatrix} \overrightarrow{u_{n+1}} \\ \overleftarrow{u_{n+1}} \end{pmatrix}, \qquad (10)$$

where $\overrightarrow{u_1}$, $\overleftarrow{u_1}$ are the waves on the input side and $\overrightarrow{u_{n+1}}$, $\overleftarrow{u_{n+1}}$ those on the output side. Using the characteristics w_z and g introduced in the previous section, it can be easily shown that the a matrix of a n-stage ladder becomes:

$$(a)_n \equiv \frac{1}{w_z - \dfrac{1}{w_z}} \begin{vmatrix} \left(w_z e^{-ng} - \dfrac{1}{w_z} e^{ng}\right) & (e^{ng} - e^{-ng}) \\ (e^{-ng} - e^{ng}) & \left(w_z e^{ng} - \dfrac{1}{w_z} e^{-ng}\right) \end{vmatrix}. \qquad (11)$$

If we introduce Tschebeyscheff's polynomials of the first kind, (see Table I) we may write:

$$\begin{aligned} \frac{1}{2}(e^{-ng} + e^{+ng}) &= \frac{1}{2}\left[(q \pm j\sqrt{1-q^2})^n \mp (q + j\sqrt{1-q^2})^n\right] \\ &= T_n(q) \\ \frac{1}{2j}(e^{-ng} - e^{+ng}) &= \frac{1}{2j}\left[(q \pm j\sqrt{1-q^2})^n - (q \mp j\sqrt{1-q^2})^n\right] \\ &= \pm\, u_n(q). \end{aligned} \qquad (12)$$

TABLE I
TSCHEBEYSCHEFF'S POLYNOMIALS FOR $n=1$ TO 4

n	1	2	3	4
$T_n(q)$	q	$2q^2-1$	$4q^3-3q$	$8q^4-8q^2+1$
$\dfrac{U_n(q)}{\sqrt{1-q^2}}$	1	$2q$	$4q^2-1$	$8q^3-4q$

The matrix (3.2) becomes:

$$(a)_n \equiv \begin{vmatrix} \left(T_n(q) - j\dfrac{p}{\sqrt{p^2-1}} U_n(q)\right) & \dfrac{-j}{\sqrt{p^2-1}} U_n(q) \\ \dfrac{j}{\sqrt{p^2-1}} U_n(q) & \left(T_n(q) + j\dfrac{p}{\sqrt{p^2-1}} U_n(q)\right) \end{vmatrix} \qquad (13)$$

with

$$q = \frac{\sin\psi}{\sin\phi}, \qquad p = \frac{\cos\psi}{\cos\phi}.$$

If the filter is inserted in a line which is terminated by its characteristic impedance, the transmission constant g_n of the filter is given by:

$$\begin{aligned} e^{g_n} &= T_n(q) - j\frac{p}{\sqrt{p^2-1}} U_n(q) \\ &= T_n(q) - j\frac{\cos\psi}{\sin\phi} \frac{U_n(q)}{\sqrt{1-q^2}}. \end{aligned} \qquad (14)$$

As long as the dissipation loss is negligible (ϕ and ψ are real), (14) leads to the following expression for the insertion loss:

$$L = 1 + \left(\cot\phi \frac{U_n(q)}{\sqrt{1-q^2}}\right)^2. \qquad (15)$$

The phase shift of the passing wave is: $\theta = Im[g_n]$, $\tan\theta$ therefore becomes:

$$\tan\theta = -\frac{p}{\sqrt{p^2-1}} \frac{U_n(q)}{T_n(q)}. \qquad (16)$$

The reflection coefficient on the input side

$$(w_1)_{\overleftarrow{u}_{n+1}=0} = -\frac{1}{p + j\dfrac{T_n(q)}{U_n(q)}\sqrt{p^2-1}}. \qquad (17)$$

If dissipation is to be taken in account, the formulas (15) to (17) become more complicated, because p and q are no longer real and the Tschebeyscheff polynomials must be developed in order to separate the real and imaginary parts.

As may be seen from (15), the insertion loss vanishes (neglecting the dissipation losses) if $\cos\phi = 0$ or $U_n(q)/\sqrt{1-q^2} = 0$. If each stage is nonreflecting for a certain frequency, $\cos\phi$ is zero (see 3)). This provides resonating filter links, which act like parallel LC circuits shunted to a two-wire line.

The formulas (13) to (17) describe the behavior of all transmission line filters with identical links, provided that the frequency response of the characteristics ϕ and ψ is known.

Example I

We apply the formulas first to a band-pass iris filter with two identical nonresonating irises (Fig. 3) with aperture ϕ. Each filter stage consists of an iris with a guide section on each side, whose length is equal to half the distance between the irises. The angle ψ in our formulas is equal to the transmission angle between the two irises $\bar{\psi}$ plus ϕ (see Section 2).

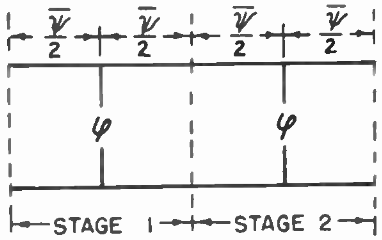

Fig. 3—Two-stage filter. each stage consisting of an iris with the aperture ϕ and guide sections with the transmission angle $\bar{\psi}/2$.

Within a certain frequency range, the frequency response of ϕ and ψ can be considered linear. Hence, we may write:

$$\phi = \phi_0 + \beta y, \quad \psi = \psi_0 + \gamma y, \quad \text{with} \quad y = \frac{f - f_0}{f_0}, \tag{18}$$

where β and γ are constants; the subscript 0 refers to the center frequency. ψ_0 has according to Section 2 (see (8)) the value $m\pi$. If dissipation losses are considered, ϕ_0, β, and γ are complex, and ψ_0 is $m\pi$ plus a small imaginary part. We calculate only the insertion loss for the dissipationless case when $m=1$. Using (15) and Table I we get:

$$L = 1 + 4\left(\frac{\cos\phi \sin\psi}{\sin^2\phi}\right)^2$$
$$\approx 1 + 4\left(\frac{\cos\phi_0}{\sin^2\phi_0}\gamma y - \frac{1+\cos^2\phi_0}{\sin^3\phi_0}\beta\gamma y^2\right)^2. \tag{19}$$

This formula is not identical to that usually given for a 2 iris or one cavity filter, because it is not restricted to small bandwidths.[3] For small bandwidths ϕ_0 becomes small, and within a certain frequency range in the neighborhood of the center frequency, the term containing $\beta\gamma y^2$ can be neglected. Thus, the insertion loss becomes quadratic in y.

Example 2

The second example which we will consider is a band rejection filter, consisting of cavities coupled by small holes in the side of a waveguide, separated by a distance of a quarter wavelength (Fig. 4(a)). If the coupling is effected by the electric field or the longitudinal component of the magnetic field of a TE-wave mode, and the field distortion is compensated by plungers (pl in Fig. 4(a)), each of these cavities behaves like a series tuned circuit in shunt to a line (Fig. 4(b)). According to (4) the aperture of an equivalent iris is given by the relation:

$$\frac{j}{2}\tan\phi = \frac{R}{Z_0}\left(1 + j2Q\frac{f - f_0}{f_0}\right), \tag{20}$$

where R is the resonance impedance of the equivalent circuit, Q the quality of the cavity, f_0 its resonance frequency, and Z_0 the characteristic impedance of the waveguide.

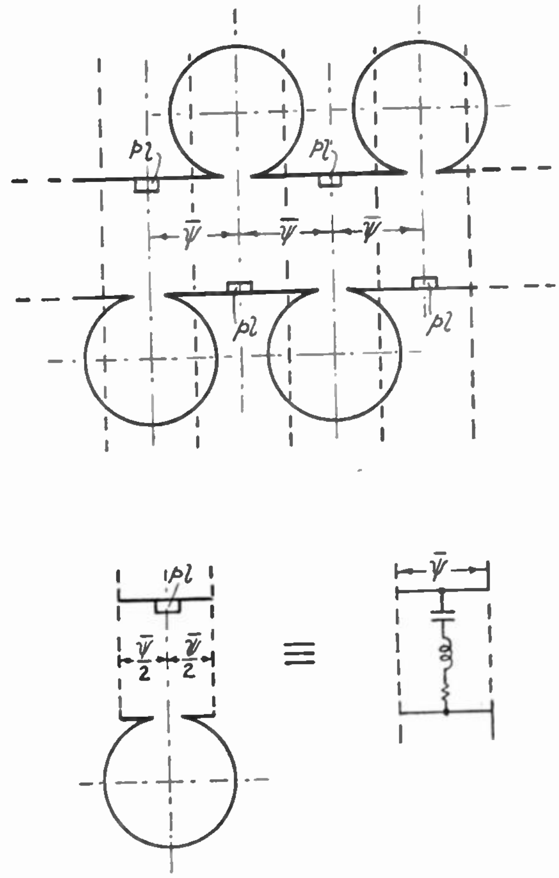

Fig. 4—(a) Band rejection filter, each stage consisting of a cavity coupled to a guide section having a length ψ. pl indicates the compensating elements. (b) Single filter stage and equivalent circuit.

Each filter link consists of a cavity and a guide section on both sides, the length of which is half the distance $\bar{\psi}$ between two cavities. As $\psi = \bar{\psi} + \phi$, p and q become:

$$p = \frac{\cos\psi}{\cos\phi} = \frac{\cos(\bar{\psi} + \phi)}{\cos\phi} = \cos\bar{\psi} - \sin\bar{\psi}\tan\phi$$
$$q = \frac{\sin\psi}{\sin\phi} = \frac{\sin(\bar{\psi} + \phi)}{\sin\phi} = \sin\bar{\psi}\cot\phi + \cos\bar{\psi}. \tag{21}$$

Because of (20) tan ϕ can be written in the form:

$$\tan\phi = x - j\sigma \quad \text{with} \quad x = \frac{4R}{Z_0} Q \frac{f - f_0}{f_0} \tag{22}$$
$$\text{and } \sigma = \frac{2R}{Z_0}.$$

As the distance between two cavities is a quater wavelength at the center frequency, $\bar{\psi}$ becomes:

$$\bar{\psi} = \frac{\pi}{2} + \beta\frac{f - f_0}{f_0} = \frac{\pi}{2} + \alpha x \text{ with } \alpha = \beta\frac{Z_0}{4RQ}. \tag{23}$$

β denotes the frequency response of $\bar{\psi}$ and has the value

$$\beta = \bar{\psi}_{f=f_0} \frac{1}{1-\left(\dfrac{f_c}{f_0}\right)^2} \quad (f_c = \text{cutoff frequency of the guide}). \tag{24}$$

Equations (21) and (22) furnish all information necessary for the description of the filter properties.

Within the rejection range, the frequency response of $\bar{\psi}$ can be neglected in general. Under this condition p and q become:

$$p = -\tan\phi = -(x - j\sigma), \quad q = \cot\phi = \frac{1}{x - j\sigma}. \tag{25}$$

The insertion loss for an n stage filter is then

$$L = \left| e^{\rho_n} \right|^2 = \left| T_n(q) + j\left(\frac{U_n(q)}{\sqrt{1-q^2}}\right) \right|^2 \text{ (see(14))}. \tag{26}$$

For $n = 2$, for instance, L becomes:

$$L = \left| e^{\rho_2} \right|^2 = \frac{(x^2 + \sigma(\sigma+2))^2 + 4(1+\sigma)^2}{(x^2+\sigma^2)^2}. \tag{27}$$

4. Filters with Matching Transformers

In general, a filter with identical links requires matching transformers on both ends. These are unsymmetrical transducers of the same type, but applied in opposite directions. (See Fig. 5.) The characteristics of these

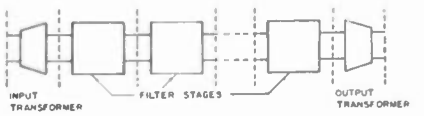

Fig. 5—Block diagram of a filter with matching transformers.

transducers influence the insertion properties of the filter, and they can be designed for various requirements. In the following, we restrict our consideration to a type of transformer with the following properties:

1. No reflection in the total filter at the center frequency of the pass band.

2. Both transformers in series connected as shown in Fig. 6 shall have the same frequency response as one filter stage.

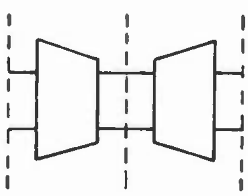

Fig. 6—Block diagram for the replacement of a filter stage by two matching transformers.

The center frequency of the pass band is defined as the frequency for which $\psi = m\pi$ (see Section 2 (8)). If dissipation losses are taken in account, only the real part of ψ can be $m\pi$. Transformers which satisfy these conditions have the matrices:

$$(a)_{\substack{i\\a}} = \frac{j}{\sin\phi'}\begin{pmatrix} -e^{j(\psi/2+\pi/4)} & -\cos\phi' e^{\mp j(\psi/2-\pi/4)} \\ \cos\phi' e^{\pm j(\psi/2-\pi/4)} & e^{-j(\psi/2+\pi/4)} \end{pmatrix} \tag{28}$$

if ϕ' is related to ϕ by:

$$\cos\phi' = \frac{1}{\cos\phi} - \sqrt{\left(\frac{1}{\cos\phi}\right)^2 - 1} \tag{29}$$

The upper subscript and the upper signs in (28) refer to the input transformer, and the lower subscript and signs to the output transformer. In order to prove that these transformers satisfy the two conditions above, we consider first the matrix $(a)_a$ for the output transformer. If the line connected with it is terminated by its characteristic impedance, the reflection factor on the filter side of the transformer is:

$$w_{(\psi=m\pi)} = -(-1)^m \cos\phi'$$
$$= -(-1)^m\left(\frac{1}{\cos\phi} - \sqrt{\left(\frac{1}{\cos\phi}\right)^2 - 1}\right). \tag{30}$$

This is the characteristic reflection factor w_z of the filter links for $\psi = m\pi$. (See (6)). The matching transformer on the input side transforms w_z for $\psi = m\pi$ into 0. Thus, condition 1 is satisfied. It may be mentioned that our consideration is not quite exact because of the imaginary part of ψ due to the dissipation losses. Its effect could be compensated by a small discontinuity in the guide on both sides of the filter which would give the required additional transformation.

To prove the second condition, we have to form the matrix product $(a)_a \times (a)_i$. Considering the relations (29), the resulting matrix becomes identical with that for one filter link (2). Only the sign becomes opposite for $Re[\phi] < 0$; however, this is of no consequence, because it means only a phase shift of 180° for the waves on one side of the transformer.

The matrix for the filter including its matching transformers is found by the following: Because of property (2) each filter link can be replaced by a pair of matching transformers as indicated in Fig. 6. Therefore, the total filter can be considered as a chain of identical symmetrical links, each of which consists of a pair of these transformers, but in the inverse arrangement (Fig. 7).

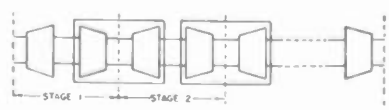

Fig. 7—The filter of Fig. 5, each stage of which has been replaced by a pair of matching transformers.

The number of these stages is one greater than the number of stages of the unmatched filter. This means the two matching transformers together form an additional stage. The matrix for one of the new stages is:

$$(a_i) \times (a)_a = -\frac{1}{\sin^2 \phi'}\begin{pmatrix} j(e^{j\psi} - \cos^2 \phi' e^{-j\psi}) & \cos \phi'(e^{j\psi} - e^{-j\psi}) \\ -\cos \phi'(e^{j\psi} - e^{-j\psi}) & -j(e^{-j\psi} - \cos^2 \phi' e^{j\psi}) \end{pmatrix}. \tag{31}$$

The corresponding characteristic reflection factor w_z' becomes, with regard to (29),

$$w_z' = -\tan\phi\left(\cot\psi \mp \frac{1}{\sin\psi}\sqrt{1 - q^2}\right);$$

$$\left(q = \frac{\sin\psi}{\sin\phi}\right). \tag{32}$$

The transmission constant g' is the same as for the original stages, because they differ only in the succession of the matching transducers of which they may be thought to consist.

Because the total filter is transformed into a ladder of identical stages, its matrix is of the type (11), w_z is replaced by w_z', and n is one more than the number of original stages. With (34) and (35), the matrix can be written in the form:

$$(a)_n' \equiv \begin{vmatrix} \left(T_n(q) - j\cos\psi \dfrac{U_n(q)}{\sqrt{1 - q^2}}\right) & -jq\cos\phi \dfrac{U_n(q)}{\sqrt{1 - q^2}} \\ jq\cos\phi \dfrac{U_n(q)}{\sqrt{1 - q^2}} & \left(T_n(q) + j\cos\psi \dfrac{U_n(q)}{\sqrt{1 - q^2}}\right) \end{vmatrix}. \tag{33}$$

The transmission constant is given by:

$$e^{g_n'} = T_n(q) - j\cos\psi \frac{U_n(q)}{\sqrt{1 - q^2}}; \tag{34}$$

the insertion loss in the dissipationless case:

$$L = 1 + \cos\phi\left(q\frac{U_n}{\sqrt{1 - q^2}}\right)^2; \tag{35}$$

the phase shift θ of the passing wave and the reflection coefficient w_1 on the input side

$$\tan\theta = -\cos\psi \frac{U_n(q)}{\sqrt{1 - q^2}} \cdot \frac{1}{T_n(q)} \tag{36}$$

$$w_1 = \frac{-q\cos\phi}{\cos\psi + j\dfrac{T_n(q)}{U_n(q)}\sqrt{1 - q^2}}. \tag{37}$$

Example:

We apply these general formulas to a special type of bandpass filter (shown in Fig. 8) for which a simplified

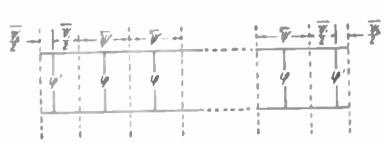

Fig. 8—Band-pass filter (direct coupled type).

design procedure is given in part II. Each filter stage consists of a nonresonating iris with guide sections of the length $\bar{\psi}/2$ on both sides. The apertures of the irises may be small, so $\sin\phi$ can be replaced by ϕ and the frequency response neglected. The matching transformers also consist of irises with guide sections on both sides, but these are of different length ($\bar{\psi}_1/2$ and $\bar{\psi}_2/2$).

The required aperture ϕ' of the matching irises is given by (29). The wave matrices of this iris $(a)_{\phi'}$ and the matrices of the line sections $(a)_{\frac{\bar\psi_1}{2}}$ and $(a)_{\frac{\bar\psi_2}{2}}$ are:

$$(a)_{\bar\phi'} \equiv \frac{j}{\sin\phi'}\begin{pmatrix} -e^{j\phi'} & -\cos\phi' \\ \cos\phi' & e^{-j\phi'} \end{pmatrix}$$

$$(a)_{\frac{\bar\psi_1}{2}} \equiv \begin{pmatrix} e^{(j/2)\frac{\bar\psi_1}{2}} & 0 \\ 0 & e^{-(j/2)\frac{\bar\psi_1}{2}} \end{pmatrix}. \tag{38}$$

If we form the product $(a)_{\frac{\bar\psi_2}{2}} \times (a)_{\phi'} \times (a)_{\frac{\bar\psi_1}{2}}$ and compare the resulting matrix with the matrix (28) of the input transformer we find $\bar\psi_2$ and $\bar\psi_1$ to be:

$$\bar\psi_2 = \frac{\pi}{2} - \phi', \qquad \bar\psi_1 = \psi - \phi'. \tag{39}$$

These relations should be satisfied over the entire frequency range. Actually they are only valid for one frequency. However, this is of no serious consequence for the following reasons: For small relative bandwidths the frequency response of ϕ and ϕ' can be neglected. (See example I, Section 3.) The frequency response of the line section $\bar\psi_2/2$ which is continued by the homogeneous guide, does not affect the insertion loss. $\bar\psi_1$ differs from ψ by only a few per cent if ϕ' is small. Therefore, the frequency response of $\bar\psi_1$ is approximately the same as that of ψ. Hence, if (39) is satisfied for the center frequency, it holds over a relatively wide frequency range.

For $\sin\phi_1 \cos\phi$, $\sin\psi$, and $\cos\psi$, we can use the approximations:

$$\sin\phi \approx \phi \qquad \cos\phi \approx 1$$

$$\sin\psi \approx (-1)^m \beta \frac{f - f_0}{f_0}, \qquad (\text{for } \beta \text{ see (24)}).$$

$$\cos\psi \approx (-1)^m \tag{40}$$

In the following we assume $m = 1$; this means that the distance between the irises should be about one-half wavelength.

For the moment we will neglect the dissipation losses. Then the insertion loss given by (35):

$$L = 1 + \left(x\frac{U_n(x)}{\sqrt{1 - x^2}}\right)^2 \text{ with}$$

$$x = -q = \frac{\beta}{\phi}\frac{f - f_0}{f_0}. \tag{41}$$

n is the number of inner irises plus one, or in other words it is the number of resonating cavities.

The transmission angle θ and the reflection factor w_1 are obtained from (36) and (37):

$$\tan\theta = \frac{U_n(x)}{\sqrt{1-x^2}}\,\frac{1}{T_n(x)} \tag{42}$$

$$w_1 = \frac{x}{1 - j\dfrac{T_n(x)}{U_n(x)}\sqrt{1-x^2}}\,. \tag{43}$$

These formulas are identical with those for the so-called quarter-wave coupled type, which is fully discussed in the literature.[8] The close relationship between the two different filter types is founded in the fact that the quarter-wave coupled type gives the iris performance of the general filter type shown in Fig. 7, in which each original filter stage is replaced by a pair of the matching transducers. Each stage of the original iris filter (Fig. 8), consisting of an iris with the aperture ϕ and the line sections $\psi/2$, is replaced by two matching irises in the distance ψ_2 with guide sections of $\psi_1/2$ on the ends (Fig. 9).

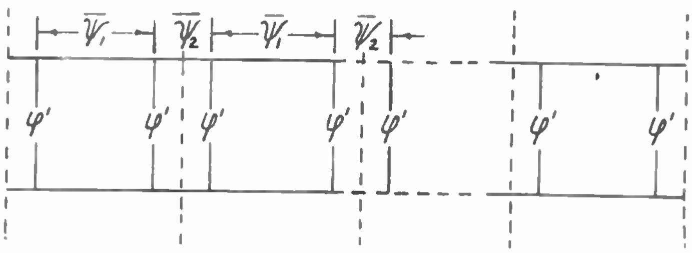

Fig. 9—Band-pass filter (quarter-wave coupled type).

We require in Part II the relative 3-db bandwidth b, for $n=1$, 2, 3 or 4 stages. It is given by the solution of the algebraic equation

$$\left(x\frac{U_n(x)}{\sqrt{1-x^2}}\right)^2 = 1. \tag{44}$$

For $n=1$, the solution is: $x=1$. Hence with (41) and (24)

$$b_1 = \frac{2\phi}{\beta} = \frac{2\phi}{\pi}\left(1-\left(\frac{f_c}{f_0}\right)^2\right).$$

The ratio τ between the relative 3-db bandwidth for n through 4 inclusive and b_1 is given in the following Table II.

TABLE II

n	1	2	3	4
$\tau = \dfrac{b}{b_1}$	1	0.707	0.762	0.827

Because the dissipation losses are small, they can be considered by assuming that only ψ has a small imaginary part—$j\epsilon$. Then, with (40)

$$q = \frac{\sin\psi}{\sin\phi} \cong -x + j\frac{\epsilon}{\phi} = -x + j\sigma. \quad p \cong -1. \tag{45}$$

Hence the transmission constant given by (34) becomes

$$\begin{aligned}
n &= 1 \quad e^{g_1} = -x + j(1+\sigma)\\
n &= 2 \quad e^{g_2} = [2x^2 - (1+2\sigma+2\sigma^2)] - j2x(1+2\sigma)\\
n &= 3 \quad e^{g_3} = -[(4x^3 - x(3+8\sigma+12\sigma^2)]\\
&\qquad + j[4x^2(1+3\sigma) - (1+3\sigma+4\sigma^2+4\sigma^3)]\\
n &= 4 \quad e^{g_4} = [8x^4 - 8x^2(1+3\sigma+6\sigma^2)\\
&\qquad + (1+4\sigma+8\sigma^2+8\sigma^3+8\sigma^4)]\\
&\qquad - j[8x^3(1+4\sigma)\\
&\qquad - x(4+16\sigma+24\sigma^2+32\sigma^3)],
\end{aligned} \tag{46}$$

σ can be expressed by the Q of a single cavity and the relative 3-db bandwidth b_1 (without dissipation):

$$\sigma = \frac{1}{b_1 Q}\,. \tag{47}$$

From the relations (46), the corresponding insertion losses can be calculated by taking the sum of the squares of the real part and the imaginary part of e^{g_n}.

PART II. APPLICATION TO FILTER DESIGN

1. Design Procedure

A. Introduction

On the basis of the theory developed, the following presents design data for band-pass iris filters which give in simplified form, the information necessary for the design of band-pass filters of the types shown in Fig. 10,

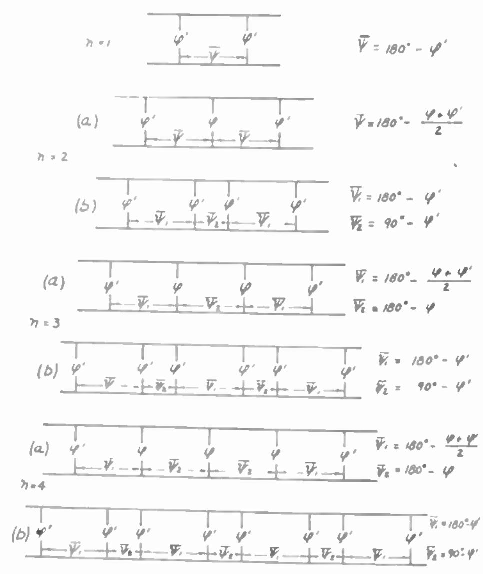

Fig. 10—Diagram showing the relation between iris distances ψ and iris aperture ϕ, for direct and quarter-wave coupled filters. ϕ' of the type (b) is identical with ϕ' of the type (a).

where n is the number of resonating cavities. For $n \geqq 2$ there are two types of filters which have approximately the same insertion properties. Type (b), is the well-known quarter-wave coupled type. The type (a), the direct coupled type, has seen little application to date, primarily because of more rigid design and manufacturing requirements. However, this type has the advantages of compactness and somewhat lower dissipation loss. Therefore, the design data presented have been examined especially for this type of filter, and the results are gratifying. The agreement between calculated and measured values is within 5 per cent.

The characteristic variables for the filter are the angles ϕ and ψ, introduced in the theoretical discussion, Part I. ϕ is a measure for the aperture of an iris. The cos ϕ and $|\sin \phi|$ are the absolute values of the reflection and passing coefficients of the iris, in a guide terminated by its characteristic impedance. It is assumed that ϕ is constant within the passing range of the filter and in the neighborhood of it. For the direct coupled type, the apertures of the irises on the ends, denoted by ϕ', differ from the inner irises (ϕ). The irises of quarter-wave coupled filters are identical, and have the same apertures as the end irises of the equivalent direct coupled filters. The irises of the one-stage filter are also denoted with ϕ', because the design procedure is identical to that of the end irises. ψ and ϕ determine the transmission angle $\bar{\psi}$ between two irises. The values for $\bar{\psi}$ indicated in Fig. 1 are referred to the center frequency.

B. Number of Stages

The first step in designing a filter is the choice of the proper number of stages. This is done with the aid of

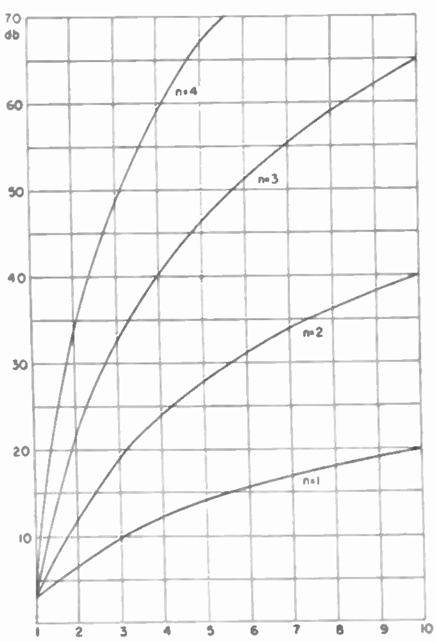

Fig. 11—Insertion loss curves for n stage filters having the same 3-db bandwidth.

Fig. 11, showing the insertion loss curves form $n=1$, 2, 3, and 4 stages with the same 3-db bandwidth. The dissipation loss is not considered in these curves, because it is of no consequence beyond the 3-db range. ν denotes the half relative 3-db bandwidth, i.e., $\nu = BW/2f_0$ where BW is the actual 3-db bandwidth, and f_0 the center frequency. The frequency scale in Fig. 11 is given in steps of ν. The curves are calculated with (46) for $\sigma = 0$. If, for instance, an attenuation of 20 db is desired for a frequency distance 3ν from the mean passing frequency, the number of stages must be at least 2.

C. Apertures

The apertures of the inner irises of the filter type (a) are found with the aid of the unbroken curves of Fig. 12. ϕ indicates the aperture in degrees, b the relative 3-

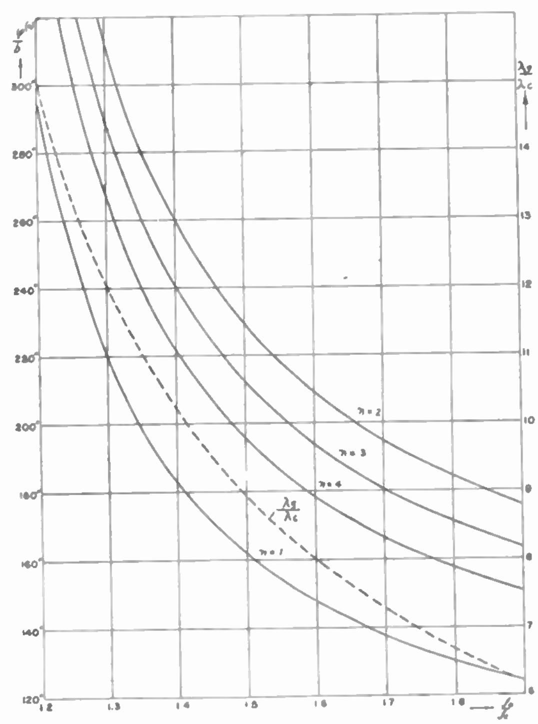

Fig. 12—Curves for determining iris aperture (solid lines), and guide wave length (broken line).

db bandwidth ($b = 2\nu$), f_0 the center frequency, and f_c the cutoff frequency of the guide. f_c for various sizes of rectangular guides is shown in Table III. The curves are calculated with the formula:

$$\phi^{(0)} = 90° \frac{1}{1 - \left(\frac{f_c}{f_0}\right)^2} \frac{b}{\tau} \tag{48}$$

based on (40) and (41) of Part I. The values of τ are given in Table II. The curves show $\phi^{(0)}/b$ as a function of f_0/f_c for the various numbers of stages. Although the one-stage filter has no iris with the aperture ϕ, the determination of ϕ is an intermediate step in obtaining ϕ'. ϕ' is connected with ϕ by the relation (29) which, for small apertures, can be simplified to

$$\phi'^{(0)} = 10.7\sqrt{\phi^{(0)}}. \tag{49}$$

D. Dimension of the Windows

The first steps require no special knowledge as to the kind of waveguide, wave mode, and form of irises. The following data are restricted to rectangular waveguides with TE_{10} mode excitation, slit-type irises with the slit parallel to the electric field and circular irises (see Table III).

For infinitely thin irises of these types, the relation between ϕ or ϕ' and the iris dimensions can be calculated with the assumption of a quasi-stationary field distribution adjacent to the openings. This assumption holds with great accuracy as long as sin ϕ can be replaced by ϕ. This is also the supposition made for the formulas above. The width d_{11} of the slit in the case of slit-iris corresponding to aperture in degrees is given by the formula:

$$d_{11}^2 = \phi^{(0)}F_{11}\frac{\lambda_g}{\lambda_c}, \quad \text{where} \quad F_{11} = \frac{a^2}{45\pi}. \tag{50}$$

The hole diameter d_0 for a circular iris is given by the formula:

$$d_0^3 = \phi^{(0)}F_0\frac{\lambda_g}{\lambda_c}, \quad \text{where} \quad F_0 = \frac{a^2b}{120}. \tag{51}$$

The values of F_{11} and F_0 have been calculated for all approved guide types which are shown in Table III. Because the inside guide dimensions a and b are given in inches, d_{11} and d_0 in the formulas above result also in inches. λ_g/λ_c is plotted in Fig. 12 as a function of f_0/f_c.

It is necessary to make a correction for the finite thickness of the irises. Because the irises with circular holes can be manufactured simply and with high accuracy, this type is preferable to the slit type for most applications; therefore, the correction for finite thickness has been measured only for this type. Fig. 13 shows a curve for this correction; d_0 is the hole diameter of an infinitely thin iris which is calculated with the design formula above. d_0' is the diameter of an iris with the thickness δ which has the same coupling effect as d_0. The curve in Fig. 13 gives d_0'/d_0 as a function of δ/d_0. If the diameter d_0 for the infinitely thin iris is determined and the thickness of the material to be used for the iris is known, δ/d_0 can be calculated. Fig. 13 gives the correc-

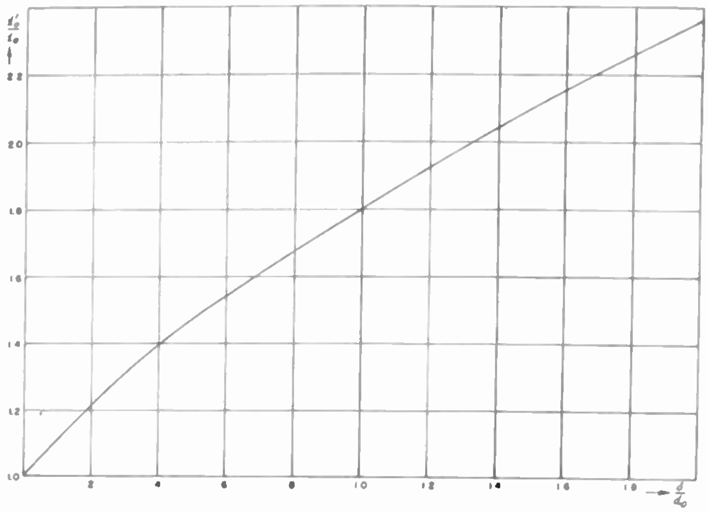

Fig. 13—Correction factor for iris thickness. d_0' is the diameter of a circular iris with the thickness δ, having the same coupling effect as an infinitely thin iris with the diameter d_0.

tion factor d_0'/d_0 with which d_0 must be multiplied to obtain the real diameter d_0'. It should be noted here that allowance for the decrease of hole diameter and increase of thickness by plating must be made when the iris dimensions are determined.

E. Distance Between the Irises

The transit angles ψ between the irises for the center frequencies are given in Fig. 10. The real distances D in cm or inches are given by the relation

$$D = \frac{\psi^{(0)}}{360°}\lambda_g = \frac{\psi^{(0)}}{360°}\left(\frac{\lambda_g}{\lambda_c}\right)\lambda_c. \tag{52}$$

λ_g/λ_c is plotted in Fig. 12. The values of λ_c are found in Table III.

TABLE III

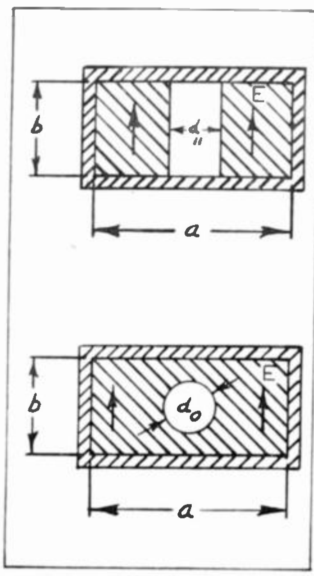

Outside Dimension (") a	Outside Dimension (") b	Inside Dimension (") a	Inside Dimension (") b	Cut Off Frequency Mc	Cut Off Wavelength cm	Cut Off Wavelength in	F_0 (d_0 in ")	F_{11} (d" in ")
6.660	3.410	6.500	3.250	908	33.04	13.01	1.144	2.989×10^{-1}
4.460	2.310	4.300	2.150	1375	21.82	8.60	3.313×10^{-1}	1.308×10^{-1}
3.000	1.500	2.840	1.340	2080	14.42	5.68	9.006×10^{-2}	5.705×10^{-2}
2.000	1.000	1.372	0.872	3155	9.51	3.74	2.557×10^{-2}	2.479×10^{-2}
1.500	0.750	1.372	0.622	4285	7.00	2.76	1.038×10^{-2}	1.332×10^{-2}
1.250	0.625	1.122	0.497	5260	5.70	2.24	5.214×10^{-3}	8.905×10^{-3}
1.000	0.500	0.900	0.400	6560	4.57	1.80	2.700×10^{-3}	7.213×10^{-3}
0.702	0.391	0.622	0.311	9490	3.16	1.24	3.224×10^{-4}	2.737×10^{-3}
0.500	0.250	0.420	0.170	14080	2.13	0.84	1.470×10^{-4}	1.248×10^{-3}

As the distances are critical (except those corresponding to $\bar{\psi}_2$ in the quarter-wave coupled type), and the guide cross section may vary somewhat, it is better to make them smaller by approximately 1 per cent, and to tune the cavities to resonance by means of a capacitive plunger.

F. Dissipation Loss

The dissipation affects the insertion loss of the filter, and also to some extent the bandwidth. The unbroken curves in Fig. 14 show the insertion loss at the center

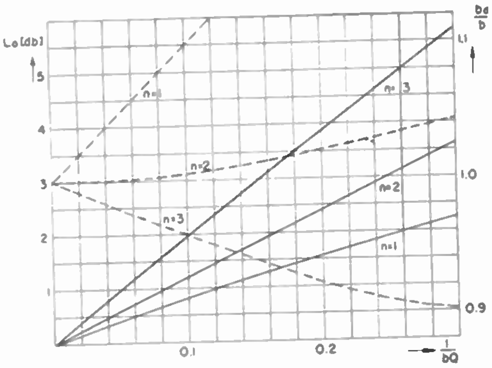

Fig. 14—Dissipation loss at the center frequency (solid lines) and ratio between relative 3-db bandwidth b_d with dissipation, to relative 3-db bandwidth b without dissipation (broken lines).

frequency for 1, 2, and 3 stages. The dissipation losses are expressed by the quantity $1/bQ$, where b is the relative 3-db bandwidth for the dissipationless case, and Q the quality of a single cavity. The broken curves in Fig. 14 show the ratio between the modified relative bandwidth b_d and b as a function of $1/bQ$. The change of bandwidth because of the dissipation losses can be considered by designing the filter for a bandwidth which is the desired bandwidth divided by b_d/b.

2. Example

The following example is given to illustrate the design procedure:

Three-stage filter of the type (a): A center frequency $f_0=9{,}350$ Mc, and 3-db bandwidth of 13 Mc is chosen. (The measured bandwidth will be a few per cent less than 13 Mc because of the dissipation losses previously discussed.) The type of guide used will be (1 inch$\times\frac{1}{2}$ inch) for which Table III gives the cutoff frequency $f_c=6{,}560$ Mc. First, the values of f_0/f_c and the relative bandwidth b must be calculated. They become $f_0/f_c=1.43$; $b=1.39\times10^{-3}$. ϕ may now be determined from Fig. 12. With $f_0/f_c=1.43$ and $n=3$, $\phi^{(0)}/b=231°$ or $\phi^{(0)}=0.325$. By (49) we find $\phi'^{(0)}$ to be 6.1°.

Table III gives the value of F_0 for 1 inch$\times\frac{1}{2}$ inch guide as 2.70×10^{-3}, and $(d^3)_{\phi'}=16.3\times10^{-3}$. Fig. 12 shows λ_g/λ_c to be 0.98. With (51) we find $(d^3)_\phi$ to be 0.860 $\times10^{-3}$ and $(d^3)_{\phi'}=16.3\times10^{-3}$. Hence: $d_\phi=0.095$ inch and $d_{\phi'}=0.252$ inch. For an iris thickness δ of 0.009 inch (including plating) $\delta/d_\phi=0.09$ and $\delta/d_{\phi'}=0.32$. Fig. 13 gives the correction factors for the iris diameters: $d_0'/d_0=1.10$ and 1.04, respectively. The real diameters are therefore $d_\phi'=0.105$ inch. $d_{\phi'}'=0.262$ inch. To find the distance D between the irises, we use (52), first determining $\bar{\psi}_1$ and $\bar{\psi}_2$ from Fig. 10; $\bar{\psi}_1=176.8°$, $\bar{\psi}_2=179.7°$. With $\lambda_g/\lambda_c=0.98$ and $\lambda_c=1.80$ inches (see Table III) we get $D_{\bar{\psi}_1}=0.864$, $D_{\bar{\psi}_2}=0.882$. To allow for tuning of the filter, we subtract approximately 1 per cent from these values to obtain the real distances.

3. Measurements

A two-stage and three-stage filter were constructed to verify the theory. The two-stage filter was designed for a bandwidth of 14 Mc ($b=1.50=10^{-3}$), centered at 9,350 Mc. The three-stage filter was constructed using the dimensions obtained in the foregoing example, 13 Mc bandwidth ($b=1.39\times10^{-3}$), and center frequency of 9,350 Mc. Fig. 15 is a plot of the measured insertion loss

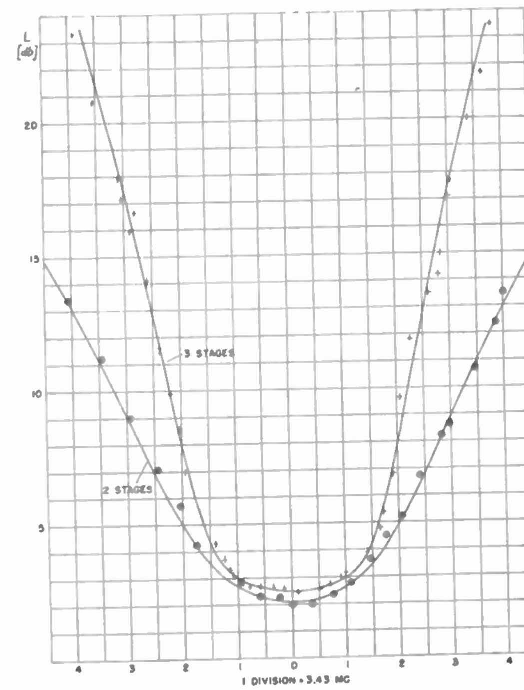

Fig. 15—Measured and calculated insertion loss curves for two- and three-stage direct-coupled filters.

of these filters. The curves shown were calculated with (46) for best fit to the measured points. The corresponding values of b and σ for the two-stage filter are $b=1.47=10^{-3}$, $\sigma=0.112$ ($Q=4{,}300$); and for the three-stage filter $b=1.25\times10^{-3}$, $\sigma=0.097$ ($Q=6{,}300$). It should be noted here that the bandwidth of the three-stage filter is about 10 per cent less than 14 Mc. Approximately one-half of this deviation is due to dissipation losses which are considered in Section 1-F (for the two-stage filter the effect of dissipation is negligible). Thickness of plating and the accuracy of measurement account for the remainder.

The measured dissipation loss at the center frequency for the three-stage filter is relatively low, compared with that of the two-stage filter. This may be due to variation in the plating of the cavities. Another reason can be the following: The dissipation loss of an iris becomes greater for larger apertures. In the two-stage filter, each cavity has one large and one small aperture. The three-stage filter, however, has one cavity with only small apertures, and therefore, the mean Q of the three-stage filter should be higher than that of the two-stage filter. The tuning of a three-stage filter can be accomplished easily in the following manner: First, one outside cavity is approximately tuned to resonance by noting the reaction on the generator. This is done to obtain some power flow through the filter. The inner cavity is then tuned far off resonance. Following this, the last cavity is tuned for maximum power transfer, and the first cavity readjusted to maximize the output. Finally, the inner cavity is tuned, and no further adjustments are required.

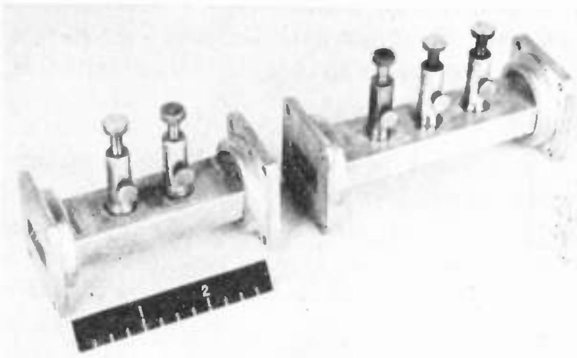

Fig. 16—Two- and three-stage filters, type A, circular iris.

Acknowledgment

Acknowledgment is due to R. E. Lacy, Chief, Radio Relay and Microwave Section, without whose encouragement this paper would not be possible; to C. E. Sharp and A. Meyerhoff for many valuable suggestions which facilitated preparation of the material; and to A. J. Colaguori, who performed much of the technical work.

Stabilization of Simultaneous Equation Solvers*

GRANINO A. KORN†

Summary—**A new stability criterion for multiple-loop feedback systems is developed and applied to the problem of stabilizing electronic simultaneous equation solvers.**

THE SOLUTION of a vast number of scientific and engineering problems involves the numerical computation of the unknowns of a system of linear simultaneous equations. Systems with as many as fifteen or twenty unknowns are frequent in many applications. The numerical solution of such systems, even by approximation methods, constitutes a formidable task. On the other hand, many engineering problems demand solutions less accurate than about 1 per cent.

Within this limit of accuracy, the problems in question have been found to lend themselves well to solutions by analogue computers of the type described.[1–4] In these devices, a physical quantity, such as a voltage, is made to correspond to each unknown by the introduction of convenient scale factors. The physical quantities representing the unknowns are then made to satisfy a set of equations analogous to the given problem. This is achieved by means of "computing elements" used to establish the desired relations between the various voltages. Once the computer is thus set up for a given problem, these voltages must then satisfy the relations established between them and must, therefore, be proportional to the unknowns. Such analogue computers are vastly cheaper than digital computers, and their accuracy is sufficient for many engineering applications.

The purpose of the computers in question is to find the set of numbers (unknowns), $x_1, x_2 \cdots, x_n$, satisfying the set of linear simultaneous equations

$$\left.\begin{array}{l} a_{11}x_1 + a_{12}x_2 + \cdots + a_{1n}x_n + b_1 = 0 \\ a_{n1}x_1 + a_{n2}x_2 + \cdots + a_{nn}x_n + b_n = 0 \end{array}\right\} \qquad (1)$$

whose determinant must be different from zero. In the following, we shall consider the case of real coefficients, a_{ik} and b_i, so that the unknowns will be real as well. It should be mentioned in passing that it will not prove difficult to extend our considerations to the case of complex coefficients.

In the computers to be discussed, the x_i's are considered as variables represented by ac or dc voltages which are proportional to the respective numerical values. We shall denote these voltages by the same symbols x_i as the respective variables.

* Decimal classification: 621.375.2. Original manuscript received by the Institute, February 25, 1948; revised manuscript received, January 12, 1949.

† Curtiss-Wright Corp., Columbus, Ohio.

[1] G. W. Brown, "The stability of feedback solution of simultaneous linear equations," *Amer. Math. Soc. Bull.*, part 1, vol. 53, p. 61; January, 1947 (abstract).

[2] E. A. Goldberg and G. W. Brown, "An electronic simultaneous equation solver," *Jour. Appl. Phys.*, vol. 19, pp. 339–345; April, 1948.

[3] C. E. Berry, D. E. Wilcox, S. M. Rock, and H. W. Washburn, "A computer for solving linear simultaneous equations," *Jour. Appl. Phys.*, vol. 17, pp. 262–272; April, 1946.

[4] F. J. Murray, "Theory of Mathematical Machines," King's Crown Press, New York, N. Y.; 1947.

Fig. 1 shows the essential features of an analog computer using feedback to establish the relations (1) between voltages x_i for the case $n=2$. An automatic feedback computer of this type is described in footnote reference 2. It is seen that voltages corresponding to

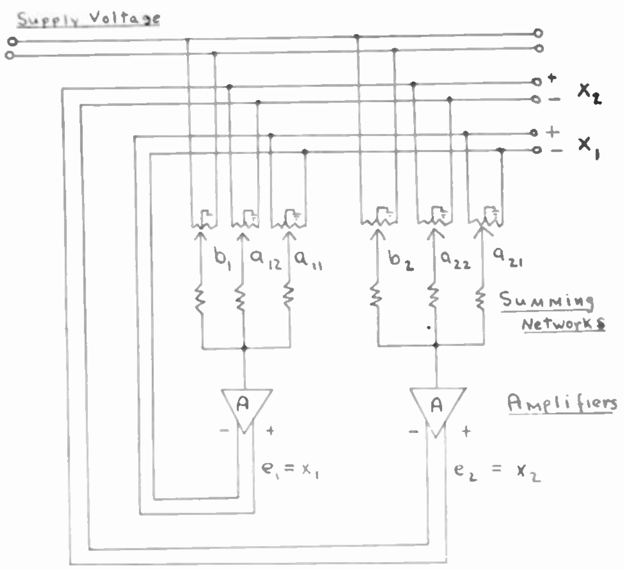

Fig. 1—Scheme of connections for solving a pair of linear simultaneous equations.

the terms b_i and $a_{ik}x_k$ are obtained by means of potentiometers and summed by means of summing amplifiers. If e_i be the output voltage of the ith summing amplifier, the device simulates the relations

$$A\left\{\sum_{k=1}^{n} a_{ik}x_k + b_i\right\} = e_i; \quad i = 1, 2, \cdots, n \qquad (2)$$

which differ from the desired relations (1) only by the amount of the error or residual e_i in each equation. The computer then attempts automatically to minimize these residuals by means of n^2 feedback connections such that $e_i = x_i$, as shown in Fig. 1. The relations (2) established by the computer now become

$$\sum_{k=1}^{n}\left(a_{ik} - \frac{\delta_{ik}}{A}\right)x_k + b_i = 0 \qquad i = 1, 2, \cdots, n \qquad \delta_{ik} = \begin{cases} 0 \text{ for } i \neq k. \\ 1 \text{ for } i = k \end{cases} \qquad (3)$$

Equation (3) approximates (1) for high amplifier gain A. The error due to finite gain is easily seen to be inversely proportional to the gain A and can be made very small. The relations (3) are satisfied by approximately the same values of the x_i as the original equations (1). The voltages x_i appearing in the arrangement of Fig. 1 will, therefore, be proportional to the desired unknowns *if and only if, the feedback system for the given set of equations is stable at all frequencies.*

Some conditions determining the stability of feedback systems of the type in question now will be discussed. If it were possible to construct the summing amplifiers so that the gain A is a negative constant for all frequencies of the input voltages, the stability of the system would depend only on the nature of the feedback networks. The net effect of the latter should be degenerative. That is to say, it should actually minimize the sum of the squares of all the residuals e_i. It is easily seen that this need not be true in every case by considering the arrangement of Fig. 1. Regeneration would surely result if $a_{11} = a_{22} = -1$ and $a_{12} = a_{21} = 0$. The nature of the feedback networks depends on the given values of the coefficients a_{ik}. Specifically, it was shown in footnote reference 2 that, *for constant negative amplifier gain A, the system will be stable if, and only if, the matrix of the coefficients a_{ik} is positive definite.* This is the case if, and only if, the equation

$$\text{determinant } |a_{ik} - \delta_{ik}\lambda| = 0 \quad \delta_{ik} = \begin{cases} 0 \text{ for } i \neq k \\ 1 \text{ for } i = k \end{cases} \qquad (4)$$

has only roots $\lambda_j (j = 1, 2, \cdots n)$ with positive real parts.[5] This condition of positive definiteness is not as stringent a limitation as it might appear. Many systems of equations related to engineering problems have positive definite matrices for physical reasons. Again, the matrix of a given set of equations can often be made positive definite by simply rearranging the equations so that the diagonal elements are large and the post-diagonal coefficients are smaller. The diagonal coefficients are then all made positive by appropriate multiplications by -1. The reference cited[3] also mentions that it is useful to arrange the equations so that, for each pair of indices i and k,

$$|a_{ii}a_{kk}| > |a_{ik}a_{ki}|. \qquad (5)$$

In any case, for any given system of linear equations (1) there exists an equivalent linear system

$$\sum_{i=1}^{n}\sum_{k=1}^{n} a_{ji}a_{ik}x_k + \sum_{i=1}^{n} a_{ji}b_i = 0, \quad j = 1, 2, \cdots, n. \qquad (6)$$

This set of equations is satisfied by the same unknowns and its matrix is necessarily always positive definite. Adcock[6] has made the relations (6) the basis of a feedback computer which is stable for all values of the coefficients a_{ik}.

In the discussion which follows, it will be assumed that the coefficients a_{ik} satisfy condition (4). It will then be found that almost all problems involved in the design of feedback computers of the type just described center about the design of the summing amplifiers. In practice, the amplifier gain A is not a negative constant, as assumed above, but a complex function $A(j\omega)$ of the angular frequency ω. Both the absolute voltage gain and the phase shift of each amplifier vary with frequency, and one must be sure that they vary in such a manner that the computer is stable at all frequencies. In other words, the amplifiers must be designed so that the feed-

[5] R. A. Frazer, W. J. Duncan, and A. R. Collar, "Elementary Matrices," Cambridge University Press, Cambridge, Mass.; 1938.
[6] W. A. Adcock, "An automatic simultaneous equation computer and its use in solving secular equations," *Rev. Sci. Instr.*, vol. 19, pp. 181–187; March, 1948.

back cannot become regenerative at any frequency, since this would result in uncontrolled oscillations.

With the performance equations of the computer given in (3), the general stability criterion[7] is that all the roots $p=j\omega$ of the so-called characteristic equation

$$\text{determinant}\left| a_{ik} - \frac{\delta_{ik}}{A(p)} \right| = 0 \tag{7}$$

must have negative real parts.

The necessity of maintaining stability imposes severe restrictions on the amplifiers to be used in feedback computers. The only known practical means of analyzing the stability of a complicated multiple-loop feedback system on the basis of (7) are Routh's rule and Nyquist analysis.[7] Both necessitate cumbersome computations for values of n larger than 2.

The writer was, however, able to develop a simple condition for stability which is useful in the case of positive definite matrices, and, therefore, applies to the present computer. An inspection of (4) and (7) shows that (7) can hold true only for such values of p which satisfy one or more of the equations

$$\frac{1}{A(p)} = \lambda, \tag{8}$$

where the λ_j are the roots in (4), often called the "eigenvalues" of the matrix of the a_{ik}. Equation (7) is, then, equivalent to the n simpler equations (8).

The general stability criterion, therefore, reduces to the much more easily tested requirement that *for a stable computer, all roots p of the n equations (8) must have negative real parts.* This criterion holds whether or not (4) is satisfied by the coefficients a_{ik}.

Assuming now that the matrix of the a_{ik} is positive definite, so that (4) holds true, it is not necessary to apply the above stability criterion to each new combination of coefficients a_{ik}, or every given problem. If (4) is to hold, the λ_j must have positive real parts, which may vary in value depending upon the nature of the problem. They will, as a matter of fact, never exceed the value 1 since that is the maximum feedback factor possible with the potentiometer arrangement shown. Thus, *the computer will be stable for all values of the coefficients a_{ik} satisfying condition (4) if, and only if, real part of $(p)<0$ for all p such that $0<$ real part of $1/A(p)1$ (9).*

It is notable that this condition is independent of the number of amplifiers or equations. Therefore, *in order to find out whether a given type of amplifier will yield a stable computer of the type considered, it is only necessary to perform analytical or experimental tests on one amplifier with simple feedback, which will solve the equation* $ax+b=0$ by the approximation $A(ax+b)=x$

or

$$x = b\frac{A}{1-aA} \approx -\frac{b}{a}, \tag{10}$$

where a is now a complex number with positive real part (passive feedback networks with less than 90° phase shift).

If this simple system, shown in Fig. 2, proves stable for all values of a between 0 and 1, the same will be the case with a computer for n equations using the same type of amplifier if the matrix of the coefficient a_{ik} is positive (except for the possible effects of stray coupling, etc.). The fundamental importance of the last-mentioned theorem lies in the fact that it reduces the design of amplifiers for the complicated multiple-loop feedback system to the design of *one* simple feedback amplifier, so that stability criteria known from experience or a simple Nyquist analysis may be applied. The analysis described can be extended to cases in which the various amplifiers are not exactly identical as has been assumed above. Other more general theorems useful for the design of multiple-loop feedback amplifiers and servomechanisms may be derived from (8).

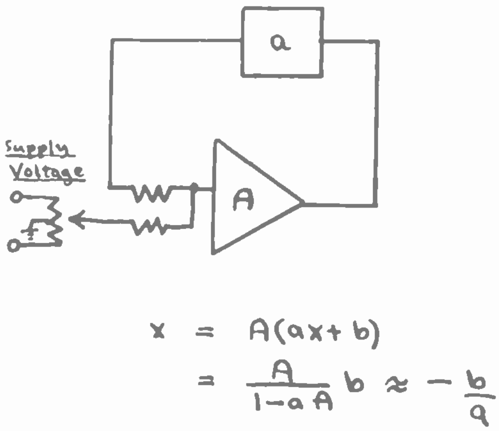

Fig. 2—Scheme of connections for testing the stability of the amplifier.

ACKNOWLEDGMENT

The author wishes to thank W. Prager, director of the Graduate Division of Applied Mathematics, Brown University, Providence, R. I., for making available the funds under which the subject research was conducted.

[7] H. W. Bode, "Network Analysis and Feedback Amplifier Design," D. Van Nostrand Co., Inc., New York, N. Y.; 1945.

Novel Multiplying Circuits with Application to Electronic Wattmeters*

M. A. H. EL-SAID†, SENIOR MEMBER, IRE

Summary—The primary relationship underlying this investigation is the exponential law relating plate current to plate voltage in a diode when operated in the so-called "retarding-field" region. By extending this classical mode of operation to multigrid tubes, the tube yielded further operating conditions in which plate current is accurately proportional to the product of a linear function of plate voltage and an exponential function of grid voltage over wide ranges.

An analysis is given of various multiplying circuits using a single multigrid tube under this mode of operation. Two methods are described for compensating accurately the inherent plate rectification due to the exponential grid curvature.

The circuits are most suited for electronic wattmeters having exceptionally good features and predictable performance over the frequency range from 20 cycles up to the neighborhood of 50 Mc.

I. Introduction

For direct measurement of power at the common frequencies of power circuits, the electrodynamometer type of wattmeter is satisfactory, but for direct measurement of small amounts of power, or for the measurement of power at the high audio frequencies or at radio frequencies, such an instrument cannot be used because of its appreciable insertion loss, inductive and capacitive qualities. For this reason, electronic wattmeters have been developed and used. With one exception,[1-3] these depend upon the use of two accurately matched tubes operating in the square-law regime. These circuits have the disadvantage that it is difficult to match the tubes sufficiently accurately and that, even when matched, the square-law relation holds over such a small range that voltage dividers are unavoidable for voltages exceeding one or two volts. It is difficult to correct the angles of these dividers at high frequencies, and the power absorbed by the divider may constitute a serious loss. The insertion unit in these instruments is a T or π configuration, and it is difficult to provide for a satisfactory ground system with these configurations.

Another type of electronic wattmeter is described by J. R. Pierce[4] in which a multigrid tube of the hexode type is used. In these instruments, the multigrid tube is arranged to operate in a regime so that its plate current versus the voltage of the first grid for various values of the voltage on the third grid is a family of straight lines, which when extended meet at one point; while at the same time the plate current varies linearly against the voltage of the third grid. Existing multigrid tubes have such a small range of linearity that the error introduced by rectification is serious enough to preclude the use of one tube in a wattmeter. When two tubes are used in a push-pull arrangement, although the error due to voltage deflection is considerably reduced, the deflections due to current alone are still appreciable. It is difficult to match the tubes under these operating conditions, and even when matched, the useful voltage range is exceedingly small.

This paper describes two types of electronic wattmeters for the measurement of ac power. The first type is mostly designed for use in circuits in which there are almost sinusoidal current and voltage relationships. Its basic multiplying circuit is of novel design and simple construction using a single vacuum tube. The second type is essentially the first, but with an additional circuit to make it generally applicable to voltages and currents having complex wave forms. The primary relationship leading to the main design equations of the incorporated multiplying circuit is the exponential law relating plate current to plate voltage in a diode when operated in the so-called "retarding-field" region. By extending this mode of operation to multigrid tubes, it was found that the tube yields further current-voltage relationships that are of importance in obtaining a predictable nonlinear performance when more than one signal is applied. These relationships are useful directly for a mathematical application to a specific type of a multiplying circuit.

II. "Retarding-Field" Characteristic of Diodes

It is known[5] that in a diode the plate current I_b is related to the temperature-limited current I_s by the expression:

$$I_b = I_s \epsilon^{bE_m}, \tag{1}$$

where E_m is the potential at the virtual cathode, $b = e/kT = 11600/T$ volts^{-1}, where e is the charge of the electron (1.602×10^{-19} coulomb), k is Boltzman's constant (1.380×10^{-23} watt/sec.), and T is the absolute temperature in degrees Kelvin. For a given diode at a fixed cathode temperature, the magnitude of E_m is a function of the plate voltage E_b. As E_b becomes sufficiently negative, E_m approaches E_b, until at a certain

* Decimal classification: R245.3. Original manuscript received by the Institute, November 24, 1948; revised manuscript received, May 31, 1949. Presented, IRE West Coast Convention, Los Angeles, Calif., October 1, 1948; and URSI-IRE Meeting, October 9, 1948, Washington, D. C.

† Fouad University, Cairo, Egypt.

[1] E. Peterson, U. S. Patent No. 1,586,533.

[2] H. M. Turner and F. T. McNamara, "An electron tube wattmeter and voltmeter and a phase-shifting bridge," Proc. I.R.E., vol. 18, pp. 1743–1748; October, 1930.

[3] E. Mallett, "A valve wattmeter," *Jour. IEE*, vol. 73, p. 295; 1933.

[4] J. R. Pierce, "A proposed wattmeter using multielectrode tubes," Proc. I.R.E., vol. 24, pp. 577–584; April, 1936.

[5] Saul Dushman, "Thermionic emission," *Rev. Mod. Phys.*, vol. 2, p. 381; 1930.

plate voltage E_b', the potential minimum is equal to E_b' and its position is at the plate. For all values of E_b more negative than E_b' a region known as "retarding-field region," $E_b = E_m$, and the $I_b - E_b$ characteristic is exponential and obeys the law:

$$I_b = I_s \epsilon^{bE_b}. \tag{2}$$

The exponential portion of the diode characteristic occurs at plate voltages more negative than those for which the three-halves power law holds, and only at plate currents determined by the Maxwellian theory of initial electron velocity distribution. The theoretical value of b corresponding to a cathode temperature of 1000° K is 11.6 volts.$^{-1}$ This exponential relationship is classical and has found practical applications; for instance, in analyzing[6] the behavior of the so-called peak-type of vacuum-tube voltmeter with small applied voltages. It is important both theoretically and practically, because it is essentially independent of variations in tube construction and processing, and therefore gives accurately reproducible results that do not demand careful selection of tubes. Fig. 1 shows this exponential

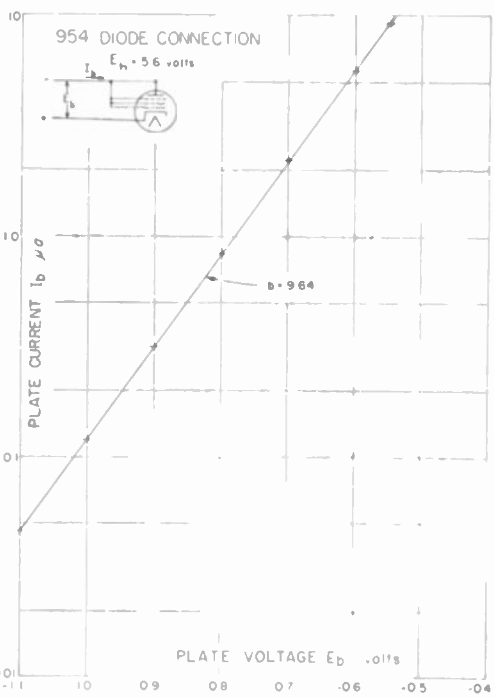

Fig. 1—"Retarding-Field" characteristic of Type 954 connected as a diode: I_b versus E_b.

characteristic for the Type 954 connected as a diode with all the grids strapped to the plate. The slope b of the $\ln - E_b$ curve is 9.64 volts^{-1}.

III. "Retarding-Field" Characteristics of Multigrid Tubes

The development of the exponential mode of operation of multigrid tubes will be presented here briefly; but some of the clarifying details are given in Appendix I. When the screen grid voltage of a tetrode or a pentode is reduced to a value near cathode potential and the grid voltage is sufficiently negative so that a virtual cathode is formed at the grid, and both grid and plate currents will vary exponentially against grid voltage. These low currents are determined by initial velocity distribution and occur at grid voltages more negative than those for which the three-halves power law holds.

Fig. 2 shows these grid and plate currents for the

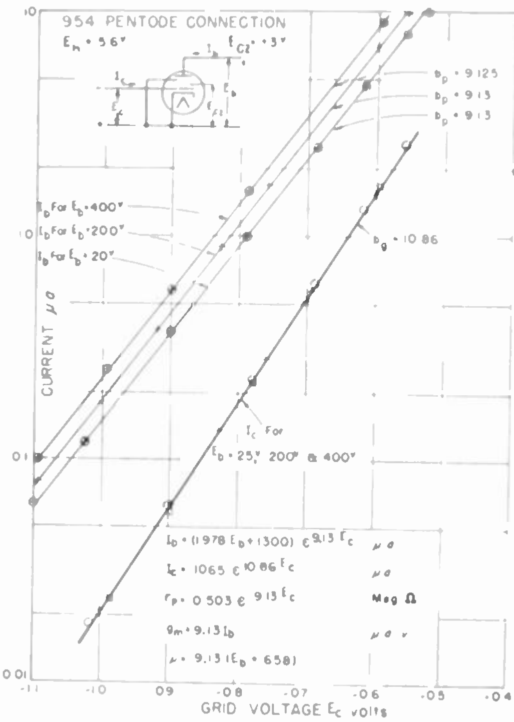

Fig. 2—"Retarding Field" characteristics of Type 954: I_b and I_c versus E_c for various values of E_b.

Type 954 plotted against grid voltage on a semilog chart. The curves are taken for plate voltages between 20 and 400 volts with the screen grid voltage held constant at +3 volts. It will be seen that the curves are accurately exponential up to about 10 microamperes and that the grid current I_c is substantially independent of plate voltage. The slope b_p of the $\ln I_b - E_c$ curves is constant, being practically 9.13 volts^{-1}. The slope b_g of the $\ln I_c - E_c$ curve is 10.86 volts^{-1}. The curves show that, over the full plate voltage range, the grid and plate currents, respectively, obey the relationships:

$$I_c = I_{c_s} \epsilon^{b_g E_c} \tag{3}$$

and

$$I_b = I_{b_s} \epsilon^{b_p E_c}, \tag{4}$$

where I_{c_s} and I_{b_s} are, respectively, the extrapolated values of grid and plate currents at $E_c = 0$. Furthermore, the plate current curves of Fig. 2 show that since b_p is fixed, the value of I_{b_s} is determined by the plate voltage only.

[6] C. B. Aiken, "Theory of the diode voltmeter," Proc. I.R.E., vol. 26, pp. 859–877; July, 1938.

Fig. 3 shows the same experimental data of Fig. 2, plate current versus plate voltage plotted on a linear chart for various constant values of grid voltage. These curves show that, over the full plate voltage range from 20 to 500 volts, the plate current varies accurately linearly with plate voltage. Also, the lines determine a

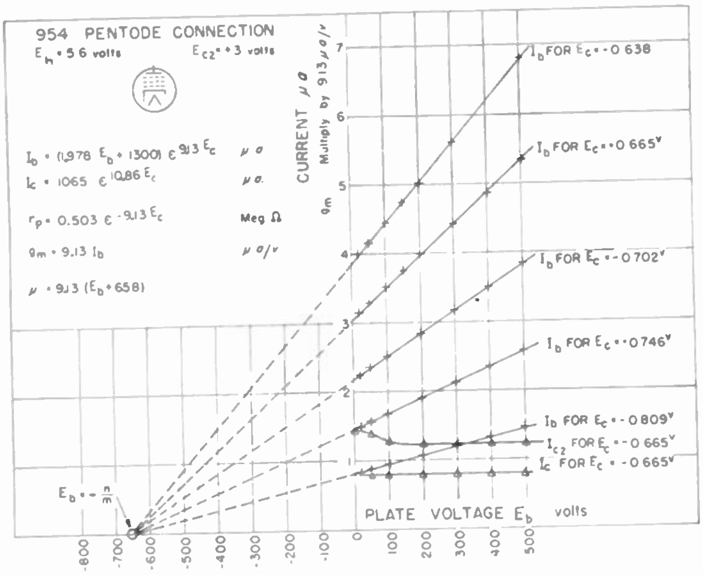

Fig. 3—"Retarding-Field" characteristics of Type 954: I_b, I_c and I_{c_2} versus E_b for various values of E_c.

common intersection on the plate voltage axis at $E_b = -660$ volts. Under these conditions, the value of I_b, varies linearly with plate voltage, and (4) for plate current can therefore be re-written as:

$$I_b = (mE_b + n)\epsilon^{b_pE_c}, \tag{5}$$

where E_b and E_c are, respectively, the plate and grid voltages, m is the slope of the extrapolated plate current-plate voltage characteristic for $E_c = 0$, and n is the extrapolated plate current for $E_b = E_c = 0$.

Referring to Fig. 2 and 3 it is evident that a multigrid tube operated under initial velocity conditions yields a plate current accurately proportional to the product of a linear function of plate voltage and an exponential function of grid voltage over wide ranges. The grid current is an exponential function of grid voltage, and substantially independent of plate voltage.

IV. Multiplying Circuits

Consider the simplified circuit of Fig. 4 in which a pentode V-1 is shown with its electrodes suitably polarized to operate in the exponential regime with (3) and (5) valid. Two ac input voltages v_p and v_g are applied in the plate and grid circuits, respectively. The source impedances of v_p and v_g are not shown, since these can be neglected compared to the corresponding high tube impedances in the operating region of Fig. 3. For the same reason, grid rectification is neglected, and only (5) will be considered. With no alternating voltages applied, let the dc plate and grid voltages be so adjusted that the direct current through the plate is given by:

$$I_b = (mE_b + n)\epsilon^{b_pE_c}, \tag{6}$$

where E_b and E_c are the dc plate and grid voltages, respectively.

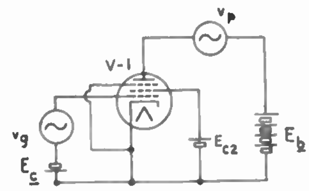

Fig. 4—Simplified multiplying circuit incorporating a pentode under initial velocity conditions.

When v_p and v_g are applied, the plate voltage becomes (E_b+v_p) while the grid voltage becomes (E_c+v_g), and the plate current becomes (I_b+i_b). Therefore:

$$i_b = I_b(\epsilon^{b_pv_g} - 1) + m_0v_p\epsilon^{b_pv_g}, \tag{7}$$

where $m_0 = m\epsilon^{b_pE_c}$ and equals the plate conductance at the quiescent operating point. Over an infinitesimal grid voltage excursion, (7) reduces to:

$$i_b = I_bb_p(v_g) + m_0(v_p) + m_0b_p(v_pv_g). \tag{8}$$

Equation (8) indicates that with infinitesimal grid voltage excursion, the change in plate current, consequent upon application of alternating plate and grid voltages, comprises a term proportional to the product of the two voltages in addition to terms proportional to each voltage. The average change in plate current equals $(i_b)_{av.}$ proportional to $(v_pv_g)_{av.}$ provided that v_p and v_g have no dc components.

In order to obtain a useful amount of output by increasing the grid voltage excursion, plate rectification occurs due to the nonlinearity inherent in the exponential curvature. The multiplying circuit of Fig. 4 would be ideal, had the plate current been proportional to the product of linear functions of plate and grid voltages. However, two methods will be described here for compensating accurately the effect of plate rectification. One method compensates for the average value of plate rectification, whereas the other compensates for the instantaneous value.

A. Compensation by Average Grid Rectification

Since plate current is exponential against grid voltage, plate rectification occurs and the average change in plate current consequent upon application of alternating plate and grid voltages contains a component determined by grid voltage only. This component is independent of plate voltage and can therefore be compensated by changing the average potential to the grid. Since, as previously indicated, the grid current is substantially independent of plate voltage, it is therefore reasonable to see if the tube can bias itself automatically to the proper operating point to compensate for average plate rectification by using the grid current to produce average grid rectification.

Consider the circuit shown in Fig. 5 (a) which is similar to that shown in Fig. 4, except that a grid leak resistor R_g by-passed by a capacitor C_g is connected in series with the grid. Also, a plate load resistance R_p by-passed by a capacitor C_p is connected in series with the plate supply E_{bb}. Let the source impedances of the alternating voltages v_g and v_p be negligibly small compared to the corresponding tube impedances in the operating region shown in Fig. 3. Let, also, the values of C_g and C_p be such that all the alternating voltages v_g and v_p are effectively applied respectively across the grid-cathode and plate-cathode spaces of the tube.

With no alternating voltages applied to the system, let the dc potential at the plate be E_b, and the direct currents flowing in the plate and grid be I_b and I_c respectively. The grid current I_c will flow through R_g, thus biasing the tube negatively; the bias depending upon R_g and its magnitude is $E_c = I_c R_g$. Also, the plate current I_b will flow through R_p, thus dropping the battery voltage to E_b at the plate.

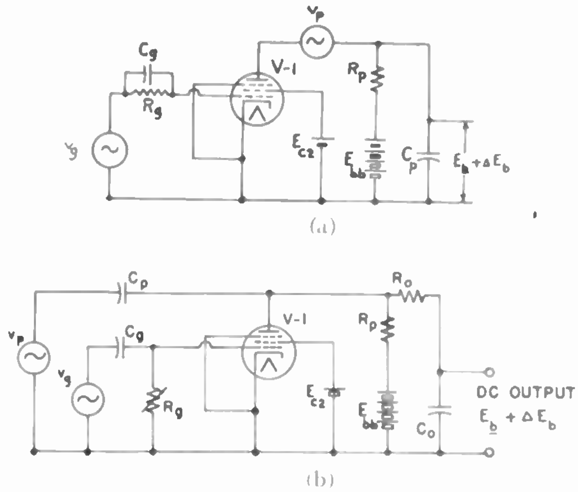

Fig. 5—Multiplying circuit incorporating a pentode under initial velocity conditions and using average grid rectification to compensate average plate rectification.

When v_g is applied, grid rectification occurs and the current through R_g increases. The total grid voltage becomes $(-E_c + v_g - \Delta E_c)$ where ΔE_c is the average rectified grid voltage depending upon the magnitude of R_g and the applied alternating grid voltage (see Appendix II).

When the alternating voltages v_p and v_g are applied simultaneously, the plate current will be $(I_b + i_b)$; the average value changing from I_b to $(I_b + (i_b)_{av.})$. The total plate voltage will be $(E_b + v_p - (i_b)_{av.} R_p)$. Therefore, substituting these values in (5), the plate current consequent upon the application of alternating voltages to the system is given by:

$$I_b + i_b = [mE_b + mv_p - m(i_b)_{av.} R_p + n]\epsilon^{(-b_p E_c + b_p v_g - b_p \Delta E_c)}$$

Taking average values of both sides and solving for $(i_b)_{av}$ we get:

$$(i_b)_{av} = I_b \frac{(\epsilon^{b_p v_g})_{av}\,\epsilon^{-b_p \Delta E_c} - 1}{1 + m_0 R_p (\epsilon^{b_p v_g})_{av}\,\epsilon^{-b_p \Delta E_c}} + m_0 (v_p \epsilon^{b_p v_g})_{av} \frac{\epsilon^{-b_p \Delta E_c}}{1 + m_0 R_p (\epsilon^{b_p v_g})_{av}\,\epsilon^{-b_p \Delta E_c}} \qquad (9)$$

Equation (9) shows that the average value of the change in plate current consequent upon the application of v_p and v_g is composed of an average product term of the form $(v_p \epsilon^{b_p v_g})_{av}$, and an additional voltage term depending upon the alternating grid voltage only. Since this additional voltage term is due to plate rectification, therefore, if by means of grid rectification the value of ΔE_c is so adjusted that the additional voltage term in (9) vanishes identically, then:

$$(\epsilon^{b_p v_g})_{av.} = \epsilon^{b_p \Delta E_c},$$

i.e., the value of ΔE_c must be given by

$$\Delta E_c = \frac{1}{b_p} \ln (\epsilon^{b_p v_g})_{av.}, \qquad (10)$$

which gives a condition for perfect grid bucking. Under this condition, (9) reduces to:

$$(i_b)_{av.} = \frac{m_0}{1 + m_0 R_p} \frac{(v_p \epsilon^{b_p v_g})_{av.}}{(\epsilon^{b_p v_g})_{av}} \qquad (11)$$

Particular interest is taken in the simple case where $v_p = V_p \cos(wt + \phi)$ and $v_g = V_g \cos wt$ (for other cases, see Appendix III). Substituting these values in (11) we get:

$$(i_b)_{av.} = \frac{m_0}{1 + m_0 R_p} \frac{-jJ_1(jb_p V_g)}{J_0(jb_p V_g)} V_p \cos \phi, \qquad (12)$$

where $-j\,J_1(jb_p V_g)$ is modified Bessel Function first kind first order, and $J_0(jb_p V_g)$ is modified Bessel Function first kind zero order. Fig. 6 shows a plot of the quotient

$$\frac{-jJ_1(jb_p V_g)}{J_0(jb_p V_g)}$$

against $b_p V_g$, and it will be seen that the deviation of this quotient from linearity is less than 3 per cent for values of $b_p V_g$ up to 0.5. Multiplying both sides of (12) by R_p and considering only the linear portion of the Bessel quotient, we obtain

$$\Delta E_b = (i_b)_{av.} R_p = \frac{m_0 R_p}{1 + m_0 R_p} \frac{1}{2} b_p V_g V_p \cos \phi, \qquad (13)$$

which shows that upon the application of pure and coherent alternating plate and grid voltages, the dc potential at the plate changes by an amount proportional to $V_p V_g \cos \phi$, provided that grid bucking is perfect. The circuit in this case can be used to measure the average value of the product of two alternating voltages. Under these conditions, when the peak ac grid voltage is limited to less than $1/2\ b_p$, the accuracy of measurement is better than ± 1.5 per cent of full output. Meanwhile, for $b_pV_g=0.5$, the full output is 12.5 per cent of the peak ac plate voltage at unity power-factor and with $m_0R_p=1$; being only doubled for $m_0R_p \gg 1$.

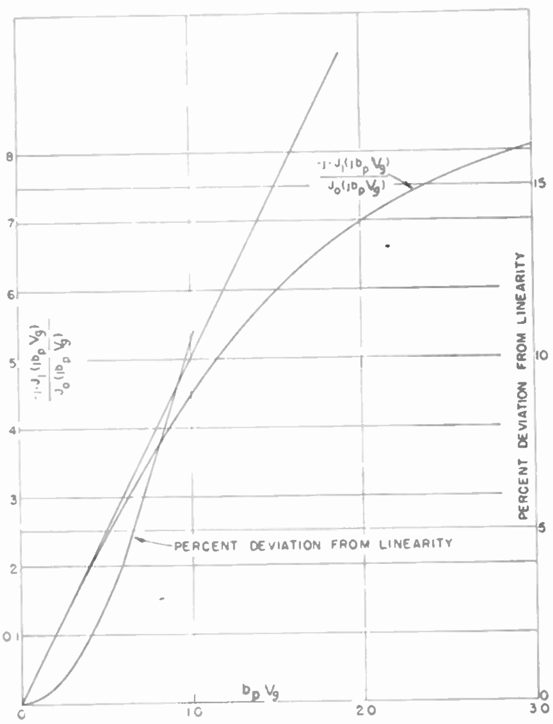

Fig. 6—A plot of the quotient $\dfrac{-jJ_1(j\,b_pV_g)}{J^0(j\,b_pV_g)}$ and its per cent deviation from linearity versus b_pV_g.

As to grid bucking, it is possible (see Appendix II) to adjust the grid rectification efficiency so that the tube biases itself automatically to such an operating point that almost perfect grid bucking is achieved. The condition for optimum grid bucking requires that the magnitude of R_g be given by:

$$R_g \cong \frac{1}{\delta b_g I_c} \quad \text{or:} \quad \delta b_g I_c R_g = 1 \tag{14}$$

where

$$\delta = \frac{b_g}{b_p} = 1$$

(see Appendix II).

However, by examining (9), it will be apparent that when $v_p=0$, the condition for perfect grid bucking demands that $(i_b)_{av.}$ should be zero independent of the magnitude of v_g. Therefore, practically, the multiplying circuit of Fig. 5 can be adjusted for optimum grid bucking by applying appropriate ac voltages to the grid with the plate input circuit short circuited, and adjusting R_g for no change in the dc component of plate current. The same result can be achieved by fixing the value of R_g and introducing a small adjustable grid bias to control the magnitude of I_c so as to fulfill the requisite grid rectification efficiency for optimum grid bucking. These practical methods of adjustment require only a fair knowledge of the parameters δ, b_g, and I_c in (14) for the particular type of tube used. It will be necessary to readjust the screen grid voltage in order to restore the plate current to its initial value before and during the adjustment.

The circuit of Fig. 5(b) is similar to that in Fig. 5(a), except that the alternating voltages v_p and v_g are fed in parallel with the plate and grid, respectively. In this arrangement, since capacitive feed is used, any dc components in the applied voltages will not reach the tube. A resistance-capacitance filter R_0-C_0 is connected across the plate and cathode; the dc potential at the plate appearing across C_0.

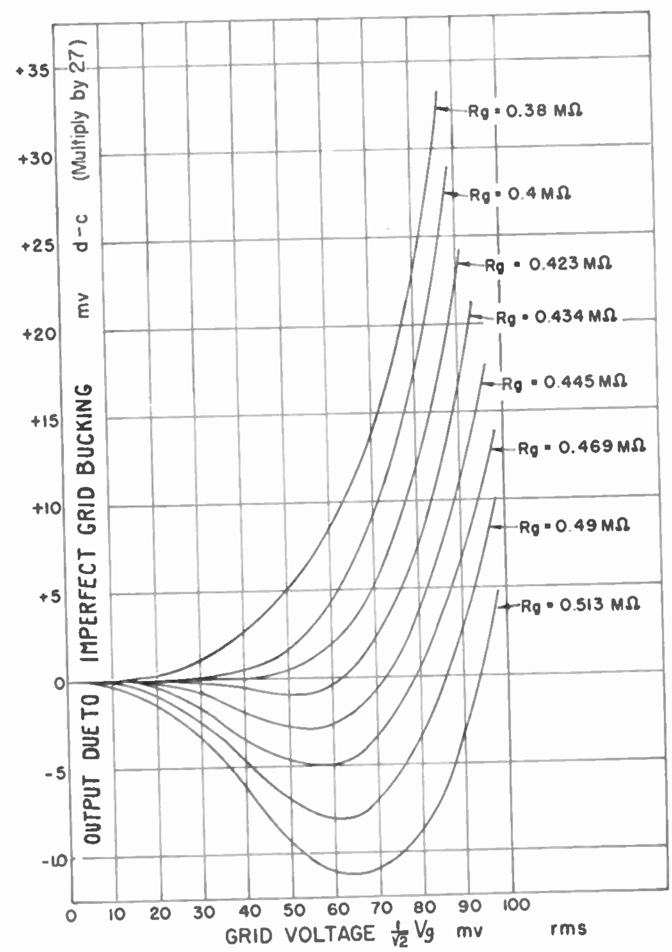

Fig. 7—Observed values of dc output voltage due to imperfect grid bucking versus rms grid voltage for various values of R_g in the circuits of Fig. 5.

Fig. 7 shows results of measurements of the dc output voltage due to imperfect grid bucking in the circuit of Fig. 5(b) using the Type 954. The measurement is made by a balanced degenerative dc voltmeter connected across C_0. These curves show that for the particular value of $R_g=0.423$ megohm, the output due to imperfect grid bucking is less than 4 millivolts over an rms grid voltage range up to 40 millivolts. For smaller values of R_g the output is positive, whereas for larger values the output displays a negative loop. The negative loop curves show that the ac grid voltage range can be increased to about 70 millivolts without having an appreciable output voltage due to imperfect grid bucking, as shown by the curve for $R_g = 0.434$ megohm.

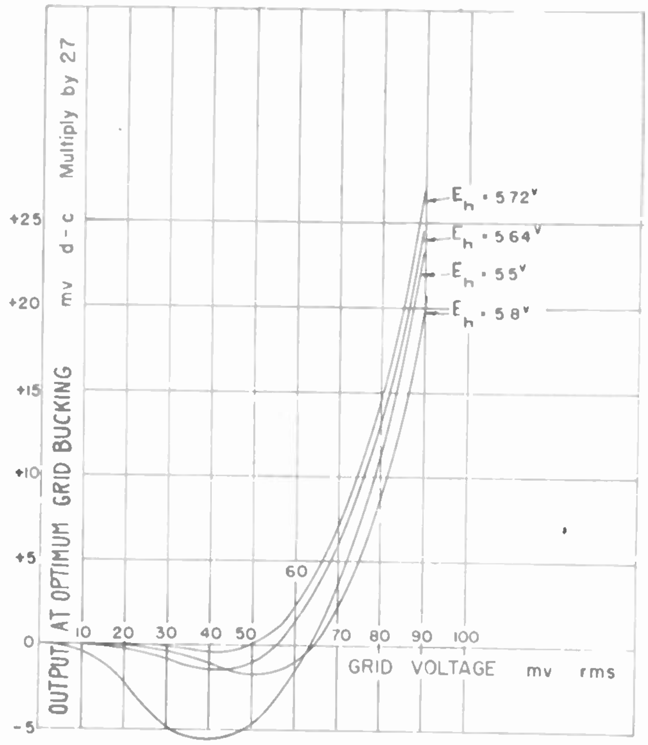

Fig. 8—Observed values of dc output voltage due to optimum grid bucking versus rms grid voltage for various values of the heater voltage in the circuit of Fig. 5.

Fig. 8 shows results of similar measurements with the circuit initially adjusted for optimum grid bucking at a heater voltage about 5.7 volts. The curves show that the circuit adjustment for optimum grid bucking is not appreciably affected by a reasonable change in heater voltage.

The pentode Type 954 is particularly suited for a large plate voltage swing without showing a serious error, due to imperfect linearity of plate current-plate voltage characteristics. For this Type, 4 microamperes is a suitable value for I_b, and 1.0 microampere for I_c. The plate conductance at 4 microamperes is of the order of 0.005 microampere per volt, corresponding to an internal resistance of 200 megohms. The requisite value of R_g for optimum grid bucking is of the order of 0.5 megohm, and a suitable value for R_p is 100 megohms. Since the dc voltage drop across R_p is 400 volts; the resistor should therefore be selected for minimum voltage coefficient. This is necessary in order to minimize resistor rectification due to dc polarization. Also, for the same reason, capacitors C_p and C_0 should preferably be of the polystyrene dielectric type. With these circuit components, and with $E_b = 250$ volts, the full output at unity power factor is about 20 volts dc for 200 volts peak ac plate voltage, and 70 millivolts peak ac grid voltage.

Circuit Performance as a Wattmeter: The circuit of Fig. 5(b) is particularly suited for a simple electronic wattmeter.

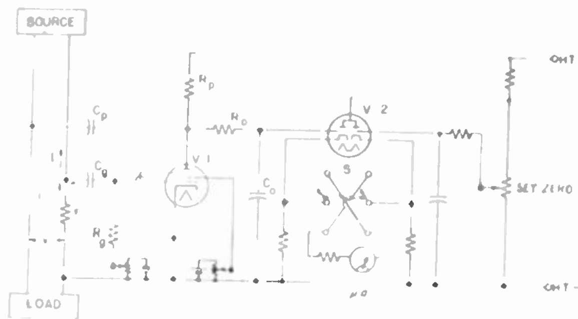

Fig. 9—Basic circuit of electronic wattmeter incorporating the multiplying circuit of Fig. 5.

Fig. 9 shows a diagram of the basic circuit of wattmeter of this type in which V-1 is the basic measuring tube, and V-2 is a twin triode connected as a conventional degenerative dc voltmeter. The indicating meter μa is connected across a reversing switch S. The voltage component of power to be measured is applied to the plate of V-1, while all the current component practically passes through the series resistor r and develops a voltage drop which is proportional to current and is applied to the grid of V-1.

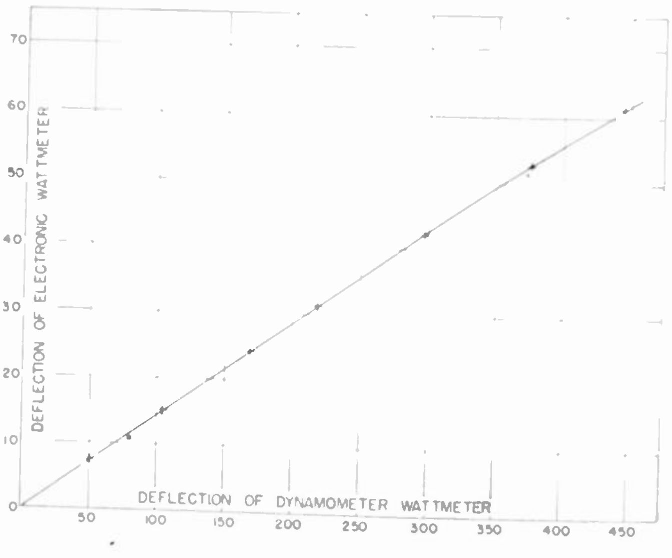

Fig. 10—Relative deflections of electronic wattmeter versus dynamometer wattmeter at unity power factor.

Assuming that $v = V \cos(wt + \phi)$ and $i = I \cos wt$, the change in the dc voltage across R_g consequent upon the application of v and i is obtained by substitution in (13), hence:

$$\Delta E_b = \frac{m_0 R_p}{1 + m_0 R_p} \cdot \frac{1}{2} \cdot b_p \cdot r \cdot (VI \cos \phi)$$

which is proportional to the mean ac power dissipated in the load.

The circuit was tested for wattmetric indication by comparing its reading with that indicated by a dynamometer wattmeter at 60 cycles. Fig. 10 shows relative results obtained at unity power factor and Fig. 11 at variable power factors. The values of power factor indicated in Fig. 11 are calculated from the reading of the

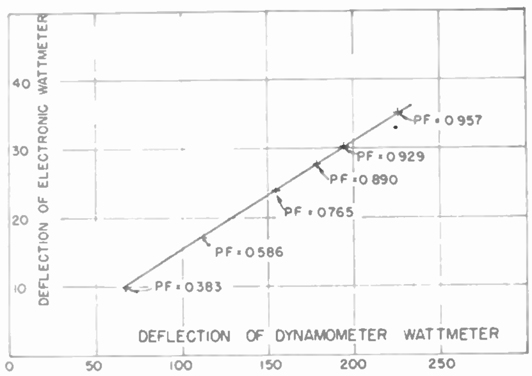

Fig. 11—Relative deflections of electronic wattmeter versus dynamometer wattmeter at various power factors.

dynamometer wattmeter, a voltmeter, and an ammeter. The curves show that both wattmeters agree closely. Fig. 12 shows that the deflection of the elec-

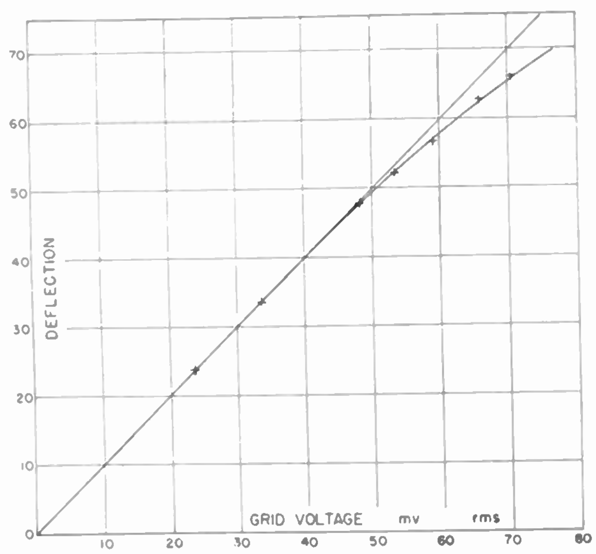

Fig. 12—Relative deflection of electronic wattmeter versus rms grid voltage with a fixed ac plate voltage.

tronic wattmeter with a constant ac plate voltage is very closely proportional to the magnitude of the ac grid voltage, as has been theoretically predicted and shown in Fig. 6.

Preliminary trials for determining the frequency characteristic of the circuit shown in Fig. 9 indicated a reasonably flat frequency response up to about 10 megacycles. Some errors were observed above this frequency indicating the presence of feedback. The circuit was then tested with the grid input circuit short circuited and a variable frequency voltage of about 150 volts rms applied to the plate. In this test, a dc output of one per cent of full scale was observed at about 5 Mc increasing approximately as the square of frequency. Since, in this type of operation, the grid-plate capacitance is insufficient to cause appreciable error at this frequency, it was found that the observed errors are due to feedback through the cathode and screen-grid lead inductances.

The effects of these two types of feedback, upon the performance of the tube under such operating conditions, are in opposite directions. One type of feedback can therefore be neutralized by means of adjusting the other. However, in the Type 954, an examination of the electrode structure showed that there are some auxiliary metallic parts, such as a top cap, a bottom ring, and a getter support, all connected to the bottom ring together with the cathode, rather than with the suppressor, as is usually the modern policy of tube construction. The resulting direct capacitance between plate and cathode is of the order of 1.5 $\mu\mu$f. In the megacycle region, and with 150 volts rms on the plate, an appreciable radio-frequency current flows through the cathode lead inductance, thus developing an in-phase voltage in the grid circuit of the order of few millivolts. In the Type 954, the amount of feedback through the screen-grid circuit is insufficient to compensate for this cathode feedback. However, with the aid of a small adjustable neutralizing capacitor of the order of 1 $\mu\mu$f connected between the plate and the screen grid it was possible to increase the feedback through the latter to an extent sufficient to compensate for the excessive cathode feedback. This arrangement extended the frequency range for the Type 954 to 20 Mc. There is a good possibility of exceeding this range by using tubes which do not have such an appreciable plate to cathode capacitance as in Type 954.

The multiplying circuit of this wattmeter is highly sensitive to supply voltage changes the power supply should be well regulated. A good degree of stability is achieved by the use of a bucking tube of the same type as the wattmeter tube and connected to the other arm of the bridged degenerative voltmeter circuit of Fig. 9. Nevertheless regulation, within 0.2 per cent is necessary at the low alternating plate voltage ranges. The circuit stability may also be improved by using tubes having tungsten or tantalum filaments since these have a value of $b = e/kT$ of the order of 3 to 4 volts^{-1}. The use of such tubes require a maximum ac grid voltage of the order of 100 millivolts rms for $b_p V_g = 0.5$. This has the further advantage of reducing effects of stray pickup and feedback at high frequencies.

In some fields of application of this wattmeter, as for instance in the measurement of power at low power-factors, the use of a two-tube push-pull arrangement may be necessary, in order to reduce the errors caused by imperfect grid bucking and imperfect linearity of plate current-plate voltage characteristics. Fortunately, such errors in this type of operation can be determined and controlled.

This wattmeter has the advantages of a wide frequency range and simplicity, in addition to the fact that it absorbs only a minute fraction of the measured power. It also enables the measurement of very small amounts of power.

B. Compensation by Instantaneous Grid Rectification

In this method of compensation, the instantaneous values of rectified plate current due to the exponential grid curvature are compensated by varying the instantaneous grid voltage on a proper logarithmic curvature. The system, in this case, obtains the product of the applied alternating voltages as if the plate current were proportional to the product of linear functions of plate and grid voltages.

Consider the circuit shown in Fig. 13 which is similar

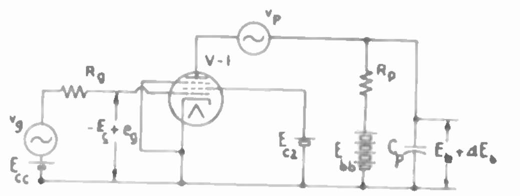

Fig. 13—Multiplying circuit incorporating a pentode under initial velocity conditions, and using instantaneous grid rectification to compensate instantaneous plate rectification.

to that in Fig. 5 except that the by-pass capacitor C_g is removed and the alternating voltage v_g is applied to the grid through the grid leak resistor R_g. An external bias E_{cc} is also shown.

With no alternating voltages applied, the direct current through the grid will bias the tube negatively; the bias will be $E_c = I_c R_g - E_{cc}$, where $I_c = I_{c_s} \epsilon^{-b_g E_c}$. Therefore: $E_{cc} + E_c = I_{c_s} R_g \epsilon^{-b_g E_c}$. When the external bias E_{cc} is much larger than E_c, the value of R_g will be practically (E_{cc}/I_c), and the relation between E_c and E_{cc} will be given by:

$$E_{cc} = I_{c_s} R_g \epsilon^{-b_g E_c}, \quad \text{i.e.,} \quad -E_c = \frac{1}{b_g} \ln \frac{E_{cc}}{I_{c_s} R_g}$$

indicating that the grid maintains a bias proportional to the logarithm of the applied external bias.

When the alternating voltage v_g is applied, grid rectification occurs, and the instantaneous voltage developed at the grid will be $(-E_c + e_g)$, where e_g is given by

$$-E_c + e_g = \frac{1}{b_g} \ln \frac{E_{cc} + v_g}{I_{c_s} R_g}$$

i.e.,

$$e_g = \frac{1}{b_g} \ln \left(1 + \frac{v_g}{E_{cc}}\right). \tag{15}$$

Let the direct current through the plate be given by (6). The rectified plate current consequent upon application of alternating voltage v_g will be given by:

$$I_b + \Delta i_b = (mE_b + n)\epsilon^{-b_p E_c + b_p/b_g \ln(1+v_g/E_{cc})}$$
$$= I_b \epsilon^{b_p/b_g \ln(1+v_g/E_{cc})}$$

Let in the ideal case $b_p = b_g$, then $\Delta i_b = I_b(v_g/E_{cc})$ indicating that the output plate current is an exact duplicate of the input voltage v_g, and that plate rectification is perfectly compensated. The system, in this case, behaves as if the plate current were accurately proportional to the product of linear functions of plate and grid voltages.

When the alternating voltages v_p and v_g are applied to the system, the plate voltage will be $(E_b + v_p - (i_b)_{av} R_p)$ and the grid voltage will be $(-E_c + e_g)$. The plate current consequent upon application of alternating voltages will be:

$$I_b + i_b = [mE_b + mv_p - m(i_b)_{av} R_p + n]\epsilon^{-b_p E_c + b_p/b_g \ln(1+v_g/E_{cc})}$$
$$= [I_b + m_0 v_p - m_0 (i_b)_{av} R_p]\left[1 + \frac{v_g}{E_{cc}}\right]^{b_p/b_g}$$

and if $b_p = b_g$, then

$$i_b = m_0 v_p + \frac{v_g}{E_{cc}}(I_b - m_0 (i_b)_{av} R_p)$$
$$+ \frac{m_0}{E_{cc}} v_p v_g - m_0 (i_b)_{av} R_p. \tag{16}$$

Equation (16) holds for all wave forms of the voltage v_p and v_g. It will be seen from (15) and (16) that, when the instantaneous voltage across the grid-cathode space of the tube is a proper logarithmic function of the applied voltage v_g, the compensation of the exponential curvature is accurate. In this case, the circuit obtains the product of the two voltages v_p and v_g without producing errors due to increasing the grid voltage excursion.

Taking average values of both sides of (16) and assuming that v_p and v_g have no dc components, the change in the dc voltage across R_p is given by:

$$\Delta E_b = (i_b)_{av} R_p = \frac{m_0 R_p}{1 + m_0 R_p} \cdot \frac{1}{E_{cc}} (v_p v_g)_{av}. \tag{17}$$

Although the circuit is extremely simple, yet it has the disadvantage that the accuracy of obtaining the product $(v_p v_g)$ depends upon the discrepancy in the ratio b_p/b_g from unity, in addition to a working frequency range limited by the frequency characteristics of R_g and its associated capacities. The circuit can be arranged to give satisfactory performance up to high audio frequencies.

However, the system is greatly improved by the addition of a radio-frequency logarithmic circuit. This additional circuit depends upon the fact that, with proper adjustments, the plate current of the pentode tube is accurately logarithmic against plate voltage; the relationship being:

$$I_b = A + K \ln E_b, \tag{18}$$

where A is a constant and K is the slope of the $I_b - \ln E_b$ curve. Fig. 14 shows the circuit diagram and operating characteristics of the Type 6AU6 for a logarithmic relation over the plate voltage range from 0.5 to 2.0 volts. In this circuit the value of K is mainly controlled by the screen grid voltage and the self-bias resistor. If the direct current voltage on the plate is adjusted to the middle of the logarithmic range and a limited alternating voltage applied to the plate through a low impedance, the consequent change in plate current will be:

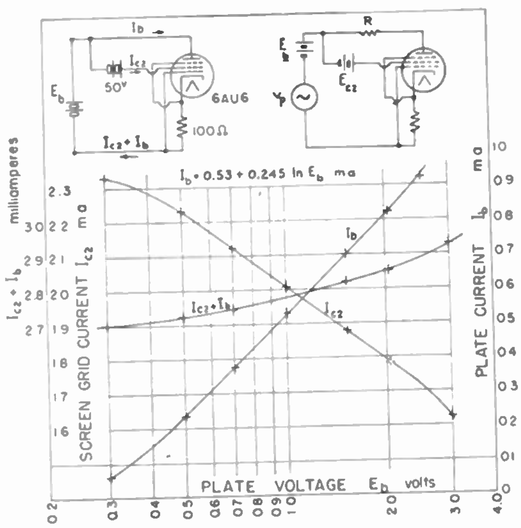

Fig. 14—A pentode arrangement for a logarithmic plate current over the plate voltage range from 0.5 to 2.0 volts.

$$i_b = K \ln\left(1 + \frac{v_p}{E_b}\right). \tag{19}$$

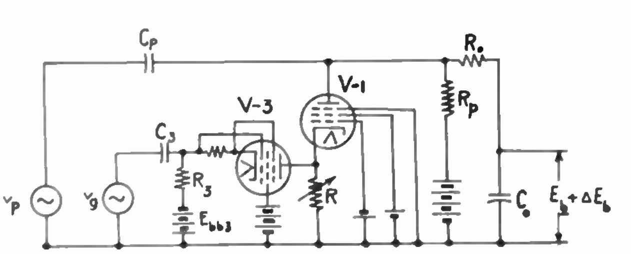

Fig. 15—Multiplying circuit incorporating a pentode under initial velocity conditions combined with a logarithmic circuit to compensate instantaneous plate rectification.

Consider the multiplying circuit shown in Fig. 15, which is similar to that in Fig. 13 except that an additional logarithmic circuit is coupled to the grid circuit of V-1 by means of the base resistor R. The alternating voltage v_g is applied between plate and cathode of V-3 through a coupling capacitor C_3 and across a resistor R_3. The voltage drop across R is injected in the grid circuit of V-1 through the cathode lead. If the plate current of V-3 is much greater than the cathode current of V-1, as is actually the case, feedback from V-1 into V-3 is negligibly small.

With no alternating voltages applied, let the system be adjusted that at any instant, the plate current of V-1 is given by (5); whereas the plate current of V-3 is given by (18). The direct current through the plate of V-3 will flow through R, whereas the sum of the screen grid and plate currents will flow through R_3, dropping the battery voltage E_{bb3} to E_{b3} at the plate.

When the alternating voltage v_g is applied, the consequent voltage drop across R sill be given by $KR \ln(1+(v_g/E_{b3}))$; the grid voltage of V-1 thus becomes

$$-E_c + KR \ln\left(1 + \frac{v_g}{E_{b3}}\right).$$

When the alternating voltages v_p and v_g are applied simultaneously, the plate voltage of V-1 will be $[E_b + v_p - (i_b)_{av.} R_p]$, and the plate current will be:

$$\begin{aligned} I_b + i_b &= [mE_b + mv_p \\ &\quad - m(i_b)_{av.}R_p + n]\epsilon^{b_p[-E_c + KR \ln(1+v_g/E_{b3})]} \\ &= [I_b + m_0 v_p - m_0 (i_b)_{av.} R_p]\epsilon^{b_p KR \ln(1+v_g/E_{b3})}. \end{aligned}$$

If by a careful pre-adjustment $b_p KR = 1$, then:

$$\begin{aligned} i_b &= m_0 v_p + \frac{v_g}{E_{b3}}(I_b - m_0(i_b)_{av.}R_p) \\ &\quad + \frac{m_0}{E_{b3}} v_p v_g - m_0 (i_b)_{av.} R_p, \end{aligned}$$

which is similar to (16). The change in the dc plate voltage consequent upon application of v_p and v_g is given by:

$$\Delta E_b = (i_b)_{av.} R_p = \frac{m_0 R_p}{1 + m_0 R_p} \cdot \frac{1}{E_{b3}} \cdot (v_p v_g)_{av.} \cdot \tag{20}$$

The requisite value of R can be calculated from $1/b_p K$. The practical method of adjusting the system is carried out experimentally by applying the alternating voltage v_g with the plate input circuit of V-1 short circuited and adjusting R so that the change in the dc output voltage is zero. The same result can be achieved by fixing the value of R and adjusting the value of K by changing the screen grid voltage of V-3. Should $b_p KR = (1 \pm \Delta)$ where Δ is a small fraction, the dc output voltage due to imperfect compensation by the logarithmic circuit is approximately $\pm(\Delta/4)(V_g/E_{b3})^2 \cdot I_b R_p$ where V_g is the peak value of v_g. This amounts to about 30 millivolts for a value of $\Delta = 0.001$, $(V_g/E_{b3}) = 0.6$ and $I_b R_p = 400$ volts. The full output is 30 volts at unity power factor and 200 volts peak on the plate for $m_0 R_p = 1$. However, provision can be easily made in the circuit for a fine adjustment of the condition $b_p KR = 1$.

In practice, values of K of the order of 1.0 milliampere are obtained from ordinary receiving tubes. The required value of R is about 100 ohms assuming $b_p = 10$ volts^{-1}. With these values the frequency range of the circuit is extended to the neighborhood of 30 Mc. However, it is necessary to compensate for the unavoidable shunting capacities across R. These usually amount to about 15 micromicrofarads and a small inductive component of R is desirable.

Appendix I

"Retarding-Field" Characteristics of Multigrid Tubes

The extension of the exponential mode of operation of diodes to multigrid tubes was accomplished by investigating—at first—the retarding-field characteristics of triodes.

In a triode, when the plate voltage is reasonably low, and the grid voltage is sufficiently negative so that a virtual cathode is formed at the grid, the grid current-grid voltage characteristic becomes exponential with a slope b_g closely equal to b. Since the plate current constitutes electrons which pass through the grid mesh, the plate current-grid voltage characteristic is also exponential, but with a slope b_p considerably less than b. Fig. 16 shows these exponential curves of the Type 954 connected as a triode with grids 2 and 3 strapped to the plate. The curves are taken for plate voltages between 5 and 40 volts. The slope b_g of the $\ln I_c - E_c$ curves is, in all cases, fairly close to that observed for the same tube connected as a diode, i.e., 9.64 volts^{-1}; but the slope b_p of the $\ln I_b - E_c$ curves is only 6.81 at $E_b = 5$ volts, decreasing to 3.62 at $E_b = 40$ volts. This considerable decrease in the observed value of b_p is due to the fact that the field distribution between grid and cathode is appreciably affected by the plate voltage.[7]

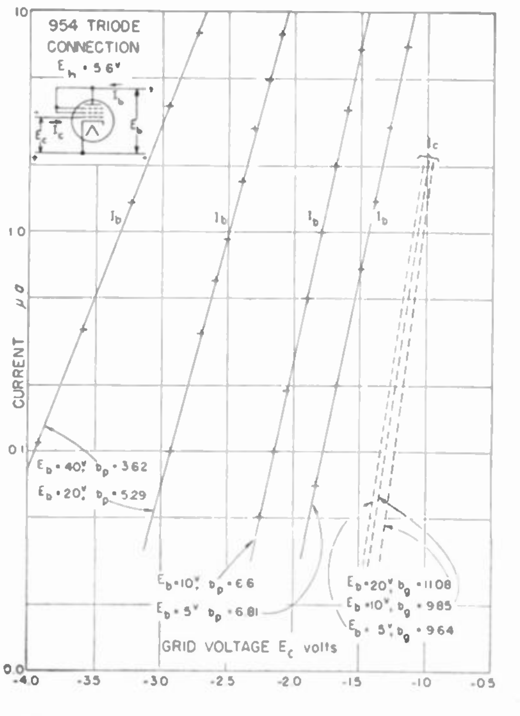

Fig. 16—"Retarding-Field" characteristics of Type 954 connected as a triode: I_b and I_c versus E_c for various values of E_b.

It was inferred that the dependence of b_p upon plate voltage can be avoided by shielding the plate from the grid-cathode region. This was proved by taking measurements of b_p for tetrodes and pentodes. Fig. 17 shows results of the measured values of b_p against E_b for the Type 954 connected progressively as a triode, tetrode, and pentode. In these measurements the screen grid potential was held constant at a value just convenient to permit a few microamperes to flow in the plate circuit. From these curves it is evident that as the plate is progressively more and more shielded from the cathode, the value of b_p increases and becomes substantially independent of plate voltage.

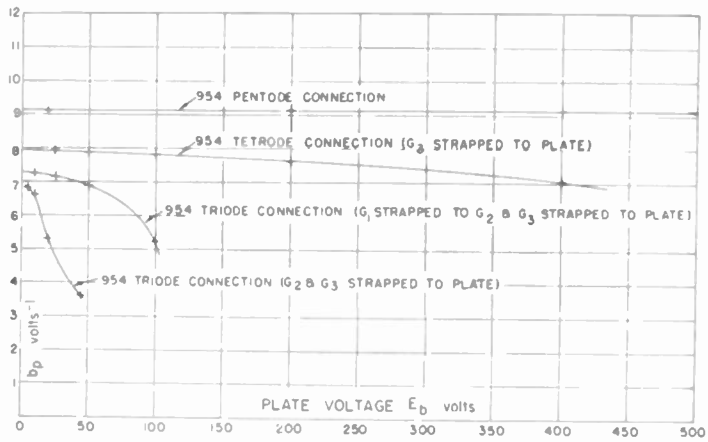

Fig. 17—Measured values of b_p versus E_b for the Type 954 connected as a triode, tetrode, and pentode.

With a fixed value of b_p, the general shape of the retarding-field characteristics of multigrid tubes are as those shown in Figs. 2 and 3 for the Type 954. These characteristics differ from those of triodes in that the slopes b_p and b_g, and the grid current are substantially independent of plate voltage. Furthermore, the plate current varies linearly with plate voltage. In general, different types of multigrid tubes have different values of the constants m, n, and I_s in (3) and (5). The values of b_g and b_p mainly depend upon the operating temperature of the cathode. For tungsten filaments, the value of b is of the order of 3 to 4 volts^{-1}. In all types, cathode stabilization is important in order to obtain consistent performance, and tube ageing for at least 100 hours may therefore be necessary.

Perhaps the most interesting feature of these characteristics is the wide range over which the plate current

[7] E. G. James, G. R. Polgreen, and G. W. Warren, "Instruments incorporating thermionic valves and their characteristics," *Jour. IEE*, vol. 85, p. 242; August, 1939.

varies linearly with plate voltage. If, however, we consider the effect of E_b upon E_m when all other electrodes are at a constant potential, it is conceivable that the plate current varies in accordance with the function $\epsilon^{bE_b/\mu}$ where μ is the amplification factor. When μ is high, the value of the exponent bE_b/μ is a small fraction of unity and the function becomes practically linear with E_b. Furthermore, as the plate voltage is increased, the position of the potential minimum moves towards the cathode causing μ to increase. This increase in μ with E_b tends to make the mode of variation of I_b with E_b more closely linear over a wider range of E_b. The curves of Fig. 3 show practically good linearity over the full plate voltage range from 20 up to 500 volts. In tubes having a higher screening factor, this linear range extends to 1,000 volts, but the internal resistance becomes excessively high.

Fig. 18 shows the values of μ and r_p for the Type 954 as calculated from the data in Fig. 2. The curves show that μ increases accurately linearly with plate voltage, but is substantially independent of grid voltage. On the other hand, r_p is independent of plate voltage, but varies exponentially with the grid voltage. The transconductance can be obtained from Fig. 2 by multiplying the value of I_b by the slope b_p. All these relations are apparent from an examination of (5).

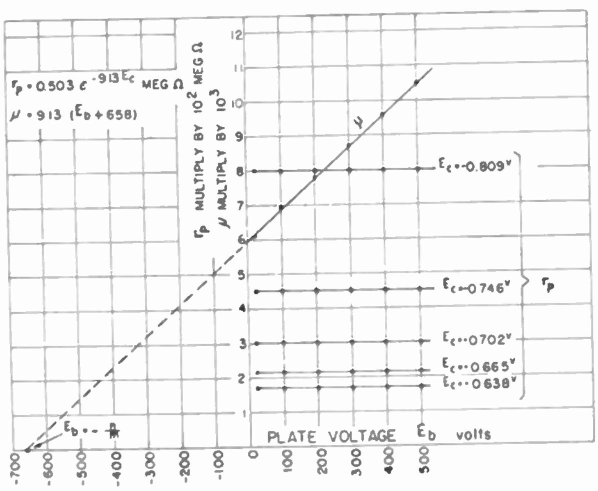

Fig. 18—Values of amplification factor and plate resistance versus plate voltage for the Type 954 under initial velocity conditions.

Appendix II

Comparison of Perfect and Practical Grid Bucking

In the description of the operation of the multiplying circuit of Fig. 5, it was assumed that the tube can bias itself automatically to the proper operating point to compensate for average plate rectification by using the grid current to produce average grid rectification. Under this assumption, the average rectified grid bias should be given by (10) for perfect grid bucking. It will be proved here that, at least for the cse where $v_g = V_g \cos wt$, perfect grid bucking can almost be achieved by a particular adjustment of the grid leak resistor. In this case the value of ΔE_c from (10) should be given by:

$$\Delta E_c = \frac{1}{b_p} \ln J_0(jb_pV_g). \tag{21}$$

Considering the grid circuit, and with no alternating voltage applied, let the direct current through the grid be given by:

$$I_c = I_{c_s}\epsilon^{-b_gE_c}.$$

When v_g is applied, the grid voltage becomes $(-E_c+v_g-\Delta E_c)$, and the grid current will be:

$$I_c + i_c = I_{c_s}\epsilon^{b_g(-E_c+v_g-\Delta E_c)},$$

giving

$$i_c = I_c\left[\epsilon^{b_gv_g}\cdot\epsilon^{-b_g\Delta E_c} - 1\right].$$

Solving for $\Delta E_c = (i_c)_{\text{av}}.R_g$ by taking average values of both sides and multiplying by R_g we get:

$$\Delta E_c = I_cR_g\left[(\epsilon^{b_gv_g})_{\text{av}}.\epsilon^{-b_g\Delta E_c} - 1\right],$$

and when $v_g = V_g \cos wt$, then:

$$\Delta E_c = I_cR_g\left[J_0(jb_gV_g)\cdot\epsilon^{-b_g\Delta E_c} - 1\right]. \tag{22}$$

Equation (22) relates the average rectified grid voltage to the applied ac grid voltage. This expression is similar to that obtained by Aiken[8] on the theory of the diode voltmeter, and has no explicit solution.

If, however, it is possible to adjust the magnitude of the grid leak resistance R_g so that the average rectified grid voltage is equal to that required for perfect grid bucking, then R_g should be determined by substituting from (21) into (22) and solving for R_g. Hence:

$$R_g = \frac{1}{b_pI_c}\cdot\frac{[J_0(jb_pV_g)]^{1+\delta}\cdot\ln\,[J_0(jb_pV_g)]}{[J_0(jb_gV_g)] - [J_0(jb_pV_g)]^{1+\delta}}. \tag{23}$$

Equation (23) shows that for the case $\delta = 0$, i.e., $b_p = b_g$, the denominator vanishes, and R_g should be infinite. But, for the case δ positive, i.e., $b_p < b_g$ which is usually true, the value of R_g becomes finite. In this latter case, it is clear from (23) that the magnitude of R_g for perfect grid bucking should depend upon the magnitude of V_g. This indicates that it is not possible with a simple linear grid-leak resistor to achieve perfect grid bucking at all values of ac grid voltages.

Let therefore the adjustment of the grid leak resistance be such that (21) and (22) are satisfied only at small values of V_g. We have then:

right-hand side of (21)

$$\cong \frac{1}{b_p} \ln\,(1 + \tfrac{1}{4}b_p{}^2V_g{}^2) \cong \tfrac{1}{4}b_pV_g{}^2,$$

and right-hand side of (22)

[8] C. B. Aiken, "Theory of the diode voltmeter," Proc. I.R.E., vol. 26, pp. 859–877; July, 1938.

$$\cong I_c R_g \frac{\frac{1}{4} b_g^2 V_g^2}{1 + b_g I_c R_g} \cong \frac{(1+\delta)\frac{1}{4} b_p V_g^2}{\dfrac{1}{b_g I_c R_g} + 1}.$$

By equating both results, we get:

$$R_g = \frac{1}{\delta b_g I_c} \quad \text{or} \quad \delta b_g I_c R_g = 1. \tag{14}$$

With the adjustment of the grid leak resistor as given by (14), it is possible to calculate the dc output voltage of the circuit of Fig. 5 due to imperfect grid bucking. Rearranging (22) we get:

$$\Delta E_c = \frac{1}{b_g} \ln (\epsilon^{b_g v_g})_{\text{av.}} - \frac{1}{b_g} \ln \left(1 + \frac{\Delta E_c}{I_c R_g}\right). \tag{24}$$

For small values of v_g the rectification efficiency is low, and $\Delta E_c / I_c R_g$ is small compared to unity, thus:

$$\ln \left(1 + \frac{\Delta E_c}{I_c R_g}\right) \cong \frac{\Delta E_c}{I_c R_g}.$$

Therefore,

$$\Delta E_c \cong I_c R_g \frac{\ln (\epsilon^{b_g v_g})_{\text{av.}}}{1 + b_g I_c R_g}$$

for a first approximation. Using successive approximation, and substituting from (14) into (24), we get:

$$\epsilon^{b_p \Delta E_c} = \left[(\epsilon^{b_g v_g})_{\text{av.}}\right]^{1/X}$$

where

$$X = 1 + 2\delta + \delta^2 - \tfrac{1}{2}\delta^2 \ln (\epsilon^{b_g v_g})_{\text{av}}$$

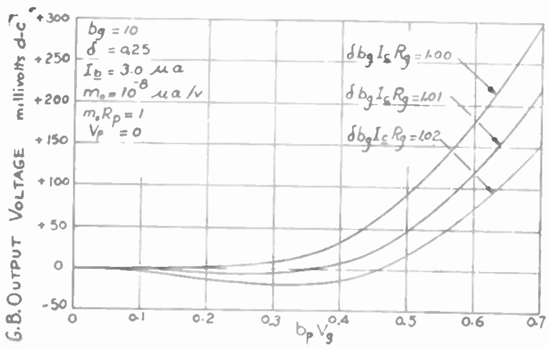

Fig. 19—Theoretical values of the dc output voltage due to imperfect grid bucking versus $b_p V_g$ for various values of $\delta b_g I_c R_g$ close to unity for the multiplying circuit of Fig. 5.

Let

$$Z = (\epsilon^{b_p v_g})_{\text{av.}} \cdot \epsilon^{-b_p \Delta E_c} = (\epsilon^{b_p v_g})_{\text{av.}} \cdot \left[(\epsilon^{b_g v_g})_{\text{av.}}\right]^{-1/X},$$

then (9) can generally be rewritten as:

$$(i_b)_{\text{av.}} R_p = I_b R_p \frac{Z-1}{1 + m_0 R_p Z} + \frac{m_0 R_p Z}{1 + m_0 R_p Z} \cdot \frac{(v_p \epsilon^{b_p v_g})_{\text{av.}}}{(\epsilon^{b_p v_g})_{\text{av.}}},$$

from which the absolute value of the dc output voltage due to imperfect grid bucking is given by:

$$I_b R_p \frac{Z-1}{1 + m_0 R_p Z}. \tag{25}$$

and the per cent error in the dc output due to imperfect grid bucking is given by:

$$\frac{I_b}{m_0} \cdot \frac{Z-1}{Z} \cdot \frac{(\epsilon^{b_p v_g})_{\text{av.}}}{(v_p \epsilon^{b_p v_g})_{\text{av.}}} \cdot 100. \tag{26}$$

Equations (25) and (26) are general and apply for any wave form of the ac grid voltage. For the case $v_g = V_g \cos wt$, Fig. 19 shows a plot of the dc output voltage due to imperfect grid bucking as calculated from (25) for various values of $\delta b_g I_c R_g$ close to unity. These curves show that for the condition $\delta b_g I_c R_g = 1$, the output is positive, increasing as $b_p V_g$ is increased; but for values slightly greater than unity, the output shows a negative loop. It is interesting to see that the curves in Fig. 19 agree in shape and order of magnitude with those obtained experimentally in Fig. 7.

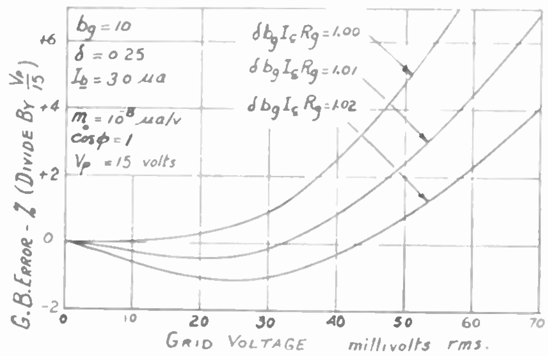

Fig. 20—Theoretical percentage error due to imperfect grid bucking versus rms grid voltage for various values of $\delta b_g I_c R_g$ close to unity for the multiplying circuit of Fig. 5.

Fig. 20 shows the per cent error in the dc output voltage due to imperfect grid bucking as calculated from (26) for unity power factor. These curves show that it is possible to adjust the grid leak resistor such that for rms grid voltages less than 40 millivolts, the order of the error is less than one per cent at unity power factor and with only 15 volts rms on the plate.

It should therefore be concluded from the above that if a linear grid-leak resistor is used, the adjustment for optimum grid bucking corresponds to a value of $\delta b_g I_c R_g$ slightly greater than unity. The requisite grid rectification efficiency for optimum grid bucking equals $\frac{1}{4} b_p V_g$ for values of $b_p V_g$ less than 0.5, decreasing slightly for higher values.

Appendix III

Accuracy of Measurement by the Multiplying Circuit of Fig. 5 under Complex Wave Forms

It was proved in the text that $(i_b)_{\text{av.}}$ of (9) is proportional to $(V_p V_g \cos \phi)$ in the simple case where $v_p = V_p \cos (wt + \phi)$, $v_g = V_g \cos wt$ and $b_p V_g \leq 0.5$. If the alternating voltages v_p and v_g have complex wave forms, the accuracy of measurement of $(v_p v_g)_{av.}$ is subject to an error caused by the fact that only average plate rectification is compensated. This type of error does not exist in the multiplying circuit of Fig. 15.

Equation (9) gives the quantities generally involved in determining the value of $(i_b)_{av.}$ under any wave form of the alternating voltages v_p and v_g. Also, (26) gives the per cent error in the indicated reading. Estimation of this error under standard wave forms—expressed in Fourrier Series—indicates that second harmonic terms contribute almost to the full value of the discrepancy in the indicated reading from that of a perfect multiplying circuit. The error will therefore be considered due to second harmonic. Two cases will be illustrated here.

Case a: $v_p = V_p \cos (wt+\phi)$, and $v_g = V_g (\cos wt + k_g \cos 2\,wt)$ where k_g is the amplitude ratio of the second harmonic to the fundamental of the ac grid voltage. The following expressions are used in the analysis:

$$(\epsilon^{bv_g})_{av.} = J_0(jbV_g) + [J_0(jbkV_g) - 1] + \tfrac{1}{8}k_g(bV_g)^3[1 + \tfrac{1}{2}k_g bV_g]$$

$$(v_p\epsilon^{bv_g})_{av.} = V_p \cos\phi\{-jJ_1(jbV_g) + \tfrac{1}{4}k_g(bV_g)^2[1 + \tfrac{1}{2}k_g bV_g + \tfrac{1}{6}(bV_g)^2]\}.$$

Fig. 21 shows the calculated per cent error versus rms value of the fundamental grid voltage for various values

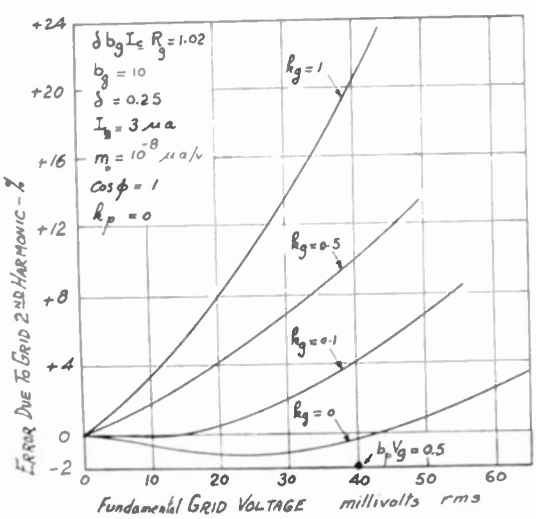

Fig. 21—Calculated error in the indicated reading of the multiplying circuit of Fig. 5 when the alternating grid voltage contains a second harmonic.

of k_g. These curves show that the error is of the order of 20 per cent for 100 per cent second harmonic at $b_p V_g = 0.5$; decreasing to about 3.5 per cent at $b_p V_g = 0.125$.

Case b: $v_g = V_g \cos wt$, and $v_p = V_p [\cos (wt+\phi) + k_p \cos (2\,wt+\phi)]$, where k_p is the amplitude ratio of second harmonic to fundamental of the ac plate voltage. The following expression is used:

$$(v_p\epsilon^{bv_g})_{av.} = V_p \cos\phi[-jJ_1(jbV_g) + k_p j^{-2}J_2(jbV_g)].$$

Fig. 22 shows the calculated per cent error versus the rms value of the ac grid voltage for various values of

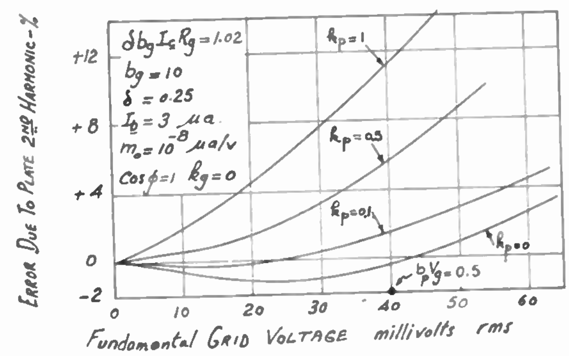

Fig. 22—Calculated error in the indicated reading of the multiplying circuit of Fig. 5 when the alternating plate voltage contains a second harmonic.

k_p. The curves show that the error is of the order of 14 per cent for 100 per cent second harmonic at $b_p V_g = 0.5$; decreasing to about 2 per cent at $b_p V_g = 0.125$.

It will therefore be concluded that though the measurement of ac power by the wattmeter circuit of Fig. 9 is subject to a reasonably serious error when the current and voltage are complex, advantage can be taken by reducing the voltage drop across the series resistor r. The accuracy is greatly improved by using the appropriate series resistor which gives a value of $b_p V_g$ about 0.125 (quarter full scale). Under this condition, the error in the measurement of the total ac power is of the order of +5 per cent when both current and voltage contain 100 per cent second harmonic; decreasing to less than 3 per cent for 50 per cent.

Acknowledgments

The author wishes to extend his appreciation to General Radio Company, Cambridge, Mass., whose co-operation made this development possible, with especial indebtedness to D. B. Sinclair, assistant chief engineer, whose constant interest has carried the investigation to a stage of development; and to R. A. Soderman, development engineer, for the able assistance in performing the experimental tests and many helpful calculations.

The author also wishes to express appreciation to Fouad University, Cairo, Egypt, for Fellowship facilities for circuit development.

Graphical Analysis of Tuned Coupled Circuits*

A. E. HARRISON†, SENIOR MEMBER, IRE, AND N. W. MATHER‡, MEMBER, IRE

Summary—**A new basis for normalizing the transfer admittance of two coupled tuned circuits permits the representation of this admittance by a single universal curve which is a parabolic locus on the complex plane. Within the limitations of the assumptions of high Q and small frequency deviations, data can be obtained from this curve for different Q ratios, as well as the usual values of coupling and relative tuning. The method also simplifies the calculation of the input admittance of coupled circuits. Extension of the method to triple tuned circuits is possible, but the applicability of a single universal curve is lost.**

ALTHOUGH THE representation of the transfer admittance of two coupled tuned circuits by a parabolic locus was published by Smith,[1] the idea has not received the attention it merited. Subsequently and independently, the same representation was worked out by Johnson,[2] Hamilton,[3] Spangenberg,[4] Chang,[5] and probably others.

This method of representing an admittance by a locus on the complex plane with the conductance as the real co-ordinate and the susceptance as the imaginary co-ordinate is quite general. A straight line parallel to the imaginary axis is the locus of the admittance of a single tuned circuit, two coupled tuned circuits have a parabolic locus, and a cubic curve represents a triple tuned circuit. The parabolic locus is the most useful, however. It is applicable only for high-Q circuits when the frequency deviation is small, but the error introduced when the Q is very low will be illustrated.

The parallel circuit of Fig. 1 has been chosen for illustration, because these circuit constants are most convenient for an admittance analysis. The results apply equally well to a circuit with a resistance in series with the inductance if the Q of the circuits is high. In low-Q circuits where the source of the losses becomes important, the circuit is usually loaded by a shunt resistance, and the circuit of Fig. 1 is generally applicable.

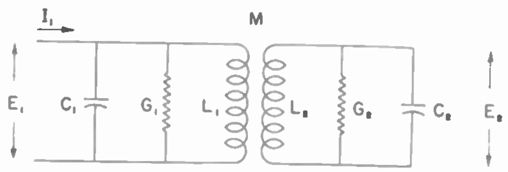

Fig. 1—Tuned coupled circuit considered in the analysis.

An analysis for the case when both circuits are tuned to the same resonant frequency ω_0 gives the following relation for the transfer admittance Y_T:

$$Y_T = \frac{k}{k_c}(1-k^2)\sqrt{G_1G_2}\left\{j\left[\frac{\omega}{\omega_0} + \frac{k^2}{k_c^2}\frac{\omega_0}{\omega}(1-k^2) - Q_1Q_2\frac{\omega_0}{\omega}\left(\frac{\omega^2}{\omega_0^2} - \frac{1}{1-k^2}\right)^2\right] - (Q_1+Q_2)\left(\frac{\omega^2}{\omega_0^2} - \frac{1}{1-k^2}\right)\right\} \tag{1}$$

$$k = \frac{M}{\sqrt{L_1L_2}} \tag{2}$$

$$k_c = \frac{1}{\sqrt{Q_1Q_2}} \text{ (coefficient for critical coupling)} \tag{3}$$

$$\omega_0 = \frac{1}{\sqrt{L_1C_1}} = \frac{1}{\sqrt{L_2C_2}} \tag{4}$$

$$Q_1 = \frac{\omega_0C_1}{G_1} = \frac{1}{\omega_0L_1G_1} \tag{5}$$

$$Q_2 = \frac{\omega_0C_2}{G_2} = \frac{1}{\omega_0L_2G_2}. \tag{6}$$

In order to convert (1) into the parabolic form, Q must be high. A Q of 100 is sufficiently high to make the parabolic locus accurate within 1 per cent for a frequency deviation corresponding to the 3 db points on the curve. The error will be larger for larger frequency deviations, but in general the parabolic locus is reasonably accurate within the values of frequency deviation of greatest interest if the Q of the circuits is 100 or more.

Under these conditions, ω/ω_0 and ω_0/ω can be replaced by unity. For small values of the coupling coefficient k, the term $(1-k^2)$ may also be considered unity and (1) becomes quadratic in terms of the quantity $[(\omega^2/\omega_0^2)-1]$. It will be more convenient to express the relationship in terms of the frequency deviation ratio $\Delta\omega/\omega_0$ or δ. The approximate relation is

$$\frac{\omega^2}{\omega_0^2} - 1 \cong 2\delta. \tag{7}$$

When these approximations are substituted in (1), the result is

$$Y_T \cong \frac{k_c}{k}\sqrt{G_1G_2}\left\{j\left[1 + \frac{k^2}{k_c^2} - 4Q_1Q_2\delta^2\right] - 2(Q_1+Q_2)\delta\right\} \tag{8}$$

* Decimal classification: R142. Original manuscript received by the Institute, January 13, 1949; revised manuscript received, May 13, 1949.

† University of Washington, Seattle, Wash.
‡ Princeton University, Princeton, N. J.

[1] F. Langford Smith, "Radiotron Designer's Handbook," Amalgamated Wireless Valve Company Pty. Ltd., Sydney, Australia, 1940.
[2] W. C. Johnson, Unpublished Lecture Notes, February, 1942.
[3] D. R. Hamilton, J. K. Knipp, and J. B. H. Kuper, "Klystrons and Microwave Triodes," McGraw-Hill Book Company, New York, N. Y., 1948.
[4] K. R. Spangenberg, "Vacuum Tubes," McGraw-Hill Book Company, New York, N. Y., 1948.
[5] S. H. Chang, "Parabolic loci for two tuned coupled circuits," Proc. I.R.E., vol. 36, pp. 1384–1388; November, 1948.

In this form, the equation for the transfer admittance is a parabola, but a different parabola will be required[3-5] for every value of the Q ratio (Q_1/Q_2). This difficulty is easily overcome by a change of variable. Consider the basic equation for a parabola with its vertex at the origin.

$$Ax^2 = By. \tag{9}$$

If both terms are multiplied by A/B^2, the result is of the form

$$X^2 = Y^2, \tag{10}$$

indicating that a change of variable can eliminate the coefficients.

A variety of possibilities exist for the new variable in the expression for the transfer admittance. If we choose $4\,Q_1Q_2\delta/(Q_1+Q_2)$, this term reduces to the familiar universal frequency deviation parameter $2Q\delta$ when Q_1 is equal to Q_2. This term may also be rewritten

$$\frac{4Q_1Q_2\delta}{Q_1+Q_2} = \frac{4\delta}{\dfrac{1}{Q_1}+\dfrac{1}{Q_2}} = \frac{2\delta}{\frac{1}{2}(D_1+D_2)}, \tag{11}$$

where D represents the dissipation factor and is the reciprocal of the circuit Q. An extension of this form of the variable to single- and triple-tuned circuits would give

$$\alpha_1 = \frac{2\delta}{D_1} \tag{12a}$$

$$\alpha_2 = \frac{2\delta}{\frac{1}{2}(D_1+D_2)} \tag{12b}$$

$$\alpha_3 = \frac{2\delta}{\frac{1}{3}(D_1+D_2+D_3)}. \tag{12c}$$

In the limiting case with extremely small coupling and equal Q for all circuits, a unity value of this parameter would correspond to the 3-db, 6-db, and 9-db points for single-, double- and triple-tuned circuits, respectively. The corresponding phase shifts from the midfrequency would be 45, 90 and 135 degrees.

Another variable can be chosen[6] which relates a unit value of the variable with the 3-db points when the coupling coefficient corresponds to transitional coupling, (maximal flatness). This parameter can also be extended to single- and triple-tuned circuits, and the relations are

$$\gamma_1 = \frac{2\delta}{D_1} \tag{13a}$$

$$\gamma_2 = \frac{2\sqrt{2}\delta}{D_1+D_2} \tag{13b}$$

$$\gamma_3 = \frac{4\delta}{D_1+D_2+D_3}. \tag{13c}$$

[6] Suggested in a Sperry Gyroscope Company report by W. W. Hansen.

In this case a unit value of γ corresponds to the 3-db point in each case, and the phase shift from the midfrequency value will be 45, 90, and 135 degrees, respectively.

It is probable that this frequency deviation parameter will be the most useful one in the analysis of coupled circuits, and it has been selected as preferable to the more familiar form. Equation (8) can be converted by introducing the frequency deviation parameter in (13b) and the result is

$$Y_T \cong \frac{k_c}{k}\sqrt{G_1G_2}\,\frac{(D_1+D_2)^2}{2k_c^2}\left\{j\left[2\,\frac{k_c^2+k^2}{(D_1+D_2)^2} - \left(\frac{2\sqrt{2}\,\delta}{D_1+D_2}\right)^2\right] - \sqrt{2}\left(\frac{2\sqrt{2}\,\delta}{D_1+D_2}\right)\right\}. \tag{14}$$

The construction of the parabola will be simplified if it is defined by a focus and a directrix. While this could be done without modifying (14), the symbols will be simpler if the dissipation factors are replaced by coupling coefficients. This can be done by relating (D_1+D_2) to the critical coupling k_c, and the transitional coupling coefficient k_T, which is the largest value of k which allows a single minimum in the magnitude of the transfer admittance. The relations are:

$$(D_1+D_2)^2 = 2(k_c^2+k_T^2) \tag{15}$$

$$k_T^2 = \frac{1}{2}(D_1^2+D_2^2) \tag{16}$$

$$\frac{k_T^2}{k_c^2} = \frac{1}{2}\left(\frac{D_1}{D_2}+\frac{D_2}{D_1}\right) = \frac{1}{2}\left(\frac{Q_2}{Q_1}+\frac{Q_1}{Q_2}\right). \tag{17}$$

Substituting these relationships in (14) gives

$$Y_T \cong \frac{k_c}{k}\sqrt{G_1G_2}\left(1+\frac{k_T^2}{k_c^2}\right)\left\{j\left[\frac{1+\dfrac{k^2}{k_c^2}}{1+\dfrac{k_T^2}{k_c^2}} - \left(\frac{2\delta}{\sqrt{k_c^2+k_T^2}}\right)^2\right] - \sqrt{2}\left(\frac{2\delta}{\sqrt{k_c^2+k_T^2}}\right)\right\}. \tag{18}$$

Several important relations can be obtained from (18). First, the parabola is determined uniquely by the term within the brace. If the transfer admittance is normalized, the distance from the vertex to the focus and the directrix is $\frac{1}{2}$, as indicated on Fig. 2. Second, the position of the origin of co-ordinates is determined by the coupling coefficients and is located a distance $(1+k^2/k_c^2)/(1+k_T^2/k_c^2)$ below the vertex. Third, the frequency scale is proportional to the real component of the admittance, and a unit value of the frequency deviation parameter $2\delta/\sqrt{k_c^2+k_T^2}$ corresponds to a distance of $\sqrt{2}$ along the horizontal axis. (Note that negative values of frequency deviation correspond to distances along the positive real axis.)

When the frequency deviation parameter has the value which makes Y_T a minimum, i.e.,

$$\frac{2\delta}{\sqrt{k_c^2+k_T^2}} = \pm\sqrt{\frac{k_c^2+k^2}{k_c^2+k_T^2}-1} \tag{19}$$

the vertical co-ordinate of the parabola has a value of unity. These two points on the curve correspond to the maximum response of the circuit. As the coupling is increased, the position of the origin of co-ordinates moves downward, but the distance between the real axis and the horizontal line determining the admittance minima remains constant and the minima occur at more widely spaced frequencies. All of these relations are illustrated by Fig. 2.

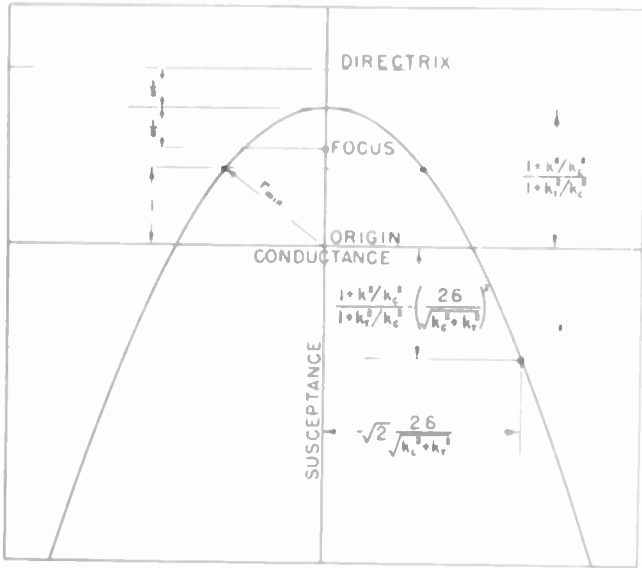

Fig. 2—Locus of the normalized transfer admittance $\frac{Y_T}{(k_c/k)\sqrt{G_1G_2(1+(k_T^2/k_c^2))}}$ on the complex admittance plane.

Fig. 3—Effect of Q on the normalized transfer admittance for two circuits of equal Q and identical tuning when the coupling is equal to the critical coupling. The co-ordinate scale represents unit values of normalized susceptance and conductance.

Low Q Circuits

It is often necessary or desirable to use low Q circuits, therefore the deviation from the simple case when the geometric mean Q of the two circuits is 100 or more is of considerable interest. A comparison of the high Q case with the loci for Q equal to 10 and 5 is shown in Fig. 3 for two circuits of equal Q and identical tuning, when the coefficient of coupling k is equal to the critical coupling k_c. Unit values of the frequency deviation parameter $2\delta/\sqrt{k_c^2+k_T^2}$ are shown as points on the curves. Note that the frequency deviation is no longer linearly related to the real component of the admittance.

Effect of Detuning

All of the previous discussion has been limited to the case when the two circuits have been tuned to the same frequency. It has been shown[3,5] that the effect of detuning is to shift the vertex of the parabola. This problem is handled by defining a midfrequency as the average of the two resonant frequencies by the relation

$$\omega_0 = \frac{\omega_1+\omega_2}{2} \tag{20}$$

where ω_1 and ω_2 are the resonant frequencies of the two circuits, respectively. A fractional detuning ratio δ_0 is defined by

$$\delta_0 = \frac{\omega_1-\omega_0}{\omega_0} = \frac{\omega_0-\omega_2}{\omega_0}. \tag{21}$$

These relations may be introduced to obtain as a final result for the detuned case

$$Y_T \cong \frac{k_c}{k}\sqrt{G_1G_2}\left(1+\frac{k_T^2}{k_c^2}\right)^{1/2}\left\{\left[\frac{1+\dfrac{k^2}{k_c^2}}{1+\dfrac{k_T^2}{k_c^2}} + \left(\frac{2\delta_0}{\sqrt{k_c^2+k_T^2}}\right)^2 - \left(\frac{2\delta}{\sqrt{k_c^2+k_T^2}}\right)^2\right]\right.$$

$$\left. - j\sqrt{2}\,\frac{1-\dfrac{D_2}{D_1}}{1+\dfrac{D_2}{D_1}}\,\frac{2\delta_0}{\sqrt{k_c^2+k_T^2}} - j\sqrt{2}\,\frac{2\delta}{\sqrt{k_c^2+k_T^2}}\right\} \tag{22}$$

Comparison of (22) and (18) shows that the effect of symmetrically detuning the two circuits adds an imaginary term which is equivalent to increasing the coupling coefficient k. In addition, if the dissipation factor D of the two circuits is not the same, there is a translation of the parabolic locus along the real axis which depends upon the ratio D_2/D_1 and the fractional detuning. The shape and size of the parabola are not affected, but the vertex follows a path in the complex plane determined by a family of curves which are also parabolas with a width depending on the ratio D_2/D_1. These relations are illustrated in Fig. 4. The location of the focus and the directrix with respect to the vertex are as given in Fig. 2, but have been deleted in Fig. 4 in order to simplify the illustration.

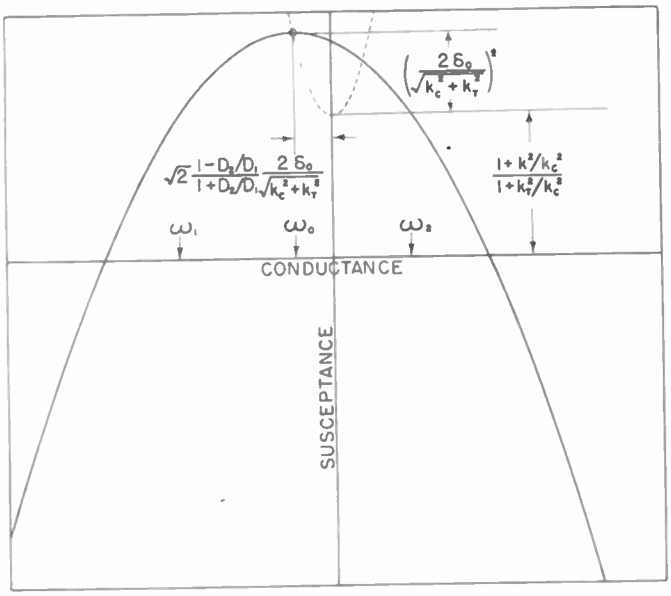

Fig. 4—Effect of symmetrical detuning on the locus of the normalized transfer admittance. The dotted parabola represents the shift of the vertex when $D_2/D_1=\frac{1}{2}$.

Input Admittance

Although the transfer admittance of two tuned coupled circuits is probably used most frequently, the input admittance is sometimes desired. It is a considerably more complicated function than the transfer admittance because the frequency deviation ratio appears in both numerator and denominator. The numerators are the same, therefore it is simple to obtain an expression for the ratio of the two admittances. This ratio permits calculation of the input admittance from the transfer admittance, which can be obtained easily from the parabolic locus, using the relation

$$Y_{\text{Input}} \cong -j\,\frac{k}{k_c}\sqrt{\frac{G_1}{G_2}}\;\frac{Y_T}{1+j\,\dfrac{1}{\sqrt{2}}\left(1+\dfrac{Q_2}{Q_1}\right)\dfrac{2(\delta+\delta_0)}{\sqrt{k_c^2+k_T^2}}}. \tag{23}$$

Triple-Tuned Circuits

The graphical method as outlined in the preceding sections can be extended, with certain modifications, to triple-tuned circuits, although it is no longer possible to represent the admittance loci by a single universal curve. The analysis will not be given in detail, since it is quite involved, but the results will be stated and illustrated.

If the discussion is limited to the high-Q case with zero coupling between the first and third tuned circuits, and all three circuits are tuned to the same resonant frequency ω_0, the expression for the transfer admittance Y_{T3} may be written[7]

$$Y_{T3} \cong \frac{\sqrt{G_1G_3}\,(D_1+D_2+D_3)^3}{8k_{12}k_{23}\sqrt{D_1D_3}}\left\{4g^4-(f^2+1)^2 + 2x^2 - j\left[2(f^2+1)x - x^3\right]\right\}. \tag{24}$$

The symbols f^2, g^4, and x are used to simplify the writing of (24) and are defined below. The parameter x is a frequency deviation parameter equivalent to γ_3 in (13c). The symbols f^2 and g^4 are functions of the coupling and the dissipation factors of the circuits and replace the coupling coefficients used in the analysis of two tuned circuits.

$$x = \frac{4\delta}{D_1+D_2+D_3} \tag{25}$$

$$f^2 = \frac{2}{(D_1+D_2+D_3)^2}(k_{12}^2+k_{23}^2+D_1D_2 + D_2D_3+D_1D_3) - 1 \tag{26}$$

$$g^4 = \frac{(f^2+1)^2}{4} - \frac{2}{(D_1+D_2+D_3)^3}(D_1D_2D_3+D_1k_{23}^2+D_3k_{12}^2) \tag{27}$$

$$k_{12} = \frac{M_{12}}{\sqrt{L_1L_2}} \tag{28}$$

$$k_{23} = \frac{M_{23}}{\sqrt{L_2L_3}}. \tag{29}$$

Inspection of (24) indicates that the form of the curve obtained by plotting (24) is fixed once the choice of the value for f^2 is made. Typical curves for the portion of (24) within the braces are shown in Fig. 5 to illustrate this point. A value of unity for f^2 has been chosen. The effect of varying g^4 only shifts the curve along the real axis and does not change the shape of the curve, provided f^2 is held constant.

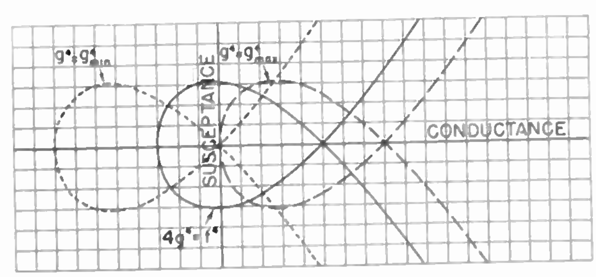

Fig. 5—Loci of the normalized transfer admittance of triple-tuned circuits illustrating the effect of the coupling factors f^2 and g^4. The co-ordinate scale represents unit values of normalized susceptance and conductance.

[7] See forthcoming paper by N. W. Mather, "An analysis of triple-tuned coupled circuits." The notation has been changed somewhat for this paper.

There is no simple geometrical construction for the locus of the transfer admittance Y_{T3} similar to the directrix for a parabola. However, there are several points on the locus which are easily located, and these points are shown in Fig. 6. If one or more curves are

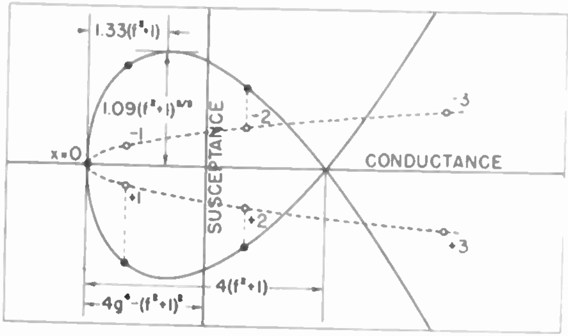

Fig. 6—Graphical construction of the locus of the transfer admittance of a triple-tuned circuit.

accurately known, it is not difficult to interpolate a curve for a different value of f^2 after the crossover point and limits to the curve are located with the aid of Fig. 6. Also, since the real component of the transfer admittance varies as the square of the frequency deviation parameter, the point on the locus corresponding to a given value of x can be located by means of a parabola with an imaginary component equal to x and the real component equal to $(2x^2)$. The vertex will be at the point on the locus corresponding to $x=0$. This construction is illustrated by the dotted curve on Fig.6 The same parabola may be used regardless of the value of f^2, provided the vertex of the parabola is located as indicated above.

The most interesting case occurs when the coupling factors are related by the equation

$$4g^4 = f^4. \tag{30}$$

This relation produces three equal magnitude minima in the magnitude of the transfer admittance Y_{T3}, provided f^2 is greater than zero.[7] The special case with

$$4g^4 = f^4 = 0 \tag{31}$$

is the transitional case between a one-minimum case and the three-minima case, i.e., the case giving "maximal flatness." When f^2 is negative, there is only one minimum.

A family of curves similar to Fig. 5 can be plotted for various values of f^2 as shown in Fig. 7. For convenience, the relation for the three equal minima case defined by (30) is illustrated, although the curves will be applicable to other values of circuit loss and choice of coupling by shifting the $x=0$ intercept along the real axis to correspond to the actual value of g^4.

Although the factors f^2 and g^4 are quite useful for obtaining the transfer admittance when the coupling coefficients and dissipation factors are known, they are not very helpful in solving the more difficult problem of determining the proper coupling to use with circuits of known losses in order to obtain the desired response

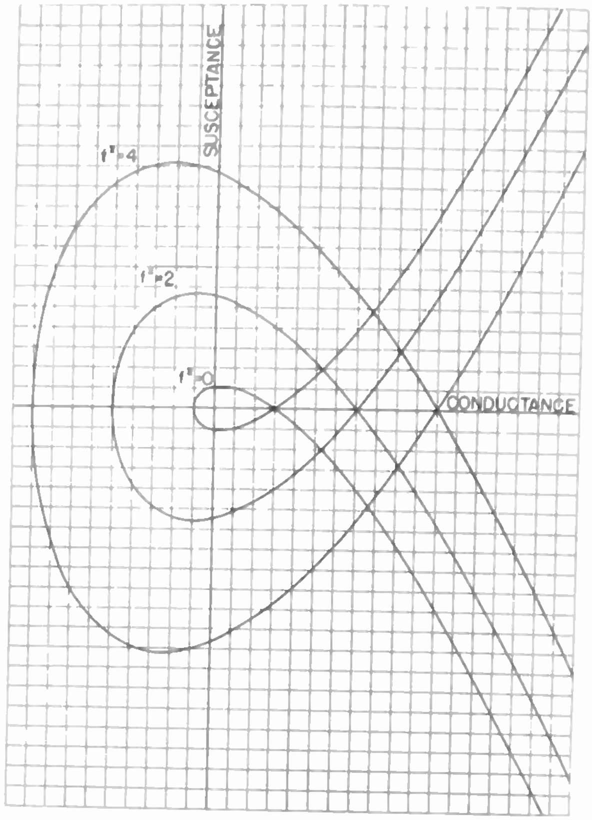

Fig. 7—Loci of the normalized transfer admittance of triple tuned circuits for the case with three equal minima. The co-ordinate scale represents unit values of normalized susceptance and conductance.

characteristic. The relation between coupling and circuit losses for the case with three equal minima may be obtained by substituting (30) in (27) and solving (26) and (27) simultaneously for k_{12}^2 and k_{23}^2:

$$k_{12}^2 = \frac{1}{8}\left[1 - \frac{D_2}{D_1 - D_3}\right]\left[(D_2 + D_3)^2 + 3D_1^2 + 2f^2(D_1 + D_2 + D_3)^2\right] \tag{32}$$

$$k_{23}^2 = \frac{1}{8}\left[1 + \frac{D_2}{D_1 - D_3}\right]\left[(D_1 + D_2)^2 + 3D_3^2 + 2f^2(D_1 + D_2 + D_3)^2\right]. \tag{33}$$

Since f^2 is positive for the case with three equal minima, it is necessary to restrict the value of D_2 in these equations in order to obtain real values for the coupling coefficients. Therefore the relation

$$D_2 \leq |(D_1 - D_3)| \tag{34}$$

must be satisfied in order to obtain three equal minima in the magnitude of the transfer admittance. It is obvious that D_2 can be greater than the value indicated by (34), but the coupling cannot be adjusted to give three equal minima.[7]

The value of f^2 used in (32) and (33) determines the type of response. If $f^2=0$, the transitional case will be obtained, while the choice of $f^2=4$ will give two maxima in the transfer admittance with a magnitude of approximately $\sqrt{2}\,Y_{T\min}$. These points would correspond to 3 db points in the response characteristic of the circuit.

An Analysis of Interlinked Electric and Magnetic Networks with Application to Magnetic Amplifiers*

D. W. VER PLANCK† AND M. FISHMAN‡, ASSOCIATE, IRE

Summary—A general system of equations is developed for the analysis of interlinked electric and magnetic networks. These equations are applied to the study of the steady-state behavior of six basic types of magnetic amplifier without feedback. The equations, which are non linear, are solved to give the currents as functions of time for certain given applied voltages and given circuit and core parameters. An experimental check is included to confirm the correctness of the analysis. A comparison of the results for the six basic types shows that the use of two separate magnetic cores has important advantages over the single three-legged core so commonly used in present practice.

Introduction

MAGNETIC AMPLIFIERS, also called dc-controlled reactors, saturable reactors, and transductors, consist of electric and saturable magnetic circuits so interlinked that a direct current controls the reactance of an ac circuit.[1–8] One form appears in Fig. 1(a). Here there are two identical iron core transformers with one pair of similar windings in series with a dc control voltage, and the other pair in series with an ac source and a load. The winding polarities are such that fundamental-frequency voltages induced in the two control windings are in opposition. The direct current determines the average saturation of the cores which, in turn, affects the inductive reactance of the ac circuit. With proper design, amplification occurs, since but a small change of control power results in a large change of load power.

Besides this simple arrangement, there are more complex schemes involving cores with constricted sections or several materials and circuits with additional coils to provide bias and feedback. Numerous variations of the elementary magnetic amplifiers, such as shown in Figs. 1 through 4, are possible, all having very similar characteristics. While some of these forms have found favor,[7,9,10] no general discussion of their relative merits could be found.

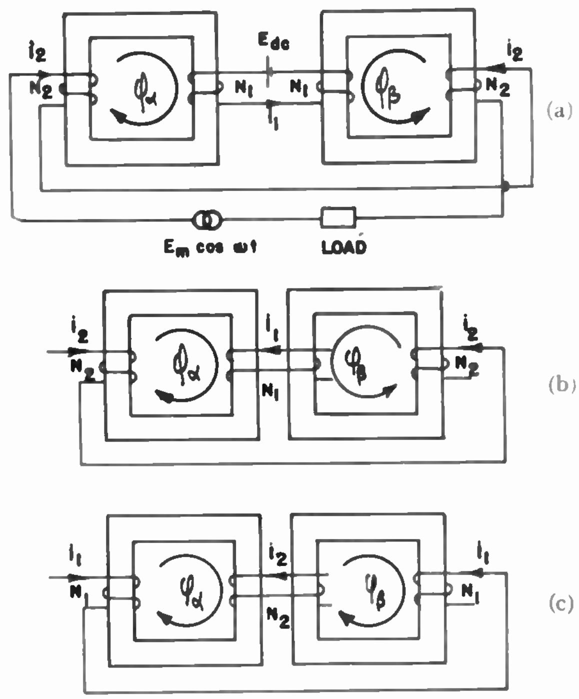

Fig. 1—Schematic representation of Type 1 magnetic amplifiers. This type has two identical but magnetically separate cores which also may be of toroidal or shell form. In (b) and (c) the cores may be placed in parallel planes with windows in line to permit uniform distribution of all windings.

The purpose of this paper is to develop a more precise analysis than those published heretofore.[4,6,11,12] While the analysis applies in general to all magnetic amplifiers in both transient and steady states, it is carried through here only for a steady-state solution of certain of the simpler circuits. Circuits employing feedback are treated in a companion paper.

Description of Some Basic Arrangements

Besides the arrangement in Fig. 1(a), already mentioned, the two others in this figure behave exactly as the first, except that in (b) the use of a single control coil

* Decimal classification: R363. Original manuscript received by the Institute, October 1, 1948. Revised manuscript received, February 24, 1949. Presented, National Electronics Conference, Chicago, Ill., November 6, 1948. This work was done in part under Office of Naval Research Contract N6ori-47 Task Order V, and in part was submitted by M. Fishman in partial fulfillment of the requirements for the degree of doctor of science at Carnegie Institute of Technology.
† Carnegie Institute of Technology, Pittsburgh, Pa.
‡ Formerly, Carnegie Institute of Technology.

[1] John B. Taylor, "Even harmonics," *AIEE Trans.*, vol. 28, p. 725; 1909.
[2] E. F. W. Alexanderson, "Controlling Alternating Currents," U. S. Patent 1,206,643, November 28, 1916, application filed December 7, 1912.
[3] E. F. W. Alexanderson and S. P. Nixdorf, "A magnetic amplifier for radio telephony," Proc. I.R.E., vol. 4, p. 101; April, 1916.
[4] A. Boyajian, "Theory of d-c excited iron-core reactors and regulators," *Trans. AIEE*, vol. 43, p. 919; 1924.
[5] E. C. Wentz, "Direct-current controlled reactor," *Electric Jour.*, vol. 28, p. 561; October, 1931.
[6] Uno Lamm, "The Transductor," Esselte Aktiebolag, Stockholm; 1943.
[7] E. C. Wentz, "Saturable core reactor now smaller, more capable," *Westinghouse Engineer*, vol. 3, p. 115; November, 1943.
[8] A. S. Fitzgerald, *Jour. Frank. Inst.*, vol. 244, p. 249; 1947.
[9] E. F. W. Alexanderson, "Means for Controlling Alternating Currents," U. S. Patent 1,328,797, January 20, 1920, application filed November 26, 1915.
[10] K. Reuss, "Die Verstärkerdrossel," *Arch. für Elekt.*, vol. 33, p. 777; December, 1939.
[11] T. Buchhold, "Über gleichstromvormagnetisierte Wechselstromdrosselspulen und deren Rückkopplung," *Arch. für Elekt.*, vol. 36, p. 221; April, 1942.
[12] A. Uno Lamm, "Some fundamentals of a theory of the transductor or magnetic amplifier," *Trans. AIEE*, vol. 66; 1947.

through both cores eliminates voltage components at power frequency from all parts of the control circuit, which may be advantageous from the standpoint of insulation.

Instead of two separate cores as in Fig. 1, a single core having two magnetic loops with a common branch may be used as in Figs. 2 and 3. In Fig. 2 the center leg carries a direct component of flux but no power-frequency component, while in Fig. 3 the reverse is true. The form in Fig. 2(b) is very common,[5] while the forms in Fig. 3 are rare, although (a) has been used.[10] Because of magnetic saturation, the behavior of a core with a common portion is quite different from that when the core is split into two separate parts as in (b) and (c) of Fig. 1, even though the cross section of the common part is twice that of each separate core.

Wherever, in Figs. 1, 2, and 3, the load circuit has two separate coils in series, additional arrangements may be derived by connecting these two coils in parallel. For example, Fig. 4 is thus derived from Fig. 1. Parallel connection of control coils is not permissible.

Altogether, there are twelve possible arrangements employing a magnetic network of two loops as in the

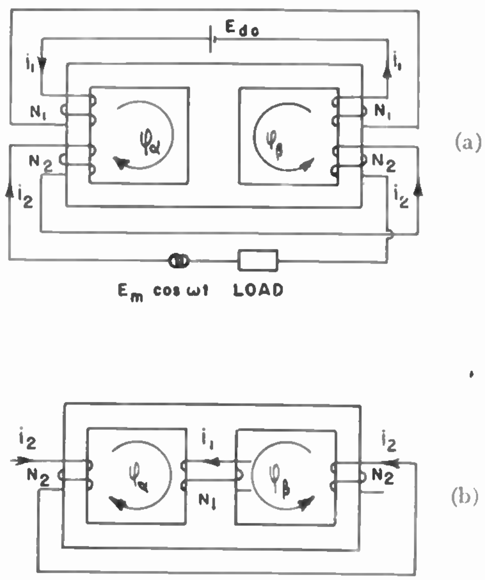

Fig. 2—Type 2 magnetic amplifiers. These have two magnetic circuits with a common branch in which there is no fundamental-frequency component of flux.

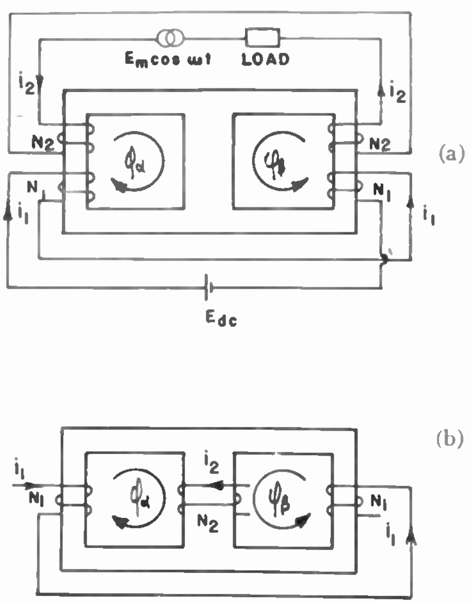

Fig. 3—Type 3 magnetic amplifiers. These have two magnetic circuits with a common branch in which there is no dc component of flux. This type is derived from Fig. 2 by interchanging the control and load windings.

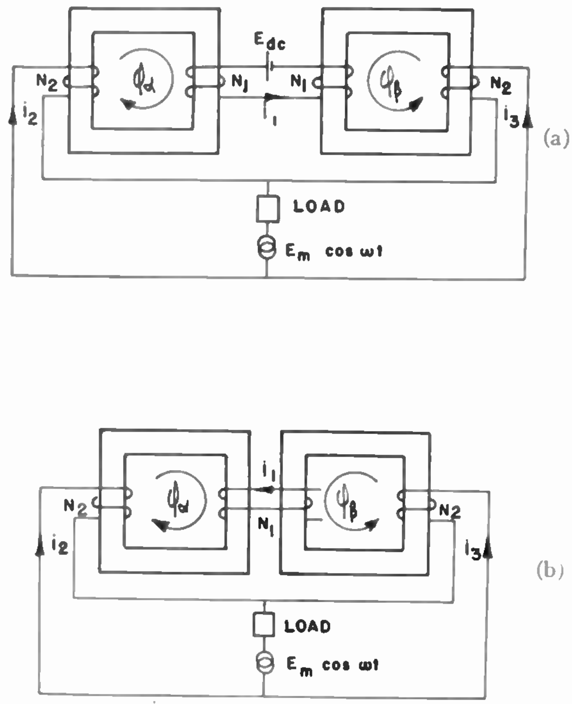

Fig. 4—Type 4 magnetic amplifiers. These are like Fig. 1, except that the load coils are connected in parallel.

TABLE I

CLASSIFICATION OF TYPES HAVING MAGNETIC NETWORKS OF TWO LOOPS

Type	Form	Magnetic Loops Have Common Branch	Fundamental Power-Frequency Components of Flux Aid or Cancel in Common Branch	Number of Control Windings	Number of Load Windings	Load-Winding Connection
1	*a*	No	—	2	2	Series
	b			1	2	Series
	c			2	1	—
2	*a*	Yes	Cancel	2	2	Series
	b			1	2	Series
3	*a*	Yes	Aid	2	2	Series
	c			2	1	—
4	*a*	No	—	2	2	Parallel
	b			1	2	Parallel
5	*a*	Yes	Cancel	2	2	Parallel
	b			1	2	Parallel
6	*a*	Yes	Aid	2	2	Parallel

foregoing examples. These twelve are of six basic types, as shown in Table I. The classification is based on the following considerations:

1. Whether or not the two magnetic circuit loops have a common branch;
2. If there is a common branch, whether the fundamental power-frequency fluxes aid or cancel in this branch; and
3. Whether the load windings (if there are two) are connected in series or in parallel.

As will be shown, these points of difference are important in the analysis. The types are subclassified into forms according to the number of coils in the load and control circuits. The forms of each type differ as to leakage reactances and winding resistances, but these differences are less important than those between types, and are neglected here, so that all forms of a given type are assumed to be equivalent.

Plan of Analysis

The object of the analysis is to predict the instantaneous currents as functions of time in terms of magnetic material characteristics, core dimensions, numbers of turns, and impressed voltages for magnetic amplifiers in general. The approach is to treat the magnetic cores as simple lumped magnetic circuits neglecting leakage fluxes, the varying cross sections at corners, and the effects of eddy currents. Thus the magnetic amplifier becomes a system of interlinked electric and magnetic networks. The procedure is to introduce the following relationships:

(a) Kirchhoff's voltage law for each loop of the electric network;
(b) Law of continuity connecting flux density, loop fluxes, and cross sectional area;
(c) The B-H characteristic of the magnetic material; and
(d) Ampere's line-integral law for each loop of the magnetic network.

While these determine the problem, a general solution would be extremely laborious, if not impossible, and useful results are obtainable only by further simplification, as will be shown for the specific group of magnetic amplifiers classified in Table I.

Voltage Equations

The voltage equations are written in terms of loop currents identified by numerals, the general indices being n and p. Similarly, in the magnetic network use is made of loop fluxes identified by Greek letters with the general index ν.

The positive directions for currents are chosen arbitrarily. The positive directions for fluxes are chosen so that they all traverse a common branch in the same direction; which is apparently always possible if the magnetic network is planar. With this convention, the sign of the number of turns of a coil may be plus or minus, and is determined after the positive directions for currents and fluxes have been chosen.

The system of equations resulting from the application of Kirchhoff's voltage law to the electric network may be written compactly in the matrix form:

$$\|e_n\| = \|N_{n\nu}\| \cdot \|\dot{\phi}_\nu\| + \|R_{np}\| \cdot \|i_p\| \qquad (1)$$

where

e_n = the instantaneous emf applied to the nth loop of the electric network (volts)

$N_{n\nu}$ = the number of turns of the coil in the nth electric loop linking the νth magnetic loop (dimensionless)

$\dot{\phi}_\nu$ = the instantaneous time rate of change of flux in the νth magnetic loop (webers/second)

R_{np} = the resistance common to loops n and p of the electric network (R_{nn} is the total resistance of loop n) (ohms)

i_p = the instantaneous value of the pth loop current (amperes).

Magnetic Equations

The magnetic network is assumed to be divisible into a finite number of parts j in each of which the flux density is sensibly uniform. Thus, to express flux density in terms of loop fluxes and cross-sectional area, one finds the total flux in a given part of the magnetic network and divides by the cross-sectional area. To express this relation in a general set of equations which will account systematically for branches common to more than one loop flux, it is convenient to introduce a matrix $\|S_{j\nu}\|$, an element of which is the reciprocal of the cross-sectional area of the jth part of the magnetic network associated with flux loop ν. As a consequence of the sign convention for loop fluxes, the elements $\|S_{j\nu}\|$ are always positive. Thus, one can write

$$\|B_j\| = \|S_{j\nu}\| \cdot \|\phi_\nu\| \qquad (2)$$

where

B_j = the magnetic flux density in the jth part of the magnetic network (webers/meter^2)

$S_{j\nu}$ = the reciprocal of the area of the jth part of the magnetic network if ϕ_ν threads that area; otherwise, zero (meter^{-2}).

In this analysis, the relation of flux density B to field intensity H need be known only in curve form. Since in the solution H will be found from B, H is said to be some known function of B, or for the jth part of the network

$$H_j = H_j(B_j). \qquad (3)$$

In the application which follows it is assumed that one magnetic material is used throughout; hence, the subscript j after H on the right of (3) may be omitted. Moreover, hysteresis is neglected, so that (3) becomes the normal magnetization curve.

Because of the assumed uniformity of field in each part j of the core, the line integral of H can be expressed as the summation of a finite number of products of magnetic field intensity and path length. Thus Ampere's law gives the system of equations:

$$\|N_{\nu p}\| \cdot \|i_p\| = \|L_{\nu j}\| \cdot \|H_j\| \tag{4}$$

where

$N_{\nu p}$ = the number of turns in the pth electric loop linking the νth magnetic loop (dimensionless)

$L_{\nu j}$ = the length of the jth part of the magnetic network if ϕ_ν traverses it; otherwise, zero (meters)

$\|N_{\nu p}\|$ in (4) can be obtained from $\|N_{n\nu}\|$ in (1) by interchanging rows and columns.

Application of the Analysis

For illustration, the foregoing analysis is applied to the magnetic amplifiers of Table I. In this application further simplifications are made, as follows:

(a) The voltage impressed on the coils in the load circuit is sinusoidal (load replaced by a short-circuit);

(b) The dc voltage impressed on the control circuit is constant and its source has no impedance to harmonic currents;

(c) Steady-state conditions exist; and

(d) Coil and circuit resistances are very small, although, as will be seen, their effects are not neglected entirely.

While these ideal conditions sometimes may be approximated only roughly in practice, results based on them are, nevertheless, useful for gaining a better understanding of magnetic-amplifier behavior and for drawing comparisons between types.

Solving for the Currents

As the first step in solving for the currents, (1) is applied, resulting in the matrices shown in Table II.

TABLE II

Matrices of (1) for the Basic Types

Type	$\|e_n\|$	$\|N_{n\nu}\|$	$\|\dot{\phi}_\nu\|$	$\|R_{np}\|$	$\|i_p\|$
1 and 2	$\begin{Vmatrix} E_{dc} \\ E_m \cos \omega t \end{Vmatrix}$	$\begin{Vmatrix} N_1 & N_1 \\ N_2 & -N_2 \end{Vmatrix}$	$\begin{Vmatrix} \dot{\phi}_\alpha \\ \dot{\phi}_\beta \end{Vmatrix}$	$\begin{Vmatrix} R_{11} & 0 \\ 0 & R_{22} \end{Vmatrix}$	$\begin{Vmatrix} i_1 \\ i_2 \end{Vmatrix}$
3	$\begin{Vmatrix} E_{dc} \\ E_m \cos \omega t \end{Vmatrix}$	$\begin{Vmatrix} N_1 & -N_1 \\ N_2 & N_2 \end{Vmatrix}$	$\begin{Vmatrix} \dot{\phi}_\alpha \\ \dot{\phi}_\beta \end{Vmatrix}$	$\begin{Vmatrix} R_{11} & 0 \\ 0 & R_{22} \end{Vmatrix}$	$\begin{Vmatrix} i_1 \\ i_2 \end{Vmatrix}$
4 and 5	$\begin{Vmatrix} E_{dc} \\ E_m \cos \omega t \\ E_m \cos \omega t \end{Vmatrix}$	$\begin{Vmatrix} N_1 & N_1 \\ N_2 & 0 \\ 0 & -N_2 \end{Vmatrix}$	$\begin{Vmatrix} \dot{\phi}_\alpha \\ \dot{\phi}_\beta \end{Vmatrix}$	$\begin{Vmatrix} R_{11} & 0 & 0 \\ 0 & R_{22} & 0 \\ 0 & 0 & R_{22} \end{Vmatrix}$	$\begin{Vmatrix} i_1 \\ i_2 \\ i_3 \end{Vmatrix}$
6	$\begin{Vmatrix} E_{dc} \\ E_m \cos \omega t \\ E_m \cos \omega t \end{Vmatrix}$	$\begin{Vmatrix} N_1 & -N_1 \\ N_2 & 0 \\ 0 & N_2 \end{Vmatrix}$	$\begin{Vmatrix} \dot{\phi}_\alpha \\ \dot{\phi}_\beta \end{Vmatrix}$	$\begin{Vmatrix} R_{11} & 0 & 0 \\ 0 & R_{22} & 0 \\ 0 & 0 & R_{22} \end{Vmatrix}$	$\begin{Vmatrix} i_1 \\ i_2 \\ i_3 \end{Vmatrix}$

Here the general values of voltages e_n and of turns $N_{n\nu}$ are replaced by specific values indicated in Figs. 1 through 4, and the general values of total circuit resistance R_{nn} are shown as R_{11} or R_{22}, as the case may be. (In types 4, 5, and 6, $R_{33}=R_{22}$.) Then, neglecting the resistance drops for the time being and noting that as a consequence E_{dc} must also be a negligibly small quantity, one can solve for ϕ_α and ϕ_β. The result for each type is that

$$\phi_\alpha = \Phi_m \sin \omega t + \Phi_0 \tag{5}$$

where Φ_m is $E_m/2\omega N_2$ for types 1, 2, and 3, and $E_m/\omega N_2$ for types 4, 5, and 6. Φ_0 is a constant of integration, as yet unknown. The other loop flux ϕ_β in types 1, 2, 4, and 5 is $-\Phi_m \sin \omega t + \Phi_0$, and in types 3 and 6, $\Phi_m \sin \omega t - \Phi_0$. Considerations of symmetry show that the time averages of ϕ_α and ϕ_β must be the same in magnitude, and thus there is but one constant of integration to be found. For types 4, 5, and 6, only two of the three equations of (1) are needed to determine the fluxes, a fact which proves useful later on.

The next step is to find the flux densities in the different parts of the core, using (2). In doing this, symmetrical cores with parts of uniform area, as indicated in Figs. 1 through 4, are assumed. In the three-legged cores, Figs. 2 and 3, the center leg is assumed to have twice the area of either of the other legs.

Having the flux densities B, the field intensities H are found using the magnetic characteristic of the material,

TABLE III

Matrices of (4) for the Basic Types

Type	$\|N_{\nu p}\|$	$\|i_p\|$	$\|L_{\nu j}\|$	$\|H_j\|$
1	$\begin{Vmatrix} N_1 & N_2 \\ N_1 & -N_2 \end{Vmatrix}$	$\begin{Vmatrix} i_1 \\ i_2 \end{Vmatrix}$	$\begin{Vmatrix} L & 0 \\ 0 & L \end{Vmatrix}$	$\begin{Vmatrix} H_+ \\ H_- \end{Vmatrix}$
2	$\begin{Vmatrix} N_1 & N_2 \\ N_1 & -N_2 \end{Vmatrix}$	$\begin{Vmatrix} i_1 \\ i_2 \end{Vmatrix}$	$\begin{Vmatrix} L' & 0 & L'' \\ 0 & L' & L'' \end{Vmatrix}$	$\begin{Vmatrix} H_+ \\ H_- \\ H_0 \end{Vmatrix}$
3	$\begin{Vmatrix} N_1 & N_2 \\ -N_1 & N_2 \end{Vmatrix}$	$\begin{Vmatrix} i_1 \\ i_2 \end{Vmatrix}$	$\begin{Vmatrix} L' & 0 & L'' \\ 0 & L' & L'' \end{Vmatrix}$	$\begin{Vmatrix} H_+ \\ -H_- \\ H_m \end{Vmatrix}$
4	$\begin{Vmatrix} N_1 & N_2 & 0 \\ N_1 & 0 & -N_2 \end{Vmatrix}$	$\begin{Vmatrix} i_1 \\ i_2 \\ i_3 \end{Vmatrix}$	$\begin{Vmatrix} L & 0 \\ 0 & L \end{Vmatrix}$	$\begin{Vmatrix} H_+ \\ H_- \end{Vmatrix}$
5	$\begin{Vmatrix} N_1 & N_2 & 0 \\ N_1 & 0 & -N_2 \end{Vmatrix}$	$\begin{Vmatrix} i_1 \\ i_2 \\ i_3 \end{Vmatrix}$	$\begin{Vmatrix} L' & 0 & L'' \\ 0 & L' & L'' \end{Vmatrix}$	$\begin{Vmatrix} H_+ \\ H_- \\ H_0 \end{Vmatrix}$
6	$\begin{Vmatrix} N_1 & N_2 & 0 \\ -N_1 & 0 & N_2 \end{Vmatrix}$	$\begin{Vmatrix} i_1 \\ i_2 \\ i_3 \end{Vmatrix}$	$\begin{Vmatrix} L' & 0 & L'' \\ 0 & L' & L'' \end{Vmatrix}$	$\begin{Vmatrix} H_+ \\ -H_- \\ H_m \end{Vmatrix}$

assumed here to be the normal magnetization curve. The time functions representing values of H which occur are indicated symbolically in the last column of Table III where the order of matrix elements is first the part of the core carrying ϕ_α alone, then the part with ϕ_β alone, and finally, if present, the part carrying their sum. The meaning of the symbols, using the notation of (3), is

$$
\begin{aligned}
H_+ &= H(B_m \sin \omega t + B_0) \\
H_- &= H(-B_m \sin \omega t + B_0) \\
H_0 &= H(B_0) \\
H_m &= H(B_m)
\end{aligned}
\tag{6}
$$

where B_m is Φ_m/A and B_0, given by Φ_0/A, replaces the unknown constant of integration.

The actual time variation of H is determined graphically for any assumed value of B_m, as illustrated in Fig. 5 by projecting the displaced sinusoids of B at the upper left across to the magnetization curve, and then down onto a new time scale to give the curves of H_+ and H_- shown at the lower right.

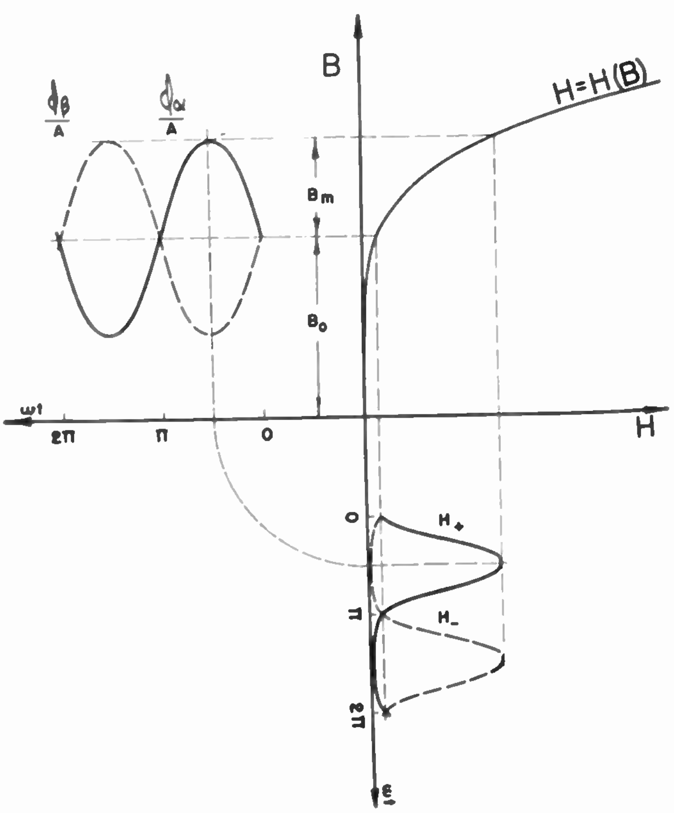

Fig. 5—Graphical construction using the normal magnetization curve of the core material to get the time variation of the field intensities.

The currents are related to the field intensities by (4), which is expanded in Table III. Here L is the total length of either flux loop, while L' represents the length of a part carrying either ϕ_α or ϕ_β alone, and L'' a part carrying their sum. For the first three types, these pairs of equations are solved for the two currents with the results shown in Table IV. For types 4, 5, and 6, however, there are three unknown currents, and so another equation is needed. It is found by manipulating the voltage equations so as to eliminate the time derivatives of flux, but now not neglecting the resistances. The resulting equation and the pair in Table III are then solved simultaneously for the three currents, with the results shown in Table IV. Here two new quantities appear: I_1, which is the average (dc) value of control current given by

$$I_1 = E_{dc}/R_{11}, \tag{7}$$

and k, given by

$$k = (2R_{22}/R_{11})(N_1/N_2)^2. \tag{8}$$

TABLE IV

Time Variation of Instantaneous Currents

Type	Current
1	$i_1 = L[H_+ + H_-]/2N_1$ $i_2 = L[H_+ - H_-]/2N_2$
2	$i_1 = L'[H_+ + H_-]/2N_1 + L''H_0/N_1$ $i_2 = L'[H_+ - H_-]/2N_2$
3	$i_1 = L'[H_+ + H_-]/2N_1$ $i_2 = L'[H_+ - H_-]/2N_2 + L''H_m/N_2$
4	$i_1 = [kL(H_+ + H_-)/2 + N_1I_1]/N_1(1+k)$ $i_2 = [kL(H_+ - H_-)/2 + LH_+ - N_1I_1]/N_2(1+k)$ $i_3 = [kL(H_+ - H_-)/2 - LH_- + N_1I_1]/N_2(1+k)$ $i_2 + i_3 = L[H_+ - H_-)/N_2$
5	$i_1 = [kL'(H_+ + H_-)/2 + kL''H_0 + N_1I_1]/N_1(1+k)$ $i_2 = [kL'(H_+ - H_-)/2 + L'H_+ + L''H - N_1I_1]/N_2(1+k)$ $i_3 = [kL'(H_+ - H_-)/2 - L'H_- - L''H_0 + N_1I_1]/N_2(1+k)$ $i_2 + i_3 = L'[H_+ - H_-]/N_2$
6	$i_1 = [kL'(H_+ + H_-)/2 + N_1I_1]/N_1(1+k)$ $i_2 = [kL'(H_+ - H_-)/2 + L'H_+ + (1+k)L''H_m - N_1I_1]/N_2(1+k)$ $i_3 = [kL'(H_+ - H_-)/2 - L'H_- + (1+k)L''H_m + N_1I_1]/N_2(1+k)$ $i_2 + i_3 = L'[H_+ - H_-]/N_2 + 2L''H_m/N_2$

The physical significance of k is that in types 4, 5, and 6 there are two low-resistance circuits linking the two flux loops similarly; the control circuit and the series path through the load coils. Then, even though the resistances otherwise may be negligibly small, their ratio is significant in fixing the division of induced currents between the paths.

Determining the Integration Constant

The expressions for the currents in Table IV depend through (6) on the average value of flux density B_0, so far unknown. To determine B_0, one finds I_1, the dc value of control current, by taking the time average of i_1; thus,

$$I_1 = \frac{1}{2\pi}\int_0^{2\pi} i_1 d(\omega t). \tag{9}$$

Evaluating this, one finds for types 1 and 4, 2 and 5, and 3 and 6, respectively, the following values of N_1I_1:

LH_{av}, $L'H_{av}+L''H_0$, and $L'H_{av}$ where

$$H_{av} = \frac{1}{2\pi}\int_0^{2\pi} H(B_m \sin \omega t + B_0)d(\omega t). \qquad (10)$$

This integral is evaluated graphically as the net area between the curve of H_+, illustrated in Fig. 5, and its time axis. Since one wishes to find B_0 for a given I_1, a process of trial and error is necessary, or a family of curves may be constructed as in Fig. 6. This family represents a property of the material independently of the frequency, the core configuration, and circuits assumed.

To obtain B_0, then, for given E_m (which determines B_m) and given I_1 one uses the curves in Fig. 6 directly, or, in the case of types 2 and 5, a trial and error procedure involving Fig. 6.

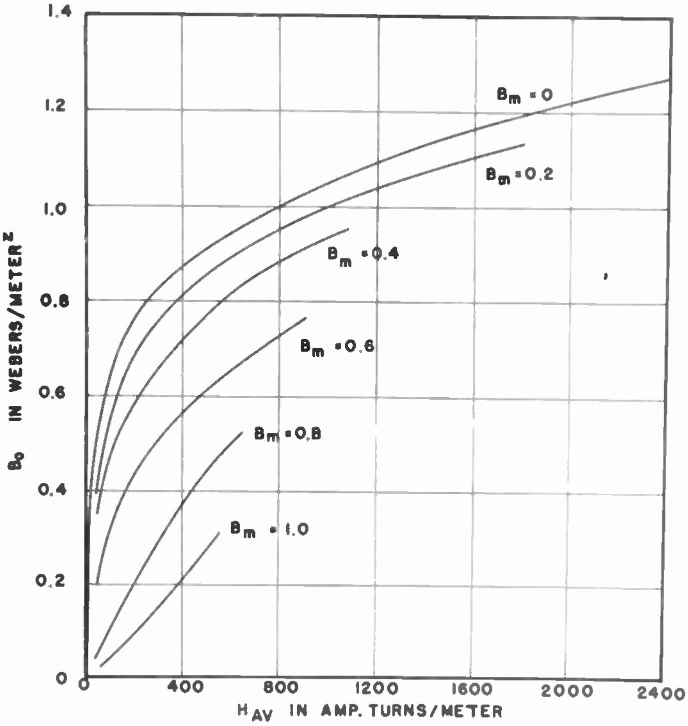

Fig. 6—Effect of superimposed alternating flux density on the dc magnetization curve. The upper curve is the measured normal magnetization curve; the others are calculated from it. This family represents a property of the core material independently of the core geometry and circuit conditions.

Experimental Check

The method of analysis has been checked by comparing the calculated currents with oscillograms for a variety of conditions. An example is given in Fig. 7 which applies to type 2, form (b), shown in Fig. 2, using the core material described by Fig. 6. The check is good, even though the conditions are such as to make the flux density reach very high values, which accounts for the large harmonics in the currents. With this material the effect of neglecting hysteresis is imperceptible in a case like this, but it is observable, though never large, in cases where the maximum flux density is low.

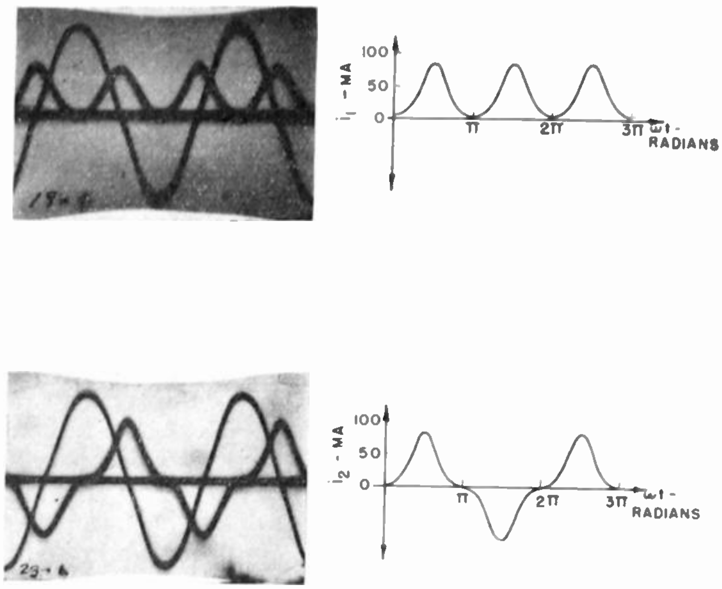

Fig. 7—Oscillograms of currents and applied ac voltage compared with calculated currents for circuit (b) in Fig. 2. The calculated curves are plotted to scales determined by the oscillograph sensitivity.

$N_1=2{,}000$ turns	$R_{11}=135$ ohms	$I_1=0.034$ amperes
$N_2=1{,}800$ turns	$R_{22}=207$ ohms	$E_m=320\sqrt{2}$ volts
$L'=0.124$ meters	$A=4.2\times10^{-4}$ (meters)²	$\omega=2\pi 60$ (sec.)$^{-1}$
$L''=0.056$ meters		

Series and Parallel Connections Compared

To compare series and parallel connection of load coils, types 1 and 4, the ones with separate cores, are considered first. All conditions are assumed identical except that N_2 for type 4 is twice that for type 1, so that the ac volts per turn is the same in both. Then the expressions for total load current (i_2 for type 1 and i_2+i_3 for type 4) shown in Table IV are identical. Moreover, the relation between B_0 and I_1 is the same for both, and thus, under these conditions, the flux densities in the respective cores of the two types are equal at every instant, and the two have identical external characteristics except for differences in the instantaneous values of i_1. The instantaneous values of mmf for each magnetic loop are the same in the two types, but because of the additional electric loop in type 4 the distribution of ampere-turns among the electric circuits differs in the two types. Analyzed in another way, it can be shown that even harmonic components of ampere-turns are necessary to produce the sinusoidal variations in the two fluxes. In type 1 these harmonics are carried entirely by the control circuit, while in type 4 they are carried in part by the series path through the two load coils. It should be noted that, had the control circuit not been assumed to have zero impedance, the series and parallel connections would not be equivalent.

Comparisons of type 2 with type 5 and of 3 with 6 also lead to the conclusion that the series and parallel connections are equivalent. Thus types 4, 5, and 6 may be eliminated from further comparisons.

Core Arrangements Compared

To study the relative merits of types 1, 2, and 3, it is assumed that the purpose of a magnetic amplifier is to cause the greatest change in reactance—that is, the greatest change in load current with constant ac voltage across the load coils—with the least change in control current. For a given type and given applied voltage, the load current i_2 is some function of the average control current I_1, and of time t. The intention is to study in the three types the effect of I_1 on $N_2i_2(I_1, t)$. Values of this function with the control current switched on and off are shown in columns 3 and 4, respectively, of Table V. Here a new quantity is introduced:

$$H_d = \frac{H_+ - H_-}{2} = \frac{H(B_m \sin \omega t + B_0) - H(B_m \sin \omega t - B_0)}{2}, \quad (11)$$

which varies in time phase with H_m. In studying Table V, it is to be noted that, because of saturation,

$$H_{av} > H_0 \quad (12)$$

$$H_d > H_m. \quad (13)$$

Also, the various H's all are functions of the flux densities, and therefore direct comparisons of items in the table must be made only with B_m and B_0 the same in all three types. Furthermore, core total lengths and areas must be the same throughout. Thus comparisons of the currents, which in general will differ from type to type, are made with applied ac voltage, B_0, N_1, N_2, and weight of core held constant.

As a first criterion, take the difference of load current produced, Table V, fifth column. This difference is identical for types 2 and 3, but requires more control excitation in type 2 than in type 3. In this respect, then, type 3 is superior to type 2. Now compare type 1 with type 3. The difference in i_2 produced in type 1 is greater than in type 3 in the ratio L/L', but the control current required by type 1 is greater in the same ratio. But type 1 is superior to type 3 because with the same amount of magnetic material a greater change in load current can be obtained, although to realize this superiority it might be necessary to increase the copper in type 1 over that in type 3.

The conclusion is different if one takes as the criterion the ratio of the load current resulting from I_1 to that with $I_1=0$, as shown in the last column of Table V. This ratio is identical for types 1 and 2, but is produced by a smaller I_1 in type 2; type 2 is thus better than type 1 in this respect. The relative standing of type 3 is not so apparent, but it is probably inferior to type 2.

These comparisons are based on theoretical considerations for one assumed kind of operation; practical considerations, however, might rule. For instance, difficulty of matching two separate cores might outweigh their theoretical advantage and dictate the use of the three-legged core where every lamination is in both magnetic circuits.

Conclusion

A general system of equations for interlinked electric and saturable magnetic networks has been developed. As an example of their application, the equations have been applied to the steady-state solution of certain common magnetic-amplifier circuits without feedback, and in this connection a systematic classification of these magnetic amplifiers into basic types was developed. Conclusions of practical interest were reached as to the relative behavior of the several types of magnetic amplifier studied.

Acknowledgments

The authors gratefully acknowledge the helpful criticisms of B. R. Teare, Jr., and L. A. Finzi of the Department of Electrical Engineering, Carnegie Institute of Technology, and the contributions of the many graduate students assigned to the project in various capacities.

TABLE V
Comparison of Types

Type	N_1I_1	$N_2i_2(I_1, t)$	$N_2i_2(0, t)$	$N_2i_2(I_1, t) - N_2i_2(0, t)$	$\dfrac{N_2i_2(I_1, t)}{N_2i_2(0, t)}$
1	LH_{av}	LH_d	LH_m	$L(H_d - H_m)$	H_d/H_m
2	$L'H_{av} + L''H_0$	$L'H_d$	$L'H_m$	$L'(H_d - H_m)$	H_d/H_m
3	$L'H_{av}$	$L'H_d + L''H_m$	LH_m	$L'(H_d - H_m)$	$\dfrac{H_d}{H_m} - \dfrac{L''}{L}\left(\dfrac{H_d}{H_m} - 1\right)$

Contributors to Proceedings of the I.R.E.

Lyle R. Battersby was born in Philadelphia, Pa., in 1904. He received his education in the Atlantic City, N. J., public schools, and through various extension and part time courses at Rutgers University. He has held either amateur or commercial radio licenses since 1919. In 1921 he became associated with the Manhattan Electrical Supply Company, pioneering in the manufacture of early radio sets and components. Here he was in charge of the radio department during the latter years of his employ, until he entered business in 1930, specializing in police aircraft, and broadcast equipment.

Lyle R. Battersby

From 1942 to date, Mr. Battersby has been engaged as a project engineer in the Signal Corps Engineering Laboratories, except for a period of approximately one year spent in the microwave laboratories of the Holmdel, N. J., unit of the Bell Telephone Laboratories. At the Coles Signal Laboratory, Signal Corps Engineering Laboratories, he has specialized in the design and development of crystal saver circuits, microwave frequency-control circuits, and microwave filters.

❖

G. Goubau was born in Munich, Germany, on November 29, 1906. He received the Dipl. Phys. degree in 1930, and the Dr.-Ing. degree in 1931, both from the Munich Technical University. From 1931 to 1939 he was employed in research and teaching in the physics department of the same University, directed by Professor Zenneck. During this time he was principally concerned with ionospheric investigations. He established the first German Ionospheric Research Station (Herzogstand/Kochel), and was in charge of the research work carried on at this station.

G. Goubau

In 1939 Dr. Goubau was appointed to the professorship of applied physics at the Friedrich Schiller University, in Jena, Germany. At the same time, he became director of the department of applied physics of this University. Before he arrived in this country, he was the senior author of the volumes on electronics of the *FIAT* Review of German Science, published by the Military Government for Germany. Dr. Goubau is now a consultant of the Signal Corps Engineering Laboratories, in Fort Monmouth, N. J.

❖

H. A. Hess was born on June 15, 1910, at Kirchheim Teck, Wuerttemberg, Germany. He attended the Technische Hochschule, Stuttgart, from 1930 to 1933, and the University of Jena from 1933 to 1935. From 1936 to 1937, he was a scientific assistant at the Heinrich Hertz Institute, Berlin, and received the Dr. Phil Nat. degree from the Friedr. Schiller University of Jena in 1937.

Hanns H. Hess

During the period from 1938 to 1940 he was employed in the research laboratories of the Telefunken Co., at Berlin, and was a contributor to the periodical *Funktechnische Monatshefte* from 1937 to 1940. From May to July, 1941, Dr. Hess was a technical assistant at the German Patent Office, Berlin and after his dismissal as a government official, he was obliged to serve as a civilian employee of the Luftwaffe. He performed research works in the field of high frequency propagation in Denmark from 1942 to 1945, together with the geophysicist, Oswald von Schmidt, now deceased.

Dr. Hess was an associate member of IRE in 1939, and a member of ARRL from 1935 to 1939. In May, 1946, the ICD of the United States Military Government in Germany gave him a recommendation as author of technical publications.

❖

M. A. H. El-Said (SM'48) was born in Aga, Egypt, in May, 1916. He was graduated from the Fouad University in Cairo in 1938, and was appointed a member of the staff of the faculty of engineering. In 1943 he received the M.Sc. degree for research work on the generation and measurement of radio frequency power, and in 1944 the Ph.D. degree was awarded for original research on the logarithmic-antilogarithmic principle and its applications to electronic wattmeters and wave analyzers.

M. A. H. El-Said

Dr. El-Said was engaged in an engineering mission to England and the United States for the Egyptian Government through a fellowship during the period 1945 to 1948. This project was made possible through the co-operation of Marconi's Wireless Telegraph Company in England, and General Radio Company in the United States. Dr. El-Said has invented various types of multiplying circuits, one of which has been developed by General Electric for a general purpose electronic wattmeter. Dr. El-Said has returned to Fouad University, where he is a senior lecturer in engineering.

Arthur E. Harrison (A'41–SM'45) was born on January 20, 1908, at San Luis Obispo, Calif. He received the B.S. degree in electrical engineering from the University of California in 1936. From 1936 to 1939 he was a teaching fellow at the California Institute of Technology, and received the M.S. degree in 1937, followed by the Ph.D. degree in 1940. From 1940 to 1946 he was employed by the Sperry Gyroscope Company in the klystron development laboratory. He joined the staff of Princeton University in 1946 as an assistant professor of electrical engineering. Since September, 1948, Dr. Harrison has been an associate professor of electrical engineering at the University of Washington in Seattle.

A. E. Harrison

❖

For a photograph and biography of M. Fishman, see page 901 of the August, 1949, issue of the Proceedings of the I.R.E.

❖

Granino Arthur Korn was born on May 7, 1922, in Berlin, Germany. He received the B.A. degree in mathematics and physics from Brown University in 1942, and the M.A. degree in physics from Columbia University in 1943. Additional graduate work was followed by two years' service in the United States Navy, mostly with the Special Devices Division, ORI.

G. A. Korn

In 1946, Dr. Korn became a project engineer with the Sperry Gyroscope Co., Great Neck, L. I. He received the Ph.D. degree in physics from Brown University in 1948. Since March, 1948, he has been assistant section head of research engineering at the Columbus plant of the Curtiss-Wright Corp., where he is in charge of the analysis group.

Dr. Korn's work is chiefly in the field of automatic controls and analogue computers, on which subject he has published a number of papers. He is a member of Sigma Xi.

N. W. Mather (A'46–M'47) was born in Upland, Calif., on April 29, 1914. He was graduated from the University of California in 1936 with the B.S. degree in electrical engineering, and was later awarded the M.S. degree from Princeton University. Until 1942 he was employed by the Otis Elevator Co., when he joined the U. S. Naval Reserve, and for twenty-eight months was connected with the Navy radar instruction program. Later he was a construction superintendent in the electronics division of the assistant industrial manager's office of the Mare Island Navy Yard. He became visiting assistant professor of electrical engineering at Princeton University in 1946, and was made associate professor in 1947, his present position.

N. W. Mather

In 1948 Mr. Mather was Chairman of the Princeton Section of the IRE. He is an associated member of the AIEE, a member of the American Society for Electrical Education, Eta Kappa Nu, and Sigma Xi.

For a photograph and biography of J. Hessel, see page 1434 of the November, 1948, issue of the Proceedings of the I.R.E.

For a photograph and biography of D. W. Ver Planck, see page 902 of the August, 1949, issue of the Proceedings of the I.R.E.

J. R. Pierce (S'35–A'38–SM'46–F'48) was born at Des Moines, Iowa, on March 27, 1910. He received the B.S. degree in electrical engineering from the California Institute of Technology in 1933, and the Ph.D. degree in 1936. Since 1936 he has been a member of the technical staff of the Bell Telephone Laboratories, where he has worked on various vacuum-tube problems.

J. R. Pierce

Dr. Pierce received the IRE Fellow award in 1948 for his "many contributions to the theory and design of vacuum tubes." He is also the recipient of the Eta Kappa Nu "Outstanding Young Electrical Engineer" award for 1942, and the IRE Morris Liebmann Memorial Prize for 1947. He has served on the IRE Papers Procurement Committee.

Correspondence

The Theory and Design of Progressive and Ordinary Universal Windings*

A paper by Kantor[1] contains several definite contributions to the science of universal coils. However, due to rather unfortunate wording, a number of statements made and conclusions reached could easily be misinterpreted. It is proposed to clarify these.

1. Accuracy of the Basic Equation of the Universal Winding

From a reading of the Summary,[1] particularly the statement that "equations are derived which are considerably simpler and at the same time more accurate than those given by Simon," one might infer that the form of the basic equation of the universal winding as given by Kantor is more accurate than that originally derived by the writer,[2] whereas, as Kantor himself points out subsequently in the body of his paper, ***both equations express absolutely identical relationships***, the particular one given by Kantor being merely an ***alternative form*** of the other. In fact, his equation can be obtained directly from that originally given by the writer merely by inverting both sides and rationalizing the denominator of the fraction appearing on the right-hand side of the resulting equation. The only new contribution made by Kantor in this connection is to show that the expression for the ***reciprocal*** of the gear ratio r, as defined by the writer, can be put into ***somewhat*** simpler form than that for this gear ratio itself. Kantor's derivation of the basic formula of the universal winding is, of course, exactly parallel to that originally given by the writer, except that the gear ratio r is replaced throughout the derivation by its reciprocal $1/R$.

Also from a reading of the Summary, particularly the statement that "the present paper offers a more thorough treatment of the subject . . . by employing theoretical expressions to replace previously required empirical rules," one might infer that the formulas given originally by the present writer for the gear ratio and the number of crossovers (throws) per turn were largely empirical. There was, however, nothing empirical about either the deduction or the form of these equations: the only empirical thing about them was that the constant k in the crossover formula had to be ***determined*** empirically. Kantor's contribution in this connection is to show how the value of this constant can be ***deduced*** from a knowledge of the coefficient of friction between the material of the insulation and that of the dowel, thus making the empirical determination of k unnecessary.

2. Selection of the Number of Crossovers (Throws) per Turn

From Kantor's theory on the factors which influence the selection of the number of crossovers per turn, it might be inferred that it is necessary in practice to vary this factor in accordance with the coefficient of friction between the surface of the dowel and that of the insulation; that is to say, with every change of material of the dowel or of the insulation. Actually, this is not the case, for the following reasons: (1) After the first layer is down, the wire is wound not on the surface of the ***dowel*** but on the surface of the ***insulation*** of the underlying layer; hence, the discussion given by Kantor applies primarily to the problem of producing a stable ***first*** layer. (2) The necessity for altering the number of crossovers per turn with every change of material of the dowel can be obviated entirely by the simple expedient of roughening the surface of all dowels (if necessary) previous to winding. In fact, it might be noted parenthetically in this connection, that winding on smooth, i.e., polished or glazed dowels, imposes an unnecessary handicap in manufacture, and should be avoided in any case. Hence, while Kantor's analysis of the factors determining the selection of the number of crossovers per turn, in particular the deduction of the constant k from the coefficient of friction μ, is a definite contribution to the science of universal coils, it is of more academic than practical importance. In the writer's experience the insertion of the empirical constant of $\frac{3}{8}$ in the crossover formula has always given satisfactory results, irrespective of the type of dowel or textile insulation used, provided only that the surface of the dowel was sufficiently rough. In fact, a value of $\frac{3}{8}$ for this constant would correspond, according to Kantor's theory,

* Received by the Institute, March 21, 1949.

[1] M. Kantor, "Theory and design of progressive and ordinary universal windings," Proc. I.R.E., vol. 35, pp. 1563–1570; December, 1947.

[2] A. W. Simon, "On the theory of the progressive universal windings," Proc. I.R.E., vol. 33, pp. 868–871; December, 1945.

Correspondence

to a value of μ of 0.21, which is in good agreement with the values actually found by him for such materials as cardboard, wood, bakelite, etc.; that is, for materials generally used.

3. Determination of the Progression

With reference to the pitch of the progression, which determines directly the number of turns per unit length of the coil, it should be pointed out that, contrary to the impression one might receive from a reading of Kantor's discussion of the subject, this factor can be arbitrarily selected in general; it is fixed or predetermined only if it is prescribed that the winding is to fulfill also a certain geometric condition; in particular, if it is to exhibit a certain ratio of width of close-packed layer to spacing between close-packed layers. Actually, however, in practice the number of turns per unit length, which will determine, for example, such factors as total band coverage in the case of permeability-tuned coils, will be of greater importance in design than the particular geometric ratio referred to; hence, the pitch will usually be selected independently and the geometric ratio allowed to take what value it may (between limits). It is true, of course, that a value of this ratio of $\frac{1}{2}$, as recommended by Kantor, is a desirable but not at all a necessary condition.

4. Accuracy of Various Approximate Formulas for the Gear Ratio (Ordinary Universal Winding)

At the outset of a discussion of the accuracy of a formula for the gear ratio, it should be pointed out that the fundamental factor to be considered in this connection is not the error in the *gear ratio* itself, but the error in the gear-ratio *parameter*, since the latter determines directly such fundamental magnitudes as the number of turns per layer, spacing between centers of adjacent wires, etc. The gear-ratio parameter P is the quantity defined by the equation:

$$r = T_C/T_D = (2/n)(1 \pm 1/P)$$

as explained in a previous paper.[3] Of the various gear-ratio formulas proposed, we have the original (accurate) form given by the author:

$$r = T_C/T_D = \frac{2}{n}\left[\frac{1 \pm \sqrt{a^2+b^2(1-a^2)}}{(1-a^2)}\right]; \quad (1)$$

the alternative (accurate) form, which can be derived merely by the inversion of (1), as given by Kantor:

$$R = T_D/T_C = \frac{n}{2}\left[\frac{1 \mp \sqrt{a^2+b^2(1-a^2)}}{(1-b^2)}\right]; \quad (2)$$

the approximate form, derived from (1), as given by the author:

$$r = (2/n)(1 \pm \sqrt{a^2+b^2} + a^2); \quad (3)$$

another approximate form derived from (3) by neglecting the a^2 term:

$$r = (2/n)(1 \pm \sqrt{a^2+b^2}); \quad (4)$$

the first approximate form of Hershey:[4]

$$r = (2/n)(1 \pm a); \quad (5)$$

and, finally, a second approximate form, given originally also by Hershey and later by Kantor:

$$R = (n/2)(1 \mp a) \quad (6)$$

where the upper sign refers in all cases to progressive layering and the lower one to retrogressive layering.

The error introduced in the gear-ratio parameter by the use of the various formulas obviously will depend on the magnitude of the quantities a and b; hence, it becomes of interest to determine what range of values these quantities take in practice. They are defined by the relations

$$a = s/qc = 1/qw \quad (7)$$

$$b = ns/q\pi d = ak/\pi \quad (8)$$

where q represents the number of crossovers per turn, w the number of wires per layer, and k the empirical constant in the crossover formula. The minimum value of q in any case is 2, so that if we let w vary from the rather extreme case of only 5 wires per layer to the more typical case of 50 wires per layer, and take for k the recommended value of $\frac{1}{3}$, we have a varying from 0.10 to 0.01 and b from 0.021 to 0.0021. The error introduced into the gear-ratio parameter under these conditions is given in Table I.

suggests that we write another approximate form, namely,

$$R = T_D/T_C = (n/2)(1 \mp \sqrt{a^2+b^2}), \quad (9)$$

thus taking the effect of diameter into account. If the corresponding parameters are found on the basis of this formula, we have for $a = 0.10$, $P = 8.78$, with an error of 0.5 per cent; and for $a = 0.01$, $P = 96.8$, with an error of 0.0 per cent. Hence this formula is to be recommended over any of the other approximate ones.

5. Accuracy of Various Approximate Formulas for the Gear Ratio (Progressive Universal Winding)

Since the quantity e occurs to the first power in the denominator of the basic formula as given by the present writer for the gear ratio in the case of a progressive universal winding, the approximate formulas derived therefrom will hold over a narrower range than those drived from the alternative form with e in the numerator as given by Kantor. Accordingly it is recommended that, in progressive universal-coil calculations, either

$$R = (n/2)[1 \mp (e + \sqrt{a^2+b^2})] \quad (10)$$

or

$$R = (n/2)[1 \mp (e + a)] \quad (11)$$

be used, depending on whether it is desired to take the effect of diameter into account or not.

6. Universal-Coil Design Procedure

In view of the foregoing, little change is recommended in universal-coil design procedure as outlined previously by the author,[6]

TABLE I

ERROR IN THE GEAR RATIO PARAMETER

a	(1)	(3)	(4)	(5)	(6)
0.10	none	1.0%	11.0%	13.4%	2.0%
0.01	none	0.0%	0.9%	3.2%	2.2%

From the Table it is seen that, for the range considered, the approximate formula (3) originally given by the author is more accurate than any of the other approximate formulas, although in the range most likely to occur in practice ($a \rightarrow 0.01$), the difference between the values given by the various formulas is not marked. The Hershey-Kantor form (6) has the advantage over the form (3) originally given by the author in that it is simpler, and over the other approximate formulas (4) and (5) in that it holds over a wider range for a given degree of accuracy. The reason for the error in (6) is, of course, that the effect of diameter (involved in b^2) has been neglected. This

with the exception, perhaps that in progressive universal-coil design the approximate formulas (10) or (11) can advantageously replace the formulas originally given by the writer; while in ordinary universal-coil design, (6) or (9) can advantageously replace (3). Varying the number of crossovers per turn with a change of material of the dowel, or selecting the pitch of the progression to produce a spacing ratio of 0.5, however, are unnecessary procedures and, accordingly, are not recommended except in special cases.

A. W. SIMON
University of Tulsa,
Tulsa, Okla.

[3] A. W. Simon, "Winding the universal coil," *Electronics*, vol. 9, pp. 22–24; October, 1936. Errata, p. 52; November, 1936.

[4] L. M. Hershey, "The design of the universal winding," PROC. I.R.E., vol. 29, pp. 442–446; August, 1941.

[6] See footnote references 2 and 3, and also: A. W. Simon, "Universal coil design," *Radio*, vol. 31, pp. 16–17; February–March, 1947.

The Duo-Mode Exciter*

During the course of an investigation at the Northwestern University Microwave Laboratory[1] of multiplexing systems using two or more modes, a device was required for independently launching the TE_{10} and TE_{20} modes in the same guide. It was necessary that this device have a low voltage-standing-wave-ratio (VSWR) over a wide frequency range with a minimum of cross talk between inputs.

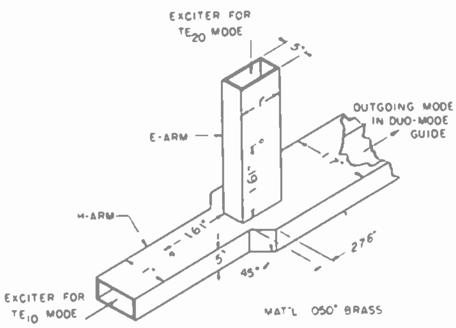

Fig. 1—Duo-mode exciter.

The duo-mode exciter is shown in Fig. 1. The vertical arm we shall designate the E arm, and the horizontal arm the H arm. When energy is transmitted down the H arm in the TE_{10} mode, it widens along the symmetrical 45° nozzle to form a TE_{10} mode in the duo-mode guide. When energy is transmitted down the E arm in the TE_{10} mode, it forms components in each side of the duo-mode guide that are 180° out of phase. This TE_{20} mode is reflected at some point along the H arm nozzle at which the width of the guide is less than cutoff for the TE_{20} mode. The distance of this nozzle from the E arm (see Fig. 1) is such that the TE_{20} mode is reinforced in the direction away from the H arm.

The TE_{10} mode from the H arm cannot propagate up the E arm, since the 0.4-inch dimension of the E arm is less than cutoff width for the TE_{10} mode. Consequently, the E arm and H arm are isolated from each other.

The results of the experimental test of the duo-mode exciter are given in Fig. 2. Without any additional matching, the VSWR remained below 1.6 from a frequency of 8,830 to 9,530 Mc. During these tests the duo-mode guide was terminated with a load having a VSWR of about 1.02 with either mode. With small posts about $\frac{3}{16}$ inch in length and positioned in the E arm and H arm as shown in Fig. 1, the VSWR remained below 1.6 from a frequency of 8,960 to 9,740 Mc. Any frequency in this range could have been chosen as center frequency for matching. Our center frequency was 9,375 Mc and the VSWR at this frequency was 1.02 looking into the E arm, and 1.04 looking into the H arm.

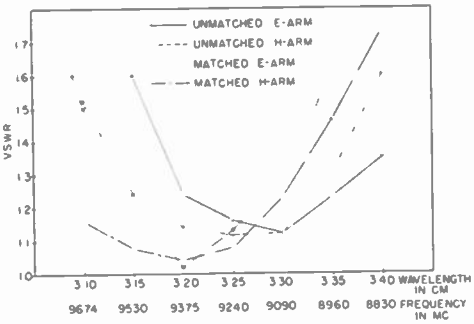

Fig. 2—Voltage-standing-wave-ratio of duo-mode exciter.

The separation between inputs was 37 db at 9,375 Mc with the duo-mode guide terminated with a load having a VSWR of 1.02 with either mode. The modes produced were very pure, the null point of the TE_{20} mode being more than 60 db below the peak value of electric intensity of the TE_{20} mode.

W. A. Hughes
Morton M. Astrahan
Northwestern University
Microwave Laboratory
Evanston, Ill.

* Received by the Institute, February 23, 1949.

[1] The duo-mode exciter was developed in a project sponsored by the U. S. Army Signal Corps, contract No. W 36-039 sc-32283.

Note on the Theoretical Efficiency of Information Reception with PPM*

For small P/N ratios, the now classical expression for the information reception capacity of a channel

$$C = W \lg_2 (1 + P/N)$$

can be written, substituting kTW for N,

$$CT_0 = WT\ P/N \lg_2 e = \frac{PT_0}{kT} \lg_2 e = \frac{E}{kT} \lg_2 e$$

where E designates the energy available for the reception of the information packet containing CT_0 binary symbols.

If quantized PPM and an ideal low-pass channel are utilized, and if the available energy E is concentrated into one pulse, the ratio of the pulse height to the rms thermal noise will be $\sqrt{2E/KT}$, and the voltage gate should be set at a proper fraction $\alpha\sqrt{2E/KT}$ of the pulse height, so as to minimize the mathematical expectation of a random positive thermal pulse exceeding this gate at any one of N prearranged sampling epochs, or of a random negative thermal pulse preventing the information carrying pulse from exceeding the gate at the proper epoch. This mathematical expectation can be written:

$$\frac{N}{\sqrt{2\pi}} \int_{\alpha\sqrt{2E/kT}}^{\infty} e^{-x^2/2} dx + \frac{1}{\sqrt{2\pi}} \int_{(1-\alpha)\sqrt{2E/kT}}^{\infty} e^{-x^2/2} dx,$$

and the minimizing operation just indicated determines the optimum value for α:

$$\alpha = \frac{1}{2} + \frac{kT}{2E} \lg_e N.$$

When this value is substituted for α in the expression given above for the mathematical expectation of errors, the first integral in this expression will always be smaller than the second. Therefore, the minimum mathematical expectation of errors will be smaller than

$$\frac{2}{\sqrt{2\pi}} \int_{1/2\sqrt{2E/kT}(1-kT/E\ \lg_e N)}^{\infty} e^{-x^2/2} dx.$$

The lower limit of this probability integral can be as large and positive as desired, provided the expression within parentheses is positive, no matter how small. This indicates that the information yielded by the position of the pulse, which is equal to $\lg_2(N+1)$, can approach the theoretical limit $E/KT \lg_2 e$, with as little equivocation as desired.

Marcel J. E. Golay
Signal Corps Engineering Laboratories
Fort Monmouth, N. J.

* Received by the Institute, February 23, 1949.

A Tribute to van der Bijl*

I have just learned of the death on December 2, 1948, in Johannesburg, of Hendrik Johannes van der Bijl. I did not know Dr. van der Bijl, but I feel a sense of personal loss at his passing, since, as a student at Cornell University, I studied his textbook on vacuum tubes. There must be thousands of radio engineers who feel as I do.

In 1920 Dr. van der Bijl was one of the few men who fully grasped the importance of the vacuum tube. As he stated so well in the introduction to his book: "The insertion of the grid into the valve resulted in a device of tremendous potentialities—one that can justly be placed in the same category with such fundamental devices as the steam engine, the dynamo, and the telephone."

Dr. van der Bijl's name will live forever in the radio art. It was he who first gave the quantitative effect of the grid in a vacuum tube, resulting in the well-known van der Bijl equation for the plate current of the triode tube. It was he who invented the modulated class-A amplifier, which is extensively used in the carrier-supression systems. A description of the operation of the van der Bijl modulator can be found in any standard radio engineering textbook. His book, "The Thermionic Vacuum Tube and its Applications," published in 1920, was the first authoritative textbook on vacuum tubes and electronics. The esteem with which his book is still held, after all the intervening years since its publication, is evidenced by its inclusion in the reading list of radio references in the current "RCA Receiving Tube Manual."

William D. Bevitt
Central Radio Propagation Laboratory
National Bureau of Standards
Washington 25, D. C.

* Received by the Institute, March 22, 1949.

Institute News and Radio Notes

Technical Committee Notes

The **Radio Transmitters Committee** met on June 13 at IRE Headquarters, with J. F. McDonald, Chairman, presiding. At present the committee is concerned chiefly with the preparation of Standards on *Methods of Testing Transmitters*. J. B. Heffelfinger has been appointed Chairman of the Radiotelephone Transmitters Subcommittee, which will operate in the midwest. Reports on the status of work were submitted by the subcommittees on Telegraph Transmitters, H. R. Butler, Chairman; Pulse Transmitters, Cledo Brunetti, Chairman; Single Side Band Transmitters, A. E. Kerwien, Chairman; and FM Transmitters. . . . A meeting of the **Wave Propagation Committee** was held on June 20 under the Chairmanship of C. R. Burrows to consider the FCC's Ad Hoc Committee's Report for *The Evaluation of the Radio Propagation Factors concerning the Television and Frequency Modulation Broadcasting Services in the Frequency Range between 50 and 250 Mc.* The results were summarized in a report submitted to the JTAC. . . . The **Committee on Electron Tubes and Solid State Devices** met at Headquarters on June 2, with L. S. Nergaard, Chairman, leading the discussion. A proposal to have this Committee sponsor a Professional Group on Electron Tubes was tabled temporarily. The relative merits of operating the Electron Tube Conference with simultaneous sessions and extending the length of the meeting as compared to having two short conferences during the year were discussed and a consensus of opinion favored extending the length of the Conference by one day. . . . On June 8 the **Electroacoustics Committee** headed by E. S. Seeley met. F. V. Hunt, H. F. Olson, W. F. Meeker, and P. S. Veneklasen were appointed members of the new subcommittee on Loudspeaker Testing, with M. J. Di Toro as Chairman. . . . B. B. Bauer, Chairman, and H. F. Olson make up the subcommittee appointed to study the proposed ASA Standard on *Secondary Microphone Calibration* for the IRE. . . . P. F. Siling, Chairman of the **Joint Technical Advisory Committee**, announced the appointment of Donald G. Fink as Chairman and John V. L. Hogan as Vice-Chairman for the coming year, July 1, 1949, to June 30, 1950 at the June 23 meeting of the Committee. It was agreed to bind the official correspondence between the FCC and the JTAC, together with the minutes of all JTAC meetings to date. This volume will be released as the PROCEEDINGS OF THE JTAC, Volume III. . . . The **Nucleonics Symposium Planning Group** for the Second Annual Joint IRE-AIEE Conference on Electronic Instrumentation in Nucleonics and Medicine met on June 15, with Harner Selvidge, Chairman, presiding. The Symposium is scheduled for October 31 and November 1 and 2, and will be held at the Hotel Commodore in New York City. The papers which will be presented at the Symposium will be published in a single volume entitled "Proceedings of the Symposium," which will be made available to those registering or upon order at an extra charge to those who did not attend the meetings. W. A. Geohegan is Chairman of the Papers Procurement and Program Committee; R. D. Chipp of the Committee on Local Arrangements; Norman Beers of the Publicity Committee. Ward Davidson is Treasurer. The Papers Procurement and Program Committee of the IRE-AIEE Planning Group for the Symposium met on June 27, and the papers to be presented will be announced at an early date.

IRE-URSI Meet

The U.S.A. National Committee of the International Scientific Radio Union (URSI) and The Institute of Radio Engineers held a joint technical meeting in Washington, D. C. on May 2, 3, and 4. General open technical sessions were held on May 2 and 3, and organization meetings of the four U.S.A. National Commissions which sponsored the meeting on May 2 and 4. Twenty-seven fundamental scientific and research papers were presented on radio standards, methods of measurement, terrestrial radio noise (natural and man-made), communication theory, antennas, and circuits.

On Monday morning, Commission One, *Radio Standards and Methods of Measurement*, headed by its chairman, J. H. Dellinger, offered papers by J. H. Rowen and V. H. Rumsey; Frank M. Greene and Max Solow; Douglas A. Venn, Joseph G. Rubenson, and W. E. Waller; A. A. Oliner; and H. E. Sorrows, W E. Ryan, and R. C. Ellenwood. In the afternoon, G. F. Metcalf, chairman of Commission 7, *Electronics, Including Properties of Matter*, presented a program including papers by Philip Parzen; Harold Jacobs, Armand LaRoche, and Alfred Mazzei; W. S. Ament; Frank S. Quinn, Jr.; George Birnbaum and D. C. and J. Franeau; Warren W. Berning; and H. A. Thomas, R. L. Driscoll, and J. A. Hipple.

Tuesday morning, Commission 4, *Terrestrial Radio Noise*, under its chairman, J. C. Schelleng, offered papers by C. F. W. Anderson, Edward W. Allen, Jr., and Leonard W. Thomas. The concluding session, held on Tuesday afternoon, was under the auspices of Commission 6, *Radio Waves and Circuits, including General Theory and Antennas*, and its chairman, L. C. Van Atta. It included papers by V. H. Rumsey; Henry J. Riblet, Charles H. Papas; R. M. Hatch, Jr. and D. K. Reynolds; David Middleton and Richard M. Hatch, Jr.; Saul Fast; M. L. Harvey, M. Leifer, and Nathan Marchand; W. M. Goodall; and John F. Brinster.

Abstracts of the papers were prepared in booklet form as a program. Copies are still available at $1.00 each, and may be obtained from Newbern Smith, Secretary, U.S.A. National Committee, URSI, National Bureau of Standards, Washington, D. C.

IRE-URSI to Meet in Fall

The regular IRE-URSI Fall Meeting, sponsored jointly by the IRE Professional Group on Wave Propagation and Antennas and the U. S. A. National Committee of the International Scientific Radio Union, will be held on Monday, Tuesday, and Wednesday, October 31, November 1 and 2, in Washington Four U. S. A. National Commissions of URSI will participate: Commission 2—Tropospheric Radio Propagation; Commission 3—Ionospheric Radio Propagation; Commission 5—Extraterrestrial Radio Noise; and Commission 6—Radio Waves and Circuits, including General Theory and Antennas.

The first two days will be devoted to individual or joint meetings of two or more Commissions, held in the National Academy of Sciences, 2101 Constitution Avenue, N. W., and the Auditorium of the New State Department Building, Twenty-first and Virginia Avenues, N. W. The third day will consist of a general assembly of all Commissions, followed by individual administrative meetings of the several Commissions.

Meetings will be of a modified symposium type, comprising invited papers, contributed papers, and informal discussions at the discretion of the chairmen.

Industrial Engineering Notes[1]

Electronic Brain Developed

A fundamental advance in the organization, storage, and dissemination of knowledge is foreseen in an "electronic brain" developed jointly by the U. S. Departments of Commerce and Agriculture. The machine stores "vast amounts of scientific information in its system," selects what is desired by its operator, and then hands him copies of the material requested. A report describing the Rapid Selector in detail (PB 97535) is available from the OTS, Department of Commerce, Washington 25, D. C., for $2.50 each copy.

Interference Suppression for Arc Welders Developed

A successful method for effectively suppressing radio interference caused by the operation of high-frequency stabilized arc welders was reported on by the Signal Corps. With the use of a double-screened room and with adequate filtering of the power lines at the point of entry into the screened room, it was possible to reduce radio interference outside the room to a point where measurement was almost impossible. The

[1] The data on which these NOTES are based were selected, by permission, from "Industry Reports," issues of June 17 and 24, and July 1 and 8, published by the Radio Manufacturers' Association, whose helpful attitude is gladly acknowledged.

report (PB 97469) may be obtained from the OTS, U. S. Department of Commerce, Washington 25, D. C.

FCC Regulations

The FCC issued an initial decision **renewing the license of Sarkes Tarzian** for a high-frequency AM experimental broadcasting station at Bloomington, Ind. The experiments in transmission and reception of high-frequency AM broadcasting have been carried on since the spring of 1946. . . . An order revising its **rules governing performance measurements of AM and FM broadcast systems** was issued recently by the FCC. The Commission rules require all AM and FM stations to make certain performance measurements at yearly intervals, with one such set of measurements being made during the four-month period preceding the date of filing application for renewal of station license. These rules were eased so that applicants for renewal of licenses expiring prior to February 1, 1950, are not required to indicate that these measurements have been made. The full requirements for AM and FM broadcast stations are contained in Part 3 of the "Commission Rules and Regulations" and the "Standards of Good Engineering Practice Concerning Both Standard and FM Broadcast Stations," which can be purchased from the Superintendent of Documents, Government Printing Office, Washington 25, D. C. . . . The FCC issued a **check list of its rules and regulations** to enable individuals possessing books of the Commission's Rules and Regulations to check for completeness. The list (Mimeograph No. 37927), which brings the rules up to date as of June 27, 1949, may be obtained from the Secretary of the FCC, Washington 25 D. C. . . . Printed copies of **the new rules governing the mobile and other nonbroadcast services** involved in the Report and Order Dockets 8658, 8965, 8972, 8973, 8974, 9001, 9018, 9046, and 9047, issued by the FCC May 3, 1949, are now available from the Superintendent of Documents, U. S. Government Printing Office.

Television News

E. U. Condon, Director of the National Bureau of Standards, is assembling a committee of independent authorities to study **the present status and future of color television.** The objective of the study will be to determine the present status of color television and to estimate when color television may be feasible for public service and commercial operation. Among those asked to serve on the committee were Donald G. Fink, JTAC Vice-Chairman and editor of *Electronics*; Stuart L. Bailey, President of the IRE; William L. Everitt, head of the University of Illinois' department of electrical engineering; and Newbern Smith, Chief of the Central Radio Propagation Laboratory at the Standards Bureau. Dr. Condon would serve as Committee Chairman . . . The FCC explained its **rule preventing the separate operation of aural and visual transmitters of a television station,** stating that it is intended to insure that television channels shall be used only for simultaneous visual and aural television programming and for incidental or test purposes, and not for separate aural broadcasts. To permit a television sound channel to be used either to duplicate AM or FM aural broadcasts, or to originate aural broadcasts only, would not be an economical use of radio frequencies and would not be in the public interest. . . . Precautionary **cathode-ray safety rules** for tube and set manufacturers, service men and dealers, and television set owners were issued by the RMA Cathode Ray Safety Committee. The Committee laid emphasis on the fact that the cathode-ray tube is not dangerous except when improperly handled, and stated further that rumors concerning the harmful effects of ultra-violet rays reputedly emitted by picture tubes are unfounded. . . . At the end of June there were 69 **commercial television stations on the air.** There were 49 construction permits outstanding, and 386 applications pending but "frozen."

Calendar of COMING EVENTS

1949 National Electronics Conference, Chicago, Ill., September 26–28

National Radio Exhibition, Olympia, London, England, September 28 to October 28

SMPE 66th Semiannual Convention, Hollywood, Calif., October 10–14

AIEE Midwest General Meeting, Cincinnati, Chio, October 17–21

Radio Fall Meeting, Syracuse, N. Y., October 31, November 1–2

1949 Nucleonics Symposium, New York, N. Y., October 31, November 1–2

1950 IRE National Convention, New York, N. Y., March 6–9

Radio and Television News Abroad

Prime Minister J. B. Chifley of **Australia** announced that his country will use a television standard of 625 lines when television is inaugurated there as a government monopoly. The use of a greater number of picture lines than either the British (405) or the American (525) should, he stated, ensure a better image than is available under either of the other two standards. Australia plans to erect stations in its six capital cities—Brisbane, Sydney, Melbourne, Adelaide, Perth, and Hobart. . . . Five television manufacturers are now producing television receivers in **Canada,** with the present Canadian market estimated at 1,500,000 persons residing along the United States border within the range of American television stations at Toledo, Buffalo, Rochester, Detroit, Cleveland, and Seattle. Sales of radio receiving sets by Canadian manufacturers in March totaled 55,283 units valued at $4,050,501, compared with 40,551 sets valued at $3,978,361 during the corresponding month in 1948.

Production Notes

Television receiver production by RMA member-companies in May was slightly under the previous month's output. May's production was 163,262 sets, as compared with 166,536 in April. For the first two months of 1949, 752,335 television sets were produced; 383,869 FM-AM and FM sets; and 2,586,135 AM only sets—all sets totaling 3,722,339.

Books

Table for Use in the Addition of Complex Numbers (Table til Brug ved Addition af Komplekse Tal) by Jørgen Rybner and K. Steenberg Sørenson

Published (1948) by Jul. Gjellerups Forlag, Copenhagen, Denmark; obtainable from Scandinavian Book Service, P. O. Box 99, Audubon Station, New York 32, N. Y. 95 pages+xiv pages. 9½×12½. $5.50.

Published in parallel Danish and English texts, this pamphlet contains a table which facilitates calculations with complex numbers by rendering possible the addition or subtraction of such numbers in polar form. It is actually a supplement to Professor Rybner's "Nomograms of Complex Hyperbolic Functions" (see page 1271 of the October, 1948, issue of the Proceedings for review), which includes the conversion between rectangular and polar co-ordinates and the function $R/\alpha = 1 + r/\phi$ represented in this table.

It was considered appropriate to prepare an extended numerical table over 90 pages long of this function, because it was found impossible to construct the corresponding nomograms with an accuracy sufficient for practical calculations. The function $R/\alpha = 1 + r/\phi$ is represented giving R and α as functions of r and ϕ for $0 \leq r \leq 1$ at intervals of 0.01 and for $0 \leq \phi \leq 180°$ at intervals of 1°. These quantities are connected by the following relations:

$$R^2 = 1 + r^2 + 2r \cos \phi$$

$$\sin \alpha = \frac{r}{R} \sin \phi$$

$$\operatorname{tg}\left(\frac{\phi}{2} - \alpha\right) = \frac{1 - r}{1 + r} \operatorname{tg} \frac{\phi}{2}.$$

Earth Conduction Effects in Transmission Systems, by Erling D. Sunde

Published (1949) by D. Van Nostrand Co., Inc., 250 Fourth Ave., New York, N. Y. 360 pages+5-page index+xiii pages. 102 figures. 6¼×9¼. $6.00.

The material in this book is primarily concerned with fundamental methods in the analysis of earth conduction effects and basic principles underlying protective devices against resultant circuit disturbances. This work will be welcomed particularly by those who are faced with interference and protection problems in wire communications systems. An orientation and exposition is provided which, in a large measure, was heretofore lacking in a field covered only by articles widely scattered throughout the literature. To engineers who are not on entirely alien ground with Maxwell's equations, boundary value problems, and transient analyses, the information is clearly presented and readable with unduly tedious mathematical treatments minimized or cited in the references.

Starting with basic electromagnetic concepts and equations, the author develops equations for evaluating earth resistivity from simple tests for a number of different assumed variations in earth structure. He next evaluates the resistance to ground for a variety of grounding electrodes and considers the effect of chemical treatment of the ground to increase the effectiveness of the electrodes. The heating effects due to large ground currents and earth potentials induced are also covered.

Theoretical analyses are made of mutual impedance and propagation characteristics of earth-return conductors. These lead into a study of inductive interferences between power lines and communications lines and between lightning channels and communications lines. An analysis of the surge characteristics of earth-return conductors is made. This is followed by the mechanism of lightning strokes and methods of protection of both overhead and underground facilities against lightning damage. There is also included a chapter on the mechanism of corrosion of buried metallic structures and methods of reducing such corrosion. Throughout the book, most of the analyses presented are based upon idealized conditions which can never be wholly realized in practice. However, since they check well with experience, they will be of great value to those who will make engineering use of the comparison.

The text proper is presented in nine chapters fortified by an extensive appendix on definitions and tables of functions, which will assist the reader, should he wish personally to work out mathematical detail omitted in the text or cited by reference. The appendix closes with a comprehensive reference list covering literature germane to the subject.

To the knowledge of the reviewers, this book is the first of its kind, covering a difficult field very well and filling a need long neglected. It should be of considerable value to practicing engineers and as a reference for graduate students majoring in communications and power system engineering.

HAROLD A. ZAHL AND GEORGE G. BOWER
Signal Corps Engineering Laboratories
Fort Monmouth, N. J.

FIRST CALL!

AUTHORS FOR NATIONAL CONVENTION

R. M. Bowie, Chairman of the Technical Program Committee for the 1950 IRE National Convention, requests that prospective authors of papers to be considered for presentation submit the following information to him as soon as possible:

(1) Name and address of author.

(2) Title of paper.

(3) Abstract of sufficient length to permit the Committee to assess the paper's suitability for inclusion in the Technical Program. Since the merit of the prospective paper must necessarily be judged by the abstract, it should be clear and informative.

Material should be mailed to R. M. Bowie, Sylvania Electric Products Inc., Box 6, Bayside, L. I., N. Y. The deadline for acceptance of abstracts is November 21, 1949.

Waveforms, edited by Britton Chance, Frederick C. Williams, Vernon Hughes, Edward F. MacNicol, and David Sayre

Published (1949) by the McGraw-Hill Publishing Co., 330 W. 42 St., New York 18, N. Y. 774 pages+9-page index+xxii pages. 763 figures. 6×9. $10.00.

This book, which is a notable addition to the Radiation Laboratory Series, should prove of great value to workers in the communication and electronics fields. Based upon wartime developments in this country and in the United Kingdom, it contains a wealth of material not previously available, and is the first book to cover completely the application of nonlinear circuit elements to the generation and shaping of current and voltage pulses and waves. The purpose of the book is to give a comprehensive survey of basic circuit techniques used in the generation and manipulation of voltages and currents by linear and nonlinear circuit elements.

An introductory discussion of operations on wave forms leads to a treatment of the generation of sinusoidal waves, pulses, and special wave forms, such as triangular waves, rectangular waves, exponentials, hyperbolas, and parabolas. Chapters on amplitude selection (clipping), comparison, and discrimination, and on time selection include the subjects of switch circuits and multiple-coincidence circuits. The subject of amplitude-modulation of electrical waves by electrical and mechanical signals is followed by a discussion of time modulation and demodulation circuits that is particularly timely. Chapters on frequency multiplication, frequency division, and counting, and on mathematical operations on wave forms should prove of special value in the field of electronic computers. The final chapters cover oscillographic techniques, storage tubes, electrical delay lines, and supersonic delay devices.

The treatment throughout the book is comprehensive and clear, and the authors and editors are to be complimented upon the excellence of style and freedom from errors. Some readers may be handicapped in places, however, by unfamiliar nomenclature. A small amount of duplication of subject matter is inevitable in a book written in so short a time by a large number of authors.

Although the book contains the first adequate analysis of the effects of tube and circuit capacitance upon the triggering of trigger circuits (multivibrators), the authors have not discussed specifically the effects of shunt tube and circuit capacitances upon the upper frequency limit and output wave form of other devices, such as clippers and differentiating circuits.

The reviewer has found the reading of this book very profitable, and will undoubtedly continue to find it an invlauable reference source. He enthusiastically recommends it to teachers and research workers in the fields of electrical engineering, physics, and applied mathematics. Since much of the subject matter is fundamental, the book will not become obsolete rapidly, and it should prove to be a bible in its field.

HERBERT J. REICH
Yale University
New Haven, Conn.

Television Antennas: Design, Construction, Installation, and Trouble-Shooting Guide, by Donald A. Nelson

Published (1949) by Howard W. Sams and Co., Inc., 2924 E. Washington St., Indianapolis 7, Ind. 166 pages. 124 figures. 5½×8½. $1.25.

This pamphlet is intended primarily for the guidance of service technicians in the selection and installation of proper television antennas and accessories. An introduction dealing with television transmission, the television receiver, frequency allocations, and television networks is followed by chapters on receiving antenna principles, antenna construction, commercial antennas, antenna installation, and common installation problems.

Tables of Generalized Sine- and Cosine-Integral Functions

Published (1949) by the Harvard University Press, Cambridge, Mass., 2 volumes, 462 and 560 pages+xxxviii pages. $20.00.

The tables in these two volumes, XVIII and XIX in the Annals of the Harvard University Computation Laboratory, were computed by the Automatic Sequence Controlled Calculator. Carried to six decimal places, the tables are timesavers in the investigation of such problems as self- and mutual impedances, radiation resistance, and distribution of current in antennas and antenna rays of various types.

Automatic Record Changer Service Manual, Volume Two (1948)

Published (1949) by Howard W. Sams and Co., Inc., 2924 E. Washington St., Indianapolis 7, Ind. 432 pages. 8½×11. $6.75.

This volume covers forty-five models of automatic record changers manufactured in 1948, including the new LP and dual-speed changers, plus wire and tape recorders. Included are change cycle data, information on adjustments, needle landing data, "hints and kinks," complete parts lists, and copious illustrations and diagrams.

Advances in Electronics, Volume I, edited by L. Marton

Published (1948) by the Academic Press, Inc., 125 E. 23 St., New York, N. Y. 451 pages+9-page author index and 14-page subject index+xii pages. 126 figures 5¾×9¼. $9.00.

The purpose of this book as stated by the editor, is to provide a series of reviews to be published annually. "It becomes more and more perplexing," he states in the preface, "for the research worker to gather all information required when attacking a new subject, or when supplementing his own knowledge by information from neighboring fields. . . . When the total number of publications is considered, it becomes imperative to produce some guide to the research worker who wishes to acquaint himself with advances in related fields."

Ten monographs by ten well-qualified authors make up this volume. "Oxide-Coated Cathodes" by Albert S. Eisenstein (65 pages) discussed the theoretical aspects of the subject very competently from the standpoint of the modern theory of semiconductors. Sections are included on properties of the coating, the interface, the complete cathode, and thin oxide film phenomena.[1]

Kenneth G. McKay's "Secondary Electron Emission" (65 pages) covers the secondary emision of pure metals, insulators, and composite surfaces thoroughly and is, to the reviewer's knowledge, the only article in English on the subject. A list of 260 references is appended.

"Television Pickup Tubes and the Problem of Vision" by A. Rose (36 pages) treats the subject from a general point of view, relating the performance of the various pickup tubes to the sensitivity and range of photographic films and the human eye. Sections are included on the relation between intelligence transmitted versus bandwidth and signal-to-noise ration; however, detailed description of the various devices is not given.

R. G. E. Hutter discusses the theory of deflection for both small and large angles quantitatively in "The Deflection of Beams of Charged Particles" (52 pages). The defocusing effects of deflection fields are described in such a manner that the various defocusing components may be examined separately.

Mark G. Inghram's "Modern Mass Spectroscopy" (50 pages) covers the basic principles of the mass spectroscope and also describes the ion sources used and the principle types of apparatus. "Particle Accelerators," by M. Stanley Livingston (48 pages), explains the participles upon which particle accelerators are designed and operated in an especially thorough manner.

A. G. McNish, in "Ionospheric Research" (30 pages), gives, for the most part, results obtained since the beginning of World War II and their correlation, but does not describe the equipment used. Early work on the problem is reviewed in Jack W. Herbstreit's "Cosmic Radio Noise" (34 pages), and the equipment used is described.

[1] Dr. Eisenstein has sent the reviewer the corrections to typographical errors in his monograph. On page 13 the fraction ½ in equation (6) is an exponent. On page 30, insert e as the denominator of the quantity in line 6 and add the exponent 5 to the effective mass m^* in equation (33). On page 50 the logarithm in equation (26) should be the natural logarithm.

Kenneth A. Norton discusses service range and the effects of factors such as antenna height, terrain, reflection, and interference in "Propagation in the FM Broadcast Band" (44 pages). "Electronic Aids to Navigation," by J. A. Pierce, covers only general aspects of the subject.

With ten contributors, each writing on ten different topics, it is not surprising that there is no uniformity in the volume; yet all the monographs are written on a completely professional level. Some of the authors, such as Eisenstein, McKay, and Hutter, assume a more specialized preparation and interest on the part of readers than do others, such as Rose and Pierce. The authenticity of the information given in all of the papers can seldom be questioned. On the other hand, some formulas in at least one paper are incomplete or there are missing terms. In another paper special symbols are used in mathematical expressions with no explanation of their meaning, while a third contains poorly composed or improperly punctuated sentences which require two readings.

Most of the papers constitute the only recently published surveys of these subjects generally available and in practically all of them the references are extensive and up-to-date. This work should, in the opinion of this reviewer, win wide recognition and become an important part of the literature of electronics.

George D. O'Neill
Sylvania Electric Products Inc.,
Bayside, L. I., N. Y.

Fundamentals of Electric Waves, by Hugh Hildreth Skilling

Published (1948) by John Wiley and Sons, Inc., 440 Fourth Ave., New York 16, N. Y. 240 pages+5-page index+vii pages. 86 figures. 6×9¼. $4.00.

This is the second edition of an excellent book which first appeared in 1942. Intended for use by individuals who have the equivalent of electrical engineering training at the college senior level, it presupposes a knowledge of static and low-frequency electric and magnetic fields, as well as of mathematics through calculus. For its purpose, that of introducing the student to vector analysis and Maxwell's equations, together with simple applications, the book has been well planned, and should serve, particularly for those who are somewhat timid, to take the chill out of that first plunge into waters often suspected of being rather icy. Some students may not need all the pictorial and pedagogic aids Professor Skilling uses so skillfully—for example, in his exposition of gradient, divergence, and curl—but many others will find them most helpful in their first introduction to vector fields.

The first half of the book treats magnetic and electric fields by vector methods, and the emphasis throughout is on imparting sound physical ideas and concepts. Maxwell's equations are subsequently introduced and used in discussing a variety of topics, such as wave propagation, reflection, radiation, antennas, waveguides, and cavity resonators. However, in a book of this size and scope, the treatment must necessarily be kept at a fairly elementary level.

The present edition differs from the first in that the mks system of units is used rather than the "Gaussian" system, and that the material used to illustrate the application of Maxwell's equations has been increased. Problems are given with each chapter, and this fact, taken in conjunction with the lucid style of writing employed, makes the book suitable both for self-study and for classroom use.

W. D. Hershberger
RCA Laboratories
Princeton, N. J.

A Textbook of Radar, by the Staff of the Radiophysics Laboratory Council for Scientific and Industrial Research, Australia

Published (1947) by Angus and Robertson, Sydney, Australia. 570 pages+9-page index. 347 figures. 5½×8½. $8.35.

This textbook, according to the publisher, "is of a standard suitable for graduate and research students of universities and technical colleges and for engineers engaged in research and development in industry." It includes chapters on fundamentals, the magnetron, triode power oscillators, modulators, microwave transmission and cavity resonator theory, transmission line and resonator techniques, aerials, aerial duplexing, receivers, local oscillators, frequency convertors, amplifiers, display circuits, automatic ranging circuits, radar systems, ground radar, shipboard radar, airborne radar, and radar navigation. Each chapter was written by a different author.

A few of these chapters, such as those on fundamentals and modulators, are very lucidly written, and are composed of material which is excellently chosen, so that practically all important considerations are mentioned and yet not treated in such minute detail that coherence and unity are lost and the balance of the book upset.

Most chapters, unfortunately, do not live up to this high standard. The chapter on microwave transmission theory is concerned with the derivation of the waveguide equations from Maxwell's equations and related subjects. It is as out of place in a book on radar as would be chapters on electron optics and network theory. The chapter on display circuits plunges into discussions of such topics as "gate generators," "clamping circuits," etc., without the benefit of any adequate discussion as to types of displays and what is to be accomplished by them. The chapter on receivers, in common with many of the others, is full of statements which are either flatly incorrect or so loosely and poorly worded that only an expert in the field could draw the correct implications from them. For instance, in this chapter on receivers, in discussing AFC, the author makes the erroneous statement (page 339) that "the basic method is to use the leakage power from the TR switch." (On page 403, however, it is pointed out correctly that it is preferable not to use TR leakage because of complications caused by the leakage "spike.") In this same chapter it is stated (on page 335) that "The fluctuation(s) in the anode current . . . cause fluctuating voltages to be developed across grid-cathode impedances, and after amplification result in noise modulation of the electron beam of the indicator." This statement is not incorrect, but the confusion to the careful student reader who will try to puzzle out why "grid-cathode impedances" and the "electron beam of the indicator" were singled out for especial mention in connection with thermal noise is unfortunate.

The book omits any mention of a number of important items, such as servo systems for antenna position or range tracking, radar altimeters, and pulse doppler techniques for moving target indication. A number of other important items, such as circuitry for automatic frequency control circuitry for automatic gain control, and waveguide rotary joints are either discussed very inadequately or are merely alluded to with no discussion at all.

Some of the material in the book is hopelessly out of date. For example, the chapter on receivers (page 340) shows "typical" receivers utilizing tube types 6AC7, 6H6, 954, and 955! Many who read this book will be exasperated by the frequent references to unpublished reports. The reviewer is puzzled to know the reason for these references; they are generally unavailable to readers and the material in the book is obviously not original, so that there is no necessity for disclaiming credit for any ingenious devices or methods described.

N. I. KORMAN
Radio Corporation of America
Camden, N. J.

Radio Wave Propagation, by the Committee on Propagation of the National Defense Research Committee; C. R. Burrows, Chairman, S. S. Attwood, Editor

Published (1949) by the Academic Press, Inc., 125 E. 23 St., New York, N. Y. 511 pages+vi pages+2-page glossary+35-page bibliography. 566 figures. 8×11.

This book should be of great interest and value to engineers concerned with radar and communication circuits operating at frequencies above 30 Mc. A vast amount of information on radio wave propagation at these frequencies has been compiled in this voluminous publication. There are excellent theoretical treatments of basic phenomena and also many good discussions of practical application problems. More than 150 charts and 30 nomographs greatly facilitate the use of the material.

The book is essentially a consolidation of the three volumes of the Summary Technical Report of the Committee on Propagation of the N.D.R.C. The work under the general supervision of this committee during World War II involved the co-operation of many groups in the United States, England, Canada, New Zealand, and Australia. Numerous wartime reports by experts from these groups are assembled in the book, the names of about forty-five of these authors being found in footnotes. Since the book is a compilation of many reports by many authors, there is understandably, a noticeable lack of co-ordination and considerable duplication, although in some cases this permits an insight into the historical development of a subject. However, the greatest inconvenience to users will probably be the lack of an index.

There are three sections or volumes into which the book is divided. Among the subjects treated in the first section are standard propagation, nonstandard propagation, diffraction, refraction, ducts, siting, and coverage. Meteorological theory and methods of forecasting propagation characteristics by meteorological measurements are presented in the second section, together with such topics as reflection coefficients, absorption, scattering, and echoes. The results of many experiments are included. The final section is a general discussion of propagation through the standard atmosphere, involving such subjects as ground reflection, atmospheric refraction, antenna gain, and the calculation of field strength and coverage diagrams. Results of a number of transmission experiments and an extensive bibliography are included in an appendix.

The chairman, editor, and publishers have done a real service by making such a wealth of information on microwave propagation available in a single book.

JOHN D. KRAUS
Ohio State University
Columbus 10, Ohio

Keys and Answers to New Radiotelegraph Examination Questions, by Alexander A. McKenzie

Published (1949) by Alexander A. McKenzie, 245 Poplar Ave., Hackensack, N. J. 62 pages. 5½×8½. $1.00.

This pamphlet, based upon the FCC's "Study Guide and Reference Material for Commercial Radio Operator Examinations, Revised July 1, 1948," and upon mimeographed supplement four, has been compiled as an interim aid to applicants for radiotelegraph first- and second class licenses. It includes answers to all Element One questions and Element Five questions 233 through 296, as well as Element Six questions 226 through 295.

Industrial Electricity, Volume II: Alternating Currents, by William H. Timbie and Frank G. Willson

Published (1949) by John Wiley and Sons, Inc., 440 Fourth Ave., New York 16, N. Y. 773 pages+7-page index+ix pages. 568 figures. 5½×9. $5.96.

This well-written book will give the high-school graduate or the lower classman in an engineering school a thorough knowledge of ac theory and ac machines. Indeed, it is well adapted for self-study, since numerous illustrative problems and diagrams are to be found throughout the text, and a basic knowledge of algebra, geometry, and trigonometry is all that is required in the way of mathematical preparation.

The text is a shorter treatment of the material covered in the author's two-volume text, "A.C. Electricity and Its Application to Industry." This indicates that the text is better adapted for the study of ac power work rather than that of electronics, in spite of the fact that at the end of the text are included two chapters on transmission lines.

However, the material given is reasonably complete and the information is well presented. The machines described are of recent design, and indicate that the text is up to date. Particularly noteworthy is the summary at the end of each chapter giving the reader a review of the chapter, as well as pointing out the highlights. The problems are very practical and relevant to the text, and help the student fix the fundamentals of the subject in his mind. Owing to the elementary nature of the treatment, however, more advanced material is treated rather sketchily. For example, rate of change is mentioned in the text, but very little is said as to just what the term means.

The book is remarkably free of errors, but one or two have been noted. On page 29, in equation (7-1) it appears that the author forgot to put 10^8 in the denominator of what is apparently intended to be a fraction; and on page 174, example 11, in the equation for Branch 1 he has written $I+(E/R_1)$, instead of $I=(E/R_1)$.

These, however, are minor matters. In general, the book covers the material indicated by the title; the table of contents and index are fairly complete; and the typography is of high quality. The text can, therefore, be highly recommended to students.

ALBERT PREISMAN
Capitol Radio Engineering Institute
Washington, D. C.

Radio Laboratory Handbook, by M. G. Scroggie

Published (1948) by Iliffe and Sons, Ltd., Dorset House, Stamford St., London, S. E. 1, England. Fourth edition. 424 pages, 6-page index. 170 diagrams, 46 photographs, 4¾×7.

The purpose of this handbook is to guide a laboratory worker in setting up and properly utilizing a laboratory. Dedicated to the use of both "home experimenters" and "dull professionals," the book comprises a compilation of data concerning laboratory techniques, instruments, and procedures. Some special instruments not commercially available are described, but a large proportion of the material is devoted to a description of commercially available British laboratory instruments.

Since practically all of the laboratory instruments considered in the book are British-made, full use of the volume for the purpose intended is somewhat limited in this country. However, it has value as a study of British Laboratory practices and instruments; furthermore, a large proportion of the material is devoted to general methods of measurement which do not consider a specific instrument. Hence, for that portion all that is required is the ability to interpret such British terms as *valve*, *H. T. accumulator*, etc.

Much of the material presented is cautionary, in that pitfalls are pointed out—"what may be neglected," "deceptive formulae," and the use of judgment in plotting results. Preferred practices, such as the use of decibels and the importance of handiness in instruments, are also stressed.

It is interesting to observe how few test instruments are exported from the United States to Great Britain. An occasional General Radio instrument and the Boonton Q meter seem to be the only ones used.

The book is presented in a clear and readable manner. Such mathematics as is used consists only of working formulas, such as inductance and capacitance formulas, and the like.

MURRAY G. CROSBY
126 Old Country Road
Mineola, L. I.
N. Y.

(*Books continued on page 1038*)

Sections

Chairman	Section	Secretary
H. I. Metz C.A.A. 84 Marietta St., N.W. Atlanta, Ga.	ATLANTA Sept. 16–Oct. 21	M. S. Alexander 2289 Memorial Dr., S.E. Atlanta, Ga.
E. W. Chapin 2805 Shirley Ave. Baltimore 14, Md.	BALTIMORE	J. V. Lebacqz Owings Mills Maryland
T. B. Lawrence 1833 Grand Beaumont, Texas	BEAUMONT-PORT ARTHUR	C. B. Trevey 2555 Pierce St. Beaumont, Texas
H. H. Scott Hermon Hosmer Scott, Inc. 385 Putnam Ave. Cambridge 39, Mass.	BOSTON	F. D. Lewis General Radio Co. 275 Massachusetts Ave. Cambridge 39, Mass.
J. P. Arnaud Guemes 827 Vte. Lopez F.C.C.A., Argentina, S.A.	BUENOS AIRES	L. Brandt Uruguay 618 Buenois Aires, Argentina, S.A.
L. P. Haner 75 Koenig Rd. Tonawanda, N. Y.	BUFFALO-NIAGARA Sept. 21–Oct. 19	K. R. Wendt Colonial Radio Corp. 1280 Main St. Buffalo 9, N. Y.
M. S. Smith 1701 10th St. Marion, Iowa	CEDAR RAPIDS	V. R. Hudek Collins Radio Co. Cedar Rapids, Iowa
E. H. Schulz Elec. Engr. Dept. Armour Research Found. Chicago, Ill.	CHICAGO Sept. 16–Oct. 21	L. H. Clardy Research Labs. Swift & Co., U. S. Yards Chicago 9, Ill.
F. W. King 6249 Banning Rd. Cincinnati 24, Ohio	CINCINNATI Sept. 13–Oct. 20	J. P. Quitter 509 Missouri Ave. Cincinnati 20, Ohio
J. F. Dobosy 31748 Lake Rd. Avon Lake, Ohio	CLEVELAND Sept. 22–Oct. 27	T. B. Friedman 2909 Washington Blvd. Cleveland Heights 18, Ohio
R. B. Jacques 227 W. Como Ave Columbus, Ohio	COLUMBUS Sept. 9–Oct. 14	S. N. Friedman 346 Lincoln Ave. Worthington, Ohio
Lawrence Grew S. N. E. Telephone Co. New Haven, Conn.	CONNECTICUT VALLEY Sept. 15–Oct. 20	J. E. Merrill 713 Montauk Ave. New London, Conn.
A. S. Levelle 801 Telephone Bldg. Dallas 2, Texas	DALLAS-FORT WORTH	E. A. Hegar 802 Telephone Bldg Dallas 2, Texas
H. E. Ruble 3011 Athens Ave. Dayton 6, Ohio	DAYTON	G. H. Arenstein 1224 Windsor Drive Dayton 7, Ohio
T. G. Morrissey Radio Station KFEL Albany Hotel Denver, Colo.	DENVER	Hubert Sharp Box 960 Denver 1, Colo
F. E. Bartlett Radio Station KSO Old Colony Bldg. Des Moines 9, Iowa	DES MOINES-AMES	O. A. Tennant 3515 Sixth Ave. Des Moines, Iowa
C. F. Kocher 17186 Sioux Rd. Detroit 24, Mich	DETROIT Sept. 16–Oct. 21	P. L. Gundy 519 N. Wilson Royal Oak, Mich
R. W. Slinkman Sylvania Elec. Prods. Emporium, Pa.	EMPORIUM	T. M. Woodward 203 E. Fifth St Emporium, Pa
H. W. G. Salinger 2527 Hoagland Ave Ft. Wayne 6, Ind.	FORT WAYNE	J. F. Conway 4610 Plaza Dr. Ft. Wayne, Ind.
C. L. Wischmeyer 808 N. Rice Ave. Bellaire, Texas	HOUSTON	Wayne Phelps 1710 Richmond Ave Houston 6, Texas
E. H. Pulliam 931 N. Parker Ave. Indianapolis 1, Ind.	INDIANAPOLIS	J. H. Schult Indianapolis Elec. School 312 E. Washington St Indianapolis 4, Ind
E. R. Toporeck Naval Ordnance Test Sta. Inyokern, Calif.	INYOKERN	R. W. Johnson 303 B. Langley China Lake, Calif.
C. F. Heister Fed. Com. Comm 838 U. S. Court House Kansas City 6, Mo.	KANSAS CITY	Mrs. G. L. Curtis 6005 El Monte Mission, Kan.
G. L. Foster Sparton of Canada London, Ont., Canada	LONDON, ONTARIO	G. R. Hosker Richards-Wilcox London, Ont., Can.
Bernard Walley Radio Corp. of Am. 420 So. San Pedro St Los Angeles 13, Calif.	LOS ANGELES	Robert L. Sink Consolidated Eng. Co. 620 N. Lake Ave. Pasadena 4, Calif.
D. C. Summerford Radio Station WKLO Henry Clay Hotel Louisville, Ky.	LOUISVILLE	R. B. McGregor 2100 Confederate Pl. Louisville, Ky.
E. J. Limpel A. O. Smith Corp. 3533 N. 27 St. Milwaukee 1, Wis.	MILWAUKEE	W. H. Elliot 3564 N. Murray Ave. Milwaukee 11, Wis.
K. R. Patrick R.C.A. Victor Co. 1001 Lenoir St. Montreal, P.Q. Canada	MONTEAL, QUEBEC Sept. 15–Oct. 12	S. F. Knights Canadian Marconi Co. Box 1690 Montreal, Que, Can.
L. A. Hopkins, Jr. 1711, 17th Loop Sandia Base Branch Albuquerque, N. M.	NEW MEXICO	T. S. Church 3079 Q 34th St. Sandia Base Branch Albuquerque, N. M.
H. F. Dart 33 Burnett St. Glen Ridge, N. J.	NEW YORK	Earl Schoenfield W. L. Maxon Corp. 460 W. 34th St. New York 1, N. Y.
J. T. Orth 4101 Fort Ave. Lynchburg, Va.	NORTH CAROLINA-VIRGINIA	C. E. Hastings 117 Hampton Roads Ave. Hampton, Va.
M. W. Bullock Capital Broadcasting Co. 501 Federal Securities Bldg. Lincoln 8, Neb.	OMAHA-LINCOLN	B. L. Dunbar Radio Station WOW Omaha, Neb.
A. W. Y. Des Brisay 240 Clemow Ave. Ottawa, Ont., Canada	OTTAWA, ONTARIO Sept. 17–Oct. 20	A. G. Sheffield 11 Fern Ave. Ottawa, Ont., Canada
A. N. Curtiss Radio Corporation of Am Camden, N. J.	PHILADELPHIA Sept. 1–Oct. 6	C. A. Gunther Radio Corp. of America Front & Cooper Sts. Camden, N. J.
M. Glenn Jarrett 416 Seventh Ave. Pittsburgh 19, Pa.	PITTSBURGH Sept. 12–Oct. 10	W. P. Caywood, Jr. 23 Sandy Creed Rd. Pittsburgh 21, Pa.
A. E. Richmond Box 441 Portland 7, Ore.	PORTLAND	Henry Sturtevant Rt. 6, Box 1160 Portland 1, Ore.
E. W. Herold RCA Laboratories Princeton, N. J.	PRINCETON	W. H. Bliss 300 Western Way Princeton, N. J.
K. J. Gardner 111 East Ave. Rochester 4, N. Y.	ROCHESTER October 20	Gerrard Mountjoy Stromberg Carlson Co. 100 Carlson Rd. Rochester, N. Y.
N. D. Webster 515 Blackwood N. Sacramento, Calif.	SACRAMENTO	J. R. Miller 3991 3rd Ave. Sacramento, Calif.
G. M. Cummings 7200 Delta Ave. Richmond Heights 17, Mo.	ST. LOUIS	C. E. Harrison 818 S. Kings Highway Blvd. St. Louis 10, Mo.
O. C. Haycock Dept. of Elec. Eng. University of Utah Salt Lake City, Utah	SALT LAKE	M. E. Van Valkenburg Dept. of Elec. Eng. University of Utah Salt Lake City, Utah
C. L. Jeffers Radio Station WOAI 1031 Navarro St. San Antonio, Texas	SAN ANTONIO	L. K. Jonas 267 E. Mayfield Blvd. San Antonio, Texas
L. G. Trolese U. S. Navy Electronics Lab. San Diego 52, Calif	SAN DIEGO	S. H. Sessions U. S. Navy Electronics Lab. San Diego 52, Calif.
W. R. Hewlett 395 Page Mill Rd. Palo Alto, Calif.	SAN FRANCISCO	J. R. Whinnery Elec. Engr. Dept. University of Calif. Berkeley, Calif.
J. M. Paterson 2009 Nipsic Bremerton, Wash	SEATTLE Sept 8–Oct. 13	J. E. Hogg General Electric Co. 710 Second Ave. Seattle 1, Wash.
R. H. Williamson 161 Parkway Dr Syracuse, N. Y.	SYRACUSE	S. E. Clements Dept. of Elec. Engr. Syracuse University Syracuse, N. Y.

Sections

Chairman		Secretary
A. M. Okum 344 Boston Pl. Toledo 10, Ohio	Toledo	R. G. Larson 2647 Scottwood Ave Toledo 10, Ohio
C. Graydon Lloyd Canadian General Electric Co., Ltd. 212 King Sq., W. Toronto, Ont., Canada	Toronto, Ontario	Walter Ward Canadian General Electric Co., Ltd. 212 King St., W. Toronto, Ont., Canada
W. G. Pree 2500 W. 66 St. Minneapolis, Minn	Twin Cities	O. A. Schott 4224 Elmer Ave. Minneapolis 16, Minn.
T. J. Carroll National Bureau of Stand. Washington, D. C.	Washington May 9–June 13	P. DeF. McKeel 9203 Sligo Creek Parkway Silver Spring, Md.
G. C. Larson Westinghouse Elec. Corp. Sunbury, Pa.	Williamsport May 4–June 1	R. C. Walker Box 414, Bucknell Univ. Lewisburg, Pa.

SUBSECTIONS

Chairman		Secretary
H. R. Hegbar 2145 12th St. Cuyahoga Falls, Ohio	Akron (Cleveland Subsection)	H. G. Shively 736 Garfield St. Akron, Ohio
H. W. Harris 711 Kentucky St. Amarillo, Tex.	Amarillo-Lubbock (Dallas-Ft. Worth Subsection)	E. N. Luddy Station KFDA Amarillo, Tex.
F. L. Hall Dept. of Elec. Engr Pennsylvania St. College State College, Pa	Centre County (Emporium Subsection)	J. H. Staten Dept. of Eng. Research Pennsylvania St. College State College, Pa.
A. H. Sievert Canadian Westinghouse Co. Hamilton, Ont., Canada	Hamilton (Toronto Subsection)	J. H. Pickett Aerovox Canada Ltd 1551 Barton St. E. Hamilton, Ont., Canada
R. B. Ayer RCA Victor Division New Holland Pike Lancaster, Pa.	Lancaster (Philadelphia Subsection)	J. L. Quinn RCA Victor Division New Holland Pike Lancaster, Pa.
H. A. Wheeler Wheeler Laboratories 259-09 Northern Blvd Great Neck, L. I., N. Y.	Long Island (New York Subsection)	M. Lebenbaum Airborne Inst. Lab 160 Old Country Rd. Box 111 Mineola, L. I., N. Y.
L. E. Hunt Bell Telephone Labs. Deal, N. J	Monmouth (New York Subsection)	G. E. Reynolds, Jr. Electronics Associates, Inc. Long Branch, N. J.
N. Young, Jr. F.C.C. Nutley, N. J.	Northern N. J. (New York Subsection)	J. H. Redington Measurements Corp. Boonton, N. J.
A. R. Kahn Electro-Voice, Inc. Buchanan, Mich.	South Bend (Chicago Subsection) January 20	A. M. Wiggins Electro-Voice, Inc. Buchanan, Mich.
R. M. Wainwright Elec. Eng. Department University of Illinois Urbana, Ill.	Urbana (Chicago Subsection)	M. H. Crothers Elec. Eng. Department University of Illinois Urbana, Ill.
R. D. Cahoon C.B.C. Winnipeg, Man., Canada	Winnipeg (Toronto Subsection)	J. R. B. Brown Suite 2 642 St. Marys Rd. Winnipeg, Man., Canada

Books (continued)

Modern Radio Technique, by A. H. W. Beck

Published (1948) by the Macmillan Co., 60 Fifth Ave., New York, N. Y. 173 pages+2-page index+2 pages of tables+1 page of symbols+1 page of bibliography+x pages. 55 figures. 5¼×8¼.

This book describes the operation of velocity-modulated tubes with considerable attention to their design. As a result, the text consists largely of mathematical equations, requiring a rather complete knowledge of existing field theory, which is not usually acquired without a corresponding predilection for certain methods. The author is English and the material is a result of his experience in England during the war, so that the methods and constructional details described may be found to be more nearly representative of British practice.

Presumably the book is intended as a guide to those entering the field. It is, however, of doubtful value for this purpose. Short books of this kind, owing to their limitations in size and scope, often tend to describe the application of concepts that have been of value to the author in meeting his particular problems, rather than covering the entire field without prejudice. As a result, some very useful and accurate design methods have been entirely omitted.

For example, the chapter on cavity resonators leads one to believe that the calculation of resonances and loss factors of even simple cylindrical shapes commonly used are subject to large errors. This is not necessarily true. Methods are available—with which the author is evidently not acquainted—which allow the calculation of resonances and loss factors to any desired degree of accuracy, for many cylindrical shapes in common use. The results have been consistently checked by tests, even including some glass as a dielectric. Thus, the author's conclusion that "the calculated loss would bear little relation to the measured loss" is obviously due to poor methods of calculation.

Again, in the chapter on velocity-modulated amplifiers, the impression is given that "debunching" as a result of space-charge effects may not be very important and cannot be calculated with any accuracy. Both of these conclusions are wrong. A wave theory has been developed which does exactly this. Although a reference to this theory was given, the author apparently did not read his own work.

W. C. Hahn
General Electric Co.
Schenectady, N. Y.

Radio Servicing: Theory and Practice, by Abraham Marcus

Published (1948) by Prentice-Hall, Inc., 70 Fifth Ave., New York 11, N. Y. 752 pages+23-page index+xix pages. 410 figures. 6×9. $5.95

Mr. Marcus' book is intended for those "who are not beginners in radio nor yet advanced enough to study the subject on an engineering level." These readers will find a clear, nonmathematical discussion of electron tubes and their use as rectifiers, AM detectors, amplifiers, and oscillators. They will also find good explanations of many practical circuits of power supplies, radio receivers, and amplifiers, such as are encountered in commercial equipment. Also included are chapters on electrical and radio theory, components and parts, special tubes, servicing procedures and techniques, and repair and alignment.

Thorough in its scope, the book discusses volume control (manual, AVC, delayed AVC, amplified delayed AVC, and quiet AVC), tuning indicators, tone compensation and control, selectivity control, band-switching and band-spread, noise suppression circuits, push-button tuning, and automatic frequency control.

One fault might be that the book is written mainly from the AM point of view. The comparison of the relative bandwidth requirements of AM and FM could be more adequately discussed.

"Radio Servicing: Theory and Practice" should be of value to those who want not only a textbook, but also a reference book.

Frank R. Arams
RCA Victor Division
Lancaster, Pa.

Television, How It Works

Published (1948) by John F. Rider, Inc., 480 Canal St., New York 13, N. Y. 194 pages+9-page "troubleshooting" chart. 229 figures. 8½×11.

Designed as an elementary textbook in television, this book, written by various staff members of the Rider Co., explains the operation of the television receivers on today's market.

The opening chapter presents an over-all picture of television, followed by a chapter on the television channels and characteristics of the video signal, operating bandwidth characteristics, and the carrier and intermediate frequencies. The third chapter discusses antennas designed for the reception of television signals, and the next eight chapters cover the receiver proper. The final chapter contains practical discussions of text instruments, signal generators, etc., used in the alignment and maintenance of receivers, alignment procedures, and "trouble-shooting" suggestions.

Auto Radio Manual

Published (1949) by Howard W. Sams and Co., Indianapolis, Inc. Over 300 pages, profusely illustrated. 8½×11. $4.95.

This volume gives uniform service data for most of the automobile radios produced since 1946. It covers 100 different postwar models put out by 24 manufacturers.

New Publications

More than 140 new American Standards approved since January of this year are included in the midyear list of standards and special publications just issued by the American Standards Association. The list shows a total of 1,124 standard specifications, methods of test, building requirements, dimensions, safety codes, and definitions and terminology in all fields of engineering, as well as for materials and equipment used by the ultimate consumer. The 28-page **list of American Standards** (July, 1949) may be obtained from the American Standards Association, 70 E. 45 St., New York 17, N. Y., without charge . . . For many years the extreme difficulty of obtaining high-accuracy tables of sines and cosines with decimal subdivisions of a degree has seriously inconvenienced workers in such fields as observational astronomy, geodesy, navigation, optical instrument design, ballistics, rocket research radar, and aircraft design. To meet this need the National Bureau of Standards has just issued a large (10¼×7¼ inches) 95-page booklet, **"Tables of Sines and Cosines to Fifteen Decimal Places at Hundredths of a Degree,"** (NBS Publication AMS 5), which is available for forty cents per copy. Here the columns of signs and cosines are arranged side by side for convenience in cases where both the sine and cosine functions are desired for the same argument, or where Taylor's theorem is to be used for interpolation. Alongside the tabular entries are presented the second central differences, which are sufficient for interpolation to the full 15 decimal places. . . . Another NBS publication, **"Accurate Determination of the Deadtime and Recovery Characteristics of Geiger-Muller Counters"** (RP 1965), by Louis Costrell, describes in nine pages an electronic gating instrument for the determination of deadtime and recovery characteristics of Geiger-Muller counters to an accuracy of two microseconds. The theory of operation of Geiger-Muller counters is briefly presented, and experimental data are given showing variation of deadtime and recovery time with counter pressure and overvoltage. The price of the booklet is ten cents. . . . Chester Snow's 22-page **"Standard of Small Capacitance,"** put out by NBS for 15 cents per copy, derives a formula for computing the electrical capacitance of an absolute standard consisting of a modification of the ordinary parallel-plate capacitor with co-planar guard. . . . All of the three aforegoing publications are available from the Superintendent of Documents, U. S. Government Printing Office, Washington 25, D. C. . . . An extensive **bibliography on the industrial uses of radioactive tracers** is available without charge from Arthur D. Little, Inc., Cambridge 42, Mass.

IRE People

The Government of the Republic of France has awarded **William Dubilier** (A'14-M'18-F'29), radio inventor and pioneer, the Diploma of Officer of the Academy and the Order of Academic Palms.

Further, at the annual meeting of the Association des Ingenieurs-Docteurs de France, held at the Sorbonne in Paris on June 1, 1949, the awards committee (consisting solely of professors of the Sorbonne and members of the French Academy of Sciences) unanimously voted to Mr. Dubilier the honorary medal of the organization. The presentation was made on June 25 at the French Embassy in New York City.

Mr. Dubilier is well-known among his fellow engineers as a long-time contributor to the fields of radio telephony; transmitting and receiving condenser theory, practice, and construction; and a successful and effective inventor in many communications and electrical fields. It was his development of the power condenser or capacitor that has made modern broadcasting and commercial radio possible.

Born in New York City on July 25, 1888, Mr. Dubilier was educated at the Cooper Institute there, as well as at European universities. When he was twenty-one, he was invited to go to the Pacific Coast by the Standard Oil Co. to build a broadcasting station for that Company's communication with Alaska. Subsequently, after an ill-fated expedition to Russia to build a broadcasting station for the Czar's palace, he founded the Dubilier Condenser Co., Ltd., in England, and later the Dubilier Electric Co. of New York, which became the Cornell-Dubilier Electric Corp.

Among the 300 patents which have been issued to him in the United States is one for his invention of the first portable electric heater. Currently he is vice-president and technical director of the Cornell-Dubilier Electronic Corp., and president of the Radio Patents Corp., both in New York City.

❖

Donald G. Fink (A'35-SM'45-F'47), editor of *Electronics* and newly appointed Chairman of the Joint Technical Advisory Board, was chosen by the Radio Manufacturers Association as technical advisor to the American delegation which attended an international meeting on television standards in Zurich, Switzerland, from July 1 through 5. The delegation was instructed to support American television standards as adopted by the FCC and to try to prevent hasty adoption by the international body of television standards not compatible with the United States system.

Mr. Fink was born in Englewood, N. J., on November 8, 1911. After receiving the bachelor of science degree from the Massachusetts Institute of Technology in 1933, he spent a year in graduate study there before joining the editorial staff of *Electronics* in 1934. During the war he took a four-year leave of absence in order to work on the development of the Loran system of long-range navigation at the Radiation Laboratory. The Loran transmitters now in use are based on his designs, and he is the author of "Microwave Radar," the first radar textbook.

Appointed head of the Loran division of the Laboratory in 1943, Mr. Fink served both in the European and Pacific areas, later being transferred to the Washington, D. C., office of the Secretary of War. In 1945 he returned to *Electronics* as executive editor. He was awarded the War Department's Medal of Freedom in 1946 and the Presidential Certificate of Merit two years later.

❖

Ross K. Gessford (A'38-M'44), formerly engineering specialist in cathode-ray tubes, has been appointed chief engineer for the television tube division of Sylvania Electric Products Inc.

Born on June 27, 1906, at Niagara Falls, N. Y., Mr. Gessford was educated at George Washington University and the University of Maryland, receiving the B.S.E.E. degree from the latter in 1929. From 1929 to 1936 he was employed by the Westinghouse Electric Corp., where he progressed from student engineer to research worker in design and development engineering. In 1936 and 1937 he worked for the Ken-Rad Tube and Lamp Corp. as a design and development engineer for radio tubes. He joined Sylvania in the latter year and has been continuously associated with the research, development, and engineering of radio and cathode tubes since that time.

Mr. Gessford is a past chairman of the Emporium Section of the IRE.

L. Jerome Stanton (A'47–M'49), staff member of the RCA Institutes' Home Study Course, has also been appointed a special consultant on communications and television problems to the Audio Facilities Corp., recently established in New York by a group of engineers, including IRE member **Lewis S. Goodfriend** (S'47–A'48).

Mr. Stanton was born in Independence, Ore., on October 10, 1910, and began his career as an engineer and writer on technical and scientific subjects while studying in the U. S. Navy Radio School during his naval service from 1929 to 1935. After working as a free-lance writer, in 1938 he was appointed chief engineer of Lorden Enterprises, Inc., in California, and there developed one of the first successful wired systems of music distribution. In 1939 he became a radio and electrical inspector at the Lockheed Aircraft Corp., Calif., leaving in 1941 to become chief radio operator on board a vessel of the Luckenbach Steamship Co.

In 1944 Mr. Stanton joined the staff of the OSRD as a technical writer. Two years later he was appointed to the staff of *Air Trails Pictorial* and *Astounding Science Fiction* as associate editor. He returned to free-lance writing in 1947, joined the Arma Corp. as a technical writer in 1948, left in 1949, and joined RCA shortly afterward.

Mr. Stanton is a member of the Audio Engineering Society, the American Radio Relay League, and the American Association for the Advancement of Science.

Mr. Goodfriend was born in New York City on May 21, 1923. In 1940 he became a technician in sound research at the Stevens Institute of Technology, leaving in 1942 to join the staff of the National Defense Research Committee's Project 17, where he remained for one year. In 1945 he became a member of the counter battery fire-control sound location unit of the U. S. Marine Corps Material Section.

He completed his course of study at the Stevens Institute of Technology in 1947, with the degree of mechanical engineer, and he thereupon joined the staff of the Stevens Institute as a research engineer. While continuing to teach at Stevens, he became a development engineer with Rangertone, Inc. in 1949. He left in the fall of the same year in order to devote full time to the Audio Facilities Corp.

❖

A. Daniel Collins (S'47), student at the University of Michigan College of Engineering, died early this year.

Born in Ohio on March 19, 1917, Mr. Collins was educated at the Celina High School in Celina, Ohio. He expected to be graduated from the University of Michigan with the B.S.E.E. degree this year.

Ralph A. Lamm (SM'46) has been appointed chief of the National Bureau of Standards' missile engineering section, where his duties will not only be the direction of guided missile engineering, including electronic, electrical, aerodynamic, servo-mechanic, and mechanical phases, but also to co-ordinate the Bureau's program with industry.

Mr. Lamm was born in Bisbee, Ariz., on July 13, 1908, and began his career as a custom radio builder in 1926. Joining the Pioneer Radio Manufacturing Co. in 1930, he left two years later to take charge of the design and production engineering of all types of electronic equipment, radio, and television receivers for the Troy Radio and Television Co. At the same time he acted as consultant for the city of Los Angeles on radio safety ordinances.

From 1942 until 1944 Mr. Lamm was a staff member of the Massachusetts Institute of Technology, conducting research and development on radar receivers and systems at the Radiation Laboratory. In 1944, as director of the MIT field experimental station at the National Bureau of Standards, Mr. Lamm was responsible for the research, development, and engineering of all electronic equipment used in automatic homing missiles, including the "Bat" and the "Pelican." He also served as consultant to the Navy Department's Ordnance Bureau on guided missile work being done by the National Bureau of Standards. He joined the NBS staff in 1947.

In recognition of his contributions to the war effort, Mr. Lamm has been awarded the Presidential Certificate of Merit, Certificates from the Office of Scientific Research and Development, the U. S Navy Bureau of Ordnance Merit Award, and the Department of Commerce Meritorious Service Award. He is a member of the Electronics Club.

❖

Directing the activities of the committee secretariat will be the task of **Fred A. Darwin** (SM'46), newly appointed executive director of the Committee on Guided Missiles of the Research and Development Board, National Bureau of Standards.

Mr. Darwin was born in Chattanooga, Tenn., on May 28, 1913. He attended the University of Chattanooga from 1929 to 1931 and the U. S. Naval Academy at Annapolis, Md., from 1931 to 1935, receiving the bachelor of science degree in the latter year. In 1936 he was granted the M.S. degree in electrical communications engineering by Harvard University, and the following year he entered the employment of the Western Union Telegraph Company as an apprentice engineer. When he left in 1941, he had risen to the rank of senior engineering supervisor.

Upon the outbreak of war, Mr. Darwin joined the services as a naval reserve commander, heading the IFF (radar identification) and radar beacon design section in the radio division of the Navy Department's Bureau of Ships. In 1946 he joined the Hazeltine Electronics Corp. at Little Neck, L. I., N. Y.

Leo Edwin Shire (A'27), former export sales representative of the Beech Aircraft Corp. in Wichita, Kansas, died last year.

He was born on October 20, 1898, in Mexico, Mo., and received the B.S.E.E. degree from the Missouri University School of Mines and Metallurgy in 1925. Immediately after graduation he started his radio career in the engineering department of the Andean National Corp., Ltd., in Cartagena, Columbia, South America, and he remained there for a number of years.

❖

New associate director of *Tele-Tech*, television and communications engineering magazine, is **John H. Battison** (M'47-SM'49). A prolific writer of scientific articles for leading publications, Mr. Battison resigned from the American Broadcasting Co., where he had been employed as assistant chief allocations engineer since July, 1947, in order to take up his new post.

Mr. Battison was born in England on August 11, 1915, and educated at the University of London, from which he received the bachelor of science degree in radio communication in 1936. Meanwhile, in 1934, he had entered the employment of the E. K. Cole Radio Corp. as a research engineer, and he continued with that organization until 1937, when he became supervisor of radio equipment production for the British Air Ministry.

In 1939, upon the outbreak of hostilities, he joined the British Royal Air Force, and served six and one-half years as bomber pilot and squadron leader. At the war's end he came to the United States as research engineer for the Midland Broadcasting Co. in Kansas City, later becoming technical director for that company. He came to New York City in 1947 and served briefly with the Federal Radio and Telephone Co. before joining the American Broadcasting Co.

❖

Victor B. Corey (A'45) has been appointed manager of the engineering physics division of Fredric Flader, Inc. Associated with the company since 1946, Dr. Corey has supervised research and development on sonic true airspeed, true air temperature, and machine number indicators; radiation physics; servomechanisms for indication and control; analogue computers; and long-range automatic navigation.

Born in Missouri on February 9, 1915, Dr. Corey received the B.A. degree from Central College in Fayette, Mo., in 1937. Until 1941 he served as a teaching assistant in the physics department of the State University of Iowa; and was a research assistant at the University for a year following. He received the M.A. degree from the University of Iowa in 1939; the Ph.D. in 1942. From 1942 until 1946 he was research physicist for the Sylvania Electric Products Inc., in Flushing, N. Y.

Dr. Corey is a member of the American Physical Society, the Acoustical Society of America, and the American Association for the Advancement of Science.

The Program for New Aids to Air Navigation*

D. W. RENTZEL†

Air navigation requires adequate communication and desirable and comprehensive guidance means. A summary of present-day practices and a schedule of future plans in this field are presented in some detail by the Administrator of Civil Aeronautics of the United States Government. Engineers working, or planning to work in this field, will be well advised to study the contents of this address.—*The Editor.*

THE ART of piloting an aircraft from one spot to another, when the earth is invisible through cloud and storm, has progressed rapidly in the past 20 years. But today, civil and military aviation jointly are entering a revolutionary new phase of air navigation which will have a major impact on the American way of living, and on our ability to defend ourselves in case of war.

Back in the days when an airplane was a novelty, a pilot could fly when and where he pleased without fear of collision, providing he maintained a safe altitude above the ground. The notion of air traffic control would have amused and amazed him.

But by the early 1930's, enough air traffic had developed to make definite airways necessary, particularly in the more congested areas. Too, the need for guidance when the pilot no longer could see the earth became more and more pressing. As a result, the Federal Government installed a system of airways throughout the country, using the best radio devices known at that time.

This air navigation system centered largely around four-course low-frequency radio ranges, plus radio-location markers, and low- and medium-frequency voice communication channels. Just before the start of World War II, the Civil Aeronautics Administration began installing very-high-frequency instrument landing systems (ILS). This system, which provides radio beams down which a pilot can fly his plane until he sights the runway, was adopted by the military forces.

The low-frequency ranges and communication systems served a useful purpose, and still are in general use today. But they have serious drawbacks, and have been outmoded by new electronic inventions which appeared before and during the war.

Those of us who travel by commercial airlines know how uncertain the schedules are during periods of bad weather. This uncertainty has been a grave handicap in the development of air travel, and has slowed down the growth of air freight and air express, It has caused the airline companies tremendous annual losses.

This outmoded air navigation system also has seriously handicapped our military air operations using the same system during instrument weather conditions. Speed is the essence of modern warfare; in case of sudden attack we must be able to move large numbers of military aircraft quickly and unerringly to the points where they are needed. The enemy will not wait for favorable weather, or give us time to acquaint our pilots with unfamiliar devices.

Fortunately, all significant groups connected with civil and military aviation have agreed on a definite program to modernize our airways and make all-weather flying a universal reality. This program was developed through the Radio Technical Commission for Aeronautics, and the plan itself is commonly referred to in aviation circles as "SC-31," because it was prepared by Special Committee 31 of the RTCA.

The first, or transition, phase of this revolutionary new air navigation program will be completed about 1953. A good start already has been made in developing and installing the new devices needed for this part of the program. The ultimate program, which envisions some devices which a highly imaginative Buck Rogers might envy, is scheduled for completion about 1963.

Omnirange and DME

Now let us look at some of the old and the new air navigation equipment. Earlier, I mentioned the four-course low-frequency range. This range offers, as the name implies, only four paths to or from the range. In order to stay on one of these courses, the pilot must listen continuously to dots and dashes which blend together when he is in the exact center of the airway. Needless to say, this is exacting, and during thunderstorms and periods of heavy static, the range becomes difficult and even impossible to hear, There is danger, too, of the pilot confusing the courses and flying on a wrong heading.

To replace this kind of range, the CAA has been installing what is known as omnidirectional, or omniranges. These offer the pilot an almost unlimited number of courses which he may fly. And the omniranges, operating in the very high-frequency part of the radio spectrum, are largely free of static and interference.

Best of all, with the omnirange, the pilot can fly by eye instead of ear. An occasional glance at a vertical needle in his cockpit is all the pilot needs to keep him on the right heading. About 250 of these omniranges are now operating in the United States, and the CAA program calls for an eventual total of about 400, blanketing most of the country with signals.

The omnirange gives the pilot simple, clear information about the course he is flying. If he is flying northeast, for example, on a course of 45 degrees, the numerals zero four five will be continuously visible. And the words "to" or "from" will tell him clearly whether he is on a course to or from the station. This course indication is entirely independent of the aircraft compass, and shows the track actually being flown, regardless of cross winds and the plane's heading. The difference betwen the omnirange course and the indicated magnetic heading continuously shows the pilot the amount of correction necessary for cross winds. But the pilot need not concern himself with this unless he wishes; if he flies by the vertical needle his wind correction is automatic.

DME

Each omnirange eventually will be equipped with a device called "distance-measuring equipment," or DME. With suitable equipment in the aircraft, the pilot always will know his exact distance to the omnirange. This information will be displayed in the cockpit by a simple pointer on a dial. With the omnirange and the DME combined, the pilot continuously will know his exact position in space, without having to work out navigational problems.

In addition to all this, an electronic brain called a course-line computer has been developed. This device solves difficult navigation problems with the speed of light. Using this computer, a pilot will not need to fly directly to or from an omnirange. He can set a course from one selected point to another, and then let the computer, which uses signals from near-by omniranges, guide him accurately to his destination.

These new devices, all of which will come into general use in the next few years, will make possible multiple airways between cities, relieving the traffic congestion which already has passed the saturation point in many parts of the country.

Very-high-frequency voice radio, which is static-free, is coming into general use along the airways. It is making a definite contribution to safer flying. For the ultimate pro-

* Decimal classification: R526. Original manuscript received by the Institute, March 8, 1949. Presented, 1949 IRE National Convention, March 8, 1949, New York, N. Y.

† Civil Aeronautics Administration, Washington, D. C.

gram, however, a private-line system will be developed for instantaneous automatic transmission of information between ground and air.

So far, we have discussed the new equipment which will guide aircraft along their routes. Equally importanc, however, is the problem of getting them safely into the air, and onto the ground, during low visibility. For all-weather flying, this is just as important as safe and reliable navigation en route.

ILS and GCA

We have available today two entirely different methods of bringing aircraft safely to a landing through low ceilings. One, mentioned earlier, is called the "instrument landing system," and uses radio beams. The second, using precision radar principles discovered during the war, is called "ground-controlled approach (GCA)." Each system has advantages, and each system has drawbacks. Each *can* be used separately. But when used together, as recommended under the RTCA program, they provide the pilot with a double check on his position at all times, and achieves the closest to ultimate safety which our present knowledge permits.

With the "instrument landing system (ILS)" two radio beams are transmitted from the airfield. Received aboard the aircraft, these beams operate a cross-pointer indicator, which is simply a dial with two needles crossing in the center. The vertical needle, which also is used with the omnirange, tells the pilot whether he is properly lined up with the center of the runway and, if not, which way he must turn. The horizontal needle tells him whether he is above or below his proper glide path, and how to correct his descent, if necessary.

The ILS system is simple, positive, and in wide use by our scheduled airlines. Already, it has permitted the CAA to lower landing minimums from 400-foot ceilings to as low as 200 feet in many locations, greatly improving schedule reliability. Similar reductions in ceiling minimums have been approved where radar systems are in use.

The radar landing system, called "ground-controlled approach (GCA)", permits a controller on the ground to "talk the pilot down" over ordinary voice radio channels. The ground controller watches two radar screens.

The first, known as the surveillance radar screen, enables the operator to locate aircraft flying within a 30-mile radius of the airport. After positively identifying the aircraft on approach as a particular dot on the screen, the controller guides him safely into and through the holding pattern.

When the plane is ready to head in for a landing, a precision radar screen comes into play. The correct path to the runway is shown by lines on the screen, and if the dot representing the plane gets off the lines, the controller tells the pilot exactly how to correct his course.

This ground-controlled approach radar may be used independently, or to monitor an approach made on the instrument landing system.

At present there are about 80 civilian instrument landing systems in operation. We have improved-type surveillance and precision radar equipment for ground-controlled approaches at LaGuardia Field in New York, at Washington National Airport, and at Chicago. As rapidly as funds and manufacturers' delivery schedules permit, we are installing additional GCA radar sets at the busiest airports.

Radar

At other large airports CAA is planning to install the surveillance radar unit alone. This will permit the traffic controller to watch all the aircraft in his vicinity through radar, even when the weather has closed in. The controller can be certain that each plane is in its reported position, thus reducing collision hazards and speeding up the landing and takeoff sequences at the airport.

There has been some misunderstanding by the public of the whole subject of radar. Many people believed that war-developed radar would, in some magic way, instantly transform aviation into an all-weather transportation system, free of hazards and navigation problems. Ultimately, it promises to do just that. But we still have quite a way to go.

For one thing, military ground radar equipment designed for use on the fighting fronts proved to be inefficient and unsatisfactory for everyday civilian use. An extensive program was necessary to design, test, and produce ground radar which is economical and equally useful for civilian and military aircraft.

Airborne radar, as produced during the war, was a heavy item of equipment. Also, it required one or more men to operate it, in addition to other members of the crew. Overseas, where there were no other navigation aids, it was a necessary piece of military equipment, well worth the extra weight and manpower.

But in a country like the United States, with adequate navigation aids, airborne radar of the wartime type cannot justify itself in commercial operation. A pilot can get far more navigational information from radio ranges, and use it more easily, than from radar equipment in his plane.

However, airborne radar does show promise in two special fields. Numerous experiments have indicated that a satisfactory light-weight radar can be produced which will help pilots to detect and fly around thunderstorms and other turbulent areas. Eventually, also, someone may develop a satisfactory radar collision warning device.

New applications of radar and television really will come into their own in the ultimate RTCA program, which will provide an air traffic system of almost inconceivable magnitude and precision. Some of the equipment needed has not yet been invented. But the specifications have been laid down, and the principles on which it will operate are understood. No one doubts the ability of American electronic engineers to produce the needed air and ground devices.

By 1963

Here, in a general way, is how this ultimate air navigation system will work:

Even before a pilot takes off on a flight, a landing time will be reserved for him at his airport of destination. As he flies along, a dial will tell him in minutes and seconds whether he is ahead or behind his exact schedule, and he will slow down or speedup accordingly.

In the cockpit the pilot will see a pictorial presentation of everything around him. This picture, probably televised to him from the ground, will show his own aircraft in relation to others in his vicinity, indicate obstructions or other hazards, and even show the location of storms and turbulent air.

At the same time, radar will be continuously watching him from the ground. By means of a block system something like that used on railroads, the pilot will be assured that he is in safe air space at all times.

The aircraft of the 1960's will carry equipment which continuously transmits to the ground the readings of the various cockpit instruments. Electronic brains on the ground will check these readings automatically against information derived from radar and other sources. If, for example, the altitude shown by ground radar differs from altimeter reading in the cockpit, the pilot will be instantly and automatically notified.

If the pilot wishes to change his altitude or his flight plan, he will be able to query the ground stations by pushing an appropriate button. Approval or disapproval will be flashed back to his cockpit in a fraction of a second, since the calculations will be made by automatic machines on the ground.

This ultimate system, fantastic though it may sound, is designed to meet the everyday needs of civil and military aviation 15 years hence. It will, of course, solve the weather problems which plague aviation today, and it will permit aircraft to fly their schedules with clocklike precision and absolute reliability.

Furthermore, the RTCA system is designed with military as well as civilian requirements in mind. In case of war, the system will give instant warning of unfriendly aircraft, and permit interceptors to be vectored to attack. It will permit quick and heavy concentration of airpower anywhere it is needed within the country, and then will assist in maintaining a continuous flow of supplies and manpower to the area.

This tremendous new program, on which the Army, Navy, Air Force, and CAA are jointly agreed, will open the way for a whole new era of aviation in which the blessings of fast, safe, reliable low-cost transportation will be shared by every American citizen.

Multipath Television Reflections*

E. G. HILLS†, ASSOCIATE, IRE

Summary—The frequency dependence of the direction from which reflected television signals reach the receiver complicates the antenna design necessary to reduce reception of these reflected signals. A formula is derived for the strength of these reflections, and an analysis is made of some reflecting areas in order to find a reason for this frequency dependence. An antenna arrangement that appears particularly useful for reflection reduction is described.

ONE OF THE most difficult types of television interference to eliminate is that causing multiple images, or "ghosts," in the picture. Although in a great number of locations the transmitting stations are all in the same direction from the receiver, the reflections causing displaced images do not generally come from the same directions for all the stations. This has resulted in the widespread use of double antennas, one for the high and one for the low television bands, which can be individually oriented.

Let us consider a building or other object located at point A in Fig. 1 as causing a reflection such that sig-

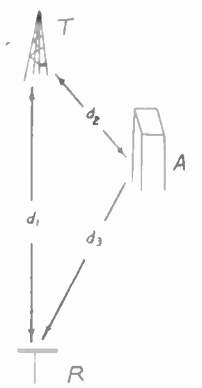

Fig. 1—Double-path transmission.

nals from the transmitter T reach the receiver R by path $d_2 - d_3$ as well as by path d_1. For an equivalent isotropic transmitter power P_t in the directions of interest the power per unit area incident on A is $P_t/4\pi d_2^2$. Let A be the equivalent isotropic reflecting area defined for incident and reflecting directions T, A and A, R, which differs from the area much used in radar calculations in which direction T, A is coincident with $-(A, R)$, while in this case of television reflection, no such relation exists between the two directions. The reflected energy incident on R will then be

$$\frac{P_t}{4\pi d_2^2} \cdot \frac{A}{4\pi d_3^2}.$$

The energy incident on R per unit area due to direct transmission from T will be $P_t/4\pi d_1^2$. The square root of the ratio of these two energy intensities will be the ratio of "ghost" field strength to signal field strength or

$$E_g/E_s = \tfrac{1}{2}(A/\pi)^{1/2} d_1/d_2 d_3. \tag{1}$$

The reflected signal will be relatively strongest when either d_2 or d_3 is a minimum and the other is nearly equal to d_1, which means that the source of reflection is near either the transmitter or the receiver. Due to the symmetry of (1) in d_2 and d_3, it makes no difference which the reflector is near. The formula can then be written

$$E_g/E_s \cong (A/\pi)^{1/2}/2d \tag{2}$$

where d is the shorter distance to either T or R when A is near one of them.

Reflections can then be divided into two categories: (1) those originating near the transmitter, all of which come from nearly the same direction as the desired signal, and (2) those that originate near the receiver, which can come from any direction. Reflections of the former type are obviously the harder to discriminate against by means of directional receiving antennas.

Since reflections do not all come from the same directions at different frequencies even though the transmitters are all located in the same direction from the receiver, if these reflections are originating in the vicinity of the receiving antenna, this must mean that the reflectors are relatively frequency sensitive. If the reflections originate in the vicinity of the transmitters no such conclusion can be drawn, since the angles at which incident waves from the various transmitters strike a given reflector would be different unless the transmitting antennas were extremely near each other relative to the distance from them to the source of reflection, which is not generally true of transmitting antennas located on tall buildings in a large city.

To see just how frequency sensitive various reflectors are, let us first consider a plane reflecting area large compared to a wavelength and oriented so as to produce the maximum reflection toward the receiver as shown in Fig. 2. The total energy incident on the plane will be equal to $S \cos \alpha_1 P_t/4\pi d_2^2$ where S is the physical area of the plane and α_1 the angle of incidence. The plane will then act as a uniformly excited plane array and will re-radiate with a beam width inversely proportional to frequency. Its isotropic gain, considering it as an antenna of area S will be[1] $4\pi S/\lambda^2$ where λ is the wave-

* Decimal classification: R583.7×R113.307. Original manuscript received by the Institute, November 26, 1948; revised manuscript received, March 21, 1949.
† Webster-Chicago Corp., Chicago, Ill.

[1] H. T. Friis, "Transmission line formula," PROC. I.R.E., vol. 34, pp. 254–256; May, 1946.

length. Its equivalent isotropic reflecting area will then be

$$A = (4\pi S^2 \cos a_1)/\lambda^2 \tag{3}$$

when the angle of incidence equals the angle of reflection. The ratio of carrier frequencies of the channel 13 and channel 2 television stations is 211.25 Mc/55.25 Mc or 3.82. The relative signal-"ghost" field strengths in the two channels for large flat reflecting surfaces would then be different by the same factor or 3.82. For reflectors several wavelengths across the angle of incidence equals the angle of reflection regardless of frequency. Therefore, if located near the receiver, such a plane should cause "ghosts" in all channels with the relative "ghost"-signal field strength changing by a factor of 3.82 as frequency is shifted from channel 2 to channel 13. If located near the transmitters, it would be coincidental if the angles of incidence and reflection were constant for more than one channel.

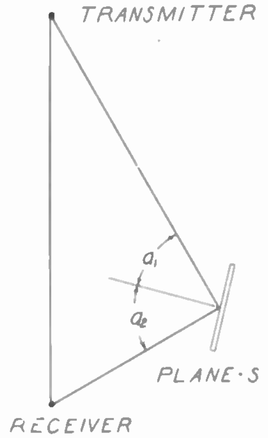

Fig. 2—Reflection from a plane surface.

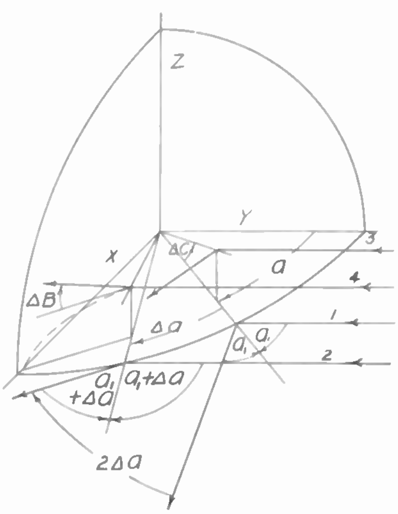

Fig. 3—Square cylinder of rays impinging on a sphere.

Let us now consider the echoing area of a sphere when the incident and reflected wave directions do not coincide. The laws of geometrical optics[2] apply if the sphere is large in wavelengths. Let us assume that a square cylinder of incident rays bounded by the lines 1, 2, 3, 4 of Fig. 3 impinges on the sphere. Assume that the rays are all parallel to the XY plane and that rays 1 and 2 lie in the XY plane. If incident ray 1 makes an angle of a_1 with the normal to the surface, its angle of reflection will also equal a_1. The angles of incidence and reflection of ray 2 are greater than those of ray 1 by Δa, so the two rays leave the surface no longer parallel but diverging at an angle $2\Delta a$.

Rays 3 and 4 are deflected both upward and to the left upon reflection. The angle ΔB that ray 4 makes with the XY plane after reflection is given by the formula from trigonometry

$$\sin \Delta B = 2 \tan \Delta C \cos (a_1 + \Delta a),$$

again assuming the angle of incidence equals the angle of reflection. This formula as Δa, ΔB, and ΔC approach zero approaches

$$B = 2\Delta C \cos a_1.$$

We see then that all of the energy incident in the square cylinder is reflected in a rectangular beam $2\Delta a_1$ wide and $2\Delta C \cos a_1$ deep. The area of the incident beam is $R^2\Delta C\Delta a \cos a_1$ where R is the radius of the sphere. If the beam has an intensity of I watts per unit area, the incident power is $IR^2\Delta C\Delta a \cos a_1$ watts. Dividing this power by the solid angle of the reflected beam we get $IR^2/4$ watts per steradian. If the sphere of radius R has an isotropic reflecting area of A, the power reflected by it in the direction of interest will be the same as if the total incident power IA were reflected uniformly over all 4π steradians. The signal intensity will then be

$$IA/4\pi = IR^2/4 \text{ watts per steradian.}$$

The echoing area of the sphere will then be, solving for A,

$$A = \pi R^2 \tag{4}$$

as is well known to be true when the directions of incidence and reflection coincide as in radar operation. Equation (4) shows that the area is independent of both frequency and the directions of incidence and reflection. Displaced images, then, caused by reflections from a spherical shaped object, should appear on all television channels with equal intensity regardless of where the object is located, provided the television transmitters are close together, compared to the distance between them and the reflector.

A similar analysis to the above for vertical cylinders, such as smoke stacks, where the radiation is always normal to the cylinder axis shows the echoing area of

[2] L. J. Chu, "Microwave Beam-Shaping Antennas," Research Laboratory of Electronics, MIT, Report 40; June, 1947.

such a cylinder to be

$$A = \frac{2\pi R h^2 \cos a}{\lambda} \tag{5}$$

where h is the cylinder height, R its radius, and a the angle of incidence with respect to a normal to the surface. This type of echoing area, like that of a flat plane, is dependent on the included angle between directions from the reflector to the transmitter and to the receiver, but is not dependent on a particular reflector orientation as is the plane reflector, and does not vary as rapidly in magnitude with frequency as does the equivalent isotropic area of a plane. The "ghost"-signal field strength ratio due to reflection from such a cylinder would then change from channel 2 to channel 13 by a factor of only $(3.82)^{1/2}$ or 1.96.

In considering smaller reflectors we might see how close an object must be for the receiver to give a visible displaced image. Assuming a "ghost"-signal field strength ratio visibility threshold for the television receiver of approximately 0.01 and an area equivalent to that of a sphere of 1.96 foot radius which, because of resonances occurring with such a small sphere, is 16.3 square feet[3] in both channels 2 and 13, the distance to the reflector would have to be

$$d = (A'/\pi)^{1/2} E_s / 2E_g = 114 \text{ feet},$$

which is so small that a displaced image caused by it would barely be visible as a "ghost." For objects smaller than this 1.96-foot sphere, the Raleigh sixth power law soon governs, and reflections quickly become negligible with decreasing reflector size, even though they are much more frequency-dependent than larger sized reflectors.

The corner reflectors so effective in radar work would, of course, be of little interest here because of the sparsity of structures simulating them, and because they would cause "ghosts" only if placed on a line passing through the receiver and transmitter, and not located on the portion of the line between the two.

Separately Orientable Array

One antenna type that can be used for countering the difficulty presented by the frequency dependence of the direction from which reflected television signals approach the receiver is one made up of several separately orientable arrays; one for each station in a particular locality. The various array outputs are fed into a filter unit which selects the desired array for a particular channel.

The antenna of Fig. 4 is made up of 7 four-element parasitic arrays. As the maximum number of stations presently to be located in any one service area is seven, and since in no area will two stations occupy adjacent channels, the arrays of Fig. 5 each cover two adjacent channels, except for the low-frequency array for each band which cover only one channel each. Fig. 5 shows a picture of the filter box used with the array. The box is

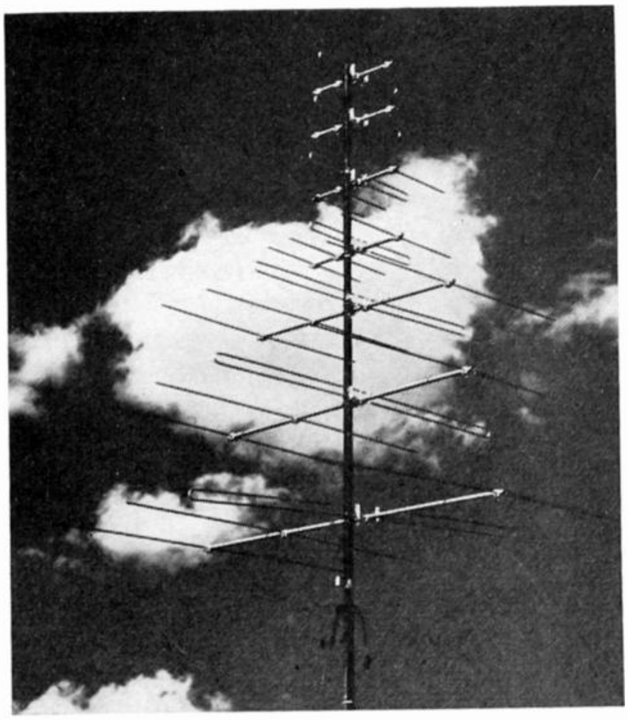

Fig. 4—An individually orientable antenna.

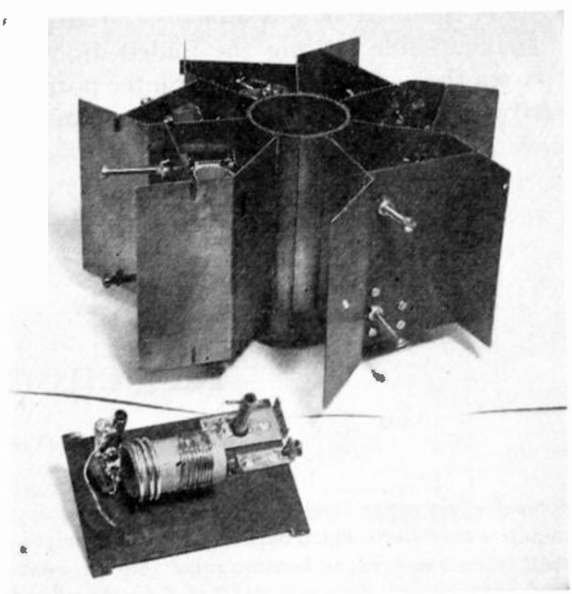

Fig. 5—A filter unit with cover removed.

designed to fit around the antenna mast so as to minimize the necessary lengths, for economic reasons, of the seven 92-ohm coaxial cables leading into the box. A single 300-ohm twin lead carries energy from the box to the receiver. The box contains seven doubly tuned filters, one of which is shown removed in the figure. The circuit of the filter unit is shown in Fig. 6. The filter unit serves to pass energy from a particular array to the main transmission line only at the desired frequencies

[3] P. J. Rubenstein, Research Laboratory of Electronics, MIT, Report 42; April 3, 1943.

of operation of the array, and to transform the 92-ohm impedance of each array up to the 300 ohms of the main transmission line.

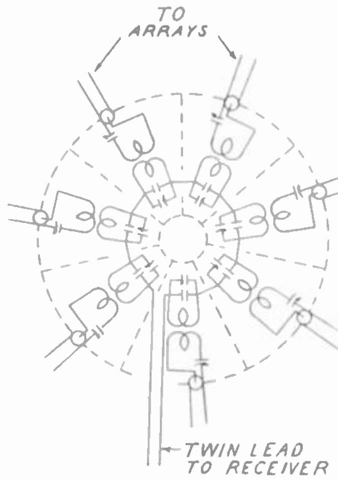

Fig. 6—Circuit of a filter unit.

Fig. 7 shows radiation patterns of the complete antenna with filter box when the arrays corresponding to the two filters in operation are oriented 90 degrees apart. These patterns were taken for two adjacent channels and at a frequency midway between the channels. The gain of the antenna is the 8 db of each array, minus the losses in the filter box at any particular frequency.

The coaxial cable feeding the folded dipole of each array passes through a hole in the center portion of the grounded part of the folded dipole and is run inside the tube of the dipole, so that the braid can be fastened to one of the dipole terminals and the central conductor of the cable to the other dipole terminal without unbalancing the normally balanced folded dipole. The seven arrays of the antenna show negligible mutual effects when two adjacent arrays are separated by a quarter wavelength at the frequency of the longer array.

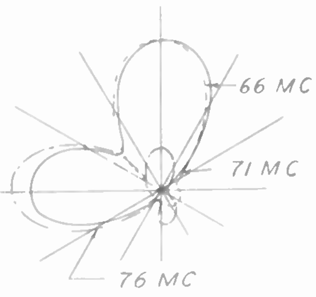

Fig. 7—Reception patterns of a complete antenna.

Conclusions

If the frequency dependence of reflected signal directions were reduced, the television receiving antenna problem would be considerably simplified. One possible solution to the problem would be to place all television transmitting antennas of a given service area on the same structure. Other possible solutions would be, of course, the development of improved receiving antennas, or improved "ghost" suppressors, such as of the delay line type, or the adoption of circularly polarized transmitting and receiving antennas.

Regenerative Amplifiers*

Y. P. YU†, ASSOCIATE, IRE

Summary—**This paper describes the principles and applications of regenerative amplifiers, which may be used, for example, to mark the instant when two voltages become equal. A peak voltmeter circuit based upon the switching properties of a regenerative amplifier is introduced to minimize the error encountered in measuring low duty-cycle pulses. The use of a regenerative amplifier in forming a pulse-width descriminator circuit is also described.**

Introduction

By EMPLOYING a large amount of regeneration, the output voltage of an amplifier can be made to change abruptly from one constant value to another when the input voltage is raised to a critical value, and to change back to its original value when the input is reduced to another critical value. A regenerative amplifier may be considered as a variant of the familiar Eccles-Jordan trigger circuit, with the difference that in the latter circuit only one switching process occurs during a single input pulse and the output voltage does not return to its original value until the arrival of the next pulse. In the regenerative amplifiers to be described two switching processes occur during a single input pulse, and the output voltage returns to its original value at the end of each input pulse.

Fig. 1 shows a typical regenerative amplifier circuit. The purpose of cathode follower T_3 is to remove the loading effect on the plate circuit of T_2 due to the screen current of T_1. Circuit constants of regenerative ampli-

* Decimal classification: R363.23. Original manuscript received by the Institute July 19, 1948; revised manuscript received, November 8, 1948.
† North Dakota State College, Fargo, N. Dak.

fiers may be determined by using Kirchhoff's law. With the calculated values listed in Fig. 1, the circuit will trigger on with $E_{out}=100$, and trigger off with $E_{out}=50$, for a difference in input voltage of one-half volt.

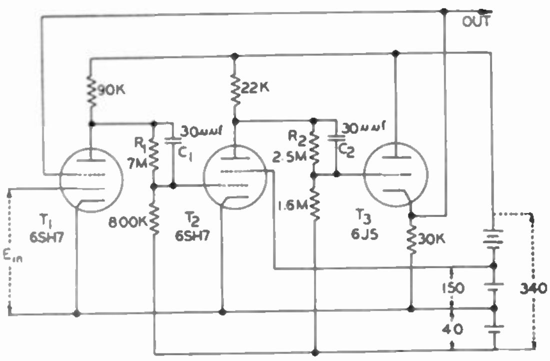

Fig. 1—A typical regenerative amplifier circuit. At the time of switching, C_1 and C_2 act as coupling capacitors.

Special Circuits

A variant of the circuit of Fig. 1 is shown in Fig. 2. This circuit can be adjusted to trigger on or off for the same critical value of input voltage, depending upon whether the input voltage is increasing or decreasing, respectively. Because positive feedback is introduced by the cathode resistor R_1, plate current can flow in only one tube at a time, and can be caused to transfer abruptly from one tube to the other by varying the input voltage. When the input voltage is zero or small, T_1 is cut off, and T_2 conducts. When the input voltage reaches a certain value, say E_c, the plate current of T_1 starts to flow, a switching process takes place and the plate current transfers from T_2 to T_1. Because the voltage across C cannot change instantly, the voltage on the screen of T_1 remains constant during the switching process. After the switching process, T_1 conducts, capacitor C discharges, and the screen voltage of T_1 reduces. The amount of reduction is governed by the magnitude of voltage E_1 because at the instant the grid of T_4 reaches E_1, diode T_3 conducts and further discharge of C is thereby stopped. This reduction lowers the operating path of T_1, i.e., causes T_1 to operate along a lower transfer characteristic. Thus the second switching process can be arranged to occur as soon as input voltage is reduced to E_c again (or even above E_c), by adjusting the magnitude of E_1. After the second switching process, T_1 is cut off and C charges back to its original value. The circuit is then ready to repeat the cycle when the input voltage reaches the same critical value. The choice of time constant R_2C is governed by the characteristics of the input voltage, such as repetition frequency, rise, and decay times.

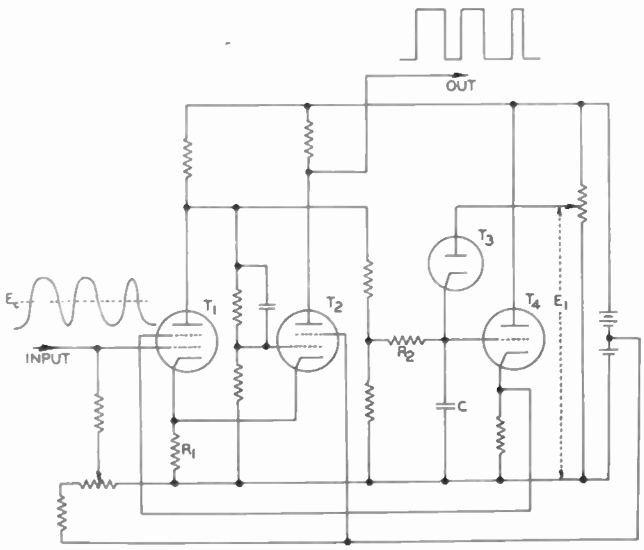

Fig. 2—Regenerative amplifier which can be adjusted to switch on and off at the same critical value of input voltage.

A somewhat different form of regenerative amplifier is shown in Fig. 3. This circuit generates a sharp positive pulse as soon as the unknown voltage equals the reference voltage. Either thermionic diodes or germanium crystals can be used for T_1 of this circuit, or for T_1 and T_2 of the circuit of Fig. 4. When the circuit is in its quiescent condition, the unknown voltage is higher than the reference voltage, and diode T_1 conducts. Thus the impedance between the grid of T_2 and ground is very small (approximately equal to the plate resistance of T_1 plus the internal impedance of the reference voltage source). The amount of regeneration is therefore very small and no oscillation can be expected. As soon as T_1 is cut off, the amount of regeneration greatly increases, and the grid voltage of T_2 reduces. Thus a switching process similar to that of other regenerative amplifiers

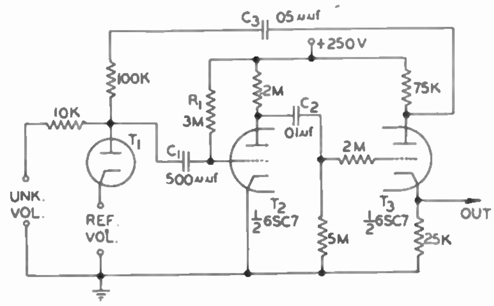

Fig. 3—In conjunction with a diode, a regenerative amplifier may be used to mark the instant when two voltages are equal.

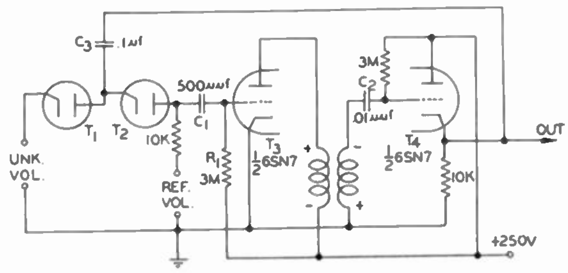

Fig. 4—Alternative method of using a regenerative amplifier for marking the instant when two voltages become equal.

takes place, and ends with T_2 cut off and T_3 carrying maximum current. Since the grid-leak resistor R_1 is returned to 250 volts, the grid voltage of T_2 increases exponentially toward 250 volts as C_1 discharges. When the cutoff point is reached, the plate current of T_2 begins to flow, a second switching process occurs, and the circuit returns to its normal condition. The sharpness of output pulse depends on the time constant R_1C_1.

The circuit of Fig. 4 generates a sharp negative pulse as soon as the unknown voltage equals the reference voltage. At this instant, diode T_2 conducts, and the amount of regeneration is hereby greatly increased. Therefore, cumulative processes will take place. The purpose of diode T_1 is to prevent C_3 from discharging through the unknown voltage source. The coupling transformer should provide a phase shift of 180 degrees. If the duration of the pulse is to be determined by the time constant R_1C_1, the mutual inductance of the coupling transformer must be large enough to support the pulse without material decay.

Peak Voltmeter Circuits

Regenerative amplifiers are well adapted to the measurement of the peak amplitude of voltage pulses. A peak voltmeter circuit, based upon the switching properties of a regenerative amplifier, is shown in block form in Fig. 5. Before the application of an input pulse, triode T is

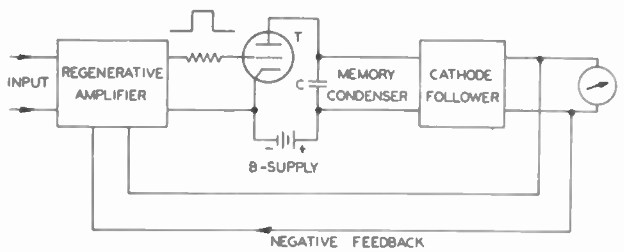

Fig. 5—Block diagram of a peak voltmeter circuit.

cut off, and the potential across C is zero. The regenerative amplifier is triggered by the leading ledge of the input pulse, and produces a positive voltage to drive the grid voltage of T to zero, or slightly positive. Then the memory capacitor C charges. The voltage across C is coupled through the cathode-follower to the indicating device which consists of a dc milliameter and a resistor in series. The input resistance of the cathode-follower is made very high in order to prolong the hold-on time of the memory capacitor C. The voltage on the indicating device is fed back negatively to the input terminal of the regenerative amplifier for the purpose of reducing the potential developed by the input pulse. Therefore the regenerative amplifier will trigger off as soon as the voltage on the indicating device equals the amplitude of the input pulse. This in turn cuts off the plate current of T and blocks C from further charging. Once triggered off, the regenerative amplifier remains so until the input voltage rises above the voltage on the indicating meter.

The principal advantages of peak voltmeters of this type are: (1) Errors encountered in measuring pulses of low repetition frequency and short duration are greatly reduced. This results because the use of the B-supply instead of the measured pulse or the output of an amplifier to charge the memory capacitor greatly shortens the charging time, and makes it possible to prolong the hold-on time by increasing the capacity of the memory capacitor. Furthermore, this meter employs a regenerative amplifier to trigger the charging current, thus permitting the final voltage of the memory capacitor to reach a value equal to the peak amplitude of the input pulse. (2) The meter reading is practically independent of circuit constants and operating voltages because the instrument is based on a comparison principle.

The circuit diagram of a practical instrument of this type is shown in Fig. 6. T_1, T_2, and T_3 are connected as a

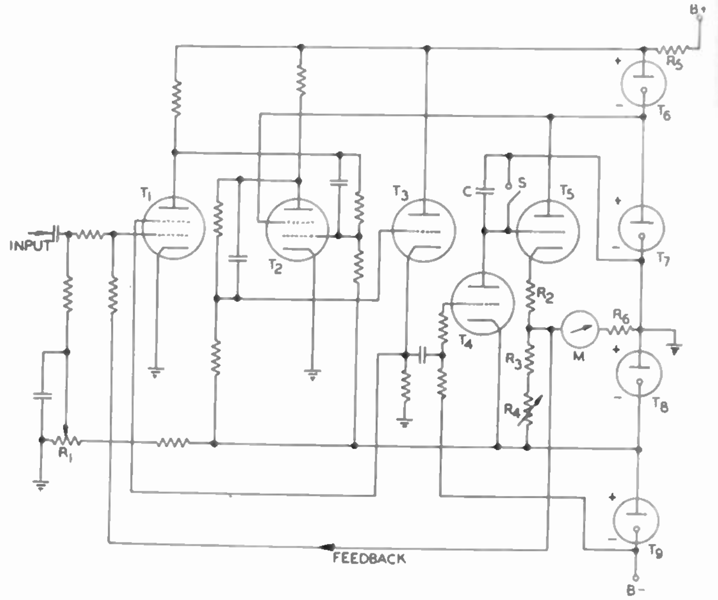

Fig. 6—Practical wiring diagram of the peak voltmeter of Fig. 5.

regenerative amplifier similar to that of Fig. 1. The function of T_4 is identical to that of triode T of Fig. 5. The negative bias voltages of T_1 to T_3 are all supplied by gas diode T_8. C functions as the memory capacitor. T_5 serves as a cathode-follower with output meter M and R_6 in series as its load. To minimize the leakage due to the grid current of T_5, resistor R_2 should be so dimensioned that T_5 operates just at its "floating-grid" potential, at which the positive grid current becomes equal to the negative (positive-ion) grid current. Switch S is used for reset, and potentiometer R_4 is the zero panel control. Before applying a signal to the input, potentiometer R_1 is adjusted so that T_1 operates just at the critical point of cutoff, a milliameter may be connected in series with the cathode of T_1 as an indicator for this adjustment. The regenerative amplifier is triggered by the application of a positive input pulse, and then T_4 conducts because the plate current of T_2 suddenly falls to zero. This in turn causes memory capacitor C to charge and develops a negative voltage across meter M and R_6. While this instrument is designed for measuring positive pulses, in conjunction with a phase inverter, it may also be used to measure negative pulses.

Pulse-Width Discriminator

The name applied to circuits whose output is proportional to the width of the input pulse is pulse-width discriminator. A regenerative amplifier may be used to augment the special circuit to be described to form a pulse-width discriminator. In Fig. 7, the input to the

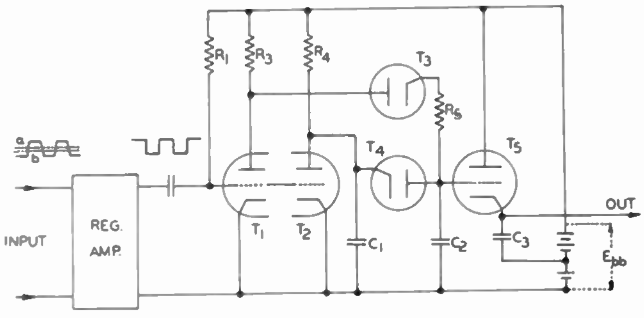

Fig. 7—Pulse-width discriminator circuit.

grids of T_1 and T_2 is taken from the plate of the normally off tube of the regenerative amplifier, which is adjusted to trigger on and off when the input voltage reaches levels a and b respectively. Thus, the regenerative amplifier acts as a pulse-slicer. When the circuit is in its quiescent condition, the grid-to-cathode potential of both T_1 and T_2 is zero, and T_5 (a sharp cutoff triode) is operating just at the critical point of cutoff. T_1 and T_2 are chosen to be identical in characteristics, and R_3 is made equal to R_4. Thus e_{c1} and e_{c2}, the potentials across capacitors C_1 and C_2 respectively, are equal to E_0 (see Fig. 8). The application of an input pulse drives the

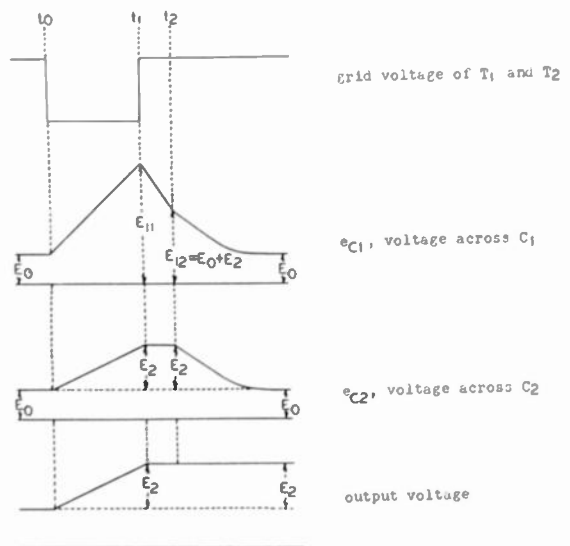

Fig. 8—Wave forms at various points of the circuit of Fig. 7.

grids of T_1 and T_2 far below cutoff. Therefore C_1 (with initial voltage E_0) charges, e_{c1} rises exponentially toward a final value of E_{bb} with a time constant of R_4C_1. We have

$$E_{11} = (E_{bb} - E_0)\left[1 - e^{-t/R_4C_1}\right] + E_0.$$

C_2 (with initial voltage E_0) also charges, but e_{c2} rises with a different time constant, namely, $(R_3+R_5)C_2$, assuming the plate resistance of diode T_3 equal to zero. We can write

$$E_2 = (E_{bb} - E_0)\left[1 - e^{-t_1/(R_3+R_5)C_2}\right].$$

After the pulse, T_1 and T_2 again conduct. C_1 (with initial voltage E_{11}) discharges, e_{c1} falls exponentially toward a final value of E_0 with a time constant equal to $C_1r_{p2}R_4/(r_{p2}+R_4)$, where r_{p2} is the plate resistance of T_2. But C_2 cannot discharge until e_{c1} reaches the value E_{12}, at which the potential across C_1 and C_2 are equal. Since t_1-t_2 is the amount of time required for C_1 to discharge from E_{11} to (E_0+E_2), we can find

$$t_2 - t_1 = \frac{C_1R_4r_{P2}}{R_4 + r_{P2}}\left[\ln\left(1 - e^{-t_1/R_4C_1}\right) - \ln\left(1 - e^{-t_1/(R_3+R_5)C_2}\right)\right].$$

After time t_2, both C_1 and C_2 discharge through triode T_2. If the plate resistance of diode T_4 is very small, the potentials across both capacitors are approximately equal and decrease exponentially toward E_0 with a time constant equal to $(C_1+C_2)r_{p2}R_4/(r_{p2}+R_4)$. During the pulse, from t_0 to t_1, triode T_5 conducts and capacitor C_3 charges because the grid of T_5 rises with e_{c2}. After the time t_2, triode T_5 is cut off and capacitor C_3 does not discharge. During the next cycle, T_5 will not conduct unless the width of the input pulse increases or the voltage across C_3 drops below that at the end of the previous cycle. The time between t_1 and t_2 serves to insure that the output voltage increases by an amount equal to E_2. Therefore (t_2-t_0) must be long enough to allow C_3 to charge up to a voltage equal to E_2. When the circuit of Fig. 7 is required to follow a series of pulsed signals of decreasing width, a proper resistance must be used to shunt capacitor C_3. In general the time constant of C_3 and its shunting resistance should be small enough to allow the output voltage to follow the decreasing of the input pulse width, and at the same time must be large enough to permit C_3 to hold most of its charge between pulses.

Acknowledgment

The author wishes to thank H. S. Dixon for his helpful suggestions in the preparation of this paper.

Bibliography

1. F. M. Colebrook, "A valve voltmeter with retroactive direct-voltage amplification," *Wireless Eng.*, vol. 15, pp. 138–142; March, 1938.
2. O. S. Puckle, "Time Baese," John Wiley and Sons, Inc., New York, N. Y., chap. 4; 1943.
3. B. Chance, "Some precision circuit techniques used in wave-form generation and time measurement," *Rev. Sci. Instr.*, vol. 17, pp. 396–415; October, 1946.

Design of Dissipative Band-Pass Filters Producing Desired Exact Amplitude-Frequency Characteristics*

MILTON DISHAL†, SENIOR MEMBER, IRE

Summary—The purpose of this paper is to present a basic method of obtaining the *exact* required values for all circuit constants in a band-pass network using *n* finite-*Q* resonant circuits to obtain either of two types of exact amplitude responses; the so-called critical shape-coupled, Butterworth, or transitional type of response, and the so-called over-coupled or Chebishev[1] type of response.

The equation giving the gain obtained with the desired response shape is derived. Equations for the exact phase characteristics associated with the above exact amplitude characteristics are also given.

Some comments are made concerning a somewhat similar method of design, which makes use of the so-called "poles" of the network.

Design sheets are presented giving the necessary equations for single-, double-, triple-, and stagger-tuned networks to produce either of the above two amplitude-response shapes.

1. Symbols

n = total number of resonant circuits in networks of Figs. 3 and 4.

N = total number of cascaded networks between which there is no coupling, e.g., separated by vacuum tubes.

$\vec{V}$ = complex voltage output at any frequency.

V = magnitude of the voltage output at any frequency. (See Fig. 7.)

V_p = magnitude of the voltage output at the frequency of peak response. (See Fig. 7.)

V_β = magnitude of the voltage output at that point on the response curve that the designer defines as the edge of the pass band. For response-shape C, this voltage output is identical with the response at the valleys of the response inside the pass band. (See Fig. 7.)

Δf = frequency bandwidth between response points whose voltage output is V. (See Fig. 7.)

Δf_p = frequency bandwidth between the peaks of response-shape C at the voltage output of V_p. (See Fig. 7.)

Δf_β = frequency bandwidth between the response points whose voltage output is V_β, i.e., the frequency bandwidth between the edges of the defined pass-band width. (See Fig. 7.)

f_0 = resonant frequency of each resonant circuit. See Section 3.2. f_0 is also the geometric mean frequency $(f_1f_2)^{1/2}$ between two frequencies f_1 and f_2 having the same voltage response.

ω_0 = resonant radian frequency $= 2\pi f_0$

F = total percentage bandwidth between two frequencies $F = (f/f_0 - f_0/f) = (f_2 - f_1)/f_0$, where $f_0 = (f_1f_2)^{1/2}$.

F_p = percentage bandwidth between peaks of response-shape $C (= \Delta f_p/f_0)$.

F_β = percentage bandwidth between edges of the defined pass-band width $[= (f_{\beta 2} - f_{\beta 1})/(f_{\beta 2}f_{\beta 1})^{1/2}]$.

d = total decrement of a resonant circuit. See Figs. 3 and 4.

G_n = *total* conductance across nth resonant circuit of node network $\left(= \frac{1}{R_n} + \frac{1}{Q_LX_{0L_n}} + \frac{1}{Q_cX_{0C_n}}\right)$. See Fig. 4(a).

R_n = *total* resistance in series with nth resonant circuit of mesh network $\left(= R_n + \frac{X_{0L_n}}{Q_L} + \frac{X_{0C_n}}{Q_c}\right)$. See Fig. 4(b).

Q = inverse of the total resonant-circuit decrement.

K = resultant coefficient of coupling between resonant circuits. (See Figs. 3 and 4, and Sections 3.1.2 and 3.2.2.

I = magnitude of the equivalent constant-current generator that drives the network of Fig. 3. For a pentode generator $I = g_mV_g$. For a "transformed" low-resistance generator, see Fig. 6.

C_n = *total* resonated capacitance in the nth resonant circuit.

L_n = *total* resonated inductance in the nth resonant circuit.

U_p = general symbol for a coefficient of some power of (jF) in the complex polynomial form of the circuit-response equations. The subscript of the U is identical with the power of (jF) for which U is the coefficient. (See Section 6.2 and (2).)

U_p^b, U_p^c = general symbol for a coefficient in that complex polynomial that produces the desired response-shape B and C, respectively. The subscript is identical with the power of (jF) for which U is the coefficient.

A_p, B_p, C_p, etc. = specific coefficient of that (jF) whose power is p, in that specific complex polynomial for a network that has as many resonant circuits as the numerical position of the letter in the alphabet, e.g., C_2 would be the coefficient of $(jF)^2$ in the polynomial

* Decimal classification: R143.2. Original manuscript received by the Institute, May 11, 1948; revised manuscript received, March 25, 1949. Presented, 1948 IRE National Convention, New York, N. Y., March 22, 1948, under the title, "Application of Tschebyscheff polynomials to the exact design of band-pass filters."

† Federal Telecommunication Laboratories, Inc., Nutley, N. J.

[1] This name is spelled variously in English, commonly as "Tchebyscheff."

for a triple-tuned network. (See Design Equations—Group 1.)

A_p^b, B_p^b; A_p^c, B_p^c; etc. = same as above, except applied to that specific polynomial that produces response-shapes B and C, respectively. (See Design Equations—Groups 2 and 4.)

$|\Delta_n|_{\min}$ = Minimum value of the magnitude of the complex polynomial for an n-resonant-circuit network. (See (3).)

$|\Delta_n^b|_{\min}$, $|\Delta_n^c|_{\min}$ = same as above, except for the complex polynomial for shapes B and C, respectively.

r_m^b, i_m^b = magnitudes of the real and imaginary parts, respectively, of the general expression for the complex roots of the equation giving response-shape B. These roots always occur in conjugate pairs and m is the pair number. (See Section 7.1 and (6).)

r_m^c, i_m^c = same as above for response-shape C. (See (26).)

θ_n^b, θ_n^c = phase angle, at the percentage bandwidth F, of the response shape (V_p/V), i.e., the θ in $(V_p/V) < \theta$, for amplitude-response-shapes B and C respectively, for an n-resonant-circuit network. (See (10).)

$T_n(F/F_\beta)$ = general Chebishev[4] polynomial in terms of the variable $(\Delta f/\Delta f_\beta)$ of highest power n. (See (17), (18), and (19).)

s_n, c_n = defined by (26).

2. Introduction

As the need increases for more and more channels in a given frequency band and as the voltage ratios between desired and undesired signals continue to increase, there will also be an increasing need for design information for band-pass filter networks that is more exact than that supplied by classical filter theory.

It is well known that when a continuously increasing attenuation is required outside of a given pass band, a straightforward method of producing a very high rate of increase in attenuation is to use a large number of correctly coupled and correctly damped resonant circuits.

For many designers, a further very important practical requirement arises at this point. For the exact design to be of practical value, *no lossless elements (no infinite Q's) should be required.* For multiple-resonant-circuit filters, this last requirement has apparently not received much attention. In general, it has been stated that any dissipation in the reactive elements of a filter degrades its performance at the edges of the pass band. With correctly designed networks, this last statement is not true. With correct circuit element values using finite Q's, the amplitude response can be made identical to that obtained with infinite-Q elements.

To show the increase in sharpness of cutoff as the number of resonant circuits is increased, the graphs of

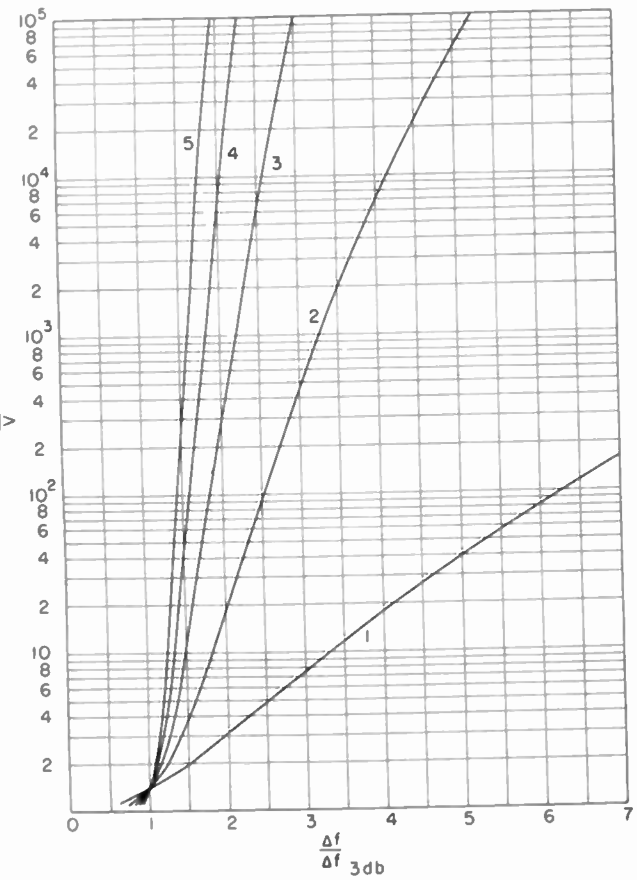

Fig. 1—Selectivity characteristic of 5 cascaded stages, each stage containing a correctly resonated n-resonant-circuit network having a proper Q distribution and being critical-shape-coupled. When f_0 and Δf are given, the two frequencies between which Δf occurs are $f_{12}=[f_0^2+(\Delta f/2)^2]^{1/2}+(\Delta f/2)$. When f_1 and f_2 are given, then $f_0=(f_1f_2)^{1/2}$. The number of tuned circuits per stage n is indicated on each curve. See (4) and (4a).

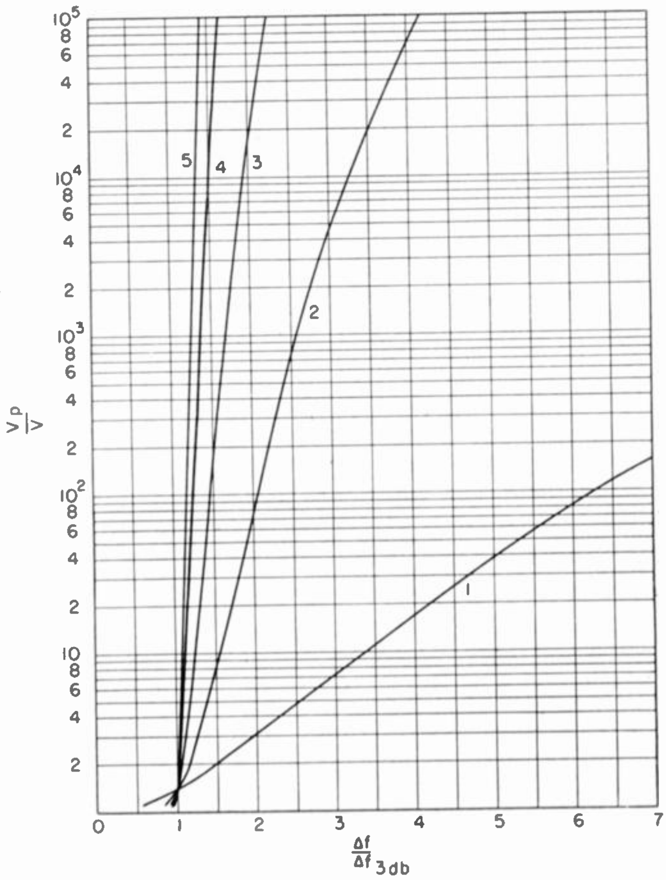

Fig. 2—Selectivity characteristic of 5 cascaded stages, each stage containing a correctly resonated n-resonant-circuit-network having a proper Q distribution and overcoupled for a 1-db peak-to-valley ratio. When f_0 and Δf are given, the two frequencies between which Δf occurs are $f_{12}=[f_0^2+(\Delta f/2)^2]^{1/2}+(\Delta f/2)$. When f_1 and f_2 are given, then $f_0=(f_1f_2)^{1/2}$. The number of tuned circuits per stage n is indicated on each curve. See (14) and (15).

takes place, and ends with T_2 cut off and T_3 carrying maximum current. Since the grid-leak resistor R_1 is returned to 250 volts, the grid voltage of T_2 increases exponentially toward 250 volts as C_1 discharges. When the cutoff point is reached, the plate current of T_2 begins to flow, a second switching process occurs, and the circuit returns to its normal condition. The sharpness of output pulse depends on the time constant R_1C_1.

The circuit of Fig. 4 generates a sharp negative pulse as soon as the unknown voltage equals the reference voltage. At this instant, diode T_2 conducts, and the amount of regeneration is hereby greatly increased. Therefore, cumulative processes will take place. The purpose of diode T_1 is to prevent C_3 from discharging through the unknown voltage source. The coupling transformer should provide a phase shift of 180 degrees. If the duration of the pulse is to be determined by the time constant R_1C_1, the mutual inductance of the coupling transformer must be large enough to support the pulse without material decay.

Peak Voltmeter Circuits

Regenerative amplifiers are well adapted to the measurement of the peak amplitude of voltage pulses. A peak voltmeter circuit, based upon the switching properties of a regenerative amplifier, is shown in block form in Fig. 5. Before the application of an input pulse, triode T is

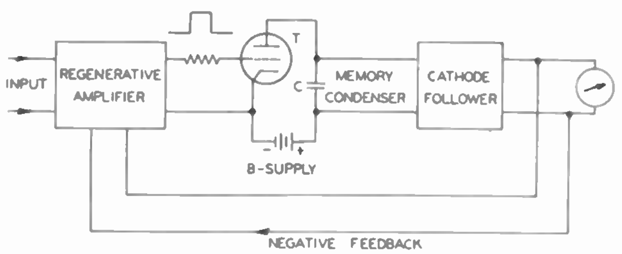

Fig. 5—Block diagram of a peak voltmeter circuit.

cut off, and the potential across C is zero. The regenerative amplifier is triggered by the leading ledge of the input pulse, and produces a positive voltage to drive the grid voltage of T to zero, or slightly positive. Then the memory capacitor C charges. The voltage across C is coupled through the cathode-follower to the indicating device which consists of a dc milliameter and a resistor in series. The input resistance of the cathode-follower is made very high in order to prolong the hold-on time of the memory capacitor C. The voltage on the indicating device is fed back negatively to the input terminal of the regenerative amplifier for the purpose of reducing the potential developed by the input pulse. Therefore the regenerative amplifier will trigger off as soon as the voltage on the indicating device equals the amplitude of the input pulse. This in turn cuts off the plate current of T and blocks C from further charging. Once triggered off, the regenerative amplifier remains so until the input voltage rises above the voltage on the indicating meter.

The principal advantages of peak voltmeters of this type are: (1) Errors encountered in measuring pulses of low repetition frequency and short duration are greatly reduced. This results because the use of the B-supply instead of the measured pulse or the output of an amplifier to charge the memory capacitor greatly shortens the charging time, and makes it possible to prolong the hold-on time by increasing the capacity of the memory capacitor. Furthermore, this meter employs a regenerative amplifier to trigger the charging current, thus permitting the final voltage of the memory capacitor to reach a value equal to the peak amplitude of the input pulse. (2) The meter reading is practically independent of circuit constants and operating voltages because the instrument is based on a comparison principle.

The circuit diagram of a practical instrument of this type is shown in Fig. 6. T_1, T_2, and T_3 are connected as a

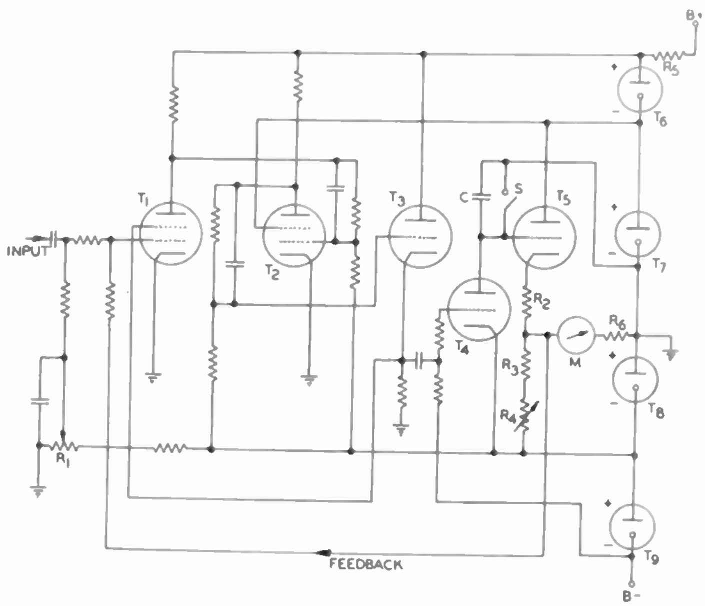

Fig. 6—Practical wiring diagram of the peak voltmeter of Fig. 5.

regenerative amplifier similar to that of Fig. 1. The function of T_4 is identical to that of triode T of Fig. 5. The negative bias voltages of T_1 to T_3 are all supplied by gas diode T_8. C functions as the memory capacitor. T_6 serves as a cathode-follower with output meter M and R_6 in series as its load. To minimize the leakage due to the grid current of T_5, resistor R_2 should be so dimensioned that T_5 operates just at its "floating-grid" potential, at which the positive grid current becomes equal to the negative (positive-ion) grid current. Switch S is used for reset, and potentiometer R_4 is the zero panel control. Before applying a signal to the input, potentiometer R_1 is adjusted so that T_1 operates just at the critical point of cutoff, a milliameter may be connected in series with the cathode of T_1 as an indicator for this adjustment. The regenerative amplifier is triggered by the application of a positive input pulse, and then T_4 conducts because the plate current of T_2 suddenly falls to zero. This in turn causes memory capacitor C to charge and develops a negative voltage across meter M and R_6. While this instrument is designed for measuring positive pulses, in conjunction with a phase inverter, it may also be used to measure negative pulses.

Pulse-width Discriminator

The name applied to circuits whose output is proportional to the width of the input pulse is pulse-width discriminator. A regenerative amplifier may be used to augment the special circuit to be described to form a pulse-width discriminator. In Fig. 7, the input to the

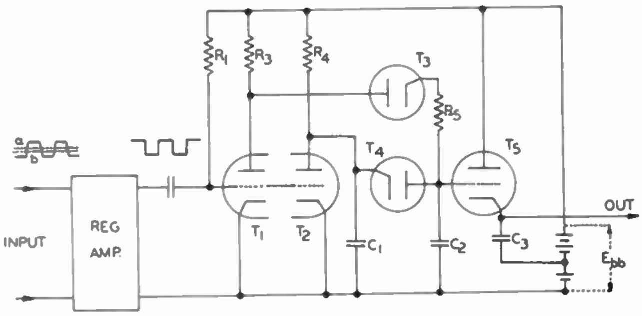

Fig. 7—Pulse-width discriminator circuit.

grids of T_1 and T_2 is taken from the plate of the normally off tube of the regenerative amplifier, which is adjusted to trigger on and off when the input voltage reaches levels a and b respectively. Thus, the regenerative amplifier acts as a pulse-slicer. When the circuit is in its quiescent condition, the grid-to-cathode potential of both T_1 and T_2 is zero, and T_5 (a sharp cutoff triode) is operating just at the critical point of cutoff. T_1 and T_2 are chosen to be identical in characteristics, and R_3 is made equal to R_4. Thus e_{c1} and e_{c2}, t he potentials across capacitors C_1 and C_2 respectively, are equal to E_0 (see Fig. 8). The application of an input pulse drives the

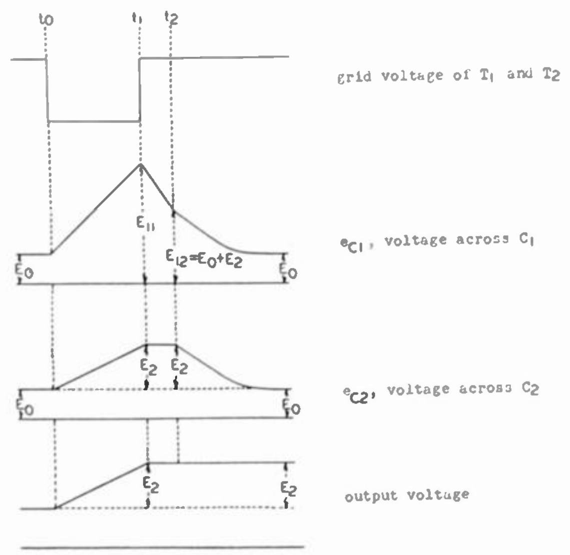

Fig. 8—Wave forms at various points of the circuit of Fig. 7.

grids of T_1 and T_2 far below cutoff. Therefore C_1 (with initial voltage E_0) charges, e_{c1} rises exponentially toward a final value of E_{bb} with a time constant of R_4C_1. We have

$$E_{11} = (E_{bb} - E_0)\left[1 - e^{-t/R_4C_1}\right] + E_0.$$

C_2 (with initial voltage E_0) also charges, but e_{c2} rises wlth a different time constant, namely, $(R_3+R_5)C_2$, assuming the plate resistance of diode T_3 equal to zero. We can write

$$E_2 = (E_{bb} - E_0)\left[1 - e^{-t_1/(R_3+R_5)C_2}\right].$$

After the pulse, T_1 and T_2 again conduct. C_1 (with initial voltage E_{11}) discharges, e_{c1} falls exponentially toward a final value of E_0 with a time constant equal to $C_1r_{p2}R_4/(r_{p2}+R_4)$, where r_{p2} is the plate resistance of T_2. But C_2 cannot discharge until e_{c1} reaches the value E_{12}, at which the potential across C_1 and C_2 are equal. Since t_1-t_2 is the amount of time required for C_1 to discharge from E_{11} to (E_0+E_2), we can find

$$t_2 - t_1 = \frac{C_1R_4r_{P2}}{R_4 + r_{P2}}\left[\ln\left(1 - e^{-t_1/R_4C_1}\right) - \ln\left(1 - e^{-t_1/(R_3+R_5)C_2}\right)\right].$$

After time t_2, both C_1 and C_2 discharge through triode T_2. If the plate resistance of diode T_4 is very small, the potentials across both capacitors are approximately equal and decrease exponentially toward E_0 with a time constant equal to $(C_1+C_2)r_{p2}R_4/(r_{p2}+R_4)$. During the pulse, from t_0 to t_1, triode T_5 conducts and capacitor C_3 charges because the grid of T_5 rises with e_{c2}. After the time t_2, triode T_5 is cut off and capacitor C_3 does not discharge. During the next cycle, T_5 will not conduct unless the width of the input pulse increases or the voltage across C_3 drops below that at the end of the previous cycle. The time between t_1 and t_2 serves to insure that the output voltage increases by an amount equal to E_2. Therefore (t_2-t_0) must be long enough to allow C_3 to charge up to a voltage equal to E_2. When the circuit of Fig. 7 is required to follow a series of pulsed signals of decreasing width, a proper resistance must be used to shunt capacitor C_3. In general the time constant of C_3 and its shunting resistance should be small enough to allow the output voltage to follow the decreasing of the input pulse width, and at the same time must be large enough to permit C_3 to hold most of its charge between pulses.

Acknowledgment

The author wishes to thank H. S. Dixon for his helpful suggestions in the preparation of this paper.

Bibliography

1. F. M. Colebrook, "A valve voltmeter with retroactive direct-voltage amplification," *Wireless Eng.*, vol. 15, pp. 138–142; March, 1938.
2. O. S. Puckle, "Time Baese," John Wiley and Sons, Inc., New York, N. Y., chap. 4; 1943.
3. B. Chance, "Some precision circuit techniques used in wave-form generation and time measurement," *Rev. Sci. Instr.*, vol. 17, pp. 396–415; October, 1946.

Design of Dissipative Band-Pass Filters Producing Desired Exact Amplitude-Frequency Characteristics*

MILTON DISHAL†, SENIOR MEMBER, IRE

Summary—**The purpose of this paper is to present a basic method of obtaining the *exact* required values for all circuit constants in a band-pass network using *n* finite-*Q* resonant circuits to obtain either of two types of exact amplitude responses; the so-called critical shape-coupled, Butterworth, or transitional type of response, and the so-called over-coupled or Chebishev[1] type of response.**

The equation giving the gain obtained with the desired response shape is derived. Equations for the exact phase characteristics associated with the above exact amplitude characteristics are also given.

Some comments are made concerning a somewhat similar method of design, which makes use of the so-called "poles" of the network.

Design sheets are presented giving the necessary equations for single-, double-, triple-, and stagger-tuned networks to produce either of the above two amplitude-response shapes.

1. Symbols

n = total number of resonant circuits in networks of Figs. 3 and 4.

N = total number of cascaded networks between which there is no coupling, e.g., separated by vacuum tubes.

$\vec{V}$ = complex voltage output at any frequency.

V = magnitude of the voltage output at any frequency. (See Fig. 7.)

V_p = magnitude of the voltage output at the frequency of peak response. (See Fig. 7.)

V_β = magnitude of the voltage output at that point on the response curve that the designer defines as the edge of the pass band. For response-shape C, this voltage output is identical with the response at the valleys of the response inside the pass band. (See Fig. 7.)

Δf = frequency bandwidth between response points whose voltage output is V. (See Fig. 7.)

Δf_p = frequency bandwidth between the peaks of response-shape C at the voltage output of V_p. (See Fig. 7.)

Δf_β = frequency bandwidth between the response points whose voltage output is V_β, i.e., the frequency bandwidth between the edges of the defined pass-band width. (See Fig. 7.)

f_0 = resonant frequency of each resonant circuit. See Section 3.2. f_0 is also the geometric mean frequency $(f_1f_2)^{1/2}$ between two frequencies f_1 and f_2 having the same voltage response.

ω_0 = resonant radian frequency $= 2\pi f_0$

F = total percentage bandwidth between two frequencies $F = (f/f_0 - f_0/f) = (f_2 - f_1)/f_0$, where $f_0 = (f_1f_2)^{1/2}$.

F_p = percentage bandwidth between peaks of response-shape $C (= \Delta f_p/f_0)$.

F_β = percentage bandwidth between edges of the defined pass-band width $[= (f_{\beta 2} - f_{\beta 1})/(f_{\beta 2}f_{\beta 1})^{1/2}]$.

d = total decrement of a resonant circuit. See Figs. 3 and 4.

G_n = *total* conductance across nth resonant circuit of node network $\left(= \frac{1}{R_n} + \frac{1}{Q_l X_{0L_n}} + \frac{1}{Q_c X_{0C_n}}\right)$. See Fig. 4(a).

R_n = *total* resistance in series with nth resonant circuit of mesh network $\left(= R_n + \frac{X_{0L_n}}{Q_L} + \frac{X_{0C_n}}{Q_c}\right)$. See Fig. 4(b).

Q = inverse of the total resonant-circuit decrement.

K = resultant coefficient of coupling between resonant circuits. (See Figs. 3 and 4, and Sections 3.1.2 and 3.2.2.

I = magnitude of the equivalent constant-current generator that drives the network of Fig. 3. For a pentode generator $I = g_m V_g$. For a "transformed" low-resistance generator, see Fig. 6.

C_n = *total* resonated capacitance in the nth resonant circuit.

L_n = *total* resonated inductance in the nth resonant circuit.

U_p = general symbol for a coefficient of some power of (jF) in the complex polynomial form of the circuit-response equations. The subscript of the U is identical with the power of (jF) for which U is the coefficient. (See Section 6.2 and (2).)

U_p^b, U_p^c = general symbol for a coefficient in that complex polynomial that produces the desired response-shape B and C, respectively. The subscript is identical with the power of (jF) for which U is the coefficient.

A_p, B_p, C_p, etc. = specific coefficient of that (jF) whose power is p, in that specific complex polynomial for a network that has as many resonant circuits as the numerical position of the letter in the alphabet, e.g., C_2 would be the coefficient of $(jF)^2$ in the polynomial

* Decimal classification: R143.2. Original manuscript received by the Institute, May 11, 1948; revised manuscript received, March 25, 1949. Presented, 1948 IRE National Convention, New York, N. Y., March 22, 1948, under the title, "Application of Tschebyscheff polynomials to the exact design of band-pass filters."

† Federal Telecommunication Laboratories, Inc., Nutley, N. J.

[1] This name is spelled variously in English, commonly as "Tchebyscheff."

for a triple-tuned network. (See Design Equations—Group 1.)

A_p^b, B_p^b; A_p^c, B_p^c; etc. = same as above, except applied to that specific polynomial that produces response-shapes B and C, respectively. (See Design Equations—Groups 2 and 4.)

$|\Delta_n|_{min}$ = Minimum value of the magnitude of the complex polynomial for an n-resonant-circuit network. (See (3).)

$|\Delta_n^b|_{min}$, $|\Delta_n^c|_{min}$ = same as above, except for the complex polynomial for shapes B and C, respectively.

r_m^b, i_m^b = magnitudes of the real and imaginary parts, respectively, of the general expression for the complex roots of the equation giving response-shape B. These roots always occur in conjugate pairs and m is the pair number. (See Section 7.1 and (6).)

r_m^c, i_m^c = same as above for response-shape C. (See (26).)

θ_n^b, θ_n^c = phase angle, at the percentage bandwidth F, of the response shape $(\overrightarrow{V_p/V})$, i.e., the θ in $(V_p/V)<\theta$, for amplitude-response-shapes B and C respectively, for an n-resonant-circuit network. (See (10).)

$T_n(F/F_\beta)$ = general Chebishev[1] polynomial in terms of the variable $(\Delta f/\Delta f_\beta)$ of highest power n. (See (17), (18), and (19).)

s_n, c_n = defined by (26).

2. Introduction

As the need increases for more and more channels in a given frequency band and as the voltage ratios between desired and undesired signals continue to increase, there will also be an increasing need for design information for band-pass filter networks that is more exact than that supplied by classical filter theory.

It is well known that when a continuously increasing attenuation is required outside of a given pass band, a straightforward method of producing a very high rate of increase in attenuation is to use a large number of correctly coupled and correctly damped resonant circuits.

For many designers, a further very important practical requirement arises at this point. For the exact design to be of practical value, *no lossless elements (no infinite Q's) should be required.* For multiple-resonant-circuit filters, this last requirement has apparently not received much attention. In general, it has been stated that any dissipation in the reactive elements of a filter degrades its performance at the edges of the pass band. With correctly designed networks, this last statement is not true. With correct circuit element values using finite Q's, the amplitude response can be made identical to that obtained with infinite-Q elements.

To show the increase in sharpness of cutoff as the number of resonant circuits is increased, the graphs of

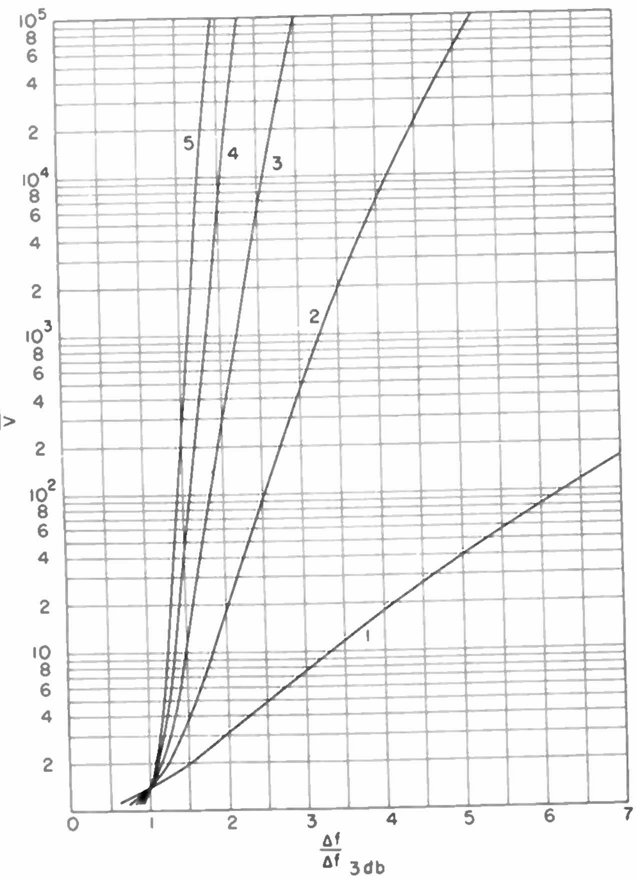

Fig. 1—Selectivity characteristic of 5 cascaded stages, each stage containing a correctly resonated n-resonant-circuit network having a proper Q distribution and being critical-shape-coupled. When f_0 and Δf are given, the two frequencies between which Δf occurs are $f_{12}=[f_0^2+(\Delta f/2)^2]^{1/2}+(\Delta f/2)$. When f_1 and f_2 are given, then $f_0=(f_1f_2)^{1/2}$. The number of tuned circuits per stage n is indicated on each curve. See (4) and (4a).

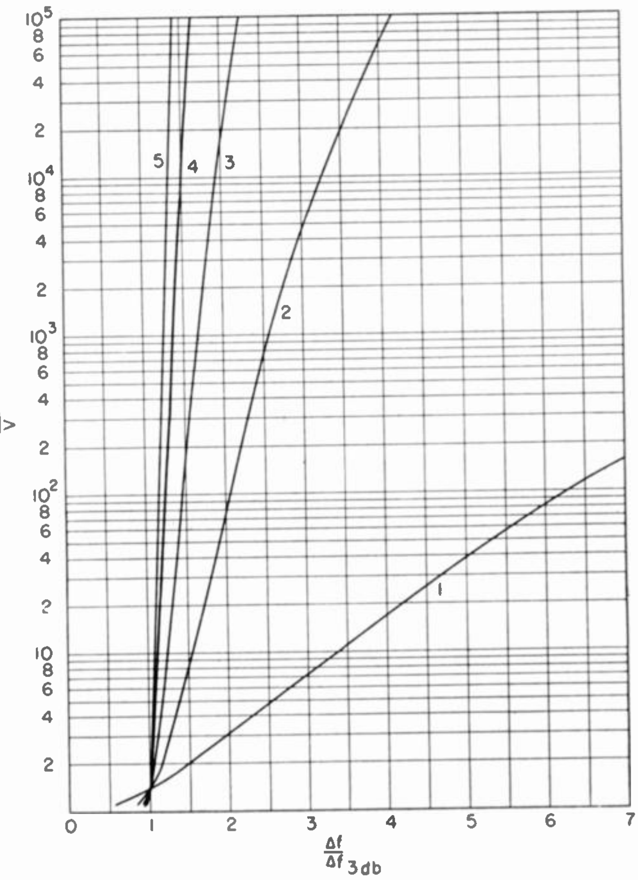

Fig. 2—Selectivity characteristic of 5 cascaded stages, each stage containing a correctly resonated n-resonant-circuit-network having a proper Q distribution and overcoupled for a 1-db peak-to-valley ratio. When f_0 and Δf are given, the two frequencies between which Δf occurs are $f_{12}=[f_0^2+(\Delta f/2)^2]^{1/2}+(\Delta f/2)$. When f_1 and f_2 are given, then $f_0=(f_1f_2)^{1/2}$. The number of tuned circuits per stage n is indicated on each curve. See (14) and (15).

Figs. 1 and 2 should be examined. For five cascaded stages, and a required adjacent-channel rejection of 100 db, the use of three resonant circuits per stage having an allowable peak-to-valley ratio in the pass band of 1 db more than doubles the available number of channels over the use of two resonant circuits per stage with critical-shape-coupled characteristics.

The major purpose of this paper is to present a method and some of the resulting equations for obtaining the necessary n simultaneous equations that must be solved to determine the exact circuit constants required for band-pass circuits that use n finite-Q resonant circuits ($n=1, 2, 3, 4, 5$, etc.) to produce either one of two types of exact response shapes; the so-called critical shape-coupled (maximally flat or transitional-shape-coupled) response, and the so-called overcoupled response.

Briefly the method proposed is as follows:

A. Express the determinant of the exact *circuit-response* equation in the form of a polynomial in $j(\Delta f/f_0)$ of highest power n, with descending consecutive powers.

B. Solve for the complex roots of the exact amplitude equation that describes the *desired-response* shape.

C. Use these roots to place the desired-response equation in the complex polynomial form described in *A*.

D. Equate the corresponding n coefficients.

3. Circuits and Circuit Constants

3.1 *Circuit Producing an Amplitude-Frequency Characteristic Having Exact Geometric Symmetry*

Fig. 3 shows the basic unbalanced band-pass "ladder network." As in the well-known constant-K filter, the

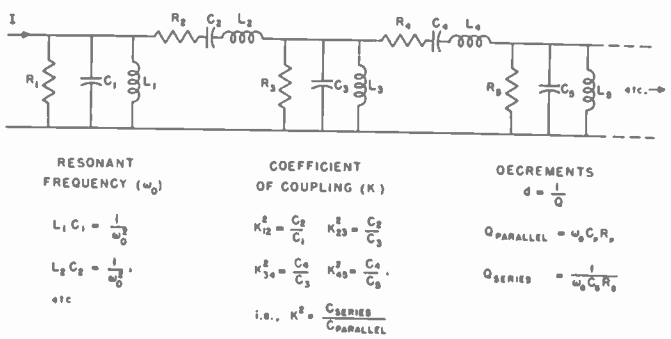

Fig. 3—The basic band-pass circuit that is analyzed and the circuit constants. The network may begin and/or end with either a series or a parallel arm. This network produces a response-frequency characteristic having perfect geometric symmetry for any percentage band width $(f_2-f_1)/(f_2f_1)^{1/2}$.

reactance structure of the series and shunt arms are inverse arms. However, it should be noted that in this paper each resonant circuit is considered to be dissipative, each circuit having its own specific Q. When correctly designed, this circuit can produce *for any percentage bandwidth* an amplitude response exactly described by the Butterworth and Chebishev equations given in sections 7 and 8. *This result can be accomplished using finite Q's in all resonant circuits.* It is worth repeating that, when this circuit can be used, no small-percentage passband approximation is required.

The chain may start and/or end with either a series or shunt arm. It should be realized that if the network starts with a series arm and a constant-current generator, e.g., pentode tube, drives the network, then the constant-current generator should be connected across the resistor that produces the required resonant-circuit decrement. Similarly, if the network ends in a series arm and output voltage is to be used, it must be obtained across the resistor that produces the correct resonant circuit decrement.

The circuit constants that exactly and conveniently describe the circuit of Fig. 3 are the resonant frequency f_0 of the series and shunt arms, the coefficient of coupling K between adjacent resonant circuits, and the decrement d of each resonant circuit. The definitions of these circuit constants are obtained from examination of the exact circuit response equations for a specific network in the form of Fig. 3 (using, for example, five resonant circuits).

3.1.1 *Resonant Frequency* f_0

In the circuit of Fig. 3, all series and shunt arms are tuned to exactly the same resonant frequency, $f_0=1/2\pi(LC)^{1/2}$. This frequency will also be the geometric mean frequency $(f_1f_2)^{1/2}$ between any two frequencies f_1 and f_2 having the same amplitude response.

3.1.2 *Coefficients of Coupling*

It is found that the determinant of the network of Fig. 3 can be expanded into the form of a polynomial in descending consecutive powers of $j[(f/f_0)-(f_0/f)]$; the coefficients of these various powers are completely independent of frequency and involve only the decrements of the resonant circuits and certain capacitance ratios. The capacitance appearing in the numerator of these ratios is always that of a series resonant circuit, and the denominator capacitance is always that of an adjacent shunt resonant circuit. In this paper, these capacitance ratios will be called coefficients of coupling (squared) because they define a required relation between adjacent resonant circuits, and also because they are exactly equivalent to the well-known coefficients of coupling in the small-percentage pass-band circuits of Figs. 4(a) and 4(b). Thus, between any two adjacent resonant circuits, $K=C_{\text{series}}/C_{\text{parallel}}$.

3.1.3 *Resonant-Circuit Decrement*

As they appear in the determinental equation, the resonant-circuit decrements d are the inverse of the well-known resonant-circuit Q's. For any series arm, $d=R_s\omega_0C_s$, where R_s is the resistance in series with that arm and C_s is the resonated capacitance of the arm. For any shunt arm, $d=1/R_p\omega_0C_p$, where R_p is the resistance in parallel with that arm and C_p is the resonated capacitance of the arm.

For high- and very-high-frequency band-pass circuits where shunt capacitance of the usual generators cannot be neglected), it should be noted that if the circuit of Fig. 3 is used only odd numbers of resonant circuits can be employed, i.e., the first and last resonant circuits must be parallel arms.

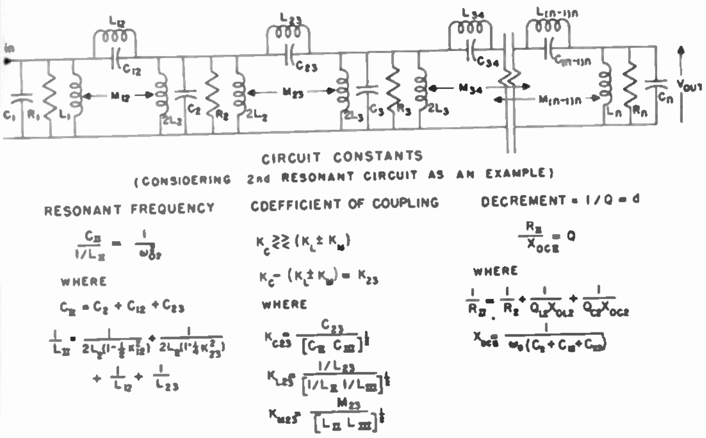

Fig. 4(a)—Basic node network to be analyzed and the resonant-circuit constants that are used. For small-percentage pass bands, this network is exactly equivalent to that of Fig. 3, when equal numbers of resonant circuits are used.

3.2 *Circuits Producing an Amplitude-Frequency Characteristic Having Geometric Symmetry for Only a Small-Percentage Bandwidth*

When the required pass band is small, the circuits of Figs. 4(a) and 4(b) are exactly equivalent to that of Fig. 3, and are usually more practical to build physically. When a small-percentage band pass is needed, the circuit of Fig. 3 is often not the most desirable. For instance, the required values for the coefficients of coupling between adjacent resonant circuits $[(C_{\text{series}}/C_{\text{parallel}})$ for Fig. 3] are approximately equal to the percentage bandwidth; thus we see that, for a 5 per cent bandwidth, the resonating capacitance of a series arm would have to be approximately 5 per cent of that used in the adjacent parallel branch; to satisfy the resonance requirement, the inductance in the series branch must be twenty times that in the adjacent shunt branch; a satisfactory inductance of this size is often undesirable or impractical.

Figs. 4(a) and 4(b) are not exactly equivalent to Fig. 3 because the effective coefficients of coupling between adjacent resonant circuits, which appear in the determinantal equations for the circuits of Figs. 4(a) and 4(b), are functions of frequency; i.e., we find that for Fig. 4(a), e.g., $K = K_C(f/f_0) - (K_L \pm K_M)(f_0/f)$. If we make the approximation that $K_C \gtrless (K_L + K_M)$ and $f/f_0 \doteq 1$, then the above K varies negligibly with frequency, and for the same number of resonant circuits the determinantal equations for Figs. 4(a), and 4(b) are identical.

The above assumption automatically means that the response null, which can be obtained with the circuits of Figs. 4(a) and 4(b), is placed far from the pass band. In the circuits of Fig. 4(a), this response null occurs exactly at $f_{\text{null}}/f_0 = [(K_L \pm K_M)/K_C]^{1/2}$. In the circuits of Fig. 4(b), this response null occurs exactly at $f_{\text{null}}/f_0 = [K_C/(K_L \pm K_M)]^{1/2}$.

Since the circuit of Fig. 4(a) has n nodes (where n is the number of resonant circuits used) and is most simply analyzed by the use of node equations, it will be called the node network, and the n-mesh circuit of Fig. 4(b) will be called the mesh network. It should be realized that these networks are physically different (thus supplying the designer with a variety of physical configurations) but are electrically related, in that wherever G, C, L, I, and V appear in the determinantal equation for Fig. 4(a), then R, L, C, E, and I appear in the corresponding determinantal equation for Fig. 4(b) (principle of duality).

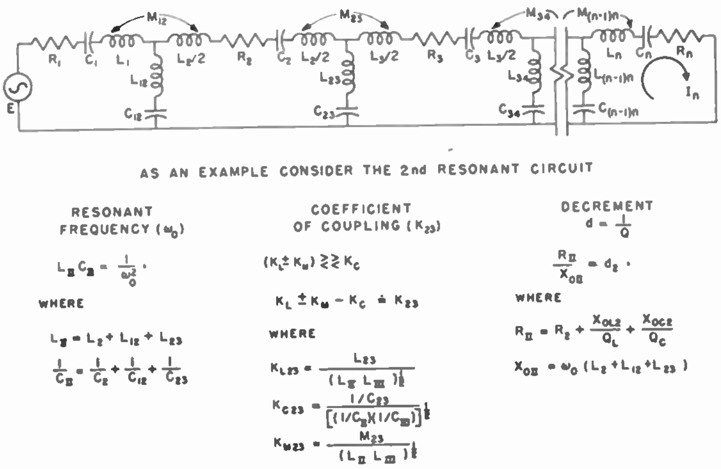

Fig. 4(b)—Basic mesh network to be analyzed and the resonant-circuit constants that describe it. For small-percentage pass bands, this network is exactly equivalent to that of Fig. 3, when equal numbers of resonant circuits are used.

It may be noted that when we use only the first two nodes of Fig. 4(a) with mutual-inductive coupling between these nodes, the familiar intermediate-frequency transformer of the common broadcast receiver is obtained.

For a small-percentage band pass, the constants that best describe the above circuits are the coefficients of coupling K between resonant circuits, the resonant frequency f_0 of the resonant circuits, the decrement d of the resonant circuits (inverse of the resonant-circuit Q).

It may be helpful for the reader to realize that the definitions of the above circuit constants are obtained from the exact node equations for a node network and from the exact mesh equations for a mesh network. Thus, if the reader will write the exact node equations for a triple-tuned circuit, then by correct manipulation, the above constants will be recognized. These constants, as they appear in the exact node and mesh equations, will now be described briefly.

3.2.1 *Exact Resonant Frequency f_0*

The resonant frequency f_0 of each node is that frequency at which the susceptance of the total capacitance (including mutual) attached to the node equals the susceptance of the *total* inductance (including mutual) attached to the node. Figs. 4(a) and 4(b) give this exact general resonance frequency.

In line with this definition, it should be noted that a fundamental and practical method of experimentally "tuning up" the resonant circuit attached to any node is effectively to short-circuit the two nodes on either side of the node in question, and then tune this resonant circuit for maximum output. In practice, the effective short-circuiting can be done by completely detuning the two adjacent nodes, thus allowing some signal transfer through the filter so that an output indicator at the end of the filter chain can be used for all the nodes. Mesh networks can be tuned up by effectively open-circuiting the two meshs on either side of the mesh in question, and then tuning the desired mesh for maximum response.

3.2.2 *Coefficient of Coupling*

The coefficient of any one type of coupling, C, L, or M, between any two nodes is the ratio of the susceptance of that type common to the two nodes in question to the geometric mean of the *total* susceptance of that type connected to each node. For the correct coefficient of coupling between any two meshes of Fig. 4(b), substitute in the above statement the word reactance for susceptance and mesh for node. Figs. 4(a) and 4(b) give these coefficients.[2]

Either inductive, capacitive, or mutual-inductive coupling, or a combination of them, may be used between the adjacent resonant circuits. The resultant coefficient of coupling is $K=[K_C(f/f_0)]-(K_L\pm K_M)(f_0/f)$ and in the analysis to be considered, the frequency at which this quantity equals zero must not occur within or near the pass band.

It should be realized that it is not necessary to use the same type of coupling between all the nodes of the network.

The designer will find that there is less chance of making an error in designing the coefficient of coupling if the following procedure is used: first, decide whether to use a node or a mesh network; second, decide what type of coupling to use; third, if a *node* network is to be used design the network *using the exact circuit configuration of Fig. 3* or if a *mesh* network is to be used use *the exact configuration of Fig. 4*; fourth, after the above design is completed then the T, π, or transformer equivalents of Fig. 5 can be used to obtain different circuit configurations that, depending on the specific problem, may be desirable.

3.2.3 *Resonant-Circuit Decrement $d=1/Q$*

For node networks, the decrement d of the resonant circuit is the ratio of the resultant equivalent conductance across the resonant circuit to the susceptance of the resonant frequency of either the total capacitance or total inductance. The term "equivalent" is used to indicate that any series resistance in the inductance or capacitance of the resonant circuit should be transformed into its equivalent shunt conductance and added to any actual shunt conductance present to obtain the total resonant-circuit conductance. Figs. 3 and 4 give the resonant-circuit decrement. Naturally any shunt conductance due to the generator and the load must be considered, when calculating the decrement of the input and output resonant circuits.

3.2.4 *Equivalent Generator*

With reference to the equivalent constant-current generator that drives the first node, there are in practice two situations to be considered. If a vacuum tube is attached directly to the input circuit, the equivalent generator is, of course, $g_m V_{kg}$. If a transforming circuit is used to couple the generator to the resonant circuit, then Fig. 6 gives the equivalent "reflected constant-current generator" for use with the node circuits (equivalent constant-voltage generator for use with the mesh circuits) and the "reflected decrement" portion of the total resonant-circuit decrement that results when a resistive generator and/or load are "transformed" into the first and last resonant circuits of the network. The equivalents of Fig. 6 thus allow application of the following analysis to the important practical cases where the actual generator is not a pentode but is, for example, the much-used equivalent 50-ohm generator and the load is, for example, a low-input-resistance crystal mixer. For this example, one could use a transforming circuit as given in Fig. 6 to couple the untuned generator and untuned load to the first and last resonant circuits of the chain.

When a certain response *shape* is to be produced, the function of the transforming circuit that couples a nonresonant generator and/or load to the first and/or last resonant circuit should be thought of in the following manner: The transforming circuit is used in conjunction with the generator and/or load resistance to couple a certain amount of decrement to the resonant circuit to make the total resulting resonant-circuit decrement equal to that value required to produce the desired-response shape. Note that one does not design the transforming circuit to produce a certain desired equivalent constant-current (or constant-voltage) generator.

The total resonant-circuit decrement is the sum of the above-considered "reflected decrement" and the "unloaded decrement" of the resonant circuit (which is the inverse of the unloaded Q of the resonant circuit). The inverse of the sum of these two decrements is then, of course, the resultant resonant-circuit Q.

4. Basic Response Shapes

When the resonant circuits are correctly tuned, there are three basic types of symmetrical band-pass shapes

[2] It should be noted that when more than two resonant circuits are in the network, this definition of coefficient of coupling is different from that given in Section IX of reference 16 of the bibliography. The required triple-tuned-circuit K given in references 16 and 17 must be divided by 1.414 to correspond to the K of this paper. The definition of coefficient of coupling given in this present paper leads to simpler numerical constants in the equations for the circuit response.

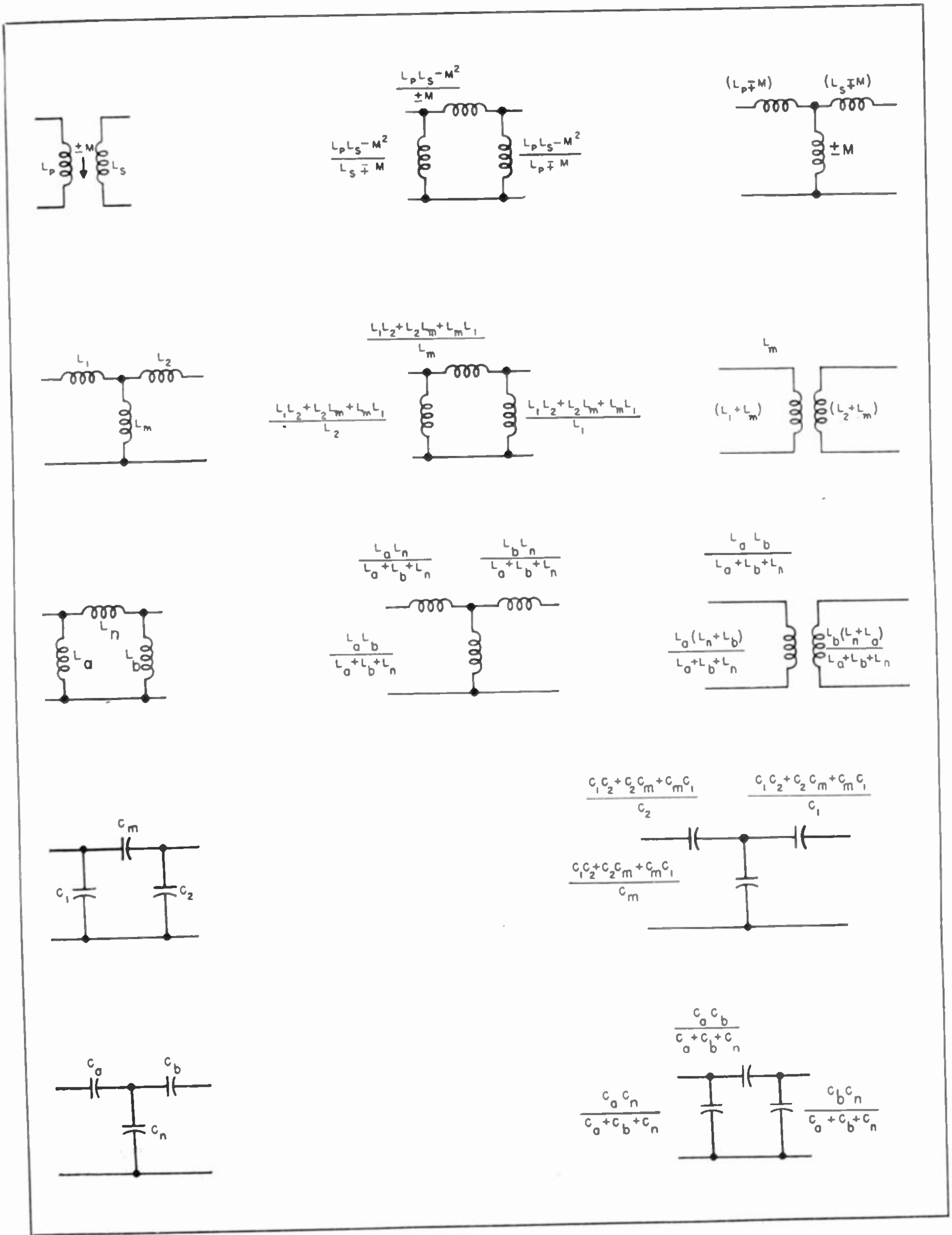

Fig. 5—Five different coupling methods and the transformer, T, and π equivalents. The use of these equivalents in the circuit of Fig. 4 enables the designer to obtain the same electrical performance with a large number of physically different circuits.

that can be used to give the same pass-band width.

Shape A: *This shape corresponds to that obtained with the well-known "undercoupled" condition for the familiar double-tuned circuit.* It may be described as a shape having a single maximum in the center of the pass band. It is not the squarest possible single maximum and the attenuation outside the pass band does not increase as rapidly as possible.

Shape B: *This shape corresponds to that obtained with the well-known "critical-shape coupled" condition for the familiar double-tuned circuit, and has also been called the "maximally flat" and the "transitional" shape.* It may be described as the type having the squarest possible single maximum in the center of the pass band and its attenuation outside the pass band increases as rapidly as possible while still maintaining a single-peaked response.

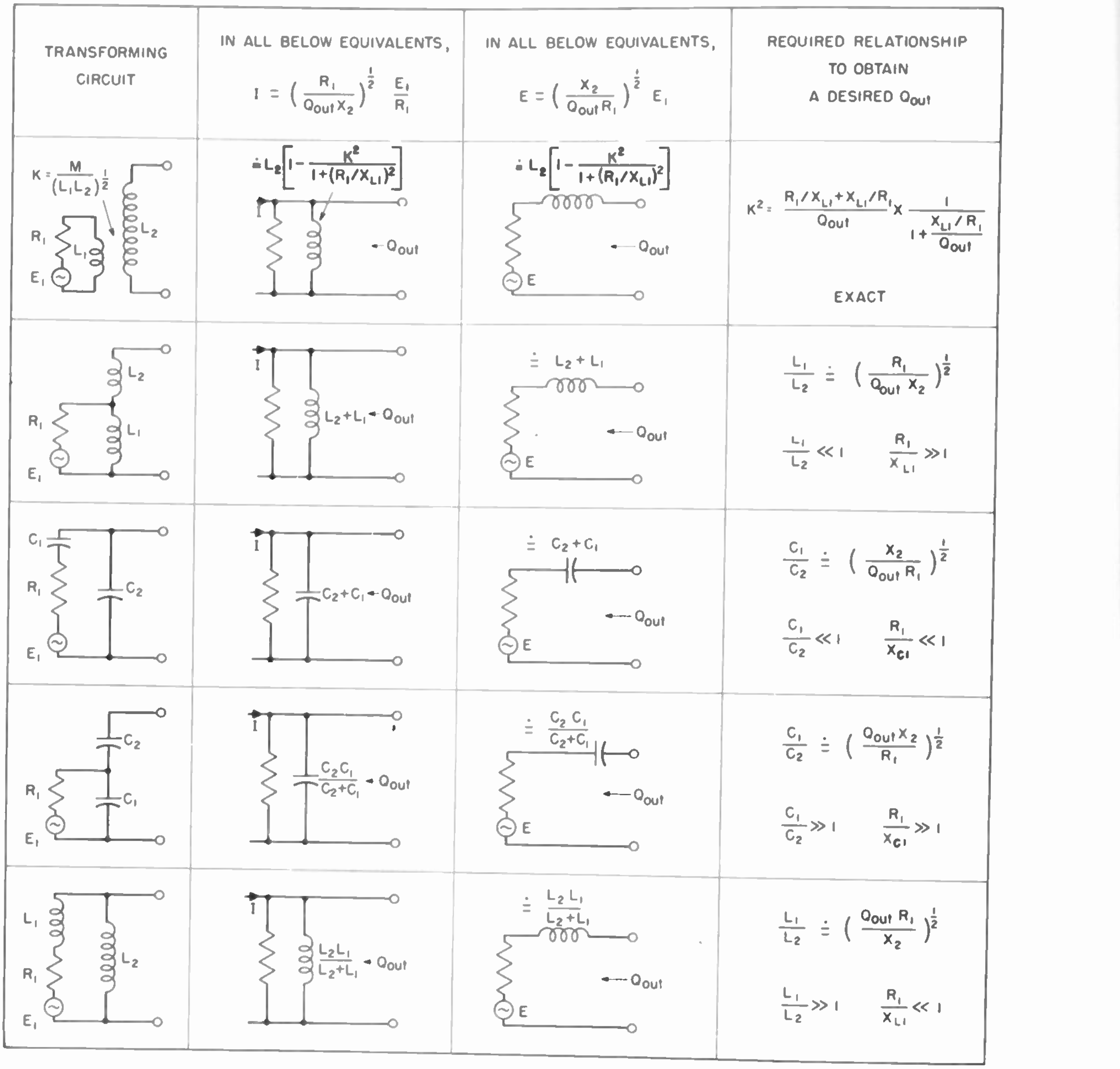

Fig. 6—Five methods of "transforming" a nonresonant generator and/or load into the first and/or last resonant circuit of the network, the equivalent constant-current (and constant-voltage) generator, and "reflected decrement." (See Section 3.)

Shape C: *This shape corresponds to that obtained with the well-known "overcoupled" condition for the familiar double-tuned band-pass circuit.* This type of shape has n maxima of equal height and $(n-1)$ minima of equal height inside the pass band, where n is the number of resonant circuits used. For a given allowable number of decibels down for the edges of the pass band, this shape gives the maximum possible rate of increase of attenuation outside the pass band.

An additional characteristic of response-shape C should be mentioned here: It will be found that no matter what the peak-to-valley ratio, there is a fixed ratio, dependent only on n, between the bandwidth across the outside peaks and the bandwidth of the skirts at that number of decibels down equal to the valley response. With response-shape C, the symbol Δf_B denotes this particular skirt bandwidth at the response value V_B that is equal to the valley response V_v.

Shape C_1: In many practical cases, the designer can allow, for example, 1-db dips inside the pass band, but would like to define the edges of the pass band as the 3-db down points. This type of response shape is a simple modification of the basic shape-C response. For example, suppose four coupled resonant circuits are to be used with an allowable peak-to-valley ratio of 1 db; the ratio between Δf_{1db} and Δf_{3db} is fixed by the above data and, if we know this ratio, we thus know that Δf_{1db} required to give the desired Δf_{3db} bandwidth. One then designs for the basic shape-C response (i.e., 1-db dips and the "pass-band edges" at 1 db down equal to the above-found Δf_{1db}).

In this paper, only response-shapes B and C will be

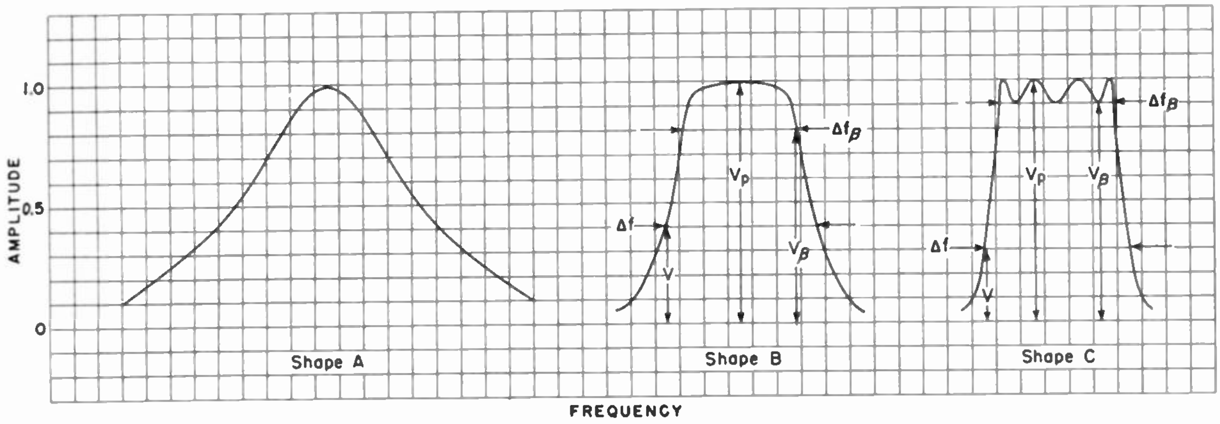

Fig. 7—The three geometrically symmetrical amplitude-response shapes considered and the shape constants to be used. These shapes are physically symmetrical when plotted on a logarithmic frequency scale.

considered. Fig. 7 gives the above described three response shapes, and the shape constants that describe the responses, for the voltage produced across the last node, when the node network of Fig. 4(a) is driven by a constant-current generator, and for the current produced in the last mesh when the mesh network of Fig. 4(b) is driven by a constant voltage generator.

5. Mathematical Procedure

The analytical procedure to be used in this paper consists of the following steps.

Step *A*. Express the general circuit response in its simplest possible form. For the networks of Figs. 3, 4(a), and 4(b), this form is that in which the determinantal equation is expressed as a polynomial in descending powers of $j[(f/f_0)-(f_0/f)]$.

Step *B*. Express the desired response equation in the same form as the general circuit-response equation.

Step *C*. Equate the corresponding coefficients in the two equations.

This will produce the necessary number of simultaneous equations.

6. Circuit Response Equations

6.1 *Polynomial Coefficients of Complex-Circuit-Response Equation*

Consider the design of the shape of the transfer impedance of the networks of Figs. 3 and 4(a), i.e., the resulting output voltage when the networks are correctly driven by a constant-current generator; and for the shape of the transfer admittance of the networks of Figs. 3 and 4(b), i.e., the resulting output current when the networks are correctly driven by a constant-voltage generator.

By the straightforward application of Kirchhoff's laws to any specific network in the form of Figs. 3 and 4, we find that the above-described transfer admittance and transfer impedance can be exactly written as

$$\left(\frac{V_{\text{out}}}{I_{\text{gen}}}\right) \text{ or } \left(\frac{I_{\text{out}}}{E_{\text{gen}}}\right) = \frac{(\text{Numerator})_n}{(jF)^n + U_{n-1}(jF)^{n-1} + U_{n-2}(jF)^{n-2}\cdots U_2(jF)^2 + U_1(jF) + U_0} \quad (1)$$

For all the node networks of Fig. 4(a) and for all the networks of Fig. 3 that begin and end with shunt arms, the numerator for $(V_{\text{out}}/I_{\text{gen}})$ of (1) is

$$(\text{Numerator})_n = \frac{1}{\omega_0(C_1C_n)^{1/2}} K_{12}K_{23}K_{34}\cdots K_{(n-1)n}, \quad (1a)$$

where the K's are defined in Figs. 3 and 4(a).

For all the mesh networks of Fig. 4(b) and for all the networks of Fig. 3 that begin and end with series arms, the numerator for $(I_{\text{out}}/E_{\text{gen}})$ of (1) is

$$(\text{Numerator})_n = \frac{1}{\omega_0(L_1L_n)^{1/2}} K_{12}K_{23}K_{34}\cdots K_{(n-1)n}, \quad (1b)$$

where the K's are defined in Figs. 3 and 4(b).

The denominator of (1) is a polynomial in consecutive powers of $j[(f/f_0)-(f_0/f)]$, the highest power being n the number of resonant circuits used and, within the limitations of the discussion of Section 3, the coefficients (U) of the polynomial are independent of frequency and are functions of only the coefficients of coupling K and decrements d as they are described in Section 3.

Since the numerator of (1) is independent of frequency within the limitations of the discussion of Section 3, *the response shape is fixed entirely by the denominator* of (1). For the same number of resonant circuits, the denominators Δ_n are identical for all the networks of Figs. 3 and 4.

In the general notation of (1), U is used to denote an arbitrary number of resonant circuits. For any specific network, the letter used in the coefficients will be that one whose numerical position in the alphabet corresponds to the number of resonant circuits in the network. Thus, for a 5-resonant-circuit network, we would use E to represent the coefficients. The subscript on any coefficient is exactly the same as the power of the (jF) for which it is the coefficient. Thus, for example, for a 4-resonant-circuit network, the coefficient of $(jF)^3$ would be represented by D_3.

Since the numerator of (1) is independent of frequency, the peak value of the transfer admittance or transfer impedance is given by

$$\left(\frac{V_{\text{out}}}{I_{\text{gen}}}\right)_{\text{peak}} \quad \text{or} \quad \left(\frac{I_{\text{out}}}{E_{\text{gen}}}\right)_{\text{peak}} = \frac{(\text{Numerator})_n}{|\Delta_n|_{\min}}, \tag{2}$$

where $|\Delta_n|_{\min}$ is the minimum magnitude of the polynomial of (1).

Equation (2) will be used in a later section of this paper to find the gain obtained at the amplitude response peaks.

Dividing (2) by (1), we obtain the ratio of the peak response to the response at any frequency; this is the basic response-*shape* equation:

$$\frac{V_p}{V} \text{ or } \frac{I_p}{I} = \frac{1}{|\Delta_n|_{\min}} \left[(jF)^n + U_{n-1}(jF)^{n-1}\right.$$
$$\left. + U_{n-2}(jF)^{n-2} + \cdots + U_2(jF)^2 + U_1(jF) + U_0\right]. \tag{3}$$

In Design Equations—Group 1, the specific circuit-response-shape equations are listed for $n=1, 2, 3$, and 4.

Careful study of the series of response equations given in Design Equations—Group 1 will show the law of formation of the coefficients, and it should now be possible to write the general exact complex response equation for a chain containing any number of resonant circuits.

Insofar as plotting of a response curve is concerned, the above equations enable us to obtain methodically the equations required to plot the amplitude- and phase-response shapes for any number of tuned circuits, once the various circuit coefficient of couplings and Q's are specified. The complex equation of Design Equations—Group 1 are, of course, expanded into their magnitude and phase-angle form when we plot the amplitude-and phase-response shapes. (All the even powers of (jF) are algebraically added together to give the real part of the determinant, all the odd powers of (jF) are added together algebraically to give the imaginary part of the determinant.)

7. Response Shape B

7.1 *Desired-Shape Equation*

Our next step is to express the desired-shape equation given below in the form of Design Equations—Group 1, so that we can equate the above coefficients (U_1, U_2, U_3, etc.) to the corresponding coefficients of the desired-response equation.

When the straightforward procedure mentioned in Section 5 of this paper is applied to single-, double-, and triple-tuned filters, we find that the magnitude equations that result are exactly given by the general equation (4). This equation and the corresponding response shape are also shown in Fig. 8.

$$\left(\frac{V_p}{V}\right)^2 = \{1 + [(V_p/V_\beta)^2 - 1][F/F_\beta]^{2n}\}. \tag{4}$$

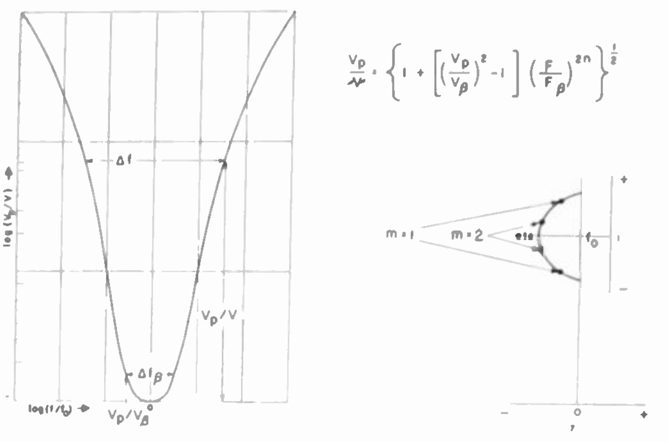

Fig. 8—The exact equation describing response-shape B and the location of the roots of this equation on a semicircle on the complex plane. Equation (6) gives the exact root values. n is the number of resonant circuits used and the response equation for an n-resonant-circuit network will have n roots.

Remember that $F = [(f/f_0) - (f_0/f)]$ has the same numerical value for two different frequencies related to each other by $f_1 = f_0^2/f_2$, i.e., the actual response-frequency curve of Fig. 4 will have geometric symmetry. To make the two sides of the response-frequency curve physically symmetrical, we should use a logarithmic frequency scale. Also, realize that

$$F_\beta = \left(\frac{f_{\beta 2}}{f_0} - \frac{f_0}{f_{\beta 2}}\right) = -\left(\frac{f_{\beta 1}}{f_0} - \frac{f_0}{f_{\beta 1}}\right) = \frac{f_{\beta 2} - f_{\beta 1}}{(f_{\beta 2} f_{\beta 1})^{1/2}} = \frac{\Delta f_\beta}{f_0}.$$

Solving for $\Delta f/\Delta f_\beta$, we have the useful equation

$$\frac{F}{F_\beta} = \left[\frac{(V_p/V)^2 - 1}{(V_p/V_\beta)^2 - 1}\right]^{1/2n} \tag{4a}$$

where n is the total number of resonant circuits used in the filter chain. Equation (4a) was used to plot the response curves of Fig. 1.

Figs. 1 and 2 (see (14) and (15)) have been plotted in terms of the *numerical* bandwidth Δf to make them independent of a particular percentage bandwidth. The two frequencies producing a given Δf are then related to the resonant frequency f_0 by $f_{12} = [f_0^2 + (\Delta f/2)]^2 \pm (\Delta f/2)$. We note from this equation that for small percentage bandwidths, i.e., $f_0 \gg \Delta f/2$ the frequency plot of the resonance curve will have arithmetic symmetry.

Insofar as cascades of networks are concerned, it should be realized, of course, that the voltage ratios of (4) and (4a) apply to one network, and when N identical networks are cascaded (i.e., separated by tubes) the voltage ratios to be used in (4) and (4a) must be the Nth root of the desired resultant voltage ratio.

We will here assume that this type of response shape given by (4) can be obtained for any number of coupled resonant circuits.

Solving for the roots of (4) we find this equation can be expressed in complex form

$$\frac{V_p}{\vec{V}} = \frac{1}{\dfrac{F_\beta^n}{[(V_p/V_\beta)^2-1]^{1/2}}}\{[jF-(-r_1^b+ji_1^b)][jF-(-r_1^b-ji_1^b)][jF-(-r_2^b+ji_2^b)][jF-(-r_2^b-ji_2^b)]\cdots\} \quad (5)$$

where the real (r_m^b) and imaginary (i_m^b) parts of the roots are given by (6a) and (6b).

$$r_m^b = F_\beta\{1/[(V_p/V_\beta)^2-1]^{1/2n}\}\sin\left(\frac{2m-1}{n}\frac{\pi}{2}\right), \quad (6a)$$

$$i_m^b = F_\beta\{1/[(V_p/V_\beta)^2-1]^{1/2n}\}\cos\left(\frac{2m-1}{n}\frac{\pi}{2}\right), \quad (6b)$$

$m = 1, 2, 3, \cdots n/2$ for n even or $(n+1)/2$ for n odd, where n is the total number of tuned circuits used.

The meaning of the letter m should be made clear by the following discussion. The complex roots of the response equation always occur in conjugate pairs, i.e., $(r+ji)$ and $(r-ji)$, and m is the *pair number* of the various pairs of roots. As plotted in the complex plane, these roots fall on a *half circle* whose center is f_0 as shown in Fig. 8 for 4 resonant circuits. It will be seen that $m=1$ *gives the pair of roots whose real-frequency component is farthest from the midfrequency,* $m=2$ gives the pair of roots whose real-frequency components is next farthest from the midfrequency, etc. The maximum value that m can reach is that which makes the cos factor equal zero and simultaneously, of course, the sin factor equals unity. Thus m_{max} is $n/2$ for an even number of resonant circuits and $(n+1)/2$ for an odd number of resonant circuits.

By multiplying out the correct number of terms of the above general equation (5), we can prepare a list of general-shape equations for $n=1, 2, 3$, etc., which are in exactly the form taken by the general-response equations of Design Equations—Group 1. *We use exactly as many factors of* (5) *as there are tuned circuits n.* These resulting equations are given in Design Equations—Group 2. We can now compare Design Equations—Groups 1 and 2 and equate the corresponding coefficients. Carrying out this procedure, we obtain the sets of simultaneous equations given in Design Equations—Group 3 which have to be solved to find the required circuit constants that will produce the B type of response shape. The simultaneous equations up to $n=4$ are listed, and the procedure for obtaining the simultaneous equations for any number of tuned circuits should now be quite clear.

7.2 *Gain Obtained with Response-Shape B*

By comparing the equations of Design Equations—Groups 2 and 1, we see that the quantity $|\Delta_n^b|_{min}$, which is the minimum value of the determinantal polynomial for response-shape B as given in (7).

$$(|\Delta_n^b|_{min} = F_\beta^n[(V_p/V_\beta)^2-1]^{1/2}. \quad (7)$$

Therefore the gain at the peak of the response obtained with response-shape B is as given in (8).

$$V_p^b = \frac{I}{2\pi\Delta f_\beta(C_1C_n)^{1/2}}[(V_p/V_\beta)^2-1]^{1/2}\left(\frac{K_{12}}{F_\beta}\right)\left(\frac{K_{23}}{F_\beta}\right)\left(\frac{K_{34}}{F_\beta}\right)\cdots\left(\frac{K_{(n-1)n}}{F_\beta}\right). \quad (8)$$

Equation (8) alone is not of much use insofar as numerical gain calculations are concerned because the values of the K's in (8) must first be determined from the solution of the simultaneous equations given in Design Equations—Group 3. The required values for coefficients of coupling as obtained from Design Equations—Group 3 will be found to be in terms of $(\Delta f_\beta/f_0)$ and $[(V_p/V_\beta)^2-1]$ and, when the expressions for the required coefficients substituted in (8), a useful gain equation will result, which is in terms of C_I, C_n, Δf_β, (V_p/V_β) and the constant-current generator I.

7.3 *Resulting Phase Response of Amplitude-Response-Shape B*

The exact phase-response shape associated with amplitude-response-shape B can, of course, be obtained from (5). We are neglecting the actual magnitude of the phase shift at the midfrequency, which from (2) is always plus or minus some multiple of 90 degrees, depending on the number of inductive and capacitive couplings used. From (5), we see that θ_n, the phase shift of $(V_p/\vec{V})$ at any percentage bandwidth F is given by

$$\theta_n^b = \tan^{-1}\left(\frac{F-i_1^b}{r_1^b}\right) + \tan^{-1}\left(\frac{F+i_1^b}{r_1^b}\right) + \tan^{-1}\left(\frac{F-i_2^b}{r_2^b}\right) + \tan^{-1}\left(\frac{F+i_2^b}{r_2^b}\right) + \cdots \quad (9)$$

where r_m^b and i_m^b are given by (6a) and (6b). *There will be exactly as many terms in* (9) *as there are resonant circuits in the network.*

As an example of the use of (9), (6a), and (6b), we see that when a triple-tuned circuit is used to produce amplitude-response-shape B, the resulting phase shift of $(V_p/\vec{V})$ at any $(\Delta f/\Delta f_\beta)$ is given by

$$\theta_3{}^b = \tan^{-1}\left\{2\left[(V_p/V_\beta)^2-1\right]^{1/6}\left(\frac{\Delta f}{\Delta f_\beta}\right)-1.73\right\}$$
$$+\tan^{-1}\left\{2\left[(V_p/V_\beta)^2-1\right]^{1/6}\left(\frac{\Delta f}{\Delta f_\beta}\right)+1.73\right\}$$
$$+\tan^{-1}\left\{\left[(V_p/V_\beta)^2-1\right]^{1/6}\left(\frac{\Delta f}{\Delta f_\beta}\right)\right\}. \qquad (10)$$

In a similar way, the exact phase-shift equation may be written for any number of coupled circuits that are correctly used to obtain response-shape B.

7.4 *Exact Design Equations for Response-Shape B* ($n=1, 2, 3$)

The design sheets given next in this paper for single-, double-, and triple-tuned circuits used to produce shape B were obtained by solving the first three sets of simultaneous equations given in Design Equations—Group 3 for the required circuit constants; substitution in (8) then gives the gain equations and substitution in (9) gives the phase-shift equation. In each case, the Q *distribution* chosen is the one that allows the designer to use the lowest possible Q value in the high-Q circuits of the network.[17] Thus for the double-tuned network, the case of $Q_1=Q_2$ is considered. For the triple-tuned network, the Q distribution $Q_1=Q_2$ (or $Q_3=Q_2$) is considered, and the coefficient of coupling distribution considered is $K_{12}=K_{23}$. The reader should realize that the equations of Design Equations—Group 3 are perfectly general and any Q distribution and coefficient of coupling distributing can be investigated.

The problem of successfully solving the simultaneous equations of Design Equations—Group 3 in the cases where there are more than three resonant circuits per network, will be considered in another paper. It should be clearly realized that the coefficients of Design Equations—Group 2 give exact ***numerical*** values to which the general coefficients of Design Equations—Group 1 are equated; thus, even though it may be impossible to obtain closed-form design equations for the required circuit-element values, it may still be possible to obtain the numerical solutions of these simultaneous equations by some form of "try-and-try-again" method. Graphs or alignment charts can then be prepared from these numerical values and thus complete and exact design information can be satisfactorily presented to the engineer.

7.4.1 *Exact Design Equations for N-Cascaded Triple-Tuned Circuits for Response-Shape B. (See Figs. 3, 4, and 7)*

$$Q_1=Q_2=\left(\frac{f_0}{\Delta f_\beta}\right)3.12\left[(V_p/V_\beta)^{2/N}-1\right]^{1/6}.$$

$$Q_3=\left(\frac{f_0}{\Delta f_\beta}\right)0.734\left[(V_p/V_\beta)^{2/N}-1\right]^{1/6}.$$

$$K_{12}=K_{23}=\left(\frac{\Delta f_\beta}{f_0}\right)0.716\;\frac{1}{\left[(V_p/V_\beta)^{2/N}-1\right]^{1/6}}.$$

$$\text{Gain}_{\text{per stage}}=\frac{G_m}{2\pi\Delta f_\beta(C_IC_{III})^{1/2}}\,0.511\left[(V_p/V_\beta)^{2/N}-1\right]^{1/6}.$$

$$V_p/V=\left\{1+\left[(V_p/V_\beta)^{2/N}-1\right](\Delta f/\Delta f_\beta)^6\right\}^{N/2}$$

$$\text{or}\quad\frac{\Delta f}{\Delta f_\beta}=\frac{\left[(V_p/V)^{2/N}-1\right]^{1/6}}{\left[(V_p/V_\beta)^{2/N}-1\right]^{1/6}}.$$

$$\theta_{\text{per stage}}=\tan^{-1}\left\{2\left[(V_p/V_\beta)^{2/N}-1\right]^{1/6}\left(\frac{\Delta f}{\Delta f_\beta}\right)-1.73\right\}$$
$$+\tan^{-1}\left\{2\left[(V_p/V_\beta)^{2/N}-1\right]^{1/6}\left(\frac{\Delta f}{\Delta f_\beta}\right)+1.73\right\}$$
$$+\tan^{-1}\left\{\left[(V_p/V_\beta)^{2/N}-1\right]\left(\frac{\Delta f}{\Delta f_\beta}\right)\right\}.$$

7.4.2 *Exact Design Equations for N-Cascaded Double-tuned Circuits for Response-Shape B (See Figs. 3, 4, and 7)*

$$Q_1=Q_2=\left(\frac{f_0}{\Delta f_\beta}\right)1.414\left[(V_\beta/V_p)^{2/N}-1\right]^{1/4}.$$

$$K_{12}=\left(\frac{\Delta f_\beta}{f_0}\right)0.707\;\frac{1}{\left[(V_p/V_\beta)^{2/N}-1\right]^{1/4}}.$$

$$\text{Gain}_{\text{per stage}}=\frac{G_m}{2\pi\Delta f(C_IC_{II})^{1/2}}\,0.707\left[(V_p/V_\beta)^{2/N}-1\right]^{1/4}.$$

$$\frac{V_p}{V}=\left\{1+\left[\left(\frac{V_p}{V_\beta}\right)^{2/N}-1\right]\left(\frac{\Delta f}{\Delta f_\beta}\right)^4\right\}^{N/2}\quad\text{or}$$

$$\frac{\Delta f}{\Delta f_\beta}=\frac{\left[\left(\frac{V_p}{V}\right)^{2/N}-1\right]^{1/4}}{\left[\left(\frac{V_p}{V_\beta}\right)^{2/N}-1\right]^{1/4}}.$$

$$\theta_{\text{per stage}}=\tan^{-1}\left\{1.414\left[(V_p/V_\beta)^{2/N}-1\right]^{1/4}\left(\frac{\Delta f}{\Delta f_\beta}\right)-1\right\}$$
$$+\tan^{-1}\left\{1.414\left[(V_p/V_\beta)^{2/N}-1\right]^{1/4}\left(\frac{\Delta f}{\Delta f_\beta}\right)+1\right\}.$$

7.4.3 *Exact Design Equations for N-Cascaded Single-Tuned Circuits for Response-Shape B*

$$Q=\left(\frac{f_0}{\Delta f_\beta}\right)\left[(V_p/V_\beta)^{2/N}-1\right]^{1/2}.$$

$$\text{Gain}_{\text{per stage}}=\frac{G_m}{2\pi\Delta f_\beta C}\left[(V_p/V_\beta)^{2/N}-1\right]^{1/2}.$$

$$V_p/V=\left\{1+\left[(V_p/V_\beta)^{2/N}-1\right]\left(\frac{\Delta f}{\Delta f_\beta}\right)^2\right\}^{N/2}$$

$$\text{or}\quad\frac{\Delta f}{\Delta f_\beta}=\frac{\left[(V_p/V)^{2/N}-1\right]^{1/2}}{\left[(V_p/V_\beta)^{2/N}-1\right]^{1/2}}.$$

$$\theta=\tan^{-1}\left\{\left[(V_p/V_\beta)^{2/N}-1\right]\left(\frac{\Delta f}{\Delta f_\beta}\right)\right\}.$$

8. Response-Shape C

8.1 Desired-Shape Equation

When the straightforward procedure given in Section 3.1 is applied to single-, double-, and triple-tuned networks, the three resulting shape equations can be generalized for n resonant circuits into the following general form

$$V_p/V = \{1 + [(V_p/V_\beta)^2 - 1][T_n(F/F_\beta)]^2\}^{1/2}, \quad (11)$$

where T_n is the Chebishev polynomial of highest power n as given by

$$T_n\left(\frac{F}{F_\beta}\right) = 2^{n-1}\left[\left(\frac{F}{F_\beta}\right)^n - \frac{n}{1!2^2}\left(\frac{F}{F_\beta}\right)^{n-2} + \frac{n(n-3)}{2!2^4}\left(\frac{F}{F_\beta}\right)^{n-4} - \frac{n(n-4)(n-5)}{3!2^6}\left(\frac{F}{F_\beta}\right)^{n-6} + \cdots\right]. \quad (12)$$

It is known that the above Chebishev polynomial is also given by (13).

$$T_n\left(\frac{F}{F_\beta}\right) = \begin{cases} \cos\left[n \cos^{-1}\left(\frac{F}{F_\beta}\right)\right], & \text{for } \left(\frac{F}{F_\beta}\right) < 1 \quad (13a) \\ \cosh\left[n \cosh^{-1}\left(\frac{F}{F_\beta}\right)\right], & \text{for } \left(\frac{F}{F_\beta}\right) > 1. \quad (13b) \end{cases}$$

Thus we can write the shape equation for type C as

Equation (15b) was used to obtain selectivity curves given in Fig. 2. The discussion following (4) and (4a) concerning the quantities F and Δf should now be reread. The voltage ratios in (14) and (15) are the ratios for one network so that for N-cascaded identical networks the voltage ratios to be used in (15) are the Nth root of the desired resultant voltage ratios.

8.2 Location of Peaks and Valleys Inside Pass Band

A little thought will show that we will obtain the location of the peaks of the response if, in (15a) we set V equal to V_p; and we will obtain the locations of the valleys of the response if in (15a) we set $V = V_\beta$.

Making the above substitutions, we obtain (16), which gives the location of the maxima of the response, and (17), which gives the location of the minima of the response.

$$\frac{\Delta f_{\text{peaks}}}{\Delta f_\beta} = \cos\left(\frac{2m-1}{n}\,\frac{\pi}{2}\right). \quad (16)$$

$$\frac{\Delta f_{\text{valleys}}}{\Delta f_\beta} = \cos\left(\frac{2m}{n}\,\frac{\pi}{2}\right). \quad (17)$$

As before, $m = 1, 2, 3 \cdots n/2$ for n even, or $(n+1)/2$ for n odd. $m = 1$ gives the location of the pair of peaks and pair of valleys that are most distant from the midfrequency; $m = 2$ gives the location of the pair of peaks and pair of valleys that are second most distant from the midfrequency, etc.

From (16), we note the interesting point that the ratio of the bandwidth between outside peaks Δf_{p1} to the bandwidth Δf_β (where the skirt response equals the valley response) is 0.707 for double-tuned circuits; 0.866 for triple-tuned circuits; 0.922 for quadruple-tuned circuits, etc.

$$V_p/V = \left\{1 + [(V_p/V_\beta)^2 - 1]\left[\cos\left(n \cos^{-1}\left(\frac{F}{F_\beta}\right)\right)\right]^2\right\}^{1/2}, \quad \text{inside pass band,} \quad (14a)$$

$$V_p/V = \left\{1 + [(V_p/V_\beta)^2 - 1]\left[\cosh\left(n \cosh^{-1}\left(\frac{F}{F_\beta}\right)\right)\right]^2\right\}^{1/2}, \quad \text{outside pass band,} \quad (14b)$$

and, solving (14) for $(\Delta f/\Delta f_\beta)$, we obtain the useful equations

$$\left(\frac{F}{F_\beta}\right) = \cos\left[\frac{1}{n}\cos^{-1}\left(\frac{(V_p/V)^2 - 1}{(V_p/V_\beta)^2 - 1}\right)^{1/2}\right], \quad \text{inside pass band,} \quad (15a)$$

$$\left(\frac{F}{F_\beta}\right) = \cosh\left[\frac{1}{n}\cosh^{-1}\left(\frac{(V_p/V)^2 - 1}{(V_p/V_\beta)^2 - 1}\right)^{1/2}\right], \quad \text{outside pass band,} \quad (15b)$$

where n is the total number of resonant circuits used in the filter chain.

8.3 Mathematical Manipulation

Solving for the roots of (14), we find it can be expressed in the complex form (18).

$$\frac{V_p}{\vec{V}} = \frac{1}{F_\beta{}^n/2^{n-1}[(V_p/V_\beta)^2 - 1]^{1/2}}\left\{[jF - (-r_1{}^c + ji_1{}^c)][jF - (-r_1{}^c - ji_1{}^c)][jF - (-r_2{}^c + ji_2{}^c)][jF - (-r_2{}^c - ji_2{}^c)] \cdots\right\} \quad (18)$$

where the real (r_m^c) and imaginary (i_m^c) parts of the roots are given by (19a) and (19b).

$$r_m^c = F_\beta|s_n| \sin\left(\frac{2m-1}{n}\frac{\pi}{2}\right),$$
$$i_m^c = F_\beta|c_n| \cos\left(\frac{2m-1}{n}\frac{\pi}{2}\right), \tag{19a}$$

where

$$s_n = \sinh\left\{\frac{1}{n}\sinh^{-1} 1/[(V_p/V_\beta)^2-1]^{1/2}\right\}$$
$$c_n = \cosh\left\{\frac{1}{n}\sinh^{-1} 1/[(V_p/V_\beta)^2-1]^{1/2}\right\} \tag{19b}$$

and $m=1, 2, 3, 4 \cdots n/2$ for n even, or $(n+1)/2$ for n odd.

Consideration of (19) shows that if plotted in the complex plane, the roots of the Chebishev or Shape-C type of response fall on a half ellipse as shown in Fig. 9.

The meaning and use of m in (19) should be clear from Fig. 8 and from the paragraph in Section 7 that gives the meaning of m in connection with (6).

By "multiplying out" the correct number of terms of the above general equation (18), we can prepare a list of general shape equations for $n=1, 2, 3$, etc., which are in exactly the form taken by general response equations of Design Equations—Group 1. These resulting equations are given in Design Equations—Group 4. (*We use exactly as many factors of (18) as the number of resonant circuits in the networks.*)

We can now compare Design Equations—Groups 4 and 1 and equate the corresponding coefficients. Carrying out this procedure, we obtain the sets of simultaneous equations given in Design Equations—Group 5, which have to be solved to obtain the exact required circuit constants (Q and K) that will produce the C type of response shape. The simultaneous equations up to $n=4$ are listed, and the procedure for obtaining the simultaneous equations for any n should now be be quite clear.

8.4 *Gain Obtained with Response-Shape C.*

Comparison of the equation given in Design Equations—Group 1 and those given in Design Equations—Group 4 shows that for response-shape C the value of $|\Delta_n^c|_{\min}$ is

$$|\Delta_n^c|_{\min} = \frac{F_\beta^n}{2^{n-1}[(V_p/V_\beta)^2-1]^{1/2}}. \tag{20}$$

and using (2) and (1a), we see that the gain obtained at the voltage response peaks with response-shape C can be written as

$$V_p^c = \frac{I}{2\pi\Delta f_\beta(C_1C_n)^{1/2}}\, 2^{n-1}[(V_p/V_\beta)^2-1]^{1/2}\left(\frac{K_{12}}{F_\beta}\right)\left(\frac{K_{23}}{F_\beta}\right)\left(\frac{K_{34}}{F_\beta}\right)\cdots\left(\frac{K_{(n-1)n}}{F_\beta}\right). \tag{21}$$

Equation (21) alone does not enable us to make any numerical gain calculations, because the required values for the coefficients of coupling K must first be found from the solution of the simultaneous equations given in Design Equations—Group 5. It will be found that the required coefficients of coupling will be a function of the desired percentage bandwidth F_β and the ratio (V_p/V_β), and when the expression for the required coefficient of coupling is substituted in (21) a useful gain equation results.

8.5 *Resulting Phase Response of Amplitude-Response-Shape C*

From (18), we can obtain the exact phase-response shape that is obtained when response-shape C is used. This will neglect the actual magnitude of the phase shift at the midfrequency, which from (2) is always plus or minus some multiple of 90 degrees, depending on the number of inductive and capacitive couplings used. From (18), we see that the phase shift θ_n of $(V_p/\overrightarrow{V})$ at any percentage bandwidth F is given by

$$\theta_n^c = \tan^{-1}\left(\frac{F-i_1^c}{r_1^c}\right) + \tan^{-1}\left(\frac{F+i_1^c}{r_1^c}\right) + \tan^{-1}\left(\frac{F-i_2^c}{r_2^c}\right) + \tan^{-1}\left(\frac{F+i_2^c}{r_2^c}\right) + \cdots \tag{22}$$

where r_m^c and i_m^c are given by (19). There will be exactly as many terms in (22) as there are resonant circuits in the network.

As an example of the use of (22) and (19), we see that when a triple-tuned circuit is used to produce amplitude-response-shape C, the resulting phase shift of $(V_p/\overrightarrow{V})$ is given by

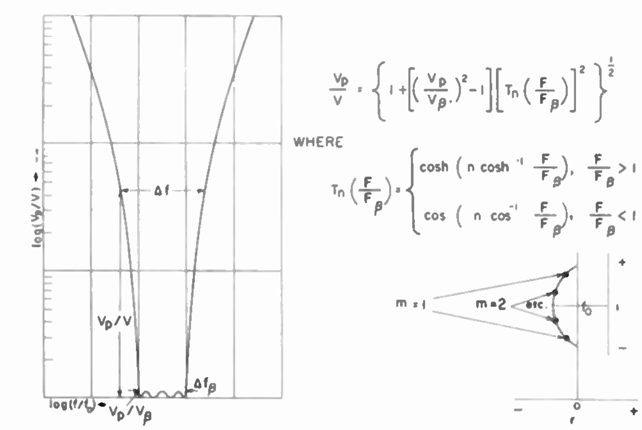

Fig. 9—The exact equation describing response-shape C and the location of the roots of the equation on a semiellipse on the complex plane. Equation (19) gives the exact root values. n is the number of resonant circuits used and the response equation for an n-resonant-circuit network will have n roots.

$$\theta_3^c = \tan^{-1}\left[\frac{2}{s_3}\left(\frac{\Delta f}{\Delta f_B}\right) - 1.73\frac{c_3}{s_3}\right] + \tan^{-1}\left[\frac{2}{s_3}\left(\frac{\Delta f}{\Delta f_B}\right) + 1.73\frac{c_3}{s_3}\right] + \tan^{-1}\left[\frac{1}{s_3}\left(\frac{\Delta f}{\Delta f_B}\right)\right].$$

where s_3 and c_3 are given by (19).

In any exactly similar way, the exact phase-shift equation may be written for any number of resonant circuits when they are used to obtain response-shape *C*.

8.6 *Exact Design Equations for Response-Shape C* ($n = 1, 2, 3$)

The design sheets given next in this paper for single-, double-, and triple-tuned circuits used to produce response-shape *C* were obtained by solving the first three sets of simultaneous equations in Design Equations—Group 5 for the required circuit constants (with the *Q* distribution and *K* distribution given below). Single-tuned design is, of course, identical for both response-shapes *B* and *C*. Substitution in (21) gives the gain equation, and substitution in (22) gives the phase-shift equation.

$$\theta_{\text{per stage}} = \tan^{-1}\frac{2}{s_3}\left[\frac{\Delta f}{\Delta f_B} - 0.87(1+s_3^2)^{1/2}\right] + \tan^{-1}\frac{2}{s_3}\left[\frac{\Delta f}{\Delta f_B} + 0.87(1+s_3^2)^{1/2}\right] + \tan^{-1}\frac{1}{s_3}\left(\frac{\Delta f}{\Delta f_B}\right).$$

In the case of the double-tuned circuit, the *Q* distribution considered is the one that allows the designer to use the lowest possible *Q*, i.e., the distribution $Q_1 = Q_2$.

In the case of the triple-tuned circuit, the *Q* distribution considered here is the one that produced the simplest mathematical solution, i.e., $Q_1 = Q_3 = Q$ and $Q_2 = \infty$; the *K* distribution considered is $K_{12} = K_{23}$. This is not the most practical useful *Q* distribution because of the infinite *Q* required in the middle resonant circuit.[17] The solution of the three simultaneous equations given in Design Equations—Group 5 for the triple-tuned circuit has been accomplished for the much more practical *Q* distribution of $Q_1 = Q_2 = Q$ (or $Q_3 = Q_2 = Q$), and this solution will be presented in a later paper.

The problem of successfully solving the simultaneous equations of Design Equations—Group 5 for the cases where there are more than three resonant circuits per network will be considered in another paper. It should be clearly realized that the coefficients of Design Equations—Group 4 give us exact numerical values to which we are equating the general coefficients of Design Equations—Group 1. Thus, even though it may be impossible to obtain closed-form design equations for the required circuit-element values, it may still be possible to obtain the numerical solution of these simultaneous equations by some form of "try-and-try-again" method. Graphs or alignment charts can then be prepared from these numerical values, and complete exact design information can thus be satisfactorily presented to the engineer.

8.6.1 *Exact Design Equations for N-Cascaded Triple-Tuned Circuits for Response-Shape C (See Figs. 3, 4, and 7)*

Let

$$s_3 = \sinh\left\{\tfrac{1}{3}\sinh^{-1} 1/\left[(V_p/V_B)^{2/N} - 1\right]^{1/2}\right\}$$

$$Q_1 = Q_3 = \frac{f_0}{\Delta f_B}\,\frac{1}{s_3}.$$

$$Q_2 = \infty$$

$$K_{12} = K_{23} = \frac{\Delta f_B}{f_0}(0.375 + 0.5 s_3^2)^{1/2}.$$

$$\text{Gain}_{\text{per stage}} = \frac{G_m}{2\pi\Delta f_B(C_I C_{III})^{1/2}}(1.5 + 2s_3^2)\left[(V_p/V_B)^{2/N} - 1\right]^{1/2}.$$

$$\frac{\Delta f}{\Delta f_B} = \cosh\left\{\tfrac{1}{3}\cosh^{-1}\left[\frac{(V_p/V)^{2/N} - 1}{(V_p/V_B)^{2/N} - 1}\right]^{1/2}\right\}$$

outside pass band,

$$\frac{\Delta f}{\Delta f_B} = \cos\left\{\tfrac{1}{3}\cos^{-1}\left[\frac{(V_p/V)^{2/N} - 1}{(V_p/V_B)^{2/N} - 1}\right]^{1/2}\right\},$$

inside pass band.

8.6.2 *Exact Design Equations for N-Cascaded Double-Tuned Stages for Response-Shape C (See Figs. 3, 4, and 7)*

Let

$$s_2 = \sinh\left(\tfrac{1}{2}\sinh^{-1} 1/\left[(V_p/V_B)^{2/N} - 1\right]^{1/2}\right).$$

$$Q_1 = Q_2 = \frac{f_0}{\Delta f_B}\,\frac{1.414}{s_2}.$$

$$K_{12} = \frac{\Delta f_B}{f_0}\,0.707(1 + s_2^2)^{1/2}.$$

$$\text{Gain}_{\text{per stage}} = \frac{G_m}{2\pi\Delta f_B(C_I C_{II})^{1/2}}\,1.414(1 + s_2^2)^{1/2} \cdot \left[(V_p/V_B)^{2/N} - 1\right]^{1/2}.$$

$$\frac{\Delta f}{\Delta f_B} = \cosh\left\{\tfrac{1}{2}\cosh^{-1}\left[\frac{(V_p/V)^{2/N} - 1}{(V_p/V_B)^{2/N} - 1}\right]^{1/2}\right\},$$

outside pass band,

$$\frac{\Delta f}{\Delta f_B} = \cos\left\{\tfrac{1}{2}\cos^{-1}\left[\frac{(V_p/V)^{2/N} - 1}{(V_p/V_B)^{2/N} - 1}\right]^{1/2}\right\},$$

inside pass band.

$$\theta_{\text{per stage}} = \tan^{-1}\frac{1.414}{s_2}\left[\frac{\Delta f}{\Delta f_B} - 0.707(1 + s_2^2)^{1/2}\right] + \tan^{-1}\frac{1.414}{s_2}\left[\frac{\Delta f}{\Delta f_B} + 0.707(1 + s_2^2)^{1/2}\right].$$

9. Comments on Method of Design that Uses Complex Roots (or "Poles") of Network Response Equation

9.1 *Mathematical Procedure*

Although perhaps not stated from quite the viewpoint given below, there has recently been presented a method of design that also finds the complex roots of the desired amplitude-response-shape equation, and then finds the complex roots or poles of the circuit-response equations given in Design Equations—Group 1. The complex roots of the desired amplitude-response equation are then equated to the corresponding complex roots of the circuit-response equation to obtain the necessary n simultaneous equations required for the solution for the n unknown circuit constants.

Now, unfortunately, as we increase the number of resonant circuits in our n resonant-circuit band-pass network, the expressions for the complex roots or poles of the network in terms of the circuit constants K and Q become more and more complicated. To generalize, we can see from (2) that it will be necessary to solve an nth order equation to find the roots or poles of an n resonant-circuit band-pass network. It is thus theoretically impossible to obtain general expressions for the poles of band-pass circuits employing more than 5 resonant circuits and, in practice, the general expression for the poles of even a triple-tuned circuit having three finite and different Q's seems almost hoplessly complicated.

To demonstrate the above fact, the pole location $(r \pm ji)$ for single-, double-, and triple-tuned networks are given below in (23), (24), (25), i.e., these are the roots of the corresponding equations of Design Equations—Group 1.

$$F_1 = -d \pm j0, \text{ single tuned,} \tag{23}$$

$$F_{12} = -\left(\frac{d_1 + d_2}{2}\right) \pm j\left[K_{12}^2 - \left(\frac{d_1 - d_2}{2}\right)^2\right]^{1/2}, \text{ double tuned.} \tag{24}$$

The roots of a triple-tuned circuit are

$$\left.\begin{aligned}
P_{1,2} &= -\left[\tfrac{1}{3}C_2 + \tfrac{1}{2}(\alpha+\beta)\right] \pm j\tfrac{3}{2}^{1/2}(\alpha-\beta),\\
P_3 &= -\left[\tfrac{1}{3}C_2 - (\alpha+\beta)\right] \pm j0,\\
&\text{where}\\
\alpha &= \left\{-\left(\frac{q}{2}\right) + \left[\left(\frac{q}{2}\right)^2 + \left(\frac{p}{3}\right)^3\right]^{1/2}\right\}^{1/3},\\
\beta &= \left\{-\left(\frac{q}{2}\right) - \left[\left(\frac{q}{2}\right)^2 + \left(\frac{p}{3}\right)^3\right]^{1/2}\right\}^{1/3},\\
&\text{where}\\
q &= C_0 - \tfrac{1}{3}C_2C_1 + \tfrac{2}{27}C_2^3,\\
p &= C_1 - \tfrac{1}{3}C_2^2,\\
&\text{where}\\
&C_0, C_1, C_2 \text{ are given in Design Equations—Group 1.}
\end{aligned}\right\} \tag{25}$$

When the above three roots of the triple-tuned-circuit response equation are simultaneously equated to the corresponding three roots of the desired triple tuned-response equation, as obtained from (6) or (19), it is readily apparent that the solution of the resulting simultaneous equations for the required values of the circuit constants (K's and Q's) will indeed be a formidable task.

9.2 *Stagger Tuning of Simple Interstage Circuits*

The great practical importance of the pole type of design method must not be overlooked, however. When we consider the case of an over-all network consisting of many simple band-pass networks (i.e., single and double tuned) *that are separated from each other by vacuum tubes, i.e., there is no coupling between the different simple circuits*, then this design method is extremely useful. For this case, the expressions for each of the many poles retain the simplicity of (23) and (24), and it is a relatively simple matter to solve the resulting simultaneous equations for the required circuit constants. (It will be noted that the expression for the poles of a double-tuned circuit (24) becomes quite simple for the case of $Q_1 = Q_2$).

9.2.1 *Single-Tuned Interstage Circuits As Used to Obtain Response-Shape B (Small-Percentage Pass Band)*

For example, let us briefly consider the case of stagger tuning of a single-tuned-interstage circuit. When obtaining the expressions for the poles of the networks, it is always important to consider the question of whether the *resonant frequency* of the networks used is identical with the *midfrequency* of the desired response shape. For the case of stagger tuning of *single-tuned* interstage circuits, it is of course obvious that this cannot be the case, and therefore it is necessary to express the equation for the pole of the network in terms of both the desired midfrequency of the response and the resonant frequency of the circuits.

A little thought will show that for the small-percentage pass-band case, the desired general expression for the pole of a single-tuned network which allows us mathematically to place the pole anywhere on the frequency axis, is given by (26)

$$P_m = d_m \pm j(\Delta f_{rm}/f_0). \tag{26}$$

where the subscript m has the same significance as in Section 7 and 8, d is the decrement (i.e., reciprocal of Q) of the single-tuned circuit being considered, and $(\Delta f_{rm}/f_0)$ is the percentage bandwidth (from the midfrequency of the desired response) between the required pair of resonant frequencies of the mth pair of single-tuned interstages. (Equation (26) can be obtained from the usual simple expression for the transfer impedance of a single-tuned circuit by effectively changing the coordinate-system reference by simply expressing the resonant frequency of the resonant circuit as $f_r = f_0(1 \pm K/2)$, where K is twice the percentage frequency difference between the desired midfrequency f_0

and the circuit resonant frequency f_r.)

By equating the above circuit pole expression of (26) to the amplitude-response-shape-B pole expression of (6), we obtain the first two design equations of the design sheet for stagger tuning to produce response-shape B.

The following equations give the desired-response-shape equation in three different forms. The final equations are the gain equations in two different forms. These gain equations are obtained by realizing that the total output voltage of the stagger-tuned chain at any frequency is given by simply multiplying together the responses of all the networks in the chain, thus obtaining (27).

or
$$\frac{\Delta f}{\Delta f_\beta}=\left[\frac{(V_p/V)^2-1}{(V_p/V_\beta)^2-1}\right]^{1/2n}$$

or
$$n=\frac{\log\left[\dfrac{(V_p/V)^2-1}{(V_p/V_\beta)^2-1}\right]^{1/2}}{\log\,(\Delta f/\Delta f_\beta)}.$$

$$\text{Gain}_{\text{per stage}}=\frac{G_m}{2\pi\Delta f_\beta C}\,[(V_p/V_\beta)^2-1]^{1/2n}$$

or
$$n=\frac{\log\left(\dfrac{\text{Gain}_{\text{total}}}{[(V_p/V_\beta)^2-1]^{1/2}}\right)}{\log\left(\dfrac{G_m}{2\pi\Delta f_\beta C}\right)}$$

$$\vec{V}=\frac{I_1/\omega_0C_1\quad I_2/\omega_0C_2\quad I_3/\omega_0C_3\quad I_4/\omega_0C_4\cdots}{\left[jF-\left(-d_1\pm j\dfrac{\Delta f_{r1}}{f_0}\right)\right]\left[jF-\left(-d_2\pm j\dfrac{\Delta f_{r2}}{f_0}\right)\right]\left[\cdots\right.}. \tag{27}$$

The gain at the peak of the response is obtained when the magnitude of the denominator of (27) has its minimum value. We have already seen that for response-shape B this minimum value is given by (8). Thus, making use of (8), we obtain the total-gain equation; the nth root of this total-gain equation gives the equation for gain per stage as included in the design sheet.

where

G_m = geometric mean of all G_m's,

C = geometric mean capacitance.

9.2.2 *Single-Tuned Interstage Circuits Used to Obtain Response-Shape C (Small-Percentage Pass Band)*

By going through exactly the same line of resoning used in Section 9.2.1, using the pole expressions of (19) for amplitude-response-shape C, and the value of $|\Delta_n^c|_{\min}$ for response-shape C given by (20), we obtain the equations given on the design sheet for stagger tuning of single-tuned interstage networks used to produce response-shape C.

It should be realized that the voltage ratios given on the stagger-tuning design sheets are the ratios for a one-staggered n-tuple design, if N of these n-tuples are to be cascaded, then the voltage ratios to be used on the design sheets should be the Nth root of the over-all resulting desired voltage ratio.

In the interests of simplicity, a general many-termed phase-shift equation has not been included on the stagger-tuned design sheets. By referring to Sections 7.3 and 8.5, the reader should be able to write the correct phase-shift equation for any specific stagger-tuned design.

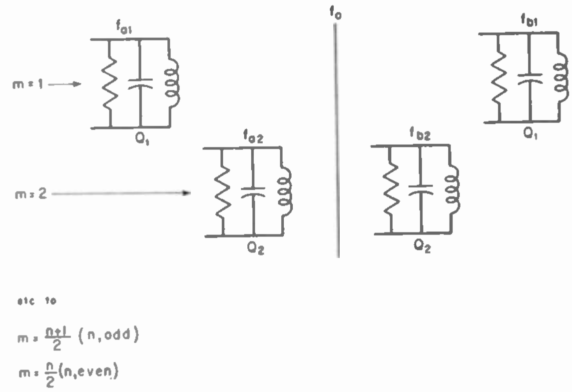

Fig. 10—Definition of symbols in the stagger-tuning design equations Thus $m=1$ gives the resonant-frequency difference and the required Q for that pair of circuits that are staggered the greatest distance from the midfrequency, $m=2$ is for the next greatest distance, to the limiting cases $m_{\max}=(n+1)/2$ for n odd and $m_{\max}=n/2$ for n even.

9.3 *Stagger Tuning of Single-Tuned Interstage Circuits for Response-Shape B (See Fig. 10)*

$$\frac{1}{Q_m}=\frac{\Delta f_\beta/f_0}{[(V_p/V_\beta)^2-1]^{1/2n}}\sin\left(\frac{2m-1}{n}\,90°\right).$$

$$(f_a-f_b)_m=\frac{\Delta f_\beta}{[(V_p/V_\beta)^2-1]^{1/2n}}\cos\left(\frac{2m-1}{n}\,90°\right).$$

$$V_p/V=\{1+[(V_p/V_\beta)^2-1](\Delta f/\Delta f_\beta)^{2n}\}^{1/2}$$

9.4 *Stagger Tuning of Single-Tuned Interstage Circuits for Response-Shape C (See Fig. 10)*

$$\frac{1}{Q_m}=\frac{\Delta f_\beta}{f_0}\,s_n\sin\left(\frac{2m-1}{n}\,90°\right).$$

$$s_n=\sinh\left\{\frac{1}{n}\sinh^{-1}\frac{1}{[(V_p/V_\beta)^2-1]^{1/2}}\right\}$$

$$(f_a-f_b)_m=\Delta f_\beta c_n\cos\left(\frac{2m-1}{n}\,90°\right).$$

$$c_n=\cosh\left\{\frac{1}{n}\sinh^{-1}\frac{1}{[(V_p/V_\beta)^2-1]^{1/2}}\right\}.$$

For shape outside the pass band,

$$\frac{V_p}{V} = \left\{1+\left[(V_p/V_\beta)^2-1\right] \cdot \left\{\cosh^2\left[n \cosh^{-1}(\Delta f/\Delta f_\beta)\right]\right\}\right\}^{1/2} \text{ or}$$

$$\frac{\Delta f}{\Delta f_\beta} = \cosh\left\{\frac{1}{n}\cosh^{-1}\left[\frac{(V_p/V)^2-1}{(V_p/V_\beta)^2-1}\right]^{1/2}\right\} \quad \text{or}$$

$$n = \frac{\cosh^{-1}\left[\dfrac{(V_p/V)^2-1}{(V_p/V_\beta)^2-1}\right]^{1/2}}{\cosh^{-1}(\Delta f/\Delta f_\beta)}.$$

For shape inside the pass band,

$$V_p/V = \left\{1+\left[(V_p/V_\beta)^2-1\right] \cdot \left\{\cos^2\left[n \cos^{-1}(\Delta f/\Delta f_\beta)\right]\right\}\right\}^{1/2},$$

$$\frac{\Delta f_{\max}}{\Delta f_\beta} = \cos\left(\frac{2m-1}{n}\, 90°\right).$$

$$\frac{\Delta f_{\min}}{\Delta f_\beta} = \cos\left(\frac{2m}{n}\, 90°\right).$$

$$\text{Gain}_{\text{per stage}} = \frac{G_m}{2^{1/n}\pi\Delta f_\beta C}\left[(V_p/V_\beta)^2-1\right]^{1/2n} \quad \text{or}$$

$$n = \frac{\log\left(\dfrac{2\,\text{Gain}_{\text{total}}}{\left[(V_p/V_\beta)^2-1\right]^{1/2}}\right)}{\log\left(\dfrac{G_m}{\pi\Delta f_\beta C}\right)},$$

where

G_m = geometric mean of all G_m's,

C = geometric mean of all C's.

Bibliography

1. S. Butterworth, "On the theory of filter-amplifiers," *Exp. Wireless and Wireless Eng.*, vol. 7, pp. 536–541; October, 1930.
2. W. Cauer, "Siebschaltungen," VDI Verlag; 1931.
3. W. R. Bennett, United States Patent No. 1,849,656; March, 1932.
4. H. W. Bode, "General Theory of Electric Wave-Filters," *Jour. Math. and Phys.*, vol. 13, pp. 275–362; November, 1934.
5. H. W. Bode and R. L. Dietzold, "Ideal wave filters," *Bell Sys. Tech. Jour.*, vol. 14, pp. 215–252; April, 1935.
6. W. Cauer, "New theory and design of wave filters," *Physics;* April, 1939.
7. S. Darlington, "Synthesis of reactance four poles which produce a prescribed insertion loss characteristic," *Jour. Math. and Phys.*, vol. 18, pp. 257–353; September, 1939.
8. V. D. Landon, "Cascade amplifiers with maximal flatness," *RCA Rev.*, Part I, vol. 5, pp. 347–363; January, 1941: Part II, vol. 5, pp. 481–498; April, 1941.
9. H. Wallman, "Stagger-tuned intermediate-frequency amplifiers," *M.I.T. Radiation Laboratory*, Report 524; February, 1944) (Presented, 1946 IRE National Convention, New York, N. Y.).
10. W. W. Hansen and O. C. Lundstrom, "Experimental determination of impedance functions by use of an electrolytic tank," Proc. I.R.E., vol. 33, pp. 528–534; August, 1945.
11. W. W. Hansen, "On maximum gain-bandwidth product in amplifiers," *Jour. Appl. Phys.*, vol. 16, pp. 528–534; September, 1945.
12. R. H. Baum, "Design of broad-band intermediate-frequency amplifiers," *Jour. Appl. Phys.*, Part I, vol. 17, pp. 519–529; June, 1946. Part II, vol. 17, pp. 721–729; September, 1946.
13. P. I. Richards, "Universal optimum-response curves for arbitrarily coupled resonators," Proc. I.R.E., vol. 34, pp 624–629; September, 1946.
14. K. R. Spangenberg, "The universal characteristics of triple-resonant-circuit band-pass filters," Proc. I.R.E., vol. 34, pp. 629–635; September, 1946. This reference makes an approximation in the triple-tuned analysis so that the expression for the poles of the network are not as exact as those considered in the present paper.
15. W. E. Bradley, "A theory of wide-band amplifier design," presented, 1947 IRE National Convention, New York, N. Y.
16. Milton Dishal, "Exact design and analysis of double- and triple-tuned band-pass amplifiers," Proc. I.R.E., vol. 35, pp. 606–626; June, 1947. Also, *Elect. Commun.*, vol. 24, pp. 349–373; September, 1947.
17. V. D. Landon and Milton Dishal, Discussion of, "Exact design and analysis of double- and triple-tuned band-pass amplifier," by Milton Dishal, Proc. I.R.E., vol. 35, pp. 1507–1510; December, 1947. Also, *Elect. Commun.*, vol. 25, pp. 100–102; March, 1948.
18. W. H. Huggins, "A note on frequency transformations for use with the electrolytic tank," Proc. I.R.E., vol. 36, pp. 421–424; March, 1948.
19. W. H. Huggins, "The natural behavior of broadband circuits," Electronics Research Laboratories (AMC). Report E5013; May, 1948.

Design Equations—Group I

Exact Circuit-Response-Shape Equations in the Complex Polynomial Form for an n Resonant Circuit Network.

Single-Tuned Circuit

$$\frac{\vec{V}_p}{\vec{V}_1} = \frac{1}{|\Delta_1|_{\min}}\left[jF + A_0\right].$$

$$A_0 = d_1.$$

Double-Tuned Circuit

$$\frac{\vec{V}_p}{\vec{V}_2} = \frac{1}{|\Delta_2|_{\min}}\left[(jF)^2 + B_1(jF) + B_0\right].$$

$$B_1 = d_1 + d_2.$$

$$B_0 = K_{12}^2 + d_1 d_2.$$

Triple-Tuned Circuit

$$\frac{V_p}{\vec{V}_3} = \frac{1}{|\Delta_3|_{\min}}\left[(jF)^3+C_2(jF)^2+C_1(jF)+C_0\right].$$

$$C_2 = d_1 + d_2 + d_3.$$

$$C_1 = K_{12}^2 + K_{23}^2 + d_1d_2 + d_1d_3 + d_2d_3.$$

$$C_0 = K_{12}^2d_3 + K_{23}^2d_1 + d_1d_2d_3.$$

Quadruple-Tuned Circuit

$$\frac{V_p}{\vec{V}_4} = \frac{1}{|\Delta_4|_{\min}}\left[(jF)^4 + D_3(jF)^3 + D_2(jF)^2 + D_1(jF) + D_0\right].$$

$$D_3 = d_1 + d_2 + d_3 + d_4.$$

$$D_2 = K_{12}^2 + K_{23}^2 + K_{34}^2 + d_1d_2 + d_1d_3 + d_1d_4 + d_2d_3 + d_2d_4 + d_3d_4.$$

$$D_1 = K_{12}^2d_3 + K_{12}^2d_4 + K_{23}^2d_1 + K_{23}^2d_4 + K_{34}^2d_1 + K_{34}^2d_2 + d_1d_2d_3 + d_1d_2d_4 + d_1d_3d_4 + d_2d_3d_4.$$

$$D_0 = K_{12}^2K_{34}^2 + K_{12}^2d_3d_4 + K_{23}^2d_1d_4 + K_{34}^2d_1d_2 + d_1d_2d_3d_4.$$

Design Equations—Group 2

Exact Complex Polynomials for Response-Shape B.

Single-Tuned Circuit

$$\frac{V_p}{\vec{V}_1} = \frac{1}{F_\beta/\left[(V_p/V_\beta)^2 - 1\right]^{1/2}}\left[jF + A_0^b\right]$$

$$A_0^b = 1\left[\frac{1}{\left[(V_p/V_\beta)^2 - 1\right]^{1/2}}\right]F_\beta.$$

Double-Tuned Circuit

$$\frac{V_p}{\vec{V}_2} = \frac{1}{F_\beta^2/\left[(V_p/V_\beta)^2 - 1\right]^{1/2}}\left[(jF)^2 + B_1^b(jF) + B_0^b\right]$$

$$B_1^b = 1.414\left[\frac{1}{\left[(V_p/V_\beta)^2 - 1\right]^{1/4}}\right]F_\beta.$$

$$B_0^b = 1\left[\frac{1}{\left[(V_p/V_\beta)^2 - 1\right]^{1/4}}\right]^2F_\beta^2.$$

Triple-Tuned Circuit

$$\frac{V_p}{\vec{V}_3} = \frac{1}{F_\beta^3/\left[(V_p/V_\beta)^2 - 1\right]^{1/2}}\left[(jF)^3 + C_2^b(jF)^2 + C_1^b(jF) + C_0^b\right].$$

$$C_2^b = 2\left[\frac{1}{\left[(V_p/V_\beta)^2 - 1\right]^{1/6}}\right]F_\beta.$$

$$C_1^b = 2\left[\frac{1}{\left[(V_p/V_\beta)^2 - 1\right]^{1/6}}\right]^2F_\beta^2.$$

$$C_0^b = 1\left[\frac{1}{\left[(V_p/V_\beta)^2 - 1\right]^{1/6}}\right]^3F_\beta^3.$$

Quadruple-Tuned Circuit

$$\frac{V_p}{\vec{V}_4} = \frac{1}{F_\beta^4/\left[(V_p/V_\beta)^2 - 1\right]^{1/2}}\left[(jF)^4 + D_3^b(jF)^3 + D_2^b(jF)^2 + D_1^b(jF) + D_0^b\right].$$

$$D_3^b = 2.61\left\{\frac{1}{\left[(V_p/V_\beta)^2 - 1\right]^{1/8}}\right\}F_\beta.$$

$$D_2^b = 3.41\left\{\frac{1}{\left[(V_p/V_\beta)^2 - 1\right]^{1/8}}\right\}^2F_\beta^2.$$

$$D_1^b = 2.61\left\{\frac{1}{\left[(V_p/V_\beta)^2 - 1\right]^{1/8}}\right\}^3F_\beta^3.$$

$$D_0^b = 1\left\{\frac{1}{\left[(V_p/V_\beta)^2 - 1\right]^{1/8}}\right\}^4F_\beta^4$$

Design Equations—Group 3

Exact Simultaneous Equations to be Solved for Circuit Constants (K's and Q's) of an n-Resonant-Circuit Network to Produce Response-Shape B when the Circuits are Correctly Resonated.

Single-Tuned Circuit

$$d_1 = \frac{F_\beta}{[(V_p/V_\beta)^2 - 1]^{1/2}}.$$

Double-Tuned Circuit

$$d_1 + d_2 = 1.414 \frac{F_\beta}{[(V_p/V_\beta)^2 - 1]^{1/4}}.$$

$$K_{12}^2 + d_1 d_2 = \frac{F_\beta^2}{[(V_p/V_\beta)^2 - 1]^{2/4}}.$$

Triple-Tuned Circuit

$$d_1 + d_2 + d_3 = 2 \frac{F_\beta}{[(V_p/V_\beta)^2 - 1]^{1/6}}.$$

$$K_{12}^2 + K_{23}^2 + d_1 d_2 + d_1 d_3 + d_2 d_3 = 2 \frac{F_\beta^2}{[(V_p/V_\beta)^2 - 1]^{2/6}}.$$

$$K_{12}^2 d_3 + K_{23}^2 d_1 + d_1 d_2 d_3 = \frac{F_\beta^3}{[(V_p/V_\beta)^2 - 1]^{3/6}}.$$

Quadruple-Tuned Circuit

$$d_1 + d_2 + d_3 + d_4 = 2.61 \frac{F_\beta}{[(V_p/V_\beta)^2 - 1]^{1/8}}.$$

$$K_{12}^2 + K_{23}^2 + K_{34}^2 + d_1 d_2 + d_1 d_3 + d_1 d_4 + d_2 d_3 + d_2 d_4 + d_3 d_4 = 3.41 \frac{F_\beta^2}{[(V_p/V_\beta)^2 - 1]^{2/8}}.$$

$$K_{12}^2 d_3 + K_{12}^2 d_4 + K_{23}^2 d_1 + K_{23}^2 d_4 + K_{34}^2 d_1 + K_{34}^2 d_2 + d_1 d_2 d_3 + d_1 d_2 d_4 + d_1 d_3 d_4 + d_2 d_3 d_4 = 2.61 \frac{F_\beta^3}{[(V_p/V_\beta)^2 - 1]^{3/8}}.$$

$$K_{12}^2 K_{34}^2 + K_{12}^2 d_3 d_4 + K_{23}^2 d_1 d_4 + K_{34}^2 d_1 d_2 + d_1 d_2 d_3 d_4 = \frac{F_\beta^4}{[(V_p/V_\beta)^2 - 1]^{4/8}}.$$

Design Equations—Group 4

Exact Complex Polynomials for Response-Shape C.

Single-Tuned Circuit

$$\frac{V_p}{\vec{V}} = \frac{1}{F_\beta/[(V_p/V_\beta)^2 - 1]^{1/2}} [jF + A_0^c].$$

$$A_0^c = \frac{1}{[(V_p/V_\beta)^2 - 1]^{1/2}} F_\beta.$$

Double-Tuned Circuit

$$\frac{V_p}{\vec{V}} = \frac{1}{F^2/2[(V_p/V_\beta)^2 - 1]^{1/2}} [(jF)^2 + B_1^c(jF) + B_0^c]$$

$$B_1^c = 1.414 s_2 F_\beta.$$

$$B_0^c = 0.5(s_2^2 + c_2^2) F_\beta^2.$$

$$s_2 = \sinh \left\{ \frac{1}{2} \sinh^{-1} \frac{1}{[(V_p/V_\beta)^2 - 1]^{1/2}} \right\}.$$

$$c_2 = \cosh \left\{ \frac{1}{2} \sinh^{-1} \frac{1}{[(V_p/V_\beta)^2 - 1]^{1/2}} \right\}.$$

Triple-Tuned Circuit

$$\frac{V_p}{\vec{V}} = \frac{1}{F_\beta^3/4[(V_p/V_\beta)^2 - 1]^{1/2}} [(jF)^3 + C_2^c(jF)^2 + C_1^c(jF) + C_0^c].$$

$$C_2^c = 2 s_3 F_\beta.$$

$$C_1^c = (1.25 s_3^2 + 0.75 c_3^2) F_\beta^2.$$

$$C_0^c = s_3(0.25 s_3^2 + 0.75 c_3^2) F_\beta^3.$$

$$s_3 = \sinh\left\{\frac{1}{3}\sinh^{-1}\frac{1}{[(V_p/V_\beta)^2 - 1]^{1/2}}\right\}$$

$$c_3 = \cosh\left\{\frac{1}{3}\sinh^{-1}\frac{1}{[(V_p/V_\beta)^2 - 1]^{1/2}}\right\}.$$

Quadruple-Tuned Circuit

$$\frac{V_p}{\vec{V}} = \frac{1}{F_\beta^4/8[(V_p/V_\beta)^2 - 1]^{1/2}}\left[(jF)^4 + D_3^c(jF)^3 + D_2^c(jF)^2 + D_1^c(jF) + D_0^c\right]$$

$$D_3^c = 2.61 s_4 F_\beta.$$

$$D_2^c = (2.41 s_4^2 + c_4^2)F_\beta^2.$$

$$D_1^c = s_4(0.923 s_4^2 + 1.69 c_4^2)F_\beta^3.$$

$$D_0^c = 0.125(s_4^4 + 6 s_4^2 c_4^2 + c_4^4)F_\beta^4$$

$$s_4 = \sinh\left\{\frac{1}{4}\sinh^{-1}\frac{1}{[(V_p/V_\beta)^2 - 1]^{1/2}}\right\}$$

$$c_4 = \cosh\left\{\frac{1}{4}\sinh^{-1}\frac{1}{[(V_p/V_\beta)^2 - 1]^{1/2}}\right\}$$

Design Equations—Group 5

Exact Simultaneous Equations to be Solved for Circuit Constants (K's and Q's) of an n-Resonant-Circuit Network to Produce Response-Shape C when the Circuits are Correctly Resonated.

Single-Tuned Circuit

$$d_1 = \frac{F_\beta}{[(V_p/V_\beta)^2 - 1]^{1/2}}.$$

Double-Tuned Circuit

$$d_1 + d_2 = 1.414 s_2 F_\beta$$

$$K_{12}^2 + d_1 d_2 = (0.5 + s_2^2)F_\beta^2.$$

Triple-Tuned Circuit

$$d_1 + d_2 + d_3 = 2 s_3 F.$$

$$K_{12}^2 + K_{23}^2 + d_1 d_2 + d_1 d_3 + d_2 d_3 = (0.75 + 2 s_3^2)F_\beta^2$$

$$K_{12}^2 d_3 + K_{23}^2 d_1 + d_1 d_2 d_3 = s_3(0.75 + s_3^2)F_\beta^3.$$

Quadruple-Tuned Circuit

$$d_1 + d_2 + d_3 + d_4 = 2.61 s_4 F_\beta.$$

$$K_{12}^2 + K_{23}^2 + K_{34}^2 + d_1 d_2 + d_1 d_3 + d_1 d_4 + d_2 d_3 + d_2 d_4 + d_3 d_4 = (1 + 3.41 s_4^2)F_\beta^2.$$

$$K_{12}^2 d_3 + K_{12}^2 d_4 + K_{23}^2 d_1 + K_{23}^2 d_4 + K_{34}^2 d_1 + K_{34}^2 d_2 + d_1 d_2 d_3 + d_1 d_2 d_4 + d_1 d_3 d_4 + d_2 d_3 d_4 = s_4(1.69 + 2.61 s_4^2)F_\beta^3.$$

$$K_{12}^2 K_{34}^2 + K_{12}^2 d_3 d_4 + K_{23}^2 d_1 d_4 + K_{34}^2 d_1 d_2 + d_1 d_2 d_3 d_4 = (0.125 + s_4^2 + s_4^4)F_\beta^4.$$

In all the above equations,

$$s_n = \sinh\left\{\frac{1}{n}\sinh^{-1}[(V_p/V_\beta)^2 - 1]\right\}.$$

CORRECTION

The authors have brought to the attention of the Editor the following error in the paper "Considerations in the Design of a Radar Intermediate-Frequency Amplifier," by Andrew L. Hopper and Stewart E. Miller, which appeared on pages 1208–1220 of the November, 1947, issue of the PROCEEDINGS OF THE I.R.E.

On page 1215, the expression $V_g = \sqrt{BKT\ \Delta f\ R_g}$ should read $V_g = \sqrt{4BKT\ \Delta f\ R_g}$.[1]

[1] Dwight O. North and W. Robert Ferris, "Fluctuations induced in vacuum-tube grids at high frequencies," PROC. I.R.E., vol. 29, pp. 49–50; February, 1941:

$$\frac{2}{i_g} = 4BKT\ \Delta f\ g_g$$

Since $V_g = i_g R_g$ and $g_g = \frac{1}{R_g}$

$$V_g = \sqrt{4BKT\ \Delta f\ R_g}.$$

Cathode Neutralization of Video Amplifiers*

JOHN M. MILLER, JR.†, ASSOCIATE, IRE

Summary—**The usual cathode bypass capacitors are eliminated, and replaced by a resistor connected from cathode to cathode of succeeding stages. It is shown that no gain need be sacrificed, and a great reduction in low-frequency phase shift is obtained. The addition of a small capacitance across a portion of the intercathode resistance gives an improvement in high frequency response and phase shift. Gain and stability equations are derived, and a circuit diagram of a practical amplifier is given.**

IN VIDEO amplifier stages having tubes of very high transconductance, it is customary to use cathode bias resistors in order to minimize variations in plate current that might be caused by variations in electrode operating potentials, replacement or aging of tubes, etc. A cathode bypass capacitor is normally used in each stage to avoid loss in amplification due to degeneration. However, even with the largest practical values of capacitance, there is usually an appreciable amount of phase shift at very low frequencies.[1]

The cathode bypass is sometimes omitted when a very small value of cathode resistance can be used. This arrangement may be moderately successful in an early stage where the signal is so small that little bias is needed to prevent the flow of grid current. However, the dc stability is not nearly so good as that which is obtained with a large cathode resistance.

In the circuit described here, the cathode bypass capacitors are omitted, and the resulting cathode degeneration is effectively eliminated or greatly reduced by the use of a neutralizing resistor connected between the cathodes of succeeding stages.

The circuit of such an amplifier is shown in Fig. 1. The high-frequency compensation is not shown. The circuit is otherwise normal, except for the resistor R_{k0} connected between the cathodes of the tubes, and the capacitor C, which serves merely to improve the performance at high frequencies. The effect of C will be neglected in the following expressions for the gain of the amplifier.

Also, the plate load resistance of each tube will be assumed to be negligible compared with the internal plate resistance of the tube; a condition that normally exists in pentode video amplifiers.

For convenience, R_L has been included in R_2 in deriving the gain equations, and R_3 has been included in R_1. It has also been assumed that there is no voltage drop across the plate and screen grid supply bypass capacitors

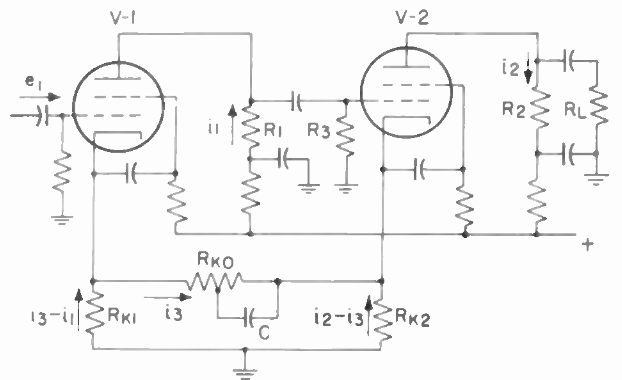

Fig. 1—Elementary schematic diagram of a two-stage video amplifier using cathode neutralization.

or across the grid blocking capacitors. While this condition does not usually hold completely true in practice, the gain equations would otherwise become very unwieldy, not only because of the complex circuit meshes that result, but because the equations would include signal frequency as a function. As a practical matter, the value of R_{k0} must be determined for proper operation at medium frequencies, unless a complex network is substituted for R_{k0} that would correct for the attenuation and phase shift in the bypass and grid blocking capacitors.

At medium frequencies, the gain of the amplifier is

$$\text{Gain} = g_{m1}g_{m2}R_2 \frac{R_1(R_{k0} + R_{k1} + R_{k2}) + R_{k1}R_{k2}}{[R_{k0} + R_{k1} + R_{k2} + g_{m2}R_{k2}(R_{k0} + R_{k1}) + g_{m1}R_{k1}(R_{k0} + R_{k2}) + g_{m1}g_{m2}R_{k1}R_{k2}(R_{k0} - R_1)]}. \quad (1)$$

When R_{k1} and R_{k2} equal zero, a situation that is equivalent to a conventional amplifier circuit having perfectly bypassed cathodes, (1) reduces to

$$\text{Gain} = g_{m1}g_{m2}R_1R_2. \quad (2)$$

In order to obtain the same gain with unbypassed cathode resistors, R_{k0} must have the value

$$R_{k0} = \frac{R_{k1}R_{k2}(1/R_1 - g_{m1} - g_{m2} + g_{m1}g_{m2}R_1)}{g_{m1}R_{k1} + g_{m2}R_{k2} + g_{m1}g_{m2}R_{k1}R_{k2}}. \quad (3)$$

The value of R_{k0} for oscillation, or infinite gain, is

* Decimal classification: R363.4. Original manuscript received by the Institute, August 2, 1948; revised manuscript received, April 20, 1949.

† Formerly, Ripley Co., Inc., Middletown, Conn., now, Bendix Radio, Baltimore, Md.

[1] F. E. Terman, "Radio Engineers' Handbook," McGraw-Hill Book Co., New York, N. Y., First Ed., Sec. 5, Fig. 6; 1943.

$$R_{k0} = \frac{g_{m1}g_{m2}R_{k1}R_{k2}R_1 - (R_{k1} + R_{k2} + g_{m2}R_{k1}R_{k2} + g_{m1}R_{k1}R_{k2})}{(1 + g_{m1}R_{k1})(1 + g_{m2}R_{k2})}. \tag{4}$$

The derivation of equations (1) through (4) is given in he Appendix.

It is of some interest to determine how close together he values of R_{k0} for oscillation and for normal gain may ome in a typical case. Let us assume that g_{m1} and g_{m2} re 0.009 mho; R_{k1} and R_{k2} are 160 ohms, and R_1 equals ,000 ohms. These are values that might exist in an amplifier using 6AC7 tubes. From (3), the value of R_{k0} for normal gain is 331 ohms, and from (4), the value for oscillation is 215 ohms. It is apparent, therefore, that a easonably close tolerance should be placed on R_{k0} in the nanufacture of amplifiers of this type. The cathode bias esistors need not be held to such close tolerances, and normal variations in tube transconductances are not roublesome. However, resistor R_1 must be held to a airly close tolerance.

Since the cathode of the first tube is at an ac potential hat is 180 degrees out of phase with its grid voltage, here will be some increase in the input capacity of the amplifier, accompanied by a decrease in the input capacitance of the second stage.[2] If desired, these effects can be corrected by shunting cathode resistors R_{k1} and R_{k2} with small capacitors of such value that the amplifier will function in the manner of conventional amplifiers with bypassed cathodes at high frequencies, but tube internal plate resistance, the output impedance of the amplifier will be reduced, as the system consists essentially of positive current feedback.[3,4]

If desired, R_{k1}, R_{k2}, and R_{k0} may be rearranged to form a wye rather than a delta, with C connected in shunt with either of the ungrounded cathode resistors.

Fig. 2 shows the circuit diagram of a portion of a practical amplifier that uses cathode neutralization. C_8 yields a considerable increase in gain and reduction in phase shift, for frequencies above 3 mc per second.

As the screen grids of the tubes in Fig. 2 are bypassed to the low potential side of the cathode resistors instead of directly to the cathodes, the screen grid alternating currents will flow through the cathode resistors, so that the expressions for gain given previously will apply only approximately.

As a practical consideration, amplifiers incorporating the circuit of Fig. 2 that were manufactured in production runs were very uniform in gain and frequency response without any individual selection of parts or tubes. Both low- and high-frequency response were greatly improved over previous designs.

The cathode neutralization principle could also be used in some audio amplifier applications. The value of R_{k0} chosen would be somewhat modified by the fact that

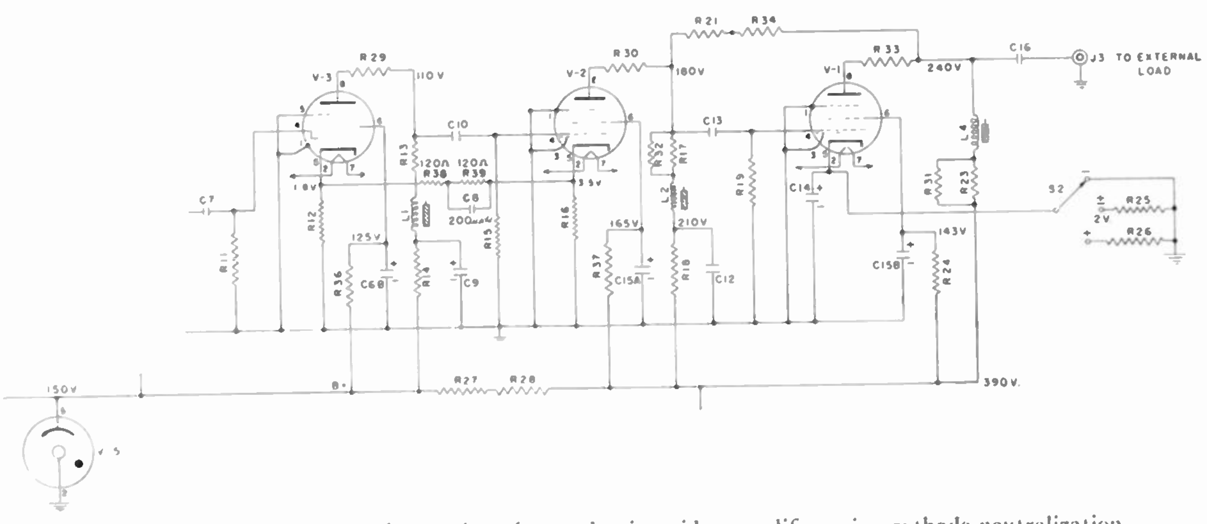

Fig. 2—Schematic diagram of a portion of a production video amplifier using cathode neutralization.

will function as a cathode neutralized amplifier at lower frequencies.

It can be seen from a comparison of (1) and (2) that the output impedance of the amplifier is not affected by the use of cathode neutralization. However, if the plate load resistance is not negligibly small compared with the in most audio amplifiers the tube plate load resistance is not negligible, compared with the tube internal plate resistance. Also, heater-cathode leakage might create a hum problem in the early stages of high gain amplifiers.

[2] MIT Radiation Laboratory Series, "Waveforms," McGraw-Hill, New York, N. Y., Vol. 19, Sec. 2.4, p. 26.

[3] See Sec. 5. Par. 11, p. 402 of footnote reference 1.

[4] H. F. Mayer, "Control of the effective internal impedance of amplifiers by means of feedback," Proc. I.R.E., vol. 27, p. 213, March, 1939.

APPENDIX

The four simultaneous equations for the operation of the circuit of Fig. 1 are:

$$i_1 = [e_1 + R_{k1}(i_3 - i_1)]g_{m1} \tag{5}$$

$$i_2 = [i_1 R_1 - (i_2 - i_3)R_{k2}]g_{m2} \tag{6}$$

$$R_{k0}i_3 + R_{k1}(i_3 - i_1) = R_{k2}(i_2 - i_3), \tag{7}$$

$$\text{Gain} = i_2 R_2 / e_1 \tag{8}$$

where g_{m1} and g_{m2} are the transconductances of V-1 and V-2.

Solving (5) for i_3 we obtain

$$i_3 = \frac{-e_1 + R_{k1}i_1 + \dfrac{i_1}{g_{m1}}}{R_{k1}}. \tag{9}$$

Dividing both sides of (6) by g_{m2}, and substituting (9),

$$\frac{i_2}{g_{m2}} = i_1R_1 - i_2R_{k2} + i_3R_{k2}$$

$$= i_1R_1 - i_2R_{k2} + \frac{R_{k2}}{R_{k1}}\left(-e_1 + R_{k1}i_1 + \frac{i_1}{g_{m1}}\right),$$

or

$$i_2\left(R_{k2} + \frac{1}{g_{m2}}\right) = i_1\left(R_1 + R_{k2} + \frac{R_{k2}}{R_{k1}g_{m1}}\right) - \frac{R_{k2}}{R_{k1}}e_1,$$

whence

$$i_1 = \frac{i_2\left(R_{k2} + \dfrac{1}{g_{m2}}\right) + \dfrac{R_{k2}}{R_{k1}}e_1}{R_1 + R_{k2} + \dfrac{R_{k2}}{R_{k1}g_{m1}}}. \tag{10}$$

Solving (7) for i_3, and substituting (9),

$$i_3 = \frac{R_{k1}i_1 + R_{k2}i_2}{R_{k0} + R_{k1} + R_{k2}} = \frac{-e_1 + R_{k1}i_1 + \dfrac{i_1}{g_{m1}}}{R_{k1}}.$$

Cross-multiplying,

$$R_{k1}^2 i_1 + R_{k1}R_{k2}i_2 = -e_1(R_{k0} + R_{k1} + R_{k2})$$
$$+ i_1\left(R_{k1} + \frac{1}{g_{m1}}\right)(R_{k0} + R_{k1} + R_{k2}). \tag{11}$$

Solving (11) for i_1, and substituting (10),

$$i_1 = \frac{R_{k1}R_{k2}i_2 + e_1(R_{k0} + R_{k1} + R_{k2})}{\left(R_{k1} + \dfrac{1}{g_{m1}}\right)(R_{k0} + R_{k1} + R_{k2}) - R_{k1}^2}$$

$$= \frac{i_2\left(R_{k2} + \dfrac{1}{g_{m2}}\right) + \dfrac{R_{k2}}{R_{k1}}e_1}{R_1 + R_{k2} + \dfrac{R_{k2}}{R_{k1}g_{m1}}}.$$

Transposing, and factoring out i_2,

$$i_2\left[\frac{R_{k1}R_{k2}}{\left(R_{k1} + \dfrac{1}{g_{m1}}\right)(R_{k0} + R_{k1} + R_{k2}) - R_{k1}^2} - \frac{R_{k2} + \dfrac{1}{g_{m2}}}{R_1 + R_{k2} + \dfrac{R_{k2}}{R_{k1}g_{m1}}}\right]$$

$$= -e_1\frac{R_{k0} + R_{k1} + R_{k2}}{\left(R_{k1} + \dfrac{1}{g_{m1}}\right)(R_{k0} + R_{k1} + R_{k2}) - R_{k1}^2}$$

$$+ e_1\left(\frac{R_{k2}}{R_{k1}}\right)\frac{1}{R_1 + R_{k2} + \dfrac{R_{k2}}{R_{k1}g_{m1}}}.$$

Cross-multiplying,

$$i_2\left\{R_{k1}R_{k2}\left(R_1 + R_{k2} + \frac{R_{k2}}{R_{k1}g_{m1}}\right) - \left(R_{k2} + \frac{1}{g_{m2}}\right)\cdot\left[\left(R_{k1} + \frac{1}{g_{m1}}\right)(R_{k0} + R_{k1} + R_{k2}) - R_{k1}^2\right]\right\}$$

$$= e_1\left\{-(R_{k0} + R_{k1} + R_{k2})\left(R_1 + R_{k2} + \frac{R_{k2}}{R_{k1}g_{m1}}\right) + \frac{R_{k2}}{R_{k1}}\left[\left(R_{k1} + \frac{1}{g_{m1}}\right)(R_{k0} + R_{k1} + R_{k2}) - R_{k1}^2\right]\right\}. \tag{12}$$

Substituting (12) into (8), we obtain

$$\text{Gain} = R_2\frac{-(R_{k0} + R_{k1} + R_{k2})\left(R_1 + R_{k2} + \dfrac{R_{k2}}{R_{k1}g_{m1}}\right) + \dfrac{R_{k2}}{R_{k1}}\left[\left(R_{k1} + \dfrac{1}{g_{m1}}\right)(R_{k0} + R_{k1} + R_{k2}) - R_{k1}^2\right]}{R_{k1}R_{k2}\left(R_1 + R_{k2} + \dfrac{R_{k2}}{R_{k1}g_{m1}}\right) - \left(R_{k2} + \dfrac{1}{g_{m2}}\right)\left[\left(R_{k1} + \dfrac{1}{g_{m1}}\right)(R_{k0} + R_{k1} + R_{k2}) - R_{k1}^2\right]}.$$

Multiplying out numerator and denominator, cancelling equal terms of opposite signs, and multiplying numerator and denominator by $g_{m1}\,g_{m2}$, we obtain equation (1) of the main text:

$$\text{Gain} = g_{m1}g_{m2}R_2\left[\frac{R_1(R_{k0}+R_{k1}+R_{k2})+R_{k1}R_{k2}}{R_{k0}+R_{k1}+R_{k2}+g_{m2}R_{k2}(R_{k0}+R_{k1})+g_{m1}R_{k1}(R_{k0}+R_{k2})+g_{m1}g_{m2}R_{k1}R_{k2}(R_{k0}-R_1)}\right]. \quad (1)$$

In order for the gain in (1) to be equal to $g_{m1}g_{m2}R_1R_2$, he fraction inside the brackets must be equal to R_1. Di- 'iding both sides of this identity by R_1, cross-multiply- ng, and solving for R_{k0}, we obtain (3) of the main ext:

$$R_{k0} = \frac{R_{k1}R_{k2}\left(\frac{1}{R_1} - g_{m1} - g_{m2} + g_{m1}g_{m2}R_1\right)}{g_{m1}R_{k1} + g_{m2}R_{k2} + g_{m1}g_{m2}R_{k1}R_{k2}}. \quad (3)$$

In order for the gain of (1) to become infinite, the denominator of the fraction in the brackets must be equal to zero. Setting up this identity, and solving for R_{k0}, we obtain (4) of the main text:

$$R_{k0} = \frac{g_{m1}g_{m2}R_{k1}R_{k2}R_1 - (R_{k1}+R_{k2}+g_{m2}R_{k1}R_{k2}+g_{m1}R_{k1}R_{k2})}{(1+g_{m1}R_{k1})(1+g_{m2}R_{k2})}. \quad (4)$$

A New Figure of Merit for the Transient Response of Video Amplifiers*

R. C. PALMER†, ASSOCIATE, IRE, AND L. MAUTNER‡, SENIOR MEMBER, IRE

Summary—**A figure of merit suitable for comparing the transient response of television video amplifiers is proposed. The parameters are adjusted so that when applied to a shunt-peaked interstage, the figure of merit reaches a maximum for an overshoot of approximately 2 per cent. Application of the suggested form to other types of interstages arranges the various networks in the order of their suitability in television amplifiers as considered from their transient responses.**

THE STUDY of amplifiers for video applications has, in the past, been considered from the viewpoints of both steady-state and transient response. In the process of developing wide-band amplifiers on a steady-state basis, it has been assumed that the desired goal is to achieve a flat amplitude characteristic for the widest band of frequencies. It has been further assumed that the accompanying phase-shift characteristic be linear within limits which will make the over-all amplifier useful for the particular application. Although the experimental verification of a given amplitude characteristic is not difficult, the determination of the accompanying phase characteristic often presents a considerable problem. For minimum phase-shift networks, and these are the types which will be considered here, Bode[1] has shown that the phase characteristic is uniquely defined by the amplitude characteristic; however, this determination, while straightforward, is nonetheless involved.

A figure of merit for comparing the relative utility of wide-band amplifiers on a steady-state basis has been generally accepted as the gain-bandwidth product. By considering the interstages alone, normalizing these to a reference midfrequency impedance level, the steady-state figure of merit degenerates to a comparison of the upper frequency limit at which the impedance of the network falls to some specified value. This cutoff frequency may be considered as that at which the interstage network impedance has decreased to 70.7 per cent of its midfrequency value, or alternatively, as that frequency which, when multiplied by the midfrequency impedance, gives the same product as the area contained under the impedance versus frequency curve. This latter value may be more useful for mathematical manipulation, as considered by Hansen[2] and DiToro.[3]

* Decimal classification: R 363.4. Original manuscript received by the Institute, April 13, 1948; revised manuscript received, January 21, 1949. Presented, 1948 IRE National Convention, New York, N. Y., March 23, 1948.

† Allen B. DuMont Laboratories, Inc., Passaic, N. J.
‡ Television Equipment Corp., New York, N. Y.

[1] H. W. Bode, "Network Analysis and Feedback Amplifier Design," D. Van Nostrand Co., Inc., New York; N. Y., 1945.
[2] W. W. Hansen, "Transient response of wideband amplifiers," *Electronic Ind.*, vol. 3, pp. 80–82, 218–220; November, 1944.
[3] M. J. DiToro, "Phase and amplitude distortion in linear networks," Proc. I.R.E. vol. 36, pp. 24–36; January, 1948.

In video applications, the fidelity of pulse reproduction is, in reality, the final criterion by which we seek to judge the utility of various interstages. Since the steady-state response only indirectly measures the fidelity of pulse reproduction, it is but an intermediate step in the evaluation of the transient response. In particular, since the steady-state figure of merit does not take cognizance of the variation of the time-delay characteristic near the cutoff frequency, it is of relatively little use in transient work.

The purpose of this paper is to analyze video interstages from a transient viewpoint solely, and to propose a figure of merit by which the relative utility of an amplifier for transient applications can be specified. Although the criterion that is proposed does not rest upon a coherent mathematical development, it, nevertheless, does consider for the first time those factors which, from both an experimental and theoretical viewpoint, must be dealt with in order to make a fair appraisal.

Some definitions are in order before proceeding further. Assume the input signal takes the form of a unit step, which is the integral of the sometimes used Δ function. An ideal amplifier from a transient standpoint will reproduce such a wave form exactly,[4] and a typical amplifier which fails to do this will, in general, reproduce the initial step with a function that has a finite slope and may also have an "overshoot" or "undershoot" which, in a simple case, will take the form of a damped sinusoid. The steepness of the maximum slope will be a measure of the rise time, and this parameter has been previously defined in several different ways. One must decide whether the rise time should be specified in a manner which is of practical value, or in a manner which lends itself to easy mathematical manipulation. Although we penalize ourselves somewhat for doing so, the former method is elected here. Kallman, Spencer, and Singer[5] have suggested that this parameter be defined in terms of the time interval within which the output amplitude wave form traverses the 10 to 90 per cent points. This has been found, in practice, to be desirable inasmuch as one is seldom concerned with the delay which may take place from the origin to the 10 per cent value, and provided the overshoot is not excessive and the wave form follows a normal shape, the 90 per cent value represents a convenient point at which the wave form excursion may be said to have been completed. If the interstage is normalized with respect to impedance level, the absolute magnitude of the maximum variation of the output wave form from its end value of unity will be defined as the overshoot. These two parameters will be referred to as the rise time τ and the overshoot γ, and are shown in Fig. 1. The Laplace transformation has been used in analyzing the interstage networks to be described here, the methods following those of Gardner and Barnes.[6] In carrying out such an analysis, it is found that the rise time varies inversely with both R and C, so that it is convenient to conduct one analysis for each network configuration and

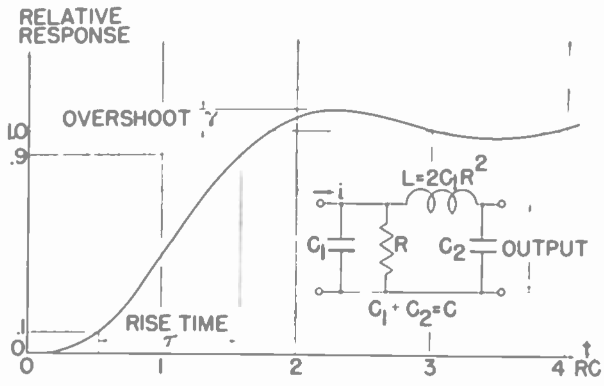

Fig. 1—Typical transient response.

specify the rise time in t/RC units. The value of shunt capacitance C, in the case of two-terminal networks, will consist of the total distributed interstage capacitance; in the case of four-terminal networks, the convention that has been followed has been to consider C as the sum of the input and output capacitances of the network. This then permits the use of recurrent filter networks without penalizing the ultimately derived figure of merit for the midpoint shunt capacitances of the system.

In comparing the performance of any interstage, one is concerned with the quantities absolute rise time, overshoot, and gain (or impedance level). In order to make the figure of merit independent of impedance level, the relative rise time τ must be introduced as a reciprocal function. It is considered important that the figure of merit also be some inverse function of the overshoot γ. The amount that the figure of merit should be penalized for increasing values of overshoot rests upon two foundations. If the figure of merit relates only to single interstages, it should be so arranged that the value of the figure of merit increases with decreasing rise time, up to a point where the overshoot becomes so large as to be objectionable from a practical standpoint. For values of overshoot greater than this value, the figure of merit should decrease rapidly. In television applications, values of overshoot greater than 2 per cent may lead to a perceptible and possibly objectionable ringing in the reproduced picture in the case of sharp black and white transitions. Consequently, such a value of overshoot should be given some weight in determining

[4] That is, excluding any delay which merely translates the wave form along the time axis.

[5] H. E. Kallman, R. E. Spencer, and C. P. Singer, "Transient response," Proc. I.R.E., vol. 33, pp. 169–195; March, 1945.

[6] M. F. Gardner and J. L. Barnes, "Transients in Linear Systems," vol. I; John Wiley and Sons, Inc., New York, N. Y.; 1942.

t what point the figure of merit will begin to become enalized with respect to increasing values of γ.

A much more important factor in establishing his alue of γ, however, occurs in relation to the use of the gure of merit for multistage applications. Kallman, et l.,[5] and Elmore[7] have shown the relation between the se time of a single interstage as compared to the over-ll rise time accruing from the recurrent use of such iterstages. If the value of γ is small, these results can e summarized by saying that the over-all rise time of n milar interstages is equal to the rise time of a single ich interstage multiplied by the square root of n. lowever, if γ is not small, this relationship does not old, and we are led to inquire as to the value of γ eyond which the approximation becomes in error. The ork of Bedford and Fredendall[8] fortunately gives us ome clue to the establishment of the value of γ from his standpoint. They have given graphical data showig the performance of 16, 32, and 64 recurrent shunteaked interstages, in each case these data being tabuated for three different values of γ of a single such iterstage. Based upon these results, it is found that if he overshoot has a value equal to or less than approximately 2 per cent, the rise time agrees fairly well ith the relationship given above, and the overshoot emains substantially constant. However, for values of greater than 2 per cent, the overshoot of the over-all mplifier increases enormously, and concurrently the iven relationship for the rise time does not hold. From his standpoint, therefore, it seems fair, in the case of a hunt-peaked amplifier, to permit the figure of merit o increase for decreasing rise time, up to a point where he overshoot approximates 2 per cent. For values of arameters in such a network that lead to greater values f γ, although the rise time may still continue to decrease, it is felt reasonable to have the figure of merit decrease sharply inasmuch as such a configuration is deemed of little use for transient work such as television, where the recurrent use of such a network would cause excessive overshoots.

It has seemed expedient, therefore, to derive the figure of merit based upon this data and to consider the shunt-peaked network first. In Fig. 2 is shown a typical shunt-peaked network, and it will be observed that there are an infinite number of variations possible, depending upon the assigned value of the parameter m, where m is given by $m = L/CR^2$. In Fig. 3 the relationship between rise time and m is given graphically, and we can see that as m is increased from a value of 0 (which corresponds to a simple RC interstage), the value of τ decreases initially at approximately a linear rate. Also, in Fig. 3 is shown the relationship between γ and m for the same network. One observes that for a value of $m < 0.25$ there is no overshoot; and as m increases beyond this value, the overshoot increases, eventually becoming approximately a linear variation. It is found that a value of $m = 0.388$ will give an overshoot of approximately 2 per cent, and based upon the data of Bedford and Fredendall for recurrent shunt-peaked interstages, this value has been selected as representing the point beyond which the figure of merit should be penalized for increasing values of γ. The expression for the figure of merit which we shall now propose will take cognizance of this fact, leading to a figure of merit for a shunt-peaked interstage which will have a maximum value for this value of m. A suitable form for the figure of merit, F, is as follows

$$F = a\tau^{-1}\epsilon^{-b\gamma^2} \tag{1}$$

where

F = a numeric specifying the relative quality of a shunt-peaked interstage from the transient viewpoint

a = a constant to give a suitable magnitude to F

τ = the rise time in units of time normalized by the factor RC

γ = the fractional overshoot

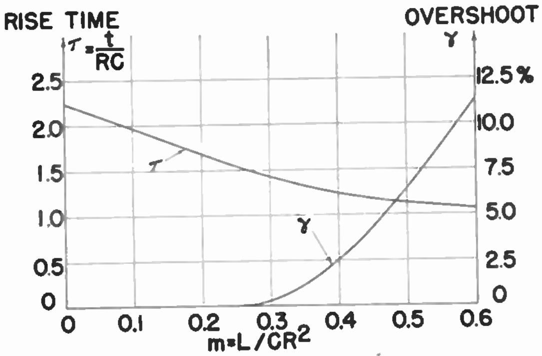

Fig. 3—Variation of τ and γ with $m = L/CR^2$ for shunt-peaked interstage.

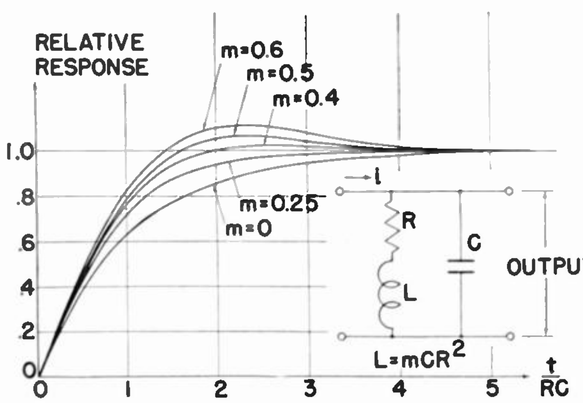

Fig. 2—Transient response, shunt-peaked interstage.

[7] W. C. Elmore, "The transient response of damped linear networks with particular regard to wideband amplifiers," *Jour. Appl. Phys.*, vol. 19, pp. 55–63; January, 1948.

[8] A. V. Bedford and G. L. Fredendall, "Transient response of multi-stage video-frequency amplifiers," PROC. I.R.E., vol. 27, pp. 277–284; April, 1939.

Appendix

The four simultaneous equations for the operation of the circuit of Fig. 1 are:

$$i_1 = [e_1 + R_{k1}(i_3 - i_1)]g_{m1} \tag{5}$$

$$i_2 = [i_1R_1 - (i_2 - i_3)R_{k2}]g_{m2} \tag{6}$$

$$R_{k0}i_3 + R_{k1}(i_3 - i_1) = R_{k2}(i_2 - i_3), \tag{7}$$

$$\text{Gain} = i_2R_2/e_1 \tag{8}$$

where g_{m1} and g_{m2} are the transconductances of V-1 and V-2.

Solving (5) for i_3 we obtain

$$i_3 = \frac{-e_1 + R_{k1}i_1 + \dfrac{i_1}{g_{m1}}}{R_{k1}}. \tag{9}$$

Dividing both sides of (6) by g_{m2}, and substituting (9),

$$\frac{i_2}{g_{m2}} = i_1R_1 - i_2R_{k2} + i_3R_{k2}$$

$$= i_1R_1 - i_2R_{k2} + \frac{R_{k2}}{R_{k1}}\left(-e_1 + R_{k1}i_1 + \frac{i_1}{g_{m1}}\right),$$

or

$$i_2\left(R_{k2} + \frac{1}{g_{m2}}\right) = i_1\left(R_1 + R_{k2} + \frac{R_{k2}}{R_{k1}g_{m1}}\right) - \frac{R_{k2}}{R_{k1}}e_1,$$

whence

$$i_1 = \frac{i_2\left(R_{k2} + \dfrac{1}{g_{m2}}\right) + \dfrac{R_{k2}}{R_{k1}}e_1}{R_1 + R_{k2} + \dfrac{R_{k2}}{R_{k1}g_{m1}}}. \tag{10}$$

Solving (7) for i_3, and substituting (9),

$$i_3 = \frac{R_{k1}i_1 + R_{k2}i_2}{R_{k0} + R_{k1} + R_{k2}} = \frac{-e_1 + R_{k1}i_1 + \dfrac{i_1}{g_{m1}}}{R_{k1}}.$$

Cross-multiplying,

$$R_{k1}^2i_1 + R_{k1}R_{k2}i_2 = -e_1(R_{k0} + R_{k1} + R_{k2})$$
$$+ i_1\left(R_{k1} + \frac{1}{g_{m1}}\right)(R_{k0} + R_{k1} + R_{k2}). \tag{11}$$

Solving (11) for i_1, and substituting (10),

$$i_1 = \frac{R_{k1}R_{k2}i_2 + e_1(R_{k0} + R_{k1} + R_{k2})}{\left(R_{k1} + \dfrac{1}{g_{m1}}\right)(R_{k0} + R_{k1} + R_{k2}) - R_{k1}^2}$$

$$= \frac{i_2\left(R_{k2} + \dfrac{1}{g_{m2}}\right) + \dfrac{R_{k2}}{R_{k1}}e_1}{R_1 + R_{k2} + \dfrac{R_{k2}}{R_{k1}g_{m1}}}$$

Transposing, and factoring out i_2,

$$i_2\left[\frac{R_{k1}R_{k2}}{\left(R_{k1} + \dfrac{1}{g_{m1}}\right)(R_{k0} + R_{k1} + R_{k2}) - R_{k1}^2} - \frac{R_{k2} + \dfrac{1}{g_{m2}}}{R_1 + R_{k2} + \dfrac{R_{k2}}{R_{k1}g_{m1}}}\right]$$

$$= -e_1\frac{R_{k0} + R_{k1} + R_{k2}}{\left(R_{k1} + \dfrac{1}{g_{m1}}\right)(R_{k0} + R_{k1} + R_{k2}) - R_{k1}^2}$$

$$+ e_1\left(\frac{R_{k2}}{R_{k1}}\right)\frac{1}{R_1 + R_{k2} + \dfrac{R_{k2}}{R_{k1}g_{m1}}}.$$

Cross-multiplying,

$$i_2\left\{R_{k1}R_{k2}\left(R_1 + R_{k2} + \frac{R_{k2}}{R_{k1}g_{m1}}\right) - \left(R_{k2} + \frac{1}{g_{m2}}\right)\right.$$
$$\left.\cdot\left[\left(R_{k1} + \frac{1}{g_{m1}}\right)(R_{k0} + R_{k1} + R_{k2}) - R_{k1}^2\right]\right\}$$
$$= e_1\left\{-(R_{k0} + R_{k1} + R_{k2})\left(R_1 + R_{k2} + \frac{R_{k2}}{R_{k1}g_{m1}}\right)\right.$$
$$\left.+ \frac{R_{k2}}{R_{k1}}\left[\left(R_{k1} + \frac{1}{g_{m1}}\right)(R_{k0} + R_{k1} + R_{k2}) - R_{k1}^2\right]\right\}. \tag{12}$$

Substituting (12) into (8), we obtain

$$\text{Gain} = R_2\frac{-(R_{k0} + R_{k1} + R_{k2})\left(R_1 + R_{k2} + \dfrac{R_{k2}}{R_{k1}g_{m1}}\right) + \dfrac{R_{k2}}{R_{k1}}\left[\left(R_{k1} + \dfrac{1}{g_{m1}}\right)(R_{k0} + R_{k1} + R_{k2}) - R_{k1}^2\right]}{R_{k1}R_{k2}\left(R_1 + R_{k2} + \dfrac{R_{k2}}{R_{k1}g_{m1}}\right) - \left(R_{k2} + \dfrac{1}{g_{m2}}\right)\left[\left(R_{k1} + \dfrac{1}{g_{m1}}\right)(R_{k0} + R_{k1} + R_{k2}) - R_{k1}^2\right]}.$$

Multiplying out numerator and denominator, cancelling equal terms of opposite signs, and multiplying numerator and denominator by g_{m1} g_{m2}, we obtain equation (1) of the main text:

$$\text{Gain} = g_{m1}g_{m2}R_2\left[\frac{R_1(R_{k0}+R_{k1}+R_{k2})+R_{k1}R_{k2}}{R_{k0}+R_{k1}+R_{k2}+g_{m2}R_{k2}(R_{k0}+R_{k1})+g_{m1}R_{k1}(R_{k0}+R_{k2})+g_{m1}g_{m2}R_{k1}R_{k2}(R_{k0}-R_1)}\right]. \quad (1)$$

In order for the gain in (1) to be equal to $g_{m1}g_{m2}R_1R_2$, the fraction inside the brackets must be equal to R_1. Dividing both sides of this identity by R_1, cross-multiplying, and solving for R_{k0}, we obtain (3) of the main text:

$$R_{k0} = \frac{R_{k1}R_{k2}\left(\frac{1}{R_1} - g_{m1} - g_{m2} + g_{m1}g_{m2}R_1\right)}{g_{m1}R_{k1} + g_{m2}R_{k2} + g_{m1}g_{m2}R_{k1}R_{k2}}. \quad (3)$$

In order for the gain of (1) to become infinite, the denominator of the fraction in the brackets must be equal to zero. Setting up this identity, and solving for R_{k0}, we obtain (4) of the main text:

$$R_{k0} = \frac{g_{m1}g_{m2}R_{k1}R_{k2}R_1 - (R_{k1}+R_{k2}+g_{m2}R_{k1}R_{k2}+g_{m1}R_{k1}R_{k2})}{(1+g_{m1}R_{k1})(1+g_{m2}R_{k2})}. \quad (4)$$

A New Figure of Merit for the Transient Response of Video Amplifiers*

R. C. PALMER†, ASSOCIATE, IRE, AND L. MAUTNER‡, SENIOR MEMBER, IRE

Summary—**A figure of merit suitable for comparing the transient response of television video amplifiers is proposed. The parameters are adjusted so that when applied to a shunt-peaked interstage, the figure of merit reaches a maximum for an overshoot of approximately 2 per cent. Application of the suggested form to other types of interstages arranges the various networks in the order of their suitability in television amplifiers as considered from their transient responses.**

THE STUDY of amplifiers for video applications has, in the past, been considered from the viewpoints of both steady-state and transient response. In the process of developing wide-band amplifiers on a steady-state basis, it has been assumed that the desired goal is to achieve a flat amplitude characteristic for the widest band of frequencies. It has been further assumed that the accompanying phase-shift characteristic be linear within limits which will make the over-all amplifier useful for the particular application. Although the experimental verification of a given amplitude characteristic is not difficult, the determination of the accompanying phase characteristic often presents a considerable problem. For minimum phase-shift networks, and these are the types which will be considered here, Bode[1] has shown that the phase characteristic is uniquely defined by the amplitude characteristic; however, this determination, while straightforward, is nonetheless involved.

A figure of merit for comparing the relative utility of wide-band amplifiers on a steady-state basis has been generally accepted as the gain-bandwidth product. By considering the interstages alone, normalizing these to a reference midfrequency impedance level, the steady-state figure of merit degenerates to a comparison of the upper frequency limit at which the impedance of the network falls to some specified value. This cutoff frequency may be considered as that at which the interstage network impedance has decreased to 70.7 per cent of its midfrequency value, or alternatively, as that frequency which, when multiplied by the midfrequency impedance, gives the same product as the area contained under the impedance versus frequency curve. This latter value may be more useful for mathematical manipulation, as considered by Hansen[2] and DiToro.[3]

* Decimal classification: R 363.4. Original manuscript received by the Institute, April 13, 1948; revised manuscript received, January 21, 1949. Presented, 1948 IRE National Convention, New York, N. Y., March 23, 1948.
† Allen B. DuMont Laboratories, Inc., Passaic, N. J.
‡ Television Equipment Corp., New York, N. Y.

[1] H. W. Bode, "Network Analysis and Feedback Amplifier Design," D. Van Nostrand Co., Inc., New York; N. Y., 1945.
[2] W. W. Hansen, "Transient response of wideband amplifiers," *Electronic Ind.*, vol. 3, pp. 80–82, 218–220; November, 1944.
[3] M. J. DiToro, "Phase and amplitude distortion in linear networks," Proc. I.R.E. vol. 36, pp. 24–36; January, 1948.

In video applications, the fidelity of pulse reproduction is, in reality, the final criterion by which we seek to judge the utility of various interstages. Since the steady-state response only indirectly measures the fidelity of pulse reproduction, it is but an intermediate step in the evaluation of the transient response. In particular, since the steady-state figure of merit does not take cognizance of the variation of the time-delay characteristic near the cutoff frequency, it is of relatively little use in transient work.

The purpose of this paper is to analyze video interstages from a transient viewpoint solely, and to propose a figure of merit by which the relative utility of an amplifier for transient applications can be specified. Although the criterion that is proposed does not rest upon a coherent mathematical development, it, nevertheless, does consider for the first time those factors which, from both an experimental and theoretical viewpoint, must be dealt with in order to make a fair appraisal.

Some definitions are in order before proceeding further. Assume the input signal takes the form of a unit step, which is the integral of the sometimes used Δ function. An ideal amplifier from a transient standpoint will reproduce such a wave form exactly,[4] and a typical amplifier which fails to do this will, in general, reproduce the initial step with a function that has a finite slope and may also have an "overshoot" or "undershoot" which, in a simple case, will take the form of a damped sinusoid. The steepness of the maximum slope will be a measure of the rise time, and this parameter has been previously defined in several different ways. One must decide whether the rise time should be specified in a manner which is of practical value, or in a manner which lends itself to easy mathematical manipulation. Although we penalize ourselves somewhat for doing so, the former method is elected here. Kallman, Spencer, and Singer[5] have suggested that this parameter be defined in terms of the time interval within which the output amplitude wave form traverses the 10 to 90 per cent points. This has been found, in practice, to be desirable inasmuch as one is seldom concerned with the delay which may take place from the origin to the 10 per cent value, and provided the overshoot is not excessive and the wave form follows a normal shape, the 90 per cent value represents a convenient point at which the wave form excursion may be said to have been completed. If the interstage is normalized with respect to impedance level, the absolute magnitude of the maximum variation of the output wave form from its end value of unity will be defined as the overshoot. These two parameters will be referred to as the rise time τ and the overshoot γ, and are shown in Fig. 1. The Laplace transformation has been used in analyzing the interstage networks to be described here, the methods following those of Gardner and Barnes.[6] In carrying out such an analysis, it is found that the rise time varies inversely with both R and C, so that it is convenient to conduct one analysis for each network configuration and specify the rise time in t/RC units. The value of shunt capacitance C, in the case of two-terminal networks, will consist of the total distributed interstage capacitance; in the case of four-terminal networks, the convention that has been followed has been to consider C as the sum of the input and output capacitances of the network. This then permits the use of recurrent filter networks without penalizing the ultimately derived figure of merit for the midpoint shunt capacitances of the system.

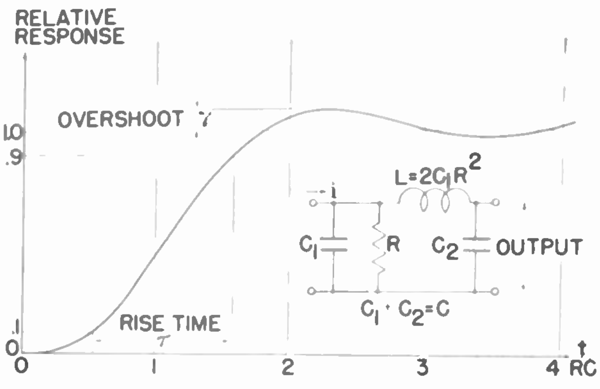

Fig. 1—Typical transient response.

In comparing the performance of any interstage, one is concerned with the quantities absolute rise time, overshoot, and gain (or impedance level). In order to make the figure of merit independent of impedance level, the relative rise time τ must be introduced as a reciprocal function. It is considered important that the figure of merit also be some inverse function of the overshoot γ. The amount that the figure of merit should be penalized for increasing values of overshoot rests upon two foundations. If the figure of merit relates only to single interstages, it should be so arranged that the value of the figure of merit increases with decreasing rise time, up to a point where the overshoot becomes so large as to be objectionable from a practical standpoint. For values of overshoot greater than this value, the figure of merit should decrease rapidly. In television applications, values of overshoot greater than 2 per cent may lead to a perceptible and possibly objectionable ringing in the reproduced picture in the case of sharp black and white transitions. Consequently, such a value of overshoot should be given some weight in determining

[4] That is, excluding any delay which merely translates the wave form along the time axis.

[5] H. E. Kallman, R. E. Spencer, and C. P. Singer, "Transient response," Proc. I.R.E., vol. 33, pp. 169–195; March, 1945.

[6] M. F. Gardner and J. L. Barnes, "Transients in Linear Systems," vol. 1; John Wiley and Sons, Inc., New York, N. Y.; 1942.

at what point the figure of merit will begin to become penalized with respect to increasing values of γ.

A much more important factor in establishing his value of γ, however, occurs in relation to the use of the figure of merit for multistage applications. Kallman, et al.,[5] and Elmore[7] have shown the relation between the rise time of a single interstage as compared to the over-all rise time accruing from the recurrent use of such interstages. If the value of γ is small, these results can be summarized by saying that the over-all rise time of n similar interstages is equal to the rise time of a single such interstage multiplied by the square root of n. However, if γ is not small, this relationship does not hold, and we are led to inquire as to the value of γ beyond which the approximation becomes in error. The work of Bedford and Fredendall[8] fortunately gives us some clue to the establishment of the value of γ from this standpoint. They have given graphical data showing the performance of 16, 32, and 64 recurrent shunt-peaked interstages, in each case these data being tabulated for three different values of γ of a single such interstage. Based upon these results, it is found that if the overshoot has a value equal to or less than approximately 2 per cent, the rise time agrees fairly well with the relationship given above, and the overshoot remains substantially constant. However, for values of γ greater than 2 per cent, the overshoot of the over-all amplifier increases enormously, and concurrently the given relationship for the rise time does not hold. From this standpoint, therefore, it seems fair, in the case of a shunt-peaked amplifier, to permit the figure of merit to increase for decreasing rise time, up to a point where the overshoot approximates 2 per cent. For values of parameters in such a network that lead to greater values of γ, although the rise time may still continue to decrease, it is felt reasonable to have the figure of merit decrease sharply inasmuch as such a configuration is deemed of little use for transient work such as television, where the recurrent use of such a network would cause excessive overshoots.

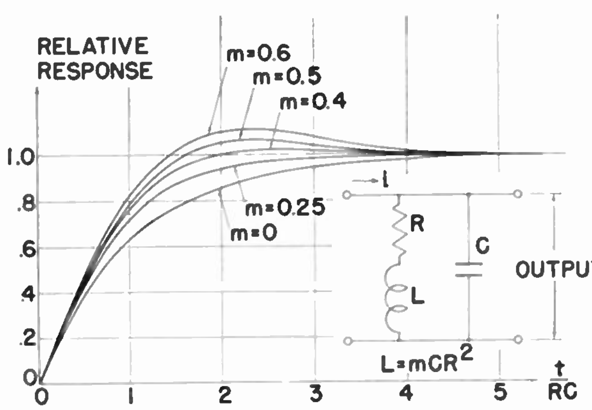

Fig. 2—Transient response, shunt-peaked interstage.

It has seemed expedient, therefore, to derive the figure of merit based upon this data and to consider the shunt-peaked network first. In Fig. 2 is shown a typical shunt-

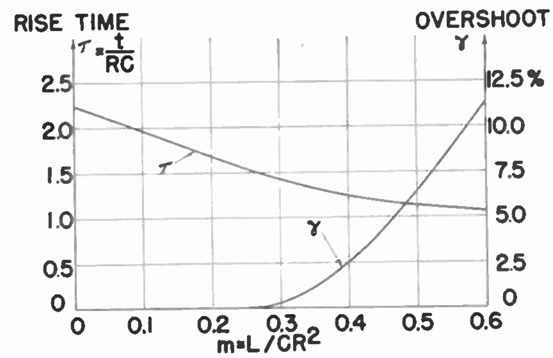

Fig. 3—Variation of τ and γ with $m=L/CR^2$ for shunt-peaked interstage.

peaked network, and it will be observed that there are an infinite number of variations possible, depending upon the assigned value of the parameter m, where m is given by $m=L/CR^2$. In Fig. 3 the relationship between rise time and m is given graphically, and we can see that as m is increased from a value of 0 (which corresponds to a simple RC interstage), the value of τ decreases initially at approximately a linear rate. Also, in Fig. 3 is shown the relationship between γ and m for the same network. One observes that for a value of $m<0.25$ there is no overshoot; and as m increases beyond this value, the overshoot increases, eventually becoming approximately a linear variation. It is found that a value of $m=0.388$ will give an overshoot of approximately 2 per cent, and based upon the data of Bedford and Fredendall for recurrent shunt-peaked interstages, this value has been selected as representing the point beyond which the figure of merit should be penalized for increasing values of γ. The expression for the figure of merit which we shall now propose will take cognizance of this fact, leading to a figure of merit for a shunt-peaked interstage which will have a maximum value for this value of m. A suitable form for the figure of merit, F, is as follows

$$F = a\tau^{-1}\epsilon^{-b\gamma^2} \tag{1}$$

where

F = a numeric specifying the relative quality of a shunt-peaked interstage from the transient viewpoint

a = a constant to give a suitable magnitude to F

τ = the rise time in units of time normalized by the factor RC

γ = the fractional overshoot

[7] W. C. Elmore, "The transient response of damped linear networks with particular regard to wideband amplifiers," *Jour. Appl. Phys.*, vol. 19, pp. 55–63; January, 1948.

[8] A. V. Bedford and G. L. Fredendall, "Transient response of multi-stage video-frequency amplifiers," Proc. I.R.E., vol. 27, pp. 277–284; April, 1939.

b = a second constant which determines the amount by which the figure of merit F is penalized for different values of γ.

Carrying out computations with such a figure of merit and utilizing the known data for shunt-peaked interstages reduces (1) to

$$F = 1000\tau^{-1}\epsilon^{-100\gamma^2}. \tag{2}$$

Plotting F versus the network parameter m in Fig. 4, it is observed that the maximum figure of merit for the shunt-peaked interstage has a value of 755. For $m=0$, corresponding to a simple RC interstage, the corresponding figure of merit is 450. The figure of merit is permitted to increase beyond the critically damped case into the

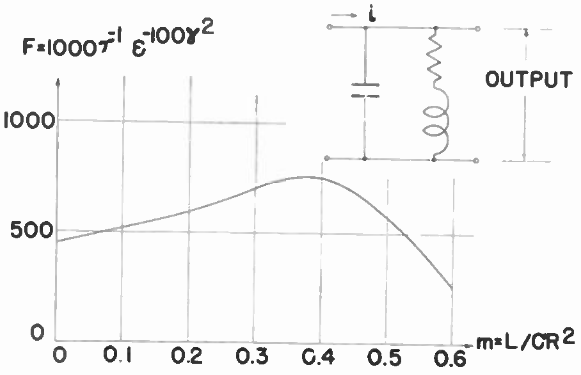

Fig. 4—Figure of merit versus $m = L/CR^2$ for shunt-peaked interstage.

region where overshoot becomes apparent, reaching a peak for a value of m corresponding to an overshoot which we consider the maximum permissible from two viewpoints:

1. The practical consideration, wherein greater overshoot may result in objectionable distortion in a transmitted picture, in the case of a television system.

2. From the standpoint that a greater overshoot will render a multistage amplifier of limited application because its over-all overshoot is then very objectionable. The logic of this arrangement becomes apparent when one realizes that the figure of merit for n similar stages of a shunt-peaked amplifier with small overshoot is given simply as the figure of merit for one interstage divided by the square root of n. It should also be clear that this figure of merit is independent of the gain of the amplifier or the corresponding impedance level of the interstage. Of course, in a given case and for a fixed value of shunt capacitance, one is always at liberty to reduce the gain by reducing R; this then makes the absolute rise time in microseconds less, but the value of F, the figure of merit, remains constant.

The figure of merit defined above, while resting on a well-established experimental background, does not have any profound mathematical basis. Nevertheless, from an engineering standpoint, it does provide a useful rule-of-thumb measure of the relative quality of such an interstage for certain video applications.

One is now led to inquire as to the application of such a figure of merit to other types of interstages, both two- and four-terminal varieties. There are two aspects to such networks: (1) their configuration, and (2) the parameter values specified for such a configuration. If we apply the figure of merit derived herein to a typical four-terminal network, for example, one has no assurance that the value thus determined represents the highest figure of merit possible with the particular configuration. However, the derivation of the optimum parameter values for a given four-terminal network represents a vast amount of effort. Since it must be additionally demonstrated that the overshoot resulting from the recurrent use of such an optimum interstage is not objectionable, there seems to be a real value at this time in appraising certain configurations for at least the parameter values which have already been investigated. There appears to be some assurance that for any network, if the overshoot resulting from its use singly is small, the recurrent use of such networks will not give rise to a poor transient response, at least from a standpoint of excessive overshoot. With this thought in mind, and assuming that a 2 per cent overshoot permits of this extrapolation, we have tabulated the figure of merit for a number of typical interstages.

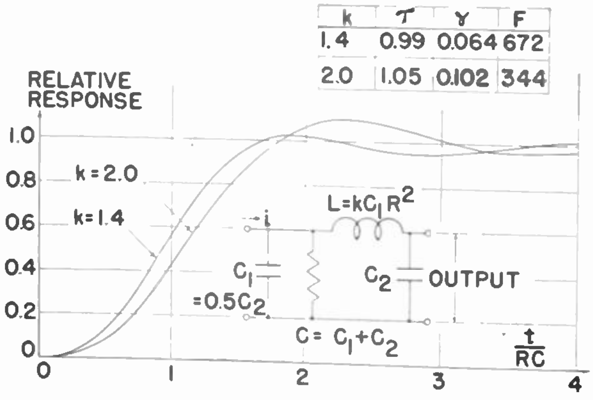

Fig. 5—Transient response, series-peaked interstage.

In Fig. 5 is given the transient response for a series-peaked network for two values of the parameter k indicated in the circuit diagram. For the value $k=1.4$, it is seen that there is a 6.4 per cent "undershoot," which, of course, may be as objectionable as an overshoot. The fact that γ appears squared in the definition of F means, of course, that an "undershoot" is considered in the same fashion as an overshoot. A value of $k=2.0$ gives a 10 per cent overshoot, further penalizing the resulting figure of merit. In Fig. 6 is given the transient response of a network which will be referred to as "Doba's network" because the particular value of parameters specified for this configuration is due, it is believed, to S. Doba of the Bell Telephone Laboratories. In Fig. 7 is shown the network referred to as the series-shunt network; and in Fig. 8, the so-called "Dietzold network," again the name being derived from the fact that the particular parameter values specified are believed to be due to R. L. Dietzold of the Bell Telephone Laboratories. By way of summary, Table I compares the figures of merit for the interstages discussed.

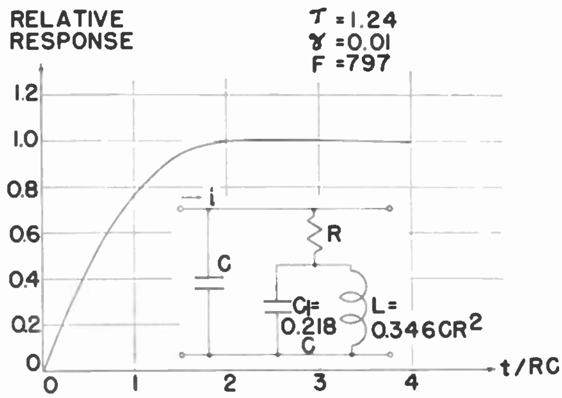

Fig. 6—Transient response, Doba's network.

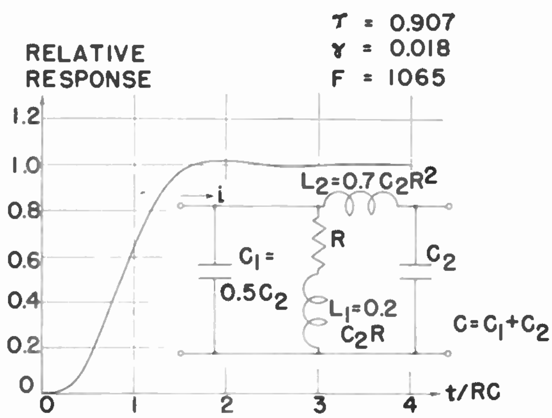

Fig. 7—Transient response, series-shunt interstage.

TABLE I

Interstage	$F = 1{,}000\tau^{-1}\epsilon^{-100\gamma^2}$
Dietzold's Network	1,128
Series-Shunt Peaking	1,065
Doba's Network	797
Shunt Peaking, $m = 0.388$	755
Shunt Peaking, $m = 0.3$	697
Series Peaking, $k = 1.4$	672
Shunt Peaking, $m = 0.5$	572
Uncompensated RC	450
Series Peaking, $k = 2.0$	344

In view of the decreased rise time that one may achieve with some of the more complicated four-terminal networks, and the concurrent increase in figure of merit, one gains the feeling that if a more complicated network may be justified from the standpoint of improved rise time, such an improvement may be gained at the expense of the more involved adjustment. There has been a tendency in the past with respect to production types of video amplifiers to adhere to the simplicity of the shunt-peaked amplifier, because the complexity of adjustment of the more involved networks has rendered their use ill advised. The justification for this feeling may well be questioned in the future as more profound methods become available for the evaluation of the sensitivity of the figure of merit to change in parameter values. However, in the light of present limited knowledge, there seems to be a definite engineering utility for the application of a simple figure of merit of the type described herein to all of the common types of video interstages. It must be borne in mind, however, that the figure of merit assigned on the basis established above, to a given interstage configuration with presently proposed parameter values, may not in fact represent the ultimate in either performance or figure of merit for such an interstage.

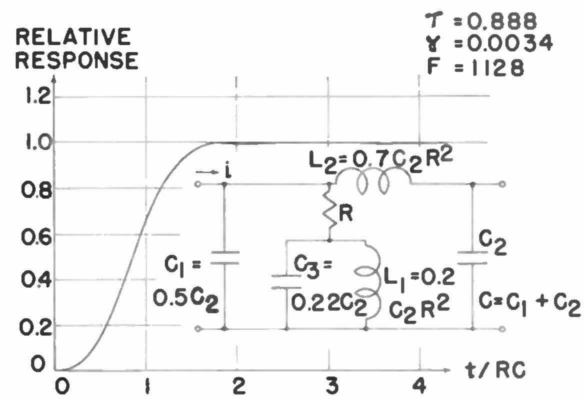

Fig. 8—Transient response, Dietzold's network.

Acknowledgment

The assistance of J. H. Mulligan, Jr., and S. Shamis in the computation of transient responses is gratefully acknowledged.

Design Equations for Reactance-Tube Circuits*

J. D. YOUNG†, ASSOCIATE, IRE, AND H. M. BECK†, MEMBER, IRE

Summary—Without assuming the usual approximations, design equations are derived for several systems of reactance-tube modulation. Empirical methods are used to derive expressions for the total band swept, in which the effect of each parameter can be directly evaluated. The analysis was completed without the use of the usually accepted simplifying relationships between the impedances of the feedback network.[1-3] The critical point where a given-type network changes from an apparent inductance to an apparent capacitance is noted.

Introduction

Variable-Impedance Circuit

THE SYSTEM under consideration is shown in Fig. 1, where

$$E_1/E_0 = Z_1/(Z_1 + Z_2) \tag{1}$$

and assuming a constant current generator

$$E_0/E_1 = -g_m Z_0(Z_1 + Z_2)/(Z_0 + Z_1 + Z_2). \tag{2}$$

From (1) and (2) it follows that

$$-g_m Z_0 Z_1 = Z_0 + Z_1 + Z_2. \tag{3}$$

Equation (3) is the general relation of the system, which, if satisfied completely, would show conditions for oscillation. For convenience, (3) will be considered in two cases, in the first of which Z_1 and Z_2 are composed of parallel capacitance and resistance, while in the second case they are parallel inductance and resistance. In both cases, it can be shown that the reals and imaginaries cannot be simultaneously satisfied at any positive frequency and, therefore, are inherently stable systems. In both cases, the part of (3) corresponding to the reactive component must vanish, and its vanishing will determine a definite frequency, very nearly, at which the system will oscillate if supplied with an external negative resistance.

Case I

The following definitions refer to Fig. 1, where Z_1 and Z_2 are parallel CR circuits:

$$Z_0 = R_0/(1 + jt_0)$$

$$Z_1 = R_1/(1 - jt_1)$$

$$Z_2 = R_2/(1 - jt_2)$$

$$t_0 = R_0(C_0/L_0)^{1/2}(\omega/\omega_0 - \omega_0/\omega)$$

$$t_1 = -\omega C_1 R_1$$

$$t_2 = -\omega C_2 R_2$$

where

$\omega_0 = (L_0 C_0)^{-1/2}$ = resonant angular frequency of the single tuned circuit Z_0 alone

$\omega = 2\pi f$ = resonant angular frequency of the entire variable-impedance circuit as shown in Fig. 1, under operating conditions.

On substituting these quantities in (3) and clearing, the following relationship will result:

$$\begin{aligned}-g_m R_0 R_1 + jg_m R_0 R_1 t_2 = {} & R_0(1 - jt_2 - jt_1 - t_1 t_2) \\ & + R_1(1 - jt_2 + jt_0 + t_0 t_2) \\ & + R_2(1 - jt_1 + jt_0 + t_0 t_1). \end{aligned} \tag{4}$$

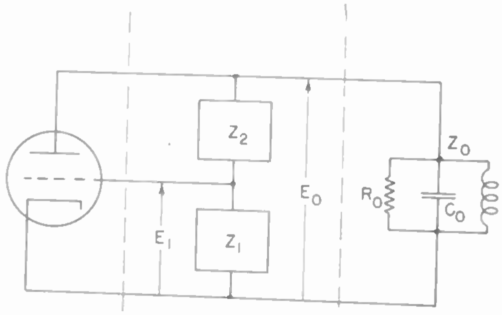

Fig. 1—Variable impedance circuit.

From the reals the following expression for ω/ω_0 is obtained:

$$\omega/\omega_0 = \left\{\frac{(g_m R_0 R_1 + R_0 + R_1 + R_2)L_0 C_0 + R_0 R_1 R_2(C_0 C_1 + C_0 C_2)}{R_0 R_1 R_2(C_0 C_1 + C_0 C_2 + C_1 C_2)}\right\}^{1/2}. \tag{5}$$

Now, in (5), let $g_m \equiv g_c$, the "Class A" operating point on the "$g_m - e_g$" curve, corresponding to the "center" angular frequency ω_c, and let the equal positive and negative increments Δg_m correspond to increments $\Delta_2\omega$ and $\Delta_1\omega$.

Then, defining $\Delta\omega \equiv \Delta_1\omega + \Delta_2\omega$, and rearranging terms, the following will result:

---

* Decimal classification: R145. Original manuscript received by the Institute, August 20, 1948; revised manuscript received, January 20, 1949.

† Naval Research Laboratory, Washington, D. C.

[1] "Reactance tube modulator," *Electronics*, Reference and Directory Issue, vol. 14, p. 47; June, 1941.

[2] August Hund, "Frequency Modulation," first edition, McGraw-Hill Book Co., Inc., New York, N. Y., 1942; pp. 155–174.

[3] N. Marchand, "Reactance tubes," *Communications*, vol. 26, pp. 42–45; March, 1946.

$$\frac{\Delta\omega}{\omega_0} = \left\{\frac{(g_cR_0R_1 + \Delta g_mR_0R_1 + R_0 + R_1 + R_2)L_0C_0 + R_0R_1R_2(C_0C_1 + C_0C_2)}{R_0R_1R_2(C_0C_1 + C_0C_2 + C_1C_2)}\right\}^{1/2} - \left\{\frac{(g_cR_0R_1 - \Delta g_mR_0R_1 + R_0 + R_1 + R_2)L_0C_0 + R_0R_1R_2(C_0C_1 + C_0C_2)}{R_0R_1R_2(C_0C_1 + C_0C_2 + C_1C_2)}\right\}^{1/2}. \quad (6)$$

Then, from (5), with $g_m \equiv g_c$ and $\omega \equiv \omega_c$, we can refer the total band swept, $\Delta\omega$, to the operating angular frequency ω_c, as follows:

$$\frac{\Delta\omega}{\omega_c} \equiv \frac{\Delta\omega}{\omega_0}\cdot\frac{\omega_0}{\omega_c}.$$

Then we see that by a number of elementary operations, the ratio of total band swept to operating center frequency is

$$\frac{\Delta\omega}{\omega_c} = \left\{1 + \frac{\Delta g_m}{\frac{1}{R_0} + \frac{1}{R_1} + \frac{R_2}{R_0R_1} + \frac{R_2C_1}{L_0} + \frac{R_2C_2}{L_0} + g_c}\right\}^{1/2} - \left\{1 - \frac{\Delta g_m}{\frac{1}{R_0} + \frac{1}{R_1} + \frac{R_2}{R_0R_1} + \frac{R_2C_1}{L_0} + \frac{R_2C_2}{L_0} + g_c}\right\}^{1/2}. \quad (7)$$

Rewriting (5) will give the necessary explicit expression for ω_0

$$\omega_0 = \left\{\omega_c^2\left[1 + \frac{C_1C_2}{C_0(C_1 + C_2)}\right] - \frac{g_cR_0R_1 + R_0 + R_1 + R_2}{R_0R_1R_2C_0(C_1 + C_2)}\right\}^{1/2}. \quad (8)$$

From (8) the quantity under the radical must be positive and (7) is then defined only for

$$\omega_c^2 > \frac{g_cR_0R_1 + R_0 + R_1 + R_2}{R_0R_1R_2(C_0C_1 + C_0C_2 + C_1C_2)}. \quad (9)$$

If the inequality in (9) is reversed, we see that ω_0 has no real definition in terms of ω_c and we must return to (4). It appears that, for the region where the inequality is reversed, apparently the significance of the imaginaries and reals interchange, and we must use the nominally imaginaries which are now the reals. It can be shown that this is legitimate as it will be found to check in the correct limits with published information.[2] In this region, then, from the "imaginaries" of (4), $\Delta\omega/\omega_c$ and ω_0 are defined as follows:

The circuits of case 1, along with the associated formulas, are listed in Fig. 2.

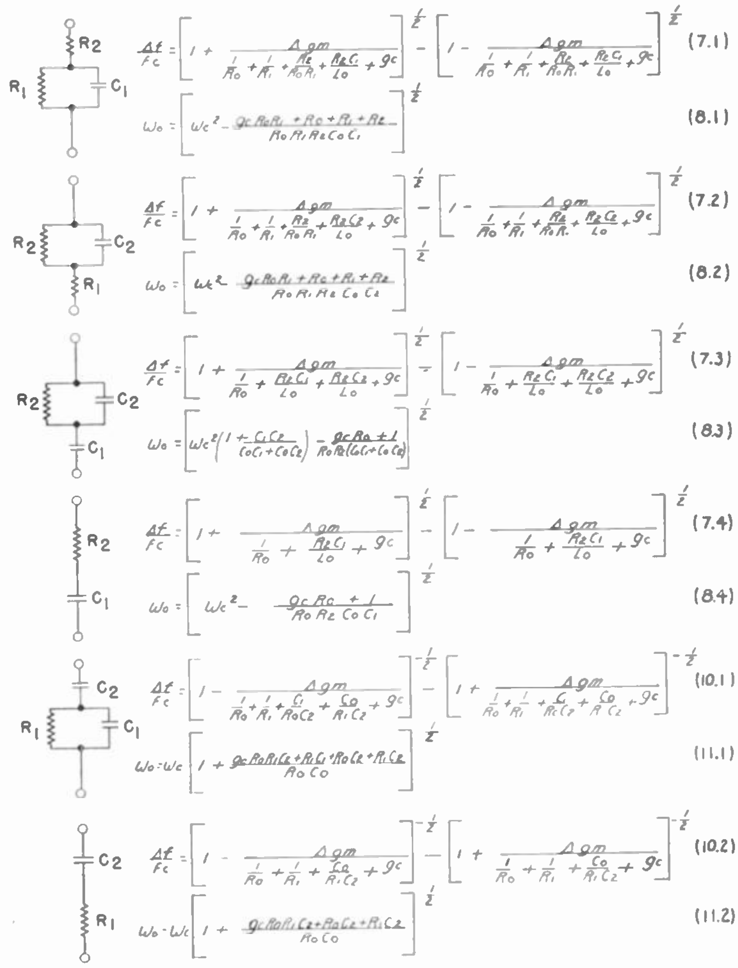

Fig. 2—Formulas for case I.

Case II

Again referring to Fig. 1, the definitions of case II are identical to case I, except that Z_1 and Z_2 are now parallel LR circuits, and the corresponding t's are

$$t_1 = R_1/\omega L_1$$

$$t_2 = R_2/\omega L_2.$$

$$\frac{\Delta\omega}{\omega_c} = \left\{1 - \frac{\Delta g_m}{\frac{1}{R_0} + \frac{1}{R_1} + \frac{C_1}{R_0C_2} + \frac{C_0}{R_1C_2} + \frac{C_0}{R_2C_2} + \frac{C_1}{R_2C_2} + g_c}\right\}^{-1/2} - \left\{1 + \frac{\Delta g_m}{\frac{1}{R_0} + \frac{1}{R_1} + \frac{C_1}{R_0C_2} + \frac{C_0}{R_1C_2} + \frac{C_0}{R_2C_2} + \frac{C_1}{R_2C_2} + g_c}\right\}^{-1/2} \quad (10)$$

$$\omega_0 = \omega_c\left\{1 + \frac{g_cR_0R_1R_2C_2 + R_1C_1(R_0 + R_2) + R_2C_2(R_0 + R_1)}{R_0C_0(R_1 + R_2)}\right\}^{1/2}. \quad (11)$$

Replacing the t's in (4) with quantities defined here the vanishing of the imaginaries this time yields the desired expression for ω/ω_0.

$$\frac{\omega}{\omega_0} = \left\{1 + \frac{R_2L_0L_1(g_mR_0R_1 + R_0 + R_1) + R_1L_0L_2(R_0 + R_2)}{R_0L_1L_2(R_1 + R_2)}\right\}^{1/2}. \tag{12}$$

Considerations similar to those used in case I, yield the following expressions:

$$\frac{\Delta\omega}{\omega_c} = \left\{1 + \frac{\Delta g_m}{\frac{1}{R_0} + \frac{1}{R_1} + \frac{L_2}{R_0L_1} + \frac{L_2}{R_1L_0} + \frac{L_2}{R_2L_0} + \frac{L_2}{R_2L_1} + g_c}\right\}^{1/2} - \left\{1 - \frac{\Delta g_m}{\frac{1}{R_0} + \frac{1}{R_1} + \frac{L_2}{R_0L_1} + \frac{L_2}{R_1L_0} + \frac{L_2}{R_2L_0} + \frac{L_2}{R_2L_1} + g_c}\right\}^{1/2} \tag{13}$$

$$\omega_0 = \left\{\omega_c^2 - \frac{R_2L_1(g_cR_0R_1 + R_0 + R_1) + R_1L_2(R_0 + R_2)}{L_1L_2C_0R_0(R_1 + R_2)}\right\}^{1/2} \tag{14}$$

and (13) will hold only as long as

$$\omega_c^2 > \frac{R_2L_1(g_cR_0R_1 + R_0 + R_1) + R_1L_2(R_0 + R_2)}{L_1L_2C_0R_0(R_1 + R_2)}. \tag{15}$$

In the region where the inequality is reversed, we must return to (4) and obtain

$$\frac{\Delta\omega}{\omega_c} = \left\{1 - \frac{\Delta g_m}{\frac{1}{R_0} + \frac{1}{R_1} + \frac{R_2}{R_0R_1} + \frac{R_2C_0}{L_1} + \frac{R_2C_0}{L_2} + g_c}\right\}^{-1/2} - \left\{1 + \frac{\Delta g_m}{\frac{1}{R_0} + \frac{1}{R_1} + \frac{R_2}{R_0R_1} + \frac{R_2C_0}{L_1} + \frac{R_2C_0}{L_2} + g_c}\right\}^{-1/2} \tag{16}$$

and

$$\omega_0 = \left\{\omega_c^2\left[1 + \frac{L_1L_2(g_cR_0R_1 + R_0 + R_1 + R_2)}{R_0R_1R_2C_0(L_1 + L_2)}\right] - \frac{1}{C_0(L_1 + L_2)}\right\}^{1/2} \tag{17}$$

in which again the quantity under the radical sign must also be positive.

Case II should not be interpreted to cover the conditions wherein the interelectrode capacitances become of primary importance. Some of the more conventional inductive circuits are listed in Fig. 3.

It should be noted that cases I and II are special developments of a more general condition in which Z_1 and Z_2 are both parallel LCR circuits.

Appendix I

Considering only the feedback network within the broken lines of Fig. 1, exclusive of the tube and tuned circuit, leads to an interesting development, the results of which may be correlated with the regions defined by the inequalities (9) and (15). From Fig. 1,

$$\frac{E_1}{E_0} = \frac{Z_1}{Z_1 + Z_2} \tag{18}$$

$$\frac{E_1}{E_0} = \frac{R_1(1 - jt_2)}{R_1(1 - jt_2) + R_2(1 - jt_1)}. \tag{19}$$

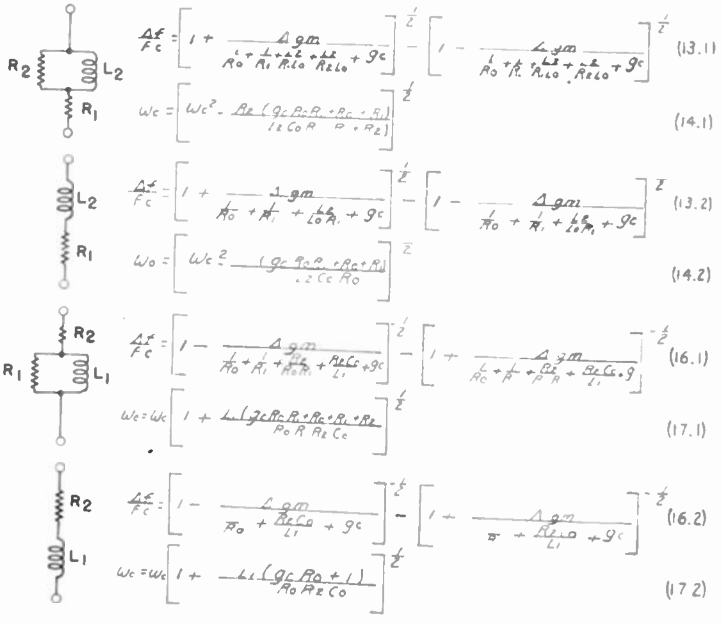

Fig. 3—Formulas for case II.

Rationalizing (19) will give

$$\frac{E_1}{E_0} = \frac{A}{D} + j\,\frac{B}{D} \tag{20}$$

where

$$A = R_1(R_1 + R_2) + R_1t_2(R_1t_2 + R_2t_1)$$

$$B = R_1R_2(t_1 - t_2).$$

Corresponding to the definitions given under case I,

$$B = R_1R_2(-\,\omega c_1R_1 + \omega c_2R_2)$$

and under case II,

$$B = R_1R_2\left\{\frac{R_1}{\omega L_1} - \frac{R_2}{\omega L_2}\right\}.$$

In both cases,

$$\tan\phi = \frac{B}{A} = \frac{R_1R_2(t_1 - t_2)}{A};$$

and, since A is always positive, if $t_2 > t_1$ the phase angle will be negative, and if $t_2 < t_1$ the phase angle will be positive.

This shows that there are distinct regions where a given phase-shift network is capable of either phase delay or of phase advance corresponding to a change-over from effective inductance to effective capacitance for that circuit. These regions are defined by the inequalities (9) and (15).

Appendix II

Numerical Example

The parameters for the following problem were chosen from an example given in footnote reference 4, the essential details of which are shown in Fig. 4, to illustrate the present method and to show that its use obviates the necessity for the more cumbersome methods of successive approximations.

The problem will be to accomplish the maximum bandwidth swept at a geometrical center frequency of 23 Mc. The oscillator is a 955 and the reactor a 6AC7. The reactance circuit of Fig. 1 for case I is chosen as the basic circuit, and use is made of the associated formulas.

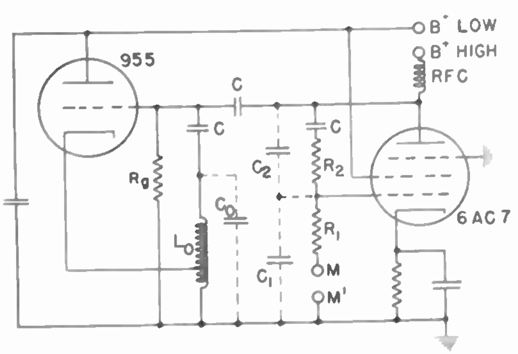

Fig. 4—Frequency-modulated oscillator circuit, M and M' are the modulation input and C are the coupling capacitors.

[4] Joseph I. Heller and Oscar Friedman, "Notes on factors affecting the selection of values for use in the phase net of reactance tubes," Panoramic Radio Corp., New York, N. Y., Report, October 23, 1944.

The following information is available:

$f_c = 23$ Mc (geometrical center frequency)

$g_c = 0.0075$ mho (since $g_c = g_{max}/2$ by definition, and maximum g_m of a 6AC7 can approach 0.015 mho)

$\Delta g_m = 0.0075$ mho (since the change in g_m is seen to be one-half of maximum)

$C_0 = 25\ \mu\mu f$ (this is the distributed capacitance of the oscillator coil plus the tube and stray capacitances)

$C_1 = 20\ \mu\mu f$ (this is the input plus stray capacitances of the 6AC7)

$C_2 = 1\ \mu\mu f$ (this order of capacitance is realizable in practice)

$R_0 = \left\{\frac{1}{R_0'} + \frac{1}{R_g} + \frac{1}{r_p}\right\}^{-1}$ (where $R_0' = \frac{Q_0}{\omega_c C_0}$, and Q_0 is the value of Q obtainable in the reactance tube at cutoff.

$R_0 \doteq 20\text{K}\ \Omega$ A practical value is $Q_0 = 110$. $R_0' \doteq 30{,}000$ ohms. $r_p = 10^6$ for a 6AC7. $R_g = 50{,}000$ ohms was used in this example)

$R_1 = 12\text{K}\ \Omega$ (this should be as large as possible. The effective R_1 is the electronic loading *c.* 13,000 ohms in parallel with the 200,000-ohm grid resistor used)

$R_2 = 2{,}000\ \Omega$ (R_2 as shown by (9) should be as small as possible for maximum bandwidth swept. The minimum of R_2 is limited by its damping effect on the oscillator.)

In solving the problem it is first necessary to find ω_0, which in turn will give the design value of L_0. From (8)

$$f_0 = \frac{\omega_0}{2\pi} = 19.17 \text{ Mc}$$

and

$$L_0 = \frac{1}{\omega_0^2 C_0} = 2.76\ \mu\text{h}.$$

For this problem the bandwidth swept is given by (7)

$$\Delta f = 7.61 \text{ Mc}.$$

The results of an approximate solution obtained by using formulas (8.4) and (7.4) are given in the Table I.

Following is a summary of the results obtained for the problem, as given by the various methods of approach.

TABLE I

Method of Solution	f_0 Mc	L_0 μh	Δf Mc
Successive approximations as given in footnote reference 4	19.7	2.62	7.60
Present design using (7), (8)	19.17	2.76	7.61
Present design using less exact equations (8.4), (7.4)	18.4	2.99	8.30

It will be noted that the solution presented here involves considerably less work than usual procedures, and this typical example will sufficiently illustrate the usefulness of the present method.

Conclusion

In approaching the solution of any reactance tube problem, it is first necessary to decide which one of the circuits given in Figs. 2 and 3 is most nearly applicable to the problem at hand. The several associated equations readily show the parameters that should be changed and the direction of the change to produce desired results. The degree of accuracy of the design depends on the particular method chosen and its respective formulas. For usual purposes, the approximate methods as shown in Figs. 2 and 3 will give sufficient accuracy. Many times when a particular system is under consideration, it is often useful to know the theoretical maximum bandwidths available; and these limits are easily obtainable as can be seen from the text. It is believed that these particular formulas might be extremely helpful in problems of reactance tube circuits wherein theoretical limits are being approached.

[2] C. F. Schaeffer, "Frequency Modulation," PROC. I.R.E., pp. 66–67; February, 1940.
[3] August Hund, "Reactance tubes in F.M. applications," *Electronics*, vol. 15, pp. 68–71, 143, October, 1942.
[4] E. Williams, "Reactance valve frequency modulator," *Wireless Eng.*, vol. 20, pp. 369–371; August, 1943.
[5] H. A. Ross and B. Sandel, "Design of electronic reactance networks," *HWA Tech. Rev.*, vol. 6, February, 1943.

Medium-Frequency Crossed-Loop Radio Direction Finder with Instantaneous Unidirectional Visual Presentation*

L. J. GIACOLETTO†, SENIOR MEMBER, IRE, AND SAMUEL STIBER‡, ASSOCIATE, IRE

Summary—A radio direction finder is described which uses a crossed-loop collector system, electronic switch, single superheterodyne receiver, and synchronous rectifier to produce an instantaneous unidirectional visual indication of the direction of arrival of an electromagnetic wave. Design data and operating characteristics are considered, with details given of the new components.

I. Introduction

THE RADIO DIRECTION FINDER to be described was a Signal Corps development calling for a direction finder covering the frequency range of 1.5 to 18 Mc. The equipment was to be transportable in a small vehicle and consist of components of such size and weight as to be readily portable by three men. Each set was to be assembled for operation in less than twenty minutes by two men, with operation being possible in the field, in the open, or under canvas. The performance requirements were that it should be as accurate and sensitive as the electronic art permitted without undue complexity of operation or compromise of transportability. It was desirable that the equipment be capable of obtaining bearings on transmissions of short duration.

Development of the radio direction finder was first begun in August, 1943, and pursued actively until August, 1945, when field tests were completed and the performance of the set demonstrated.

The initiation of development first required a decision as to the basic mode of direction finding to be employed. The requirements of transportability and operation limited the collector system to loop antennas. For direction finding on transmissions of short duration, direction finders requiring a manually or motor-rotated collector system were ruled out; the dual-channel instantaneous direction finder was eliminated because of difficulties of providing equalized phase and gain. This narrowed the field of possible modes of operation to the selective-modulation type of direction finder[1] in which radio-frequency voltages proportional to the direction of arrival of a signal are suitably "tagged" at the input, pass through a common receiver, and are then decoded. Some prior successful work[2] on a left-right, square-wave-switched, cardioid type of direction finder led to a further examination of this method of operation. A brief examination indicated that, provided certain circuit characteristics could be achieved, a crossed-loop square-wave-switched cardioid type of direction finder would work satisfactorily.

II. Theory of Operation

The over-all operation of the set can best be understood from the block diagram in Fig. 1. The collector system is a set of crossed balanced loops with a vertical sense antenna. Under ideal conditions, loop *A* receives a radio-frequency signal proportional to $\sin\theta$ (θ is azimuth angle of arrival of signal). This voltage is fed push-

* Decimal classification: R501×561. Original manuscript received by the Institute, July 27, 1948; revised manuscript received, November 18, 1948.

† Formerly, Signal Corps Engineering Laboratories, Fort Monmouth, N. J., where the work described herein was completed; now, Radio Corporation of America, RCA Laboratories Division, Princeton, N. J.
‡ Signal Corps Engineering Laboratories, Fort Monmouth, N. J.

[1] C. W. Earp, U. S. Patent 2,213,273, September 3, 1940. C. F. A. Wagstaffe, U. S. Patent 2,213,874, September 3, 1940.
[2] E. Cole and R. E. McCoy, U. S. Patent 2,397,128, March 26, 1946. A few prior patents on related art are: C. C. Jones, U. S. Patent 2,146,745, February 14, 1939; F. J. Hooven, U. S. Patent 2,190,787, February 20, 1940; and W. S. Hinman, U. S. Patent 2,266,038, December 16, 1941.

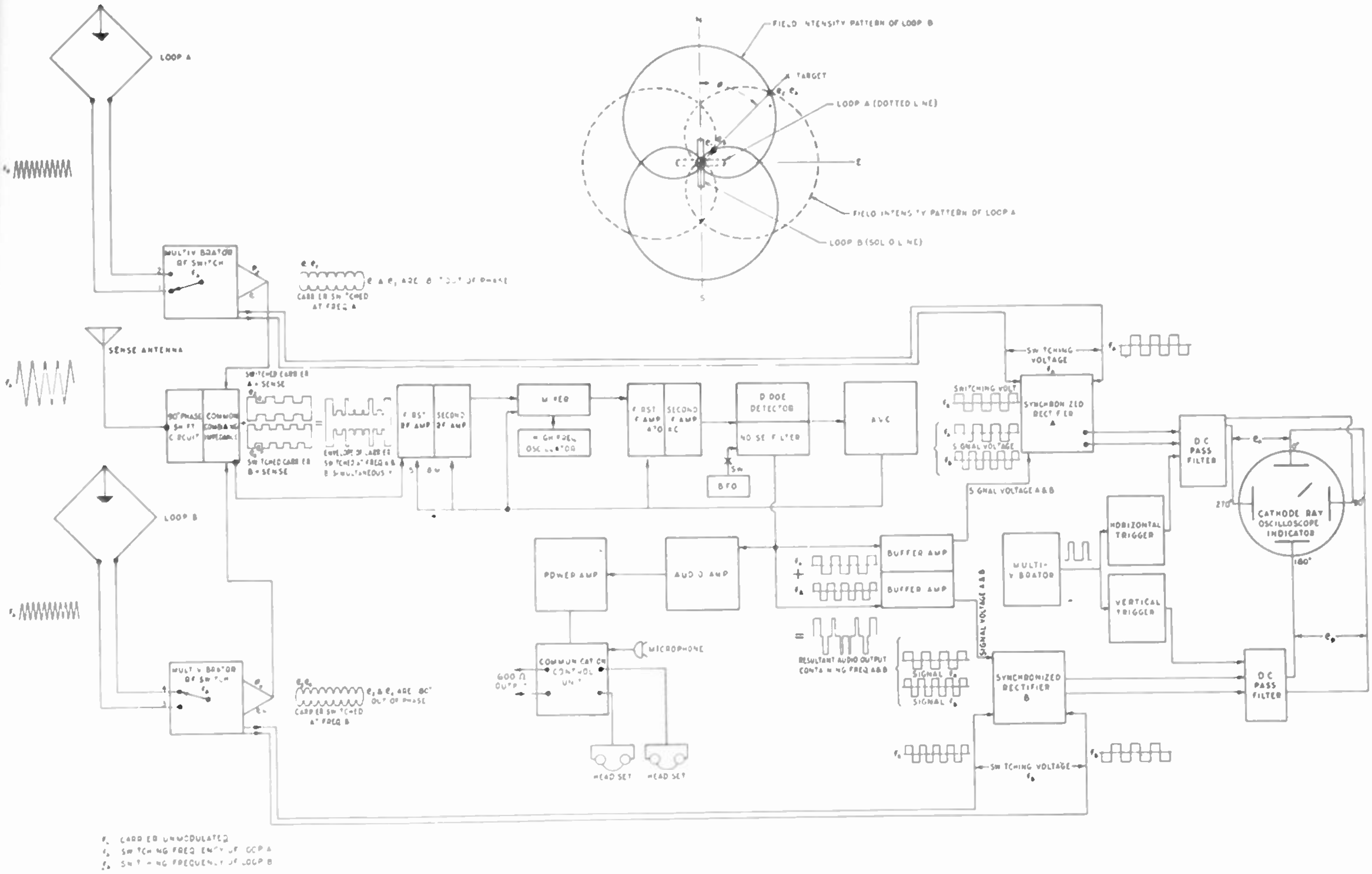

Fig. 1—Block diagram of the radio direction-finder set.

pull into a radio-frequency switch, switching at a frequency f_A (approximately 253 cps). The output of this switch (voltages e_1 and e_1 as shown in Fig. 1) is essentially a constant-amplitude radio-frequency voltage with e_1 and e_2 180 degrees out of radio-frequency phase, since the switch receives input voltage from either end of the loop to ground. Loop B operates similarly, except that its radio-frequency signal is proportional to cos θ and the radio-frequency switching frequency is f_B (approximately 340 cps). Generally, e_1 and e_1 are not equal in amplitude to e_3, e_4, although for the case illustrated in Fig. 1 $\theta = 45°$) the amplitudes are equal. The outputs of the A and B switches are combined with the sense-antenna voltage, which has been shifted through 90 degrees in order that it will be in phase with either e_1 or e_2. Ideally, the sense antenna voltage should be just equal to the maximum loop-antenna voltage, although practically it is sufficient to insure that the sense-antenna voltage always be larger than the loop-antenna voltages. When voltages e_1, e_2 are added to the sense-antenna voltage, the result is a square-wave modulated signal; similarly, e_3, e_4 added to the sense-antenna voltage, gives a square-wave modulated signal. The combination of these two signals produces a signal with a complex envelope which is nonrecurernt in shape, since f_A and f_B are purposely chosen to have a nonintegral relationship. The resulting radio-frequency signal passes through a conventional receiver composed of two rf stages, pentagrid converter, two if stages, diode detector with provision for beat-frequency oscillator injection; and an audio amplifier and power amplifier. Automatic-volume-control and pulse noise-suppression circuits are also provided for optional use. The output of the diode detector, consisting of the combination of two square waves of frequencies f_A and f_B also, goes to buffer amplifiers which feed into synchronized rectifiers A and B. Each rectifier is switched synchronously with its associated rf input circuit. Consider first the nonsynchronous square-wave signal, which is applied in parallel to both grids of the synchronous rectifier; the net result is that the output is balanced out due to the push-pull action of the circuit. In the case of a square-wave signal which is in synchronism with the switching frequency, a difference voltage is produced at the anodes which is proportional in magnitude to the peak amplitude of the input square wave of like frequency. The polarity of this difference frequency is determined by the relative phase of signal and synchronous switching voltage applied to the grids of the synchronous rectifier. The charging time constant in the anode circuit of the synchronous rectifier is made long compared to the switching frequency, so that the difference voltage is largely direct current with a small superimposed alternating component. The output voltage passes through additional dc filters to remove the remaining alternating components, and is then connected to an appropriate pair of oscilloscope deflection plates.

The oscilloscope electron beam is deflected out in an X and Y direction proportional to $\cos\theta$ and $\sin\theta$ and therefore indicates the direction of arrival of the signal. Since dc voltage polarities change for a signal coming from a direction 180 degrees from θ, an unambiguous direction of arrival is shown on the oscilloscope. For improved presentation, the deflected oscilloscope spot is converted into a line by having a trigger discharge circuit periodically short the oscilloscope deflection plates to ground.

In order to permit net operation of several direction finders for position location, a communication control unit is incorporated in the set; this control unit permits talking and listening over an interconnecting line as well as the connection of the receiver output to the line for remote monitoring. A third position permits signal matching by connecting one earphone to the receiver and the other earphone to the line.

In the above discussion, audio modulation on the radio-frequency signal was not considered. Audio modulation will have no effect on the operation of the direction finder as long as it does not contain a component that is synchronized with either switching frequencies A or B or any harmonics thereof; this condition is unlikely to exist in practice. Since the square-wave switching voltages are also present in the audio output, some loss in intelligibility is experienced. In practice, it is found that this is not too serious, particularly for code signals; simultaneous direction finding and monitoring are therefore possible. A switch is provided for disabling the switching circuit; the receiver is then connected directly to the sense antenna and serves as a sensitive intercept receiver. When mounted on a turret-head mounting plate, the set can also be operated as a manually rotated aural null direction finder (one loop only directly connected to the input), or a visual null direction finder (only one rf switch in operation; null indicated by electron beam at center).

A rotating crossed-hair alidade and a reverse illuminated angular scale are provided to facilitate reading bearings. A two-position switch is provided for varying the time constant of the dc filter. The short-time-constant filter allows bearings to be taken on shorter-duration signals, as well as giving a clearer picture of the character of the bearing. The longer-time-constant filter acts to "freeze" a bearing in position; i.e., tends to read the average bearing for a "swinging" reading. In addition, the longer time constant removes more of the noise.

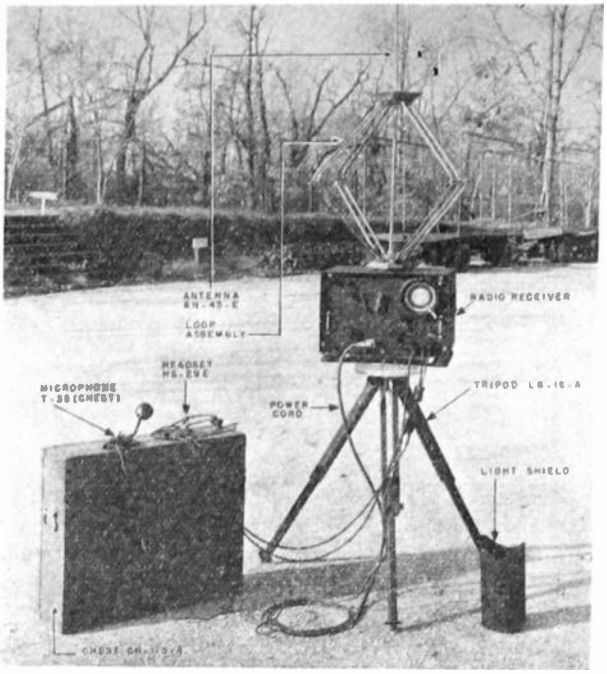

Fig. 2—The radio direction-finder set up for operation.

A typical ground installation of the set is shown in Fig. 2. Vehicular installation is also possible.

III. Component Performance

Since the operation of the set is essentially dual channel up to the input of the first rf stage, considerable attention was devoted to the design of this portion of the set. It was considered inadvisable to tune or resonate the loop antennas, as tracking problems are severe; loop mistuning could produce large bearing errors, as well as reversal of sense. Although untuned loops provide a smaller pickup voltage and require somewhat larger dimensions, freedom from unbalance is obtained due to their inherent low impedance; placement of antenna and position of operator and near-by objects become relatively unimportant. For improved voltage pickup, two sets of loops are used, one self-resonant at 14.5 Mc for use from 1.5 to 8 Mc, and the second self-resonant at 22.5 Mc for use from 8 to 18 Mc. Physically, each collector system consists of two square two-turn loops at right angles to each other mounted on one corner with a vertical sense antenna mounted on the opposite corner with a shielded lead passing along the vertical common diagonal of the squares. The low- and high-frequency

TABLE I
Radio-Frequency-Switch Performance Data of 7F8

Frequency (Mc)	1.5	2.0	6.5	9.0	12.5	16.0	18.0
Rf voltage gain	8.0	6.0	2.3	1.5	0.7	1.3	5.0
Switching ratio	75	70	35	25	13	10	9
Grid input impedance (ohms)	2,000	2,200	750	360	200	55	—
Grid rf input (μv) for receiver $(S+N/N)=10$	3.2	5.0	4.0	4.0	6.5	4.5	4.0

Note: For all tests, the multivibrator was operating and measurements were made from one grid to the common output. Signal modulation was 400 cps, 30 per cent.

loops are 22 and 16 inches on a side, respectively. The center of each loop antenna is grounded and the loop terminals are capacitively coupled to the balanced rf switch input. The sense antenna is inductively coupled to the tuned receiver input in order to provide the 90° phase shift required to bring the sense-antenna voltage in phase with the loop-antenna voltage.

In the development of the rf switch,[3] the following characteristics are important:

(1) A high switching ratio.[4]
(2) Large balanced rf gain with good stability and minimum noise.
(3) Adequate square-wave output voltage of good shape for use in operating synchronous rectifier circuit.

The following four types of rf switches were designed and tested.

1. *Grounded Anode* (*Fig. 3(a)*). This circuit utilizes a dual triode connected as a conventional multivibrator[5] oscillating at a low frequency. Additional resistors are added in series with anode-to-grid coupling capacitor in order to maintain a large rf impedance at the grids. The rf is connected to the triode grids, with the output taken from a common cathode impedance. This circuit exhibited good switching ratios but its rf gain (0.3 for a 6SN7GT) was poor.

2. *Grounded Grid* (*Fig. 3(b)*). This circuit is similar to the one above except that small capacitors serve to ground the grid at radio frequency, and the input is to separate cathodes with the output from a common impedance coupled to the anode by means of small rf coupling capacitors. This circuit exhibited excellent switching ratios and moderate gain, but was considered inadequate because of small square-wave output voltage and poor square-wave shape.

3. *Grounded Cathode* (*Fig. 3(c)*). This circuit was found to have the best operating characteristics and was incorporated in the final design. Detailed performance data as a function of frequency are tabulated in Table I. Potential instability of the triode necessitated careful choice of circuit constants and placement of parts. Small resistors in series with the control grid together with large resistors in series with anode-grid coupling capacitor serve to reduce regeneration. Several types of dual triodes were tried, including the 7F8, 6SN7GT, 6SU7GT, and 6SL7GT; of these the 7F8 was found to be the best. In order to insure equal rf gains both between triode sections and between tubes, it was necessary to test tubes and utilize only those tubes that had transconductances matched within 5 per cent.

4. *Dual Tetrode* (*Fig. 3(d)*). This circuit is similar to Fig. 3(c) except for the addition of the two screen grids.

[3] H. M. Wagner and J. F. Herrick, "Self-switching amplifier," *Electronics*, vol. 20, pp. 128–131; June, 1947. This article contains an analysis of a switch similar to those described herein except designed for operation at higher radio frequencies.

[4] Switching ratio is defined at the ratio of radio-frequency output voltage during on and off half-cycle of the multivibrator.

[5] O. S. Puckle, "Time Bases," John Wiley and Sons, Inc., London, p. 25, 1943.

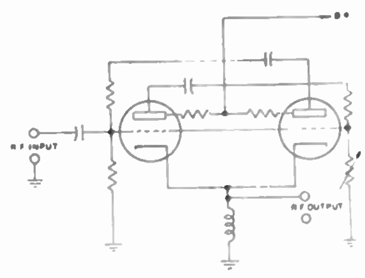

(a)

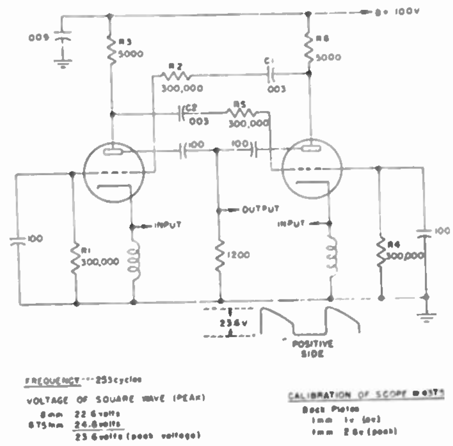

(b)

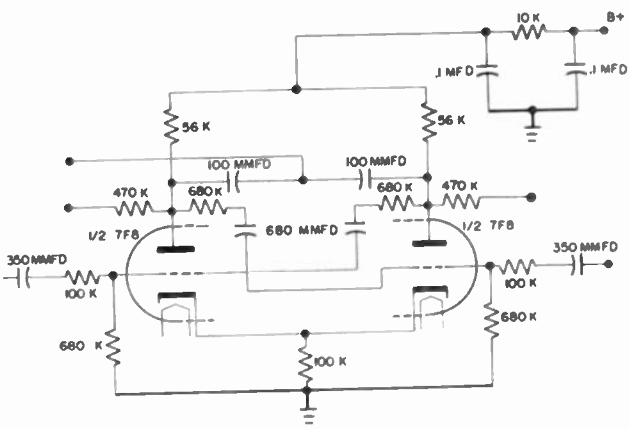

(c)

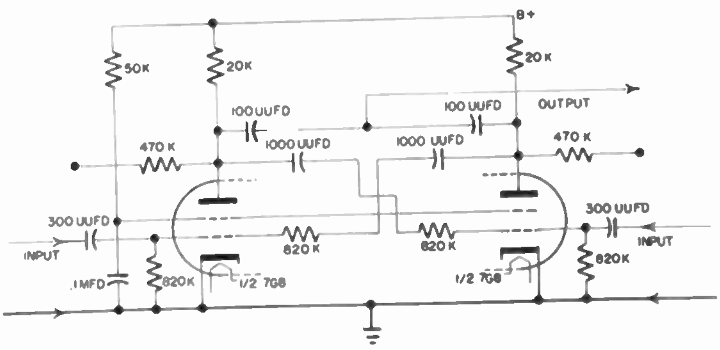

(d)

Fig. 3—Electronic switch circuits.

(a) Triode grounded-anode circuit. The constants in this circuit are determined chiefly by the frequency desired. The one variable resistor controls the symmetry of the square wave. The value of the plate resistors determines the flatness of the positive cycle. The resistor between plate of one section and grid of the other section offers impedance to rf which is necessary for better switching ratios.
(b) Triode grounded-grid circuit.
(c) Triode grounded-cathode circuit.
(d) Tetrode grounded-cathode circuit.

Development of this circuit was initiated with the object of improving the grounded cathode circuit, both from the standpoint of improved stability and improved operating characteristics. Comparitive tests using 7F8 dual triode and 7G8 dual tetrode tubes indicated that (a) the 7F8 had a signal plus noise-to-noise ratio averaging three times better than the 7G8 over the frequency range of 1.5 through 18 Mc; (b) the radio-frequency gain characteristics were about the same for both tubes; (c) switching voltage stability and wave shape were satisfactory for both tubes; and (d) the square-wave output voltage of the 7F8 averaged 30 per cent higher than for the 7G8. The choice of the 7F8 tube was due primarily to (a) above, and, in addition, to the fact that the 7G8 was considered a developmental tube at the time.

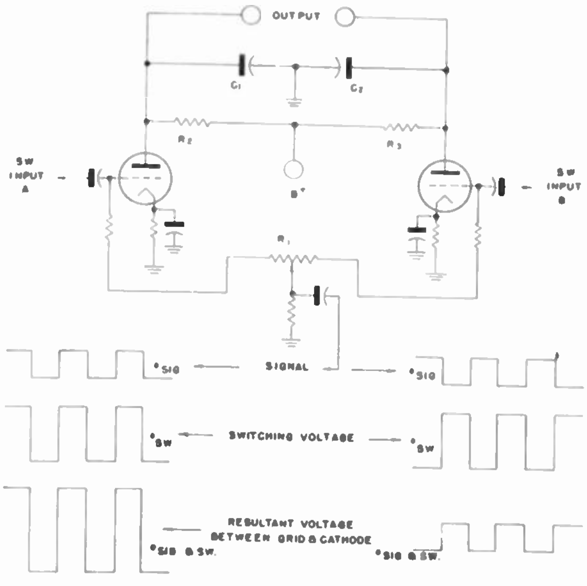

Fig. 4—Synchronous rectifier circuit.

TABLE II

SENSITIVITY VERSUS FREQUENCY DATA

Frequency (Mc)	Signal Input		
	A (μv)	B (μv)	C (μv)
2.2	0.5	1.3	1.0
3.0	0.8	1.3	
4.0	0.3	1.0	0.7
5.0	0.3	1.0	
6.5	0.7	0.7	0.6
8.0	0.4	1.0	
9.5	0.4	0.9	0.8
11.0	0.4	1.4	
12.5	0.9	0.9	1.0
14.0	0.9	1.2	
16.0	1.0	0.9	1.0
18.0	1.0	0.6	

NOTE: (a) Signal input A is the input at the sense antenna with the switching tubes off for 4:1 signal-plus-noise to noise ratio. Signal modulation is 400 cps, 30 per cent.

(b) Signal input B is the input at the grid of the switching tube with the switching tube on, for 4:1 signal-plus-noise to noise ratio. Signal modulation is 400 cps, 30 per cent.

(c) Signal input C is the same as for signal input B but for full-scale deflection on the oscilloscope tube (approximately 150 volts between plates).

(d) Phantom antenna consists of a 100 $\mu\mu$f capacitor in series with the input to the receiver.

The superheterodyne receiver covered the frequency range of 1.5 to 18 Mc in six bands. It was believed at first that, because of the necessity of passing square-wave modulated signal with small envelope distortion, a flat-top if response curve was desired. Tests indicated, however, that a bell-shaped response curve, center frequency at 470 kc with 3 kc bandwidth (at the half-power point), was sufficient for passing the carrier and sidebands and, in addition, was convenient in alignment. A narrower bandwidth of, perhaps, 1 kc would be more desirable for separation of communication channels, but is insufficient for passing the direction finder intelligence. Because of the existence in the if stages of direction-finder intelligence at several amplitude levels, the linearity of these stages is also of considerable importance. For this reason, the automatic volume control can be used only when the receiver is operated for intercept purposes.

Sensitivity versus frequency data at both sense-antenna and switching-tube inputs are tabulated in Table II.

The set was designed to operate with a dynamotor unit driven from a 12-volt storage battery. In addition, a 180-cps resonant-reed vibrator was used in conjunction with a transformer to furnish 6.3 volts at 0.6 ampere, insulated for 3,000 volts from ground, for the oscilloscope heater; $-1,200$ volts at 1 ma dc (rectified by means of 110 small disk selenium rectifiers) for oscilloscope acceleration and focus; and $+500$ volts, 10 ma dc (selenium rectifier) for the anode voltage of the synchronous rectifier tubes. Careful shielding and filtering was used to reduce rf noise.

In order to eliminate radar, ignition, and similar impulse noises, an automatic noise limiter was provided. The circuit was adjusted to provide automatic limiting when impulse noise peaks exceed the average carrier level. Square-wave direction-finder intelligence modulation is, accordingly, passed without distortion.

The function of the synchronous rectifiers is to segregate the N-S and E-W direction-finder intelligence and to provide dc voltages proportional thereto. The basic circuit consists of a pair of triodes operating as balanced modulators, as shown in Fig. 4. The detected signal voltage is introduced to the triode grids in parallel, while the square-wave switching voltage is applied in push-pull. For proper operation, the grid bias is chosen so that each tube operates as a class-A amplifier during the "on" portion of the switching cycle and is completely cut off during the "off" portion of the cycle. If this is done, the push-pull dc output voltage is proportional only to the amplitude of an input voltage of frequency synchronous with the switching frequency. The polarity of the dc voltage difference is dependent upon the relative phase (established at the associated input switch) of the square-wave switching voltage and synchronous input signal voltage. Proper "sense" is thus obtained.

Since large output dc voltage differences are required for full oscilloscope deflection, the problem of linear operation is a severe one. Some consideration was given

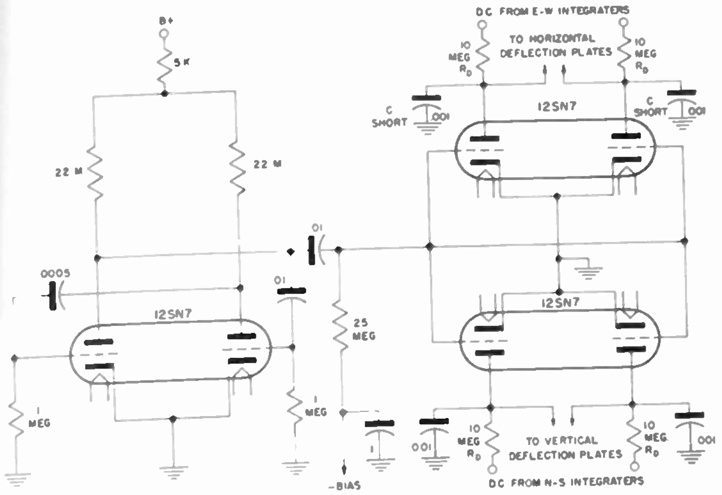

Fig. 5—Oscilloscope line formation circuit.

to the use of dc amplifiers, but due to additional complexity and potential instability, this was discarded. Instead, the problem was resolved by exhaustive circuit and tube studies together with use of a high B+ voltage (500 volts). Of the various tubes tested (7F8, 6SN7GT, 6SL7GT, 7G8, 6N7, 6E6, and 6SC7), the 6SN7GT gave the best performance. As in the case of the rf switching tubes, matched performance of the four triodes is required, and tubes are selected with transconductances matched to 1 per cent. A screwdriver-adjustable gain control is also provided, mainly to compensate for variation in transconductance due to aging.

A three-section resistance-capacitor filter network couples each synchronous rectifier anode to the corresponding oscilloscope deflection plate and acts to remove any ac variations in the anode voltage. The total time constant of this circuit is 50 milliseconds; by paralleling additional capacitance using a panel control, this time constant can be increased to 0.1 second.

The method used for forming a radial line from the deflected oscilloscope spot consists in using triodes to short, periodically, the oscilloscope deflector plates to ground, as shown in Fig. 5. Three dual triodes are used; one acting as an unbalanced multivibrator, and the other two as electronic switches. Dissimilar tube characteristics caused the discharge trace to differ from the charge trace, but since the discharge trace was hardly visible, this was not objectionable and the resulting line presentation was considered very acceptable.

Since manufacturing tolerances on the oscilloscope (3BP1) permit perpendicularity of the deflection plates to be off by as much as $\pm 3°$, it is necessary to check tubes; no difficulty was experienced in obtaining tubes in which the plates were perpendicular within $\pm \frac{1}{2}°$. The unequal horizontal and vertical deflection sensitivities were compensated for by using different load resistors and providing screwdriver-adjustable controls in the switching rectifiers.

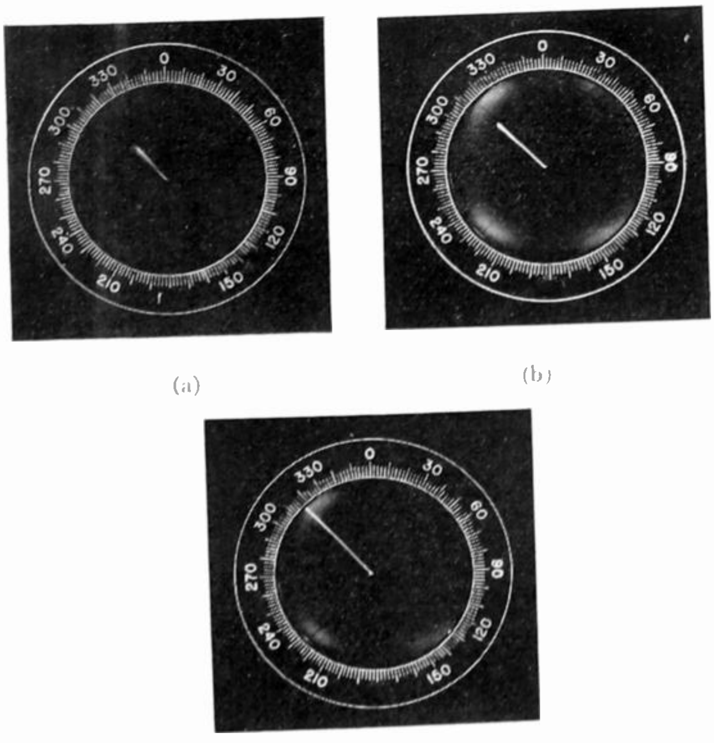

(a) (b) (c)

Fig. 6—Bearing indication.
(a) Signal strength, below noise level.
(b) Signal strength, weak.
(c) Signal strength, good.

IV. System Performance[6]

The over-all performance of a direction finder is probably best summed up by data presenting the field strength required for a given quality of bearing. The data for a bearing readability of $\pm 1°$ are shown in Table III; calibrated fields were obtained by operating the equipment in a calibrated screen room. Some indication of the character of the instantaneous bearing can be obtained from Fig. 6(a), (b), and (c). By using the long-time-constant integrating circuit, moderately good bearings can be obtained on signals well below the input noise level.

TABLE III

Field Strength versus Frequency Data for $\pm 1°$ Bearing Readability

Frequency (Mc)	Loop Antenna	Field Strength for $\pm 1°$ Readability (μv/m)
1.5	Low frequency	8.0
2.2	Low frequency	6.0
4.0	Low frequency	3.5
6.5	Low frequency	2.0
8.0	Low frequency	1.0
9.5	High frequency	2.4
12.5	High frequency	1.4
14.0	High frequency	1.4
16.0	High frequency	1.5
18.0	High frequency	1.5

The evaluation of the field performance of the set in the lower frequency range (1.5–3.0 Mc) can be ascertained from Fig. 7, in which is plotted the percentage of

[6] The most recent and most comprehensive attempt to specify direction-finder performance was work done by NDRC Division 13.1, E. D. Blodgett, Chairman. The last provisional draft was published July 12, 1945, entitled "Standard Direction Finder Measurements." Performance data in this report were taken only in part in accordance with the proposed standards.

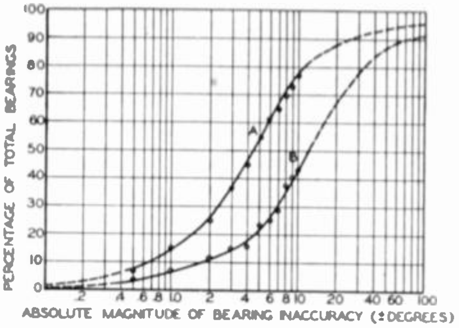

Fig. 7—Percentage bearing accuracy in the frequency range of 1.5 to 3.0 Mc.

Test condition A: 442 signals received when ground wave only was known to be present. Of these, 4.8 per cent (21 signals) were received but no bearings taken.

Test condition B: 70 signals received when sky wave only was known to be present. Of these, 8.6 per cent (6 signals) were received but no bearings taken.

total bearings whose inaccuracy was less than the indicated value. These data were taken using test signals produced under a variety of conditions, including the following:

(a) Ranges from 5 to 50 miles.

(b) Different target transmitter antennas from vertical whip to long horizontal doublet producing conditions of mixed vertical and horizontal polarization.

(c) Signal strengths from below the noise level to those capable of overloading the receiver.

(d) Target located on flat clear terrain to locations below line of sight with intervening small hills.

(e) Operation during daylight, twilight, and night time, producing conditions of good ground-wave and mixed ground and sky-wave.

(f) Both interrupted, continuous wave, radiotelephone, and commercial signals.

In view of the fact that the set was designed primarily for ground-wave reception, the test conditions specified above are considered quite severe. In operation, it is found that, because of the instantaneous visual bearing indication provided in the set, fairly accurate bearings can be obtained under some conditions of mixed polarization producing swinging bearings.

Using an SCR536 (handy-talkie, Frequency = 3.64 Mc) as a target at a distance of 200 to 600 yards, the average error with different antenna orientations was 0.8°; for distances from 600 to 1,200 yards, the average error was 0.87°.

Although this set, together with other similar sets, is known as an instantaneous direction finder, practically, since data are coded at the input, it is necessary to receive for a finite time before a bearing of a given reliability can be obtained. With the switching rates employed in this set, a theoretical minimum time (without dc filter) of 7 milliseconds is required.

No performance data were obtained for operation as an aural- or visual-null direction-finder set. It was believed desirable to incorporate these additional features since they did not add in weight or complexity and, in the case of aural null, advantage could be taken of the possibility of direction finding on two continuous signals very close in frequency but separated in azimuth. Individual bearings can, of course, be resolved instantaneously if the two signals are interrupted in random fashion. The visual-null facility provided a means of very accurate direction finding under ideal conditions.

Limited screen room tests indicated that the instrumental error was less than ±1° for all frequencies and azimuths.

V. Conclusions

It is believed that the method of operation described represents a new approach to an instantaneous direction finder. It is the purpose of this paper to record the work that has been accomplished, so that it will be readily available to anyone contemplating similar development.

While this equipment was designed primarily for radio communication direction finding, it is believed that it may also have important application to homing and navigation of ground, sea, and air vehicles, for position finding for rescue or control operations, and for wave-propagation studies. With a suitable collector system and receiver, the same method of direction finding could be employed at frequencies other than the 1.5 to 18 Mc range employed in this set. Of particular interest would be the adaptation of the set to an Adcock-type collector system to reduce bearing errors on abnormally polarized radio waves. Further development work could be spent advantageously on the electronic switching circuits; and, in particular, the improvement to be realized in separating the switching and wave-generation functions in the input tubes should be studied. Other methods of "tagging" or modulating the input signal should be investigated; of the alternate methods available, the following were considered but not tried:

(a) The sequential switching (electronic single-pole four-position switch)[7] of the four loop voltages to the phase-shifted sense voltage with synchronously switched rectifiers. With this mode of operation, only a single fundamental switching voltage is employed.

(b) The switching of the loop voltages directly to the quadrature sense voltage to produce phase modulation[8] instead of amplitude modulation. Synchronously switched phase detectors are then employed to decode the data.

Acknowledgments

The development work described in this paper was conducted under the leadership of the authors and Aldo Scandurra, formerly of the Signal Corps Engineering Laboratories. Others who contributed in a substantial manner to the project are Benjamin Bernstein, Julia Herrick, Josephine Hollingsworth, Gustave Shapiro, and Cosimo Testa.

[7] N. A. Moerman, "Four-channel electronic switch," *Electronics*, vol. 19, pp. 150–153; April, 1946.

[8] A single loop operated in this matter is described by F. J. Hooven, U. S. Patent 2,190,787, issued February 20, 1940.

Contributors to Waves and Electrons Section

H. M. Beck (A'37–M'48) was born on January 18, 1912, at Jefferson, Wis. After graduation from RCA Institutes, Inc., of Chicago, he worked for broadcasting station WHBL of Sheboygan, Wis., from 1937 to 1939. He was with RCA Victor Distributing Corp. in Chicago and went to Zenith Radio Corp. in 1940 as test equipment engineer.

H. M. BECK

In 1942 Mr. Beck came to the Naval Research Laboratory, where he is now employed as radio engineer in the Radio Countermeasures Branch of the laboratory.

❖

For a biography and photograph of MILTON DISHAL, see page 530 of the May, 1949, issue of the PROCEEDINGS OF THE I.R.E.

❖

E. Guy Hills (A'41) was born in El Paso Texas, on February 1, 1918. He received the B.S. degree in electrical engineering from the New Mexico State College in 1939, and the M. S. in mathematics from the University of Michigan, where he had a teaching assistantship in 1940. After five months as a test engineer for the General Electric Company in Schenectady, N. Y., he became a radio instructor for the U. S. Air Corps. During the following two years, Mr. Hills worked at night toward the Ph.D. degree in mechanics, at Washington University.

E. GUY HILLS

In 1934, Mr. Hills joined the engineering staff at the Belmont Radio Corporation in Chicago, Ill., and spent the next six years in radar and television development work. At present he is the manager of the Government Engineering Division of the Webster-Chicago Corp.

❖

L. J. Giacoletto (S'37–A'42–M'44–SM'48) was born in Clinton, Ind., on November 14, 1916. He received the B.S. degree in electrical engineering from Rose Polytechnic Institute, Terre Haute, Ind., in 1938, and the M.S. degree in physics from the State University of Iowa in 1939, where he was a research assistant. From 1939 to 1941, while holding an appointment as teaching fellow, he completed graduate course requirements for a doctorate degree at the University of Michigan.

L. J. GIACOLETTO

Mr. Giacoletto was associated with Collins Radio Company during the summers of 1937 and 1938, and with the Bell Telephone Laboratories in the summer of 1940. From 1941 to 1945 he was on active military duty with the Signal Corps, engaged in development activities in the field of radio, navigational, and meteorological direction-finding equipment. In 1945 and 1946 he was on duty in Japan, concerned with technical intelligence work, after which he returned to inactive status as a major in the Signal Corps Reserve. In December, 1947, and January, 1948, he returned to temporary active duty with the Thermionics Branch, Evans Laboratory.

Since June, 1946, Mr. Giacoletto has been a research engineer with the Radio Corporation of America, RCA Laboratories Division, Princeton, N. J., engaged in research and development on electron tubes and electronic equipment. He has served on IRE New York Section committees, and helped to organize the Monmouth Subsection, serving as Chairman. He is now Secretary-Treasurer of the Princeton Section.

Mr. Giacoletto is a member of the American Association for the Advancement of Science, Gamma Alpha, Iota Alpha, Phi Kappa Phi, Sigma Xi, and Tau Beta Pi.

❖

Leonard Mautner (M'46–SM'47) was born on October 30, 1917, in New York, N. Y. He received the degree of B.S. in electrical engineering from the Massachusetts Institute of Technology in 1939. He did graduate study at the Stevens Institute of Technology from 1940 to 1941, and at the Massachusetts Institute of Technology in 1942.

LEONARD MAUTNER

In 1939, Mr. Mautner was an illuminating engineer at the Macbeth Daylighting Corp., New York, N. Y., later joining the Army Signal Corps, as radio engineer. In 1942 he joined the television department of the National Broadcasting Co., and when broadcasting was curtailed because of the war, he became a staff member of the Radiation Laboratory at the Massachusetts Institute of Technology. Here he was a member of the Indicator Group, which developed a variety of indicator units for radar equipment. In 1944, Mr. Mautner was asked to serve as a Radiation Laboratory member of the Combined Research Group at the Naval Research Laboratory, Washington, D. C., where he took charge of the display section. In this capacity, he supervised the development of all of the display and interconnection equipment for the Mark V IFF/UNB Project. In 1945, he joined the Research Division of the Allen B. DuMont Laboratories, and in 1947 became manager of their television transmitter division. He recently organized a new firm, Television Equipment Corp., where he is president and director.

Mr. Mautner is a member of Eta Kappa Nu and is active on several committees of the Radio Manufacturers Association, serving as chairman of the Television Studio Facilities Subcommittee of the Television Transmitter Dept. He is author of a number of technical papers, as well as a text book entitled "Mathematics for Radio Engineers."

❖

John M. Miller, Jr. (A'41) was born in Washington, D. C., on July 6, 1910. He was graduated from the University of Pennsylvania in 1932, with the degree of B.S. in electrical engineering, and received the E.E. degree in 1947 from the same University.

JOHN M. MILLER, JR

From 1933 to 1939 Mr. Miller was associated with the Philco Radio & Television Corporation, first as a test equipment engineer, and later as head of the physical laboratory. He joined the RCA Victor Division in 1939 as a broadcast receiver design engineer, leaving in 1940 to become a member of the Naval Research Laboratory and Bureau of Ships, where he specialized in radio receiver and radar test equipment design. Mr. Miller remained with the Naval Research Laboratory until 1944, when he accepted a position as chief engineer with the Ripley Company, Inc., in Middletown, Conn. In 1947 he joined the Bendix Radio Division of Bendix Aviation

Contributors to Waves and Electrons Section

Corporation, in Baltimore, Md., where he is a radar principal research engineer at present, having been previously concerned with television receiver engineering, and formerly in charge of audio engineering for radio, phonograph, and television.

Mr. Miller is a member of the Acoustical Society of America.

❖

Richard C. Palmer (S'42–A'43) was born on October 9, 1922, in Washington, D. C. After graduation from the University of Virginia in 1943, he entered the student test program of the General Electric Co. From 1944 to 1946, he did developmental work on automatic controls for the Tennessee-Eastman Corp., at Oak Ridge, Tenn., leaving to engage in television camera development with Remington Rand, Inc., at South Norwalk, Conn. Since 1946, Mr. Palmer has been associated with the Allen B. DuMont Laboratories, Inc., doing developmental work on television and oscillographic equipment.

Richard C. Palmer

Mr. Palmer is an associate of the AIEE, and a member of Sigma Xi and Tau Beta Pi.

❖

Delos W. Rentzel was born in Houston, Tex., on October 20, 1909. He was graduated from the Engineering School of Texas Agricultural and Mechanical College in 1929. He worked on radio station installations for the United States Navy until 1931, when he joined American Airways, Inc., as a radio operator and station manager. He was promoted successively to system chief operator, assistant director of communications, and finally to director of communications.

Delos W. Rentzel

In 1943 Mr. Rentzel became president of Aeronautical Radio, Inc., where he was active in helping to develop improved aviation equipment and techniques as chairman of the Radio Technical Planning Board's Aeronautical Radio Panel and vice-chairman of the Radio Technical Commission for Aeronautics. During this period he was also a member of the Board of Aeronautical Radio of Mexico, serving as its president in 1948; and as a member of the Board of the Airborne Instrument Laboratory.

Mr. Rentzel was appointed Administrator of Civil Aeronautics on April 8, 1948, and was confirmed by the Senate on May 5. As Administrator, he is continuing his interests in improving airway and airline operations by his committee memberships on the Telecommunications Co-ordinating Committee, the Radio Technical Commission for Aeronautics, the National Advisory Committee for Aeronautics, and the Committee on Navigation of the National Military Establishment Research and Development Board.

Mr. Rentzel is a member of the Institute of Aeronautical Sciences, Society of Automotive Engineers, Aircraft Owners and Pilots Association, American Ordnance Association, National Press Club, and the Aero Club.

❖

Samuel Stiber (A'43) was born in New York, N. Y., in 1909. He received the B.S. and M.S. degrees from the College of the City of New York, in 1931 and 1933, respectively. From 1935 to 1940 he was an instructor in physics and mathematics in Puerto Rico. Returning to the United States in 1941, he became an instructor in radio engineering at the Air Force Technical Training Command, at Scott Field, Ill. Since 1943, Mr. Stiber has been a radio engineer at the Evans Signal Laboratories, Belmar, N. J.

Samuel Stiber

Mr. Stiber has made numerous inventions pertaining to communications and direction-finding, such as the instantaneous direction finder, resonant structures for panoramic receivers, and new receivers for detecting radio signals over wide frequency bands.

Jack D. Young (S'42-A'45) was born in Council Bluffs, Iowa, on April 17, 1916. He received the B.S. degree in electrical engineering from the University of Iowa in 1942. During the time he was an undergraduate, he undertook certain developmental work in connection with the recording of speech as an aid to students taking courses in public speaking. He was employed by the Nebraska Power Company of Omaha, Neb., during summer vacations.

J. D. Young

Shortly after graduation he entered the Naval Research Laboratory in Washington, D. C., as a radio engineer, and was closely associated with various projects involving the development of Naval radar equipment and special electronic devices. During 1945 Mr. Young undertook certain specialized work in the Radio Countermeasure Branch of the Naval Research Laboratory. This work is primarily concerned with research and design of electronic circuits utilizing cathode-ray tubes and their applications in various naval electronic systems.

❖

Yeo Pay Yu (A'48) was born on August 27, 1917, in Canton City, China. He received the M.S degree in electrical engineering from Lehigh University. From 1942 to 1947 he was engaged in the development of special electronic instruments, FM-AM receivers, and television with industries, as a project engineer. Since 1947, Professor Yu has been associated with the School of Engineering, North Dakota Agricultural College, as an associate professor in charge of the electronics option.

Yeo Pay Yu

Professor Yu has published various articles in the electronics and communication field. He is a member of the American Institute of Electrical Engineers and the Society for American Engineering Education.

Abstracts and References

Prepared by the National Physical Laboratory, Teddington, England, Published by Arrangement with the Department of Scientific and Industrial Research, England, and *Wireless Engineer*, London, England

NOTE: The Institute of Radio Engineers does not have available copies of the publications mentioned in these pages, nor does it have reprints of the articles abstracted. Correspondence regarding these articles and requests for their procurement should be addressed to the individual publications and not to the IRE.

The Institute of Radio Engineers has made arrangements to have these Abstracts and References reprinted on suitable paper, on one side of the sheet only. This makes it possible for subscribers to this special service to cut and mount the individual Abstracts for cataloging or otherwise to file and refer to them. Subscriptions to this special edition will be accepted only from members of the IRE and subscribers to the Proc. I.R.E. at $15.00 per year. The Annual Index to these Abstracts and Refernces, covering those published from February, 1948, through January, 1949, may be obtained for 2s. 8d. postage included from the *Wireless Engineer*, Dorset House, Stamford St., London S. E., England.

The number in heavy type at the upper left of each Abstract is its Universal Decimal Classification number and is not to be confused with the Decimal Classification used by the United States National Bureau of Standards. The number in heavy type at the top right is the serial number of the Abstract. DC numbers marked with a dagger (†) must be regarded as provisional.

ACOUSTICS AND AUDIO FREQUENCIES

016:534 2114
References to Contemporary Papers on Acoustics—A. Taber Jones. (*Jour. Acous. Soc. Amer.*, vol. 21, pp. 273–280; May, 1949.) Continuation of 924 of May.

534:061.3 2115
A Report on the International Conference on Acoustics, London, 1948—L. L. Beranek. (*Jour. Acous. Soc. Amer.*, vol. 21, pp. 264–269; May, 1949.)

534.143:538.652 2116
Motional Impedance Measurements on a Magnetostrictive System—F. P. Finlon. (*Jour. Acous. Soc. Amer.*, vol. 21, pp. 177–182; May, 1949.) Describes a method of mounting a nickel toroid coil in a block of Permafil, a nonmagnetic plastic, so that motion due to magnetostriction can be damped out. The motional impedance can then be obtained as the difference between the clamped and unclamped impedances. Frequency range, 5 to 45 kc.

534.21 2117
Interactions between a Plate and a Sound Field—R. D. Fay. (*Jour. Acous. Soc. Amer.*, vol. 21, p. 272; May, 1949.) Corrections to 605 of April.

534.22-13+534.231.3-13]:534.321.9 2118
Ultrasonic Velocities and Absorption in Gases at Low Pressures—I. F. Zartman. (*Jour. Acous. Soc. Amer.*, vol. 21, pp. 171–174; May, 1949.) Improvements in an interferometer of the Hubbard type (1932 *Wireless Eng.*, Abstracts, p. 171) are described and measurements of velocity and absorption in air, CO_2, H_2, and N_2 are given for frequencies from 500 kc to 2.16 Mc, temperatures from 9°C to 36.6°C and pressures from 82.17 cm Hg to 0.45 cm Hg.

534.321.9 2119
Visual Methods for Studying Ultrasonic Phenomena—R. B. Barnes and C. J. Burton. (*Jour. Appl. Phys.*, vol. 20, pp. 286–294; March, 1949.) A brief review of the applications and methods of schlieren photography. A simple technique is described, with many photographs of the reflection and diffraction of ultrasonic waves in liquids.

534.7:611.85 2120
The Structure of the Middle Ear and the Hearing of One's Own Voice by Bone Conduction—G. v. Békésy. (*Jour. Acous. Soc. Amer.*, vol. 21, pp. 217–232; May, 1949.) A detailed discussion of the construction of the animal ear and throat as an acoustic system shows how the ear's sensitivity is not upset by sounds originating in the throat.

534.7:611.85 2121
The Vibration of the Cochlear Partition in Anatomical Preparations and in Models of the Inner Ear.—G. v. Békésy. (*Jour Acous. Soc. Amer.*, vol. 21, pp. 233–245; May, 1949.) Translation of an article published in *Akust. Z.*, vol. 7, pp. 173–186; 1942.

An account of experimental methods (acoustic and optical) by which the vibrations of the round window (cochlear partition) were studied. A working model of the cochlea is described.

534.7:611.85 2122
On the Resonance Curve and the Decay Period at Various Points on the Cochlear Partition—G. v. Békésy. (*Jour. Acous. Soc. Amer.*, vol. 21, pp. 245–254; May, 1949.) Translation of an article published in *Akust. Z.*, vol. 8, pp. 66–76; 1943.

534.833 2123
Absorption by Sound-Absorbent Spheres—R. K. Cook and P. Chrzanowski. (*Jour. Acous. Soc. Amer.*, vol. 21, pp. 167–170; May, 1949.) Theory and measurement show that the absorption coefficient of a sphere covered with hair felt can be greater than unity. The normal impedance assumption does not appear to be valid.

534.842 2124
Concert Hall Acoustics—P. H. Parkin. (*Nature* (London,) vol. 163, pp. 122–124; January 22, 1949.) Report of Physical Society discussion.

534.86:534.322.1 2125
Influence of Reproducing System on Tonal-Range Preferences—H. A. Chinn and P. Eisenberg. (Proc. I.R.E., vol. 37, pp. 401–402; April, 1949.) Discussion on 2695 of 1948.

534.861.1+534.862.1 2126
A Demonstration Studio for Sound Recording and Reproduction and for Sound Film Projection—(*Philips Tech. Rev.*, vol. 10, pp. 196–204; January, 1949.) Description of the construction and special features of a new studio at Eindhoven. The reverberation time at the higher frequencies (0.9 second at 2,000 cps) is only slightly less than at the lower frequencies (1.3 second at 100 cps); this has a good effect on high-note response.

621.395.61 2127
The Miniature Electrodynamic Microphone of the Société indépendante de T.S.F.—(*Ann. Radioélec.*, vol. 4, pp. 161–163; April, 1949.) A short description of Type S.I.F. Md. 8, which is 30 mm in diameter, 18 mm thick, and weighs 30 gm. Response is linear to within ±7.5 db in the frequency band 300 to 6,000 cps and signal to-noise ratio and sensitivity are good. Impedance is 70Ω±10 per cent at 1,000 cps.

621.395.61+681.85:621.315.612.4 2128
Application of Activated Ceramics to Transducers—H. W. Koren. (*Jour. Acous. Soc. Amer.*, vol. 21, pp. 198–201; May, 1949.) The conditions are examined under which titanate ceramics can be made to have pronounced piezoelectric properties. Methods of applying the necessary stress to ceramic strips are described. Various applications are mentioned, including a sensitive phonograph pickup.

621.395.61:534.773 2129
Interactions between Microphones, Couplers and Earphones—K. C. Morrical, J. L. Glaser, and R. W. Benson. (*Jour Acous. Soc. Amer.*, vol. 21, pp. 190–197; May, 1949.)

621.395.61:621.317.32 2130
The Substitution Method of Measuring the Open Circuit Voltage Generated by a Microphone—M. S. Hawley. (*Jour. Acous. Soc. Amer.*, vol. 21, pp. 183–189; May, 1949.) Analysis shows that the "normal" substitution voltage equals the open-circuit voltage for all types of acoustic measurement and for any value of the electrical impedance loading the microphone.

621.395.625.2 2131
The Design of a Balanced-Armature Cutter-Head for Lateral-Cut Disc Recording—F. E. Williams. (*Proc. IEE*, part III, vol. 96, pp. 145–158; March, 1949.) The theory of cutter heads is developed with particular reference to the control of mechanical resonance by inertia, stiffness, and damping. Moving-coil and moving-iron systems are considered. The limitations set by the magnetic circuit make it impracti

cable to obtain modulation velocities of the order of 15 cm per second at 400 cps unless the fundamental resonance frequency of the mechanical system is made less than 3,000 cps.

621.395.625.3:534.76 2132

A Stereophonic Magnetic Recorder—M. Camras. (Proc. I.R.E., vol. 37, pp. 442–447; April, 1949.) An experimental 3-channel recorder and play-back unit is described and results obtained with it are discussed. Best results for a small room are obtained with a dihedral mounting of two loudspeakers.

621.395.625.3 2133

Graphical Analysis of Linear Magnetic Recording Using High-Frequency Excitation—M. Camras. (Proc. I.R.E., vol. 37, pp. 569–573; May, 1949.) "The addition of a high-frequency component to an audio signal which is to be recorded magnetically results in a low-distortion, linear recording characteristic under certain conditions. This paper gives a graphical method for constructing the recording characteristic from the B_R versus H curve of the record material. An analysis accounts for such magnetic-recording characteristics as variation in sensitivity with bias, linearity at low recording levels, adjustment for maximum sensitivity, and adjustment for minimum distortion."

621.395.665.1 2134

Contrast Expansion—Wheeler. (*See* 2171).

621.395.813:621.395.623.7 2135

Non-Linear Distortion in Dynamic Loudspeakers due to Magnetic Effects—W. J. Cunningham. (*Jour Acous. Soc. Amer.*, vol. 21, pp. 202–207; May, 1949.) An analysis of two kinds of distortion; that due to (a) the force between the voice coil and the magnet iron, and (b) the nonuniformity of the magnetic field. Distortion produced may be several tenths of 1 per cent. To minimize (b), the voice coil and the magnet gap should have unequal lengths.

621.396.611.21:534.6 2136

Low Loss Crystal Systems—W. J. Fry. (*Jour. Acous. Soc. Amer.*, vol. 21, p. 272; May, 1949.) Corrections to 1326 of June.

ANTENNAS AND TRANSMISSION LINES

621.315.2 2137

High-Impedance Cable—S. Frankel. (Proc. I.R.E., vol. 37, p. 406; April, 1949.) An approximate expression for the inductance of a long solenoid surrounded by a cylindrical shield is derived by consideration of the multiwire transmission line obtained when coil and shield are cut lengthwise and unwrapped. Results obtained appear to confirm the value of the correction coefficient given by Winkler. The formula obtained for the distributed capacitance of the system agrees with that for a coaxial line. See also 1278 of June (Hodelin).

621.315.212 2138

Influence of Nonuniformity in a Coaxial Cable on its Parameters—L. A. Zhekulin. (*Bull. Acad. Sci.* (URSS), pp. 1089–1105; September, 1947. In Russian.)

621.392.26† 2139

Disk-Loaded Wave Guides—E. L. Chu and W. W. Hansen. (*Jour. Appl. Phys.*, vol. 20, pp. 280–285; March, 1949.) Dimensions of such waveguides for use in a linear accelerator are calculated with high accuracy by Schwinger's method, of which a qualitative explanation is given. Comparison with the work of J. C. Slater (MIT Technical Report No. 48, September 19, 1947) shows perfect agreement.

621.392.26† 2140

Geometrical Representation of the Characteristics of an Active Obstacle inserted in a Waveguide—J. Ortusi and P. Fechner. (*Ann. Radioélec.*, vol. 4, pp. 131–135; April, 1949.) In waveguide problems, it is often necessary to consider the reflections caused by impedances thrown back into the main waveguide by shunt or series matching stubs, which may be variable. A simple geometrical method is described for determining the coefficients of reflection, transmission, and energy loss corresponding to such impedances and, conversely, for determining the impedance from measured values of the coefficients. The shunt and series cases are considered separately.

621.392.26†:621.3.09 2141

The Conditions of Propagation of H_0 Waves, and their Applications—J. Ortusi. (*Ann. Radioélec.*, vol. 4, pp. 94–116; April, 1949.) H_0 waves are defined as those for which the longitudinal current in the waveguide wall is everywhere zero. Discussion of: (a) mathematical theory for such waves in waveguides of circular section, (b) methods of producing them practically free from parasites, (c) filters of various types favoring the propagation of H_0 waves, (d) measurement methods, (e) attenuation, (f) the effects of waveguide deformation or curvature and of the dielectric filling the waveguide, (g) curves showing the attenuation in circular waveguides compared with that for propagation in the open air by diffraction, and (h) applications to the construction of cavity wavemeters with very high Q and to problems connected with radar scanning.

621.396.67 2142

Antennas for Circular Polarization—W. Sichak and S. Milazzo. (*Elec. Commun.*, vol. 26, pp. 40–45; March, 1949.) Reprint of 3343 of 1948.

621.396.67 2143

U.H.F. Aerials—J. Maillard. (*Onde Élec.*, vol. 29, pp. 110–123; March, 1949.) The general characteristics of antenna radiation are outlined and the special features of uhf antennas are considered. Various types are described and their use for particular services is discussed.

621.396.67:538.56:535.13 2144

The Radiation and Transmission Properties of a Pair of Parallel Plates: Part 2—A. E. Heins. (*Quart. Appl. Math.*, vol. 6, pp. 215–220; October, 1948.) Formulas are derived for the reflection coefficient at the mouth of a semi-infinite parallel-plate system excited by a plane wave. Fields are expressed by integral equations of the Wiener-Hopf type and the Fourier transforms are determined. Part 1, 1920 of August.

621.396.67:621.396.41:621.396.65 2145

Use of a Reflecting Mirror and of Simple Electromagnetic Lenses for the Experimental 23-cm Link between France and Corsica—J. Hugon. (*Ann. Radioélec.*, vol. 4, pp. 157–160; April, 1949.) Communication could be effected by a link with direct visibility between Mont Agel and Calenzana or between Grasse and Calenzana (a) directly, with part of the path beyond optical range, or (b) indirectly, using a reflector installed on Monte Grosso (Corsica), with direct visibility to Grasse and oriented so as to reflect signals from Grasse to the receiving antenna at Calenzana, or vice versa. The reflector was of perforated sheet-iron and had an aperture of 10×4 m. Tests showed that it gave a gain of 20 db compared to the direct link beyond optical range. The electromagnetic lenses used with the Mont Agel transmitter had rectangular waveguides, of dimensions decreasing from center to sides, fitted along the top and bottom. The propagation velocities in these waveguides were so calculated as to correct the phase shifts in the aperture plane and to give an effective plane wave output, resulting in improved directional characteristics. See also 3508 of 1948 (Rivère).

621.396.671:621.396.97 2146

Directional Antennas for A.M. Broadcasting—J. H. Battison. (*Electronics*, vol. 22, pp. 101–103; April, 1949.) A simplified, practical method of calculating radiation patterns for 2-tower and 3-tower arrays.

621.396.677 2147

Analysis of the Metal-Strip Delay Structure for Microwave Lenses—S. B. Cohn. (*Jour. Appl. Phys.*, vol. 20, pp. 257–262; March, 1949. See also 2176 of 1948 (Kock).

621.396.677 2148

Aerial Arrays with Horizontal Beams without Side Lobes—O. Schmidl. (*Bull. Schweiz Elektrotech. Ver.*, vol. 38 pp. 15–20; January 11, 1947. In German, with French summary.) General theory is developed by considering the resultant obtained by superposition of the radiation distributions from each element. Technical requirements demand a minimum number of such elements with optimum efficiency. Practical design formulas are derived and applied in two numerical examples.

CIRCUITS AND CIRCUIT ELEMENTS

538.1:621.392.26†:621.396.611.4 2149

Narrow Gaps in Microwave Problems—W. R. Smythe. (*Rev. Mod. Phys.*, vol. 20, pp. 175–180; January, 1948.) An explicit expression, $E_x=f(x)$, is given for the x-component of the electric field between two infinite, oppositely charged conducting masses bounded by the $y=0$, $x=b$ planes and the $y=0$, $x=-b$ planes, respectively. The coefficients of the Fourier expansion of E_x and the potential function V are used to determine a rapidly convergent series for the potential in the narrow gap between two right circular, coaxial, conducting cylindrical electrodes. The resonance frequency of a reentrant cylindrical cavity with a narrow gap is computed within about 0.03 per cent. The shape of the field radiated from the open end of a rectangular waveguide, terminating in an infinite conducting plane and transmitting only the TE_{10} mode, is calculated with 4-figure accuracy.

621.3.012.2:621.392.5 2150

Circle Diagrams of Impedance or Admittance for Four-Terminal Networks—J. Rybner. (*Proc. IEE*, part III, vol. 96, p. 132; March, 1949.) Discussion on 3357 of 1948.

621.3.012.8:621.385.2 2151

Diode Circuit Analysis—R. H. Dishington. (*Elec. Eng.* vol. 67, pp. 1043–1049; November, 1948.) The nonlinear tube characteristic is analyzed and an equivalent circuit is suggested to which most ordinary applications can be reduced. This method of analysis is less complex than other methods hitherto used and can be applied to various diode and multi-element tube circuits, such as the diode modulator.

621.3.012.8:621.385.2:518.4 2152

Graphical Analysis of Diode Circuits—G. L. Hamburger. (*Wireless Eng.*, vol. 26, pp. 147–153; May, 1949.) Analysis of the basic diode-rectifier circuit leads to an integral equation which has no formal explicit solution; it can, however, be solved by a simple graphical method which is applicable to periodic input voltages of arbitrary wave form. The method is applied to a typical AM detector, and to squaring and clipping circuits. Circuits involving reactance are considered briefly.

621.314.2 2153

Design of I.F. Transformers—B. Sandel. (*Radiotronics*, no. 131, pp. 43–59; May and June, 1948.) Design procedure can be reduced to a few routine operations with the aid of charts and tables if certain assumptions are made. Only the 2-winding transformer with mutual inductance coupling is here considered; the added capacitance coupling is taken into account by adjusting the coefficient of coupling k. Numerical examples are included. FM trans formers are discussed as well as undercoupled overcoupled, and critically coupled transformers. Practical construction details and methods of measuring k are also considered.

621.314.2.015.33 2154
Considerations on Pulse Transformers—F. Blaché. *Ann. Radioélec.*, vol. 4, pp. 149–156; April, 1949). Simple calculation and design methods are presented for transformers of high power. The methods are based on the response to an ideal rectangular pulse. The effects of the various transformer constants on the pulse shape are shown graphically, and methods of measuring primary inductance, core permeability, and losses are indicated.

621.316.718:621.396.9:371.3 2155
The Velodyne—F. C. Williams and A. M. Uttley. (*Proc. IEE*, part III, vol. 96, p. 168; March, 1949.) Discussion on 962 of 1948.

621.316.86 2156
Thermistors—F. E. Butler. (*Radio News, Radio-Electronic Eng. Supplement*, vol. 10, pp. 15–18, 31 and 10–12, 30; May and June, 1948.) Detailed discussion of their properties and applications. Materials used are oxides of Mn, Ni, Co, Cu, U, etc. Resistance can be varied by several powers of 10 by introducing impurities or by other treatment. Manufacturing methods are discussed. Applications considered include compensation of resistance changes, automatic control, timing devices, and voltage regulators.

621.318.423.011.3(083.3) 2157
The Use of Bessel Functions for Calculating the Self-Inductance of Single-Layer Solenoids—E. B. Moullin. (*Proc. IEE*, part III, vol. 96, pp. 133–137; March, 1949.) Continuation of 2077 of 1947. The general Bessel formulas lead to the well-known expression for the field at the center of a solenoid. The Bessel treatment has special advantages for calculating the field just inside the winding. Formulas are derived for the inductance of an isolated solenoid and also of a solenoid symmetrically placed between two infinite metal sheets perpendicular to its axis.

621.318.423.011.3(083.3) 2158
A Note on the Inductance of Screened Single-Layer Solenoids—F. M. Phillips. (*Proc. IEE*, part III, vol. 96, pp. 138–140,; March. 1949.) The change of inductance which occurs when a single-layer solenoid is placed inside a coaxial cylindrical screening can is calculated by Moullin's method (2157 above) and compared with that obtained from Bogle's empirical formulas (821 of 1941.)

621.318.572 2159
Scaler Circuits—W. M. Couch, Jr. (*Radio News, Radio-Electronic Eng. Supplement*, vol. 10, pp. 3–5, 28 and vol. 11, pp. 10–12, 30; June and August, 1948.) Comparison of (a) trigger-type circuits, with special reference to the Eccles-Jordan binary-scale unit, (b) ring circuits, and (c) capacitor accumulation circuits, and discussion of their design and operation. A bibliography of 47 references is included.

621.318.572 2160
High-Speed Trigger Circuit—W. B. Lurie. (*Electronics*, vol. 22, pp. 85–87; April, 1949.) For photographic and other applications which require triggering pulses in a predetermined time pattern after a given event (sound, flash of light, etc.). The event is used to generate a keying pulse which, after inversion and clipping is applied to three delay lines, with independent delays ranging up to 26.6 µsecond, to derive positive high-level firing pulses. The undelayed pulse is also applied, after sharing and clipping, to a thyratron generator to produce a pulse of square form with a maximum current of 10 amperes through 1 Ω.

621.319.4 2161
Resonances in Capacitors—C. F. Muckenhoupt. (Proc. I.R.E., vol. 37, pp. 532–533; May, 1949.) In a parallel-plate capacitor whose leads emerge at opposite ends, the higher resonance and antiresonance frequencies are very close together; near such points the capacitor may be very frequency sensitive and exhibit anomalous effects.

621.319.4 2162
Ceramic Capacitors—W. G. Roberts. (*Jour. Brit. I.R.E.*, vol. 9, pp. 184–199; May, 1949. Discussion, pp. 199–200.) A general survey. Properties of the various types of material, and the construction, manufacture and uses of the capacitors are discussed.

621.392 2163
Transfer Functions for R-C and R-L Equalizer Networks—E. W. Tschudi. (*Electronics*, vol. 22, pp. 116–120; May, 1949.) Transfer functions and gain-curve asymptotes are shown for 30 different types of network.

621.392:003.62 2164
Drawing Circuit Diagrams—L. Bainbridge-Bell. (*Wireless World*, vol. 55, pp. 179–180; May, 1949.) Discussion of representation of leads which cross without connection. See also 664 of April.

621.392:621.3.015.3 2165
The Effect of Pole and Zero Locations on the Transient Response of Linear Dynamic Systems—J. H. Mulligan. (Proc. I.R.E., vol. 37, pp. 516–529; May, 1949.) The conditions for a monotonic time response are expressed in terms of the location of transfer-function poles and zeros, for stable low-pass systems having only first-order poles and no poles on the $j\omega$ axis. A simplified method of computing maxima and minima in the time response is explained. Under certain conditions, the normalized time response is well represented by a single dominant time term. A method of determining whether these conditions exist is discussed. When they do exist, a method is outlined for designing pole and zero patterns to yield given time-response characteristics of a certain kind for step-function inputs. Constant overshoot-factor curves and charts are provided for this purpose. The results can be applied to networks, amplifiers, servomechanisms, etc.

621.392:621.3.015.3 2166
Transient-Response Equalization Through Steady-State Methods—W. J. Kessler. (Proc. I.R.E., vol. 37, pp. 447–450; April, 1949.) Only a sinusoidal signal generator and a cro are used. The frequency of the signal generator is slowly swept through the transmission ranges of the networks, and amplitude and phase adjustments are made so that a closed line of unit slope is displayed on the cro at all frequencies. Photographs of patterns displayed on the cro and methods of determining the required network adjustments rapidly are discussed.

621.392.5 2167
The "Phantastron" Control Circuit—J. R. McDade. (*Elec. Eng.* vol. 67, pp. 974–977; October, 1948.) The construction and operation of the pentagrid converter tube used in these radar delay circuits are described. The action of a typical phantastron circuit is explained in detail by considering separately the six periods corresponding to the discontinuous portions of the voltage wave form. For another account see 2478 of 1948 (Close and Lebenbaum).

621.392.5:621.385.3:512.831 2168
The Application of Matrices to Vacuum-Tube Circuits—J. S. Brown and F. D. Bennett. (Proc. I.R.E., vol. 37, pp. 403–404; April, 1949.) Discussion on 3043 of 1948.

621.392.5.029.64:621.392.26† 2169
A Consideration of Directivity in Waveguide Directional Couplers—S. Rosen and J. T. Bangert. (Proc. I.R.E., vol. 37, pp. 393–401; April, 1949.) 1947 IRE National Convention paper. An explanation of the behavior of a two-hole coupler is given in terms of an infinity of interaction processes between two waveguides. Expressions based on Bethe's theory are derived for the directivity ratio in terms of the transmission factor and the distance between the holes. Solutions are also obtained for two and for four pairs of holes. The directivity ratio usually reaches a nonzero minimum for a single pair of holes, and has multiple minima, one of which is almost independent of pair spacing, for the multiple-pair systems. Comparison with experiment shows good agreement for transmission factors up to 0.01. See also 675 of 1948 (Riblet).

621.392.52 2170
Resonant-Section Band-Pass Filters—S. Frankel. (*Elec. Commun.*, vol. 26, pp. 76–83; March, 1949.) An explicit formula is obtained for the ratio η of the power transferred to the resistive load to the maximum power transferable under matched conditions; the filter is assumed to consist of a chain of n identical resonators coupled by identical reactances to the preceding and following resonators. When $n=10$, η is constant within 3 db over 85 per cent of the pass band, but has undesirable fluctuations at the edges of the band.

621.395.665.1 2171
Contrast Expansion—L. J. Wheeler. (*Wireless World*, vol. 55, pp. 211–215; June, 1949.) A review of different methods and of means for eliminating their defects. Circuit diagrams of several systems are given, including a modified negative-feedback circuit giving improved results in reproduction from phonograph records.

621.396.61 2172
Parasitic Oscillations—"Cathode Ray." (*Wireless World*, vol. 55, pp. 206–210; June, 1949.) Discussion of conditions favorable to the production of unwanted oscillations and of means of preventing them.

621.396.611.21 2173
Cathode-Coupled Crystal Oscillators—F. Butler. (*Short Wave Mag.*, vol.. 7, pp. 258–262; June, 1949.) Simple explanations are given of the operation of the basic circuit (32 of 1945) and of the derivatives described by Goldberg and Crosby (333 of March and 3048 of 1948.)

621.396.611.3:621.365.5 2174
On Circuits with Electromagnetic Coupling and their Appplication in H.F. Induction-Heating Equipment—F. P. Pietermaat. (*HF*, (Brussels), no. 2, pp. 35–44; 1949. In French.) The importance of a knowledge of the Q factor of the oscillatory circuit of an oscillator used for high-frequency induction heating is stressed. The case is considered where the oscillatory circuit and the work are coupled by means of an aperiodic transformer. Abacs are given which enable Q to be determined rapidly. The effect of partial tuning of the work coil is examined and also the case where only a part of the oscillatory circuit inductance is coupled to the work coil. Numerical examples are included.

621.396.615 2175
Generation of Oscillations—R. Urtel; F. W. Gundlach; J. Frey; W. O. Schumann; E. Marx; G. Hettner (*FIAT Review of German Science 1939–1946. Electronics, incl. Fundamental Emission Phenomena*, part 1, pp. 147–250; 1948, In German.)

Sections 1, 2, and 3, by Urtel, briefly consider (a) general questions and stability, (b) feedback, and (c) kipp oscillations.

Section 4, by Gundlach, gives a full account of theoretical and experimental work in Germany in connection with transit-time tubes for uhf work, including diodes, retarding-field tubes, tubes with space-charge or velocity control, and magnetrons.

Section 5, by Frey, outlines work on frequency multiplication.

Section 6, by Schumann, discusses plasma oscillations.

Section 7, by Marx, deals briefly with spark transmitters for centimeter waves.

Section 8, by Hettner, discusses the production of waves in the range 0.1 to 0.3 mm with the high-pressure Hg-vapor lamp.

621.396.615 2176

Oscillation Amplitude in Simple Valve Oscillators—A. S. Gladwin. (*Wireless Eng.*, vol. 26, pp. 159–170 and 201–209; May and June, 1949.) A method is derived of calculating this amplitude in oscillators of the regenerative type where grid leak bias is used. The amplitude is found in terms of parameters which are functions of the tube and circuit constants, and the solution is presented graphically.

Two types of amplitude instability are studied and criteria for their existence are deduced. The first type is dynamical instability or squegging; the second type gives rise to the effect known as oscillation hysteresis.

The analysis is applicable to all the common types of oscillator circuit, subject to the conditions that the tube should operate always in the space-charge-limited condition, and that the anode voltage should never fall to the point where the anode current is rapidly diverted to the grid or screen.

621.396.615 2177

Wide-Range Deviable Oscillator—M. E. Ames. (*Electronics*, vol. 22, pp. 96–100; May, 1949.) A cathode follower working into a capacitive load will produce a phase shift dependent on the anode ac resistance, which, in turn, depends on the grid bias. The type of oscillator described uses four such phase-shift stages following an amplifier. The system oscillates at the frequency for which the phase shift per stage is 45° and this shift is effected by making the capacitive reactance of each stage equal to its equivalent resistance. FM is accomplished by simultaneous variation of the anode current to all the four phase-shift stages. Each time the effective resistance is altered by changing the grid bias, the oscillation frequency changes to a new value at which the reactance of the fixed capacitors is equal to the new effective resistance. The voltage loss of the phase-shift stages remains constant because the amplification factor of the triodes does not change and because the phase-shift required is also constant. With careful design, a linear frequency versus modulating-voltage characteristic is obtained. One oscillator constructed has a frequency range from 150 cps to 15 kc; frequencies than are usually possible with this type of oscillator. Circuit diagrams are given.

621.396.615:621.396.619.13 2178

A simple Method of Producing Wide-Band Frequency Modulation—Rakshit and Sarkar. (*See 2362.*)

621.396.615.17 2179

Blocking Oscillators—W. T. Cocking. (*Wireless World*, vol. 55, pp. 230–233; June, 1949.) A method is described for improving the linearity of the sawtooth output by eliminating the high-frequency transients superimposed on the wave at the commencement of each stroke. This enables the circuit to be used as an oscilloscope time base at higher repetition frequencies than are usually possible with this type of oscillator. Circuit diagrams are given.

621.396.615.17 2180

Pulse Generation—S. Moskowitz and J. Racker. (*Radio News, Radio-Electronic Eng. Supplement*, vol. 11, pp. 14–19, 30; July, 1948.) Discussion of circuits and techniques. Both active and passive networks are considered.

621.396.615.17 2181

Symmetrical Multivibrators—R. Feinberg. (*Wireless Eng.*, vol. 26, pp. 153–158; May, 1949.) "Formulae are derived from an equivalent circuit diagram to give the frequency and waveform of oscillation of a symmetrical multivibrator circuit with pentodes operating on the coalescent part of their characteristic. It is assumed that the interelectrode capacitances of the valves and any self-inductances and self-capacitances of the circuit elements have no effect on the circuit performance. The waveform of oscillation is rectangular when the time constant of capacitor charge is relatively small, and is triangular when the time constant is relatively large. The frequency is governed by the d.c. supply voltage, the type and screen grid voltage of the pentodes and essentially by the values of the reservoir capacitance and the grid-shunting resistance. Predicted frequencies and waveforms are verified by experiment."

621.396.619.13 2182

Frequency Swing with Variable-Reactance Valves—R. Leprêtre. (*Onde Élec.*, vol. 29, pp. 130–136 and 167–174; March and April, 1949.) The equivalent impedance of a reactance tube and its *RC* circuit, when *R* is connected between grid and anode, is shown theoretically to be inductive. Formulas are derived, in a manner as rigorous as possible, for the frequency swing and the damping. An approximate equation for the reactive admittance is given for the general case and for a pentode, with a simplified formula for the frequency swing and with numerical examples. When *C* is connected between grid and anode the equivalent impedance is capacitive. Comparison shows that the capacitive arrangement gives a greater frequency swing for a given damping than the inductive connection. Circuits in which the damping is zero, or even negative, are discussed, with particular reference to a circuit described by Helfrich (2489 of 1948.) A circuit insensitive to supply-voltage variations is also given.

621.396.619.23 2183

The Serrasoid F.M. Modulator—Day. (*See 2363.*)

621.396.619.23 2184

Non-Linear Effects in Ring Modulators—V. Belevitch. (*Wireless Eng.*, vol. 26, p. 177; May, 1949.) The operation of a 4-rectifier ring modulator is considered for signal voltages of arbitrary value, and the amplitude of the general modulation product is given as a hypergeometric function. Curves are drawn for the lowest products, illustrating the departure from linearity with increasing signal voltage.

621.396.619.23:621.396.615.17 2185

A Modulator Producing Pulses of 10^{-7} Second Duration at a 1-Mc Recurrence Frequency—M. G. Morgan. (PROC. I.R.E., vol. 37, pp. 505–509; May, 1949.) A modulator for use with a spark transmitter, of pulse duration about 2×10^{-8} second, for radar countermeasures. A large 1-Mc voltage wave is applied to the grid of a triode with low internal resistance and a sinusoidal 1-Mc signal is applied to the anode. Suitable phase adjustment results in the production of steep-fronted positive pulses which are applied to the grid of the modulator. The modulating voltage is built up across a capacitive load of 125 pF. The occurrence of a spark reduces the load impedance to a low value and assists in producing a rapid drop of the modulating voltage.

621.396.645+621.396.621.53 2186

Increase of Sensitivity of Amplifier and Mixer Stages for Metre and Decimetre Waves—Strutt. (*See 2312.*)

621.396.645 2187

On the General Theory of Linear Amplifiers: Part 1—S. P. Strelkov. (*Avtomatika i Telemekhanika*, vol. 9, pp. 233–244; May and June, 1948. In Russian.) In a linear amplifier, the input and output are related by a linear differential equation. A general analysis is given of the problem of finding such parameters of this equation as will ensure amplification without excessive distortion. Means of obtaining an approximate estimate of the distortion will be discussed in part 2.

621.396.645 2188

Note on the Sensitivity of an Amplifying Stage—W. Kleen. (*Ann. Radioélec.*, vol. 4, pp. 136–137; April, 1949.) Discussion of the grounded-anode circuit shows that, at low frequency, the sensitivity is the same whether cathode, grid, or anode is grounded, though at high frequency, the optimum sensitivity of the grounded-anode circuit differs slightly from that of the other two. See also 1338 of June.

621.396.645 2189

Amplification of Pulses of Gating Methods—J. A. Fejer. (*Trans. S. Afr. Inst. Elec. Eng.*, vol. 40, part 2, pp. 39–49, February, 1949. Discussion, pp. 49–50.) The limitations of conventional methods of pulse amplification are discussed, with reference to (a) the minimum pulse length for which amplification is possible, (b) ringing effects, and (c) internal noise. Three gating methods, whose principles are explained, all eliminate ringing and enable very short pulses to be amplified. Neglecting fluctuation noise in tubes, the improvement in signal-to-noise ratio obtained by any of the three methods is equal to the ratio of pulse recurrence frequency to the bandwidth of the amplifier following the gate. An experimental double-gate amplifier is described for which the measured signal-to-noise ratio showed an improvement of 31 db compared with the ratio for an amplifier not using gating technique. The application of gating technique to ac pulses is also considered and methods of locking to the leading edges of the dc modulating pulses are described.

621.396.645 2190

Stabilized Decade-Gain Isolation Amplifier—J. F. Keithley. (*Electronics*, vol. 22, pp. 98–100; April, 1949.) An input impedance of over 200 MΩ and less than 6 pF shunt capacitance is obtained by enclosing the input circuit in a shield which is at almost the same instantaneous potential as the test signal conductor. The low dynamic output impedance enables several measuring instruments to be connected to it in parallel, for simultaneous observation of various characteristics of signals in high-impedance circuits. See also 2281 of 1945 (Daniels).

621.396.645 2191

A Coaxial 50-kW F.M. Broadcast Amplifier—Balthis. (*See 2365.*)

621.396.645 2192

Square-Wave Analysis of Compensated Amplifiers—P. M. Seal. (PROC. I.R.E., vol. 37, p. 382; April, 1949.) Correction to 1626 of July.

621.396.645 2193

Stagger-Tuned Amplifiers—L. J. Libois. (*Onde Élec.*, vol. 29, pp. 124–129; March, 1949.) Formulas are derived which enable the number of stages and the values of the various circuit components to be calculated directly, without the use of abacs, for an amplifier with (a) the minimum number of tubes, (b) a given gain, and (c) as flat a response curve within the pass band as possible.

621.396.645.012.8 2194

Network Representation of Input and Output Admittances of Amplifiers—L. M. Vallese. (PROC. I.R.E., vol. 37, pp. 407–408; April, 1949.) A clear picture of circuit performance is obtained if these admittances are represented by networks derived from the equivalent circuit of the amplifier, together with certain series or parallel branches whose elements are functions of μ. Such networks are shown for grounded-cathode, grounded-grid, and grounded-anode amplifiers and for reactance tubes. Results are discussed.

621.396.645.37 2195
Combined Current and Voltage Feedback—K. R. Sturley. (*Electronic Eng.* (London), vol. 21, pp. 159–161; May, 1949.) When voltage feedback is applied in the usual way, current feedback occurs simultaneously and cannot be ignored. The over-all amplification and equivalent output impedance are here derived theoretically. Interaction between the sources of voltage and current feedback tends to reduce slightly the over-all amplification.

621.396.645.371 2196
Negative Feedback Amplifiers—T. S. McLeod. (*Wireless Eng.*, vol. 26, pp. 176–177; May, 1949.) Comment on 1910 of August. (Brockelsby).

621.396.645.371 2197
When Negative Feedback Isn't Negative—"Cathode Ray." (*Wireless World*, vol. 55, pp. 189–193; May, 1949.) Elementary discussion of the cause and prevention of oscillation and distortion.

621.396.69+621.317.7+621.38 2198
The Physical Society's Exhibition—(*Engineering* (London), vol. 167, pp. 313–316 and 337–340, 348; April 8 and 15, 1949. *Engineer* (London), vol. 187, pp. 382–385, 407–409, and 446–448; April 8, 15, and 22, 1949. *Wireless World*, vol. 55, pp. 182–186; May, 1949. *Wireless Eng.*, vol. 26, pp. 171–176; May, 1949.) Descriptions of selected exhibits.

621.396.69 2199
Recent Trends in Radio Technique—M. Adam. (*Tech. Mod.* (Paris), vol. 41, pp. 163–165; May 1 to 15, 1949.) Discussion of (a) miniaturization of all types of components, (b) the use of printed circuits in subminiature assemblies, (c) methods of ensuring satisfactory performance of equipment under extreme conditions of humidity, temperature, and altitude, and (d) component design to withstand shock, vibration, or rapid acceleration.

621.397.645.371 2200
Nonlinearity in Feedback Amplifiers—A. B. Thomas. (PROC. I.R.E., vol. 37, p. 531; May, 1949.) Comment on 2766 of 1948.

GENERAL PHYSICS

534.21+538.566]:537.228.1 2201
Wave Propagation in Piezoelectric Crystals—J. J. Kyame. (*Jour. Acous. Soc. Amer.*, vol. 21, pp. 159–167; May, 1949.)

535.37 2202
A Report on the Second Conference on Luminescence (held in Moscow, 12th–22nd May 1948)—(*Uspekhi Fiz. Nauk.* vol. 36, pp. 557–566; December, 1948. In Russian.)

535.37 2203
Polarized Luminescence—P. P. Feofilov. (*Uspekhi Fiz. Nauk*, vol. 36, pp. 417–455; December, 1948. In Russian.)

537.291+538.691 2204
Some Properties of Tubular Electron Beams—N. Wax. (*Jour. Appl. Phys.*, vol. 20, pp. 242–247; March, 1949.) Approximate expressions are obtained for the potential distribution, maximum current density, and spread of beams of finite thickness. Results are compared with those of Haeff (127 of 1940) and of Smith and Hartman (2409 of 1940).

537.533+621.385.83 2205
Electron Emission and Electron Currents—H. Mayer; M. Knoll. (*FIAT Review of German Science 1939–1946. Electronics, incl. Fundamental Emission Phenomena*, part 1, pp. 1–42; 1948. In German.) Section 1, by Mayer, reviews theoretical and experimental investigations on various aspects of the photoelectric effect. Section 2, by Knoll, in collaboration with E. Kinder, discusses electron optics, with particular reference to cro deflection systems, electron lenses, and the electron microscope.

538.122:621.385 2206
An Electron Tube for Viewing Magnetic Fields—Lutz and Tetenbaum. (*See* 2375.)

538.3 2207
Nonlinear Theories of the Electromagnetic Field—F. Bertein. (*Rev. Sci.* (Paris), vol. 86, pp. 349–356; April 1, 1948.) The difficulties presented by Maxwell's theory are reviewed, the principles of the Born-Infeld theory are outlined and brief reference is made to the theories of Dirac and L. de Broglie.

538.3 2208
Development in Series of the Retarded Potentials of Classical Electromagnetism—É. Durand. (*Jour. Phys. Radium*, vol. 10, pp. 41–48; February, 1949.) One of the fundamental problems of classical electromagnetism is the calculation of the electromagnetic field produced by a given distribution of electricity variable in time. According as one adopts the hypothesis of a space-time distribution of electricity or the hypothesis of point charges, the solution of the problem is represented either by the integrals of retarded potentials or by the potentials of Liénard-Wiechert. The fields can then be easily deduced. These expressions cannot, in general, be used directly, since they involve the retard time, which cannot be expressed in terms of the usual analytical functions. Expressions are derived for the potentials as functions of actual time, using a new type of series development related to Lagrange series. Complete formulas are derived for the radiation potential of a linear sinusoidal oscillator and for the radiation field.

538.56:535.13:621.396.67 2209
The Radiation and Transmission Properties of a Pair of Parallel Plates: Part 2—Heins. (*See* 2144.)

538.566 2210
A Note on Singularities Occurring at Sharp Edges in Electromagnetic Diffraction Theory—C. J. Bouwkamp. (*Physica*, *'s Grav.*, vol. 12, pp. 467–474; October, 1946. In English.) The existence of singularities is demonstrated explicitly in the case of Sommerfeld's well-known solution for diffraction at the edge of a perfectly conducting semiplane. Möglich's solution for the 3-dimensional problem of diffraction by a circular screen is shown to be erroneous.

538.691 2211
Motion of an Electrified Particle in the Magnetic Field of a Current—A. Brunel. (*Rev. Sci.* (Paris), vol. 86, pp. 345–347; April 1, 1948.) Solutions are obtained for the motion of positively or negatively charged particles, with an initial velocity in any direction, in the field of a rectilinear current.

621.39.001.11 2212
Theoretical Limitations on the Rate of Transmission of Information—Tuller. (*See* 2319.)

GEOPHYSICAL AND EXTRATERRESTRIAL PHENOMENA

523.53:621.396.9 2213
A Phenomenological Theory of Radar Echoes from Meteors—D. W. R. McKinley and P. M. Millman. (PROC. I.R.E., vol. 37, pp. 364–375; April, 1949.) Echoes from meteors are classified into basic types according to their appearance on the range versus time record of the radar display. These types include echoes indicating approach or recession, echoes of long duration, and echoes with a complex structure. A qualitative explanation of the various types is given.

523.72.029.6:621.396.822 2214
Electromagnetic Solar Radiation on 158 Mc/s—Y. Rocard. (*Rev. Sci.* (Paris), vol. 86, p. 348; April 1, 1948.) A table is given of the solar energy radiated at this frequency, and the corresponding solar temperature, assuming the radiation to be of thermal origin, for various dates from June 7, to July 7, 1948. The records were obtained with a superheterodyne receiver, using a dipole antenna at the focus of a reflector 8 m in diameter, in open country 30 km south of Paris. The temperatures range from 4.4×10^5 to 8×10^5 degrees K.

523.72.029.64:621.396.822 2215
Circularly Polarized Solar Radiation on 10.7 Centimeters—A. E. Covington. (PROC. I.R.E., vol. 37, p. 407; April, 1949.) Radiation from the quiet sun appears to be randomly polarized, whereas sunspots can produce circularly polarized radiation. See also 2513 of 1948.

523.746"1948.10/.12" 2216
Provisional Sunspot-Numbers for October to December, 1948—M. Waldmeier. (*Jour. Geophys. Res.*, formerly *Terr. Mag. Atmo. Elec.*, vol. 54, p. 64; March, 1949.)

523.854:621.396.822 2217
Origin of the Radio Frequency Emission and Cosmic Radiation in the Milky Way—A. Unsöld. (*Nature* (London), vol. 163, pp. 489–491; March 26, 1949.) The interpretation of galactic rf radiation as due to free-free transitions of electrons in the interstellar gas is unsatisfactory because (a) an electron temperature of 100,000 to 200,000°K is needed to account for results at 20 to 30 Mc, (b) the observed spatial distribution of the radiation does not fit. The alternative hypothesis is discussed that the radiation originates in late-type stars showing eruption activity like that of the sun, but on a scale perhaps 10^{11} times as great.

523.854:621.396.822 2218
Cosmic Radio Noise—G. Reber. (*Radio News, Radio-Electronic Eng. Supplement*, vol. 11, pp. 3–5, 29; July, 1948.) Historical review, with discussion of intensity as a function of galactic longitude at zero galactic latitude and of apparatus used for measurement and recording.

538.12:521.15 2219
Rotation and Terrestrial Magnetism—T. Gold. (*Nature* (London), vol. 163, pp. 513–515; April 2, 1949.) Report of a geophysical discussion of the Royal Astronomical Society on February 25, 1949, on the present state and observational justification of various theories.

550.38"1948.07/.09" 2220
Selected Days, Preliminary Mean *K*-Indices, and Preliminary *C*-Numbers for Third Quarter, 1948—E. K. Weisman. (*Jour. Geophys. Res.*, formerly *Terr. Mag. Atmo. Elec.*, vol. 54, pp. 66–67; March, 1949.)

550.38"1948.10/.12" 2221
Cheltenham [Maryland] K-Indices for October to December, 1948—P. G. Ledig. (*Jour. Geophys. Res.*, formerly *Terr. Mag. Atmo. Elec.*, vol. 54, p. 65; March, 1949.)

550.38"1948.10/.12" 2222
Daily Magnetic-Activity Figures *C*, Three-Hour-Range Indices *K*, and List of Sudden Commencements, October to December, 1948. at Abinger—H. Spencer Jones. (*Jour. Geophys. Res.*, formerly *Terr. Mag. Atmo. Elec.*, vol. 54, pp. 67–68; March, 1949.)

550.385"1948.10/.12" 2223
Principal Magnetic Storms [Oct.–Dec., 1948]—(*Jour. Geophys. Res.*, formerly *Terr. Mag. Atmo. Elec.*, vol. 54, pp. 80–95; March, 1949.)

551.510.4 2224
The Vertical Distribution of Atomic Oxygen in the Upper Atmosphere—R. Penndorf. (*Jour. Geophys. Res.*, formerly *Terr. Mag. Atmo. Elec.*, vol. 54, pp. 7–38; March, 1949.)

551.510.52 2225
The Ionic Equilibrium of the Lower Atmosphere—J. Bricard. (*Jour. Geophys. Res.*, formerly *Terr. Mag. Atmo. Elec.*, vol. 54, pp. pp. 39–52; March, 1949. In French, with English summary.)

551.510.535 2226
Measurement of Sporadic E-Layer Ionization—K. Rawer. (*Nature* (London), vol. 163, pp. 528–529; April 2, 1949.) The critical frequency is insufficient as a measure of sporadic E-layer ionization, because this layer consists of ionized clouds and is not homogeneous. At the Service Ionosphérique de la Marine Française (SPIM) station at Freiburg, the frequencies are observed for which the ratio of the strength of the sporadic-E reflection to the strength of the F-layer reflection has the values 100, 10, 1, 0.1, and 0.01. Results for August, 1948, are shown graphically and discussed.

551.510.535 2227
On Long-Term Forecasts of the Critical Frequencies of the Ionosphere and of the Occurrence of Disturbances in It—G. M. Bartenev. (*Bull. Acad. Sci.* (URSS) pp. 1139–1152; September, 1947. In Russian.)

LOCATION AND AIDS TO NAVIGATION

621.396.9 2228
Spiral-Phase Fields—E. K. Sandeman. (*Wireless Eng.*, vol. 26, pp. 96–105; March, 1949.) The general properties of such fields are examined theoretically. They are produced if four vertical antennas are placed at the corners of a horizontal square of side $<\lambda/4$, and each diagonal pair is driven in antiphase and in quadrature with the other diagonal pair. Three main applications are outlined: (a) an aircraft could obtain its bearing relative to the center of the field, (b) a lighthouse or talking beacon could be operated so that continuous characteristic signals were sent out on various bearings, and (c) narrow interrogating beams could be produced for secondary radar and possibly also for primary radar.

621.396.9 2229
Doppler Radar—E. J. Barlow (Proc. I.R.E., vol. 37, pp. 340–355; April, 1949.) The principle of Doppler radar systems is that a frequency change is produced when radio waves are reflected from moving targets, which can thus be distinguished from stationary ones. The application of this principle to cw systems is described and compared with its use in pulse systems. Quantitative calculations are made of sensitivity, range error, fixed-target rejection, and system stability.

621.396.9:371.3 2230
Aids to Training—The Design of Radar Synthetic Training Devices for the R.A.F.—G. W. A. Dummer. (*Proc. IEE*, part III, vol. 96, pp. 101–112; March, 1949. Discussion, pp. 113–116.) The training devices described are of two main types, a bench trainer of simple design, and a complete crew trainer. The former was required as an aid to the introduction of new radar systems, while the latter provided accurate presentation of moving targets, complete operational practice, and also error-recording facilities.

621.396.9:523.53 2231
A Phenomenological Theory of Radar Echoes from Meteors—McKinley and Millman. (*See* 2213.)

621.396.93 2232
Some Relations between Speed of Indication, Bandwidth, and Signal-to-Random-Noise Ratio in Radio Navigation and Direction Finding—H. Busignies and M. Dishal. (Proc. I.R.E., vol. 37, pp. 478–488; May, 1949.) The total bandwidth required for navigation and direction-finding systems is quite small ($\leq +100$ cps or so), because rates of change of observed phenomena are small and required speeds of indication slow. A small total bandwidth is possible even with a complex waveform provided that a filter can be designed with a number of very narrow pass bands occurring at the steady-state Fourier components of the complex signal. Such a "comb" filter is discussed briefly.

Systems for which the output signal-to-noise ratio is better than the input carrier-to-noise ratio have improvement thresholds, but many navigation systems can give satisfactory information at output signal-to-noise ratios below these thresholds. Single-sideband and double-sideband AM produce the most sensitive systems under such conditions.

The phenomenon of "apparent demodulation" is discussed for systems having the post-detection bandwidth Δf_v narrower than the predetection bandwidth Δf_{IP} and carrier-to-noise ratio appreciably less than unity at the input to the final detector. A relation between the available power, the output signal-to-noise ratio $(S/N)_v$ required for satisfactory indication, the percentage modulation m, Δf_{IP}, and Δf_v is obtained for a double-sideband AM system with a linear final detector; this relation depends markedly on whether the quantity $4(\Delta f_{IP}/\Delta f_v)\ (N/S)_v{}^2m^2$ is greater than or less than unity.

621.396.93 2233
Radio Direction-Finding by the Cyclical Differential Measurement of Phase—C. W. Earp and R. M. Godfrey. (*Elec. Commun.*, vol. 26, pp. 52–75; March, 1949.) Reprint, with minor additions, of 1059 of May.

621.396.93 2234
Rotating H-Adcock Direction Finder—B. G. Pressey. (*Wireless Eng.*, vol. 26, pp. 85–92; March, 1949.) The instrument has a frequency range of 4 to 30 Mc; the antenna system is about 4 feet over-all. Spheres are fixed to the ends of the antennas to increase their effective height and measures are taken to balance the system throughout the frequency range. By splaying the points of connection of the antenna coil to the horizontal feeders, the polarization error is appreciably reduced. The minimum usable field strength varies between 8 and 2.5μvolts per meter. The instrumental error is not greater than $\frac{1}{2}°$ and the polarization error is of the same order as that of a U-type Adcock system.

621.396.932 2235
Marine Navigation Radar—G. Kniazeff. (*Onde Élec.*, vol. 29, pp. 202–215; May, 1949.) Technical requirements are discussed and tests with prototype equipment leading to the design of the RNMII set are described. This set operates at any frequency between 9,000 and 9,550 Mc. Power output is 30 kw, pulse duration 0.3μseconds and repetition frequency 1,000 per second. The beam angle is 1.8° in horizontal and 17° in the vertical direction; the antenna, of the cylindro-parabolic reflector type with horn feed, rotates at about 30 rpm. The receiver has a panoramic display on a 22.5-cm screen. Four range scales are provided, with maxima of 1, 3, 9, and 27 miles respectively, and five circles on the screen facilitate accurate ranging. On the liner *Jean Bart* the performance of the equipment has proved very satisfactory.

621.396.933 2236
System of Air Navigation and Traffic Control Recommended by the Radio Technical Commission for Aeronautics—P. C. Sandretto. (*Elec. Commun.*, vol. 26, pp. 17–27; March, 1949.) An outline of a completely integrated system to be developed and brought into use in the United States over a period of 15 years. The system is designed to meet a number of predetermined operational requirements. The basic techniques required have been developed during the war, but the exact technical character and design parameters of the apparatus required cannot yet be given.

621.396.933.2 2237
Radio Beacons of the Consol Type—H. Portier. (*Onde Élec.*, vol. 29, pp. 57–65; February, 1949.) The basic principles are outlined and the effects of antenna spacing, antenna current and phasing, and signal cycle are discussed and illustrated by data for the transmitter at Bush Mill, N. Ireland. Proposals for new stations in Europe and America are mentioned.

621.396.933.23 2238
Radio Aids for Approach and Landing Control of Aerial Traffic—A. Violet. (*Onde Élec.*, vol. 29, pp. 91–109; March, 1949.) Present facilities are briefly reviewed and the requirements which future systems should satisfy are discussed, with special reference to the recommendations of the American Radio Technical Commission for Aeronautics. The principles and operation of the navar, navaglide, and navascreen systems are also described.

621.396.9 2239
Radar Primer [Book Review]—J. L. Hornung. McGraw-Hill, New York, N. Y., 1948, 210 pp., $3.50. (Proc. I.R.E., vol. 37, p. 543; May, 1949.) A nonmathematical presentation of the fundamental principles upon which the operation of pulsed radar is based. Various practical applications are discussed briefly.

MATERIALS AND SUBSIDIARY TECHNIQUES

531.788 2240
Radiometer Vacuum Gauge of Compensation Type—A. Rostagni and I. Filosofo. (*Nuovo Cim.*, vol. 4, pp. 74–84; February 1, 1947. In Italian, with English summary.) An instrument using two narrow strips of Al foil, one fixed at both ends and carrying a heater current, the other suspended freely from one end a few millimeters away from the first. Deflection of the suspended foil is compensated by rotation of the containing tube about a horizontal axis; the angle of rotation α is approximately proportional to the gas pressure p up to 10^{-2} tor and independent of the nature of the gas (for H_2, He, Ne, Ar, air). Above 10^{-2} tor the (α, p) curves for the different gases diverge; all reach a maximum and then fall off slowly. The useful pressure range is $10^{-1}=10^{-6}$ tor. Sensitivity can be varied widely by adjusting the heater current.

535.5:621.385.832 2241
Modern Vacuum-Pump Design—G. L. Mellen. (*Electronics*, vol. 22, pp. 90–95; May, 1949.) Detailed description of a vapor-type pump for television cathode-ray tubes. Automatic controls are suggested for further improvement of cathode-ray-tube production rates.

535.37 2242
Temperature Quenching of Photoluminescence of Sublimated KI-Tl Phosphors—K. V. Shalimova. (*Zh. Eksp. Teor. Fiz.*, vol. 18, pp. 1045–1048; November, 1948. In Russian.) An experimental investigation of films prepared in air by a simultaneous condensation of KI and metallic Tl on a quartz plate. The quenching process conforms to Mott's theory. The energy of activation U depends on the wavelength of the exciting light and on the concentration of the activator; the higher the concentration, the lower is the value of U. The coefficient indicating the degree of binding of the mixture with the crystalline lattice remains constant, for a given concentration of the ac-

tivator, for all wavelengths of the excitation light, and decreases with increase in the concentration of the activator. See also 230 of 1939 (Mott).

538.213:538.221 2243
High-Frequency Permeability—J. Smidt. (*Appl. Sci. Res.*, vol. B1, no. 2, pp. 127–134; 1948.) Experimental results for the permeability of iron at frequencies between 360 and 580 Mc are discussed.

538.569.3/.4].029.64 2244
High-Frequency Absorption Phenomena in Liquids and Solids—W. Jackson and J. A. Saxton. (*Proc. IEE*, part III, vol. 96, pp. 77–80; March, 1949.) The paper discusses briefly the work on liquid and solid dielectrics carried out in England during the war and immediate post-war periods. The work was concerned mainly with substances of technical importance such as polythene, water, and ice; the results emphasize the limitations of existing theories of dipolar absorption. Summary noted in 366 of March.

620.179.14 2245
Magnetic and Inductive Non-Destructive Testing of Metals—I. R. Robinson. (*Metal Treat.*, vol. 16, no. 57, pp. 12–24; Spring, 1949. Bibliography, p. 24.) Two general methods of testing are discussed: (a) The field set up by eddy currents in a ferrous or nonferrous sample is compared with that due to a standard of the same size and shape; apparatus for testing bar stock by this method is described. (b) The sample is sprayed with ferromagnetic powder whose distribution over the surface of the magnetized material indicates leakage fields and hence flaws. Bridges and crt techniques are considered.

621.3.015.5:546.217 2246
The Electrical Breakdown Strength of Air at Ultra-High Frequencies—J. A. Pim. (*Proc. IEE*, part III, vol. 96, pp. 117–129; March, 1949.) The measurements were made in the frequency range 100 to 300 Mc, using parallel-plate gaps up to 1 mm wide. The apparaus and method of measurement are described and a theoretical analysis of the results is given. See also 3141 of 1948.

621.315.221 2247
Continuous Lead-Extrusion Machine for Electric Cables—(*Engineering* (London), vol. 167, pp. 319–321; April 8, 1949.) Illustrated description of a machine made by the Pirelli-General Cable Works to overcome the difficulties inherent in stroke-type presses operating intermittently.

621.315.61:621.317.37.029.64 2248
Measurements on Dielectric Materials in the Centimetre-Wave Region at High Temperatures—F. Borgnis. (*Helv. Phys. Acta*, vol. 22, pp. 149–154; April 20, 1949. In German.) A cavity resonator constructed of calit, with its inner surface silvered, was used to measure the dielectric constant and loss of rods of various glasses and ceramics at temperatures up to 400°C. The results are tabulated. The loss factor of the ceramics (ergan, calit, frequenta, tempa *S*, condensa *C* and *F*) and of quartz, uviol glass, and supremax glass showed no variations greater than the possible errors of measurement. The loss factor for selected examples of the large number of glasses tested increased 2 to 3 times between room temperature and 350°C.

621.315.616:679.5 2249
Electrical Properties of Plastics—A. J. Warner. (*Elec. Commun.*, vol. 26, pp. 33–39; March, 1949. Discussion, p. 39.) Reprint of 3443 of 1948.

621.316.86 2250
Study of Uranium-Oxide Thermistors—J. Prigent. (*Jour. Phys. Radium*, vol. 10, pp. 58–64; February, 1949.) Methods of preparing UO_2 powder and beads are described and test results are given showing the effect of applied voltage and of temperature on the resistance of the beads. On account of its variability and high resistivity, the use of UO_2 is likely to be limited to bolometer detectors for infrared radiation; for such a purpose it is necessary to use a very thin layer of the oxide.

666.3:621.315.612 2251
Ceramics and their Manufacture—R. A. Ijdens. (*Philips Tech. Rev.*, vol. 10, pp. 205–213; January, 1949.) A survey of the different ceramic materials manufactured at Eindhoven, the methods used in their preparation, and also their applications. The relation between the characteristics of a material and its composition is discussed, with particular reference to the ternary system MgO-Al_2O_3-SiO_2.

669.718:534.321.9.001.8 2252
Supersonic Tinning of Aluminum Wires—(*Machinery* (London), vol. 74, pp. 546–547; April 28, 1949.) Discussion of apparatus for making soldered joints without using flux. A Ni striker is immersed beneath the surface of molten solder in an electrically heated crucible. The striker is made to oscillate at about 18 kc. The wire to be tinned is held by hand near or touching the striker, and becomes tinned over the short length immersed in a few seconds. For full details see B.I.O.S. Report No. 1844 (2253 below).

621.791 2253
Some Aspects of German Soldering, Brazing and Welding Methods [Book Notice]—B.I.O.S. Final Report No. 1844. H. M. Stationery Office, London, 66 pp., 7s. A collection of miscellaneous data on metal joining processes, including the ultrasonic tinning of Al referred to in 2252 above.

MATHEMATICS

517.5 2254
Remarks on the Harmonic Analysis of Aleatory Functions—A. Blanc-Lapierre. (*Rev. Sci.* (Paris), vol. 85, pp. 1027–1040; November 1 to 15, 1947.) Aleatory functions of the second kind are defined and the method of filters is applied to their analysis. See also 1666 of 1948 (Blanc-Lapierre and Fortet).

517.512.2:578.088.7 2255
Fourier Analysis in Relation to the Electrocardiogram—W. E. Benham. (*Jour. Brit. I.R.E.*, vol. 9, pp. 170–183; May, 1949.)

517.93:53 2256
Non-Linear Vibrations—M. L. Cartwright. (*Advanc. Sci.*, vol. 6, pp. 64–69; April, 1949. Bibliography, pp. 69–74.) Discussion of (a) general methods of solving nonlinear differential equations, including methods involving differential analyzers, (b) special types of second-order equation, (c) difficulties of formulating the equation for a physical problem, (d) standards of rigor, (e) subharmonics, (f) relaxation oscillations, (g) numerical and graphical solutions, (h) topological methods, and (i) miscellaneous recent work. The bibliography is arranged according to the above sections, which are mainly a commentary upon it. See also 156 of 1948 (Minorsky).

518.5 2257
Electronic Digital Counters—W. H. Bliss. (*Elec. Eng.*, vol. 68, pp. 309–314; April, 1949.) Discussion of a circuit consisting of a binary chain of four multivibrators, with modifications that convert it to a decade system. The associated switching circuit is also considered. Various applications are mentioned.

518.5:621.385.832 2258
A Storage System for Use with Binary-Digital Computing Machines—F. C. Williams and T. Kilburn. (*Proc. IEE* part II, vol. 96, pp. 183–200; April, 1949. Discussion, pp. 200–202. Also published *ibid.*, part III, vol. 96, pp. 81–98, March, 1949. Discussion, pp. 98–100.) Full paper; summary abstracted in 1110 of May.

MEASUREMENTS AND TEST GEAR

531.763 2259
An Electronic Stopclock—K. J. Brimley. (*Electronic Eng.* (London), vol. 21, pp. 180–183; May, 1949.) Fundamentally, the arrangement is a high-speed mechanical counter in which a Scophony torque motor Type BTM is used, together with two thyratron inverters. This combination counts the quarter-cycles of a standard oscillator within the interval defined by the operation of two trigger circuits. Full circuit details are included, and the principle of the motor drive is explained.

621.3.018.41(083.74) 2260
Some Electromechanical Methods for Producing Low Frequencies from a Primary Frequency Standard—D. W. R. McKinley. (*Canad. Jour. Res.*, vol. 27, sec. F, pp. 49–54; February, 1949.) The primary-standard crystal frequency of 50 kc is divided by the conventional chain of multivibrators to 10 kc, 1 kc, 100 cps, and 10 cps. At the 1-kc stage, power is supplied to a 1-kc phonic clock motor, one shaft of which rotates at 10 rps and carries sector disks or needle disks whose elements generate pulses in the winding of an electromagnet as they pass between its poles. These pulses are used as gate pulses to select pulses of higher timing precision at the desired repetition rate.

621.317.32+621.317.34]:621.396.11 2261
A Simple Method of Measuring Electrical Earth-Constants—E. W. B. Gill. (*Proc. IEE*, part III, vol. 96, pp. 141–144; March, 1949.) An incoming ground-wave is received in succession on two short sloping antennas of equal length, one in the vertical plane α containing the transmitter and the other in a vertical plane at right angles to α. The eccentricity of the ground-wave ellipse, and hence the earth constants, are calculated from the antenna slopes when the slopes are adjusted for equal signal amplitudes. Some measurements for S. England are tabulated.

621.317.323(083.74) 2262
A Primary High-Frequency Voltage Standard—(*Tech. Bull. Nat. Bur. Stand.*, vol. 33, pp. 43–44; April, 1949.) A thermistor bridge, using very small thermistors of diameter only 0.015 inch, has been developed for measurements from 20 mvolts to 1.5 volts at all frequencies from af to 800 Mc. Careful design of a special mount for a 2-thermistor arrangement eliminated the need for frequency corrections and reduced the time required to balance the bridge. Up to 200 Mc measurements by means of a cro, thermoelement, or electrostatic voltmeter agreed with the bridge measurements to within 1 per cent. Above 200 Mc the accuracy of available data is limited by inadequate precision of the slotted transmission lines used for power measurement. Up to 50 Mc the voltage range was extended to 10 volts by use of thermistor beads of considerably larger diameter.

621.317.336:621.314.2 2263
Measurement of Transformer Impedance using Low-Current Bridge Techniques—K. Goldsmith. (*Elec. Times*, vol. 115, pp. 522–526; April 21, 1949.) Bridge methods have definite advantages, but if carried out at the usual frequency of 1,000 cps the results obtained may differ so greatly from those which would be obtained at the 50-cps operating frequency that they would give an entirely wrong idea of the transformer performance. Bridge measurements should, therefore, be carried out at the normal operating frequency, using a vibration galvanometer or other suitable detector.

621.317.34 2264

Transmission-Line Impedance Measurement—R. J. Lees, C. H. Westcott and F. Kay. (*Wireless Eng.*, vol. 26, pp. 78–84; March, 1949.) Balance-to-unbalance devices are discussed briefly. Early impedance measurements, carried out by observation of the detuning and damping of *LC* circuits, had an upper frequency limit of about 200 Mc. Measurements at somewhat higher frequencies were made on balanced lines by a standing-wave method. The voltage distribution was measured by means of a thermocouple at the end of a $\lambda/4$ stub. For the range 500 to 600 Mc, a special measuring section was designed, consisting of a length of line of similar dimensions to the feeder, but with a slot along which the measuring stub could slide. A capacitance was used instead of a shorting bar. Experimental results discussed include admittance measurements on various slots.

621.317.35 2265

The Optimum Performance of a Wave Analyser—N. F. Barber. (*Electronic Eng.* (London), vol. 21, pp. 175–179; May, 1949).

621.317.372 2266

***Q* Measurements—Two- and Four-Terminal Networks**—M. C. Pease. (Proc. I.R.E., vol. 37, pp. 573–577; May, 1949.) Formulas are derived for calculating the resonance frequency and *Q* values of simple shunt-resonant networks from measurements of voltage SWR at three frequencies. If these frequencies are suitably chosen, the formulas are greatly simplified. They are general and exact within the range for which the equivalent circuits are valid with due regard to loss. For two-terminal networks, an ambiguity exists which can be resolved only with simple phase data, but in practice, the correct solution is usually obvious.

621.317.372 2267

***Q*-Meter Controversy**—P. H.: H. G. M. S.: V. A. Sheridan. (*Wireless World*, vol. 55, pp. 216–218; June, 1949.) Comment on 1121 of May (Spratt).

621.317.7+621.38+621.396.69 2268

Physical Society's Exhibition—(*See* 2199.)

621.317.71:621.385 2269

Electrometer Tubes for the Measurement of Small Currents—Victoreen. (*See* 2376.)

621.317.73:621.396.67:629.135 2270

Measurement of Aerial Impedances in Aircraft—P. Durand. (*Onde Élec.*, vol. 29, pp. 73–78; February, 1949.) A coaxial cable of characteristic impedance 55 Ω and length 25 meters is coiled round a drum of circumference 1 meter. The polythene insulation is pierced at intervals of 10 cm to admit the probe of a high-impedance tube voltmeter; this instrument has a recording milliammeter in its cathode circuit. The standing waves along the cable, terminated by the antenna impedance to be measured, are shown by the voltages obtained by insertion of the probe successively in each of the holes, to make contact with the central conductor. A 150-watt generator covering the range 300 kc to 30 Mc is used. The resistive and reactive components of the impedance are determined from the reflection coefficient by means of Smith circle diagrams. An example shows the results obtained on an 8-meter antenna in a Junkers-52 aircraft.

621.317.733 2271

Pulse Excitation of Impedance Bridges—J. G. Yates. (*Nature* (London,) vol. 163, p. 132; January 22, 1949.) Measurements can be made in many practical cases with rectangular pulses of duration 1 to 10μseconds and of suitable recurrence frequency; sinusoidal excitation would require frequencies as low as 150 cps, under similar conditions, to make the quadrature component in the bridge output negligible. A number of bridges can be excited in sequence by pulses and their output applied to a common amplifier. Pulse excitation can be used for capacitance as well as resistance bridges.

621.317.761 2272

A Compact Direct-Reading Audio-Frequency Meter—A.A.McK. (*Electronics*, vol 22, pp. 108–109; April, 1949.) A cascade amplifier is followed by a squaring amplifier, the output from which is differentiated; the resultant pips are used to trigger a blocking oscillator. The integrated space current in the final triode driven by the positive half of the oscillation is read by a microammeter and is proportional to the frequency. Maximum readings of the three scales are 1,000, 5,000, and 10,000 cps.

621.317.761.029.56/.58 2273

The Additive Frequency Meter—G. Grammer. (*QST*, vol. 33, pp. 32–37; May, 1949.) A suitable harmonic of a 100 kc crystal oscillator is fed to a mixer, together with the output of a variable-frequency oscillator covering a 50-kc range. The sidebands so generated supply a series of signals that can be used like the signal from an ordinary heterodyne meter. Dial errors are only of the order of 50 cps and are independent of the frequency being measured. Errors due to instability of the variable-frequency oscillator are also small. Errors due to instability of the variable frequency oscillator are also small. Measurements can be made in any part of the spectrum where 100-kc harmonics can be heard. A similar principle has been used at the National Bureau of Standards for uhf measurements.

621.317.784.088 2274

Some Sources of Error in Microwave Milliwattmeters—G. F. Gainsborough. (*Proc. IEE*, part III, vol. 96, p. 130; March, 1949.) Discussion on 3466 of 1948.

621.317.79:621.396.615:621.396.619.11 2275

Low-Distortion A.M. Signal Generator—E. S. Sampson. (*Electronics*, vol. 22, pp. 118–120; April, 1949.) The outputs of an af amplifier and a rf oscillator are combined in a modulator to produce a signal with 75 per cent modulation. By adding an out-of-phase component of the carrier signal through a cancellation amplifier, a signal is obtained with an effective modulation of 100 per cent. Negative feedback is used in both the af amplifier and the modulator, and an exalted-carrier detector is used in an over-all feedback circuit.

621.317.79:621.396.822 2276

Atmospheric Noise Measurement—H. Reiche. (*Electronics*, vol. 22, pp. 110–113; April, 1949.) A description of equipment for continuous measurement of noise levels down to 0.3 μvolts per meter over the frequency range 75 kc to 30 Mc. Three remotely situated wide-band preamplifiers, each covering about 10 Mc of the frequency range, have antennas attached and feed six receivers through coaxial cables. Each receiver is sampled in turn and the noise is recorded. The design of the first stage of the preamplifiers to give a low noise figure is discussed.

621.317.79:621.396.9.089.6 2277

Radar Range Calibrator—R. L. Rod. (*Electronics*, vol. 22, pp. 114–117; April, 1949.) Design of an instrument for production calibration of the concentric rings used for estimating distance with a PPI. Range ring pulses generated in the radar are compared on a triggered cro with spaced pulses from a crystal-controlled calibrator.

621.396.645 2278

Stabilized Decade-Gain Isolation Amplifier—(*See* 2190.)

621.396.69.001.4(083.75) 2279

Climatic and Durability Tests for Radio Components—(*Engineer* (London), vol. 187, p. 393; April 8, 1949.) Brief details of specification No. RIC/11, obtainable (price 1s.) from the Radio Industry Council, 59, Russell Square, London, W.C.1. It covers approximately the same ground as the Inter Services Specification No. RCS/11.

621.317.755 2280

Elektronenstrahloszillographen (Electron-Beam Oscillographs.) [Book Review]—P. E. Klein. Weidmannsche Verlagsbuchhandlung, Frankfurt am Main, 210 pp., 19 DM. (*Wireless Eng.*, vol. 26, p. 107, March, 1949.) Describes the tube itself and the auxiliary devices necessary for the practical application of cro methods of measurement; the applications themselves will be discussed in a second volume to appear later. Recommended for anyone wishing to study German cro development.

OTHER APPLICATIONS OF RADIO AND ELECTRONICS

534.321.9.001.8 2281

New British Ultrasonic Generator—(*Electronic Eng.* (London), vol. 21, pp. 154, 161, May, 1949.) Designed as a laboratory tool for research workers in industry. A rf output of 1 kw is generated directly by a silica triode. Interchangeable coil assemblies are provided for operation at frequencies around ¼, ½, 1, and 2 Mc. The quartz crystal oscillator can safely be immersed in liquids at temperatures up to 150°C.

538.569.2.047:621.315.61.011.5 2282

Dielectric Properties of the Human Body in the Microwave Region of the Spectrum—T. S. England and N. A. Sharples. (*Nature* (London), vol. 163, pp. 487–488; March 26, 1949.) Homogeneous specimens were inserted in a waveguide cell between a metal plunger and a plug of polystyrene. Measured values of the absorption coefficient and phase constant for various body substances are tabulated and discussed.

538.569.2.047:621.38.001.8 2283

Investigations on the Biological Effects of Microwaves in view of their Therapeutic Application—L. de Séguin, G. Castelain, and M. Pelletier. (*Rev. Sci.* (Paris), vol. 86, pp. 335–344; April 1, 1948.) Experiments are described which show that microwaves can modify, and even stimulate, certain biological processes. They provide a convenient and precise means for the therapeutic application of heat.

538.569.2.047:621.38.001.8 2284

Exposure [of animals] to Microwaves—W. W. Salisbury, J. W. Clark, and H. M. Hines. (*Electronics*, vol. 22, pp. 66–67; May, 1949.) Experiments to find the effect of high-intensity 12-cm radiation on rabbits are briefly described. An intensity greater than 3 watts per cm² can cause damage to certain tissues, such as those of the eye, without accompanying pain. The most vulnerable parts of the body are those not abundantly supplied with blood.

539.16.08 2285

Laboratory Pulse Counter—L. E. Greenlee. (*Radio News, Radio-Electronic Eng. Supplement*, vol. 10, pp. 6–8, 31; June, 1948.) Design and construction of an experimental radiation counter for rates up to 600 pulses per minute.

620.179.16 2286

Location of Internal Defects by Supersonics—J. W. Dice. (*Instruments*, vol. 19, pp. 718–722; December, 1946.) An account of the Sperry ultrasonic reflectoscope, which provides (a) square waves of frequency continuously variable from 5 to 130 kc, serving as a distance marker, and (b) 1,000-volt pulses of recurrence frequency variable from 0.5 to 12 Mc and of duration 1μsecond or more, which are applied to the crystal search unit and thence to the test piece through a film of oil. Illustrations are given of the pulse echoes seen on the screen of the associated cro in the case of cracks or similar defects in the material under investigation.

621.365.5:621.396.611.3 2287
On Circuits with Electromagnetic Coupling and their Application in H. F. Induction-Heating Equipment—(*See* 2174.)

621.365.92.029.64 2288
Some Possibilities of Heating by Centimetric Power—R. Keitley. (*Jour. Brit. IRE* vol. 9, pp. 97–121; March, 1949.) Discussion of basic principles, range of applications, and methods suitable for frequencies above 500 Mc, for which the linear dimensions of the system and load are large compared to λ. Stationary-wave patterns in the load, methods of preventing consequent nonuniform heating, and methods of avoiding or automatically correcting mismatch due to reflected waves which reach the generator are considered in detail. Methods of localizing the dissipation of high-frequency power are analyzed; three basic systems—resonator, beam, and transmission-line—are distinguished. Typical arrangements for heating thin films, threads or strips, and bulky objects are shown.

621.38 2289
Electronic Apparatus—Schaffernicht; Knoll Schwartz; Rukop—(*See* 2368.)

621.38.001.8 2290
Electronic Classifying, Cataloging, and Counting Systems—J. H. Parsons. (PROC. I.R.E., vol. 37, pp. 564–568; May, 1949.)

621.384.611.1† 2291
The Betatron—J. Dosse. (*Rev. Sci.* (Paris), vol. 86, pp. 357–367; April 1, 1948. Bibliography, pp. 367–368.) Discussion of basic principles, orbital stability, electron injection and extraction, effects of eddy currents in the magnet material, and practical examples. Mathematical theory is given in five appendices.

621.385.833 2292
Distortion-Free Electrostatic Lenses—T. Mulvey and L. Jacob. (*Nature* (London), vol. 163, pp. 525–526; April 2, 1949.) Distortion in symmetrical electrostatic lenses of the 3-aperture type is eliminated by a suitable choice of the thickness of the central electrode.

621.385.833:535.371.07 2293
A New Fluorescent Screen for the Electron Microscope—K. B. Merling. (*Nature* (London), vol. 163, pp. 541–542; April 2, 1949.) Discussion of a screen made of Ag-activated Zn/Cd sulphide, which is much brighter than the conventional willemite screen.

621.385.833:535.61-15:621.383 2294
Electron-Optics of the Image Converter—W. Veith. (*Rev. Sci.* (Paris), vol. 86, pp. 67–76; January 15, 1948.) The question of electrostatic focusing in the image converter is discussed, different practical methods of effecting it are compared and optimum conditions for plane focusing without distortion are stated. A description of a corrected electrostatic lens is also given.

621.38.001.8 2295
Applied Electronics [Book Review] D. H. Thomas. Blackie and Son, London, 132 pp., 7s. 6d. (*Beama Jour.*, vol. 56, p. 96; March, 1949.) Based on a course of lectures to students in the final year of the Higher National Certificate course.

621.38.001.8 2296
Elementary Industrial Electronics [Book Review]—W. R. Wellman. Macmillan, London, 371 pp., 22s. (*Beama Jour.*, vol. 56, pp. 96 97; March, 1949.) For the beginner rather than the advanced student or engineer. ". . . . [the book] is admirably suited to those with an interest in electronics and its applications but who possess little mathematical and technical knowledge."

621.38.001.8 2297
Techniques in Experimental Electronics [Book Review]—C. H. Bachman. J. Wiley and Sons, New York, 243 pp., $3.50. (PROC. I.R.E., vol. 37, p. 542; May, 1949.) Concentrates on the conduction of electricity in a moderately high vacuum. " . . .the inclusion of many simple but pertinent details is the very feature that should make this book most valuable."

PROPAGATION OF WAVES

538.566 2298
On an Important Formula in the Theory of the Propagation of Radio Waves—M. I. Ponomarev. (*Bull. Acad. Sci.* (URSS) pp. 1191–1192; September, 1947. In Russian.) It is claimed that M. V. Shuleikin proposed in 1923 a formula for the current in a receiving antenna similar to that of van der Pol (1930 Abstracts, *Wireless Eng.*, pp. 560–561 and 1931 Abstracts, *Wireless Eng.*, p. 375).

621.396.11 2299
A New Solution to the Problem of Vertical Angle-of-Arrival of Radio Waves—E. W. Hamlin, P. A. Seay, and W. E. Gordon. (*Jour. Appl. Phys.*, vol. 20, pp. 248–251; March, 1949.) A practical mathematical solution of the case of a signal consisting of direct and reflected waves arriving from different directions. The measurement of the amplitudes and relative phase of the field at three equally spaced positions in a vertical line gives sufficient information to enable the angle of arrival and intensity of each wave to be calculated. The formulas are applied to 3-cm transmissions over a 27-mile desert path in Arizona.

621.396.11:551.510.52 2300
Radar Reflections in the Lower Atmosphere—A. B. Crawford. (PROC. I.R.E., vol. 37, pp. 404–405; April, 1949.) Simultaneous radar and visual observations suggest that "angels" are due to echoes from flying insects and birds. For other views, see 2769 of 1947 (Friis), 722 of 1948 (Gould), and 1761 of July (Gordon).

621.396.11:551.510.535 2301
Ionospheric Absorption and the Calculation of Fields at a Distance—A. Haubert. (*Onde Élec.*, vol. 29, pp. 152–159 and 216–226; April and May, 1949.) A review of the theories and experimental results of many authors, aiming at the presentation of the principal conclusions and results as a concise whole. Semi-empirical methods of calculating the minimum usable frequency for a given link and a given time of day, or, for a given fréquency, the received field as a function of distance and time, will be considered in a subsequent paper.

621.396.11:[621.317.32+621.317.34 2302
A Simple Method of Measuring Electrical Earth-Constants—(*See* 2261.)

621.396.812 2303
Propagation of V.H.F. Electromagnetic Waves over the Sea—G. de Burlet. (*HF* (Brussels), no. 2, pp. 53–60; 1949. In French.) The general conditions for the propagation of very short waves are reviewed and a formula is established for the decrease of field strength E with distance d, taking account of refraction and of the plane of polarization. Curves are given showing the dependence of E on d for waves of frequency from 40 to 300 Mc, polarized vertically or horizontally and extending beyond the electromagnetic horizon. Charts are also given showing the values of E which can be expected over the North Sea at distances up to 150 km from a 1-kw transmitter at Ostende, operating on a frequency of either 43 or 75 Mc. Practical suggestions are made regarding optimum frequency, choice of antenna and plane of polarization, and power requirements.

621.396.812 2304
Calculation of Ground-Wave Field Strength over a Composite Land and Sea Path—H. L. Kirke. (PROC. I.R.E., vol. 37, pp. 489–496; May, 1949.) Three possible methods are discussed—those of P. P. Eckersley (1930 Abstracts, *Wireless Eng.*, p. 621), Somerville, and Millington (1753 of July and 2307 below). The methods are applied to paths between Start Point (Devon) and two points in Norfolk, and to a path in Denmark. Theoretical results obtained are compared with observations on these paths. The Eckersley method agrees less well with observation than the other two. The Somerville method is the simplest and is probably adequate for rough calculations where the conductivity data are of doubtful accuracy. The Millington method has the best theoretical justification. The differences between the three methods are small at low frequency and when the effect of the land-sea discontinuity is not large, but no one empirical method can be regarded as established for all conditions.

621.396.812:551.510.535 2305
The Absorption of Short Radio Waves in the Ionosphere and the Electric Field Intensity at the Point of Reception—A. N. Kazantsev. (*Bull. Acad. Sci.* (URSS) pp. 1107–1136; September, 1947. In Russian.) The structure of the ionosphere and the chief properties of its various layers are considered. The absorption of radio waves by these layers is discussed and curves showing their coefficients of absorption are given. Methods are indicated for calculating the received field intensity and for determining the maximum and minimum operating frequency. The discussion is illustrated by numerous experimental curves. The need for further investigations, especially in the polar regions, is emphasized.

621.396.812:621.396.97:551.524.3 2306
Temperature Variations of Ground-Wave Signal Intensity at Standard Broadcast Frequencies—F. R. Gracely. (PROC. I.R.E., vol. 37, pp. 360–363; April, 1949.) Measurements over six paths of lengths from 76 to 558 miles at frequencies from 640 to 1,170 kc show that variations of ground-wave signal intensity appear to be more closely related to changes in temperature than to changes in any other single commonly observed meteorological quantity. The main conclusions are that there is a marked decrease in the intensity at the higher temperatures and that this decrease is approximately proportional to the path length in wavelengths. See also 2308 below.

621.396.812.029.62 2307
Ground-Wave Propagation Across a Land/Sea Boundary—G. Millington. (*Nature* (London), vol. 163, p. 128; January 22, 1949.) A 77.575-Mc 10-watt transmitter-receiver was situated at sea level about 1.4 km south of the Blackwater, Essex. A similar transmitter-receiver was moved toward the shore, across the Blackwater (a 2.2-km sea path) and beyond the opposite shore. Field-strength readings taken at intervals confirm the marked rise of field strength expected theoretically under certain conditions at a land-sea boundary. See also 1753 of July and 2304 above.

621.396.812.3 2308
Tropospheric Propagation on Lower Radio Frequencies—D. W. Heightman. (*Nature* (London), vol. 163, pp. 527–528; April 2, 1949.) Tropospheric effects should not be ignored even at frequencies below 1 Mc. Signal-strength measurements at 59 Mc, 3.58 Mc, 877 kc, 668 kc, and 804 kc are shown graphically and correlated with the greatest change in relative humidity per 50-mb step of the corresponding Larkhill balloon soundings and the height of this change. Comparable ionospheric sounding records did not account for the variations noted.

RECEPTION

621.396.621 2309
Superregeneration—An Analysis of the Linear Mode—H. A. Glucksman. (PROC. I.R.E. vol. 37, pp. 500–504; May, 1949.) The effect of a sinusoidally varying damping factor on the behavior of a tuned circuit is considered. The

amplitude and frequency of this variation are the fundamental parameters distinguishing the superregenerator from the ordinary resonant circuit. Sensitivity and selectivity are considered as functions of these parameters. Multiple resonance and other circuit properties are deduced from the solution of the differential equation. See also 3501 of 1948 (Macfarlane and Whitehead).

621.396.621 2310

G.E.C. Model BRT400—(*Wireless World*, vol. 55, pp. 171–174; May, 1949.) An 11-tube superheterodyne receiver with an integral ac supply unit which can operate from mains voltages between 95 and 130 volts or 195 and 250 volts at 40 to 80 cps. Frequency coverage is 150 to 350 kc and 550 kc to 33 Mc in six switched ranges. Six alternative bandwidths between 0.5 kc and 9 kc are provided.

621.396.621:621.396.619.13 2311

The Response of Frequency Discriminators to Pulses—E. F. Grant. (Proc. I.R.E., vol. 37, pp. 387–392; April, 1949.) The time response of a simple shunt resonant circuit is analyzed, and the results are applied to the behavior of the Round-Travis and Foster-Seeley frequency discriminators. The condition for the discriminator to have only one crossover frequency in the desired frequency band is derived.

621.396.621.53+621.396.645 2312

Increase of Sensitivity of Amplifier and Mixer Stages for Metre and Decimetre Waves—M. J. O. Strutt. (*Bull. Schweiz. Electrotech. Ver.*, vol. 38, pp. 363–371; June 28, 1947. In German, with French summary.) Formulas for the maximum power amplification are derived for narrow and for wide frequency bands in the decimeter-wave range. Theory relative to interference factors is developed and three rules are given whose application enables such factors to be reduced considerably and in ideal cases even eliminated. Practical application of these rules to grounded-grid amplifier stages and to multigrid mixers results in a reduction of the noise factor of about 15 db.

621.396.622+621.314.6 2313

Rectification—Möller; Seiler; Sachse—(*See* 2330.)

621.396.822:621.396.619.16 2314

Noise-Suppression Characteristics of Pulse-Time Modulation—S. Moskowitz and D. D. Grieg. (*Elec. Commun.*, vol. 26, pp. 46–51; March, 1949.) Reprint of 2607 of 1948.

621.396.822:621.396.621 2315

Noise Figures for Receiver Input Circuits—P. G. Sulzer. (*Tele-Tech*, vol. 8, pp. 40–42, 57; May, 1949.) The following six circuits are compared from the noise standpoint and suggestions for the proper application of each are made (a) single-ended grounded-cathode amplifier, (b) push-pull grounded-cathode amplifier, (c) cathode-follower circuit, (d) grounded-grid amplifier, (e) cathode-coupled amplifier, and (f) Wallman circuit. Circuits (a), (b), (c), (d), and (f) all have essentially the same noise figure with modern high-μ tubes. The cathode-coupled amplifier is definitely inferior to the other circuits. The choice of the best circuit for a given application depends largely upon whether a pentode or a triode tube is to be used. The pentode type of circuit is satisfactory for low-frequency narrow-band applications, but triode circuits are usually preferable for high-frequency wide-band receivers.

621.396.828 2316

Suppression of Electrical Interference to High-Frequency Apparatus in Naval Vessels—A. Hunter. (*Proc. IEE*, part III, vol. 96, pp. 159–165; March, 1949.) Screening and bonding, and internal and external suppression are considered for the range 10 kc to 150 Mc. Details and performance of π-type filter boxes with air or dust-core chokes rated up to 150 amperes at 220 volts are given. Vhf ignition suppressors of the capacitor type and lead-through bushing capacitors are described. The use of π-networks in the internal brushgear leads of machines is advocated if shunt capacitance is inadequate.

621.396.621.004.67 2317

Most-Often-Needed 1949 Radio Diagrams and Servicing Information [Book Review]—M. N. Beitman. Supreme Publications, Chicago, 1949, 160 pp., $2.50. (Proc. I.R.E. vol. 37, p. 418; April, 1949.) Continuation of 256 of 1948. Diagrams and repair data for 1949 radio sets made by 39 different manufacturers are included.

STATIONS AND COMMUNICATION SYSTEMS

621.39 2318

Telegraphy Service during the 5th Olympic Winter Sports, St Moritz, 30th January 8th February 1948—H. Wyss. (*Tech. Mitt. Schweiz. Telegr.-Teleph. Verw*, vol. 26, pp. 255–258; December 1, 1948. In German.) A short account of the general arrangements and special services, including Telex teletype and picture transmission facilities. See also 3243 of 1948 (Wettstein).

621.39.001.11 2319

Theoretical Limitations on the Rate of Transmission of Information—W. G. Tuller. (Proc. I.R.E., vol. 37, pp. 468–478; May, 1949.) A theory is developed which takes account of first-order noise effects. The transmission of a quantity of information H over a given circuit is governed by the relation

$$H \leq 2BT \log (1+C/N)$$

where B is the transmission-link bandwidth, T the time of transmission, and C/N the carrier-to-noise ratio. For large signal-to-noise ratios S/N, this formula leads to $S/N \leq (C/N)^{B/f}$, f being the channel bandwidth. Coded transmission is capable of realizing the fullest capabilities of the general system, but in uncoded transmission $S/N \leq (C/N) \times (B/f)$. The inefficiency of existing communication systems is discussed. The advantages to be gained by the removal of internal message correlations and by analysis of the information content of a message are mentioned. The theory is applied to radar relays, telemeters, voice communication systems, servomechanisms, computers, etc. See also 1057 of 1947 (Gabor) and 1649 of July (Shannon).

621.39.001.11 2320

Communication Theory—T. Roddam. (*Wireless World*, vol. 55, pp. 162–164; May, 1949.) An elementary discussion of the validity of the Hartley law and of absolute criteria of performance for the transmission of coded messages in noise.

621.39.001.11 2321

A Note on the Theory of Communication—J. D. Weston. (*Phil. Mag.*, vol. 40, pp. 449–453; April, 1949.) A basis for a general quantitative theory is suggested. A coded message is represented as a vector in a space of an infinite number of dimensions; the process of transmission over an ideal signaling system is equivalent to a projection of this vector on to a sub-space. A message will be accurately transmitted if, and only if, it is coded so that its associated vector lies entirely in the sub-space characterizing the signaling system.

621.395.34:621.385.032.212 2322

Application of Gas-Filled Tubes for Storage and Sending—F. H. Bray, D. C. Ridler, and W. A. G. Walsh. (*Elec. Commun.*, vol. 26, pp. 28–32; March, 1949.)

621.395.365.3 2323

Automatic Change-Over to an Emergency Apparatus in a Communication System—G. Hepp. (*Philips Tech. Rev.*, vol. 8, pp. 310–314; October, 1946.) Two methods for automatic change-over to an emergency oscillator when the output signal falls below a certain amplitude are discussed. Where low-frequency amplifiers are involved, a constant auxiliary signal outside the band of the signal to be amplified is added; this auxiliary signal brings about the change-over to the emergency amplifier.

621.396.619.16 2324

Pulse Communication Systems—S. Van Mierlo. (*HF* (Brussels), nos. 1 and 2, pp. 16–25 and 45–51; 1949. In French.) The principal pulse-amplitude, pulse-position, and pulse-code systems are reviewed and discussed with particular reference to bandwidth and signal-to-noise ratio. Different types of distributors, modulators, and demodulators are mentioned; two pulse-position systems and two commercial equipments are also discussed.

621.396.619.16 2325

Signal-to-Noise-Ratio Improvement in a P.C.M. System—A. G. Clavier, P. F. Panter, and W. Dite. (Proc. I.R.E., vol. 37, pp. 355–359; April, 1949.) The output signal-to-noise power ratio (expressed in decibels) is approximately twice the corresponding input ratio, and is independent of the number of code digits provided this is large enough. The distortion due to quantization varies greatly with the number of code digits. A relation is found showing the number of digits for which the output noise power is equal to the distortion power for a given input signal-to-noise ratio.

621.396.65 2326

Directional Transmission Investigations in the Alps—W. Klein. (*Tech. Mitt. Schweiz. Telegr.-Teleph. Verw.*, vol. 27, pp. 49–69; April 1, 1949 In German.) A detailed account of experiments carried out between Monte Generoso at the southern end of Lake Lugano, and the Jungfraujoch, using wavelengths of 15 cm and 2 meters, and with 90-cm equipment linking Chasseral, Jungfraujoch, Monte Generoso, and Lugano Central. For many of the tests, relay stations on the NE ridge of the Jungfrau, or on neighboring peaks, were used to provide line-of-sight paths between stations. Power for the relay stations was supplied by means of rubber-insulated cables connected to a point on the nearest available ac network. The equipment used and its installation are described and the results of field-strength measurements for the various links are tabulated and discussed. Typical field strength records are reproduced. The results show that a multichannel telephony system with stations on the Jungfraujoch and Monte Generoso is quite practicable. A possible system of line-of-sight links connecting all the north of Switzerland with the south via the Jungfraujoch is illustrated and discussed.

621.396.931 2327

Radio-Telephony at Whitemoor Marshalling Yard—(*Engineer* (London), vol. 187, pp. 326 327; March 25, 1949. *Engineering* (London), vol. 167, p. 306; April 1, 1949.) A two-way 85.425-Mc system having a fixed 12-watt transmitter-receiver station in the control tower and a remote control unit in the foreman's cabin, and mobile 12-watt transmitter-receiver units in the engine cabs, where 12-volt batteries are fitted.

621.396.97 2328

Broadcasting at the 5th Olympic Winter Sports, St Moritz—F. Dupuis. (*Tech. Mitt. Schweiz. Telegr.-Teleph. Verw.*, vol. 26, pp. 258–263; December 1, 1948. In French.) Details of the arrangements for Switzerland and also of the international connections with many European countries and with the United States. Altogether 359 transmissions were arranged, 116 in Switzerland and the remainder abroad, the total duration of the transmissions being 273 hours. See also 3243 of 1948 (Wettstein).

SUBSIDIARY APPARATUS

621.526:061.3 2329
I.E.E. Convention on Automatic Regulators and Servomechanisms—(*Jour. IEE*, part IIA, vol. 94, nos. 1 and 2; 1947.) These two issues contain the full text of all the papers mentioned in 4039 of 1947 and 829 of 1948, together with the following papers:—A Method of Analysing the Behaviour of Linear Systems in Terms of Time Series, by A. Tustin. The Effects of Backlash and of Speed-Dependent Friction on the Stability of Closed-Cycle Control Systems, by A. Tustin. A Method of Analysing the Effect of Certain Kinds of Non-Linearity in Closed-Cycle Control Systems, by A. Tustin. Hydraulic Remote Position-Controllers, by J. E. M. Coombes. Electrical Remote Position-Indicating Systems as Applied to Aircraft, by R. J. Garvey. Method of Testing Small Servo Mechanisms and Data-Transmission Systems, by E. W. Marchant and A. C. Robb. Some Characteristics of a Human Operator, by J. A. V. Bates.

621.314.6+621.396.622 2330
Rectification—H. G. Möller; K. Seiler; H. Sachse. (*FIAT Review of German Science 1939–1946. Electronics, incl. Fundamental Emission Phenomena*, part 1, pp. 259–295; 1948. In German.)

Part 1, by Möller, discusses tube rectification and heterodyne reception, with particular reference to Döhler's method of rectification (see 4383 of 1939) and also rectification and reception by means of Barkhausen oscillations.

Part 2, by Seiler, on detectors, outlines the Schottky theory of blocking-layer and point rectifiers and describes the synthesis and properties of sensitive, low-resistance detector materials and also the construction of the Telefunken detector Type ED705.

Part 3, by Sachse, briefly reviews work on oxide rectifiers for high frequency.

621.316.7 2331
Application of the Method of Logarithmic Frequency Characteristics to the Investigation of the Stability of Monitoring and Regulating Systems and to the Estimation of their Efficiency—V. V. Solodovnikov. (*Avtomatika i Telemekhanika*, vol. 9, pp. 85–103; March and April, 1948. In Russian.)

621.316.72 2332
Carrier Communication Level Regulator—W. S. Chaskin. (*Electronics*, vol. 22, pp. 104–107; April, 1949.) For correcting twist and maintaining the signal level constant within 2 db for 3-channel carrier telegraphy or telephony on open-wire lines.

621.316.722 2333
An Analysis of the Stability of an Electronic-Ionic Voltage Regulator—L. S. Gol'dfarb. (*Avtomatika i Telemekhanika*, vol. 9, pp. 245–250; May and June, 1948. In Russian.) The operation of the usual type of electronic-ionic voltage regulator (Fig. 1), consisting of an exciter with variable feedback coupling, a voltage generator and a measurement element, is discussed. Equations for various circuits are given and it is shown that while the use of variable feedback coupling ensures stability, it also increases the time constant of the exciter and reduces the speed of the regulation process. A discussion of the circuit equations shows that it is advantageous to use higher amplification in the feedback channel and lower amplification in the measuring element. Design formulas and curves for the feedback coupling circuit are given.

621.316.722:621.3.013.1 2334
Rectifier Voltage Control using Saturable-Core Reactors—F. Butler. (*Wireless World*, vol. 55, pp. 227–229; June, 1949.) The principle is outlined and different methods of winding the reactors are discussed. A circuit diagram and performance figures are given for a full-wave Hg-vapor rectifier with reactor control; the output voltage remains between 970 and 1,000 volts for a current range of 0 to 400 mamp, while the voltage change for a current range of 100 to 400 mamp does not exceed 1.5 per cent.

621.316.726 2335
An Electronic Frequency Regulator—I. S. Bruk, S. S. Chugunov, and N. V. Pautin. (*Avtomatika i Telemekhanika*, vol. 9, pp. 144–151; March and April, 1948. In Russian.) A description of a regulator employed to control the frequency of a 400-cps oscillator feeding a circuit analyzer. The regulator uses a tuning fork as a frequency standard and its accuracy is within 0.1 per cent. A circuit diagram is given with values of the components, and the operation is discussed in detail. Experimental curves are also included.

621.316.726.078:621.397.6 2336
Automatic Frequency Phase Control of Television Sweep Circuits—E. L. Clark. (PROC. I.R.E., vol. 37, pp. 497–500; May, 1949.) Circuit diagrams are given and discussed for three types of afc system, namely: (a) a sawtooth system in which the sawtooth is formed from the pulse present across the deflection yoke, and the phase of this sawtooth is compared with that of the synchronizing pulse to produce a voltage to control the sweep circuit, (b) a sinusoidal system in which a stable oscillator is controlled in phase and frequency by the synchronizing pulse, and in turn controls the sweep circuit, and (c) a pulse-time system in which the area of the synchronizing pulse, which is changed by phase variations, is used to develop a control voltage.

621.319.3 2337
Powerful Electrostatic Machines—N. J. Feleci. (*Jour. Phys. Radium*, vol. 10, pp. 137–144; April, 1949.) Discussion of the energy loss in electrostatic machines at the commutator and due to gas friction leads to the conclusion that for the production of low or medium power electrostatic machines are superior to electromagnetic generators. Although great progress has been made recently in the design of electrostatic generators, they are not likely to supersede electromagnetic generators for very high power.

TELEVISION AND PHOTOTELEGRAPHY

621.397.21.3 2338
Experimental Transmitting and Receiving Equipment for High-Speed Facsimile Transmission—H. Rinia, D. Kleis, and M. van Tol. (*Philips Tech. Rev.*, vol. 10, pp. 189–195; January, 1949.) Drawings, printed matter etc., up to 22 cm wide and of any length are electrically "stuck" on an endless belt and scanned by a rapidly rotating optical system. A document of quarto size can be transmitted in 8 seconds. The image signals may be sent over either cable or radio links. At the receiving end, positive or negative reproductions, of one-sixth the size of the original, are "written" on film, which can be rapidly processed to provide enlarged prints. Resolving power is 5 lines per mm. Applications are suggested and comparative advantages of the system assessed.

621.397.24 2339
Television Distribution over Short Wire Lines—P. Adorian. (*Jour. Brit. I.R.E.*, vol. 9, pp. 89–94; March, 1949.) Reception in closely populated areas, and particularly in blocks of flats, could be improved by using a common antenna and a local wire distribution system. In the system described, the complete carrier and sidebands of the transmitted programs are received, amplified, and distributed over concentric cables. The amplifier, of which a circuit diagram is included, has a uniform gain of 55 db for frequencies between 42 and 48 Mc. Input voltage to receivers is between 7.5 mvolts and 0.75 mvolts for not more than 30 receivers on each line at distances up to 480 meters.

621.397.26 2340
Ultrafax—D. S. Bond and V. J. Duke. (*Jour. Brit. I.R.E.*, vol. 9, pp. 146–156; April, 1949.) Reprint of 2055 of August. See also 1203 of May.

621.397.331.2 2341
High-Speed Production of Metal Kinescopes—H. P. Steier and R. D. Faulkner. (*Electronics*, vol. 22, pp. 81–83; May, 1949.) New techniques used in the manufacture of the RCA 16-inch metal-cone cathode-ray tube Type 16 AP4.

621.397.5 2342
Wideband Television Transmission Systems—E. Labin. (*Electronics*, vol. 22, pp. 86–89; May, 1949.) A survey of the difficulties of obtaining bandwidths in excess of 40 Mc in the various elements of a television service. Video amplifiers, if amplifiers, discriminators, FM klystrons, and microwave antennas having the required performance are discussed. The limiting factors are considered to be transmitter output-stage bandwidth, propagation irregularities, and the cost of the domestic receiver.

621.397.5 2343
Televising the 1949 Oxford and Cambridge Boat Race—T. C. Macnamara and P. A. T. Bevan. (*Electronic Eng.* (London), vol. 21, pp. 165–168; May, 1949.) A single camera and associated apparatus was mounted in a river launch following the race. A small portable 25-watt transmitter at a frequency between 50 and 60 Mc was used to transmit the picture signals to a shore station from which they could be relayed to Alexandra Palace. Power was supplied by a special petrol-electric generator. Pictures from shore cameras were used while the launch was near bridges.

621.397.5(083.74) 2344
Contribution to the Discussion of Television [line] Standards—R. Barthélemy. (*Onde Élec.*, vol. 29, pp. 181–184; May, 1949.) A review leading to the conclusion that the logical solution of the problem lies in the adoption of a standard of 945 lines, with a video-frequency bandwidth of 15 Mc.

621.397.5(083.74) 2345
Reasons for the Choice of the 819-Line [standard]. Reply to Some Criticisms—Y. L. Delbord. (*Onde Élec.*, vol. 29, pp. 185–192; May, 1949.)

621.397.5(083.74) 2346
Theoretical Basis of the Choice of Television [line] Standards—J. L. Delvaux. (*Onde Élec.*, vol. 29, pp. 193–201; May, 1949.) Discussion of the various factors which led to the selection of the 819 line standard for France.

621.397.6:621.396.65 2347
New York-to-Schenectady Television Relay—F. M. Deerhake. (*Elec. Eng.*, vol. 68, pp. 419–422; May, 1949.) For an earlier account see 1792 of 1948.

621.397.6-182.3 2348
The WOW-TV Television Field Car—J. Herold. (*Communications*, vol. 29, pp. 12–13; April, 1949.) A console dolly is included so that the whole equipment can be operated at a distance from the car, which has also a hydraulic leveling unit.

621.397.6-182.3 2349
Mobile TV Studio for WDTV—W. I. McCord. (*FM-TV*, vol. 9, pp. 20–21; March, 1949.) An illustrated description.

621.397.645 2350
Television Front-End Design: Parts 1 and 2—H. M. Watts. (*Electronics*, vol. 22, pp. 92–97 and 106–110; April and May, 1949.) Design equations are derived and illustrated for

several types of rf amplifier stage for television receivers, including a cathode-coupled amplifier, and for several types of mixer. Emphasis is placed on the problem of obtaining the optimum signal-to-noise ratio while satisfying gain, bandwidth, and adjacent-channel rejection requirements.

621.397.7 2351
Low-Cost TV Operation—G. W. Ray. (*FM-TV*, vol. 9, pp. 24–27; March, 1949.) The video signals of selected programs from New York are relayed by a microwave link to New Haven, the relay station being located on Oxford Hill, 8 miles from the New Haven transmitter. Audio signals are transmitted by telephone line. Reception in the New Haven area is quite satisfactory. Equipment is described.

621.397.8(494) 2352
First Practical Tests of Television Reception in Switzerland—J. Dufour. (*Tech. Mitt. Schweiz. Telegr.-Teleph. Verw.*, vol. 26, pp. 241–249; December 1, 1948. In French, with German summary.) An account of trials carried out in and near Zürich during the 20th Swiss radio exhibition, August 26 to 31, 1948, when television demonstrations were given by Philips-Lampen AG., Eindhoven. Field-strength measurements and subjective estimations of picture quality were made at many points up to a maximum distance of 16 km from the 80-watt transmitter, which was installed on the Zürichberg, about 110 meters above the center of the town. The results obtained are tabulated and discussed. For field strengths >3 mvolts per meter reception was generally good, but reception was not possible for fields < 0.7 mvolts per meter. The most common interference was that from car ignition systems, but some industrial high-frequency generators were troublesome; one in particular, operating on 60.5 Mc, rendered reception in its neighborhood quite impossible, as the video frequency used was 61.6 Mc. Analysis of the results shows that a 2-kw transmitter on the Uetliberg should give good reception over the whole of Zürich.

621.397.8(73) 2353
A Field Survey of Television Channel 5 Propagation of New York Metropolitan Area—I. T. Goldsmith, Jr., R. P. Wakeman, and J. D. O'Neill. (Proc. I.R.E., vol. 37, pp. 556–563; May, 1949.)

621.397.92 2354
TVI Patterns—G.G. (*QST*, vol. 33, pp. 43–45; May, 1949.) Photographs are reproduced and discussed which show the interference to television caused by a 28 Mc amateur transmitter, and the improvement effected by various remedial measures.

621.397.823 2355
Ignition Interference—M. V. Callendar. (*Wireless Eng.*, vol. 26, p. 106; March, 1949.) To reduce ignition interference with television sound, it is quite as important to reduce the number of pulses in the train as to reduce the field radiated. See also 3741 of 1946 (Eaglesfield) and 1779 of July (Pressey and Ashwell).

621.397.828 2356
Further Advances in T.V.I. Suppression—L. Varney. (*RSGB Bull.*, vol. 24, pp. 268–273; May, 1949.) It was found possible to operate various commercial television receivers close to a 14-Mc transmitter when suitable harmonic-suppression devices were used in the transmitter. The initial tests and means of suppression are discussed in detail. A harmonic monitor is described.

621.397.5 2357
Television [Book Review]—M. G. Scroggie. Blackie and Sons, Glasgow, 2nd edition, 77 pp., 6s. (*Wireless World*, vol. 55, p. 233; June, 1949.) ". . . a very simple and lucid explanation of how television works. . . . an excellent introduction to television."

621.397.62 2358
Television Receiver Construction [Book Review]—Iliffe and Sons, London, 1948, 47 pp., 2s.6d. (Proc. I.R.E., vol. 37, p. 417; April, 1949.) Reprint of ten articles in *Wireless World* noted in 1186 of 1948 and back references.

TRANSMISSION

621.396.61 2359
The Development of German Broadcasting Transmitter Equipment during the War—E. Wolf (*Tech. Mitt. Schweiz. Telegr.-Teleph. Verw.*, vol. 27, pp. 24–33 and 78–85; February 1, and April 1, 1949. In German.) A review of developments in all kinds of high-power transmitting equipment, including (a) the transmitters, their high-frequency and output stages, modulators and measurement and monitoring racks, (b) power supplies and auxiliary equipment, and (c) antennas. The provision of a network of unattended low-power common-wave transmitters is also considered.

621.396.61 2360
High Power U.H.F. Transmitter—H. C. Lawrence. (*Radio News, Radio-Electronic Eng. Supplement*, vol. 10, pp. 3–5, 29; May, 1948.) Two similar pulsed transmitters using Type 4C33 triodes and coaxial-line tuning elements give peak outputs of 300 kw over frequency bands of 390 to 465 Mc and 510 to 720 Mc respectively. The pulse duration is 5 μseconds and repetition rate 200 per second. Mechanical layout, circuit details, and the mode of operation of the tuning system are described.

621.396.619 2361
Modulation and Keying—L. Pungs and K. Lamberts. (*FIAT Review of German Science 1939–1946. Electronics, incl. Fundamental Emission Phenomena*, part 1, 1948, pp. 251–258. In German.) Review of work in Germany on AM and FM.

621.396.619.13:621.396.615 2362
A Simple Method of Producing Wide-Band Frequency Modulation—H. Rakshit and N. Sarkar. (*Nature* (London), vol. 163, pp. 572–573; April 9, 1949.) FM can be produced in an oscillator with three identical stages by shunting one of the tubes by a triode, and applying the modulating af voltage to the grid of this triode. Results obtained with 6SK7 tubes, using a 6C5 tube as the modulator, are shown graphically and discussed. A linear variation of over 3 kc was obtained with an oscillator frequency of about 1 Mc. See also 2356 of 1947 (Rakshit and Bhattacharyya).

621.396.619.23 2363
The Serrasoid F.M. Modulator—J. R. Day. (*Proc. Radio Club Amer.*, vol. 26, no. 1, pp. 3–13; 1949.) For another account see 342 of March.

621.396.619.23:621.396.615.17 2364
A Modulator Producing Pulses of 10^{-7} Second Duration at a 1-Mc Recurrence Frequency—Morgan. (See 2185.)

621.396.645 2365
A Coaxial 50-kw F.M. Broadcast Amplifier—D. L. Balthis. (*Electronics*, vol. 22, pp. 68–73; May, 1949.) Describes the design and construction of the Symmetron amplifier for the 88 to 108-Mc FM band. Eight triodes, Type 3X2500A3, are connected in parallel. The anode and cathode tuned circuits are formed by two coaxial-cylinder resonators, one outside the other, the common intermediate cylinder being connected to the grid. Input, 12.5 kw, is between the cathode and the earthed resonator shorting bars, and output is between anode and grid. See also 592 of 1948 (Norton, Ballou, and Chamberlin), *FM-TV*, vol. 9, pp. 16–17; March, 1949; and *Tele Tech.*, vol. 8, pp. 42–43, 57; April, 1949.)

621.397.828 2366
Further Advances in T.V.I. Suppression—Varney—(See 2356.)

VACUUM TUBES AND THERMIONICS

621.314.6+621.396.622 2367
Rectification—Möller; Seiler; Sachse—(See 2330.)

621.38 2368
Electronic Apparatus—W. Schaffernicht; M. Knoll; E. Schwartz; H. Rukop. (*FIAT Review of German Science 1939–1946. Electronics, incl. Fundamental Emission Phenomena*, part 1, pp. 43–146; 1948. In German.)

Section 1, by Schaffernicht, deals with photo cells, including discussion of electron multipliers and of the properties of different light-sensitive layers.

Section 2, by Knoll, in collaboration with M. Stark, describes electron-microscope developments.

Section 3, by Schaffernicht, gives a detailed account of various types of infrared image converter.

Section 4, by Schwartz, reviews work on cathode-ray tubes.

Section 5, by Rukop, gives construction and functional details of a wide variety of transmitting and receiving tubes, gas-filled tubes and stabilizers, with a short review of recent technical developments in materials and methods of construction.

621.383.4 2369
Temperature Coefficient of Sensitivity of Lead Sulphide Photo-Conductive Cells at Room Temperature—S. S. Carlisle and G. Alderton. (*Nature* (London), vol. 163, pp. 529–530; April 2, 1949.)

621.383.4 2370
Lead Sulfide Photoconductive Cells—S. Pakswer. (*Electronics*, vol. 22, pp. 111–115; May, 1949.) Practical operating data, characteristics, and applications.

621.383.5 2371
The Efficiency of the Selenium Barrier-Photocell When Used as a Converter of Light into Electrical Energy—E. Billig and K. W. Plessner. (*Phil. Mag.*, vol. 40, pp. 568–572; May, 1949.) Discussion shows that an efficiency of the order of 1 to 4 per cent is to be expected for monochromatic light of frequency near that for peak sensitivity, slightly lower efficiency for white light, and much lower for the light from an incandescent lamp, which includes a good deal of infrared radiation to which the Se cell is not sensitive. Measurements confirmed these conclusions. Houstoun's very low results (900 of April) are criticized.

621.385 2372
New Series of Miniature Valves of the Société Française Radioélectrique—(*Ann. Radioélec.*, vol. 4, pp. 163–164; April, 1949.) The bulb diameter is 19 mm and connections are sealed through the glass base. The principal electrical characteristics are tabulated for HM 04 heptode frequency changer for AM or FM receivers, PM.05 low-capacitance high-frequency pentode, BPM.04 output beam-tetrode, TM.12 uhf triode (for use as grounded-grid amplifier up to 500 Mc), T2.M.05 uhf double triode (for use as mixer or oscillator up to 600 Mc, and D2.M9 uhf double diode. Equivalent American tubes are respectively 6BE6, 6AK5, 6AQ5, 6J4, 6J6, and 6AL5.

621.385 2373
Planar Electrode Valves for V.H.F.—(*Wireless World*, vol. 55, pp. 165–167; May, 1949.) Discussion of various tubes with low interelectrode capacitance and transit time, with particular reference to disk-seal tubes and an experimental triode, Type E1714.

621.385:519.283 2374
Quality Control in Radio-Tube Manufacture—J. A. Davies. (Proc. I.R.E., vol. 37, pp.

548–556; May, 1949.) A general survey of methods used. Typical mount-inspection service, the use of statistical control charts, and sampling procedures are discussed.

621.385:538.122 2375

An Electron Tube for Viewing Magnetic Fields—S. G. Lutz and S. J. Tetenbaum. (*Elec. Eng.*, vol. 67, pp. 1143–1146; December, 1948.) The development of the special tubes is discussed, tubes with 5 cathodes and 8 anodes respectively are described, with illustrations, and design improvements are suggested. For another account see 1919 of August.

621.385:621.317.71 2376

Electrometer Tubes for the Measurement of Small Currents—J. A. Victoreen. (Proc. I.R.E., vol. 37, pp. 432–441; April, 1949.) An account of the American VX series of tubes, used to measure currents of order 10^{-12} amp. Special problems discussed include the low anode voltage required to keep grid current very small, and the high-stability requirements for cathode emission. Curves show emission and anode and control-grid current characteristics. Typical circuits are given.

621.385-712 2377

Study and Realization of a New System of Forced-Air Cooling for Transmitting Valves—J. Prévost, J. Boissière, and A. Loukovski. (*Ann. Radioélec.*, vol. 4, pp. 138–148; April, 1949.) Cooling by means of air currents is discussed theoretically. Various methods hitherto used and an improved method, developed by the Société indépendante de T.S.F. (S.I.F.) are considered. Special circular vanes of Cu, fitting round the cylindrical anode, have certain portions bent downward to touch the vanes below so as to provide channels for the flow of air from two diametrically opposed sources. Alternate vanes are rotated through 180°. All are slightly conical, so that temperature differences between center and edge only vary the angle of the cone. The cooling with this system is particularly efficient and allows continuous operation of tubes at maximum dissipation for long periods.

621.385.01 2378

On the Co-Ordination of Circuit Requirements, Valve Characteristics and Electrode Design—I. A. Harris. (*Jour. Brit. I.R.E.*, vol. 9, pp. 125–143; April, 1949.) "A comprehensive theory is developed, combining the relevant parts of present-day circuit requirements with parts of the theories of electronic, mechanical, and thermal limitations to tube electrode design, from which data on optimum design emerge. The scope includes amplifier tubes with indirectly heated cathodes. Illustrations of theoretical design show general agreement with current practice and indicate directions in which improvement may be sought. Whilst not being a cut-and-dried formulation of tube design, its method may prove a powerful tool in facilitating further development." See also 2406 of 1946 (Liebmann) and 937 of 1947 (Ford).

621.385.029.63/.64 2379

Theory of the Travelling-Wave Valve—J. Laplume. (*Onde Élec.*, vol. 29, pp. 66–72; February, 1949.) The method of Blanc-Lapierre, Lapostolle, Voge, and Wallauschek (3421 of 1947 and back references) is extended to the more complex problem of the helix circuit, making use of results established by Roubine (3036 of 1947) for the case of no interaction between the electron beam and the helix. The pitch of the helix is assumed small enough for the field to be considered as symmetrical about the axis; the actual distribution of the helix current is replaced by a purely superficial helicoidal distribution on the surface of the generating cylinder, and resistance losses are neglected. The electron density and velocity are uniform over the beam cross-section and the velocity is everywhere parallel to the axis. Small-signal theory applies to the interaction between helix and beam.

The conditions prevailing (a) within the beam, (b) between the beam and helix, and (c) outside the helix are considered and formulas giving the field distribution are derived. Boundary conditions lead to six linear and homogeneous relations between six integration constants, and finally to an equation which defines implicitly the propagation constant and thus indicates the waves which can be propagated in the system. Particular cases are considered which result in considerable simplification of the wave equation and other formulas. The principal properties of the traveling-wave tube deduced from the wave equation are summarized and the effect of increased beam width is discussed quantitatively.

621.385.029.63/.64 2380

Travelling-Wave Valve—V. M. Lopukhin. (*Uspekhi Fiz. Nauk*, vol. 36, pp. 456–477; December, 1948. In Russian.) The theory of the tube is discussed.

621.385.029.63/.64 2381

Effect of the Transverse Electric Vector in the Delay Line of the Travelling-Wave Valve: Part 2—O. Doehler and W. Kleen. (*Ann. Radioélec.*, vol. 4, pp. 117–130; April, 1949.) The form of the delay line affects the intensity of the radial field and hence, as explained in part 1 (2089 of August), the tube gain. A simplified form of the gain equations is given, taking account of the radial field, and the equations are developed for a helix system with a central conductor; such a system has an increased transverse field. Numerical results for this case are discussed. A qualitative explanation is given of the effects of space charge and of electron absorption by the line walls due to the existence of the high-frequency electric vector. The effect of the displacement of the electrons in the radial electric field is negligible in comparison with other factors contributing to the gain. Oscillation of the electrons about their original trajectory in the absence of the high-frequency field causes, in a longitudinal electric field, a displacement of the electrons which varies with the radius. Electron bunching results and the wave propagation constant is altered, with a consequent increase of gain. In the case of a simple helix the gain increase is small, but in systems with intense radial fields the increase may be large and even predominant. The variation of the radius of the electron beam due to the radial high-frequency field reduces the effect of the space charge on the gain. The resulting gain increase is considerable even for simple helix systems without a central conductor. Any diminution of gain due to electron absorption by the line walls is negligible.

621.385.029.63/.64 2382

Circuits for Traveling-Wave Tubes—J. R. Pierce. (Proc. I.R.E., vol. 37, pp. 510–515; May, 1949.) Phase velocity v_ϕ, group velocity v_g, and stored energy W per unit length are parameters which can be used for comparing different types of traveling-wave tubes and associated circuits. Given W, lowering v_g relative to v_ϕ increases circuit impedance and gain, increases attenuation, and narrows the band. The effect of gap length in filter-type circuits consisting of pillbox resonators is discussed and the attenuation for such circuits is calculated. They are electrically much inferior to helix circuits.

621.385.029.64 2383

Beam-Deflection Mixer Tubes for U.H.F.—E. W. Herold and C. W. Mueller. (*Electronics*, vol. 22, pp. 76–80; May, 1949.) These tubes have an electron gun producing a thin rectangular beam, two pairs of deflector plates and an anode. An intercepting electrode is placed between deflector plates and anode so that voltages applied to the deflector plates cause variation in the current reaching the anode. One pair of deflectors receives the signal input, and the other pair receives the oscillator output. Advantages include a lower noise factor than that of a crystal mixer in the 1,000-Mc region, very small oscillator coupling and radiation, and high input impedance.

621.385.032.29 2384

The Virtual Cathode Problem for Cylindrical Electrodes—A. van der Ziel. (*Appl. Sci. Res.*, vol. B1, no. 2, pp. 105–118; 1948.) The effect of space charge on the potential distribution between parallel electrodes is discussed. The current versus voltage characteristics are then calculated for cylindrical electrodes; results are similar to those for plane electrodes. The theory may be useful for the development of cylindrical tetrodes and pentodes, especially transmitting tubes.

621.385.032.29 2385

Resistive Films in Valves: Effect on Interelectrode Capacitance—E. G. James and B. L. Humphreys. (*Wireless Eng.*, vol. 26, pp. 93–95; March, 1949.) The capacitance of such films varies as the square root of the frequency at high frequency and tends to a limit at low frequency.

621.385.2:621.396.822 2386

Nonlinear Distortion and Noise in a Diode acted upon by U.H.F. Signals—Yu. I. Kaznacheev. (*Bull. Acad. Sci.* (URSS), pp. 1173–1189; September, 1947. In Russian.) Equations are derived for the current in the circuit of a plane diode for the most general initial conditions, using a method similar to that proposed by Müller (1933 Abstracts, *Wireless Eng.*, p. 433). In passing over from electron equations to current equations, a different method from that proposed by Benham (148 of 1939) is used; a clearer physical interpretation of the theory is thus achieved. From the current equations, general equations are derived determining the nonlinear distortion occurring in the amplification of uhf signals, intermodulation of signals and noise, and the effect of the transit time of electrons on noise. The cases of weak and strong signals are treated separately. The results obtained can be applied to multi-electrode tubes which can be regarded as consisting of a number of diodes.

621.385.2:621.396.822 2387

Measured Noise Characteristics at Long Transit Angles—N. T. Lavoo. (Proc. I.R.E., vol. 37, pp. 383–386; April, 1949.) Tests on diodes at 3,000 Mc indicate that the space-charge reduction of noise is of the order of 10 to 1 when the transit time exceeds 1 rf cycle. This applies to diodes having tungsten, thoriated-tungsten, or oxide emitters. The observed magnitude of the noise and its variation with transit time agree qualitatively with theory.

621.385.3 2388

Current Distribution in Triodes Neglecting Space Charge and Initial Velocities—H. C. Hamaker. (*Appl. Sci. Res.*, vol. B1, no. 2, pp. 77–104; 1948.) A theory of current distribution, originally due to de Lussanet de la Sabloniere (1933 Abstracts, *Wireless Eng.*, p. 507) is clarified and developed for positive-grid triodes. A graphical method of checking the applicability of this theory to any set of observations is discussed; the different distribution functions which are involved in the equations can easily be determined from the graphs given. In some cases theory and experiment are in excellent agreement; discrepancies occurring in other cases are discussed. The basic assumptions underlying the theory are examined in the light of the experimental results.

621.385.3:621.396.619.13.029.64 2389

Certain Aspects of Triode Reactance-Tube Performance for Frequency Modulation at Ultra-High Frequencies—C. L. Cuccia. (*RCA Rev.*, vol. 10, pp. 74–98; March, 1949.) Investigation of the properties of reactance tubes is extended to uhf, taking account of such factors as transit time and interelectrode capacitance. Formulas for the frequency deviation and Q of a transmission-line versus reactance-tube system are derived. The grid swing limits the magnitude of the rf voltages in any such system. Mechanical detail, design, and performance are discussed for a particular case in which a frequency deviation of 5 Mc was obtained.

621.385.3.029.64 2390
New Microwave Triode—(*Electronics*, vol. 22, pp. 171, 177; April, 1949.) Description of a close-spaced planar triode, Type BTL 1553, for operation at 4,000 Mc.

621.385.38:621.396.619.23 2391
Thyratrons in Radar Modulator Service—H. H. Wittenberg. (*RCA Rev.*, vol. 10, pp. 116–133; March, 1949.) The relations between performance and various characteristics and circuit parameters are shown.

621.385.38.032.213 2392
The Hot Cathode Hydrogen-Filled Thyratron—H. de B. Knight and O. N. Hooker. (*Brit. Thomson-Houston Activities*, vol. 20, pp. 47–49; March and April, 1949.) The hydrogen filling permits operation as an electronic switch at frequencies much higher than those possible with Hg vapor, but a voltage drop of 50 to 70 volts is required, instead of 10 to 15 volts for Hg.

621.385.4/.5 2393
Increasing the Power Output of Vacuum Tubes—B. M. Hadfield. (*Radio News, Radio-Electronic Eng. Supplement*, vol. 10, pp. 10–11; May, 1948.) The circuit of a pentode or tetrode, connected for use as a triode or diode, can be arranged so that a large part of the anode dissipation is transferred to an external resistance R without affecting the triode or diode characteristics. The conditions governing the maximum value of R and the reduction in anode dissipation obtainable are discussed. Application to voltage stabilizers of the cathode-follower type is considered.

621.385.5 2394
The Choice of Operating Conditions for Resistance-Capacitance-Coupled Pentodes—F. Langford-Smith. (*Radiotronics*, pp. 63–69; July and August, 1948.) Discussion of: (a) the optimum value of the anode load resistor for minimum distortion, (b) the optimum anode current for minimum distortion under given conditions, (c) the relative distortion characteristics of a pentode and a triode for given output voltage, and (d) pentode operating conditions.

621.385.5:621.397.645 2395
Variation of the Input Impedance of Television-Amplifier Pentodes—F. Juster. (*Télév. Franç.*, pp. 23–26, 36; April, 1949.) Discussion of the dependence of input-impedance variations on frequency and on tube characteristics. Results for specified tubes are shown graphically. Methods of reducing such variations are indicated.

621.385.83+537.533 2396
Electron Emission and Electron Currents—Mayer; Knoll. (*See* 2205.)

621.385.832 2397
Cathode-Ray Tubes with Post-Deflection Acceleration—W. G. White (*Electronic Eng.* (London), vol. 21, pp. 75–79; March, 1949.) The outstanding advantage of post-deflection acceleration (p.d.a.) is the increase in brightness obtainable for a given accelerating voltage. One form of p.d.a. electrode is a band of graphite on the inner circumference of the cathode-ray-tube envelope near the fluorescent screen. Several such electrodes can be used. P.d.a. causes a slight reduction in sensitivity, and the electric fields near the p.d.a. electrode lose their radial symmetry. Various quantities are comparatively tabulated for p.d.a. and ordinary tubes with electrostatic or with electromotive deflection, but no general formula expressing the over-all advantage of a p.d.a. tube can be deduced. The work of Pierce (1965 of 1941) is critically discussed.

621.385.832:533.5 2398
Modern Vacuum-Pump Design—Mellen. (*See* 2241.)

621.385.832:621.397.6 2399
Development of a Large Metal Kinescope for Television—H. P. Steier, J. Kelar, C. T. Lattimer, and R. D. Faulkner. (*RCA Rev.*, vol. 10, pp. 43–58; March, 1949.) Discussion of a 16-inch cathode-ray tube Type $16AP_4$, and the associated design and construction problems.

621.396.615 2400
Generation of Oscillations—Urtel; Gundlach; Frey; Schumann; Marx; Hettner. (*See* 2175.)

621.396.615.141.2:621.396.619.11 2401
A Spiral-Beam Method for the Amplitude Modulation of Magnetrons—J. S. Donal and R. R. Bush. (PROC. I.R.E., vol. 37, pp. 375–382; April, 1949.) A beam of electrons spiralling in a longitudinal magnetic field varies the conductance presented by a resonant cavity coupled to the magnetron, and so varies the power delivered to the load. The method has been applied to a 900-Mc continuous-wave magnetron, giving a peak power output of 500 watts, with a modulating power of only about ½ watt. Satisfactorily linear voltage modulation is obtained up to a maximum depth of about 85 per cent, while the frequency variation during the AM cycle is only ±15 kc. The system has been used to give a satisfactory reproduction of a television resolution pattern. Theory indicates that the method should be applicable at frequencies higher than 900 Mc.

621.396.615.142.2 2402
Klystrons—H. Döring. (*Fernmeldetech. Z.*, vol. 2, pp. 105–118; April, 1949.) Basic principles of operation are discussed and many types are described, with special reference to construction details and methods. The special features of all-metal reflex klystrons for wavelengths of about 3.2 cm and 6.5 mm respectively are described and clearly shown in section diagrams.

621.396.615.142.2:621.396.619.13 2403
Klystrons for F.M.—W. Henderson. (*FM-TV*, vol. 9, pp. 17–19; May, 1949.) The special features of the Sperry SRL-17 reflex klystron are described, with a cut-away view showing the internal construction. The continuous-wave output is 3 watts and the frequency range 920 to 990 Mc. For low-power local-oscillator service, the beam voltage is +250 volts and the reflector voltage −150 volts. FM of the output is simply obtained by applying the signal to the reflector.

621.396.645:537.311.33:621.315.59 2404
The Transistor—A New Semiconductor Amplifier—J. A. Becker and J. N. Shive. (*Elec. Eng.*, vol. 68, pp. 215–221; March, 1949.) The construction of the Type-A transistor is described and the conventions regarding sign of current and voltages are given. Both large-signal and small-signal performance are discussed mathematically and the useful power obtainable, the internally generated noise, the useful frequency range and the effect of changes in ambient temperature are considered. For coaxial transistors, see 2406 below.

621.396.645:537.311.33:621.315.59 2405
The Type-A Transistor—R. M. Ryder. (*Bell Lab. Rec.*, vol. 27, pp. 89–93; March, 1949.) The type described is less than ½ inch long and under ¼ inch in diameter. The static characteristics of the transfer properties between the contacts are shown graphically.

621.396.645:537.311.33:621.315.59 2406
The Coaxial Transistor—W. E. Kock and R. L. Wallace, Jr. (*Elec. Eng.*, vol. 68, pp. 222–223; March, 1949.) The construction and characteristics of a transistor having point contacts placed on opposite sides of a thin Ge crystal plate are discussed. Advantages over the type-A transistor (2404 above) are briefly indicated.

621.396.645:537.311.33:621.315.59 2407
Coaxial Transistor—(*Electronics*, vol. 22, p. 128; March, 1949.) Satisfactory results are obtained when the two point contacts on a Ge disk are placed on opposite faces instead of the same face as in previous designs. The coaxially mounted contacts rest in polished spherical depressions in the disk. Improved mechanical stability, complete electrostatic screening between input and output, and easier construction are claimed.

621.396.822 2408
Transit-Time Deterioration of Space-Charge Reduction of Shot Effect—D. K. C. MacDonald. (*Phil. Mag.*, vol. 40, pp. 561–568; May, 1949.) When space charge is present in a tube, the emission current from the cathode exhibits less fluctuation than in the absence of space charge. If this current drifts for some distance, as in a v.m. tube, it is to be expected that the fluctuation will increase until, after a sufficient time, the full shot noise is reached again. Analysis of this problem leads to a curve which shows the progressive increase of noise with drift time.

621.385 2409
Radio Valve Data [Book Notice]—Iliffe and Sons, London, 80 pp., 3s.6d. (*Wireless Eng.*, vol. 26, p. 84; March, 1949.) The characteristics of 1,600 British and American receiving tubes are tabulated. The booklet is the post-war successor to the *Wireless World* Valve Data Supplements which used to appear annually.

MISCELLANEOUS

001.891 2410
The Radio Research Board—(*Wireless Eng.*, vol. 26, pp. 145–146; May, 1949.) A historical review of its work (a minor part of which is the preparation of these abstracts) and of its relationship with the Department of Scientific and Industrial Research.

061.3:621.396 2411
International Radio Conferences—R. L. Smith-Rose. (*Nature* (London), vol. 163, pp. 493–495; March 26, 1949.) A general survey of the main conclusions of various conferences held in the summer of 1948.

621.3.018.4:001.4 2412
Proposed Standard Frequency-Band Designations—(PROC. I.R.E., vol. 37, p. 467; May, 1949.) Discussion of a system in which "Band n" includes all frequencies from 10^n cps up to, but not including, 10^{n+1} cps. Standard abbreviations for frequency and length units are also listed. For an alternative system see 2413 below.

621.3.018.4:001.4 2413
Nomenclature of Frequencies—C. F. E. Booth. (*P.O. Elec. Eng. Jour.*, vol. 42, part 1, pp. 47–49; April, 1949.) A new classification is proposed in which frequencies between 0.3×10^n cps and 3×10^n cps are defined to constitute "Band n." This is capable of unlimited extension. See also 2412 above.

5+6](43) 2414
FIAT Review of German Science 1939–1946. Electronics, incl. Fundamental Emission Phenomena: Part 1. [Book Notice]—G. Goubau and J. Zenneck (Senior Authors). Office of Military Government for Germany, Field Information Agencies Technical, British, French, U. S., 1948, 295 pp.

ADVENTURES IN ELECTRONIC DESIGN

Centralab Announces the NEW MODEL 2 RADIOHM CONTROL!

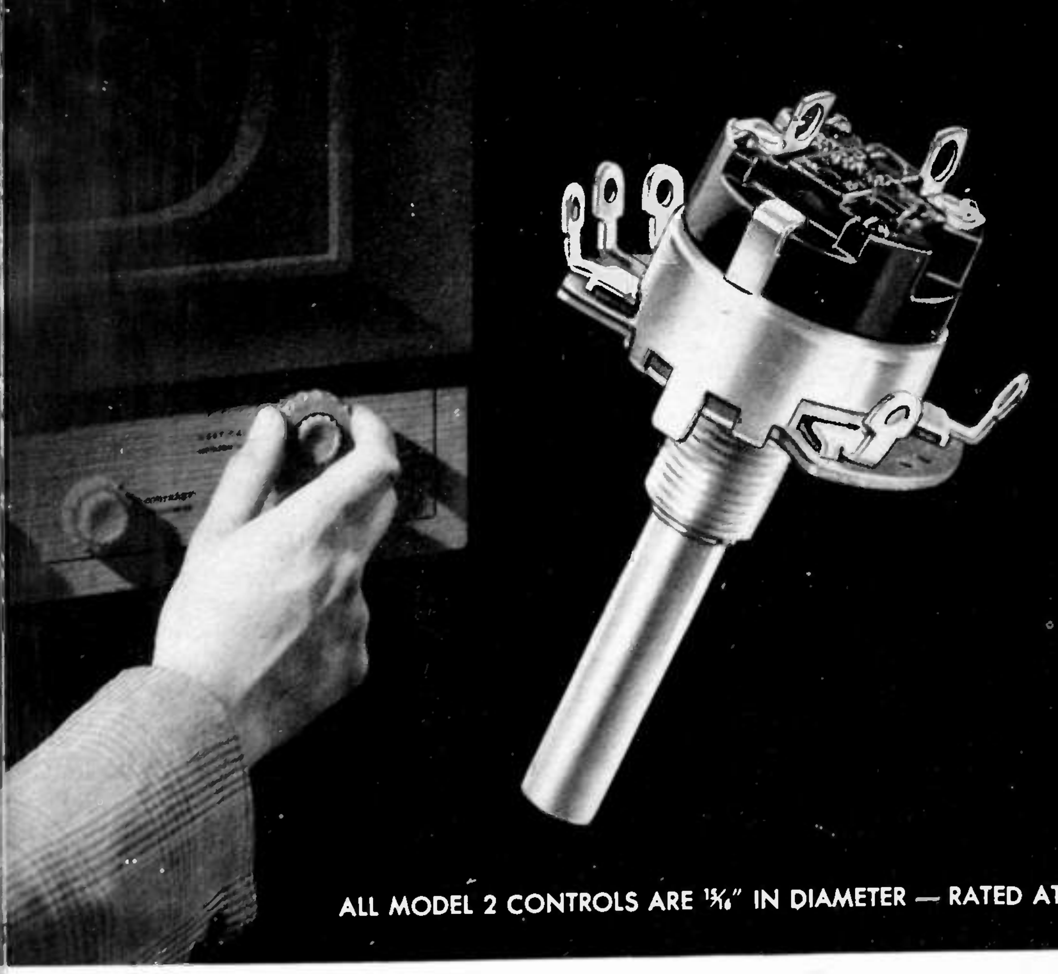

OTHER MODEL 2
RADIOHM CONTROLS

Left: plain type. *Right:* plain type — concentric shaft, twin with taps.

Left: switch type—with taps.
Right: switch type—twin.

ALL MODEL 2 CONTROLS ARE $\frac{15}{16}$" IN DIAMETER — RATED AT ½ WATT.

HERE THEY ARE! Centralab's Model 2 Radiohm Controls. Designed by skilled Centralab engineers, these new quality controls are used in television, radio, sound, motion picture and other electronic equipment. Precision-built with a special composition resistance material securely bonded to a high quality phenolic base, they give you lower noise level . . . longer life. Yes — examine the new CRL Model 2 Radiohms and see why it will pay you to use these finer controls in the equipment you manufacture. See how Model 2's clinched terminals insure firm, positive connections. See how Model 2's complete line of 3 basic switches (5, 8 and 1 amp.) gives you 24 switch combinations for real flexibility in application and design. See how Model 2's tap positions at 37½, 50 and 62½ percent of rotation simplify wiring problems. Yes — check *all of the outstanding advantages* of Centralab's fine new Model 2 Radiohm Controls and you'll agree they're the right controls for you. For complete information, see your Centralab representative or write direct.

Centralab — **DEVELOPMENTS THAT CAN HELP YOU**

Division of GLOBE-UNION INC. • Milwaukee

Centralab reports to

SEPTEMBER, 1949

Exploded View Shows Why Centralab's New Model 2 Radiohm is Today's Finest Control!

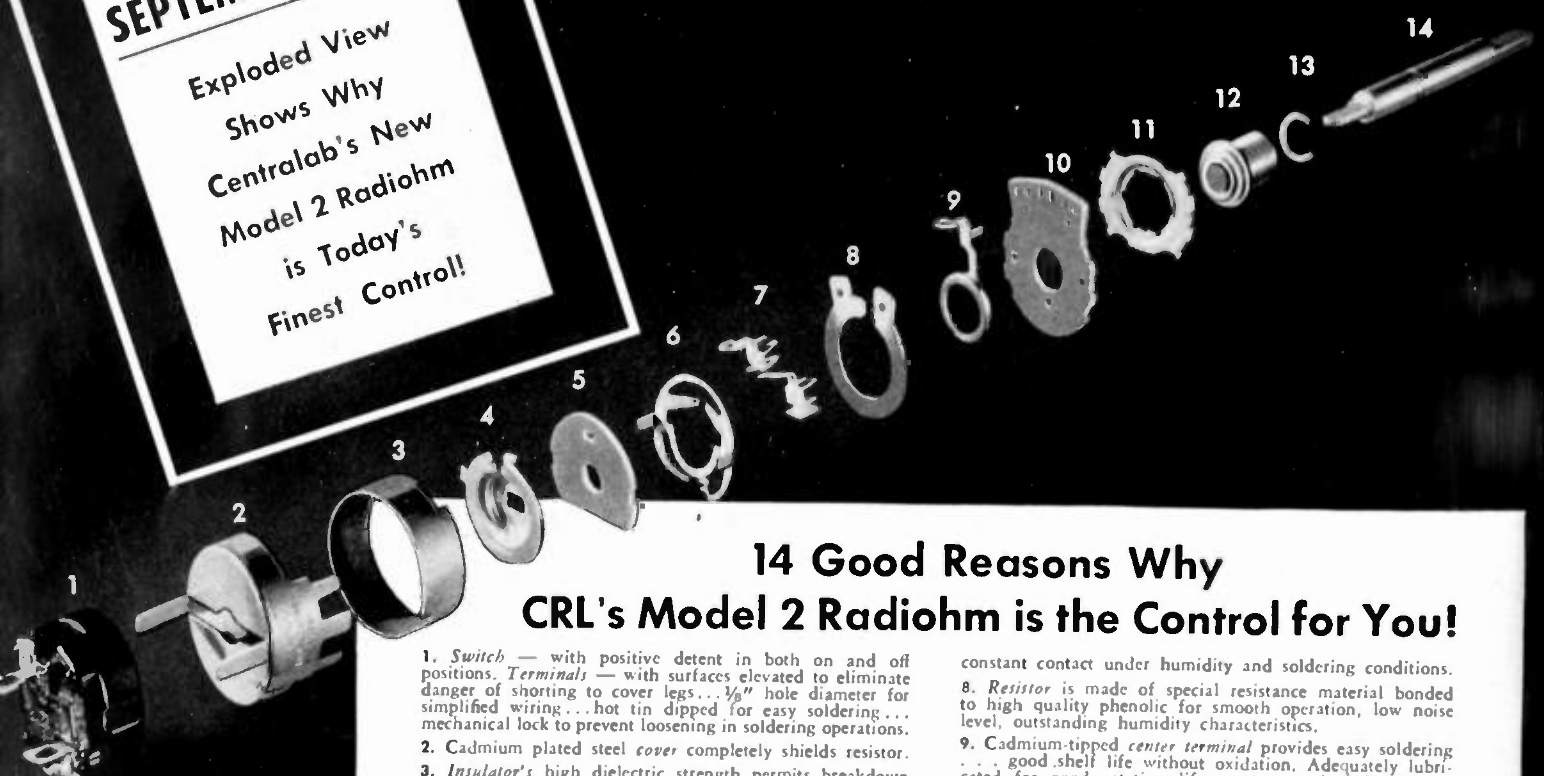

14 Good Reasons Why CRL's Model 2 Radiohm is the Control for You!

1. *Switch* — with positive detent in both on and off positions. *Terminals* — with surfaces elevated to eliminate danger of shorting to cover legs . . . 1/8" hole diameter for simplified wiring . . . hot tin dipped for easy soldering . . . mechanical lock to prevent loosening in soldering operations.

2. Cadmium plated steel *cover* completely shields resistor.

3. *Insulator's* high dielectric strength permits breakdown test at 1000 volts R. M. S. Dust and dirt can't get in.

4. *Stop*, of cup design, provides superior switch shielding . . . gives you excellent torque strength without distortion.

5. High grade laminated phenolic *shoe* maintains high insulation resistance (under humidity conditions.)

6. Contact Spring gives you double wiping contacts on both resistor and center terminal ring . . . is accurately formed to maintain uniform pressures and minimize noise.

7. Electro tin-plated *terminals* provide soldering ease. Tightly crimped, terminals give you direct contact to resistor . . . assure constant contact under humidity and soldering conditions.

8. *Resistor* is made of special resistance material bonded to high quality phenolic for smooth operation, low noise level, outstanding humidity characteristics.

9. Cadmium-tipped *center terminal* provides easy soldering . . . good shelf life without oxidation. Adequately lubricated for good rotation life, center terminal is finished to give you smooth take-off . . . minimum noise.

10. Laminated phenolic *base* maintains high insulation resistance (under humidity conditions.)

11. Cadmium-plated steel *ground plate* assures positive grounded cover.

12. Cadmium-plated steel *bushing* is accurately finished and fit to shaft for smooth rotation.

13. *Retaining ring.*

14. *Shaft.* Unlimited variations available to meet your specifications.

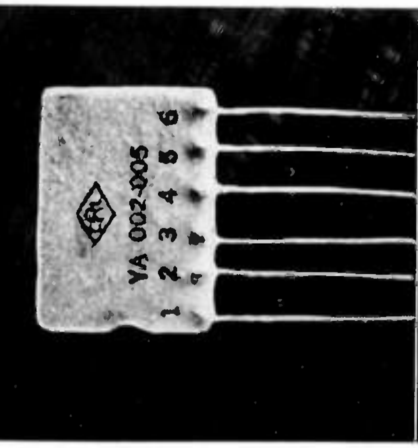

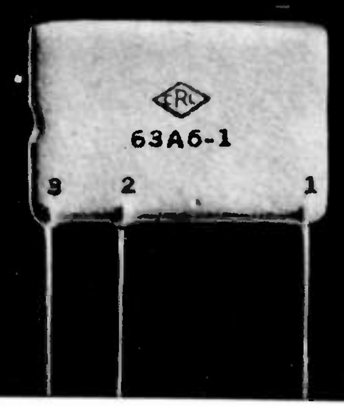

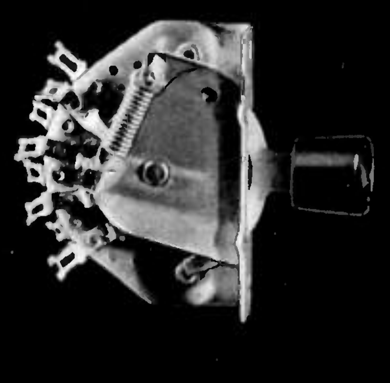

1 *Pentode Couplate* consists of plate lead and grid resistors, plate by-pass and coupling capacitors. Minimum soldered connections speed production.

2 This is the new CRL *Vertical Integrator Network* used in TV sets. Variations of this Centralab *Network* are available on special order.

3 In its *Lever Switch*, Centralab guarantees a minimum life of 50,000 cycles. Here's the reason: an exclusive new coil spring index.

Electronic Industry

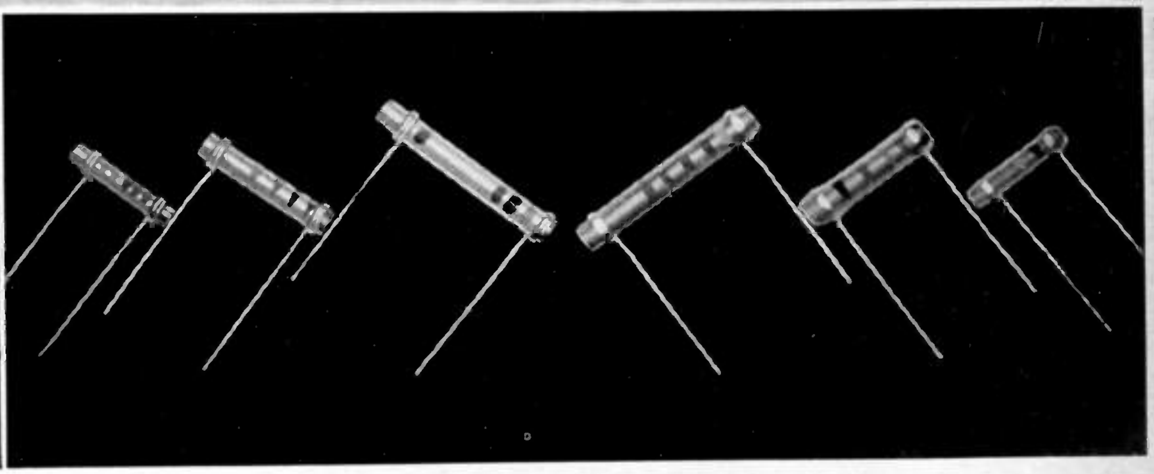

4 Model "1" *Radiohm* control — plain and switch types — is no larger than a dime. Especially designed for miniature applications.

5 Centralab's TC (Temperature Compensating) Tubular *Hi-Kaps*, left, are the most stable capacitors available. With TC *Hi-Kaps*, there's practically no variation due to aging or changes in temperature or humidity. For applications where temperature compensation is unimportant, use Tubular BC *Hi-Kaps*, right.

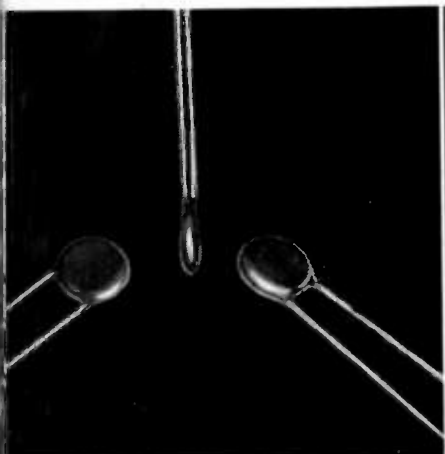

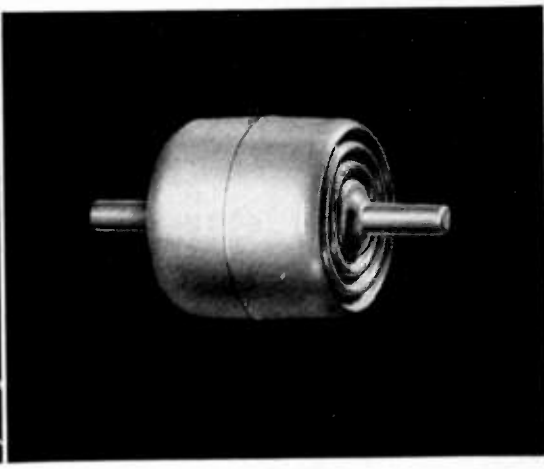

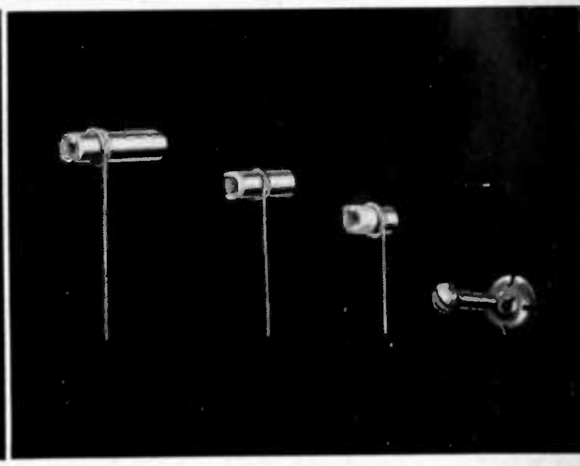

6 For by-pass or coupling applications, check Centralab's original line of ceramic disc *Hi-Kaps*. Disc *Hi-Kaps* are smaller than a dime!

7 *Hi-Vo-Kaps* are filter and by-pass capacitors combining high voltage, small size and variety of terminal connections to fit most TV needs.

8 CRL's new Tubular *Trimmers* come in 3 basic types, 3 capacity ranges. Tinnerman locknut and adjusting screw available on special request.

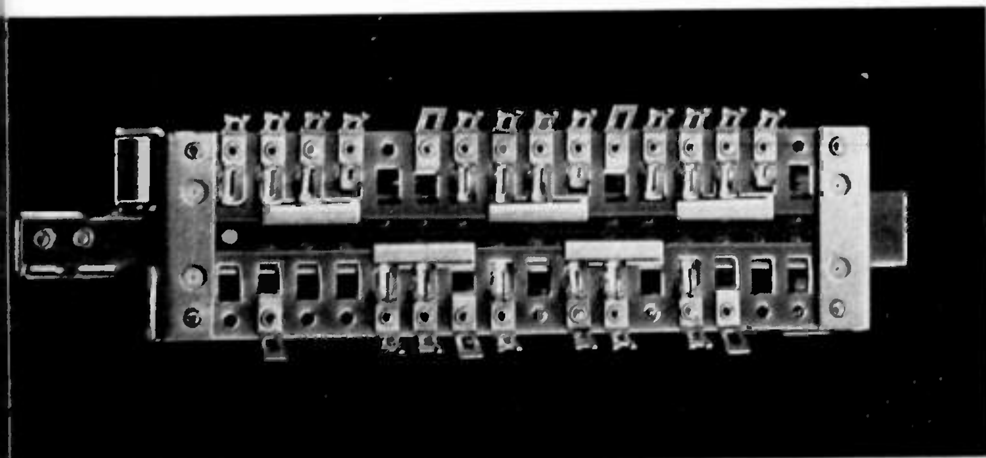

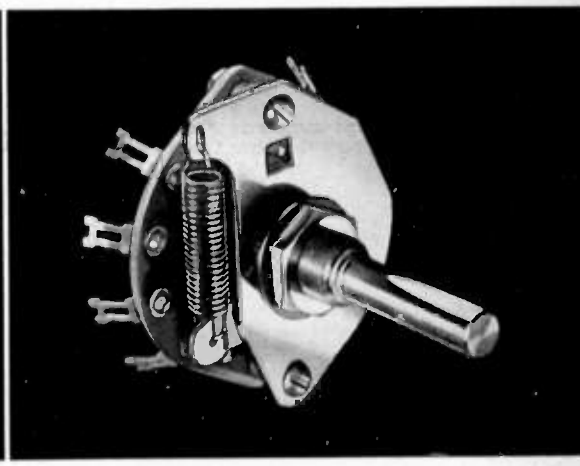

9 Centralab's development of a revolutionary, new *Slide Switch* gives you improved AM and FM performance! Flat, horizontal design saves valuable space, allows short leads, convenient location to coils, reduced lead inductances for increased efficiency in low and high frequencies. CRL *Slide Switches* are rugged and dependable.

10 Great step forward in switching is CRL's New *Rotary Coil and Cam Index Switch*. Its coil spring gives you smoother action, longer life.

STUDENT BRANCH
MEETINGS

FENN COLLEGE—IRE BRANCH

"Microwave Relay Systems for Television with Demonstration," by O. Henderson, Ohio Bell Telephone Company; June 24, 1949.

SECTION MEETINGS

ATLANTA

"History and Program for Development and Operation of WGST-FM," by Ben Akerman, Chief Engineer, Radio Station WGST-FM; June 24, 1949.

BALTIMORE

Inspection Tour of Television Station WAAM; June 20, 1949.

BEAUMONT-PORT ARTHUR

"The IRE and You," by J. C. Petkovsek, Past Chairman, Beaumont-Port Arthur Section; June 23, 1949.

COLUMBUS

"Theoretical and Experimental Studies of Radio Interference Transients from Precipitation Static and Corrective Measures," by M. M. Newman, Lightning and Transients Research Institute; April 15, 1949.

"Television Transmitting and Microwave Pickup," by C. Sloan, Chief Engineer, Radio Station WLWC; Tour of Radio Station WLWC; May 25, 1949.

"The Problem of Producing a Television Program," by R. Rider, Radio Station WLWC; Election of Officers; June 8, 1949.

DES MOINES-AMES

"Programming for College FM Stations," by R. B. Hull, Radio Station WOI; May 18, 1949.

HOUSTON

"Theory and Application of Radar in Marine Geophysical Prospecting," by O. E. Haley, McCollum Laboratories, Inc.; June 15, 1949.

LOS ANGELES

"Magnetic Tape Sound Recording for Kinescope Transcriptions," by R. H. Ranger, Rangertone Inc.; "The Aims and Purposes of the Motion Picture Research Council, Inc.," by W. V. Wolfe, President, Motion Picture Research Council; June 21, 1949.

MILWAUKEE

"Atomic Power Plants," by Dr. Kingdon, General Electric Company; April 6, 1949.

"A Radio Engineer Looks at Industrial Electronics," by Dr. Cook, General Electric Company; April 13, 1949.

"Engineering Aspects of the Transistor," by J. A. Morton, Bell Telephone Laboratories; April 27, 1949.

"Application of Proximity Effects in Induction Heating," by E. Bennett, Faculty of University of Wisconsin; May 4, 1949.

"Sixteen-inch Kinescope," by H. Steier, RCA; May 11, 1949.

"Electronic Control of DC Motors," by J. B. Reeves, Cutler-Hammer Inc.; May 25, 1949.

"Audio-Frequency Transformers and Their Functions in High-Fidelity Amplifiers," by D. Schwennesen, Chief Engineer, Chicago Transformer Corporation; May 31, 1949.

(Continued on page 40A)

SECTION MEETINGS

(Continued from page 38A)

Ladies Night; Ventriloquist; Movies; and Election of Officers; June 9, 1949.

NEW MEXICO

"Theory and Practice of Strategic Bombing in World War II," by A. W. Baldyreff, Faculty of University of New Mexico; Election of Officers; June 17, 1949.

NORTH CAROLINA-VIRGINIA

"Electrical Measurements of Force and Pressure," by D. H. Newby, National Advisory Committee for Aeronautics; "Application of Radio Telemetering to Aeronautical Research," by C. A Taylor, National Advisory Committee for Aeronautics; Inspection Trip of Instrument Laboratories, National Advisory Committee for Aeronautics; June 24, 1949.

PHILADELPHIA

"A Record Changer and Record of Complimentary Design," by H. I. Reiskind and A. D. Burt, RCA Victor Division; May 5, 1949.

SAN DIEGO

"The Ultrasonics Research Program at Brown University," by R. B. Lindsay, Faculty of Brown University; July 12, 1949.

SAN FRANCISCO

"Electronic Digital Computors," by P. L. Norton, Faculty of University of California; May 11, 1949.

Student Papers Competition; "Ion Beam Integrator," by K. D. Jenkins, Student, University of California; "Electronic Flux Meter," by F. B. Gallagher, Student, Santa Clara University; "High-Power Limitations of a Traveling-Wave Tube," by D. Dunn, Student, Stanford University; Election of Officers; June 8, 1949.

TWIN CITIES

"Music Reproduction," by J. D. Goodell, President, The Minnesota Electronics Corporation; June 16, 1949.

WASHINGTON

"Stratovision," by C. E. Nobles, Westinghouse Electric Corporation; June 13, 1949.

SUBSECTIONS

LONG ISLAND

Election of Officers; April 27, 1949.

MONMOUTH

"Image Quality in Photography and Television," by O. H. Schade, RCA, June 15, 1949.

LANCASTER

Tour of Safe Harbor Dam and Power Plant; May 11, 1949

MEMBERSHIP

The following transfers and admissions were approved and will be effective as of September 1, 1949.

Transfer to Senior Member

Chapin, R. S., 383 Lake St., Lake Garda, Unionville, Conn.

Finney, W. J., Bldg. 1, Rm. 213, Naval Research Laboratory, Washington 25, D. C.

(Continued on page 42A)

2 new metal "Big Picture" tubes by Rauland!

AVAILABLE WITH NEW HIGH-CONTRAST LUXIDE SCREEN

Gives 60% greater contrast! Reduces glare! Gives sharper, easier-to-view pictures!

50% LIGHTER WEIGHT

Can be safely shipped installed in sets, reducing field installation costs.

LARGER SCREEN

105 square inches useful screen area

LOWER PRICE

Lower bulb cost permits lower prices

BETTER FACE QUALITY

Optical quality of metal tube faces is superior to the pressed faces of all-glass tubes.

SHORTER LENGTH

2⅝″ shorter than the 16AP4

USES AVAILABLE OPERATING COMPONENTS

Same focus and deflection coils as used with the 16AP4

ALLOWS IMPROVED CABINET DESIGN AND LOWER CABINET COST

Because of reduced cabinet depth requirement

Other Available Types—10BP4, 10FP4, 12LP4, 12KP4, 16AP4

WRITE FOR TECHNICAL BULLETINS

"Perfection through Research"

THE **Rauland** CORPORATION

4245 N. Knox Avenue · Chicago 41, Illinois

MEMBERSHIP

(*Continued from page 40A*)

Hammond, G. H., 66 Old Billerica Rd., Bedford Mass.
Hebenstreit, W. B., Hughes Aircraft Company, Culver City, Calif.
Hodgson, A. D., Barnes Bldg., Bridge St., Bridgetown, Barbados, B.W.I.
Linder, E. G., RCA Laboratories, Princeton, N. J.
Margosian, J. W., 75-34 113 St., Forest Hills, L. I., N. Y.
Miller, G. A., 30 Sunset Blvd., Ottawa, Ont., Canada
Ottemiller, W. H., Jr., R.D. 1, Seneca Falls, N. Y.
Robins, B. W., 6021 Upsal St., Pennsauken, N. J.
Suffield, F. G., 333 15 St., Manhattan Beach, Calif.
Todd, S. R., 4711 Woodlawn Ave., Chicago 15, Ill.
Winter, H., 3514 E. Thaxton Ave., Albuquerque, N. Mex.

Admission to Senior Member

Brueckmann, H. L., 372 W. Park Ave., Oakhurst, N. J.
Franklin, W. S., 3123 N. Pulaski Rd., Chicago 41, Ill.
Harrison, C. E., 4530a W. Papin, St. Louis 10, Mo.
Horton, A. W., Jr., 463 West St., New York 14, N. Y.
Pearce, J. M., Electronics Section #355, The Glenn L. Martin Company, Baltimore 3, Md.
Stiles, K. P., 106 Prospect St., Summit, N. J.

Transfer to Member

Ahrens, G. W., 2402 Avenue P, Galveston, Tex.
Anderson, R. M., 4315 Virginia, Kansas City, Mo.
Eastman, J. W., 4607 Harwood Dr., Des Moines 12, Iowa
Flynn, G., Radio Station WOW, Insurance Bldg., Omaha 2, Neb.
Franco, M., 527 N. Mott St., Los Angeles 33, Calif.
Hoff, K., c/o Stremsheim, Vei 2884, Oslo, Norway
Karanjia, K. F., Patel Mansion, DeLisle Rd., Lower Parel, Bombay, India
McFadden, H. W., 1244 Dufferin St., Toronto 4, Ont., Canada
Monroe, W. J., Box 1581, New Orleans, La.
Moore, H. H., 3601 College Ave., Kansas City 3, Mo.
Nicholson, T., 3614 E. 57 St., Kansas City 4, Mo.
Phillips, F. S., 809 W. 32 St., Houston 8, Tex.
Russ, W. E., 1503 S. Harvey Ave., Berwyn, Ill.
Seigle, R. K., 1 Ash Dr., Great Neck, L. I., N. Y.
Srivastava, T. N., Asst. Divisional Engineer Telegraphs, Eastern Court, New Delhi, India
Threadgill, A. R., 103 Kenwyn Rd., Oak Ridge, Tenn.
White, M. F., 465 W. 162 St., New York 32, N. Y.

Admission to Member

Basavaraju, T. V., 500 Riverside Dr., New York 27, N. Y.
Capron, R. W., 3407 Trumbull Ave., Detroit 8, Mich.
Chaffee, M. A., 5 Brookwood St., Glen Head, N. Y.
Crain, C. M., Engineering Bldg. 149, University of Texas, Austin, Tex.
Deise, L. F., 1901 E. 31 St., Baltimore 18, Md.
Durkee, C. H., 1 Sylvan Lane, Old Greenwich, Conn.
Firestone, W. L., 846 W. Montrose, Chicago 13, Ill.
Gerhold, R. A., 1680 Metropolitan Ave., New York 62, N. Y.
Goerke, V. H., National Bureau of Standards, APO 942, c/o Postmaster, Seattle, Wash.
Greene J. C., 2327 Rosedale St., Baltimore 16, Md.
Hart, S. V., Industrial Electronics, Inc., 2457 Woodward Ave., Detroit 1, Mich.

(*Continued on page 44A*)

MEMBERSHIP

(*Continued from page 42A*)

Ingraham, K. R., Director Telecommunications, Box 48, Nassau, Bahamas
Keyes, J. C., 414A Nimitz Ave., China Lake, Calif.
Kubicek, W. G., Dept. of Physical Medicine, Medical School, University of Minnesota, Minneapolis 14, Minn.
Lambert, C. O., 758-B Crane Walk, Akron 11, Ohio
Neelands, L. J., 117 Parkside Ave., Syracuse, N. Y.
Neubauer, J. R., 3118 Dillon Ave., Cheyenne, Wyo.
Obermuller, W. F., Caixa Postal 2726, Rio De Janeiro, Brazil
Shama Rao, P. L., 124 Sri Krishnarajendra Rd., Basavangudi, Bangalore, South India
Toufexis, S., The Delehanty Radio Institute, 105 E. 13 St., New York 3, N. Y.
Wembold, R. F., 480 E. 23 St., Brooklyn 26, N. Y.

The following admissions to Associate were approved and are effective as of August 1, 1949:

Aarons, C. R., 631 W. Ellet St., Philadelphia, Pa.
Arnold, A., Jr., 6026 Madison St., West New York, N. J.
Bantin, W. F., 4166 St. Catherine St., W., Montreal, Que., Canada
Beiser, F. D., 532 Thatcher, River Forest, Ill.
Bell, W. L., R.D. 1, Coatesville, Pa.
Bergman, L. C. H. M., Government Radio and Telephone Administration, Willemstad Curacao, Netherlands West Indies
Boyd, D. B., General Delivery, Hilliards, Pa.
Bryant, R. M., Jr., Pines Lake E., Box 307, Paterson, N. J.
Buck, D. T., 37-41 Marcy St., Freehold, N. J.
Dula, J. E., 10217 Ave. M, Chicago 17, Ill.
Edens, R. L., 1015 S. Fifth St., Waco, Tex.
Eslava, E. R., Apartado Postal No. 1106, Bogota, Columbia
Fujimoto, J. J., 5327 N. Winthrope Ave., Chicago 40, Ill.
Gatch, C. E., Box 444, St. George, S. C.
Ghose, B. N., 11-42 Panditia Rd., Ballygunge, Calcutta 29, India
Goddard, C. A., 6517 Kimbark Ave., Chicago 37, Ill.
Gudzin, M. G., 3259 Queenstown Dr., Mt. Rainier, Md.
Hall, F. C., 5331 W. Congress, Chicago 44, Ill.
Hall, R. E., 43 Leon St., Boston 15, Mass.
Harris, R. B., Taylor Instrument Co., 95 Ames St., Rochester 1, N. Y.
Hodgkinson, W. S., 58 Adella Ave., West Newton, Mass.
Holt, C., III, Box 1372, Wright Patterson A.F.B., Dayton, Ohio
Hooper, F. E., 1120 19 St., S., Arlington, Va.
Iannotti, J. D., 606 W. South St., Angola, Ind.
Johnston, J. L., 223 W. Park, Pittsburg, Kan.
Kilpatrick, L. L., 3981 Menlo Ave., Los Angeles 37, Calif.
King, R. L., Box 313, Lockbourne A.F.B., Columbus 17, Ohio
Knox, R. M., 818-B S. Catalina Ave., Redondo Beach, Calif.
Kofler, E. J., 1409 Franklin St., Racine, Wis.
Lambert, R. L., 550 Arlington Pl., Chicago 14, Ill.
Lombard, W. A., 2560 Lalla St., Beaumont, Tex.
Marchetta, P., ASW Branch, Aeel Nads, Johnsville, Pa.
Marheine, E. A., 2173 N. 70 St., Wauwatosa 13, Wis.
Marsh, S. V., 1308 W. Rosedale St., Chicago 40, Ill.
Mattern, J., 1724 Patton Dr., Schenectady 7, N. Y.
Mehta, O. N., 2 Royal Hotel, Jubbilpore C. P., India
Mohan, M. A., Tech. Officer, Civil Aviation Dept., Radio Development Unit, Factory Rd., New Delhi, India

(*Continued on page 47A*)

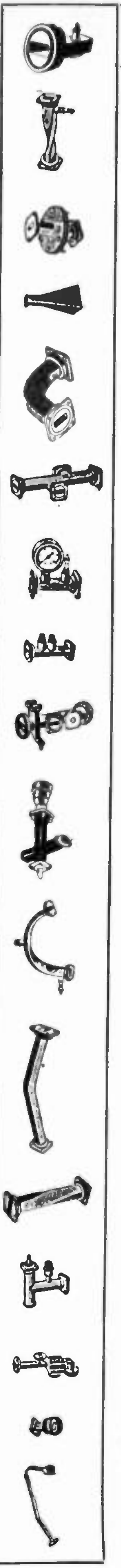

MICRO WAVE PLUMBING & ACCESSORIES

1.25 CENTIMETER

"K" BAND DIRECTIONAL COUPLER CU104/ APS-34 20 DB .... $49.50 ea.
"K" BAND FEEDBACK TO PARABOLA HORN, with pressurized window $30.00
MITRED ELBOW cover to cover $4.00
TR/ATR SECTION choke to cover $4.00
FLEXIBLE SECTION 1" choke to choke $5.00
ADAPTER, rd. cover to sq. cover $5.00
MITRED ELBOW and S sections choke to cover $4.50
WAVE GUIDE ½ x ¼ per ft. $1.00
K BAND CIRCULAR FLANGES .... 50¢

10 CENTIMETER

WAVEGUIDE TO ⅞" RIGID COAX "DOOR-KNOB" ADAPTER. CHOKE FLANGE. SILVER PLATED. BROAD BAND .... $49.50 EACH
WAVEGUIDE DIRECTIONAL COUPLER. 27 db. Navy type CABV-47AAN, with 4 in. slotted section $42.50
SQ. FLANGE to rd choke adapter, 18 in. long OA 1½ in. x 3 in. guide, type "N" output and sampling probe $32.00

10 cm. waveguide to ⅞" rigid coax doorknob transition, 21" high with 8" slotted section .... $52.50 ea.
10 cm. flexible section 4 feet long .... $42.50 ea.
10 CM. FLANGES, UG65/U $8.50
UG65/U 10 CM. FLANGE $8.50
ADAPTER 1½ x 3 TO 1" x 2". SQ. 10 CM FLANGE TO SQ 5 CM CHOKE $57.50
KLYSTRON MOUNT W/TUNABLE MATCHING OUTPUT TO TYPE "N" CONNECTOR SOCKET & TUBE CLAMP INCLUDED $12.50
"S" BAND CRYSTAL MOUNT, gold plated, with 2 type "N" connectors $12.50
PICKUP LOOP, Type "N" Output $2.75
TR BOX Pick-up Loop $1.25
POWER SPLITTER: 726 Klystron input, dual "N" output $5.00
MAGNETRON TO WAVEGUIDE coupler with 721-A duplexer cavity, gold plated $27.50
10 CM WAVEGUIDE SWITCHING UNIT, switches 1 input to any of 3 outputs. Standard 1½" x 3" guide with square flanges. Complete with 115 vac or dc arranged switching motor. Mfg. Raytheon. CRP 24AAS. New and complete $150.00
10 CM END-FIRE ARRAY POLYRODS .... $1.75 ea.
"S" BAND Mixer Assembly, with crystal mount, pick-up loop, tunable output $3.00
721-A TR CAVITY WITH TUBE. Complete with tuning plungers $12.50
10 CM McNALLY CAVITY Type SG $3.50
WAVEGUIDE SECTION, MC 445A, rt. angle bend. 5½" ft. OA. 8" slotted section $21.00
10 CM OSC. PICKUP LOOP, with male Home-dell output $2.00
10 CM DIPOLE WITH REFLECTOR in lucite ball, with type "N" or Sperry fitting $4.50
10 CM FEEDBACK DIPOLE ANTENNA, in lucite ball, for use with parabola ⅞" Rigid Coax Input $8.00
PHASE SHIFTER. 10 CM WAVEGUIDE. WE TYPE ES-683816. E PLANE TO H PLANE MATCHING SLUGS $95.00
721A TR cavities. Heavy silver plated .... $2.00 ea.
10 cm. horn and rotating joint assembly, gold plated .... $65.00 ea.
10 cm. right angle bend "E" or "H" plane, less flanges .... $17.50 ea.

⅞" RIGID COAX—¼" I.C.

⅞" RIGID COAX. Bead Supported $1.20
SHORT RIGHT ANGLE BEND $2.50
Rotating joint, with deck mounting $15.00
RIGID COAX, slotted section CU-60/AP $5.00
"S" BAND "Y" JUNCTION. SQ. FLANGES $65.00

⅞" RIGID COAX—⅜" I.C.

⅞" RIGID COAX ROTARY JOINT. PRESSURIZED. SPERRY #810613. GOLD PLATED $27.50
Dipole assembly. Part of SCR 584 .... $25.00 ea.
Rotary joint. Part of SCR-584 .... $35.00 ea.
RIGHT ANGLE BEND, with flexible coax output pick-up loop $8.00
SHORT RIGHT ANGLE bend, with pressurizing nipple $3.00
RIGID COAX to flex coax connector $3.50
STUB-SUPPORTED RIGID COAX, gold plated 5' lengths. Per length $5.00
RT. ANGLES for above $2.50
RT. ANGLE BEND 15" L. OA $3.50
FLEXIBLE SECTION. 15" L. Male to female $4.25
MAGNETRON COUPLING to ⅞" rigid coax, with TR pickup loop, gold plated $7.50
FLEX COAX SECT. Approx. 30 ft. $16.50

MISCELLANEOUS

Type "N" patching cord UG11/U female to UG9/U using RG5/U cable 12" long .... $2.25 ea.
AN/TPS-1B flanged nipple and insert assembly for rotary coupling .... $3.75 ea.
Pulse connector Navy type 49579 .... $1.50 ea.
Transmission line pressure gauge, 2" 15 lbs. .... $1.85 ea.
Pulse cable assembly Western Electric type D163262. 10 feet long .... $4.50 ea.
Holmdell Jack Western Electric #8O-12962-1 D.B. #J-102X .... $3.75 ea.
Adaptor type "N" RG8/U to RG17/U or 18/U cable .... $4.50 ea.
ADAPTER TYPE "N" TO RG-17/U CONNECTOR $5.50
F-29/SPR-2 HIGH PASS FILTER P/O AN/APR-5AX. TYPE "N" CONNECTORS $12.50
Magnetron coupling to ⅝ rigid coax .... $5.00 ea.
Hand pumps for pressurizing transmission line with humidity indicator .... $12.50 ea.

MARINE RADAR

SO-1 AND SO-8 RADAR SETS, Complete, in Used but Excellent Condition. 10 CM Surface Search using 2J26 or 2J27 Magnetron, 707B Mixer. PPI Indicator. Input 115VDC. Used on Merchant Ships throughout the world. FCC Approved. Guaranteed. $1250.00.

TEST EQUIPMENT

TS-268/U crystal test set for checking 1N21, 1N21A, 1N21B, 1N23, 1N23A, 1N23B crystals. New $35.00
TS-117GP 10 CM WAVEMETER TEST SET. Mfg. "Sperry". 2400-3400 MC. Micrometer Adj. Coaxial Cavity. Freq. Meas by absorption or transmission method. Mounts Crystal Current Meter & Calib. Chart $145.00
VSWR AMPLIFIER TS-12/AP. Unit 1 3 stages of Amplif. and Diode Rectifier w/direct VSWR. reading on meter. 115 volts 60 cyc. AC operation w/Inst. BK and CCT diag. New $235.00
SLOTTED LINE PROBE and Matched Termination incld'g Accessories TS-12/AP Unit 2 incl. UG81/U, CG92/U, CG91/U, CG89/U, UG79/U, CG87/U, MX158/U, CG-88/U, CG/90U, UG/80U plus Tools. New $135.00
COMPLETE TS-12/AP UNITS 1 AND 2 .... $350.00
10 CM ECHO BOX CABV 14ABA-1 of OBU-3. 2890 MC to 3170 MCS. direct reading micrometer head. Ring prediction scale plus 9% to minus 9%. Type "N" input. Resonance indicator meter. New and Comp. w/access. Box and 10 CM Directional Coupler $350.00
3 CM RECEIVER. SO-3. Complete with W.G. Mixer Assy (723 A/B) Reg. Fil. Power Supply, 6 Stages IF (6AC7) $99.50
10 cm. horn assembly consisting of two 5" dishes with dipoles feeding single type "N" output. Includes UG28/U type "N" "T" junction and type "N" pickup probe. Mfg. Bernard Rice, RGH/U cable. New .... $15.50 ea.
10 cm. cavity type wavemeters 6" deep 6¼" in diameter. Coax. output. Silver plated .... $64.50 ea.
10 cm. echo box. Part of SF-1 Radar with 115 volt DC tuning motor Sub Sig 1118A $47.50 ea.
TS33AP WAVEMETER. MICROMETER ADJ. TYPE "N" FITTINGS $125.00
THERMISTOR BRIDGE: Power meter 1-203-A. 10 cm. mfg. W.E. Complete with meter, interpolation chart, portable carrying case $72.50
W. E. I. 138. Signal generator. 2700 to 2900 Mc. range. Lighthouse tube oscillator with attenuator & output meter. 115 VAC input, reg. Pwr. supply. With circuit diagram $50.00
3 cm. Wavemeter: 9200 to 11,000 mc. transmission type with square flanges $15.00
3 cm. stabilizer cavity, transmission type $20.00
3 cm. Wavemeter, Micrometer head mounted on X-Band guide. Freq. range approx. 7900 to 10,000 Mc $75.00
TS-238 GP. 10 cm. Echo box with resonance indicator and micrometer adjust cavity, 2700 to 2900 Mcs calibrated as shown $85.00
Bell Labs. Dual Mount mixer-beacon assemblies. 2 complete mixer-beacon mounts on gold plated waveguide section $50.00
"X" band klystron mount, shielded with rough attenuator output $65.00
TS-108A/P DUMMY LOAD $65.00
3 CM. HORN AT-48/UP Model 710. Type "N" input. Hvy. Silver Plated $6.50

MICROWAVE ANTENNAS

SO-3 RADAR 3 CM. SURFACE SEARCH ANTENNA. Complete with 24 VDC Drive Motor, Selsyn, Gear Mechanisms, "X" Band Slotted "Peel" Reflector. Less Plumbing $135.00
As Shown
APS-15 Antennas. New $99.50
AN MPG-1 Antenna. Rotary feed type high speed scanner antenna assembly, including horn parabolic reflector. Less internal mechanisms. 10 deg. sector scan. Approx. 12'L x 4'W x 3'H Unused. (Gov't Cost—$4500.00) $250.00
APS-4 3 cm. antenna. Complete. 14½ dish. Cutler feed dipole directional coupler, all standard 1" x ½" waveguide. Drive motor and gear mechanisms for horizontal and vertical scan. New, complete $65.00
AN/TPS3. Parabolic dish type reflector approx. 10' diam. Extremely lightweight construction. New in 3 carrying cases $89.50
RELAY SYSTEM PARABOLIC REFLECTORS: approx. range: 2000 to 6000 mc. Dimensions: 4' x 3' rectangle, now $35.00
TDY "JAM" RADAR ROTATING ANTENNA. 10 cm. 30 deg. beam. 115 v.a.c. drive. New $100.00
SO-13 ANTENNA, 24" dish with feedback dipole 360 deg. rotation, complete with drive motor and selsyn. New $128.00
Used $45.00
DBM ANTENNA. Dual, back-to-back parabolas with dipoles. Freq. coverage 1,000-4,500 mc. No drive mechanism $65.00
AS125/APR Cone type receiving antenna, 1080 to 3208 megacycles. New $4.50
140-600 MC. CONE type antenna, complete with 25' sectional steel mast, guys, cables, carrying case, etc. New $49.50
ASD 3 cm. antenna, used, ex. cond. $49.50
YAGI ANTENNA AS-46A. APG-4, 5 elements .... $14.50 ea.

R. F. EQUIPMENT

LHTR. LIGHTHOUSE ASSEMBLY. Part of RT-39/APG-5 & APG-15. Receiver and Transmitter Lighthouse Cavities with assoc. Tr. Cavity and Type N CPLG. To Rcvr. Uses 2C40, 2C43, 1B27. Tuneable APX 2400-2700 MCS. Silver plated $49.50
Receiver transmitter. Rt-39A/APG-5 10 cm. gun laying RF package using 2C40 and 2C43, new .... $150.00 ea.
APS-2 10CM RF HEAD COMPLETE WITH HARD TUBE (715B) Pulser, 714 Magnetron 417A Mixer all ⅞" rigid coax, incl. rcvr. front end $210.00
Beacon lighthouse cavity 10 cm with miniature 28 volt DC FM motor. Mfg. Bernard Rice .... $47.50 ea.
T-128/APN-19 10 cm. radar Beacon transmitter package, used, less tubes .... $59.50 ea.
SO-3 "X" banc 3 cm RF package, new complete, including receiver unit as illustrated on Page 337, Volume 23 RAD LAB Series .... $375.00 ea.
Pre-amplifier cavities type "M" 7410590GL to use 446A lighthouse tube. Completely tunable. Heavy silver plated construction .... $37.50 ea.
RT32/APS 6A RF HEAD. Compl. with 725A Magnetron magnet pulse xfmr. TRA-ATR. 723 A/B local osc. and beacon mount, pre amplifier. Used but exc. cond. $97.50
AN/APS-15A "X" Band compl. RF head and modulator, incl. 725-A magnetron and magnet, two 723A/B klystrons (local osc. & beacon), 1B24, TR, rcvr-ampl. duplexer, HV supply, blower, pulse xtmr. Peak-Pwr Out: 45 KW apx. Input: 115, 400 cy. Modulator pulse duration .5 to 2 micro-sec. apx. 13 KV Pk Pulse. Compl. with all tubes incl. 715-B, 829B, RKR 73, two 72's. Compl. pkg., new $210.00
APS-15B. Complete pkg. as above, less modulator $150.00
"S"BAND AN/APS-2. Complete RF head and modulator, including magnetron and magnet, 417-A mixer, TR, receiver, duplexer, blower, etc., and complete pulser. With tubes, used, fair condition $75.00
10 CM, RF Package. Consists of: SO Xmtr.-receiver using 2J27 magnetron oscillator, 250 KW peak input. 707-B receiver-mixer $150.00

WRITE FOR LATEST FLYER!

ALL MERCHANDISE GUARANTEED. MAIL ORDERS PROMPTLY FILLED. ALL PRICES F.O.B. NEW YORK CITY. SEND MONEY ORDER OR CHECK ONLY. SHIPPING CHARGES SENT C.O.D. RATED CONCERNS SEND P. O. MERCHANDISE SUBJECT TO PRIOR SALE

COMMUNICATIONS EQUIPMENT CO.

131 "I 8" Liberty St., New York, N.Y.

Cable "Comsupo" Ph. Digby 9-4124

MEMBERSHIP

(Continued from page 44A)

Neilsen, I. R., Microwave Laboratory, Stanford University, Stanford, Calif.
Palmer, C. E., Jr. 1039 Investment Bldg., 15 & K Sts., N.W., Washington 5, D. C.
Platter, A. V., R.D. 1, Salt Point Rd., Poughkeepsie, N. Y.
Pope, L. A., 6040 N. Winthrop, Chicago 40, Ill.
Prouty, G. S., Jr., Wauwinet House, Nantucket Island, Mass.
Rayasa, N. G., Asst. Works Manager, Indian Ordnance Service, Gun Carriage Factory, Jubbulpore, C.P., India
Rayasa, R. G., Radio Sonde Section Observatory, Lodi Rd., New Delhi, India
Robinson, T., 15392 12 Detroit 3, Mich.
Rous, W. H., 1830 S. 54 Ave., Cicero 50, Ill.
Seaton, A. F., 1126 W. 17 St., Los Angeles 15, Calif.
Seid, E., 3011 Fourth Ave., Los Angeles 16, Calif.
Squires, C., 36 Bedford Park Blvd., New York 58, N. Y.
Steward, R. H., 315 Second St., Angola, Ind.
Stimson, R. L., 318 Rockdale Ave., Cincinnati 29, Ohio
Stone, P. E., Lendrick, 45 St. Mark's Crescent, Maidenhead, Berks., England
Taylor, A. D., Shell Oil Company, Inc., 3737 Bellaire Blvd., Houston 5, Tex.
Taylor, E. S., 227 E. 57 St., New York 22, N. Y.
Underberger, G. M., 1819 Cota Ave., Long Beach, Calif.
Valentine, P. T., 250 Myrtle Ave., Boonton, N. J.
Weiss, S. B., Hq. 1804 AACS Group, APO 942, c/o Postmaster, Seattle, Wash.
Welch, C. A., 3778 St. Johns Terr., Cincinnati, Ohio
Willson, W. C., Jr., Radio Station KCLO, Leavenworth, Kan.
Yashin, N., 9524 Dungan Rd., Bustleton, Philadelphia 15, Pa.

The following transfers to the Associate grade were approved to be effective as of May 1, 1949:

Arfin, B., 2088 Mohegan Ave., New York 60, N. Y
Austin, C. S., 3 Remington St., Dorchester 24, Mass
Brooks, R. W., c/o Engineering Department, Barber-Colman Co., Rockford, Ill.
Ellowitz, H. I., 38-3 Garden Circle, Waltham, Mass.
Fairbanks, L. F., 11 Everett St., East Boston 28, Mass.
Farrell, C., BOQ Bldg. 600, Naval Air Station, Pensacola, Fla.
Fowler, B. V., 159 Osage Alley, San Francisco 10 Calif.
Fristensky, C. A., 802 Prospect Ave., Ridgefield, N. J.
Gardener, G. F., 214 Maple Ave., Hollidaysburg, Pa.
Goldfisher, J., 5629 North 16 St., Philadelphia 41, Pa.
Hanft, H., 711 New Jersey Ave., Brooklyn 7, N. Y.
Hansen, R. C., 809 South Fifth St., Champaign, Ill.
Helgeson, W. B., General Electric Co., 2231 E. State St., Trenton 9, N. J.
Jacob, F. C., 48 College Park, Davis, Calif.
Lethin, J. E., 702 Orange St., New Haven, Conn.
Moore, S. F., 637 Sixth St., Huntington, W. Va.
Morita, T., 92 Beals St., Brookline, Mass.
Naylor, A. F., 147-D Wallworth Park, Haddonfield, N. J.
Nemcovsky, R., R.F.D. 1, East Haddam, Conn.
Neubert, H. A., Jr., 414 Morris St., Woodbury, N. J.
Novick, G., 768 Rockaway Ave., Brooklyn 12, N. Y.
Portz, G., 2633 First Private Rd., Flossmoor, Ill.
Quateman, M. H., 6151 N. Winthrop Ave., Chicago 40, Ill.

(Continued on page 49A)

NEW! small

d-c capacitors for use in ambient temperatures up to 125°C

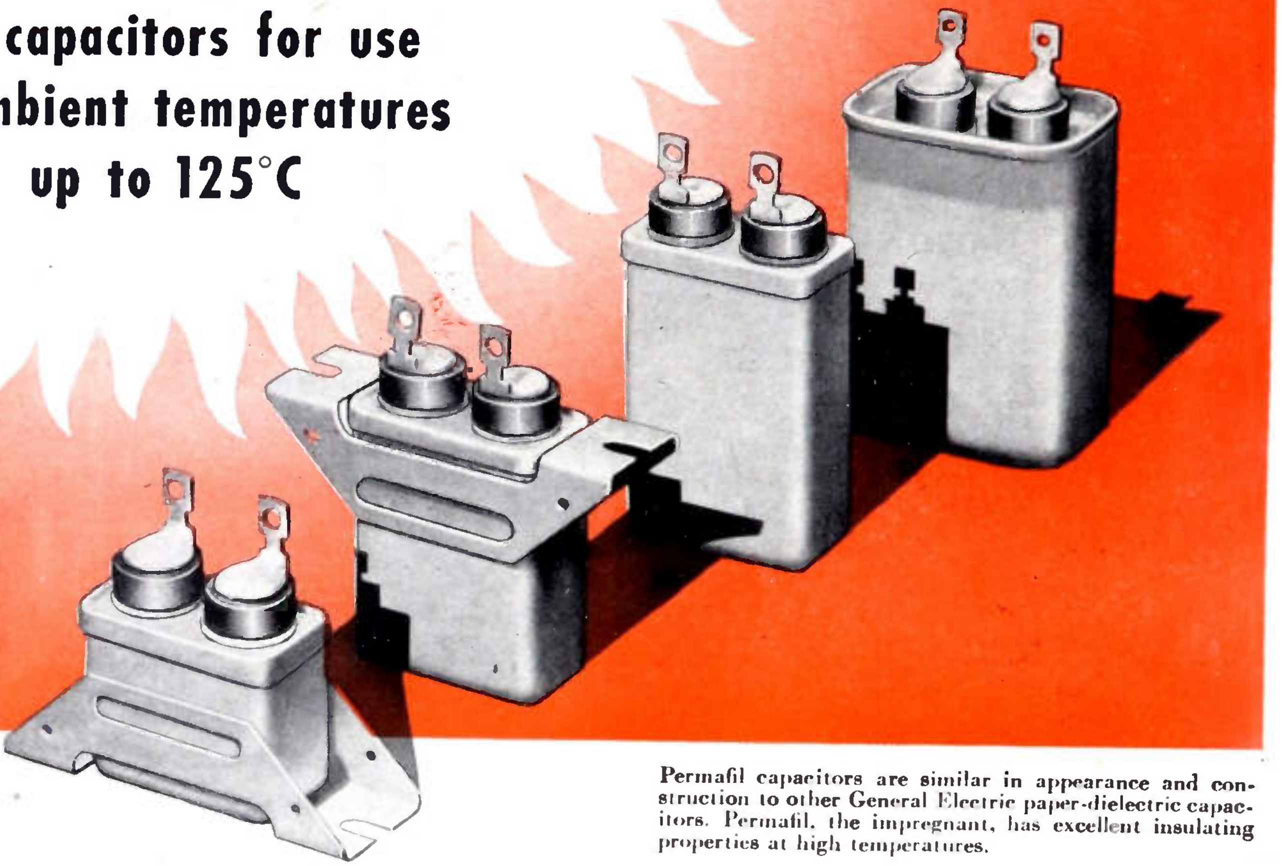

Permafil capacitors are similar in appearance and construction to other General Electric paper-dielectric capacitors. Permafil, the impregnant, has excellent insulating properties at high temperatures.

General Electric announces a new line of Permafil d-c paper-dielectric capacitors designed especially for operation in high ambient temperatures. They require no derating for temperatures up to 100°C and can be used up to 125°C.

Hermetically sealed in metallic containers, these new units are available in case styles 61, 63, 65 and 70, as covered by Joint Army-Navy Specifications JAN-25-C, in ratings of 0.10 to 4.0 muf 600-, 1000- and 1500-volts. Permanently sealed silicone bushings are provided on all types.

Permafil capacitors were developed to provide suitable components for the many new applications involving continual operation at ambient temperatures above 85°C—another example of capacitors "designed for the job" by G-E engineers. For further information on these or on capacitors for other applications, write *Capacitor Sales Division, General Electric Company, Pittsfield, Mass.*

GENERAL ELECTRIC

407-162

Specialty Capacitors FOR

- Motors
- Luminous-tube transformers
- Fluorescent lamp ballasts
- Industrial control
- Radio filters
- Radar
- Electronic equipment
- Communication systems
- Capacitor discharge welding
- Flash photography
- Stroboscopic equipment
- Television
- Dust precipitators
- Radio interference suppression
- Impulse generators

AND MANY OTHER APPLICATIONS

MEMBERSHIP

(Continued from page 47A)

Shelton, J. T., 1507 10 St., Alamogordo, N. Mex.
Slaughter, J. E., 1715 Avenue B, Schenectady, N. Y.
Stanko, E. S., 828 Distel St., Detroit 9, Mich.
Verven, S. J., 50 Academy St., Poughkeepsie, N. Y.
Wagner, R., Jr., 422 Robeson St., Reading, Pa.
Winningstad, C. N., 706 56 St., Oakland 9, Calif.
Zimmerman, R. L., 3243 Sepulveda Blvd., Los Angeles 34, Calif.

The following transfers to the Associate grade were approved to be effective as of June 1, 1949:

Albin, F. I., 44 Totten Pl., Babylon, L. I., N. Y.
Anderson, F. J., 824 Beacon St., Boston, Mass.
Babbitz, H. B., Philco TECH. REP., BOQ Bldg. 256, U. S. Naval Station, San Diego 36, Calif.
Day, L. R., 112 Harding Rd., Red Bank, N. J.
Dosch, T. J., 3417 Tibbett Ave., New York 63, N. Y.
Folsom, W. A., 263 Harvard St., Cambridge 39, Mass.
Gilbertson, S. R., 5556 17 Ave. St., Seattle 8, Wash.
Hammack, J. W., 2507 Locust St., Texarkana, Ark.
Hegar, D. T., 718 S. First St., Temple, Tex.
Hutto, J. T., 2040 Peachtree Rd., Apt. B-2, Atlanta, Ga.
Jacobson, H. P., Jr., Radio Station HCJB, Casilla 691, Quito, Ecuador, S. A.
Jain, P. L., 45 River Dr., Passaic, N. J.
Kilpatrick, J. R., 1471 Rose Ave., Long Beach 13, Calif.
Kress, O. C., 721 Wellmeier Ave., Dayton 10, Ohio
Lindner, N. J., 85 Von Reypen St., Jersey City 6, N. J.
Mueller, R. P., Physics Research Laboratory, University of Illinois, Champaign, Ill.
Pierce, E. W., 516 Eastern Ave., Toledo 9, Ohio
Rickert, H. H., 57 Grace Ave., Great Neck, L. I., N. Y.
Roberts, B. J., 1648 S. 160 St., Seattle 88, Wash.
Schauer, J. D., 408 S. Cornell, Albuquerque, N. Mex.
Schmidt, D. P., Pyle National Co., 1334 N. Kostner Ave., Chicago 51, Ill.
Shapiro, H., 2128 Cleveland Ave., Chicago 14, Ill.
Sherman, S., 1886 Harrison Ave., New York 53, N. Y.
Smith, J. S., 302 Shaver Ave., N. Syracuse, N. Y.
Somerville, J. R., Jr., 511 Griffith Ave., Owensboro, Ky.
Studnicka, G. J., 8866 Burnette, Detroit 4, Mich.
Thompson, C. G., American Telephone & Telegraph Co., District Office 4100, Bryan St., Dallas, Tex.
Weaver, J. A. c/o Sohio Pipe Line Co., 407 North Eighth St., P.O. D-15, St. Louis 1, Mo.
Wolff, R. E., 5616 N. Wayne Ave., Chicago 40, Ill.
Zeines, B., 645 Barretto St., New York 59, N. Y.

POSITIONS OPEN

The following positions of interest to I.R.E. members have been reported as open. Apply in writing, addressing reply to company mentioned or to Box No. . . . .

The Institute reserves the right to refuse any announcement without giving a reason for the refusal.

PROCEEDINGS of the I.R.E.
1 East 79th St., New York 21, N.Y.

ELECTRONICS TEACHER

Electronics Teacher to take charge of electronics option at accredited state land grant college in Northwest. Salary to $4800.00 for nine months. Write giving picture, education, experience, references, and complete personal data to Box 572.

ELECTRICAL ENGINEER—PHYSICIST

Graduate electrical engineer or physicist experienced on microwaves and servomechanism for design and layout of electronic circuits. Write Chance Vought Aircraft, Division United Aircraft Corp., Box 5907, Dallas, Texas.

INSTRUCTOR

There will be an opening in September for an instructor to teach electronics, transmission line and waveguide theory. Salary depends on qualifications and is up to $5600.00 for nine months. Possibility of later appointment at lower rank and salary. Box 573.

ELECTRONIC ENGINEERS—RESEARCH ANALYST

Research and development positions open at Army Security Agency, Washington 25, D.C., in the field of electronics and mathematics. B.S. degree in appropriate field from an accredited university necessary. Salaries for electronics engineers—P-1, $2974.80 to P-3, $4479.60 per annum. Salaries for research analysts are P-1, $2974.80 and P-2, $3727.20 per annum. Positions are permanent in so far as the Agency is concerned. Those qualified communicate immediately with Chief, Army Security Agency, CSGAS-61, The Pentagon, Washington 25, D.C.

ENGINEER

Large active midwestern quartz crystal plant needs first class quartz crystal engineer, well grounded in theory and with complete experience in manufacturing and testing procedures all types quartz units. Send complete detailed information on experience and background in first reply. Salary open. Our employees know of this ad. Box 574.

TECHNICAL WRITER

An opportunity for an experienced technical writer. Preferably an electrical engineering graduate with experience in the field of electronic development. Research laboratory located adjacent to Washington, D.C. Salary commensurate with experience. Box 576.

ENGINEER

Excellent opportunity for a man with experience in servo mechanisms and cir-

(Continued on page 51A)

POSITIONS OPEN

(Continued from page 50A)

cuit theory work. Opportunity for graduate work available. Write Box 30, State College, Pennsylvania.

DEVELOPMENT PHYSICIST ENGINEER

Experienced in theory, design and construction of attenuators, D. C. to 3 KMC. and associated test equipment, well versed in physics, chemistry and application of conductive films, operation of power tools, advanced mathematics. Write giving complete education and experience to Weinschel Engineering Co., 123 William Street, New York 7, New York.

★ ★ ★ ★

Positions Wanted By Armed Forces Veterans

In order to give a reasonably equal opportunity to all applicants, and to avoid overcrowding of the corresponding column, the following rules have been adopted:

The Institute publishes free of charge notices of positions wanted by I.R.E. members who are now in the Service or have received an honorable discharge. Such notices should not have more than five lines. They may be inserted only after a lapse of one month or more following a previous insertion and the maximum number of insertions is three per year. The Institute necessarily reserves the right to decline any announcement without assignment of reason.

ELECTRICAL ENGINEER

16 years experience in design, development, research in connection with electronic and electrical components such as capacitors and transformers. Desires location in New York City or immediate vicinity. B.E.E. degree and 3 years graduate work. Box 283 W.

ENGINEER

B.E., E.E. major, University of Toledo, graduated June 1949. Age 32. Single. Technical experience Air Force communications and navigation aids. Desires position in electronics anywhere in U. S. Box 284 W.

ELECTRONICS ENGINEER

Graduated June 1949, Polytechnic Institute of Brooklyn, B.E.E. in electronics. Member Tau Beta Pi, Eta Kappa Nu. Married. Age 22. Electronics experience in Navy. Desires position in electronic development or production. Prefer East Coast. Box 285 W.

JUNIOR ENGINEER

B.E.E., University of Louisville, June 1949. Age 26, married, one child. First phone and Class A amateur licenses. Some teaching and broadcast experience. 3 years in Army radio intelligence. Desires position in radio or T. V. research and design. Box 286 W.

(Continued on page 52A)

Positions Wanted

(Continued from page 51A)

BROADCAST ENGINEER

Specializing in broadcast station construction. 20 years experience in broadcasting and aviation radio. History and picture sent on request. Go anywhere. T. L. Kidd, P. O. Box 866, Fredericksburg, Texas.

SENIOR ENGINEER

B.S.E.E. 8 years experience. Army electronics training at Harvard, and M.I.T. Research at Radiation Laboratory, M.I.T. Radar project officer Aircraft Radio Laboratory, Wright Field. Postwar electronic research engineer. Also broadcast installation, operation, and maintenance experience. Married, children, require family housing. Prefer west, southwest, middlewest. Box 287 W.

JUNIOR ENGINEER

B.E.E. University of Louisville 1946. M.A. in mathematics. University of Michigan 1948. Age 24. Experience in telegraphy and amateur radio. Desires position in electronics and communications. Box 288 W.

ELECTRONIC ENGINEER

M.E.E. expected August 1949 Polytechnic Institute of Brooklyn. B.E.E. Cooper Union. Age 24. 2 years as electronic technician U.S.N. 1½ years design and development of radar receivers and microwave components. Prefer position in vicinity of New York City. Box 289 W.

(Continued on page 54A)

LOCKHEED
AIRCRAFT CORPORATION
has positions available
for
RESEARCH ENGINEERS in PHYSICS and ELECTRONICS

These openings are for men who have achieved advance status as researchers in either of these fields and who possess the following qualifications:

1. Advanced degree (preferably Ph.D.);
2. 7-10 years industrial or graduate research experience;
3. Ability to perform mathematical analysis in field of specialization.

Lockheed's research and development facilities are among the most advanced in the aircraft field. The accomplishments of Lockheed's research staff have resulted in the acquisition of new far reaching scientific studies.

Immediate openings available. Salary commensurate with ability.

If you are interested, and meet the qualifications listed above, send a resume of your training and experience to—

LOCKHEED AIRCRAFT CORPORATION
Employment Manager
Post Office Box 551
BURBANK, CALIFORNIA

Your Best Buy!

DU MONT Type 16FP4

Fully in keeping with the trend towards larger, direct-viewing tubes originally pioneered by Dr. Allen B. Du Mont—and also the lower price range for higher grade TV offerings.

Type 16FP4 is a 16-inch magnetic focus and deflection television picture tube designed to give high brilliance and sharp definition. Electron gun design utilizes a bent electrode structure to be used with a single external magnet for the elimination of ion spot blemishes. The exclusive Du Mont screen depositing technique assures the longest pleasurable usage.

CHECK LIST OF 16FP4 ADVANTAGES...

- All glass! No mounting problems.
- A mass-produced standard TV tube for maximum value at minimum cost.
- Overall length of only 20¼ inches.
- Deflection angle: 62°.
- Maximum diameter: 16⅛ inch ± ⅛ inch.
- Bent-gun ion trap requiring but a single magnet.
- Accelerating potential: Maximum 16 KV; (Design Center Value).
- New type small shell duodecal 5-pin instead of 7-pin base, for use with economical half-socket.
- Ideal compromise between large picture size and moderate tube cost.

Detailed Specifications on request. Let us quote on quantity requirements.

FIRST WITH THE FINEST IN TELEVISION TUBES

DUMONT *Teletrons*

ALLEN B. DU MONT LABORATORIES, INC., TUBE DIVISION, PASSAIC, N. J.

Positions Wanted

(*Continued from page 52A*)

ELECTRONIC ENGINEER

B.E.E. 1946. Age 24. 2½ years varied electronic experience including radar development work. Desires electronic development work in New York City area. Box 290 W.

JUNIOR ENGINEER

B.S.E.E. 1948 University of Illinois. Age 23. Married. Specialized training in television at RCA Institutes. One year experience commercial television receiver servicing. Desires position as research or development engineer. First class radiotelephone license. Box 291 W.

JUNIOR ENGINEER

Graduated June 1949 from Manhattan College with a B.E.E. degree. 2 years training and experience as Radio-Mechanic-Gunner in the AAF. Age 26, single. Desires employment as electrical or electronic engineer particularly in the television field, anywhere in the U. S. Box 292 W.

ENGINEER—MATHEMATICIAN

M.E.E.; B.S.E.E. (communications). G.S.E. mathematics 1 year research in magnetic amplifiers Fluent knowledge of German. Age 25, married, no children. Desires research or development in magnetic amplifiers, mathematical design, engineering mathematics instructorship, or technical writing. Available September 1949. New York City or vicinity preferred. Box 293 W.

(*Continued on page 56A*)

SUPERINTENDENT *for* ELECTRONICS LABORATORY

Qualifications Required

Post graduate training to Ph.D. level or equivalent, British Subject. Considerable experience in directing research or development groups in one or more of the following or related fields: Communications, Radar, Radio Engineering, Servomechanisms.

Salary

The appointment will be made in one of the following grades, commensurate with experience and ability. \$6,800-\$7,300; \$7,300-\$7,800; \$7,500-\$8,000.

Apply to—Director of Research Personnel, Defence Research Board, Department of National Defence, Ottawa, Canada.

Positions Wanted

(Continued from page 54A)

TECHNICAL WRITER—COMMUNICATIONS ENGINEER

Technical writer-communications engineer, Military Intelligence Service officer, B.S.R.E. licensed FCC, 1st class phone, amateur radio. Experienced in mobile radio telephony, X-ray, export trade. Speaks fluently French and Spanish. Desires position in same or allied fields. Box 294 W.

ELECTRONIC PHYSICIST

B.A., M.A., in Physics, Harvard-M.I.T. Radar School. Radar officer 3 years. Now studying for Ph.D. at Harvard in engineering sciences. Age 28, married, 2 children. Desires research in electron physics. Box 295 W.

ELECTRONIC ENGINEER

Stanford University, B.S.E.E., communications major. Age 24. 1 year broadcasting, 2 years navy electronics experience. 1st class license. Prefer position in broadcasting or electronic development and production. Box 296 W.

SALES ENGINEER

Desires selling or distributing products of electronic industries. Graduate of RCA Institutes, education at Bowdoin College, Harvard and M.I.T. in radio engineering. Holder of all FCC commercial radio licenses. 7 years experience in industry. Presently on staff of a state college. Box 297 W.

SALES ENGINEER

B.S. in G.E., Naval Academy. One year P. G. in applied communications. Five years Naval experience as radar, radio and communication officer. Telephone, electrical design and production experience. Extensive background in electrical and electronic equipment. Widely traveled with positive aggressiveness and firmly settled on a sales career. Age 32. Married. Box 311 W.

TELEVISION ENGINEER

B.S.T.E., May 1949, American Television Institute of Technology, age 29, married. 3 years communication maintenance U. S. Marine Corps. 2 years U. S. Border Patrol radio laboratories. 7 years bench and field electronics. 1st class FCC license. At present engaged in post graduate work on micro-waves. Desires position in electronic laboratory or TV station engineer. Locate anywhere. Resume upon request. Box 312 W.

TECHNICAL WRITER

B.S.E.E. September 1949, Lawrence Institute of Technology. Honor graduate with aptitude for technical writing. Managing editor college newspaper, instructor in radar electronics in Air Corps. Box 313 W.

RADIO (BROADCAST) ENGINEER

B.S.E.E. 1939. Over 5 years' experience in broadcast work includes AM, FM, Television, 50kw. transmitters. Last position chief engineer construction large station with complex directional antenna. Signal Corps radar staff officer during war. Box 314 W.

(Continued on page 58A)

DC AMPLIFIER

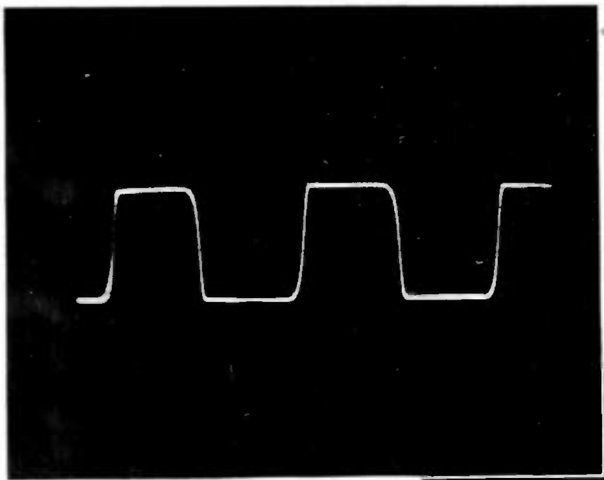

INPUT 70 KC

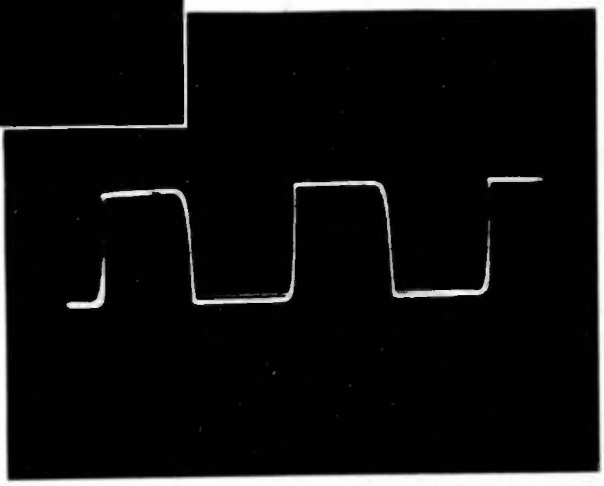

OUTPUT 70 KC

ELECTRO-MECHANICAL RESEARCH INC
EMR
RIDGEFIELD, CONN

- STABLE
- WIDE BAND
- HIGH GAIN
- NO OVERSHOOT
- LOW OUTPUT IMPEDANCE
- LARGE OUTPUT VOLTAGE SWING
- HIGH INPUT IMPEDANCE
- FOUR STAGES PLUS CATHODE FOLLOWER
- DC CALIBRATING SIGNAL
- DC OUTPUT VOLTMETER
- COMPACT
- ECONOMICAL

This new moderately-priced DC Amplifier combines a great number of desirable features. Designed for minimum overshoot, rather than maximum band width, it is, nevertheless, useful for steady-state operation at frequencies up to 1.5 megacycles. The response to steep wave fronts is excellent, as indicated by the above photographs. Balanced or unbalanced outputs may be used as desired. There is no need to compensate for a fixed dc voltage between output terminals and chassis, since the output is at ground potential. An undistorted voltage swing of 220 volts peak-to-peak makes it possible to obtain large patterns on a cathode ray tube connected directly to the amplifier output. On the other hand, a peak power of a watt into 6000 ohms, together with a low effective output impedance, make the amplifier useful for driving a variety of devices. An exceptionally well-regulated power supply furnishes plate power to all stages except the cathode-follower output, and heater power to the first three stages. This, together with careful circuit design, reduces the drift to the order of 0.5 millivolts per hour, after a 30-minute warm up. A low capacity input cable and probe make connection to driving circuits convenient, and reduce the danger of feedback between external elements connected to input and output. This amplifier offers the circuit engineer a new tool of unusual scope and versatility.

Voltage Gain: 6000.

Rise Time: 0.4 microseconds.

Stability: Drift is usually less than 0.5 millivolts per hour referred to the input, after 30-minute warm up.

Voltmeter and Calibrating Signal: A zero center voltmeter of ±15, 50 and 150 volts is provided for measuring dc output. Associated with this meter is a calibrating signal circuit for checking the gain.

Output Balanced: Internal impedance of 450 ohms. 220 volts peak-to-peak into a high impedance. Maximum undistorted output into 6000 ohms, 500 milliwatts ac, or 1 watt dc.

Output Unbalanced: Internal impedance of 450 ohms. 110 volts peak-to-peak into a high impedance. Maximum undistorted output into 3000 ohms, 250 milliwatts ac, or 500 milliwatts dc.

Input: Unbalanced. 1 megohm shunted by 40 μμf maximum. This includes capacitance of the flexible input cable.

Gain Control: Continuously variable over a range of 11 db, plus six 10 db steps.

Shock Proofing: The first two stages are mounted on a spring suspended chassis, offering excellent protection against microphonics.

Cabinet Dimensions: 11" high x 17¼" wide x 13¼" deep.

Power Supply: Approximately 300 watts of 60-cycle power is required.

ELECTRO-MECHANICAL RESEARCH, INC.
RIDGEFIELD, CONNECTICUT

Positions Wanted

(*Continued from page 56A*)

ENGINEER

MS Communications Engineering Harvard University February 1948. BS Physics, Harvard 1944. Married. 2 years communications officer U.S. Navy. 1 year experience electronic design. Desires position in New York area, electronic controls, computers or microwaves. Box 315 W.

ELECTRONIC ENGINEER

B.S.E.E. University of Connecticut. June 1949. Communications major. 3 years U.S.M.C. Radio Materiel School and experience as communication technician. Age 27. Married, no children. Desires position in electronic engineering. Prefer New England. Box 316 W.

ELECTRICAL ENGINEER

B.E.E. January 1949, City College of New York. Several months experience in psycho-acoustics and medical electronics in leading medical institutions. Will consider any offer in other fields. Box 317 W.

ELECTRONIC ENGINEER

Communications, B.E.E., recent graduate, ranked ninth, former Navy electronic technician; design, development, and research preferred. Anywhere in the U. S. Salary secondary. Box 318 W.

COMMUNICATIONS ENGINEER

B.S.E.E., December 1948, Michigan State College; age 24, married. 1 year electrical test equipment maintenance in Navy; experienced in audio and mobile high frequency communication. Desire position in development in west or southwest United States. Box 319 W.

ADMINISTRATIVE ENGINEER

Schools Harvard, NCE University of Dayton, Columbia and M.I.T. Ex-flying officer, industrial engineer with wide background in electronic research, development and production. Substantial experience in military UHF and aircraft development. Presently assistant to President of medium size concern. Desires industrial management or government contractual management position. Box 320 W.

JUNIOR ENGINEER

Honor graduate, B.S.E.E., June 1949. Age 26. University of Illinois. 4 years varied electronics experience with emphasis on radar and audio. Prefers electronic design and development position in New York City area. Box 324 W.

News—New Products

These manufacturers have invited PROCEEDINGS readers to write for literature and further technical information. Please mention your I.R.E. affiliation.

(*Continued from page 30A*)

RECENT CATALOGS

• • • The current issue of *Tracerlog*, which always contains articles of general interest to those engaged in utilizing radioactivity for research or industrial control problems, with a product listing and various other office addresses of **Tracerlab, Inc.**, 55 Oliver St., Boston 10, Mass.

(*Continued on page 60A*)

RCA scientists develop new *direct-reading* Loran instrument which simplifies problems of navigation.

The **homing pigeon** *goes to sea*

Now science gives the navigator an improved "homing pigeon instinct," a way which—without checking the sun or the stars—he can head his ship directly home.

Already thoroughly proved, *Loran equipment* has been simplified through RCA research and engineering, so that almost anyone can learn to use it in a few minutes. Free of human error, readings appear *directly* on the instrument. A quick check gives position.

Brain of this Loran system is a circuit developed at RCA Laboratories which splits seconds into millions of parts—and accurately measures the difference in the time it takes a pair of radio signals to travel from shore to ship.

Given this information, the navigator, hundreds of miles from shore, can determine his position quickly and accurately. Loran's simplicity adapts it to every type of vessel from merchant ship to yacht. Manufactured by Radiomarine Corporation of America, a service of RCA, it is already being installed in U. S. Coast Guard rescue ships.

The meaning of RCA research

RCA's contribution to the development of this new direct-reading Loran is another example of the continued leadership in science and engineering which adds *value beyond price* to any product or service of RCA.

* * *

The newest advances in television, radio, and electronics can be seen in action at RCA Exhibition Hall, 36 West 49th St., N. Y. Admission is free. Radio Corporation of America, RCA Building, Radio City, N. Y. 20.

RCA

RADIO CORPORATION of AMERICA

World Leader in Radio — First in Television

News—New Products

These manufacturers have invited PROCEEDINGS readers to write for literature and further technical information. Please mention your I.R.E. affiliation.

(Continued from page 58A)

New FM and TV Sweep Signal Generator

A new Model #SG, a sweep signal generator with a range from 0–227 Mc with no band switching, has been designed and developed by **Transvision, Inc.,** 385 North Ave., New Rochelle, N. Y.

The Model #SG has a sweep width from 0–12 Mc completely variable, and has a calibrated built-in marker generator.

The dial is calibrated in frequency. There is sufficient voltage output to permit stage-by-stage alignment. The crystal controlled output makes possible any crystal controlled frequency from 5–230 Mc. Unmodulated rf signal provides marker pips simultaneously with the main variable oscillator; these markers can be controlled as to output strength in the pip oscillator.

Magnetic Tape Recorder

A new magnetic tape recorder for studio and broadcast station use is being offered by **Presto Recording Corp.,** P.O. Box 500, Hackensack, N. J., plant, Paramus, N. J.

A desireable feature of this recorder is the accessability to all working parts. The entire top panel hinges upwards, so that the lower side may be easily serviced. Both

(Continued on page 61A)

News—New Products

These manufacturers have invited PROCEEDINGS readers to write for literature and further technical information. Please mention your I.R.E. affiliation.

(Continued from page 60A)

recording and playback amplifiers, as well as a separate regulator power supply, are vertically mounted on the front door of the cabinet. Access to both front and back of the amplifiers can be had without removal.

Keyboard-Type Oscillator

The Model 150-AO-1/100K Keyboard oscillator, improved and redesigned, is at present being marketed by **Weinschel Engineering Co.**, Dept. I., 123 William St., New York 7, N. Y.

This instrument covers a range from 0.3 cps to 100 kc with decades of push buttons. In both lower ranges frequency is selected with four decades of push buttons, and in the top range with three decades together with a continuous control which covers a deviation of approximately ±1 per cent.

Between 100 and 100,000 cps, frequency may be varied in steps smaller than 0.1 per cent. Between 10 and 100 kc in steps smaller than 1 per cent, however adjustment to 1 cps is obtainable.

Description: 19 inches long, 17½ inches high, and 13 inches deep. Weight, 29 lbs.; power supply, 105–125 volts, 50–60 cps.

Improved AF Measurement Equipment

The Model GA-1002A, sound pressure measurement equipment with major improvements which include a specially isolated socket tip which effectively separates the microphone clamping structure from the preamplifier extension tube, is being manufactured by **Massa Laboratories, Inc.**, 3868 Carnegie Ave., Cleveland 15, Ohio.

The M-101 standard microphone which is part of the equipment has also been redesigned to provide increased polar symmetry of the mechanical structure, resulting in exact acoustic symmetry about the normal axis of the microphone even at frequencies above 20 kc. The range of the

(Continued on page 62A)

News—New Products

These manufacturers have invited PROCEEDINGS readers to write for literature and further technical information. Please mention your I.R.E. affiliation.

(Continued from page 61A)

instrument is such that sound pressures from less than 1 dyne/cm² to 20,000 dynes/cm² (160 db level) may be directly measured. A multiplier is available for extending the upper range to 200,000 dynes/cm² (180 db level). A built-in calibrating circuit permits setting the system gain so that 1 millivolt/dyne/cm² is delivered across the 10,000 ohm output circuit.

New Interlocking Relay

A new interlocking relay, series 30500, consisting of two Type 2 Phil-trol relays, is the newest addition to the relays offered by **Phillips Control Corp.** 612 N. Michigan Ave., Chicago 11, Ill.

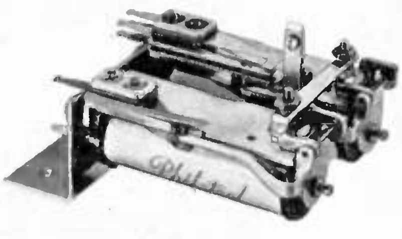

(Continued on page 64A)

News—New Products

These manufacturers have invited PROCEEDINGS readers to write for literature and further technical information. Please mention your I.R.E. affiliation.

(Continued from page 62A)

Interlocking relays may be furnished to operate on either ac or dc. When the lock-up relay is energized, it automatically locks in mechanically by means of a tension spring catch, which holds the armature in the energized position even though the circuit has been opened.

When the second relay, known as the release relay, is energized, the lock-up relay is automatically released from its mechanically held position. Other features are: relays may be equipped with as many as 12 springs; dc relays may be provided with copper slug coils, making them slow either to operate or release; contacts may be supplied either single or twin, and with contacts of various precious metals having ratings as high as 6 amperes, 110 volts ac, noninductive; relays may operate over a wide pressure range. A new descriptive catalog in color gives coil characteristics, contact assembly, and weight.

Peak Pulse Voltmeter

The new Model 80, a Peak Pulse Voltmeter that is capable of readings at pulse widths under 1 microsecond and at 10 pps, has recently been designed and developed by **C. G. S. Laboratories, Inc.**, 36 Ludlow St., Stamford, Conn.

The Model 80 is an automatic slide-back type, and provides direct peak voltage readings of positive or negative pulses of widths from 0.25 microsecond to 20 milliseconds at repetitive rates from 10 to 50,000 pps, provided the duty cycle is under 50 per cent. Ranges of 10, 50, 100, 500, 1,000, and 5,000 volts are provided. Accuracy is 3 per cent full scale on any scale.

For detailed information consult H. Langstroth at **C. G. S.**

RECENT CATALOGS

• • • A new "Commercial Radio Operators Q & A Manual," by Milton Kaufman, containing the questions used by the FCC in the April 1949 examination, with their answers, is to be released in August, by **John F. Rider, Publisher, Inc.**, 480 Canal St., New York 18, N. Y.

• • • A comprehensive catalog, #300, containing the most up-to-date information on the electronic and electrical components and their costs of **Cambridge Thermionic Corp.**, 445 Concord Ave., Cambridge 38, Mass.

(Continued on page 67A)

S·S·White MOLDED RESISTORS

The "All-Weather" Resistors

Of particular interest to all who need resistors with inherent low noise level and good stability in all climates

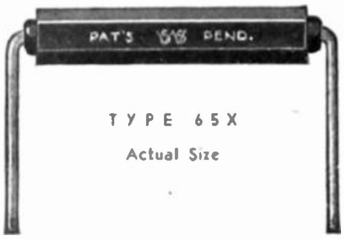

TYPE 65X

Actual Size

STANDARD RANGE

1000 OHMS TO 9 MEGOHMS

Used extensively in commercial equipment including radio, telephone, telegraph, sound pictures, television, etc. Also in a variety of U. S. Navy equipment.

HIGH VALUE RANGE

10 to 10,000,000 MEGOHMS

This unusual range of high value resistors was developed to meet the needs of scientific and industrial control, measuring and laboratory equipment—and of high voltage applications.

SEND FOR BULLETIN 4906

It gives details of both the Standard and High Value resistors, including construction, characteristics, dimensions, etc. Copy with Price List mailed on request.

S.S.WHITE INDUSTRIAL DIVISION

THE S. S. WHITE DENTAL MFG. CO.

DEPT. GR, 10 EAST 40th ST., NEW YORK 16, N. Y.

FLEXIBLE SHAFTS AND ACCESSORIES

MOLDED PLASTICS PRODUCTS—MOLDED RESISTORS

One of America's AAAA Industrial Enterprises

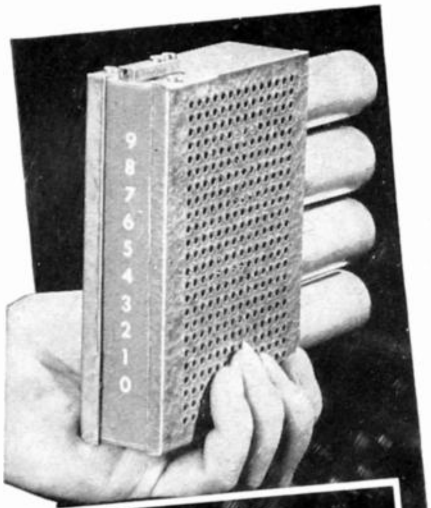

THE NEW BERKELEY MODEL 700 DECIMAL COUNTING UNIT

This unique packaged component is *easily built into* your apparatus. It has *true decimal reading*, and simple binary circuit with reliable *automatic interpolation*. Miniature size. Moderate price. Immediate shipment.

Send for Bulletin DCU-116

Berkeley Scientific Company

SIXTH AND NEVIN AVE · RICHMOND, CALIFORNIA

TEST EQUIPMENT

FOR

RADAR AND TV

MODEL 705

WOBBULATOR

SIGNAL GENERATOR

Center Frequ: 2-500 mc.
Frequ. Sweep: 0-100 mc.
Output: 0.1 volt at 50 ohms
Integral Detectors and amplifier direct viewing 5" scope.

MODEL 708

SPECTRUM ANALYZER

Frequ. Range: 8500-9600 mc.
Min. Frequ. Dispersion: 1 mc/in.
Max. Frequ. Dispersion: 10 mc/in.
Sweep frequ. 10-25 cps
Overall Gain: 125 db
Input Attenuator: 100 db
Power Input 115/230 v. 50-800 cps.

CANOGA CORPORATION

P.O. BOX 361

VAN NUYS, CALIFORNIA

Cramer TYPE SX SYNCHRONOUS MOTORS

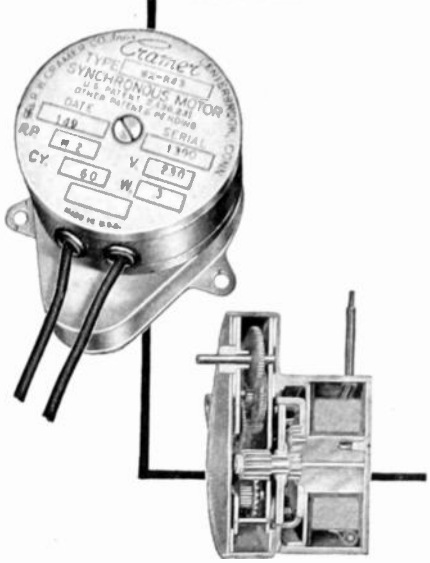

Cramer Type SX Synchronous Motors are highly efficient permanent magnet type motors that produce an exceptionally high torque. Self-starting . . . quick start and stop . . . operate at synchronous speed only. Close tolerance of magnetic field construction and precision alignment of gear train assure long, uninterrupted service.

APPLICATION

Designed for applications requiring a constant speed at a given frequency, Cramer Type SX Motors are widely used throughout the instrument and control fields to fill the gap between the low torque clock motors and the fractional horsepower group.

CHARACTERISTICS

High Torque: 30 in. oz. at 1 RPM, 60 cy. *Quick Response:* Reach synchronous speed within ½ to 2 cy. Stop within 1 pole of motion on 240 RPM rotor shaft (1/60 sec.). *Speeds:* Standard gear trains from 60 RPM through 1/24 RPH. *Cycles:* Available for 25, 50 and 60 cy. operation. *Coils:* Easily replaceable. *Lubrication:* Sealed within housing containing rotor and gear train.

SEND FOR BULLETIN 10B
THE R. W. CRAMER COMPANY, INC.
Box #12, Centerbrook, Conn.

INTERVAL – CYCLE – IMPULSE – PERCENTAGE TIMERS
RUNNING TIME METERS – GEARED SYNCHRONOUS MOTORS

8CR49

News—New Products

These manufacturers have invited PROCEEDINGS readers to write for literature and further technical information. Please mention your I.R.E. affiliation.

(Continued from page 64A)

Low Power Transmitter Mica Capacitors

A new line of transmitter mica capacitors with universal mounting, which are intended for use in low power transmitters for plate or grid coupling, filament, and plate by-pass applications, is announced by **Cornell-Dubilier Electric Corp.,** South Plainfield, N. J.

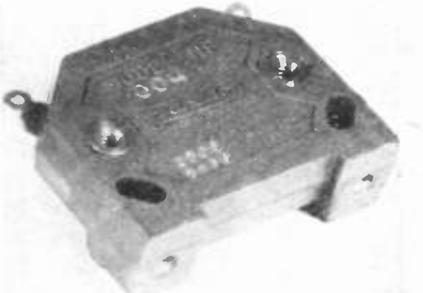

This line, the Faradon NF series, is similar to Type 9 except for different case style and mounting arrangement. The dimensions of these capacitors are $1\frac{13}{16}'' \times \frac{9}{16}'' \times 1\frac{7}{16}''$ over all, with a choice of a vertical mounting with insulated mounting holes tapped for $\frac{6}{32}''$ screw, or a horizontal mounting with brass terminal bushings tapped for a $\frac{8}{32}''$ screw. The latter type has insulated slotted mounting holes and insulated spacer feet to permit assembly against a chassis. Solder lug terminals and brass terminal bushings tapped for $\frac{8}{32}''$ screws provide an optional method of making connections. They are rated in a range from 0.00005 $\mu\mu$f with 2,500 volts dc to 0.03 $\mu\mu$f with 600 volts dc.

New Pin Riveter For Light Operations

Keller Tool Co., Grand Haven, Mich., announces production of a Pin Riveter, for very light riveting operations, with soft-metal tubular and standard rivets.

The new Pin Riveter is said to be suited to a variety of special jobs, such as setting small drive screws, driving brads in the assembly of wood, light peening and scaling operations on thin sheet-metal sections and bakelite.

The net weight of the Pin Riveter is 13 ounces; length, 6 1/16 inches. Piston diameter is 19/32 inch; stroke, ½ inch. Tool has a speed of 9,000 blows per minute. Standard equipment consists of one blank rivet set, with special rivet sets available on order.

(Continued on page 68A)

News—New Products

These manufacturers have invited PROCEEDINGS readers to write for literature and further technical information. Please mention your I.R.E. affiliation.

(Continued from page 67A)

Vertical Lead Shield for Radiation Protection

A new vertical lead shield, Model 800, that incorporates new designed principles, has been developed by **Atomic Instrument Co.**, 160 Charles St., Boston 14, Mass.

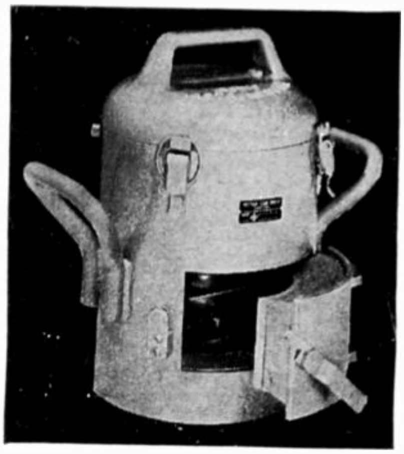

The Model 800 is steel-cased, aluminum-lined and, the manufacturer claims, offers at least 1½ inch equivalent of lead shielding in all directions. The top is of aluminum and lead construction and, while removable, can be securely locked. The connector opening, located near the top of the cylinder, is aluminum-lined.

The interior is equipped with a lucite holder and is specially designed to be completely light-proof and background-proof.

Dimensions are as follows: inside, 5 inches diameter by 8½ inches high; outside, 9 inches by 14½ inches; door opening, 3½ inches by 4 inches; weight, 250 lbs.

New Microvolt Signal Generator

The new Model 292X, signal generator, a microvolt generator designed to cover both upper channel TV and mobile band frequencies on fundamentals, is announced by **Hickok Electrical Instrument Co.**, 10551 Dupont Ave., Cleveland 8, Ohio.

The manufacturer states that its major use will be in the coverage of mobile band frequencies for taxicabs, police departments, railways, ships, etc., for which no expanded scale instrument with accuracy to 0.05 per cent was previously available.

Model 292X covers all AM, FM, TV, and mobile frequencies; measures both input and output of units under test; has modulated and unmodulated output from 1 to 100,000 microvolts; may be externally modulated from 15 to 10,000 cps; employs decibel meter for faster servicing—over 100 inches of scale; and a self-contained crystal oscillator circuit.

Dimensions are $14'' \times 16\frac{1}{2}'' \times 8''$, weight 29 lbs.

For information write to H. D. Johnson at Hickok.

New 2-Watt Fixed Resistor

The development of new 2-watt molded carbon composition resistors is announced by The **Electronic Components Div., Stackpole Carbon Co.**, St. Marys, Pa.

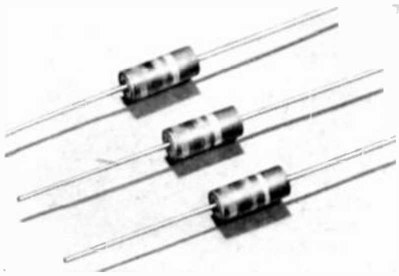

(Continued on page 69A)

News—New Products

These manufacturers have invited PROCEEDINGS readers to write for literature and further technical information. Please mention your I.R.E. affiliation.

(Continued from page 68A)

These resistors are available in a complete range from 10 to 100,000 ohms and in standard tolerances of ±5, 10 or 20 per cent as required. The new resistors have been designed to meet JAN specifications. They are fully insulated and moisture resistant. A new anchoring method assures that lead strength will exceed the standard 10-lb. pull test. Standard RMA color coding is employed. The new resistors are 11/16 inches long by 0.312 inch in diameter.

TV Antenna With Four Driven Elements

A new antenna designed to decrease cochannel interference, is announced by **Technical Appliance Corp.**, Sherburne, N. Y.

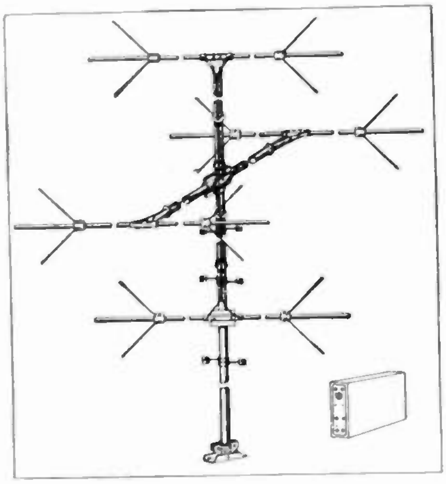

The Type 900 TV antenna has four driven elements, two in the vertical and two in the horizontal plane.

The manufacturer claims that with this new antenna it is now possible by means of a diplexer network to eliminate the cochannel interference present in many locations where two stations are on the same channel or adjacent channels and are located about 180° apart.

Type 900 is supplied with diplexer, which is mounted at the receiver. The diplexer serves as a matching transformer between the line and the receiver, eliminating any standing waves due to mismatch. It also serves as a reversing switch for switching directivity lobes.

Precision Micrometer Head

The announcement of production of a new type precision micrometer head, designed for the electronics industry is made by the manufacturer, **Frequency Standards Corp.**, P.O. Box 66, Eatontown, N. J.

(Continued on page 70A)

News—New Products

These manufacturers have Invited PROCEEDINGS readers to write for literature and further technical Information. Please mention your I.R.E. affiliation.

(Continued from page 69A)

The size of the thimble in all models is $2\frac{1}{8}$ inches in diameter. Readability is assisted by contrasting colors on the scale. The antibacklash screw thread, which compensates for thread wear, provides a positive spindle reading in either direction or rotation. The head is avilable in either English or Metric scales with either 1 inch or ½ inch thread offered in either scale.

New Four-Beam Oscillograph

A new four-beam cathode-ray indicator, capable of simultaneously displaying four related or unrelated independent phenomena on a single screen, has been made commercially available by the designer, **Special Products Section, Allen B. Du-Mont Labs., Inc.** 1000 Main Ave., Clifton, N. J.

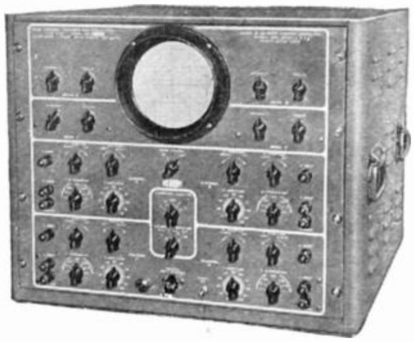

This oscillograph is equipped with Type K1027P11 C-R tube, which contains 4 independent electron guns. It also contains its own power supply and horizontal amplifier for each channel. Sweep circuits and vertical amplifiers are not provided because the instrument was not intended for use with a record camera of the moving-film type.

The horizontal amplifiers are directly coupled, with conductive or capacitive inputs to the four channels. Each channel may be individually calibrated by means of an internal voltage calibrator. Selector switches permit either conductive or capacitive input couplings.

Index and Display Advertisers

Display Advertisers

ROLLING UP THEIR SLEEVES

TYPE 1001-A

Standard-Signal Generator

- MODERATE COST THROUGH SIMPLIFIED DESIGN
- UNUSUALLY LOW LEAKAGE

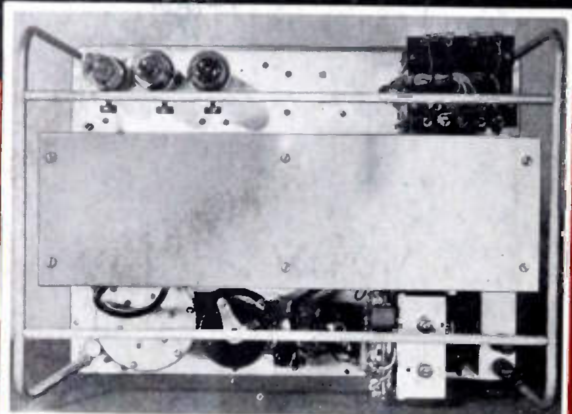

Rear view, removed from metal cabinet. Semi-unit construction with power supply along top, completely enclosed shielded and filtered carrier oscillator in center, and attenuator, carrier control, audio oscillator and modulation control at bottom.

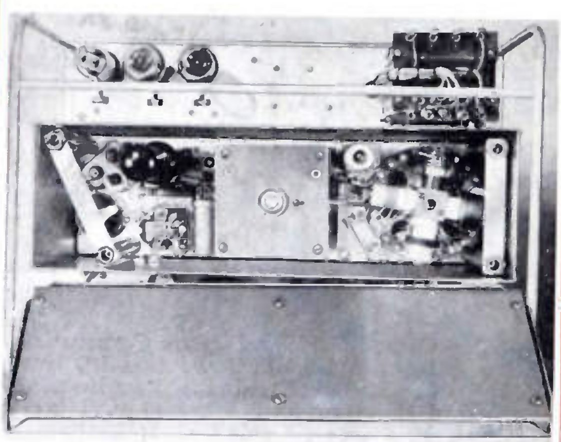

Cover removed from oscillator compartment. Note two-piece construction of cover, each being insulated from the other and making contact with both surfaces of the metal box housing the oscillator. All leads to this box are carefully filtered to prevent leakage.

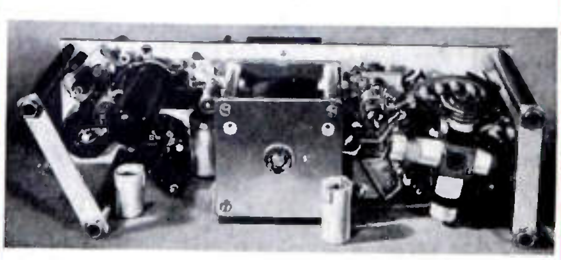

The complete oscillator plugs in and out of the metal box shown above, making testing and servicing particularly easy. The oscillator can be operated when removed from its shielding box. Extra precautions have been taken to insure excellent contact between the pre-loaded contact springs and the cylindrical contacts on the oscillator coil turret shown at extreme right.

With many mechanical and electrical improvements, the Type 1001-A Standard-Signal Generator replaces the once-popular Type 605.

Ruggedly designed, with unique mechanical construction and simplified circuits, this generator has exceptionally low leakage. Through the elimination of a number of circuit frills it has been possible to keep its cost to a moderate figure.

ABRIDGED SPECIFICATIONS

CARRIER-FREQUENCY RANGE: 5 kc to 50 Mc in eight logarithmic, direct-reading ranges.

FREQUENCY CALIBRATION: accurate to ±1%.

INCREMENTAL-FREQUENCY DIAL: indicates increments of 0.1 per cent of frequency per division up to 15 Mc.

OUTPUT VOLTAGE: open-circuit voltage adjustable from less than 0.1 microvolt to 200 millivolts. Two-volts output available from a second jack.

AMPLITUDE MODULATION: adjustable from 0 to 80% either with 400-cycle built-in source, or over 20 to 15,000 cycles from an external source.

LEAKAGE: stray fields are substantially less than 1 microvolt per meter two feet from the generator.

INCIDENTAL FREQUENCY MODULATION: varies from 10 to 100 parts per million, at 80% a.m., over each range except 15-50 Mc where it may be three times this amount.

ENVELOPE DISTORTION: about 6% at 80% modulation.

NOISE LEVEL: carrier noise level corresponds to about 0.1% modulation.

Fully 90 per cent of the needs for a standard-signal generator for general laboratory use are adequately met in this carefully designed G-R instrument, where the ultimate in accuracy and stability is not required.

TYPE 1001-A STANDARD-SIGNAL GENERATOR......$595.00

GENERAL RADIO COMPANY

Cambridge 39, Massachusetts

NEW YORK CHICAGO LOS ANGELES